Mohammad Jawaid
Abou el Kacem Qaiss
Rachid Bouhfid *Editors*

Nanoclay Reinforced Polymer Composites

Nanocomposites and
Bionanocomposites

Springer

Engineering Materials

The "Engineering Materials" series provides topical information on innovative, structural and functional materials and composites with applications in optical, electronic, mechanical, civil, aeronautical, medical, bio and nano engineering. The individual volumes are complete, comprehensive monographs covering the structure, properties, manufacturing process and applications of these materials. This multidisciplinary series is devoted to professionals, students and all those interested in the latest developments in the Materials Science field.

More information about this series at http://www.springer.com/series/4288

Mohammad Jawaid · Abou el Kacem Qaiss
Rachid Bouhfid

Editors

Nanoclay Reinforced Polymer Composites

Nanocomposites and Bionanocomposites

Springer

Editors
Mohammad Jawaid
Laboratory of Biocomposite Technology,
 INTROP
Universiti Putra Malaysia
Serdang
Malaysia

Rachid Bouhfid
Laboratory of Polymer Processing
MAScIR Foundation
Rabat
Morocco

Abou el Kacem Qaiss
Laboratory of Polymer Processing
MAScIR Foundation
Rabat
Morocco

To Our Parents

Parents of Dr. Mohammad Jawaid
Ziaur Rahman (Father)
Late Razia Rahman (Mother)

Parents of Dr. Abou el Kacem Qaiss
Mohammed Qaiss (Father)
Khadija Ghazouli (Mother)

Parents of Dr. Rachid Bouhfid
Lahcen Bouhfid (Father)
Khadija Lograi (Mother)

Preface

Nowadays nanoclay-based polymeric materials display better utilization in different applications. The nanoclay as inorganic fillers results from the exfoliation or the dispersion at nanoscale into polymeric matrices, which allows the improvement of nanocomposites properties by adding small quantities of clay due to the high specific area and the possibility to reach an affinity between the nanoclay and the polymeric matrix. Recent studies reported about fabrication and characterization of nanoclay-based nanocomposites and bionanocomposites, which illustrated better mechanical and thermal properties as compared to nanoclay-reinforced polymer composites. The proposed book is focused on nanoclay-based nanocomposites and bionanocomposites fabrication, characterization, and applications. It will also include the classification of the clay which can be nano-sized, chemically modified, processing techniques of the nanocomposites based on nanoclay. The readers will find complete information about nanoclay modification and functionalization, modification of nanoclay systems, characteristic properties of nanoclay and nanoparticulate-based nanocomposites, modification of nanoclay systems, geological and mineralogical research on clays suitability, role of various polymers and shape of nanoclays on bionanocomposites, effect of nanoclays on gas barrier properties of polymers and co-polymers nanocomposites and different properties of tropical wood polymer nanocomposites, bionanocomposites based on modified montmorillonite and nanocrystaline cellulose, synthesis of natural rubber/palygorskite nanocomposites, hybrid polymer layered silicate nanocomposites, mechanical and thermal properties of halloysite nanotube based nanocomposites, nanoclay-based hybrid composites for advanced functional materials, 3D Smart Materials, biodegradable nanocomposites for soil erosion mitigation and nanoclay reinforced three-phase sandwich composite laminates.

We are highly thankful to all authors who contributed book chapters and provided their valuable ideas and knowledge to this edited book. We attempt to gather all the scattered information of authors from diverse fields in nanoclay-based

nanocomposites and bionanocomposites and finally produce this venture that will hopefully become a success. We greatly appreciate contributors' commitment to support us in formulating ours idea in reality.

We thank Springer Science+Business Media Singapore Pte Ltd. team for their generous cooperation at every stage of the book production.

Serdang, Malaysia   Mohammad Jawaid
Rabat, Morocco   Abou el Kacem Qaiss
Rabat, Morocco   Rachid Boufid

Contents

About the Editors

Dr. Mohammad Jawaid is currently working as Fellow Researcher (Associate Professor), at Biocomposite Technology Laboratory, Institute of Tropical Forestry and Forest Products (INTROP), Universiti Putra Malaysia, Serdang, Selangor, Malaysia and also Visiting Professor at Department of Chemical Engineering, College of Engineering, King Saud University, Riyadh, Saudi Arabia since June 2013. He is also Visiting Scientist to TEMAG Laboratory, Faculty of Textile Technologies and Design at Istanbul Technical University, Turkey. Previously he worked as Visiting Lecturer, Faculty of Chemical Engineering, Universiti Teknologi Malaysia (UTM) and also worked as Expatriate Lecturer under UNDP project with Ministry of Education of Ethiopia at Adama University, Ethiopia. He received his Ph.D. from Universiti Sains Malaysia, Malaysia. He has more than 10 years of experience in teaching, research, and industries. His areas of research interests include hybrid-reinforced/filled polymer composites, advanced materials: graphene/nanoclay/fire retardant, lignocellulosic-reinforced/filled polymer composites, modification and treatment of lignocellulosic fibers and solid wood, nanocomposites and nanocellulose fibers, polymer blends. So far he has published six books, 14 book chapters, and more than 140 international journal papers and five published review papers under Top 25 hot articles in science direct during 2013–2015. He is also the Deputy Editor-in-Chief of Malaysian Polymer Journal and Guest Editor of Special issue-Current Organic Synthesis & Current analytical chemistry, Bentham Publishers, UK. Besides he is also reviewer of several high-impact ISI journals of Elsevier, Springer, Wiley, Saga publishers. Presently he is supervising 15 Ph.D. students and five Master students in the field of hybrid composites, green composites, nanocomposites, natural fiber-reinforced composites, etc., and three Ph.D. and two Master students have graduated under his supervision in 2014–2015. He has several research grants at University and National level on polymer composites of around RM 575,000 (USD 159, 722). He also delivered plenary and invited talks at international conferences related to composites in India, Turkey, Malaysia, Thailand, and China. He is also member of technical committee of several national and international conferences on composites and materials Science.

Dr. Abou el Kacem Qaiss is currently working as Director of polymer processing laboratory, at Moroccan Foundation for Advanced Science, Innovation and Research (MAScIR), Institute of Nanomaterials and Nanotechnology (Nanotech), Rabat, Morocco since october 2010. He received his Ph.D. from Université Laval, Québec, Canada. He has more than 20 years of experience in teaching, research, and industries. His areas of research interests include hybrid-reinforced/filled polymer composites, advanced materials: graphene/nanoclay, lignocellulosic-reinforced/filled polymer composites, modification and treatment of lignocellulosic fibers, nanocomposites and nanocellulose fibers, polymer blends. So far he has published one book, four book chapters, and has published more than 30 international journal papers during 2011–2015. He is also reviewer of several high-impact ISI journals of Elsevier, Springer, Wiley publishers. Presently he is supervising four Ph.D. students in the field of hybrid composites, green composites, nanocomposites, natural fiber-reinforced composites, etc., and four Ph.D. and six Master students graduated under his supervision during 2012–2015. He has research grants at MAScIR and Minister of Higher Education, Scientific Research and Training, Morocco (MESRSFC) of around USD 690000. He was a co-chair of the International Polymer Processing Society Meeting (PPS-27) that was held for the first time in Africa and in the MENA region (Middle East and North Africa), in the City of Marrakech, Morocco, during May 10–14, 2011.

Dr. Rachid Bouhfid is a researcher at Moroccan Foundation for Advanced Science, Innovation and Research (MAScIR), Institute of Nanomaterials and Nanotechnology (NANOTECH), Rabat, Morocco. He obtained his Ph.D. in Organic Chemistry under the supervision of Mohammed V. Following his Ph.D., he joined Artois University, France as ATER, and then became Assistant Professor. Dr. Rachid Bouhfid's research are mainly in the field of organic synthesis of functional molecules to use them as modifiers of inorganic fillers and the development of new polymeric nanocomposites based on clay and nanoclay, graphene and natural fibers. He is author/coauthor of more than 65 international scientific publications, one book, four book chapters, and more than 12 patents. He is also reviewer of several high-impact ISI journals of Elsevier, Springer, RSC, Bentham Science, etc. He has co-organized several international conferences in the field of heterocyclic chemistry (Trans Mediterranean Colloquium on Heterocyclic Chemistry TRAMECH-7, Rabat, 2013) and polymer processing (The International Polymer Processing Society Meeting PPS-27, Marrakech, 2011).

Nanoclay Modification and Functionalization for Nanocomposites Development: Effect on the Structural, Morphological, Mechanical and Rheological Properties

Marya Raji, Mohamed El Mehdi Mekhzoum, Abou el Kacem Qaiss and Rachid Bouhfid

Abstract During the last decades, a widespread research has been devoted to organically modified clay minerals as reinforcements for polymer matrices. The most commonly used procedure to prepare organophilic clay is the cation exchange reaction with ammonium surfactant. Nevertheless, this kind of surface modification does not provide an efficient covalent bond between clay minerals and polymer matrices. For these reason, wide variety of silane coupling agents has been used to achieve compatibility and good dispersion between the hydrophilic clay and hydrophobic polymer. In this respect, the obtained polymer/organoclay nanocomposites exhibit significant improvements in their physical and mechanical properties over those of raw polymers. Herein, this chapter is divided into two parts. In the first part, it focus on the effect of silane modification of different clays minerals namely Halloysite, Montmorillonite and Sepiolite by various organosilanes such as 3-aminopropyltrimethoxysilane (A), 3-iodopropyltrimethoxysilane (I), 3-mercaptopropyltrimethoxysilane (S) and triethoxyvinylsilane (T). Although the silylation method, characterization and properties of the silane grafted clays are discussed. The second part is devoted to the preparation of polymer/silane grafted clay nanocomposites by melt compounding using polypropylene as polymer matrix. From the nanocomposites with 3wt% concentration in terms of silane grafted clay produced, the morphological, physical, mechanical, and rheological properties were measured. The results showed that the overall properties of silane grafted clays nanocomposites were increase which is attributed to better interfacial adhesion.

M. Raji · M.E.M. Mekhzoum · A.e.K. Qaiss · R. Bouhfid (✉)
Moroccan Foundation for Advanced Science, Innovation and Research (MAScIR),
Laboratory of Polymer Processing, Rabat Design Center, Institute of Nanomaterial
and Nanotechnology (NANOTECH), Rue Mohamed El Jazouli, Madinat Al Irfane,
10100 Rabat, Morocco
e-mail: r.bouhfid@mascir.com

1 Introduction

Because of the surge in the field of nanotechnology, polymer matrix based nanocomposites have recently become a promising current research field in the worldwide. These new kinds of materials have attracted steadily growing interest in numerous industrial applications, mainly in the transportation sector, building/ construction industries and food packaging plastics (Galpaya 2012). They often exhibit remarkable properties, including unique mechanical and electrical conductivity, high gas and liquid barrier, flame retardant and thermal properties as compared to the neat polymers (Yeh and Hwang 2006).

The development and progression of environmentally friendly/green nanocomposites materials, will not only benefit on the plastic industry, but would lead to reduce the percentage of the expensive polymer used in the manufacture of materials, such as polypropylene, polyacrylic, polyester and epoxies etc. (Alonso et al. 2012). They are hazardous to the environment, non-degradable and take a long time to decompose, which generates huge many environmental problems associated with their disposal, including damage to the environment eco-system, water supplies, and sewer systems as well as to the lakes, rivers and streams. Furthermore, they are non-renewable; and their high price and unstable with impending depletion of petroleum resources (Majeed et al. 2013).

The incorporation of nano-sized particles in the polymer nanocomposites can reduce their production cost, through the substitution of small amount of polymer by a cheap and abundant resource may be organic or inorganic include layered materials such as graphite, and some clay types, or fiber-like materials namely carbon nano-tubes and nano-fibers, cellulose nano-fibers or other types of clay (Šupová et al. 2011). Among these particles loading, the different kinds of clay reinforcement have been proven an unavoidable synergistic impact on the overall performance of the nanocomposites, due to its special structure, which are most thermally stable and it arranged on the nanometer scale with a high aspect ratio and/or an enormously large surface interface with polymer. In this regard, the low cost, less weight, and low moisture absorption and also the low density makes the clay an attractive alternative to organic or petrochemical-based loading (El Achaby et al. 2013).

Since, discovered the possibility to build a polymer clay nanocomposite in the late 1980s (Nguyen and Baird 2007). Several investigations have also been conducted regarding on the development of new advanced and find further applications. The Toyota Research team began the investigations into reinforcing polymers; they found that the incorporation of moderate mineral clay charge into Nylon 6 marked the stimulus for subsequent theoretical and applied over the last decades, followed by Vaia observations (Vaia et al. 1993), that reported it is

possible to melt mixing polymers and clays without organic solvents. These two important results have motivated both academic and industrial labs to focus their attention on the polymer/clay nanocomposites.

2 Clay Minerals: Structure, Properties and Applications

To fully understand the effect of clay reinforcement on the polymer matrix properties, it is important to highlight the clay definition and their structure. The term clay mineral is difficult to define. From chemical point of view, this term signifies a class of the broad category of hydrated phyllosilicates, likewise, based on geological knowledge, this clay making up the fine-grained fraction of rocks, sediments, and soils (Velde 1985). Far from this definition which create some ambiguity until the moment, and for roughly speaking, clay minerals are essentially hydrous aluminosilicates with very fine particle size and a general chemical formula $(Ca, Na, H)(Al, Mg, Fe, Zn)_2(Si, Al)_4O_{10}(OH)_{2-x}H_2O$, where x represents the variable amount of water. Generally, the clay minerals may be broadly classified into two categories: natural and synthetic clays Include Montmorillonite, Hectorite, sepiolite, laponite, saponite, rectorite, bentonite, vermiculite, biedellite, kaolinite, chlorite, as a natural clays and the synthetic one such as various layered double hydroxides, synthetic Montmorillonite, Hectorite, etc. (Kotal and Bhowmick 2015). Figure 1 summarizes the major class of clay.

Generally, The different structures of clay minerals are basically composed of alternating of tetrahedral silica sheets "SiO_2" and alumina octahedral layers "AlO_6" in ratios of 1:1 when one octahedral sheet is linked to one tetrahedral sheet as Kaolinite, Halloysite, or in ratios of 2:1 this structure created from two tetrahedral sheets sandwiching an octahedral sheet such as Montmorillonite and Sepiolite, finally the proportion of 2:1:1 (chlorite), this latter are not always considered as
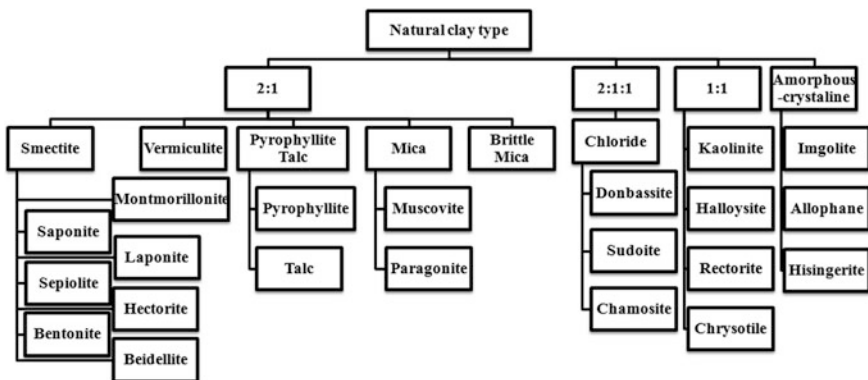
Fig. 1 Natural clay type

clay, sometimes being classified as a separate group within the phyllosilicates (García-López et al. 2010). One side of this lamella remains linked to each other through common oxygen atoms as seen in Fig. 2.

In consequently, the clay platelet undergoes a structural rearrangement to give different structures (nano-fibers, nano-tubes, and plate-like filler) as presented in Fig. 3.

The physical dimension of each platelet may be about 1 nm in thickness and the lateral dimension is varied from 30 nm to several micrometers or even larger, depending on particular silicate, due to an isomorphic substitution of alumina cation (Al^{3+}) within the silicate layers (Nguyen and Baird 2007). For example, in the case of 2:1 structure, the trivalent Al-cation in the octahedral layer is partially substituted by the divalent Mg-cation to form the Montmorillonite structure, given to each layer a net negative charge generated by their difference in valence (Paul and Robeson 2008). The negative charge is counter balanced by the interlayer alkali or alkaline earth metal cation as sodium and calcium ions, when these charges do not balanced and these ions do not fit in interlayer space, the mica will be formed and/or the layers organize themselves to form clay stalks and held together by relatively weak bonding forces of attraction between them as van der walls force, interstitial water and other polar molecules can placed inside the galleries, these latter can be then able to replace by organic cations, via a cationic-exchange reaction in the synthetic

O

OH

Al

Si

Fig. 2 Clay structure
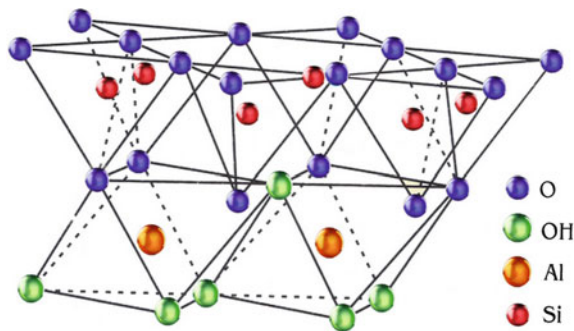
Sepiolite   Montmorillonite   Halloysite
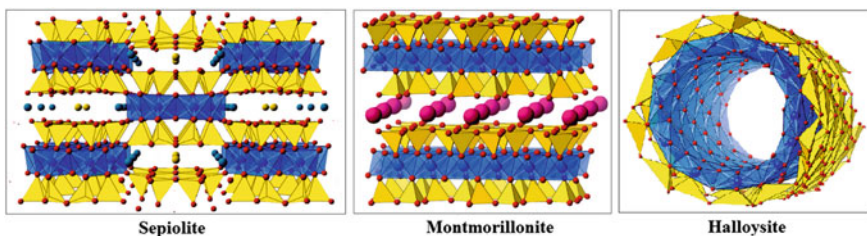
Fig. 3 Clay structures (nano-fibers, plate-like filler, and nano-tubes)

rout to transforms the hydrophilic-clay organophilic (Taxiarchou and Douni 2014). The gallery or the interlayer space of each kind of expansible clay is depend on the size and type of charge compensating cation and polar molecules on interior surfaces within the crystal clay structure itself, their presence on the basal planar rendering the clay hydrophilic in the nature (Bergaya and Lagaly 2013). Expansion of the space between two consecutive layers termed interlayers space, imparts high cation exchange capacity (CEC) relative to non-expansible phyllosilicates and most other secondary minerals (Yui et al. 2013).

Cation Exchange Capacity (CEC) is found to be an approximate measure of the amount of readily exchangeable cations neutralizing negative charge in the clay. Otherwise, it designed the capacity of the clay to hold cations, like Al^{3+}, Ca^{2+}, Mg^{2+}, Mn^{2+}, Zn^{2+}, Cu^{2+}, Fe^{2+}, Na^+, K^+ and H^+[14], it usually expressed formerly as milliequivalents per 100 g (meq/100 g), the CEC value differs from one clay to the other (Yui et al. 2013). A comparison of CEC values for some clay variety is provided in Table 1.

There are many methods available to determine the cation exchange capacity (CEC) of clay; any one is reliable employed for all clay powder. However, one possible technique that is used more effectively for all clay types is not dependent on the pH of saturation but is based on cation saturation, primarily the ammonium, sodium, and barium etc. as the index cation (Sanchez-Martin et al. 2006).

One main potential advantage of cation present between the clay layers is to be able therefore effectively replaced by organic cationic surfactant molecules, leads to renders clay useful in the large part of human existence (Hoidy et al. 2009). The initial application of clay minerals was more than 5000 years ago, for rheological additives, as thickeners in coating products, glues, platisols, drilling fluids and for wastewater treatment organoclays are used as thickeners in paints, greases, oil-base drilling muds, polymer composites and nanocomposites also for the purpose of gelling various organic liquids (Hoidy et al. 2009). Although there has been much work in the field of polymer/clay nanocomposites since their appearance (Liu and Wu 2001; Zeng et al. 2005; Mansoori and Hadi 2015), that will be detailed in the next paragraph.

Historical examples of clay nanocomposites applications are abundant in literature. Since antiquity, when Johnston had develop the fundamental concept of active sites and had also identified all the types of sites contributing to clay interaction with other substances, as in organoclays synthesis, include "broken edge" sites and exposed surface aluminol and silanol groups, isomorphic substitutions, exchangeable cations, hydrophobic silanol surfaces, hydration shell of exchangeable cations, and hydrophobic sites on adsorbed organic molecules (Rytwo 2008). The clay minerals become attractive to researchers, engineers and scientists as charge in many polymer industrial applications for commercial use. Thus, the era of clay/polymer nanotechnology can truly be said to have begun. The initial commercial application of clay nanocomposites was the use of clay, especially the Montmorillonite clay system to reinforce nylon-6 nanocomposites (He et al. 2010), used then as timing belt covers for Toyota cars, in collaboration with Ube in 1990 (Gao 2004). Unitika become the second producer of nylon-6 nanocomposites for

Table 1 Ranges of cation exchange capacities for clay

Clay types	Structure type	CEC (meq/100 g)	d-spacing (Å)	Chemical formula	R
Kaolinite	1:1(TO)	3–15	7.14	$[Si_4]Al_4O_{10}(OH)_8 \cdot nH_2O$ (n = 0 or 4)	(Alkan et al. 2005)
Halloysite	1:1(TO)	5–50	7	$[Si_4]Al_4O_{10}(OH)_8 \cdot nH_2O$ (n = 0 or 4)	(Sánchez-Fernández et al. 2014)
Illite	2:1(TOT)	10–40	10	$M_x[Si_{6.8}Al_{1.2}]Al3Fe_{0.25} Mg_{0.75}O_{20}(OH)_4$	(Euigyung et al. 2011)
Chlorite	2:1:1(TOT)	10–40	14	$(Al(OH)_{2.55})4[Si_{6.8}Al_{1.2}] Al_{3.4}Mg_{0.6}O_{20}(OH)_4$	(Bergaya and Lagaly 2013)
Montmorillonite	2:1(TOT)	60–150	12.4–17	$M_x(Al_{4-x}Mg_x)Si_8O_{20}(OH)_4$	(Navrátilová et al. 2007)
Vermiculite	2:1(TOT)	100–150	9.3–14	$M_x[Si_7Al]Al_3Fe_{0.5} Mg_{0.5}O_{20}(OH)_4$	(Kotal and Bhowmick 2015)
Hectorite	2:1(TOT)	120	12.4–17	$M_x(Mg_{6-x}Lix)Si_8O_{20}(OH)_4$	(Nguyen and Baird 2007)
Saponite	2:1(TOT)	86.6	12.4–17	$M_xMg_6(Si_{8-x}Alx)Si_8O_{20}(OH)_4$	(Hussain et al. 2006)
Sepiolite	2:1(TOT)	11–12	12	$Mg_4 Si_6 O_{15} (OH)_2 \cdot 6(H_2O)$	(Santos and Boaventura 2008)

engine covers on Mitsubishi's GDI engines in 1996 by using synthetic mica as the nano-fillers (Hussain et al. 2006). After that Chevrolet Impalas developed doors with thermoplastic polyolefin nanocomposite (TPO) (Hussain et al. 2006). This was followed by the announced of a step assistant component for GMC Safari and Chevrolet Astro vans16 as the first application of clay/polyolefin nanocomposites of General Motors and Basell (Tjong 2006). More recently, Noble Polymers has developed clay/polypropylene nanocomposites for structural seat backs in the Honda Acura17, while Ube is developing clay/nylon-12 nanocomposites for automotive fuel lines and fuel system components; the following table summarizes some commercial polymer nanocomposites (Gao 2004).

As summarized in the Table 2, the clay nanocomposites are really commonly used in the wide plastic industry due to its attractive versatility in terms of properties, precisely the synthetic one named organoclay, for instance, the great mechanical nanocomposites (tensile, stress, strain) properties together with a high thermal stability (Singla et al. 2012). The clay nano-fillers also can reduce the gas and liquid permeability (Soheilmoghaddam et al. 2014). Moreover, it can improve the dynamic mechanical performances, as well as the flame retardancy while retaining optical clarity of pure polymer (Ahmed Ben Hassan et al. 2014). Finally, the low cost and density, even at low filler loading (Pavlidou and Papaspyrides 2008).

As already mentioned in last paragraphs, there are six kinds of active sites which are important for explaining the mechanism during the synthesis of an organoclay (Pavlidou and Papaspyrides 2008). This reaction called functionalization is based on the interaction between clay minerals surface and organic components named surfactant through three different possible arrangements for their attachments to clay particles; firstly; the surfactant cations may are intercalated into the interlayer spaces by way of cation exchange and adhere to surface sites via electrostatic bonding-charge interaction, secondly; the surfactant cations and/or molecules are physically adsorbed onto the external surfaces of the particles to better coating the clay particles and finally; the surfactant molecules are located within the interlayer spaces (Pavlidou and Papaspyrides 2008). The studies on the organic surfactant grafted clay have been conducted after the introduction of X-ray diffraction in 1913 using different types of surfactant include (de Paiva et al. 2008): Anionic Surfactants, Nonionic, Cationic ones, and finally a single surfactant molecule display both anionic and cationic dissociations it is called amphoteric or zwitterionic.

These organic components can attach to the clay particles by different way is in depend on clay structure, the first one, is as organic surfactant which goes via ion exchange presented between clay layers (generally sodium and calcium ions) resulting in occupation of an interlayer space of the clay structure by organic molecules that hold positive chains and that will neutralize the negative charges from the clay layers (Beauvais et al. 2009). In order to introduce hydrophobicity and increase the clay basal space, which facilitate their exfoliation in the matrix and also improve the compatibility between the hydrophilic clay and hydrophobic polymer during extrusion. This clay modification called as organomodification, or also organophilization (Mejía et al. 2013). The second way of organic components attachment is as a compatibilizing agent if the clay structure does not contain an

Table 2 Commercial polymer nanocomposites. (Zeng et al. 2005)

Product	Characteristics	Applications	Producer
Nylon nanocomposites	Improved modulus, strength, heat distort temperature, barrier properties	Automotive parts (e.g., timing-belt cover, engine cover, barrier fuel line), packaging (e.g., cosmetics, food, medical, electronics), barrier film	Bayer, Honeywell Polymer, RTP Company, Toyota Motors, Ube, Unitika
Polyolefin nanocomposites	Stiffer, stronger, less brittle, lighter, more easily recycled, improved flame retardancy	Step-assist for GMC Safari and chevrolet Astro vans, heavy-duty electrical enclosure	Basell, Blackhawk Automotive Plastics, General Motors, Gitto Global Corporation, Southern Clay Products
M9™ Mitsubishi's MXD6 nylon	High barrier properties	Juice or beer bottles, multi-layer films, containers	Mitsubishi Gas Chemical Company
ORMLAS	High barrier performance, impact resistance, flame resistance, high clarity	Long-life food tray	Triton Systems
Durethan KU2-2601 (nylon 6)	Doubling of stiffness, high gloss and clarity, reduced oxygen transmission rate, improved barrier properties	Barrier films, paper coating	Bayer
Aegis™ NC (nylon 6/barrier nylon)	Doubling of stiffness, higher heat distort temperature, improved clarity	Medium barrier bottles and films	Honeywell Polymer
Aegis™ OX (nanoclay nylon 6 resins)	Highly reduced oxygen transmission rate, improved clarity	High barrier beer bottles	Honeywell Polymer
Aegis HFX	Highly reduced oxygen transmission rate	High barrier juice, tea, and condiments bottles	Honeywell Polymer
AEGIS CSD	High level of a passive carbon dioxide barrier	High barrier bottles weight	Honeywell Polymer
Specialty Film	Excellent barrier properties to oxygen, flavors, and aromas Provide toughness, strength, tear, and puncture resistance, and resistance to grease and gas penetration	Packaging applications: meat, fresh red meat, poultry, fish, cheese, dried food, and chilled fruit juices	Honeywell Specialty Polymers

Table 2 (continued)

Product	Characteristics	Applications	Producer
SET™ nanocomposite nylon 12	Improved stiffness, permeability, fire retardancy, transparency and recycling	Catheter shafts and balloons, tubing, film and barriers, flexible devices	Foster Corporation
Forte™ nanocomposite	Improved temperature resistance and stiffness, very good impact properties	Automotive, furniture, appliance	Noble Polymer

exchangeable cation, which is a graftization of the chemical element that has reactive groups compatible with another reactive groups existing on polymer chain to form the nanocomposite (Ferreira et al. 2011). The overall properties of the nanocomposites based on modified clay characteristics, commonly related on organic molecular mass, type and content of functional groups, organic components/clay proportion, and the manufacturing method (Lee et al. 2012). Among others, the chemical composition and the chain length of the functional groups that interact with the surface of the clays may improve many nanocomposites performance (Xie et al. 2010). The renowned using organic functional groups are Ammonium, phosphonium, imidazolium, Pyridinium, Sulfoniom, and the organosilanes (Leszczyńska et al. 2007). Amongst these latter the organosilanes are known as most favorable compatiblizers or coupling agents for clay fillers because they generally used for providing covalent bonding between clay fillers and polymer matrices, which enhance their interfacial adhesion, and then improve the mechanical properties of the nanocomposites (Sánchez-Fernández et al. 2014). A brief overview on organosilane chemistry and silylation of clay mineral is given below.

3 Oragnosilane Chemistry

Silicon is an essential element which has received a great attention due to is remarkably reactivity and its variety bonding possibilities (Bissé et al. 2005). Silicon is the second most ubiquitous element after oxygen, first, discovered in 1824 by Berzelius (Berzelius 1824). In fact, it is naturally found in the silica (SiO_2) or silicate forms (SiO_4) (Mai and Militz 2004). Silicon as a member of Group 14 in the periodic table shares numerous common characteristics with carbon, but also exhibits different chemical reactivity compared to carbon. Besides, much like carbon atoms, silicon can form four stable bonds with itself and other atoms. In contrast, silicon is more electropositive than carbon, which is much more susceptible of very special and unique chemical reactions. Owing to its dual reactivity, silicon molecule can be synthesized with the ability to bond both organic and

1

M. Raji et al.

inorganic reactivity (Witucki 1993). Therefore, the unique chemical properties and performance characteristics of silicones give rise to variety of infinite silicon-based materials containing hybrid system of silicon/carbon known as 'Organosilane' (Verdejo et al. 2008).

Historically, it was not until 1907 that Kipping and coworkers reported the first synthesis of organosilane. They initially used organozinc, followed by Wurtz-type coupling (Na), before the use of the famous Grignard reagents to make the silicon-carbon bond as shown in Scheme 1. In 1943, Dow Corning Company began commercial development of organosilane technology, opening a new world in silicone chemistry and applications (Thomas 2011). In order to understand the interaction mechanisms between silane and clay minerals called "silylation", it is first necessary to look on the chemical structure of organosilane as coupling agent. See Scheme 1.

A silane is a monomeric silicon chemical similar to hydrocarbon. It has chemical formula $(R_1R_2R_3R_4)Si$ in which four chemical groups attached to the silicon atom. These groups can be the same or different, inorganic or organic and reactive or nonreactive (Halvorson et al. 2003). To be classified as an organosilane, at least one silane substituent must be an organic group linked to silicon through Si–C bond. Alternatively, organosilanes are currently available and unique class of organic silicon compounds; they can be classified according to their molecular and spacial structures. Organosilanes characterized by the $(R_1R_2R_3)SiX_n$ formula where n can have a value between 1 and 3, they possess a hydrolytically sensitive silicon based functional group SiX_n. Organosilanes compounds can form a variety of different hybrid organic-inorganic structures; they can react with other silanes, with themselves and with both inorganic and organic substrates via complex hydrolysis/condensation reactions. The R groups in organosilanes can be either nonreactive (hydrocarbon chain) or reactive substituent with terminal organofunctional groups (methacrylate, epoxy). These latter types of organosilanes compounds are bifunctional molecules and are referred to as silane coupling agents (Plueddemann 1991). In general, silane-coupling agents can be represented by the chemical formula, $Y–(R_1R_2R_3)–SiX_n$ in which at least one of the organic substituents R_1, R_2 and R_3 has a reactive organofunctional group Y. The most common silane coupling agent structures are functional organotrialkoxysilanes $(Y–R–SiX_3)$. Whereas sometimes, the trifunctional SiX_3 group can have only two or one X substituent namely

$$SiCl_4 \ + \ R_2Zn \ \longrightarrow \ SiR_4 \ \longleftarrow \ SiCl_4 \ + \ RMgBr$$

$$\uparrow Na \qquad R = C_2H_5, C_6H_5$$

$$SiCl_4 \ + \ RBr$$
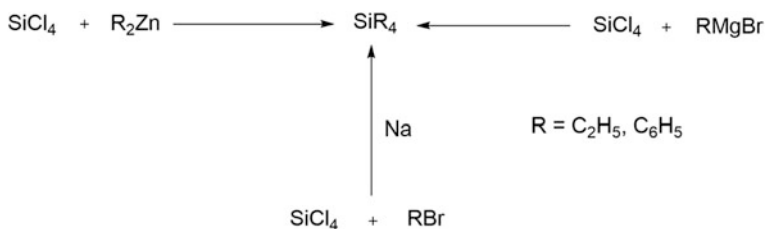
Scheme 1 Synthesis pathway for the preparation of organosilane compounds

Scheme 2 Different types of Functional organosilanes with varying numbers of hydrolyzable substituents on silicon

Trialkoxysilane　　　Dialkoxysilane　　　Monoalkoxysilane

Dipodal Silane
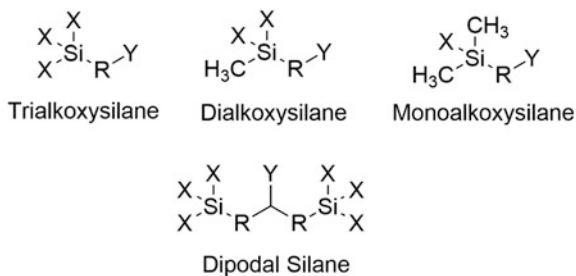
$Y–R_1R_2SiX_2$ and $YR_1R_2R_3SiX$ (Scheme 2). Silylating agents have usually three hydrolysable inorganic-reactive alkoxy groups, e.g., $–OCH_3$, $–OCH_2CH_3$, and one non-hydrolyzable organofucntional group such as amino, vinyl, mercapto. They have also an organo spacer group typically aryl or alkyl separates the organofunctional group from the silicon atom (Ishida and Kumar 1985). Typical commercial examples of silane coupling agents are illustrated in Table 3.

4　Silylation of Clay Minerals

As stated above, silane coupling agents are hybrid compounds with inorganic and organic constituents, they exhibit affinity for both organic and inorganic surfaces and act as a sort of intermediary to form a durable covalent bond between inorganic substrates (namely minerals, metals, cellulose and fillers) and organic polymer (such as thermoplastics or thermosets, rubber) (Weissenbach, Kerstin and Mack 2005). Figure 4 show the bifunctional silane coupling agent mechanism. Due to its unique dual reactivity, silylating agent can be useful for improving the adhesion between the two dissimilar materials (Matinlinna et al. 2013). Such silylating agent can find valuable application in the manufacture of pharmaceutical products, agro-chemicals and in electronics manufacturing (Blum 2003). In addition, any application where silane coupling agents are involved requires the silane molecule to be hydrolyzed and condensed.

Recently, silylation or silane grafting has proved to be an efficient way to modify clay minerals surfaces (Avila et al. 2010). Although, the interaction between hydrophobic molecules and clay could be greatly enhanced by simple grafting of hydrophibic silane groups onto the clay minerals (Takahashi and Kuroda 2011). As a result, the obtained silylation products exhibit suitable application in material science especially in polymer/clay nanocomposites (Isoda et al. 2000). In general, the interactions of silane coupling agents with clay minerals are mainly proceed through different steps. As shown in Scheme 3. Initially, the silane monomers react in the presence of water (hydrolysis) to form reactive, hydrophilic, acidic silanol groups Si–OH followed by partial condensation in which oligomers are formed; during the condensation, silane molecules react with each other forming dimers and

Table 3 Some Commercial silanes coupling agents with different organofunctional groups

Functional group	Chemical name	Structural formula
Epoxy	3-Glycidoxypropyltrimethoxysilane	
Amino	3-Aminopropyltriethoxysilane	
Mercapto	3-Mercaptopropyltrimethoxysilane	
Isocyanate	Tris-(trimethoxysilylpropyl) isocyanurate	
Chloroalkyl	3-Chloropropyltrimethoxysilane	
Diamino	Diaminopropyltrimethosysilane	
Methacryloxy	3-Methacryloxypropyltrimethoxysilane	
Vinyl	Vinyltrimethoxysilane	
Styryl	*p*-Styryltrimethoxysilane	
Acryloxy	3-Acryloxypropyl trimethoxysilane	

Fig. 4 Silane coupling agent mechanism
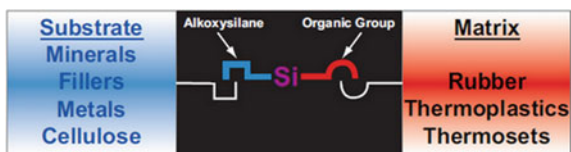
then condense to form siloxane oligomers. Next, the oligomers or monomers silanol are physically adsorbed to hydroxyl groups of clay minerals by hydrogen bonds on the clay surfaces. Finally, under dehydration condensation reaction a robust covalent bond –Si–O–Si– between silanols and hydroxyl groups of clays are formed during a drying process. Moreover, the covalent bond enables a durable

Hydrolysis :

$$R'\text{—}\underset{\underset{OR}{|}}{\overset{\overset{OR}{|}}{Si}}\text{—}OR \;+\; 3\,H_2O \;\xrightarrow{H^+ \text{ or } OH^-}\; R'\text{—}\underset{\underset{OH}{|}}{\overset{\overset{OH}{|}}{Si}}\text{—}OH \;+\; 3\,ROH$$

Self-condensation :

$$R'\text{—}\underset{\underset{OH}{|}}{\overset{\overset{OH}{|}}{Si}}\text{—}OH \;+\; R'\text{—}\underset{\underset{OH}{|}}{\overset{\overset{OH}{|}}{Si}}\text{—}OH \;\longrightarrow\; R'\text{—}\underset{\underset{OH}{|}}{\overset{\overset{OH}{|}}{Si}}\text{—}O\text{—}\underset{\underset{OH}{|}}{\overset{\overset{OH}{|}}{Si}}\text{—}R' \;+\; H_2O$$

$$R'\text{—Si—O—Si—R'} \;+\; x\,H_2O$$
$$R'\text{—Si—O—Si—R'}$$

Adsorption :

Clay platelet + HO—Si—R' structures → adsorbed (hydrogen-bonded) silane species on clay platelet

Chemically grafting :

hydrogen-bonded silane on clay platelet $\xrightarrow{\Delta}$ grafted Si—O structures $+\; x\,H_2O$

$+$

Polymer

→ grafted clay platelet —O—Si—R'······ polymer

Scheme 3 A plausible mechanism of coupling reaction between silane grafted clay mineral and thermoplastic matrices

immobilization of the organic moieties in the silane grafted products which prevents their leaching into the surrounding solutions. In addition, the R' organofunctional group remains available can react with the polymer matrix, resulting in the

formation of a network among silane, clay mineral and polymer through covalent bonds. Therefore, the resultant polymer/clay nanocomposite exhibits a substantial improvement in their properties including mechanical, rheological and other handling properties (Shanmugharaj et al. 2006; Ha et al. 2007; Shen et al. 2007; Sánchez-Valdes et al. 2009). Certainly, the silanization of the clay mineral can take place at three basic models namely at the interlayer space, external surface and at the edges. The interlayer and edges grafting can increase the distance between the layers. For the external surface, the silylation has no effect on the basal spacing of the clay. Such successful silylation of clay minerals surfaces has been reported, in this case, a great attention was paid to the kind of silanes, the clay mineral structure as well as the influence of the solvents on the grafting reaction. In addition, the silanization reaction can also take place onto organoclay minerals to improve their compatibility with the polymer matrix (Park et al. 2004; Chen and Yoon 2005).

5 Preparation and Characterization of Silane Grafted Clay

In the present chapter, three different clay minerals were reported namely Montmorillonite lamellar structure, nano-fiber sepiolite and tubular Halloysite, a 1:1 layer silicate with rolled structural layers and interlayer water. Initially, the modifications of clays were carried out using four different commercial organosilanes. Although. Toluene was used as solvent for dispersing medium. Scheme 4 shows the chemical structure of the used silanes. Certainly, the choice of organosilane as coupling agent is determined by the nature and chemical structure of the thermoplastic matrices used. In our case, each silane differs by its organic functional groups such as vinyl (T), amino (A), iodo (I), and mercapto (S). These reactive groups can form chemical bonds with polymer materials. In addition, the interaction and the interfacial properties between polymer/clay depend on the type of the non-hydrolyzable organic moiety, which can affect the final macroscopic properties of the material obtained. The method of modifying clays presents; as an example; in this work has been performed in one step. The procedure consisted on dispersing an

Scheme 4 The schematic of the used silanes
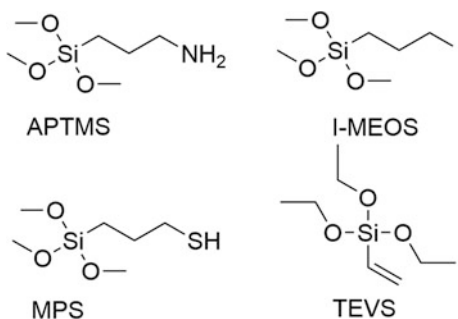
excess of clay (3 g) in 300 ml of toluene at 25 °C under constant stirring followed by sonication for at least 30 min. 3 ml of organosilane was introduced into the above-mentioned mixture and sheared for 24 h at 80 °C. After that, the modified clay was separated from solution by centrifugation at 10.000 rpm. The resultant product was washed using the mixture of ethanol/water for 3 times in order to remove the residual silane and dried at 60 °C in a vacuum oven. The final product was grinded and sieved before use.

5.1 X-Ray Diffraction (XRD)

Once the appropriate silane modified clays were prepared, a number of analysis techniques have been performed including XRD, FTIR, TGA analysis. First, XRD analysis was used to identify the chemical composition and crystallographic structure of the silane grafted clays. Figure 5 present the diffractograms of XRD of clay namely Halloysite, sepiolite and Montmorillonite as well as their four silane grafted -clays samples. As can be depicted from Fig. 5a, all diffractograms of the silane modified-Halloysite are almost identical and show no difference to the raw clays. The five solids are composed principally of two polymorphs of the bilaminar
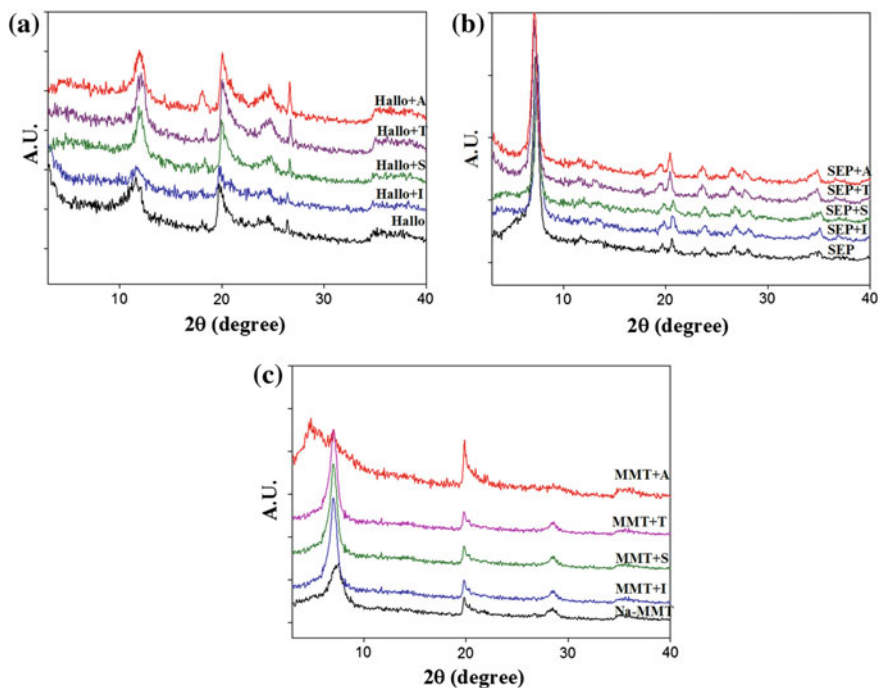
Fig. 5 XRD spectrum of montmorillonite, halloysite, sepiolite, and their silane grafted ones

clay (1:1) dioctahedral Halloysite, in the presence of SiO_2 and $Al(OH)_3$. In addition, both Halloysite-7A, and Halloysite-14A phases were identified. Therefore, during the process of silylation, the modification of Halloysite with different organosilanes did not cause any structural chemical changes compared to other clay minerals (Sánchez-Fernández et al. 2014). On the other hand, Fig. 5b show the XRD pattern of sepiolite which is affected by modification with organosilane. It can be seen that the intensities of some original peaks changed in the position range of 20–40 upon silylation. The variations in XRD diffractograms before and after the silylation of sepiolite show that there is a covalent bond formed by the interaction between sepiolite and different organosilanes, which can be confirmed by FTIR and TGA results (Belver et al. 2013). Figure 5c shows the XRD pattern of raw and silane grafted Montmorillonite. The MMT-A clay display a broad band around of $2\theta = 4.6°$. The interlayer spacing corresponding of the peak of MMT-Na around 1.21 nm which increased to 1.9 nm for the MMT-A clay, according to Bragg's equation (Eq. 1)

$$2\mathrm{dsin}\theta = n\lambda \tag{1}$$

where,

λ is the wavelength of X-Ray, θ is diffraction angle and d is interlayer distance.

It can be concluded that, after clay modification by the organosilane (A), the ATPES molecule was intercalated and grafted to interlayer surface silanol groups. It can be mentioned that d-spacing value indicates a monolayers or paraffin-type arrangement between the aluminosilicate layers. This intercalation constitutes an efficient way to increase surface hydrophobicity which is a fundamental prerequisite for good compatibility between the polymer matrix and the Montmorillonite surface (Shen et al. 2007). For the others silane grafted Montmorillonite spectrum exhibits a broad band in the region between $d = 1.31°$, $d = 1.32°$ and $d = 1.26°$ for MMT-T, MMT-S and MMT-I, respectively. No significant differences were observed in the basal spacing of the latter modified clays. This observation may indicate that there are no interlayers or edges grafting, therefore, the silylation take place at the surface of the Montmorillonite which can be verified by FTIR and TGA results.

5.2 Structural Characteristics (FTIR)

The FTIR spectra of raw clays and the silane grafted ones by A, I, S and T silane molecules are presented in Fig. 6. Figure 6a shows the FTIR spectra of the Halloysite skeleton, The transmittance bands at 3697 and 3623 cm^{-1} in the FTIR spectrum were assigned to the stretching vibration due to O–H stretching of inner-surface hydroxyl groups, O–H stretching of inner hydroxyl groups of the Halloysite, respectively (Frost and Vassallo 1996). The interlayer water is indicated by the H–O–H (adsorbed water) deformation band appears at 1635 cm^{-1} (Bobos et al. 2001). The 1113 cm^{-1} peak was assigned to the stretching mode of Si–O, while
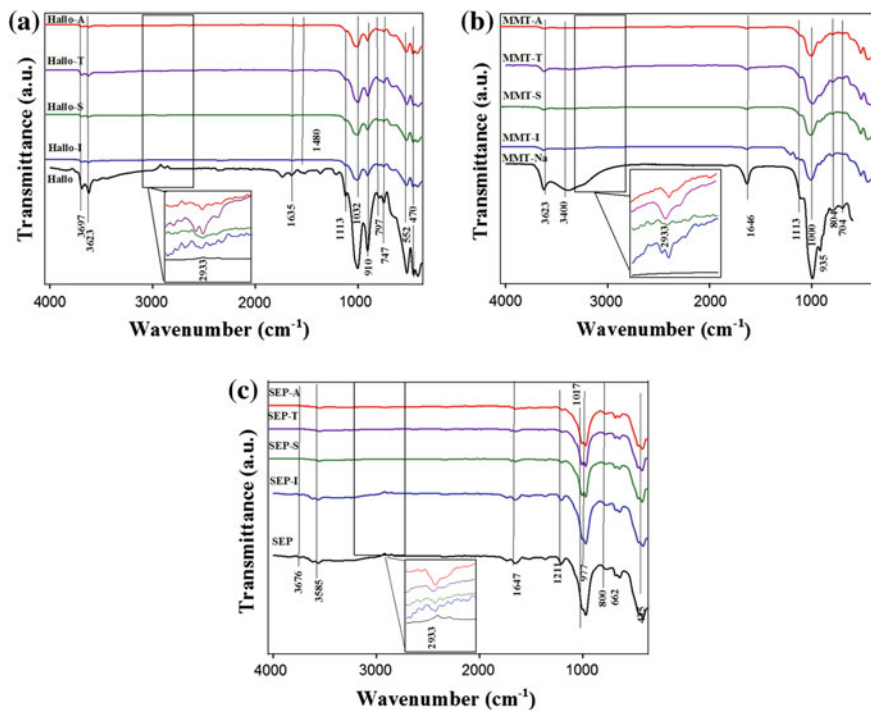
Fig. 6 FTIR spectra of montmorillonite, halloysite, sepiolite, and their silane grafted ones

the band at 1032 cm^{-1} was caused by the stretching vibration of Si–O–Si (Bordeepong et al. 2011). The O−H bending vibrations of the hydroxyl groups are observed at 910 cm^{-1} and Si–O–Si at 470 cm^{-1} confirm the existence of corresponding groups (Szczepanik et al. 2015). The bands attributed to the Al–OH vibrations of the surface hydroxyl groups are observed at 747 and 797 cm^{-1}. The band observed at 538 cm^{-1} was due to the vibration of Al–O–Si (Frost 1995). The Montmorillonite IR spectrum presented in Fig. 6b shows two important bands around 3623 and 3400 cm^{-1} which are indicative to O–H stretching for the silicate and water. The FTIR spectrum of clays, shows a band in the region of 1646 cm^{-1} which is attributed to the –OH bending mode of the adsorbed water (Xie et al. 2011). The characteristic band at 1113 cm^{-1} is assigned to Si–O stretching, and out-of-plane Si–O stretching mode of raw clays (Xie et al. 2011). The band at 1000 cm^{-1} is ascribed to Si–O stretching (in plane) vibration for layered silicates. The IR bands at 935, 804 and 704 cm^{-1} are attributed to Al–Al–OH, and Al–Mg–OH bending vibrations, respectively (Bhattacharya and Aadhar 2014). Figure 6c illustrates the FTIR spectrum of the sepiolite it shows the characteristic band at 3676 cm^{-1}, which is attributed to Mg–OH stretching of hydroxyl groups in octahedral Mg ions located in the interior blocks of natural sepiolite (Alan and İşçi 2014). The coordinated water corresponds of O–H stretching band appeared at 3585 cm^{-1}

and O–H stretching and deformation of zeolitic water bands observed for Sepiolite at 1647 cm^{-1} (Soheilmoghaddam et al. 2014). The Si–O coordination bands at 1211, 1017, 977 cm^{-1} are observed as a result of the Si–O vibrations (Ahmed Ben Hassan et al. 2014). The bands presented around 800 and 662 cm^{-1} are responsible from the O–H deformations and translations, respectively. The two peaks at 1017 and 435 cm^{-1} represent the stretching and bending of Si–O respectively in the Si–O–Si groups of the tetrahedral (Alan and İşçi 2014).

The FTIR spectrum of all silane grafted clays (sepiolite, halloysite and montmorillonite) detect other characteristic signals bands such as two weaker characteristics bands at 2933 cm^{-1} and at 2865 cm^{-1} attributed to aliphatic stretching of CH_2 and CH_3 groups, respectively. Another band at 1480 cm^{-1} which can be associated to the deformation vibration of CH_2 (Herrera et al. 2004), normally present in the mono- and the trifunctional silane molecules. Finally, the presence of silane in the all silane grafted clays spectrum is confirmed, which implies that silane has been grafted into the Montmorillonite, Halloysite and sepiolite structure.

5.3 Thermogravimetric Analysis (TGA)

The thermal degradation of the raw and silane grafted clays were evaluated by thermogravimetric analysis (TGA) to compare the degradation profiles of the different types of clay used as essential parameter in the choice of the technical applications of nanocomposite materials. The thermal decomposition of raw clays and the silane grafted ones by A, I, S and T silane molecules are superposed in Fig. 7. Firstly, the decomposition curves of the raw and silane grafted Halloysite can be divided in three steps as described in the following paragraph. Figure 7a shows the first weight loss for raw Halloysite in the range of 40–140 °C, which is reduced for the silane grafted ones, this lessen indicate an increase in the organophilicity of the Halloysite, while the adsorbed water content at the surface was reduced due to the presence of organosilanes. The second one in the range 200–320 °C can be attributed to the decomposition of silane bonded in the clay, and the decomposition of the oligomerized silane network that was not removed during washing. The last step is between 350–650 °C can be related to the structural dehydroxylation of the Al–OH and Si–OH groups and some additional organic decomposition of the silane grafted onto the Halloysite. Moreover, the higher weight loss shown from silane grafted Halloysites compared to raw Halloysite is consistent with the hydrocarbon chain of the alkyl group from the grafted silane molecules. This also supports the strong chemical interaction of the organosilanes with the Si–O and Al–O groups of Halloysite. The remaining materials at 800 °C (85 %) are of aluminum oxides and silicon oxides present in Halloysite structure. These results confirm the grafting of the silanes on the Halloysite (Carli et al. 2014).
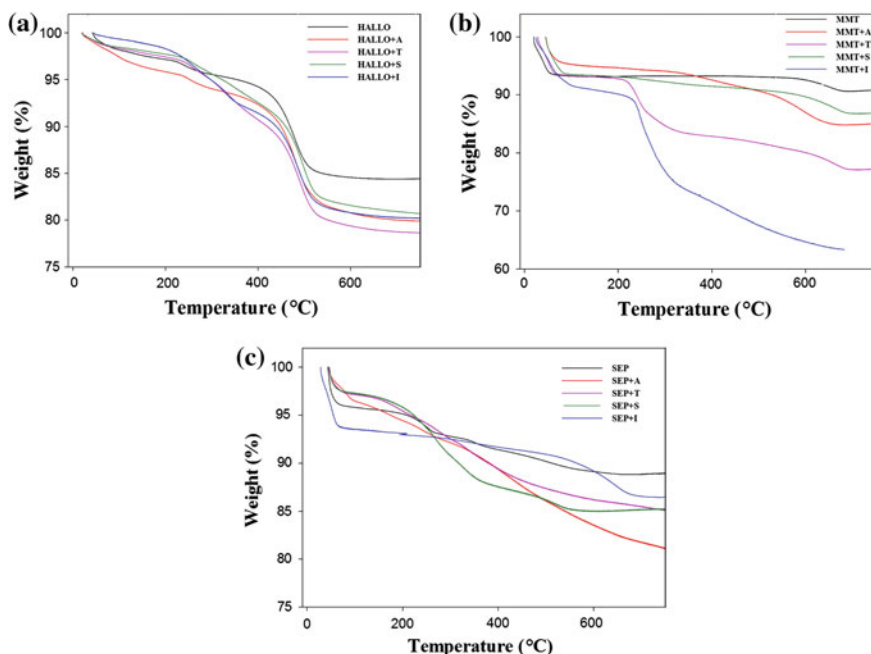
Fig. 7 TGA curves for the different raw and silane grafted clays used

The Montmorillonite thermal decomposition presented in Fig. 7, b) occurs in two steps: around 41 °C (7 % weight loss) and 651 °C (3 % weight loss) are due to the loss of physisorbed water and the loss of interstitially water, respectively. Another band appeared for silane grafted Montmorillonite ranging from 233 °C to 295 °C, in this region where the intercalated silane and all organic substances thermally decompose with a total weight loss varied from 2 % for MMT-A, 3 % for MMT-S, 10 % for MMT-T and 20 % for MMT-I.

The Grafted amount (mequiv/g), which corresponds to the amount of intercalated molecules which effectively participated in the silylation reaction, can be determined using Eq. 2 from the weight loss, W200–600, between 200 and 600 °C corresponding to silane degradation. The results show that the amount is varied from 1.17 for MMT-I, 0.37 for MMT-A, 0.53 for MMT-T and 0.74 for MMT-S (Zhao et al. 2009). (See Table 4)

$$\text{grafted amount (mequiv/g)} = 10^3 \frac{W_{200-600}}{(100 - W_{200-600})M} \tag{2}$$

where M (g/mol) is the molecular weight of the grafted silane molecules.

Table 4 DTG bands of montmorillonite

Step	Bands	Characteristics	Sample name				
			Na-MMT	MMT-A	MMT-I	MMT-S	MMT-T
First step	loss of physisorbed water	T (°C)	41	56	78	75	56
		Mass loss (%)	7	5	9	7	7
Second step	decomposition of the intercalated silane	T (°C)	–	433	295	274	287
		Mass loss (%)	–	2	20	3	10
		Grafted amount (mequiv/g)	–	0.37	1.17	0.74	0.53
		Grafting yield (%)	–	25.1	27.35	35.9	30.1
Third step	loss of interstitially water	T (°C)	651	623	590	663	638
		Mass loss (%)	3	6	9	5	5

The grafting yield, which corresponds to the percentage of silane molecules which effectively participated in the silylated reaction, the following equation (Eq. 3) is employed, where [silane] (mequiv/ g) is the silane concentration in feed

$$\text{grafting yield } (\%) = \frac{\text{grafted amount } \times 100}{[\text{silane}]} \qquad (3)$$

where [silane] (mequiv/g) designates the initial silane concentration.

Figure 8 shows the changes on sepiolite structure with thermal treatment, showing the importance of its water molecules. The thermal decomposition of neat sepiolite was carried out in four steps. First, below 250 °C, both zeolitic and adsorbed water could be eliminated in which the sepiolite structure remains

Fig. 8 DTG bands of sepiolite
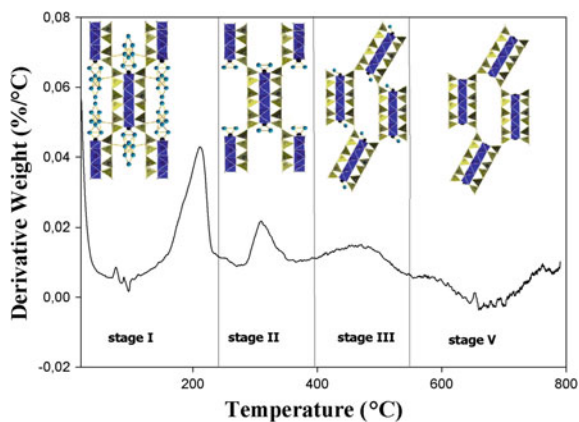
unchanged. Coordinated water is lost in two stages: between 250 and 350 °C and between 400 and 550 °C. Therefore, the coordination water loss involves structural changes reduction where a new channel cross-section of the zeolitic is reduced and an irreversible loss of water is produced. In this state, the mineral is called as anhydrous sepiolite. Between 550 and 1100 °C, the clay has lost all the water molecules and retains their Si–OH groups along its fiber. Above 1100 °C, the Si–OH was destroying after total dihydroxylation (Núñez et al. 2014). The TGA curves of both raw and silane grafted sepiolite are similar but an additional decomposition appears around 200–205 C. This new step close to the decomposition area of zeolitic water corresponds to the degradation of organosilane molecule, which is usually related to silane grafted on the silicate surface; these results confirm the silylation of sepiolite (Basurto et al. 2012), see Fig. 7c.

6 Nanocomposites Preparation

The characterization of each organoclays proved that all silane functionalization can modify the morphological and structural characteristics of the organoclay to better improve the mechanical and rheological properties of their nanocomposites, for revealing the successful surface modification and to evaluate the effect of silylation of organoclay nanocomposites, Herein we use the tensile and dynamic mechanical analysis (DMA) test results to reveal that both clay and the organoclay reinforced PP nanocomposites exhibited better properties than neat PP. The melt flow index (MFI) values will help to distinguish between the different grades of nanocomposite. Indeed, the scanning electron microscopy (SEM) images will be utilized to determine the particle size, morphological properties and their distribution/ dispersion into polymer matrix. Finally, the rheological test values will be also exploiting to characterize their visco-elastic behavior.

PP/unmodified and PP/ silane grafted clay nanocomposites were prepared by simple melt compounding using a Leistritz ZSE-18 twin-screw extruder (Leistritz Extrusiontechnik GmbH, Germany), under the following the temperature profile of the extruder barrel's seven zones was set from hopper to die at 170, 170, 175, 180, 180, 175, 170 and 170 °C, at 3wt% of each nano-clay were incorporate into PP via masterbatch process (10 % wt. nano-particles) obtained by the combination of PP with either MMT-Na, Halloysite, and Sepiolite and their organoclay by 3-aminopropyltrimethoxysilane (A) and triethoxyvinylsilane (T). After extrusion and pelletizing in a precision grinder (FRITSCH Pulverisette 19) into pieces of 2–3 mm, the compounds were injection molded using an Engel e-Victory injection molding machine with a 40 tons platen capacity. The process temperature of the injection press barrel was fixed at 180 °C while the nozzle temperature was set at 170 °C and mold at 45 °C. Then, the unmodified and the modified clay (A, T) nanocomposites were tested using different characterization methods as described next.

6.1 Dynamic Light Scattering

The clay nano-particles were evaluated by dynamic light scattering (DLS) to determine the particle size of different kind of clay which then may compared by modified clay particles size. The measurements were performed on a Zetasizer Nano ZS from Malvern Instruments Ltd. The Fig. 9 shows the dynamic light scattering of Halloysite, montmorillonite and sepiolite. The DLS result of Halloysite assumes that the particles have nanotube stricter with an average effective thickness around of 39 nm and a length about of 171 nm. In the other hand, the DLS result of the sepiolite and Montmorillonite clay, present that the both clay having the size about 264 nm and 171 nm, respectively.

6.2 Scanning Electron Microscopy (SEM)

In order to evaluate the effect of silylation treatments on clay morphology and the dispersion- distribution of the nanoclay in the matrix, scanning electronic microscopy (SEM) was used as a routine for morphology analysis of the nanocomposites polymer and provides much valuable information at the microscale level.
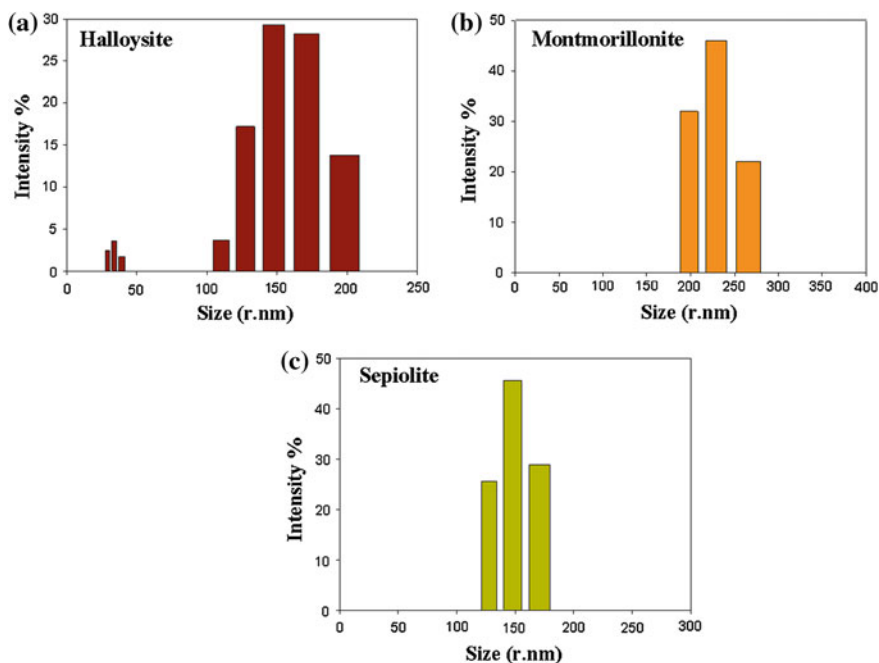
Fig. 9 Dynamic Light Scattering of a halloysite; b montmorillonite; c sepiolite

Some physical changes such as the size of nano-particles can be observed in Fig. 10, which illustrates the SEM images of the cry fracture surface of the nanocomposites reinforced by the raw and silane grafted clays. The all micrographs of silane grafted clays show that the clays nano-particles are uniformly dispersed in the PP matrix with a small amount of agglomerates, in contrast, it is observed on raw clays nanocomposites micrographs that there are a high number of agglomerations, resulting from the strong particle-particles interaction; the less aggregation and the lack of the voids around the clays nano-particles in the case of silane grafted clays nanocomposites indicate that the use of silane functionalization can improve the interfacial adhesion between the clays nano-particles and PP polymer matrix. Indeed, the use of melt compounding process to manufacture the nanocomposites is evident and enabled better nano-particles clay distribution. Based on these images, the size of 50 particles can be measured to get an average nanoparticles size summarized as follow in the Table 5. The particles sizes of all clays were decreased as compared to raw ones, attributed to the change of the clay structure by the silylation. The sizes of each clay particles measured by SEM are near of that measured by zetasizer, which means that they are no obvious agglomeration.

6.3   Melt Flow Index

The melt flow index (MFI) or melt flow rate (MFR) test was used to measures the uniformity of the flow rate of extrusion of a thermoplastic material through an orifice of specific length and diameter under prescribed conditions of temperature and load. The reported melt flow index values of each test specimen which was in the form of granules help to distinguish between the different grades of the nanocomposites. The MFI test was carried out following ASTMD1238-04, using the total load including the piston was 2.16 kg and melting temperature equal to 230 °C.

Figure 11, Shows that the MFI values of nanocomposites are increased compared to that of neat PP one, the addition of clay nano-particles illustrate an increase in flow of the polymers, this is due to the fact that the incorporation of clay nano-particles hinders plastic flow and decreases the viscosity of PP composites at the melt state. The MFI values of nanocomposites is then decreased by the chemical modification of clay, which may indicate that the structure of nano-particles was interconnected to hinder the molecular motion of polymer chains (Wang et al. 2013).
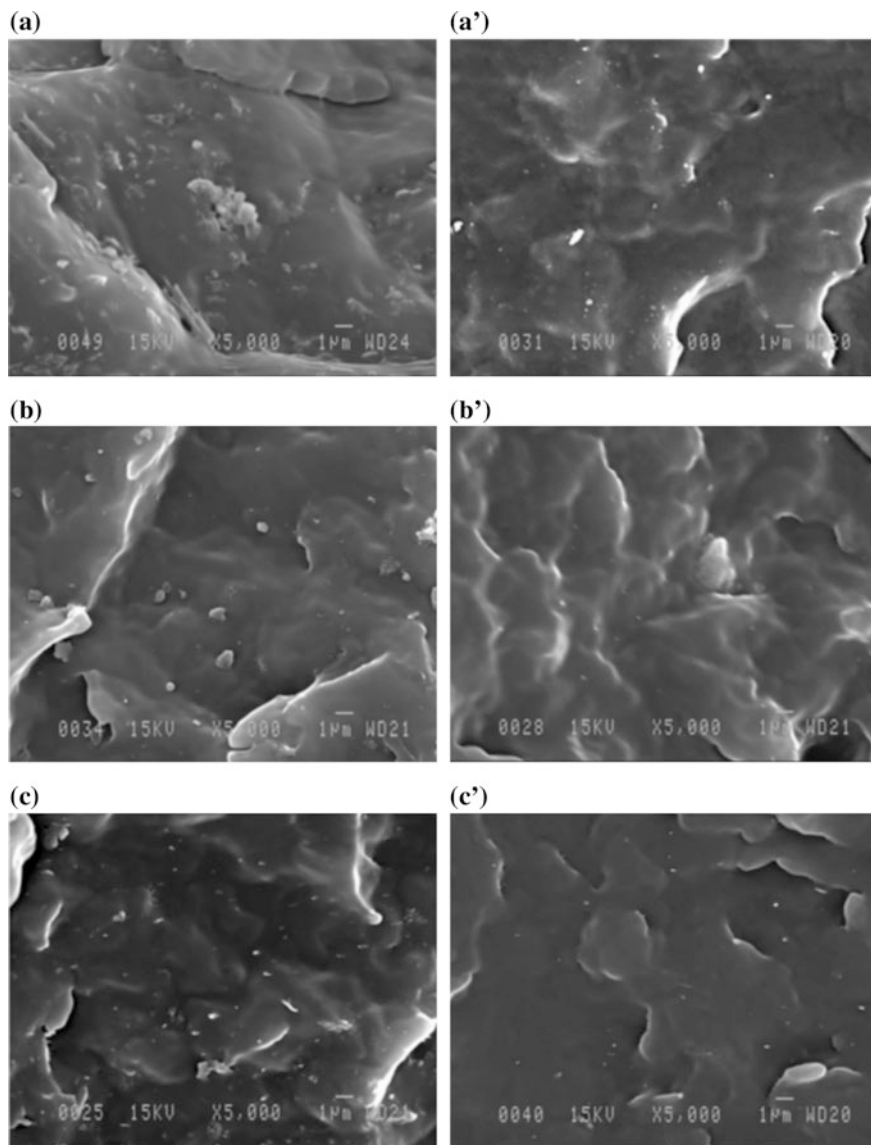
Fig. 10 SEM of **a** Halloysite; **b** grafted silane Halloysie; **c** Montmorillonite; **d** silane grafted Montmorillonite; **e** sepiolite; **f** silane grafted sepiolite

6.4 Tensile Testing

The mechanical test has been used to evaluate the improvement achieved by the silylation treatments of different clay on the nanocomposites properties. The device

Table 5 The average particles size of raw and modified clays nanocomposites from SEM analyses

Clay nanocomposites		Particles size (nm)
Montmorillonite	Raw	305,73
	Modified	146,37
Halloysite	Raw	341,36
	Modified	257,16
Sepiolite	Raw	248,50
	Modified	134,21

Fig. 11 Effect of clay nano-particles and their chemical modification on the melt flow index of PP
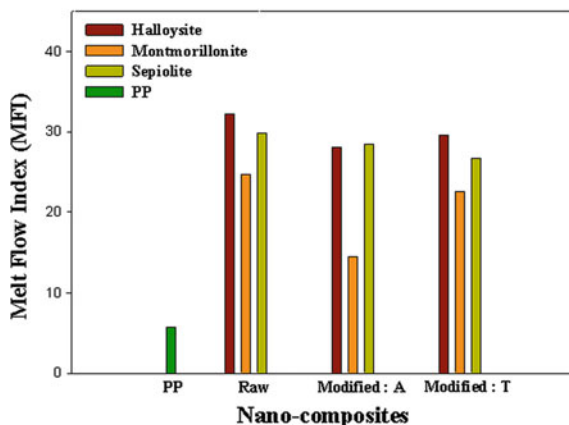
provides access to the force F exerted on the sample according to its elongation ΔL. The results can then be expressed in terms of the strain ε and stress σ. The tensile properties as Young's modulus, tensile strength and strain at yield of the nanocomposites were obtained from the stress-strain curves.

All specimens were tested using a universal test machine (H10KT, Tinius Olsen) with a cross head speed of 5 mm/min at room temperature. To investigate the effect of nanoclays loading and the effect of silane grafted clay on the mechanical properties of the manufactured nanocomposites, the tensile properties have been evaluated on terms of Young's modulus, tensile strength and strain at yield obtained from the stress-strain curves.

The Young's modulus of raw and silane grafted clays are showing in Fig. 12a. The Young's modulus values of each clay increase by the incorporation of clay and better by the silylated treatments of clay, the differences between silylated systems depending on the organosilane functional group responsible for interaction with the polymer matrix. The improvement of Young's modulus values in the case of unmodified clay from 1034 MPa of PP to 2176 MPa, 3220 MPa and 3117 MPa for Halloysite, Montmorillonite and sepiolite, respectively, is due to restricted mobility of polymer chains and their degree of freedom. These behaviors can be explained by the fact that there might be plenty of intermolecular covalent bonds formed between the surface of the clay and the polymer matrix, which enhance the
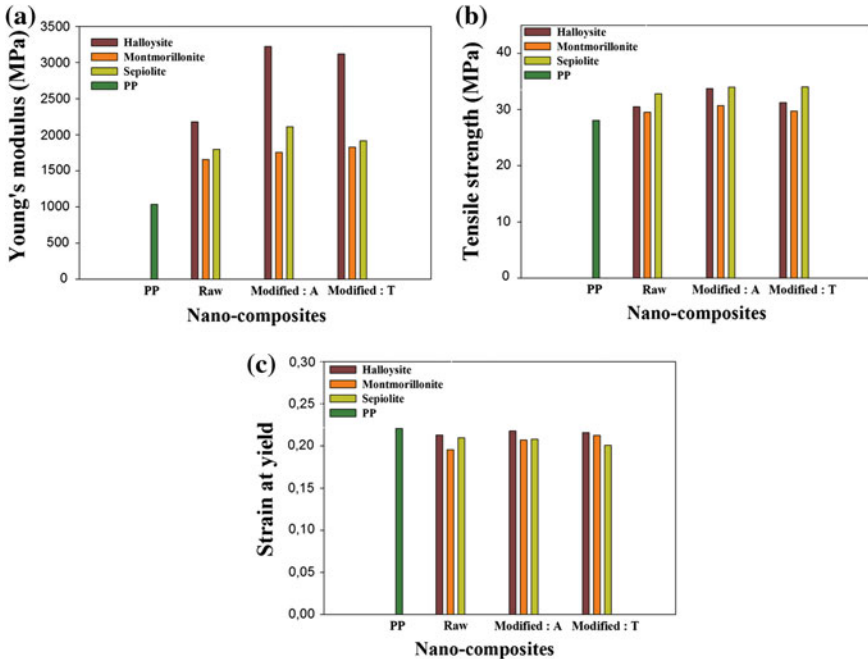
Fig. 12 Young's modulus, tensile strength and strain at yield of clay nano-particles and their chemical modification

adhesion between the composite components by the formation of a strong linkage between the organic and the inorganic phase (Kickelbick 2003).

The tensile strengths of raw and silane grafted clays with 3wt% clay content are shown in Fig. 12b. It's illustrated in Fig. 12b a marked increase in the tensile strength was observed for all nanocomposites Na-MMT, raw Halloysite and raw sepiolite at 3wt% up to 29.52 MPa, 30.05 MPa and 32.76 MPa, respectively, when compared to the neat polymer (28 MPa) which corresponds to a gain of 5 %, 7 % and 17 %, respectively. After silylation treatment, a clear increase of tensile strength values has been noticed compared to unmodified clay nanocomposites. This considerable enhancement in the tensile strength of the manufacturing nanocomposite cannot be explained only by uniformly dispersed clay particle with high aspect ratio and high intrinsic stiffness, but also can be ascribed to the strong interaction between nano-clay particles and polymer matrix (Zeng et al. 2005).

The dissimilar result has been observed from the clay nanocomposite for which the strain at Yield was be stable by the incorporation of nano-clay particles, the decrease of the strain at yield values from 22 % of the polymer composite to 21 %, 20 % and 21 % for Halloysite, Na-MMT and Sepiolite at 3 wt% clay content, respectively, correspond to a reduction of 3.48 % for Halloysite, 11.37 % Na-MMT and 5.09 % for Sepiolite, This can be allowed to concluded that the incorporation of clay at nanoscale does not affect the ductility of the produced nanocomposite. On

the other hand, Fig. 12c shows that, the strain at Yield was increase by the silylated treatments for all nanocomposites, It is believed that the improvement in stiffness and ductility of the nanocomposites is due to the homogenous dispersion of clay inside the polymer as well as the strong interaction between them, which facilitates enhancement of resistant to crack propagation so that higher strain can be tolerated by the nanocomposites (Carastan et al. 2013).

6.5 Torsional Test

Torsion tests were performed on an ARES-LS Rheometer using the rectangular torsion mode, with the following sample dimension: 5.5 mm width, 58 mm length, and 2 mm thick. Firstly, the strain sweep test was performed at 1 Hz frequency. Then, the torsion modulus is obtained in oscillatory tests performed at room temperature in sweep frequency mode (0.1–40 Hz) at strain of 2×10^{-3}, taken from the linear region of the strain sweep.

To investigate the nanocomposites response to shear stress; Fig. 13a–a'' shows the torsion modulus for raw and silane grafted clays nanocomposites, for all systems, the torsion modulus increase with the incorporation of clay nano-particles. The addition of clay improved noticeably the G*values for all nanocomposite systems. Thus, the uses of silane organoclay nanocomposites increase the torsion modulus values as compared to raw clay nanocomposite, due to the improvement of the interfacial adhesion between the PP matrix and the nano-particles clays by the grafted silane. The variation of the torsional modulus is also marked by the variation of frequency from 0.1 to 40 Hz, leading to conclude that the nanocomposites response is like an elastic solid (Ganß et al. 2009).

To investigate the elastic and viscous behaviors of raw and silane grafted clay based nanocomposites, the evolution of tan δ versus frequencies and different kinds of clay nanocomposites (raw and modified clays) in Fig. 13b–b'', for all nanocomposites tan δ decrease with increasing frequencies. Noteworthy is the curves in each system have the same shape with increasing frequency from 0.1 to 40 Hz. The elastic character of the nanocomposites prevails over a viscous behavior at high frequency. In the case of silane grafted clays, the tan δ values are lower than that of raw clay, which means that the silane grafted clays reduces the elastic character of nanocomposite and lead to a lower shear stress (Nekhlaoui et al. 2014).

6.6 Melt Rheological Test

The last paragraph is addressed to study the viscoelastic behavior of polymer nanocomposites in the solid state; nevertheless, it is necessary to analyze rheological behavior of specimen produced in the molten state to complete the observation made during compounding and to evaluate the microstructure and the
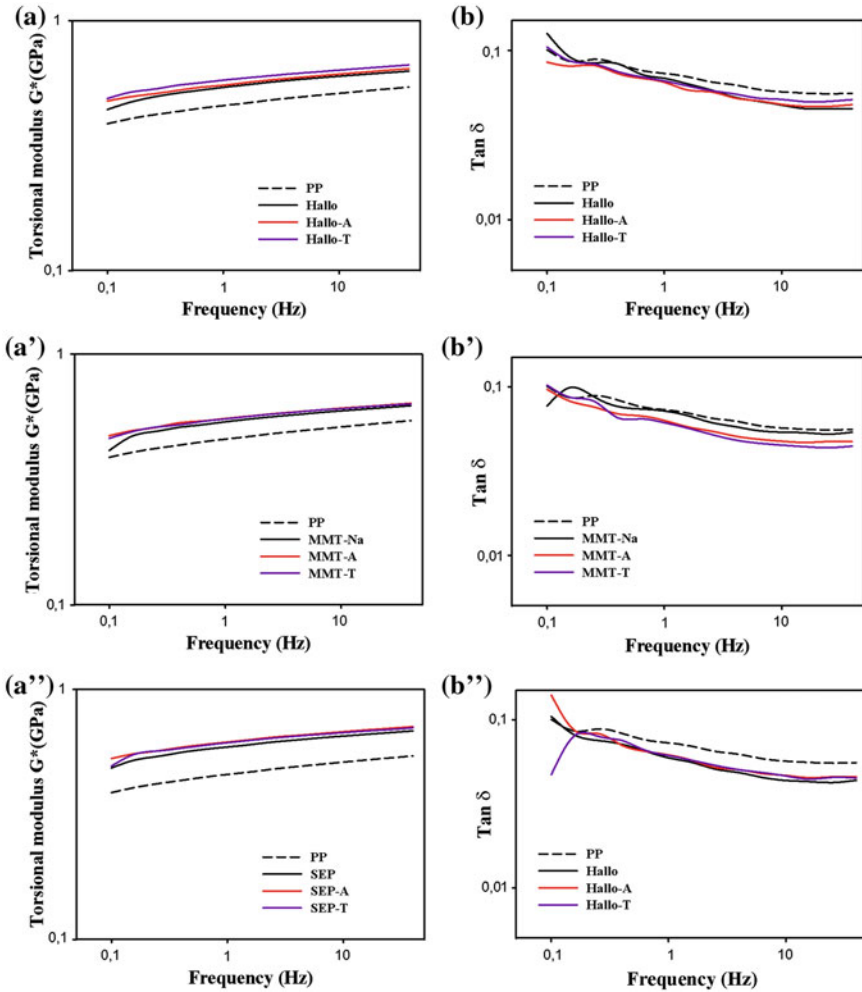
Fig. 13 The torsion modulus and tan δ of PP composites made with the raw and silane grafted clays at different frequencies

dispersion of nano-clay particles in the polymer matrix. The study of viscoelastic properties was made by means of the oscillatory melt rheology performed on an MCR 500 (Physica) rheometer equipped with a CTD600 device. The rheological measurements include the storage modulus G', loss modulus G" and tan δ were carried out at 190 °C under small amplitude oscillatory shear mode using 25 mm parallel plate-plate geometry with 1 mm thick samples. Frequency sweeps between 500 and 0.05 Hz were performed at a strain of 5 % (linear viscoelastic regime).

The rheological properties of the nanocomposites were also investigated in the melt state. Figure 14a–b" plots the storage modulus (G') and loss modulus (G") of
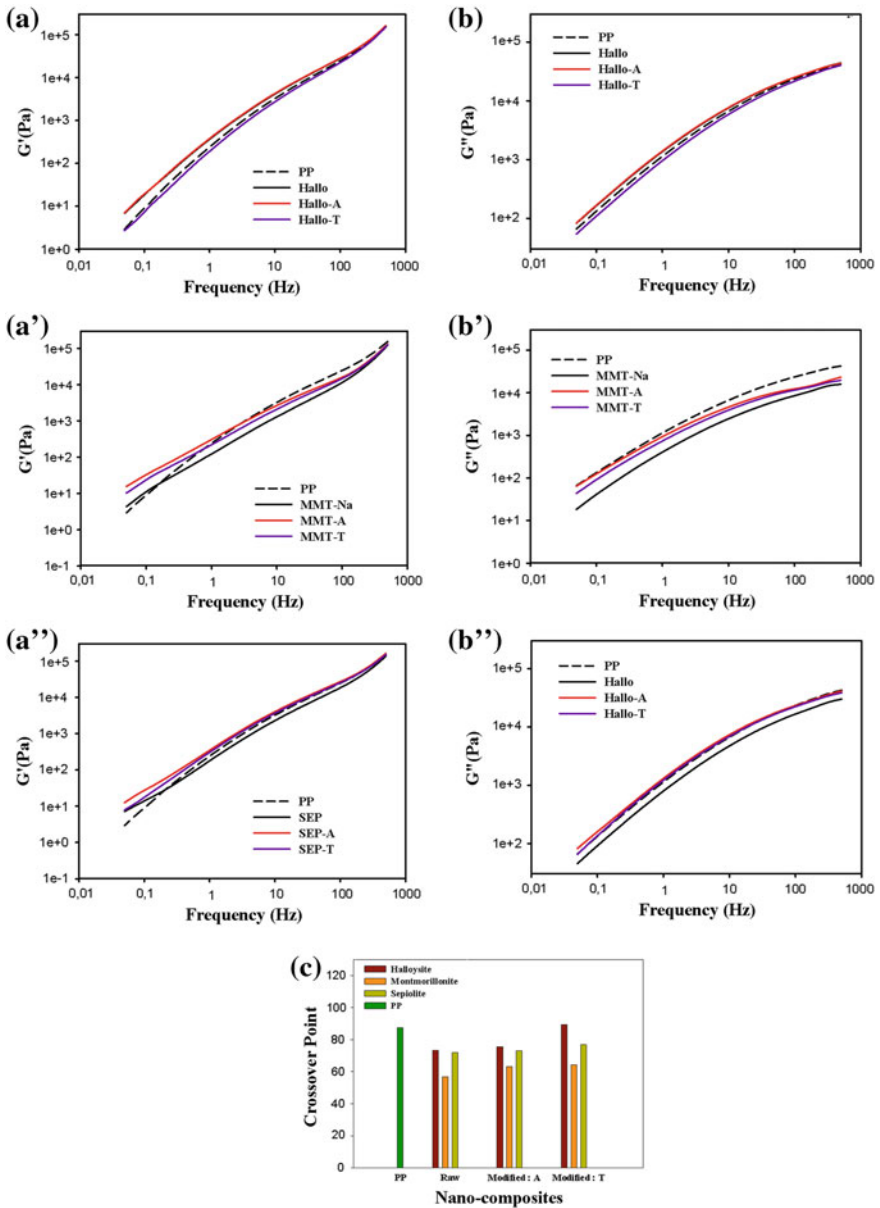
Fig. 14 Rheological properties as a function of PP composites made with the raw and silane grafted clays at different frequencies: **a**, **a'**, **a"** storage modulus, **b**, **b'** **b"** loss modulus, **c** crossover point

virgin PP nanocomposites made with the raw and silane grafted clays as function of frequencies. It is evident that both G' and G" increase linearly with an increase in angular frequency and it's clearly shows that G' values of the raw clays

nanocomposites are higher than that of pure and silane grafted clays nanocomposites. This can be explained by structural changes in the polymer nanocomposites, which being more elastic with rigid particle addition. However, in the presence of silane molecules grafted clays particles, the nanocomposites exhibit a high viscosity behavior due to the presence of organic chain grafted on nano-clays particles, and also due to the good dispersion, distribution and affinity of the rigid nano-clays inside the polymer blend, all these phenomena can prevent the melt to flow which is reflected by an increase in loss modulus/viscosity (Yürüdü et al. 2005). It also observed in Fig. 14a–b", for all nanocomposite at high frequency, that the G' values are higher than G" which indicates a solid-like response in the molten state. In fact, the insufficient time at higher frequency to allow polymer chains to relax contributing to an increase in the elastic nature of the melt (El Achaby et al. 2013).

Figure 14c shows the crossover frequency (G' = G") as a function of nanocomposites. The crossover point decreases by the incorporation of nano-clay particles indicating that the elastic behavior prevails over the viscous character due to the elastic character of nano-clays particles. However, in the case of silane grafted clays nanocomposites, the crossover point increase which meaning that the viscous behavior prevails over the elastic behavior as compared to raw clays nanocomposites, this reduction in nanocomposites rigidity can be explained by the grafted silane molecules on clays nano-particles and may be by the interaction between nano-clays particles and polymer matrix.

7 Conclusions

In summary, Polypropylene (PP)/organoclay nanocomposites have been prepared via melt compounding using a variety of clays such as raw and silane grafted Montmorillonite, Halloysite and sepiolite for purpose of comparison. First, various organosilanes were employed to produce organoclays structures with organophilic molecules in the presence of toluene solution. The dried organophilic clays were then melt-compounding with PP to obtain the corresponding PP/silane grafted clays nanocomposites. The successful silylation of different organosilanes onto the surfaces of clays were examined by various physico-chemical techniques, including FTIR, XRD, and TGA. Thus, suggesting the formation of chemical covalent bonding between the hydroxyl groups of clay minerals and alkoxy groups of silane grafted agent. In addition, the obtained SEM results showed clearly that the all clays were successfully modified using the silane molecules confirmed by lessen of the clay nano-particles size. Indeed, the MFI values was use to distinguish between the different grades of the nanocomposites. Finally, the silane grafted clays nanocomposites shows an improvement of the interfacial adhesion and random dispersion/distribution of clay nano-particles by the use of silane chemical modification afford remarkable composites property enhancements represented by high mechanical and torsional properties. It can be concluded that the functionalization

of nanoclay is mandatory to reach a high properties of nanocomposites and to benefit on the advantages of the nanoclays.

References

Ahmed Ben Hassan, S., Stojanović, D.B., Kojović, A., Janković-Castvan, I., Janaćković, D., Uskoković, P.S., Aleksić R.: Preparation and characterization of poly(vinyl butyral) electrospun nanocomposite fibers reinforced with ultrasonically functionalized sepiolite. Ceram. Int. **40**, 1139–1146 (2014)

Alan, N., İşçi, S.: Surface modification of sepiolite particles with polyurethane and polyvinyl alcohol. Prog. Org. Coat. **77**, 444–448 (2014)

Alkan, M., Hopa, Ç., Yilmaz, Z., Güler, H.: The effect of alkali concentration and solid/liquid ratio on the hydrothermal synthesis of zeolite NaA from natural kaolinite. Microporous Mesoporous Mater. **86**, 176–184 (2005)

Alonso, A., Bastos-Arrieta, J., Davies, G.: Ecologically friendly polymer-metal and polymer-metal oxide nanocomposites for complex water treatment. Nanocomposites—New Trends Dev. 187–213 (2012)

Avila, L.R., de Faria, E.H., Ciuffi, K.J., Nassar, E.J., Calefi, P.S., Vicente, M.A., Trujillano, R.: New synthesis strategies for effective functionalization of kaolinite and saponite with silylating agents. J. Colloid Interface Sci. **341**, 186–193 (2010)

Basurto, F.C., García-López, D., Villarreal-Bastardo, N., Merino, J.C., Pastor, J.M.: Nanocomposites of ABS and sepiolite: study of different clay modification processes. Compos. Part B Eng. **43**, 2222–2229 (2012)

Beauvais, M., Serreau, L., Heitz, C., Barthel, E.: How do silanes affect the lubricating properties of cationic double chain surfactant on silica surfaces? J. Colloid Interface Sci. **331**, 178–184 (2009)

Belver, C., Aranda, P., Ruiz-Hitzky, E.: Silica–alumina/sepiolite nanoarchitectures. J Mater. Chem. A **1**, 74–77 (2013)

Bergaya, F., Lagaly, G.: General Introduction: Clays, Clay Minerals, and Clay Science, 2nd edn. Elsevier Ltd (2013)

Berzelius, J.J.: Untersuchungen über die Flussspathsäure und deren merkwürdigsten Verbindungen. Ann. Phys. **77**, 169–230 (1824)

Bhattacharya, S.S., Aadhar, M.: Studies on preparation and analysis of organoclay nano particles. Res. J. Eng. Sci. **3**, 10–16 (2014)

Bissé, E., Epting, T., Beil, A., Lindinger, G., Lang, H., Wieland, H.: Reference values for serum silicon in adults. Anal. Biochem. **337**, 130–135 (2005)

Blum, F.D.: Silane Coupling Agents, Encyclopedia of Polymer Science and Technology, pp 38–50. Wiley, Inc. (2003)

Bobos, I., Duplay, J., Rocha, J., Gomes, C.: Kaolinite to halloysite-7 Å transformation in the kaolin deposit of São Vicente De Pereira, Portugal. Clays Clay Miner. **49**, 596–607 (2001)

Bordeepong, S., Bhongsuwan, D., Pungrassami, T., Bhongsuwan, T.: Characterization of halloysite from thung yai district, Nakhon Si Thammarat Province, in Southern Thailand. Songklanakarin J. Sci. Technol. **33**, 599–607 (2011)

Carastan, D.J., Amurin, L.G., Craievich, A.F., Gonçalves, C., Demarquette, N.R.: Morphological evolution of oriented clay-containing block co-polymer nanocomposites under elongational flow. Eur. Polym. J. **49**, 1391–1405 (2013)

Carli, L.N., Daitx, T.S., Soares, G.V., Crespo, J.S., Mauler, R.S.: The effects of silane coupling agents on the properties of PHBV/halloysite nanocomposites. Appl. Clay Sci. **87**, 311–319 (2014)

Chen, G.X., Yoon, J.S.: Clay functionalization and organization for delamination of the silicate tactoids in poly(L-lactide) matrix. Macromol. Rapid Commun. **26**, 899–904 (2005)

De Paiva, L.B., Morales, A.R., Valenzuela Díaz, F.R.: Organoclays: properties, preparation and applications. Appl. Clay Sci. **42**, 8–24 (2008)

El Achaby, M., Ennajih, H., Arrakhiz, F.Z., El Kadib, A., Bouhfid, R., Essassi, E., Qaiss, A.: Modification of montmorillonite by novel geminal benzimidazolium surfactant and its use for the preparation of polymer organoclay nanocomposites. Compos. Part B Eng. **51**, 310–317 (2013)

Euigyung, J., Won, L.J., Kyeong-won, S., Lee, Y.-S.: Effects of physicochemical treatments of illite on the thermo-mechanical properties and thermal stability of illite/epoxy composites. J. Ind. Eng. Chem. **17**, 77–82 (2011)

Ferreira, J.A.M., Reis, P.N.B., Costa, J.D.M., Richardson, B.C.H., Richardson, M.O.W.: A study of the mechanical properties on polypropylene enhanced by surface treated nanoclays. Compos. Part B Eng. **42**, 1366–1372 (2011)

Frost, R.L.: Fourier transform Raman spectroscopy of kaolinite, dickite and halloysite. Clays Clay Miner. **43**, 191–195 (1995)

Frost, R.A.Y.L., Vassallo, A.M.: The dehydroxylation of the kaolinite clay minerals using infrared emission spectroscopy. Clays Clay Miner. **44**, 635–651 (1996)

Galpaya, D.: Recent advances in fabrication and characterization of graphene-polymer nanocomposites. Graphene **01**, 30–49 (2012)

Ganß, M., Satapathy, B.K., Thunga, M., Staudinger, U., Weidisch, R., Jehnichen, D., Hempel, J., Rettenmayr, M., Garcia-marcos, A., Goertz, H.H.: Morphology and mechanical response of S —B star block copolymer—Layered silicate nanocomposites. Eur. Polym. J. **45**, 2549–2563 (2009)

Gao, F.: Clay/polymer composites: the story. Mater. Today **7**, 50–55 (2004)

García-López, D., Fernández, J.F., Merino, J.C., Santarén, J., Pastor, J.M.: Effect of organic modification of sepiolite for PA 6 polymer/organoclay nanocomposites. Compos. Sci. Technol. **70**, 1429–1436 (2010)

Ha, S.R., Ryu, S.H., Park, S.J., Rhee, K.Y.: Effect of clay surface modification and concentration on the tensile performance of clay/epoxy nanocomposites. Mater. Sci. Eng. A **448**, 264–268 (2007)

Halvorson, R.H., Erickson, R.L., Davidson, C.L.: The effect of filler and silane content on conversion of resin-based composite. Dent. Mater. **19**, 327–333 (2003)

He, A., Wang, L., Yao, W., Huang, B., Wang, D., Han, C.C.: Structural design of imidazolium and its application in PP/montmorillonite nanocomposites. Polym. Degrad. Stab. **95**, 651–655 (2010)

Herrera, N.N., Letoffe, J.M., Putaux, J.L., David, L., Bourgeat-Lami, E.: Aqueous dispersions of silane-functionalized laponite clay platelets. A first step toward the elaboration of water-based polymer/clay nanocomposites. Langmuir **20**, 1564–1571 (2004)

Hoidy, W.H., Ahmad, M.B., Al Mulla, E.A.J., Ibrahim, N.A.B.: Synthesis and characterization of organoclay from sodium montmorillonite and fatty hydroxamic acids. Am. J. Appl. Sci. **6**, 1567–1572 (2009)

Hussain, F., Hojjati, M., Okamoto, M., Gorga, R.E.: Review article: polymer-matrix nanocomposites, processing, manufacturing, and application: an overview. J. Compos. Mater. **40**, 1511–1575 (2006)

Ishida, H., Kumar, G. (eds.): Molecular Characterization of Composite Interfaces, 1st edn. Springer, US (1985)

Isoda, K., Kuroda, K., Ogawa, M.: Interlamellar grafting of γ-methacryloxypropylsilyl groups on magadiite and copolymerization with methyl methacrylate. Chem. Mater. **12**, 1702–1707 (2000)

Kickelbick, G.: Concepts for the incorporation of inorganic building blocks into organic polymers on a nanoscale. Prog. Polym. Sci. **28**, 83–114 (2003)

Kotal, M., Bhowmick, A.K.: Polymer nanocomposites from modified clays: recent advances and challenges. Prog. Polym. Sci. **51**, 127–187 (2015)

Lee, J., Man, S., Kim, J., Min, C.: Sensors and actuators B: chemical novel sulfonated styrenic pentablock copolymer/silicate nanocomposite membranes with controlled ion channels and their IPMC transducers. Sens. Actuators B Chem. **162**, 369–376 (2012)

Leszczyńska, A., Njuguna, J., Pielichowski, K., Banerjee, J.R.: Polymer/montmorillonite nanocomposites with improved thermal properties. Part II. Thermal stability of montmorillonite nanocomposites based on different polymeric matrixes. Thermochim. Acta **454**, 1–22 (2007)

Liu, X., Wu, Q.: PP/clay nanocomposites prepared by grafting-melt intercalation. Polymer **42**, 10013–10019 (2001)

Mai, C., Militz, H.: Modification of wood with silicon compounds. Inorganic silicon compounds and sol-gel systems: A review. Wood Sci. Technol. **37**, 339–348 (2004)

Majeed, K., Jawaid, M., Hassan, A., Abu Bakar, A., Abdul Khalil, H.P.S., Salema, A.A., Inuwa, I.: Potential materials for food packaging from nanoclay/natural fibres filled hybrid composites. Mater. Des. **46**, 391–410 (2013)

Mansoori, Y., Hadi, S.: Nanocomposite hydrogels composed of cloisite 30B-graft-poly(acrylic acid)/poly(acrylic acid): Synthesis and characterization. Poly. Sci. Ser. B **57**, 167–179 (2015)

Matinlinna, J.P., Choi, A.H., Tsoi, J.K.H.: Bonding promotion of resin composite to silica-coated zirconia implant surface using a novel silane system. Clin. Oral Implants Res. **24**, 290–296 (2013)

Mejía, A., García, N., Guzmán, J., Tiemblo, P.: Confinement and nucleation effects in poly (ethylene oxide) melt-compounded with neat and coated sepiolite nanofibers: modulation of the structure and semicrystalline morphology. Eur. Polym. J. **49**, 118–129 (2013)

Navrátilová, Z., Wojtowicz, P., Vaculíková, L., Šugárková, V.: Sorption of alkylammonium cations on montmorillonite. Acta Geodyn. Geomater. **4**, 59–65 (2007)

Nekhlaoui, S., Essabir, H., Kunal, D., Sonakshi, M., Bensalah, M.O., Bouhfid, R., Qaiss, A.: Comparative study for the talc and two kinds of Moroccan clay as reinforcements in polypropylene-SEBS-g-MA matrix. Polym. Compos. **36**, 675–684 (2014)

Nguyen, Q.T., Baird, D.G.: Preparation of Polymer—Clay Nanocomposites and Their Properties **25**, 270–285 (2007)

Núñez, K., Gallego, R., Pastor, J.M., Merino, J.C.: The structure of sepiolite as support of metallocene co-catalyst during in situ polymerization of polyolefin (nano)composites. Appl. Clay Sci. **101**, 73–81 (2014)

Park, M., Shim, I.K., Jung, E.Y., Choy, J.H.: Modification of external surface of laponite by silane grafting. J. Phys. Chem. Solids **65**, 499–501 (2004)

Paul, D.R., Robeson, L.M.: Polymer nanotechnology: nanocomposites. Polym. (Guildf) **49**, 3187–3204 (2008)

Pavlidou, S., Papaspyrides, C.D.: A review on polymer–layered silicate nanocomposites. Prog. Polym. Sci. **33**, 1119–1198 (2008)

Plueddemann, E.P.: Fundamentals of Adhesion. In: Lee, L.-H. (ed.) Fundamentals of Adhesion, pp. 279–290. Springer, US, Boston, MA (1991)

Rytwo, G.: Clay minerals as an ancient nanotechnology: historical uses of clay organic interactions, and future possible perspectives. Macla **9**, 15–17 (2008)

Sánchez-Fernández, A., Peña-Parás, L., Vidaltamayo, R., Cué-Sampedro, R., Mendoza-Martínez, A., Zomosa-Signoret, V., Rivas-Estilla, A., Riojas, P.: Synthesization, characterization, and in vitro evaluation of cytotoxicity of biomaterials based on halloysite nanotubes. Materials **7**, 7770–7780 (2014)

Sanchez-Martin, M.J., Rodriguez-Cruz, M.S., Andrades, M.S., Sanchez-Camazano, M.: Efficiency of different clay minerals modified with a cationic surfactant in the adsorption of pesticides: influence of clay type and pesticide hydrophobicity. Appl. Clay Sci. **31**, 216–228 (2006)

Sánchez-Valdes, S., Méndez-Nonell, J., Medellín-Rodríguez, F.J., Ramírez-Vargas, E., Martínez-Colunga, J.G., Soto-Valdez, H., Muñoz-Jiménez, L., Neira-Velázquez, G.: Effect of PEgMA/amine silane compatibilizer on clay dispersion of polyethylene-clay nanocomposites. Polym. Bull. **63**, 921–933 (2009)

Santos, S.C.R., Boaventura, R.A.R.: Adsorption modelling of textile dyes by sepiolite. Appl. Clay Sci. **42**, 137–145 (2008)

Shanmugharaj, A.M., Rhee, K.Y., Ryu, S.H.: Influence of dispersing medium on grafting of aminopropyltriethoxysilane in swelling clay materials. J Colloid Interface Sci. **298**, 854–859 (2006)

Shen, W., He, H.P., Zhu, J., Yuan, P., Frost, R.L.: Grafting of montmorillonite with different functional silanes via two different reaction systems. J. Colloid Interface Sci. **313**, 268–273 (2007)

Singla, P., Mehta, R., Upadhyay, S.N.: Clay modification by the use of organic cations. Green Sustain. Chem. **2**, 21–25 (2012)

Soheilmoghaddam, M., Wahit, M.U., Yussuf, A.A., Al-Saleh, M.A., Whye, W.T.: Characterization of bio regenerated cellulose/sepiolite nanocomposite films prepared via ionic liquid. Polym. Test. **33**, 121–130 (2014)

Šupová, M., Martynková, G.S., Barabaszová, K.: Effect of nanofillers dispersion in polymer matrices: a review. Sci. Adv. Mater. **3**, 1–25 (2011)

Szczepanik, B., Słomkiewicz, P., Garnuszek, M., Czech, K., Banaś, D., Kubala-Kukuś, A., Stabrawa, I.: The effect of chemical modification on the physico-chemical characteristics of halloysite: FTIR, XRF, and XRD studies. J. Mol. Struct. **1084**, 16–22 (2015)

Takahashi, N., Kuroda, K.: Materials design of layered silicates through covalent modification of interlayer surfaces. J. Mater. Chem. **21**, 14336–14353 (2011)

Taxiarchou, M., Douni, I.: The effect of oxalic acid activation on the bleaching properties of a bentonite from Milos Island, Greece. Clay Miner. **49**, 541–549 (2014)

Thomas, N.R.: Frederic Stanley Kipping-Pioneer in silicon chemistry: his life & legacy. Silicon **2**, 187–193 (2011)

Tjong, S.C.: Structural and mechanical properties of polymer nanocomposites. Mater. Sci. Eng. R Rep. **53**, 73–197 (2006)

Vaia, R.A., Ishi, H., Giannelis, E.P.: Synthesis and properties of two-dimensional nanostructures by direct intercalation of polymer melts in layered silicates. Chem. Mater. **5**, 1694–1696 (1993)

Velde, B.: Clay Minerals A Physico-Chemical Explanation of their Occurrence (1985)

Verdejo, R., Barroso-Bujans, F., Rodriguez-Perez, M.A., Antonio de Saja, J., Lopez-Manchado, M.A.: Functionalized graphene sheet filled silicone foam nanocomposites. J. Mater. Chem. **18**, 2221–2226 (2008)

Wang, K., Bahlouli, N., Addiego, F., Ahzi, S., Rémond, Y., Ruch, D., Muller, R.: Effect of talc content on the degradation of re-extruded polypropylene/talc composites. Polym. Degrad. Stab. **98**, 1275–1286 (2013)

Weissenbach, K., Mack, H.: Functional fillers for plastics. In: Silane Coupling Agents, in Functional Fillers for Plastics, pp 57–83. Wiley-VCH Verlag GmbH & Co. KGaA (2005)

Witucki, G.: A silane primer—chemistry and applications of alkoxy silanes. J. Coat. Technol. **65**, 57–60 (1993)

Xie, Y., Hill, C.A.S., Xiao, Z., Militz, H., Mai, C.: Silane coupling agents used for natural fiber/polymer composites: a review. Compos. Part A Appl. Sci. Manuf. **41**, 806–819 (2010)

Xie, A., Yan, W., Zeng, X., Dai, G., Tan, S., Cai, X., Wu, T.: Microstructure and antibacterial activity of phosphonium montmorillonites. Bull. Korean Chem. Soc. **32**, 1936–1938 (2011)

Yeh, M.-H., Hwang, W.-S.: High mechanical properties of polychloroprene/montmorillonite nanocomposites. Mater. Trans. **47**, 2753–2758 (2006)

Yui, T., Fujii, S., Matsubara, K., Sasai, R., Tachibana, H., Yoshida, H., Takagi, K., Inoue, H.: Intercalation of a surfactant with a long polyfluoroalkyl chain into a clay mineral: Unique orientation of polyfluoroalkyl groups in clay layers. Langmuir **29**, 10705–10712 (2013)

Yürüdü, C., S I., Ünlü, C., Atici, O., Ece ,Ö.I., Güngör, N.: Synthesis and characterization of HDA/ NaMMT organoclay. Bull. Mater. Sci. **28**, 623–628 (2005)

Zeng, Q.H., Yu, A.B., Lu, G.Q., Paul, D.R.: Clay-based polymer nanocomposites: research and commercial development. J. Nanosci. Nanotechnol. **5**, 1574–1592 (2005)

Zhao, Y., Zhang, S.L., Zhang, C.F., Zhou, Z., Wang, G.B.: Study on poly(ether ether ketone)/ organically modified montmorillonite composites. Plast. Rubber Compos. **38**, 279–283 (2009)

Characteristic Properties of Nanoclays and Characterization of Nanoparticulates and Nanocomposites

Muhammad Shahid Nazir, Mohamad Haafiz Mohamad Kassim,
Lagnamayee Mohapatra, Mazhar Amjad Gilani,
Muhammad Rafi Raza and Khaliq Majeed

Abstract Clays have been one of the more important industrial minerals; and with the recent advent of nanotechnology, they have found multifarious applications and in each application, nanoclays help to improve the quality of product, economize on the cost and saves environment. The chapter describes key characteristics of nanoclays and their classification on the basis of the arrangement of "sheets" in their basic structural unit "layer". Major groups include kaolin–serpentine, pyrophyllite-talc, smectite, vermiculite, mica and Chlorite. The structural, morphological and physicochemical properties of halloystite and montmorillonite nanoclays, representative of the 1:1 and 2:1 layer groups, respectively, are discussed as well. After briefly introducing the surface modification of clay minerals by modifying or functionalizing their surfaces and their incorporation into polymer matrices to develop polymer/clay nanocomposites, techniques that are being employed to characterize these nanoclays, in general, and the sample preparation for these techniques, in particular, are also reviewed in this chapter.

M.S. Nazir · M.A. Gilani · K. Majeed (✉)
Department of Chemical Engineering,
COMSATS Institute of Information Technology, Lahore, Pakistan
e-mail: khaliqmajeed@ciitlahore.edu.pk; khaliqmajeed@gmail.com

M.H. Mohamad Kassim
School of Industrial Technology, Universiti Sains Malaysia,
11800 George Town, Penang, Malaysia

L. Mohapatra · K. Majeed
Center for Advanced Materials, Qatar University, PO Box 2713, Doha, Qatar

M.A. Gilani
Department of Chemistry, College of Science and Humanities,
Prince Sattam bin Abdulaziz University, P.O. Box 83, Alkharj 11942
Saudi Arabia

M.R. Raza
Department of Mechanical Engineering,
COMSATS Institute of Information Technology, Sahiwal, Pakistan

Keywords Nanoclays · Montmorillonite · Halloystite · Structural · Morphological properties

1 Nanoclays

Nanoclays are ubiquitous nanofiller and belong to a wider group of clay minerals. They are not new to humankind and ceramists have been using them in the development of clay products since prehistoric times. For instance, several clay products had been prepared using Kaolin, with the traditional name China clay, and its use is dated to the 3rd century BC in China. Even though the structure of nanoclays and their nature is being explored for decades and are being used since antiquity, their exact definition is an ongoing subject of debate (Fernandes et al. 2014; Uddin 2008). Clay minerals are hydrous silicates and may simply be described as fine-grained particles with sheet like structure stacked over one another. Owing to this geometry, they are commonly known as phyllosilicates, sheet-structured silicates. Phyllosilicates are mainly composed of fine grained aluminosilicates and are formed as a result of chemical weathering of silicate minerals at the surface of the earth (Majeed et al. 2013; Zhang et al. 2010). Nanoclays are commonly dominated by phyllosilicates and may be separated from the clay fraction or the bulk clay material by different approaches. Methods used for extracting and processing of nanoclays include energetic stirring followed by centrifugation and freeze-drying; centrifugation and cross-flow filtration; and ultracentrifugation (Floody et al. 2009).

Clay minerals are the basic constituents of clay raw materials and platy structure is the dominant morphology. Depending on the clay type, the individual layers could be composed of two, three or four sheets of either $[SiO_4]^{4-}$ tetrahedra or $[AlO_3(OH)_3]^6$ octahedra. The aluminosilicate layers organize themselves over one another like pages of a book, with a regular van der Waals gap between them, called an 'interlayer'. Interlayer possess net negative charge which is due to the ionic substitutions in the sheets of clay minerals. The layer charge is neutralized by cations which occupy the inter-lamellar. These inter-lamellae cations can be easily replaced by other cations or molecules as per required surface chemistry and hence called exchangeable cations. Na^+, K^+, Mg^{2+}, and Ca^{2+}, are among common exchangeable cations present in the interlayer which are exchanged with other required cations. In general practice, to evaluate a material performance and its classification, chemical behavior is paid more importance. On the contrary to this general practice, the physical characteristics of clays are more important in defining various clay groups. Therefore, the clay minerals are broadly classified on the basis of the number and arrangement of sheets in a clay layer. Depending on the number and the way that the tetrahedral and octahedral sheets are packed into layers, the clay minerals can be classified into three classes, i.e., two-sheet layer, three-sheet layer and four-sheet layer (Lee and Tiwari 2012).

Nanoclays are easily available, environment friendly, low cost chemical substances and a large volume of literature has accumulated on various perspectives of

nanoclays' research over the past few decades. Major research domains include (i) synthesis and characterization; (ii) surface properties and stability; (iii) fabrication of nanoclay-filled nanocomposites; and (iv) the use of nanoclays as precursors for the development of novel materials. Nanoclays have found applications in many fields, including medicine (Ambre et al. 2010; Suresh et al. 2010), pharmacy (Carretero and Pozo 2009, 2010), cosmetics (Carretero and Pozo 2010; Patel et al. 2006), catalysis (Garrido-Ramírez et al. 2010; Nagendrappa 2011), food packaging (Azeredo 2009; Majeed et al. 2013) and textile industry (Floody et al. 2009; Shahidi and Ghoranneviss 2014). In addition to these mentioned application, nanoclays are also helpful in environmental protection and remediation. Their potential as adsorbents for volatile organic compounds, and organic/inorganic contaminants in waste water is well documented (Lee and Tiwari 2012; Ouellet-Plamondon et al. 2012; Yuan and Wu 2007). This multifariousness in applications can be attributed to (1) the amazing amenability of nanoclays for change/modification, and (2) the dispersion/delamination of clay layers into individual lamellae. Amenability of nanoclays for modification lies in the fact that inter-lamellae cations can be replaced by desirable cations or other molecules. Simple procedures are required to modify the surface chemistry of nanoclays. This surface modification provides tremendous scope for altering the properties of clays like their polarity, surface area, interlayer spacing, acidity, and pore size and many others that govern their performance in different applications. Nanoclays' tendency to delaminate into individual nanosheets that results in high aspect ratio is their other exploited characteristic behind diverse applications.

1.1 Structural and Physical Properties of Nanoclays

Nanoclays are fine-grained crystalline materials. A layer is the basic structural unit of nanoclays and these layers are prone to arrange themselves over one another like pages of a book. Individual layers are composed of the tetrahedral and/or octahedral sheets and this arrangement of sheets plays a vital role in defining and distinguishing these clay minerals. In tetrahedral sheet, the silicon-oxygen tetrahedra are linked to neighboring tetrahedra by sharing three corners while the fourth corner of each tetrahedron forms a part to adjacent octahedral sheet. The octahedral sheet is usually composed of aluminum or magnesium in six-fold coordination with oxygen from the tetrahedral sheet and with hydroxyl. The sheets form a layer, and several layers may be joined in a clay crystallite. Vander Waals force, electrostatic force, or hydrogen bonding between the layers are the main drivers to clutch these layers with one another and form stacks of parallel lamellae. This stacking results in regular Van der Waal gaps between the adjacent layers. These spaces between the layers are called interlayer or gallery and can be accessed by water, organic cations or polar organic liquids. This intercalation weakens the forces clutching these layers with one another and causes the lattice to expand. The clay minerals' ability to accept changes in surface chemistry and delaminate into individual lamellae are

their pertinent characteristics that have been widely exploited in the development of novel composites.

The tetrahedral and octahedral sheets are building blocks for clay layers and these building blocks are capable of being assembled in a variety of arrangements. Thus the classification of nanoclay structure can be related to the arrangement of these building blocks; and the Table 1 presents grouping of clay minerals on the basis of their sheet arrangement. Clay minerals would have one tetrahedral and one octahedral sheet; one octahedral sheet merged between the two tetrahedral sheets; and one octahedral sheet adjacent to one octahedral sheet merged between the two tetrahedral sheets per layer arrangements and are denoted as 1:1, 2:1 and 2:1:1 sheet arrangement. Examples of 1:1 sheet arrangement include kaolinite, halloysite and serpentine. The 2:1 phyllosilicates are comparatively larger group including Vermiculite, Pyrophyllite, mica etc. as sub groups. Among various expanding and non-expanding 2:1 phyllosilicate groups, smectites, strongly expanding 2:1 phyllosilicates also belong to this layer structure. The term smectite is used to represent a family of expansible 2:1 phyllosilicate silicate minerals having a general formula (Ca, Na, H) (Al, Mg, Fe, Zn)$_2$(Si Al)$_4$O$_{10}$(-OH)$_2$-xH$_2$O, where x represents varying level of water attached to the mineral. Many well known natural and synthetic nanoclays viz. saponite, hectorite, montmorillonite, fluorohactite, and laponite belong to smectite family (Floody et al. 2009; Lee and Tiwari 2012; Majeed et al. 2013; Uddin 2008; D. Zhang et al. 2010). It is worth noting that despite sheet arrangement similarity of the member clays of a particular clay group, the lateral dimensions of all the members are different. In addition, the layer dimensions vary not only for each member clay, but also for the same clay from different origins. Depending upon the number of factors, including source of clay, method of preparation and particulate clay, the thickness of each layer is about 1 nm with lateral dimensions ranging from 300 Å to several microns (Lee and Tiwari 2012; Pavlidou and Papaspyrides 2008).

1.1.1 Halloysite

Halloysites are types of naturally occurring multiwalled aluminosilicates with 1:1 sheet arrangement. The halloysite layer structure is composed of octahedrally coordinated Al^{3+} and tetrahedrally coordinated Si^{4+} in a 1:1 arrangement with water molecules between the layers. A schematic diagram of crystalline structure of halloysite is shown in Fig. 1.

Halloysites were firstly discovered by Berthier as a clay mineral of the kaolin group in 1826, and were named "halloysite" after Omalius d'Halloy who analyzed the mineral first time. These nanoclays are found worldwide and their deposits have been reported in countries such as Australia, China, Belgium, Brazil, France, Spain, New Zealand, Mexico, America and others (Du et al. 2010; Liu et al. 2014; Yuan et al. 2015). Halloysites' aluminosilicate sheets are rolled into tubes and nanosized tubular halloysite, also called halloysite nanotube (HNT) is morphologically similar to multiwalled carbon nanotubes. Even though platy and spheroidal morphologies

Table 1 Classification of clay minerals and their major groups (Floody et al. 2009; Lee and Tiwari 2012; Majeed et al. 2013; Uddin 2008; Zhang et al. 2010)

Layer type	Tetrahedral-octahedral sheet arrangement	Interlayer material	Group	Species	Layer charge per formula unit
1:1	T: O	None or H_2O only	Kaolin–serpentine	Lizardite, berthierine, amesite, cronstedtite, nepouite, kellyite, fraipontite, brindleyite, Kaolinite, dickite, nacrite, halloysite, Odinite	<0.01
2:1	T:O:T	None	Pyrophyllite-Talc	Talc, willemseite, kerolite, pimelite, pyrophyllite, ferripyrophyllite	0
		Hydrated exchangeable cations	Smectite	Saponite, hetorite, sauconite, stevensite, swinefordite, montmorillonite, beidellite, nontronite, volkonskoite	0.2–0.6
		Hydrated exchangeable cations	Vermiculite	Vermiculite	0.6–0.9
		Non-hydrated monovalent cations	True (flexible) mica	Biotite, phlogopite, lepidolite, Muscovite, illite, glauconite, celadonite, paragonite, etc.	0.6–1.0
		Non-hydrated divalent cations	Brittle mica	Clintonite, kinoshitalite, bityite, anandite, Margarite	1.8–2.0
2:1:1	(T:O:T):O	Variable	Chlorite	Amesite, chamosite, cookeite, nimite etc.	Variable

T = tetrahedral, O = octahedral

Fig. 1 Chemical structure of halloysite (Yah et al. 2012)
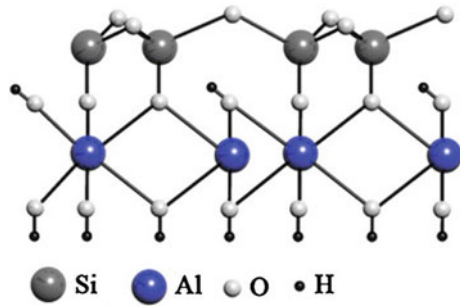
have also been reported in literature, the tubular structure is the dominant mor-phology of HNTs in nature and has attracted researchers from different scientific fields. HNTs are being used for long and the production of high-quality ceramics such as porcelain or crucible products have been among their traditional applica-tions. However, with the recent advent of nanotechnology, these natural occurring materials with nano-scale lumens are being studied for a large range of new applications such as nano-containers for drug delivery, nano-templates for the fabrication of nanowires and nanoparticles, catalyst carriers, sorbents for contam-inants and pollutants and nanofillers for polymers' reinforcement. Among these application of HNTs, their use as an encapsulation vessel for the storage and controlled release of active agents; and load bearing constituents in nanocomposites have been major focus of research in last two decades. In order to evaluate the potential of HNTs for these two aforementioned applications, the general require-ments for each of these two potential applications and the halloysite attributes owing to whom it is considered as a potential material are summarized in Table 2.

The structural formula for HNTs is $Al_2(OH)_4Si_2O_5 \cdot nH_2O$ where n represents number of water molecules and could be 2 or 0. HNTs with 2 water molecules are named as hydrated or otherwise dehydrated. When halloysite is mined from

Table 2 Halloysite attributes for its application as encapsulation vessel ad load bearing constituent (Pasbakhsh et al. 2013)

Use:	As additive to polymers	As carriers and templates
Desirable properties:	Tubular	Tubular
	Good dispersion in polymers	Chemical inertness/biocompatibility
	Strong binding with polymers	Easy availability of OH groups
	High aspect ratio	Easy availability of OH groups
		Negatively charged at appropriate pH (or) one positively charged surface
		Large volume in lumen

deposits, there is a layer of water molecules present between the halloystite multilayers (n = 2) and is called HNTs-10 Å (the "10 Å" designation indicates the d_{001}-value of the layers). Dehydrated halloysite (HNT-7 Å when n = 0) or just commercial halloysite may be obtained through the loss of the interlayer water molecules under mild heating and/or a vacuum environment. It is worth noting that the dehydration of HNTs does not affect its morphology, however the removal of inter-layer water results in changes in lattice parameters. Chemical composition of HNTs is same as platy clay kaolinite with water molecules and the unit layers in halloysites are separated by a monolayer of water molecules. Thus the interlayer water in HNTs is one of the main differences distinguishing halloysites from kaolinite. This interlayer water reduces the magnitude of electrostatic forces between adjacent layers of HNTs at the time of formation. Also, there differences in lattice parameters of alumina and silica in both a and b directions (for silica a = 5.02 Å, b = 9.16 Å, and for alumina a = 5.07 Å, b = 8.66 Å). These differences lead to dimensional mismatch of the sheets. In addition to lessen the electrostatic force between the adjacent layers, the presence of inter-layer water facilitates curvature of the layers to accommodate the dimensional mismatch of the octahedral and tetrahedral sheets. Consequently, halloysite crystallizes with the Al–OH sheet forming the inside and the Si–O sheet forming the outside of a unit layer. (Lvov and Abdullayev 2013; Pasbakhsh et al. 2013).

In dehydrated halloysite structure, 15–20 aluminosilicate sheets are rolled over and over; and the structure resembles multi-walled carbon nanotubes. Geometric dimensions of the HNTs are source dependent and ranges from 0.2 to 2 µm in length, 40–100 nm in outer diameter and 10–40 nm in lumen diameter. Typical properties of halloystite nanotubes are compiled in Table 3. In addition to differences in wall-length of HNTs, tubular HNTs with different wall thickness and different spiral structures (power spiral, logarithmic spiral) have also been reported.

Table 3 Typical properties of halloystite nanotubes (Liu et al. 2014)

Property	Value
Length	0.2–2 µm
Outer diameter	40–100 nm
Inner diameter	10–40 nm
Aspect ratio (L/D)	10–50
Elastic modulus (theoretical value)	140 GPa (230–340 GPa)
Mean particle size in aqueous solution	143 nm
Particle size range in aqueous solution	50–400 nm
BET surface area	22.1–81.6 m^2/g
Pore space	14–46.8 %
Lumen space	11–39 %
Density	2.14–2.59 g/cm^3
Average pore size	79.7–100.2 Å
Structural water release temperature	400–600 ˚C

These morphological differences can be due to the formation of HNTs under various crystallization conditions and geological occurrences (Du et al. 2010; Liu et al. 2014; Lvov and Abdullayev 2013; Mitra 2013; Pasbakhsh et al. 2013; Yuan et al. 2008; Yuan et al. 2015).

1.1.2 Montmorillonite

Smectite nanoclays are among heavily researched nanofillers in the field of nanocomposites. Among these smectite nanoclays, montmorillonite (MMT) has got prominence over other member nanoclays owing to its abundance, environmentally friendliness and well-studied chemistry. MMT is a dioctahedral nanoclay with the 2:1 layer linkage. They are the most efficient reinforcement fillers and their reinforcing potential is well documented in literature. The studies revealed that larger surface area and large aspect ratio are the salient attributes responsible for the reinforcement (Arora and Padua 2010; Azeredo 2009). Besides reinforcing effect of MMT, it is also viewed as rigid, impermeable filler. It creates a maze structure when dispersed in polymers, forces the moving gases/vapors to follow a tortuous path, and finally lowers their permeation rate.

Each individual MMT layer having lateral dimensions of 200–600 nm and thickness of a few nanometers is composed of two tetrahedral sheets and an octahedral sheet. The sheets are linked to each other in such a way that the silicon oxide tetrahedron (SiO_4) shares its 3 out of 4 oxygen atoms with the central octahedral sheets as shown in Fig. 2. MMT layers in its pristine from organize themselves over one another where the layered platelets are stacked with different levels of stacking within the clay mineral. Depending upon the stacking level, they could be primary particles or layered aggregates (micro-aggregates and aggregates). During the isomorphic substitution of Al^{+3} by Fe^{+2} or Mg^{+2}; and Mg^{+2} by Li^{+1} in the layer structure, the difference in the valences induces an overall negative charge on each three sheets layer. Different metal cations (Na^{+1}, Ca^{+2}) present between three sheets layers/in the galleries accommodate charge imbalance, thus increasing
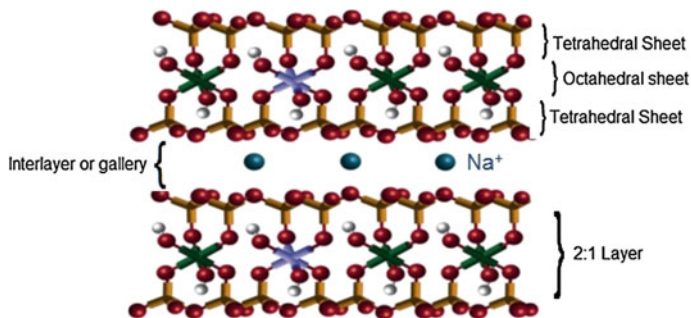
Fig. 2 Structure of Na-MMT (Paul and Robeson 2008)

Table 4 Chemical formula, cation exchange capacity and particle length of commonly used smectites (Ray and Okamoto 2003)

Smectite	Chemical formula	CEC (mequiv/100 g)	Particle length (nm)
Montmorillonite	$M_x(Al_{4-x}Mg_x)Si_8O_{20}(OH)_4$	110	100–150
Hectorite	$M_x(Mg_{6-x}Li_x)Si_8O_{20}(OH)_4$	120	200–300
Saponite	$M_xMg_6(Si_{8-x}Al_x)Si_8O_{20}(OH)_4$	86.6	50–60

M: monovalent cation; x: degree of isomorphous substitution (between 0.5 and 1.3); CEC = Cation exchange capacity

the hydrophilic behavior (Bordes et al. 2009; Paul and Robeson 2008; Pavlidou and Papaspyrides 2008). Owing to this hydrophilic behavior, the hydration of MMT causes the galleries to expand and the clay to swell. In addition, the pristine clays are readily dispersed only in hydrophilic polymers (vinyl alcohol, ethylene oxide). To beaten this hydrophilic behavior and to make the clay compatible with hydrophobic polymers, the Na^{+1} present in the clay galleries can also be exchanged with organic cations, such as alkylammonuim or alkyphosphonium/onium ions. Murray (2000) reported that the charge imbalance called as cation exchange capacity (CEC) in smectite is about 0.66 per unit cell due to the isomorphic substitution. The CEC depends on the nature of isomorphic substitutions and varies from layer to layer, hence an average value on the complete crystal is considered (Alexandre and Dubois 2000). It is expressed as mequiv/100 g (meq/100 g) and is reported to range from 80 to 150 mequiv/100 g for smectites (Pavlidou and Papaspyrides 2008). The chemical formula, cation exchange capacity and particle length of commonly used smectites are listed in Table 4.

1.2 Organophilization of Nanoclays

Clay minerals reinforced polymer nanocomposites (CPNs) have received substantial recognition in the field of composites owing to their potential to exhibit remarkable improvements in the mechanical, thermal and barrier properties even at small loadings when compared with their micro-scale counterparts. However, the enhanced performance properties could only be recognized at nanoscale dispersion. To achieve nanoscale dispersion, delamination and, thereby exfoliation of these nanofiller platelets is prerequisite. As discussed in previous section, the clay minerals have strong tendency to form stacks owing to wander walls' forces. Delamination is achieved when there is affinity between the filler and polymer matrix, polymer chains intercalate to clay galleries and delaminate them. However, most of the petroleum based polymers are not compatible with clay minerals owing to the differences in their surface energies; and the exfoliation of clay platelets is one of the main problems encountered while preparing nanocomposites (Kádár et al. 2006). To solve this

problem, the surface energy of clay layers is lowered by their surface modification. In surface modification, surfactants having compatibility with the organic polymers are exchanged with exchangeable cations present in the clay, thereby expanding clay galleries and increasing spacing between the layers (d-spacing). The cations present in MMT galleries are usually exchanged with as alkylammonuim or alkyphosphonium/onium ions (Dadbin et al. 2008; Pavlidou and Papaspyrides 2008; Yoon et al. 2007). The surfactants might also have long hydrocarbon tails. The surface modification is usually accomplished through replacing the alkali cations present in the interlayer (gallery), called exchangeable cations with onium ions connected to hydrocarbon chains (non-polar tail) as shown in Fig. 3 (Majeed et al. 2013). Primary, secondary, tertiary and quaternary alkyl ammonium cations or phosphonium cations having various substituents can be employed as surfactants. The chemical structures of different surfactants that are being commonly used to modify MMT are presented in Fig. 4 (Bhattacharya and Aadhar 2014; Majeed et al. 2013).

Many intact and modified types of clays are commercially provided by a lot of suppliers. A list of commercially available nano clays along with their organo modifier and other characteristics are provided in Table 5 (Bordes et al. 2009; Cui and Paul 2011; Hemati and Garmabi 2011; Morawiec et al. 2005; Su et al. 2011; Tjong 2006). Structure of organo-modifier plays a vital role in delaminating and dispersing a nanoclay in a particular matrix. Thus, the selection criterion of organoclay depends majorly on the type of polymer matrix used. The effect of structure of organomodifier on the dispersion of MMT in a series of EVA based copolymers have been considered by the researchers. Cui and Paul (2011) studied the effect of modifier structure in dispersing MMT in EVA matrix and reported that the clay modified with surfactants having two alkyl tails was more dispersed than that having one alkyl tail. The researchers also observed that there should be a long chain carbon of 12 or more atoms to organophilize the natural clay mineral for exfoliation. Exfoliation of the clay in polyolefin is upgraded by increase in the number of long alkyl chains on the surfactant. On the other side, the nanocomposites formed by polyamides show an opposite trend. As for the polyamides, the surfactants having a single long alkyl tail gives the excellent exfoliation, and increase in alkyls gives undesirable polyamide alkyl interaction, as a result of which

= Exchangeable Cations
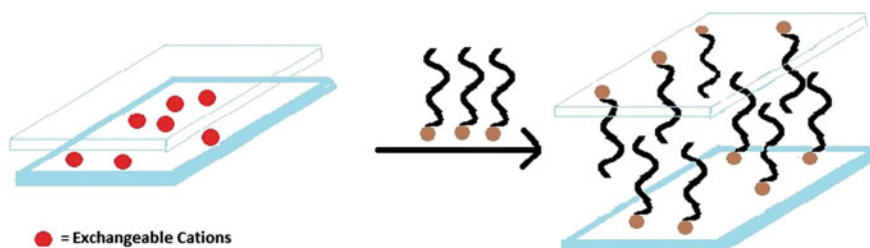
Fig. 3 Organophilization of montmorillonite (Majeed et al. 2013)
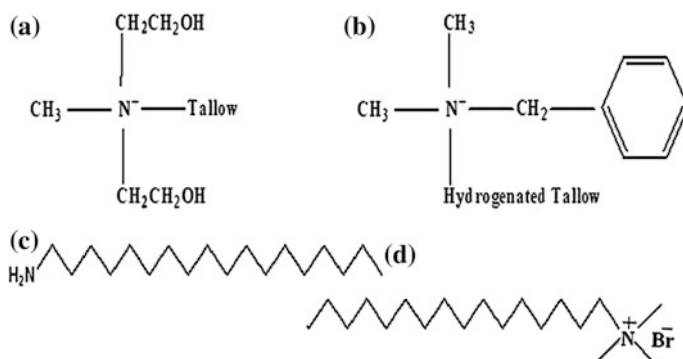
Fig. 4 Chemical structure of commonly used organomodifiers: **a** methyl, tallow, bis-2-hydroxyethyl, quaternary ammonium, **b** dimethyl, benzyl, hydrogenatedtallow, quaternary ammonium, **c** octadecylamine, and **d** Cetyl trimethyl ammonium bromide (Bhattacharya and Aadhar 2014; Majeed et al. 2013)

exfoliation decreases (Hotta and Paul 2004). In short, increment in d-spacing depends on the cation exchange capacity of layers, content and structure of surfactant and on the way the surfactants arrange themselves in the clay.

1.3 Nanoclays as Nano Fillers for Polymer-Clay Nanocomposites

Nanocomposites are a fairly new class of composite materials where a filler having at least one dimension in the nanometer (10^{-9} m) range is dispersed in a continuous matrix. They got recognition after the first successful development of Nylon nanocomposites having enhanced mechanical properties by the Toyota researchers. Since then, nanocomposites have been major area of research. The nanocomposites have shown improved mechanical and thermal properties; decreased flammability and barrier properties than both micro and macro composite materials. The filler loading; their shape, aspect ratio and their affinity towards matrix material are among distinctive parameters that play a vital role in modifying the properties (Goettler et al. 2007). The nanocomposites could be prepared by different methods including in situ polymerization, melt intercalation and direct mixing. The dispersed filler can be of the shape of sphere, tube, fiber or lamellae. The correlation of properties of materials with filler size has gained a great deal of importance with the recent advancement in the field of nanotechnology. Owing to their exceptional potential to exhibit peculiar characteristics that could not have been achieved with their traditional micro-scale counter parts, they have attracted a great deal of interest to exhibit enhanced and novel properties. There have been studies on the incorporation of nanoparticles having differences in shape, size, aspect ratio, structure

Table 5 Commercially available clay minerals along with surface modifiers (Bordes et al. 2009; Cui and Paul 2011; Hemati and Garmabi 2011; Morawiec et al. 2005; Su et al. 2011; Tjong 2006)

Supplier/ commercial designation	Clay	Surface-modifier	Modifier concentration (meq/100 g clay)	d_{001} (Å)
Southern clay products (USA)				
Cloisite®Na$^+$	MMT	–	–	11.7
Cloisite®10A	MMT	dimethyl, benzyl, hydrogenatedtallow, quaternary ammonium	125	19.2
Cloisite®15A	MMT	dimethyl, dihydrogenatedtallow, quaternary ammonium	125	31.5
Cloisite®20A	MMT	dimethyl, dihydrogenatedtallow, quaternary ammonium	95	24.2
Cloisite®25A	MMT	dimethyl, dehydrogenated tallow, 2-ethylhexyl quaternary ammonium	95	18.6
Cloisite®93A	MMT	methyl, dihydrogenatedtallow ammonium	95	23.6
Cloisite®30B	MMT	methyl, tallow, bis-2-hydroxyethyl, quaternary ammonium	90	18.5
Nanofil®15	MMT	dimethyl, dihydrogenated tallow alkyl quaternary ammonium	93	28
Nanofil®SE3000	Bentonite	dimethyl, dihydrogenated tallow alkyl quaternary ammonium	–	–
NanocorInc. (USA)				
Nanomer®1.30P	MMT	Octadecylamine (ODA)	120	22
Nanomer®1.44P	MMT	dimethyl dialkyl ammonium halide	–	–
Laviosa Chimica Mineraria (Italy)				
Dellite®43B	MMT	dimethyl benzylhydrogenated tallow ammonium	32−35	18.6
Dellite®72T	MMT	dimethyl dihydrogenated tallow ammonium	–	–

and geometry; and several nanoparticles have been recognized as possible additives to enhance performance properties (Arora and Padua 2010). Nanoclays are rigid fillers and improvement in the moduli of matrix material with the incorporation of these nanoclays is generally attributed to their high stiffness. Polymeric matrices are soft materials and their reinforcement with rigid nanoclays impede the free movement of polymer chains neighboring to the filler and if the interfacial adhesion

between the filler and the chains is satisfactory, the filler behaves as load bearing constituent. Improvement in the mechanical properties of polymer matrices with the addition of nanoclays have been published in many reviews (Patel et al. 2006; Paul and Robeson 2008; Pavlidou and Papaspyrides 2008). Beside improvement in the mechanical properties of polymers, nanoclays also have potential to reduce the permeability of gases, like oxygen and carbon dioxide; organic vapors and moisture through the nanocomposite films (Duncan 2011; Silvestre et al. 2011). Uniform dispersion of rigid impermeable nanoclays impede the diffusion of permeating molecules by forcing them to follow a tortuous path (Grunlan et al. 2004; Khaliq Majeed et al. 2015; Majeed et al. 2014; Nazarenko et al. 2007; Sanchez-Garcia et al. 2007). Increased flammability resistance (Tabuani et al. 2011; Zanetti and Costa 2004; J. Zhang et al. 2009) and enhanced thermal stability (Bertini et al. 2006; Durmuş et al. 2007; Giannakas et al. 2008; Santos et al. 2009) of nanocomposites are among the various other benefits attributed to the nanoclays.

2   Characterization

The appropriate characterization of nanoparticles exhibit a wide range of challenges and the selection of suitable technique is considerably substantial. Nanoparticles characterization is carried out to determine the surface area, porosity, solubility, particle size distribution, aggregation, hydrated surface analysis, zeta potential, wettability, adsorption potential, shape, size of the interactive surface, crystallinity, fractal dimensions, orientation, intercalation and dispersion of nanoparticles and nanotubes in nanocomposite materials. Some of the significant characterization techniques carried out for functional group identification (FT-IR); and the morphology and particle size determination (SEM & TEM) are discussed in the subsequent sections.

2.1   *Fourier Transfer Infrared Spectroscopy (FTIR)*

FTIR analysis of a chemical substance shows marked selective absorption in the infrared (IR) region. After absorption of IR radiation, the molecules of a chemical substance vibrates giving rise to close packed absorption bands called IR absorption spectrum which will correspond to the characteristic functional group and bands present in a chemical substance. Thus an IR spectrum of a chemical substance is a finger print for its identification. FTIR technique used to identify the different silicon bonds in clay structure. Specific bond produces characteristics vibrational peaks. Sample is prepared by adding 1–2 mg clay in equal amount of KBr and ground to fine powder. This mixture is placed in 13 mm casting dye and pressed about 9000 kg to make the fine shape of pellet. Solid casted pellet is placed in the path of light source at wave number ranges from 400 to 4000 cm^{-1} with scan rate of 40

Table 6 Characteristics peaks of the clays (Abdullah et al. 2015; Muthu et al. 2016)

Clay	Characteristics peak (cm^{-1})
Bentonite	3415 -OH Peaks, 471 Si-O-Al and 523 Si-O-Mg
Halloysite	1033 Si-O-Si, 3695 Al-OH
Montnorillonite	3422 (Water), 3624 (Al-OH)
Kaolinite	3696, 3671, 3650
Illite	3600
Smectite	3622
Saponite	3740 (Si-OH), 3670 (Mg(OH)$_2$)
Sepiolite	3719 (Si-OH) 3689 (Mg$_3$OH)
Nacrite	3701 and 3647 (out-of-plane), 3647 (in-plane)
Dickite	3708, 3654, 36228 (inner surface OH)
Lizardite	3686 (Mg-OH)

depending upon the desired resolution. As KBr and clay both are hygroscopic material, it may swell after absorbing moisture from air. To minimize the moisture effect samples are placed in oven at 130 °C overnight. Then samples are placed in the desiccator for further analysis. As the moisture is there, it may cause to change the chemical nature of clay by shifting K$^+$ ions from KBr to clay [15] and affect the clay spectra. It has been reported that peak intensity at 3415 and 1638 cm^{-1} may be due to presence of water molecules from moisture. Si-O-Si bond is confirmed from 1053 cm^{-1} (Abdullah et al. 2015). The peaks at 471 and 523 cm^{-1} ascribe the presence of bonds such as Si-O-Al and Si-O-Mg. The limitation of photo-acoustic mode for clay characterizations is overcome by using attenuated total reflection (ATR) mode. In ATR-FTIR analysis clay is spread completely over the diamond crystal for functional group investigation. Strong absorbance of moisture from the sample could be resolved by heating sample at 80°C and covered the sample with parafilm (Echegoyen et al. 2016). Clays and its characteristics peaks are presented in Table 6.

2.2 Scanning Electron Microscopy (SEM)

SEM technique does not affect the chemical nature of clay samples. It is very informative technique to identify the structure and chemical composition of any material including raw clay, pure clay materials and its derivatives.

Sample preparation is most important step to observe the morphology and to explore the relative composition of metals present in the sample. Solid sample is placed onto the carbon tap which is fixed at copper grid. Air is puffed on the surface of sample for uniform distributions. Clay material is non-conductor which is made conductor after platinum (Pt) coating for ten min in sputter coater. Coating may reduce the charging of sample. In solution migration technique the clay suspension

is prepared and a drop is spread onto the silicon chip where it is allowed to dry in air. Usually 5 kV accelerating potential is used to study the morphology and elemental composition of clay sample. Relative chemical composition of clay could be obtained by using energy dispersive X-ray (EDX) analysis. Nanoclay shows diversity of size and diameter of the particles. It has been reported that diameter may sometimes below or at 1–10 µm or even higher. Defining criteria for nanoparticle has been set by European Commission on October 2011; nanomaterial must have at least one dimension in range of 1–100 nm (Echegoyen et al. 2016).

SEM technique helps to explore the clay/PP nanocomposite structure. These samples are molded using injection molding technique. Layer structure of the composite material could be identified as: upper layer, middle layer and inner most layer. Thickness of layer depends on cooling while mold filling. Layer structure has been reported in Fig. 5a–f (Yu et al. 2015). In multilayer composite structure, different components are appeared as parallel layers to the flow direction of injected material into the mold. A uniform thickness of layers is observed at 70–400 nm with a little deposition of nanoclay agglomerates.

For energy dispersive X-ray studies live image is selected using SEM software. The part of image is selected and focused; where one wants to know the relative chemical composition of the material. The relative abundance of elements is mapped and these elements are segregated on the basis of energy requirements for Kα emission. EXD profile is obtained by selecting energy requirement (in KeV) at x-axis and relative abundance on y-axis. Kα emission of element is the specific characteristic which corresponds to the absorption of energy as difference of
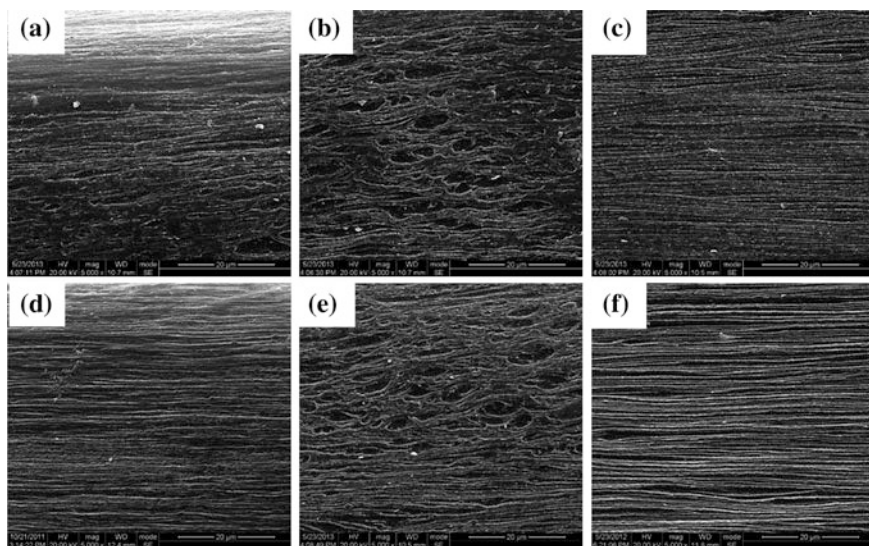
Fig. 5 Shows morphology of composite structure **a**, **d** outer layers, **b**, **e** middle layer, **c**, **f** inner layer (Yu et al. 2015)
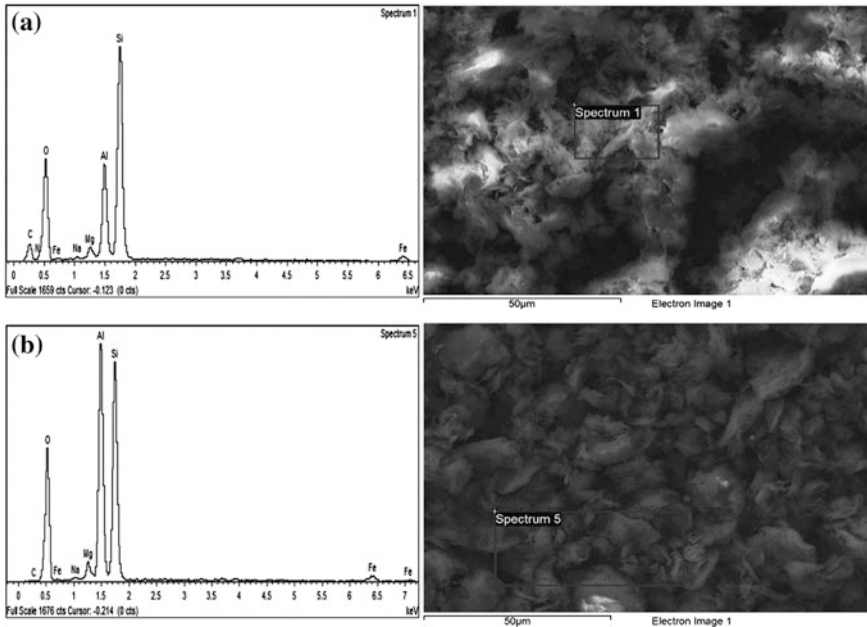
Fig. 6 **a** EDX spectra of nanoclay, **b** selected live image (Hakamy et al. 2015)

K-energy level is used to identify the element. While the peak height corresponds to the abundance of the element. Hakamy et al. (2015) studied EDX profile of nanoclays while characterizing nanoclays and calcined nanoclays/cement nanocomposites and the spectra is shown in Fig. 6. The figure attributes the selection of spot for analysis and furthermore image process is applied. EDX profile concludes that skeleton of nanoclay is composed of elements: first mostly of silicon, second most oxygen, third most aluminum and other includes are: carbon, magnesium, iron and sodium.

2.3 Transmission Electron Microscopy (TEM)

TEM is non-destructive technique used to study the morphology and diffraction pattern of nanoclay. TEM samples are prepared using solution dispersion and extrusion method. In solution dispersion method; nanoclay sample could be dispersed in ether, ethanol or isopropyl alcohol (IPA). Less than 2 mg of sample is suspended in 5–10 mL of dispersion medium which is placed in the beaker and allowed to sonicate for 15 to 30 min to ensure the complete dispersion of nanoclay. A drop of sample solution is placed onto the copper grid and allowed to dry in

vacuum oven to avoid any particulate contamination. After 24 h copper grid mounted with sample is placed on the sample holder and fixed with screw. Sample holder is carefully and gently placed in the TEM column and waited for pressure adjustment. This sample preparation method could be used for pure, raw and modified nanoclay. Extrusion and casting method is used for sample preparation of nanoclay composites. Furthermore this sample is cut into 130 nm slice using ultra-microtome and fixed on the holder. Morphology of samples is recorded using different magnification and potential where image gives the significant information.

Morphology of different clay materials has been reported by Jeong et al. and is shown in Fig. 7a–c (Jeong and Achterberg 2014). The figure shows the compact arrangement in clay layers of illite, chlorite, kaolinite etc. with deposition of different particle sizes. These particles are compactly and tightly packed in layers structure as suggested from TEM micrograph.

Transmission electron microscope at high resolution mode called HRTEM describes the diffraction pattern and layer orientation in structure. Different layers structure and deposition of different material could be distinguished apparently from micrograph. This approach has been reported in Fig. 8a–c (Jeong and Achterberg 2014), diffraction pattern shows the alignment of lattice fringes. Parallel lattice spacing suggested the presence of similar particle with regular geometrical orientation and darker spots may suggest the deposition of different particle in under layers of thin slice of clay particle.
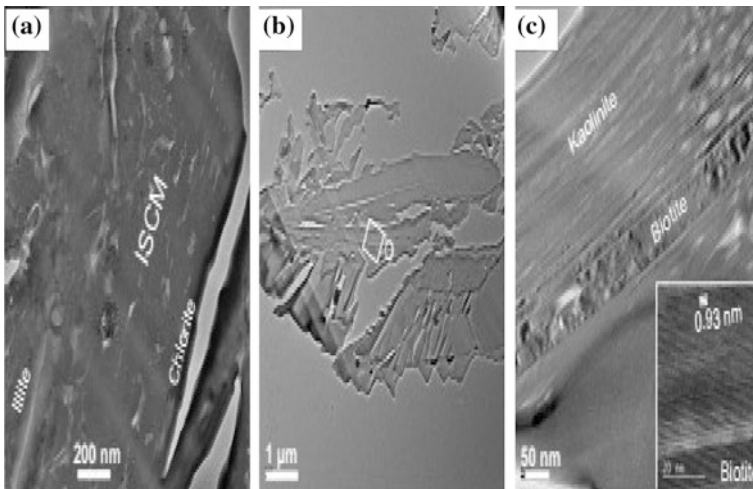
Fig. 7 Clay shows the deposition different particle sizes (Jeong and Achterberg 2014)
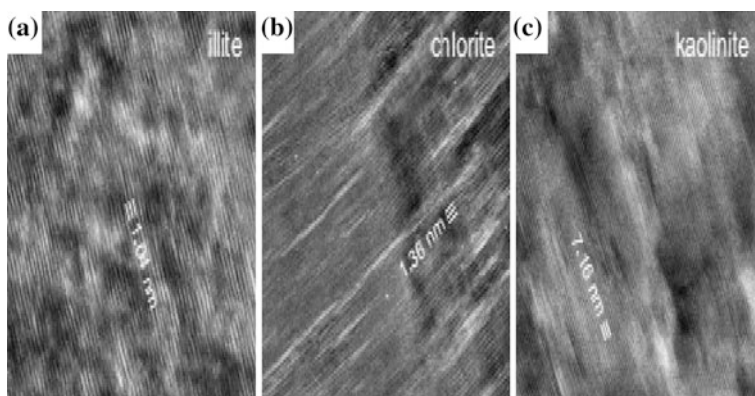
Fig. 8 HRTEM of clay particles which shows the lattice fringe (Jeong and Achterberg 2014)

3 Conclusion and Future Perspective

The study of nanoclays is a large field and shows an immense potential to be explored. Nanoclays have long been used in several applications and their uses are based on their structural and physical characteristics that are discussed in detail in this chapter. Introduction of nanoclays as fillers or additives in polymers for various desired effects has been of enormous interest for research and development studies. An interesting concern, along with the studies addressing how nanoclays change the behavior of polymeric materials, is to discover more about nanoclays. Various techniques that are used to characterize nanoclays are described in detail in this chapter and further studies could pay more attention to deep analysis with new advanced techniques. Despite clay minerals are ubiquitous in nature, several interesting nanoclays are not available in sufficient quantities therefore their synthesis will be a highlighted field of clay science and may lead to a breakthrough in the field of nanocomposites. Finding new applications of such synthetic clay minerals, including pillared clay minerals, porous clay hetero-structures, and nanocomposites, will be another promising work. Information on occupational exposure to nanoclays during extraction, development, and application is limited and is highly desirable. An additional demanding area is the potential of nanoparticles (from packaging material) to migrate to packaged food and their eventual toxicological effects, if any.

References

Abdullah, M., Afzaal, M., Ismail, Z., Ahmad, A., Nazir, M., Bhat, A.: Comparative study on structural modification of Ceiba pentandra for oil sorption and palm oil mill effluent treatment. Desalin. Water Treat. **54**, 3044–3053 (2015)

Alexandre, M., Dubois, P.: Polymer-layered silicate nanocomposites: preparation, properties and uses of a new class of materials. Mat. Sci. Eng. R **28**, 1–63 (2000)

Ambre, A.H., Katti, K.S., Katti, D.R.: Nanoclay based composite scaffolds for bone tissue engineering applications. J Nanotechnol. Eng. Med. **1**, 031013 (2010)

Arora, A., Padua, G.: Review: nanocomposites in food packaging. J. Food Sci. **75**, R43–R49 (2010)

Azeredo, H.M.C.D.: Nanocomposites for food packaging applications. Food Res. Int. **42**, 1240–1253 (2009). doi:10.1016/j.foodres.2009.03.019

Bertini, F., Canetti, M., Audisio, G., Costa, G., Falqui, L.: Characterization and thermal degradation of polypropylene–montmorillonite nanocomposites. Polym. Degrad. Stab. **91**, 600–605 (2006)

Bhattacharya, S., Aadhar, M.: Studies on preparation and analysis of organoclay nano particles. Res. J. Eng. Sci. **3**, 10 (2014)

Bordes, P., Pollet, E., Avérous, L.: Nano-biocomposites: biodegradable polyester/nanoclay systems. Prog. Polym. Sci. **34**, 125–155 (2009)

Carretero, M.I., Pozo, M.: Clay and non-clay minerals in the pharmaceutical industry: part I. Excipients and medical applications. Appl. Clay Sci. **46**, 73–80 (2009)

Carretero, M.I., Pozo, M.: Clay and non-clay minerals in the pharmaceutical and cosmetic industries part II. Active ingredients. Appl Clay Sci. **47**, 171–181 (2010)

Cui, L., Paul, D.: Polymer nanocomposites from organoclays: Structure and properties. Paper presented at the Macromol Sy (2011)

Dadbin, S., Noferesti, M., Frounchi, M.: Oxygen Barrier LDPE/LLDPE/Organoclay Nano-Composite Films for Food Packaging. Paper presented at the Macromol Sy (2008)

Du, M., Guo, B., Jia, D.: Newly emerging applications of halloysite nanotubes: a review. Polym. Int. **59**, 574–582 (2010)

Duncan, T.V.: Applications of nanotechnology in food packaging and food safety: Barrier materials, antimicrobials and sensors. J. Colloid Interface Sci. **363**, 1–24 (2011)

Durmuş, A., Woo, M., Kaşgöz, A., Macosko, C.W., Tsapatsis, M.: Intercalated linear low density polyethylene (LLDPE)/clay nanocomposites prepared with oxidized polyethylene as a new type compatibilizer: structural, mechanical and barrier properties. Eur. Polym. J. **43**, 3737–3749 (2007)

Echegoyen, Y., Rodríguez, S., Nerín, C.: Nanoclay migration from food packaging materials. Food Addit Contam. Part A (2016)

Fernandes, F.M., Baradari, H., Sanchez, C.: Integrative strategies to hybrid lamellar compounds: an integration challenge. Appl. Clay Sci. **100**, 2–21 (2014). doi:10.1016/j.clay.2014.05.013

Floody, M.C., Theng, B., Reyes, P., Mora, M.: Natural nanoclays: applications and future trends–a Chilean perspective. Clay Miner. **44**, 161–176 (2009)

Garrido-Ramírez, E., Theng, B., Mora, M.: Clays and oxide minerals as catalysts and nanocatalysts in Fenton-like reactions—a review. Appl. Clay Sci. **47**, 182–192 (2010)

Giannakas, A., Spanos, C., Kourkoumelis, N., Vaimakis, T., Ladavos, A.: Preparation, characterization and water barrier properties of PS/organo-montmorillonite nanocomposites. Eur. Polym. J. **44**, 3915–3921 (2008)

Goettler, L., Lee, K., Thakkar, H.: Layered silicate reinforced polymer nanocomposites: development and applications. Polym. Rev. **47**, 291–317 (2007)

Grunlan, J.C., Grigorian, A., Hamilton, C.B., Mehrabi, A.R.: Effect of clay concentration on the oxygen permeability and optical properties of a modified poly (vinyl alcohol). J. Appl. Polym. Sci. **93**, 1102–1109 (2004)

Hakamy, A., Shaikh, F., Low, I.: Characteristics of nanoclay and calcined nanoclay-cement nanocomposites. Compos. Part B-Eng. **78**, 174–184 (2015)

Hemati, F., Garmabi, H.: Compatibilised LDPE/LLDPE/nanoclay nanocomposites: I. Structural, mechanical, and thermal properties. Can. J. Chem. Eng. **89**, 187–196 (2011)

Hotta, S., Paul, D.: Nanocomposites formed from linear low density polyethylene and organoclays. Polymer **45**, 7639–7654 (2004)

Jeong, G., Achterberg, E.P.: Chemistry and mineralogy of clay minerals in Asian and Saharan dusts and the implications for iron supply to the oceans. Atmos. Chem. Phys. **14**, 12415–12428 (2014)

Kádár, F., Százdi, L., Fekete, E., Pukánszky, B.: Surface characteristics of layered silicates: influence on the properties of clay/polymer nanocomposites. Langmuir **22**, 7848–7854 (2006)

Lee, S.M., Tiwari, D.: Organo and inorgano-organo-modified clays in the remediation of aqueous solutions: an overview. Appl. Clay Sci. **59–60**, 84–102 (2012). doi:10.1016/j.clay.2012.02.006

Liu, M., Jia, Z., Jia, D., Zhou, C.: Recent advance in research on halloysite nanotubes-polymer nanocomposite. Prog. Polym. Sci. **39**, 1498–1525 (2014)

Lvov, Y., Abdullayev, E.: Functional polymer–clay nanotube composites with sustained release of chemical agents. Prog. Polym. Sci. **38**, 1690–1719 (2013)

Majeed, K., Hassan, A., Abu Bakar, A.: Barrier, Biodegradation, and mechanical properties of (Rice husk)/(Montmorillonite) hybrid filler-filled low-density polyethylene nanocomposite films. J. Vinyl and Addit. Technol. (2015)

Majeed, K., Hassan, A., Bakar, A., Jawaid, M.: Effect of montmorillonite (MMT) content on the mechanical, oxygen barrier, and thermal properties of rice husk/MMT hybrid filler-filled low-density polyethylene nanocomposite blown films. J. Thermoplast. Compos. 0892705714554492 (2014)

Majeed, K., Jawaid, M., Hassan, A., Abu Bakar, A., Abdul Khalil, H.P. S., Salema, A.A., Inuwa, I.: Potential materials for food packaging from nanoclay/natural fibres filled hybrid composites. Mater. Des. **46**, 391–410 (2013). doi:http://dx.doi.org/10.1016/j.matdes.2012.10.044

Mitra, G.B.: Spiral structure of 7 Å halloysite: mathematical models. Clay Clay Miner. **61**, 499–507 (2013)

Morawiec, J., Pawlak, A., Slouf, M., Galeski, A., Piorkowska, E., Krasnikowa, N.: Preparation and properties of compatibilized LDPE/organo-modified montmorillonite nanocomposites. Eur. Polym. J. **41**, 1115–1122 (2005)

Murray, H.H.: Traditional and new applications for kaolin, smectite, and palygorskite: a general overview. Appl. Clay Sci. **17**, 207–221 (2000)

Muthu, R.N., Rajashabala, S., Kannan, R.: Synthesis, characterization of hexagonal boron nitride nanoparticles decorated halloysite nanoclay composite and its application as hydrogen storage medium. Renew. Energ. **90**, 554–564 (2016)

Nagendrappa, G.: Organic synthesis using clay and clay-supported catalysts. Appl. Clay Sci. **53**, 106–138 (2011)

Nazarenko, S., Meneghetti, P., Julmon, P., Olson, B., Qutubuddin, S.: Gas barrier of polystyrene montmorillonite clay nanocomposites: effect of mineral layer aggregation. J Polym. Sci. Polym. Phys. **45**, 1733–1753 (2007)

Ouellet-Plamondon, C., Lynch, R.J., Al-Tabbaa, A.: Comparison between granular pillared, organo-and inorgano–organo-bentonites for hydrocarbon and metal ion adsorption. Appl. Clay Sci. **67**, 91–98 (2012)

Pasbakhsh, P., Churchman, G.J., Keeling, J.L.: Characterisation of properties of various halloysites relevant to their use as nanotubes and microfibre fillers. Appl. Clay Sci. **74**, 47–57 (2013)

Patel, H.A., Somani, R.S., Bajaj, H.C., Jasra, R.V.: Nanoclays for polymer nanocomposites, paints, inks, greases and cosmetics formulations, drug delivery vehicle and waste water treatment. B Mater. Sci. **29**, 133–145 (2006)

Paul, D.R., Robeson, L.M.: Polymer nanotechnology: nanocomposites. Polymer **49**, 3187–3204 (2008). doi:10.1016/j.polymer.2008.04.017

Pavlidou, S., Papaspyrides, C.: A review on polymer–layered silicate nanocomposites. Prog. Polym. Sci. **33**, 1119–1198 (2008)

Ray, S.S., Okamoto, M.: Polymer/layered silicate nanocomposites: a review from preparation to processing. Prog. Polym. Sci. **28**, 1539–1641 (2003)

Sanchez-Garcia, M., Gimenez, E., Lagaron, J.: Novel PET nanocomposites of interest in food packaging applications and comparative barrier performance with biopolyester nanocomposites. J. Plast. Film Sheeting **23**, 133–148 (2007)

Santos, K., Liberman, S., Oviedo, M., Mauler, R.: Optimization of the mechanical properties of polypropylene-based nanocomposite via the addition of a combination of organoclays. Compos. Part A-Appl. S **40**, 1199–1209 (2009)

Shahidi, S., Ghoranneviss, M.: Effect of plasma pretreatment followed by nanoclay loading on flame retardant properties of cotton fabric. J. Fusion Energ. **33**, 88–95 (2014)

Silvestre, C., Duraccio, D., Cimmino, S.: Food packaging based on polymer nanomaterials. Prog. Polym. Sci. **36**, 1766–1782 (2011)

Su, F.-H., Huang, H.-X., Zhao, Y.: Microstructure and mechanical properties of polypropylene/poly (ethylene-co-octene copolymer)/clay ternary nanocomposites prepared by melt blending using supercritical carbon dioxide as a processing aid. Compos. Part B-Eng. **42**, 421–428 (2011)

Suresh, R., Borkar, S., Sawant, V., Shende, V., Dimble, S.: Nanoclay drug delivery system. Int. J. Pharm. Sci. Nanotechnol. **3**, 901–905 (2010)

Tabuani, D., Ceccia, S., Camino, G.: Polypropylene nanocomposites, study of the influence of the nanofiller nature on morphology and material properties. Paper presented at the Macromol Sy (2011)

Tjong, S.: Structural and mechanical properties of polymer nanocomposites. Mater. Sci. Eng. R **53**, 73–197 (2006)

Uddin, F.: Clays, nanoclays, and montmorillonite minerals. Metall. Mater. Trans. A **39**, 2804–2814 (2008)

Yah, W.O., Xu, H., Soejima, H., Ma, W., Lvov, Y., Takahara, A.: Biomimetic dopamine derivative for selective polymer modification of halloysite nanotube lumen. J. Am. Chem. Soc. **134**, 12134–12137 (2012). doi:10.1021/ja303340f

Yoon, K.-B., Sung, H.-D., Hwang, Y.-Y., Noh, S.K., Lee, D.-H.: Modification of montmorillonite with oligomeric amine derivatives for polymer nanocomposite preparation. Appl. Clay Sci. **38**, 1–8 (2007)

Yu, F., Deng, H., Bai, H., Zhang, Q., Wang, K., Chen, F., Fu, Q.: Confine clay in an alternating multilayered structure through injection molding: a simple and efficient route to improve barrier performance of polymeric materials. ACS Appl. Mater. Interfaces **7**, 10178–10189 (2015)

Yuan, G., Wu, L.: Allophane nanoclay for the removal of phosphorus in water and wastewater. Sci. Technol. Adv. Mater. **8**, 60–62 (2007)

Yuan, P., Southon, P.D., Liu, Z., Green, M.E., Hook, J.M., Antill, S.J., Kepert, C.J.: Functionalization of halloysite clay nanotubes by grafting with γ-aminopropyltriethoxysilane. J. Phys. Chem. C **112**, 15742–15751 (2008)

Yuan, P., Tan, D., Annabi-Bergaya, F.: Properties and applications of halloysite nanotubes: recent research advances and future prospects. Appl. Clay Sci. **112**, 75–93 (2015)

Zanetti, M., Costa, L.: Preparation and combustion behaviour of polymer/layered silicate nanocomposites based upon PE and EVA. Polymer **45**, 4367–4373 (2004)

Zhang, D., Zhou, C.-H., Lin, C.-X., Tong, D.-S., Yu, W.-H.: Synthesis of clay minerals. Appl. Clay Sci. **50**, 1–11 (2010). doi:10.1016/j.clay.2010.06.019

Zhang, J., Hereid, J., Hagen, M., Bakirtzis, D., Delichatsios, M., Fina, A., Bourbigot, S.: Effects of nanoclay and fire retardants on fire retardancy of a polymer blend of EVA and LDPE. Fire Saf. J. **44**, 504–513 (2009)

Modification of Nanoclay Systems: An Approach to Explore Various Applications

Mohd Amil Usmani, Imran Khan, Naheed Ahmad, A.H. Bhat,
Dhananjay K. Sharma, Jahangir Ahmad Rather
and Syed Imran Hassan

Abstract Nanoclay has a great potential in various fields. Small amount of nanoclay can change the whole physical and chemical properties of polymers, paints, inks and lubricants by dispersing nanoclay layers into the polymer matrices. The flexibility of interlayer gallery of nanoclay helps in the release of drugs to the targeted place. The controlled release of drugs takes place on account of the drug incorporated within the nanoclay galleries. This makes these nanomaterials as potential materials with its application in pharmaceutical field. Organoclays, a type of nanoclay are also being utilized for waste water treatment in junction with other sorbents viz. activated carbon and alum. Organoclays have been found to be the finest material for water treatment especially when the water contains enough amounts of oil and grease or humic acid. The use of nanoclays as reinforcing agent or additives in polymers for various properties is exploited for various applications. This chapter provides an overview of nanoclays or types of nanoclays with significance on the utilization of nanoclays as the filler in polymer matrices for the synthesis/fabrication of polymer nanocomposites, drug delivery agents, viscosity modifier for coatings, inks and lubricants and nanoclays for industrial effluent as well as potable water treatment.

M.A. Usmani
Department of Chemistry, Eritrea Institute of Technology,
P.O. Box 12676, Asmara, Eritrea

I. Khan (✉) · J.A. Rather · S.I. Hassan
Department of Chemistry, College of Science, Sultan Qaboos University,
P.O. Box 36, PC 123 Muscat, Oman
e-mail: imrank@squ.edu.om; imran.pchr@gmail.com

N. Ahmad
Department of Botany, Patna University, Patna 800013, India

A.H. Bhat
Department of Fundamental and Applied Sciences, Universiti Teknologi Petronas,
31750 Bandar Seri Iskandar, Tronoh, Perak Darul Ridzuan, Malaysia

D.K. Sharma
TEMA-CICECO, University of Aveiro, 3810-193 Aveiro, Portugal

1 Introduction

Clay is generally a fine material made of natural rocks or soil stuff that consists of more than one mineral with small amount of metal oxides and organic matter. Clay is chemically small crystallites of alumino-silicates of various proportions, with substitutions of iron and magnesium by alkalis and alkaline earth elements (Pavlidou and Papaspyrides 2008). It differs from other fine materials by size and composition. The loading of nanoclays in clay based nanocomposites are optimized with many better properties as compared to the matrix materials with an eye on a specific application. Nanoclays are being commonly used for the fabrication of polymer clay nanocomposites (PCN). The loading of the clay to the polymers makes it a value added product with an increment in the properties as compared to the filled polymers at a very low addition. The incorporation of organoclay in the coatings ameliorates the rheological properties of the coatings. The final material so synthesized would prevent pigment settling and sagging on vertical surfaces (Patel et al. 2006). The extensive potential of nanoclay to improve the material properties of polymer matrix, have been proven in various studies (Chu 2006; Nguyen 2007; Ray and Okamoto 2003). The high aspect ratio enhances the interaction between matric-nanoparticles and particle-particle as compared to the interaction to conventional fillers. The incorporation of little amount of organoclays enhances the thermal stability of grease (Kandola et al. 2008; Tcherbi-Narteh 2013). Furthermore, the color retention by nanoclay, opens the avenues for it to be applied in cosmetics and inks (Natarajan 2015; Patel et al. 2006). The petroleum industry also makes use of organoclays for the removal of hydrocarbons from refineries (Natarajan 2015). The removal of toxic chemicals from pharmaceuticals and pesticides industries is being carried by organoclays (Chen et al. 2011). Other area of application are in adsorption applications for removing oil, grease, heavy metals, polychlorinated biphenyl; and organic components (Stagnaro 2015), eliminating radionuclides/pertechnetate from water (Khater et al. 2013; Mota et al. 2011) and application as therapeutic agent drug vehicle (Suresh et al. 2010). The Toyota company research group report (Usuki et al. 1993) were the pioneers of nanocomposite science or nanotechnology. This group developed nanoclay based nylon-6 nanocomposites with improved properties. In this chapter we focused on types, preparation, properties and applications of nanoclay or phyllosilicates which encompasses all silicates with layered sheets and their chemical composition which makes it so versatile for various fields.

2 Development in Clay Studies

The clay mineral studies got significant progress during 1925 to 1940. As a result, a committee for the investigation of clay minerals under the national research council had been appointed. First of all, American geologist, Heinrich Ries studied clays from many of the eastern states (Ries 1920). After that in 1924, Ross and shannon (1925) started studies of the mineral composition of clays and published a number of research papers on the clay mineral (Ross and Kerr 1930, 1931). Simultaneous, (Ross and Kerr 1928) studied the small clay particles by means of X-ray powder diffraction. In 1930, Pauling (1930) investigated the atomic structure of layer silicates which explored basic ideas about the structure of many clay minerals. Subsequent in 1932, Gruner (1932) worked out a structure for kaolinite and Hofmann et al. (1933) in 1933, suggested an atomic arrangement for MMT. Meanwhile in 1935, Mehmel (1935) was the first to indicate clearly that two forms of halloysite existed. Later in 1940, Ardenne et al. (1940) showed the electron microscope to be another powerful tool for the investigation of clay minerals and in 1942, Hendricks and Teller (1942) presented the theory of X-ray powder diffraction for interstratified minerals. Clay mineral research was developing rapidly in many European countries in the 1940s as it was in the United States. About in 1945, the U.S. National Research Council established a committee on clay minerals. The main cause of world-wide search for this clay was its extensive commercial use as bentonite mineral (Grim and Guven 1978).

The era of polymer nanocomposites got a drastic change in 1987 when Fukushima et al. (Fukushima and Inagaki 1987) discovered the possibility of synthesizing polymer nanocomposites based on nylon-6/organophilic montmorillonite clay that showed significant improvements in the material properties at very low content of layered silicate. After that, Vaia et al. (1993) in 1993, showed the possibility to melt-mix polymers with layered silicates, without the use of organic solvents which caused high momentum in the field of polymer/layered silicate nanocomposites. Nanoclays provide color retention as well as good coverage in cosmetics and inks (Tatum 1988). Thermal stability of grease is greatly enhanced by the addition of small amount of organoclays (Somani 2000). Recently, it has been shown that nanoclay is important nano additives/nano fillers due to its large availability, biodegradable nature and cost effectiveness (Heydari 2013; Sadegh-Hassani 2014; Torabi 2013; Voon 2012). Nanoclays are also potentially useful materials in the field of controlled release of therapeutic agent to patients, where it acts as a drug vehicle. MMT could adsorb dietary toxins, bacterial toxins associated with gastrointestinal disturbance, hydrogen ions in acidosis, and metabolic toxins such as steroidal metabolites associated with pregnancy (Dong and Feng 2005). The important highlights have been presented in the Table 1.

Table 1 Important highlights in the history of clay development

1898	A clay like mineral named as bentonite found (Knight 1898)
1917	Bentonite confirmed a product of volcanic ash (Hewitt 1917)
1920	Commercial production of bentonite began in the United States (Grim 1988)
1926	MMT found as major component of bentonite (Ross and Shannon 1926)
1927	Optical and x-ray research on clay minerals came into existence (Ross and Kerr 1928)
1930	A variety of clays investigated (Ross and Kerr 1930)
1930	Layered structure of silicates clay investigated (Pauling 1930)
1931	Crystalline nature of clay investigated and named as clay mineral (Ross and Kerr 1931)
1933	Atomic arrangement for montmorillonite investigated (Hofmann et al. 1933)
1935	Two forms of halloysite investigated (Mehmel 1935)
1939	Clay proved an excellent bonding material for molding sands (Grim and Bradley 1939)
1935	Clay minerals synthesised (Ewell and Insley 1935)
1949	Organo MMT for paints, greases, drilling fluids, and other materials developed (Jordan 1949)
1938	Catalyst was developed from bentonite (Houdry et al. 1938)
1945	U.S. National Research Council established a Committee on Clay Minerals (Grim 1988)
1987	The possibility of synthesizing polymer nanocomposites based on nylon-6/organophilic MMT clay that showed dramatic improvements in mechanical and physical properties and heat distortion temperature at very low content of layered silicate discovered (Fukushima and Inagaki 1987)
1990	Firstly reported use of MMT clay for preparing polymer-clay nanocomposites (Okada et al. 1990)
1993	First time exfoliated Nylon-6/clay hybrid successfully prepared via in situ ring-opening polymerization of ε-caprolactam (Usuki et al. 1993)
2002	Development of organoclay as nanofillers started (Lepoittevin et al. 2002)
2007	Organoclay has been practised as reinforcing agents (Deshmanea et al. 2007; Subramani et al. 2007)

3 Structure and Types of Nanoclay Particles

Clays are mostly consists of hydrous silicates or alumina–silicates, which have a layered structure, comprising silicon, aluminium or magnesium, oxygen and hydroxyl with various associated cations where ions and OH groups are arranged into two dimensional structures as silicates layered sheets consisting of silica and alumina. On the basis silica to alumina sheet ratio, these clay minerals can be divided into three different types as follows (Ke 2005; Theng 1979).

3.1 Type 1:1 Phyllosilicates

This type of clay mineral consists of one octahedral alumina sheet and one tetrahedral silica sheet compressed in 1:1 ratio. The sheet of this type of clay mineral

Table 2 Major groups of clay minerals

Family	Group	Layer	Family	Group
Phyllosilicates	Kaolinite	1:1	Kaolinite, dickite, nacrite	$Al_2Si_2O_5(OH)_4$
Phyllosilicates	MMT or Smectite	2:1	MMT, Pyrophyllite, talc, Vermiculite, Sauconite, Saponite, Nontronite	$(Ca,Na,H)(Al,Mg,Fe,Zn)_2$ $(Si,Al)_4O_{10}(OH)_2$-XH_2O
Phyllosilicates	Illite	2:1	Illite	$(K,H_3O)(Al,Mg,Fe)_2$ $(Si,Al)_4O_{10}[(OH)_2(H_2O)]$
Phyllosilicates	Chlorite	2:1:1	(i) amesite, (ii) chamosite, (iii) cookeite, (iv) nimite	(i) $(Mg, Fe)_4Al_4Si_2O_{10}(OH)_8$ (ii) $(Fe,Mg)_3Fe_3$ $AlSi_3O_{10}(OH)_8$ (iii) $LiAl_5\ Si_3O_{10}(OH)_8$ (iv)$(Ni,Mg,Fe, Al)_6AlSi_3O_{10}(OH)_8$

does not hold any charge in both silica and alumina sheets owing to absence of isomorphic substitution. The hydrogen bonding interaction between OH group of octahedral sheets and oxygen in tetrahedral sheets held the layers together; therefore, water molecules occupied the space between the layers. Type 1:1 clay minerals included Kaolinite, Perlite, Hallosite, etc. (Table 2).

3.1.1 The Kaolinite Group

Kaolinite is 1:1 type clay mineral which is made up of one tetrahedral (silica) sheet combined with one octahedral (alumina) sheet. The tetrahedral and octahedral sheets in a layer of a kaolinite crystal are joint by oxygen atoms (hydrogen bonding), which are mutually shared by the silicon and aluminium cations in their respective sheets. As the result with fixed structure and no expansion between layer when clay is wetted. Kaolinite particles cannot break into extremely thin plates due to the strong binding forces between their structural layers. Hence, kaolinite exhibits very little plasticity, cohesion, shrinkage and swelling capacity.

3.2 Type 2:1 Phyllosilicates

In 2:1 type clay minerals, an alumina sheet is sandwiched between two silica sheets also known as smectite. Stacking between these clay layers generate a van der Waals gap and therefore isomorphic substitution of Al^{3+} with Fe^{2+}, Mg^{2+}, Li^+ in the octahedron sheets and/or Si^{4+} with Al^{3+} in the tetrahedron sheets creates negative charge on each layer. And the metal cations in the interlayer spacing counterbalance this negative charge. Various examples are given in Table 2.

3.2.1 The MMT/Smectite Group

The clays used for the preparation of nanoclays belong to smectite group (2:1 phyllosilicates) among them, MMT is typically used for the preparation of PCN (Alexandre and Dubois 2000; LeBaron 1999; Pavlidou and Papaspyrides 2008; Ray and Okamoto 2003; Zeng et al. 2005). Among the smectite group, MMT shows extensive inter layer expansion or swelling (Fig. 1). MMT structure consists of layers sandwiching an edge shared octahedral sheet of alumina between two silica tetrahedral sheets so that the apical oxygen atoms of the tetrahedral sheets are all shared with the octahedral sheet. Aluminium for silicon in the tetrahedral sheet and iron or magnesium for aluminium in the octahedral sheet creates an overall negative charge to the crystal lattice due to isomorphous substitution and hence, positively charged cations get attracted between these layers. These layers organize themselves in a parallel way to form stacks with a regular van der Waals gap in between them, called as interlayer which in turn show high cation exchange capacity, swelling and shrinkage properties (Azeez et al. 2013).

Complete dispersion or exfoliation of nanomers into a resin matrix result in the formation of nanocomposite (He et al. 2009). These clays are used as fillers in ceramics, paint, rubber, paper, and plastics.

3.2.2 The Vermiculite Group

Vermiculites (2:1 type minerals) is a naturally occurring group of hydrated aluminium/iron/magnesium silicates with a laminate structure. Vermiculites are generally trioctahedral or sometimes dioctahedral in structure with a negative layer charge. In the tetrahedral sheet of most vermiculite, aluminum is substituted by
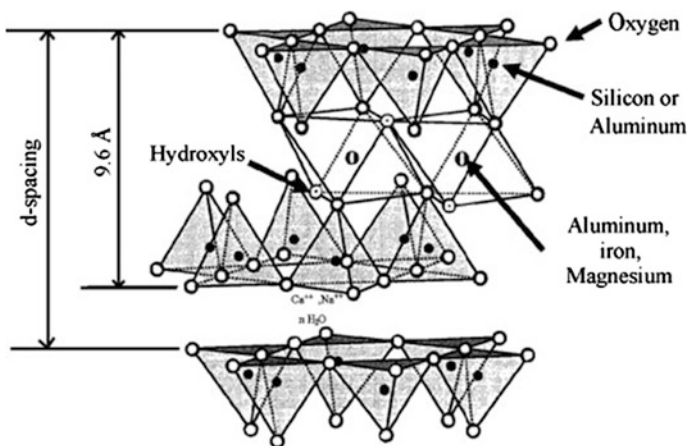
Fig. 1 Structure of montmorillonite (Azeez et al. 2013)

silicon in most of the sites which in turn creates net negative charge associated. Also, water molecules with magnesium and other ions are adsorbed in the interlayer space of vermiculites which act as bridge holding the units together rather than as wedges driving them apart. The degree of swelling is, therefore considerable less for vermiculites than for MMT because of which vermiculites have limited expansion clay minerals, expanding more than kaolinite but much less than the MMT. These clays are used in makings boards, panels, pre-mixed coatings, packaging, making lightweight concretes and vermiculite plasters (Reichenbach and Bayer 1994)

3.2.3 The Illite Group

Illite is non-expanding 2:1 type layered alumino-silicate clay mineral and also known as Micas like Muscovite and biotite. Structurally illite group is similar to the MMT/smectite, but the particles are much larger than those of the MMT/smectite. Most of the charge is counted in the tetrahedral sheet and other from aluminum atoms (20 % of the silicon sites) which creates a net negative charge in the tetrahedral sheet and the charge is higher than that found in vermiculites. To counterbalance this charge, potassium ions are strongly attracted in the interlayer space and have just the right size to fit into interlayer spaces in the adjoining tetrahedral sheets. The potassium thereby acts as a binding agent, preventing swelling of the crystal. Therefore, the illite group clay minerals are quite nonexpanding. The properties such as hydration, cation adsorption, swelling, shrinkage and plasticity are less intense in illite than in MMT/smectite but are more than kaolinite due to the presence of interstratified layers of MMT or vermiculite. Clay mineral illite is commonly used as filler in some drilling mud as well as they are common constituent of shales.

3.3 Type 2:2 or 2:1:1 Phyllosilicates

The layer structure of 2:2 type formed by the condensation of silica tetrahedron sheets and alumina or magnesium octahedron sheets. They are also known as tetramorphic of four sheet minerals like Chlorite (Table 2).

3.3.1 The Chlorite Group

These minerals are the major component formed from igneous rocks. Chlorites are basically Fe, Mg, phyllosilicates having some aluminum presence with a layered structure similar to the illite/mica. The crystal unit chlorite contains two silica tetrahedral sheets and two magnesium-dominated trioctahedral sheets (2:1:1 or 2:2 type structure). In terms of charge, negative charge of chlorites is nearly comparable

to illite but less than smectite or vermiculites. Both the particle size and surface area are nearly same for chlorites and illite. Since, there is no water adsorption between the chlorite crystal units which makes non-expanding nature (Abdel-Rahman 1995).

4 Properties of Clay

Clay has many distinct properties which have to be understood before they can be efficiently used for industrial and technological applications. They are explained below.

4.1 Cation Exchange Capacity (CEC)

Clay minerals usually tends negative charge causing from the isomorphous substitution of silica cation (Si^{4+}) by aluminum cation (Al^{3+}) which creates a capacity to clamp positive charges. And in case of soil which consists of clay and organic matters gives some characteristic feature of the soil to hold the cations, and the capacity to hold is cation exchange capacity (CEC). Therefore, CEC of the soil is said as the quantity of positively charged ions which are held by the negatively charged surface of clay minerals. The charge of the soil is expressed as centimol positive charge/Kg of soil or milliequivalent (meq) of positive charge/100 g of soil (Uddin 2008). The soil fertility can be measured with the help of CEC value of the soil in terms of the plant nutrient retention capacity and capacity of preventing cation contamination in ground water (Stagnaro et al. 2015). However, there is a need of research to explore the effect of CEC in terms ofthe functional performance of nanoclay additives. If the CEC values are available, the amount of various cations present in a given mass of soil can be measured (Uddin 2008).

4.2 Electrical Conductivity

The higher surface area per unit volume of clay minerals, due to fine particles, results in the absorption of a large number of cations owing to electrical conductivity. And the dispersal of electrical ions around mineral clay pores is known as membrane polarization. Electrical conductivity and membrane polarization, being the function of clay content, are used in soil studies to determine the clay fraction. On average clay conductivity is due to the matrix material in the presence of low conductivity pore fluid like air or water, while because of higher conductivity pore fluid like saline water, the bulk conductivity is mainly due to the pore fluid. The electrical conductivity of soil caused due to water content, salinity, soil, soil structure and the mineral phase conductivity. The important contribution of clay

saline water in the soil conductivity can be realized with the help of soil contents and measuring their conductivity (Uddin 2008). The high amount of clay minerals in soil with a 2:1 sheet structure caused an increase in the major electrical conductivity for nonsaline soils (Hunt et al. 2006). This result was observed by the exchangeable cations or proton transfer from the dissociation of interlayer water content. A reduced level of interlayer water contents in clays resulted in the lowest electrical conductivity. The estimation of electrical conductivity of reservoir rock may be used to calculate approximately clay content, pore fluid, clay type, saline water and water saturation influence because these factors effects the soil conductivity (Niwas et al. 2007).

4.3 Thermal Barrier, Flame Retardancy and Anticorrosive Properties

Nanoclays exhibit thermal stability and flame retardancy and hence they are extensively used for nanoclay-polymer composites. Clay minerals are inorganic materials and are almost stable in the temperature ranges in which organic polymers degrade into volatile compounds. It has been observed that more or less the polymer/clay nanocomposites are thermally more stable than pure polymers (Becker et al. 2004) and improvement in thermal stability observed on incorporation of clay fillers into the polymer matrices. The improvement in thermal-expansion magnitude of these materials follows order as polymer > metal > ceramic. This order can be expressed with the help of linear thermal-expansion coefficient values and therefore, the enhancement in polymer thermal stability is influenced by the aspect ratio (Reddy 2011). When impermeable clay sheets are incorporated in the polymer matrix it results in considerable improvement of barrier properties of the polymers. The barriers properties of polymers clay composite is formed by the formation of a web like structure or haphazard path that retards the diffusion of gas molecules through the polymer matrix (Pavlidou and Papaspyrides 2008).The degree of enhancement in the barrier properties depends on the degree of haphazard path created by clay layers in the diffusion way of molecules through the polymer film. Increasing the lateral length of clay sheet as well as increasing of exfoliation or dispersion degree cause to the more barrier enhancement in the polymer matrix.

Different chemical additives are being used as safety measures to retard ignition and control burning of polymers due to their applications in domestic life. Clay minerals have been used together with a low fraction of conventional flame retardants. The mixture of clay minerals and traditional flame retardants have shown to have synergistic effect in the reduction of ignitability of polymers with halogenated flame retardants and phosphorous flame retardants (Reddy 2011). The clays modified with such phosphorous compounds have been used in the preparation of nanocomposites with various polymers (Kashiwagi et al. 2004). Furthermore, an

improvement in the flammability properties of polymers has been achieved with polymer–clay nanocomposites, which could provide an alternative to conventional flame retardants.

Clay materials due to their platelet structure and high aspect ratio, in well dispersed state, decrease the permeability of polymer coating films by increasing the diffusion pathways. They are thus incorporated with polymers used to prevent corrosion. The nanocomposite of various polymeric materials such as polystyrene, poly (styrene-coacrylonitrile), polyaniline, polypyrrole, polysulfone, polyacryltes, polyimide and epoxy with unmodified and organically modified clays have been investigated as anticorrosive coating on metals (Olad and Rashidzadeh 2008; Yeh and Chang 2008).

4.4 Characterization of Clay

In the preparation of a polymer/clay nanocomposite it is important to know the degree of intercalation/exfoliation and its effect on the nanocomposite moderate properties. In other word there is need to analyze the micro structure of the prepared nanocomposite. Characterization of clays and their modified organic derivatives has been established by using simple as well as modern instrumental techniques which include mainly wide angle X-ray diffraction (WAXD) analysis, transmission electron microscopy (TEM), inductively coupled plasma (ICP) or XRF, determination of chemical compositions by gravimetric analysis, CEC using standard ammonium acetate method, powdered X-ray diffraction (PXRD), surface area measurement, Fourier transform infrared spectroscopy (FT-IR). Generally, layered silicates have been characterized on the basis of their ionic formula computed on behalf of its chemical compositions, charge density and CEC of clays. Clays and organoclays show a characteristic peak in XRD analysis due to their regular layered structures. The peak is indicative of the platelet separation or d-spacing in clay structure. Using the peak width at half maximum height and peak position (2θ) in the XRD spectra the inter layer space can be calculated utilizing Bragg's law given by the following equation.

$$\text{Sin}\,\theta = n\,\lambda/2d$$

where λ is wave length of X-ray radiation used in the diffraction experiments, d is the space\between layers in the clay lattice and θ is measured diffraction angle. Any change in the inter-layer or d-spacing of a clay lattice by organic modification or polymer intercalation causes to the change in the position, broadness and intensity of the characteristic peak in XRD spectra. According to the Bragg law, increasing of d-spacing result to the broadening and shifting of related XRD peak toward lower diffraction angles (2θ). By monitoring the position (2θ), shape and intensity of the characteristic peak for organoclay in nanocomposite structure it is possible to determine the degree of intercalation/exfoliation.

A direct way to visually observe the nanostructure of nanocomposites and clay d-spacing is to the use of TEM technique. TEM micrographs allow a qualitative understanding of the internal structure, exfoliation or spatial distribution of layers within the polymer matrix and their structural defects. In the TEM micrographs, the darker lines in the brighter matrix shows the clay layers because of the presence of heavier elements including Al, Si and O in the composition of clay sheets or layers compared the lighter atoms such as C, H, N and Na present in the polymer matrix or inter layer spacing of clay sheets. Therefore the distance between darker liner sections presented in the TEM micrographs can qualitatively show the d-spacing and dispersion status. Therefore the overall structure of the nanocomposite including intercalation, exfoliation, dispersion and defects of clay layer can be conclusively obtained using TEM technique.

The instrumental techniques mainly, FT-IR and PXRD are also basic methods for identification of clay structure. (Patel et al. 2006) studied the FTIR spectrum for MMT clay and reported the presence of –OH groups contributing in the clay structure as well as the chemical composition of MMT. Additionally, PXRD is also one of the most important techniques to determine impurities impurities like kaolin, quartz, calcite, etc. present in clay and to illustrate the structural geometry and texture in layered silicates. Figure 2, for PXRD pattern, clearly shows the presence of impurities such as kaolin (K) and quartz (Q) in raw MMT which have been removed (partly or fully) on further purification by sedimentation (Patel et al. 2006) (Fig. 3).

However both XRD and TEM techniques are essential tools for evaluation of the nanocomposite structure and complementary show the structural features of

Fig. 2 Showing the presence of impurities kaolin (K) and quartz (Q) in raw MMT, purified MMT and organoclay (Patel et al. 2006)
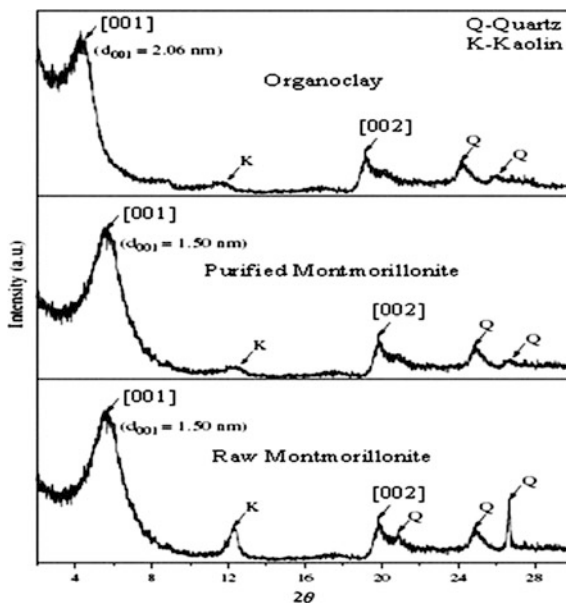
Fig. 3 Schematic diagram showing organic modification of clay (Azeez et al. 2013)
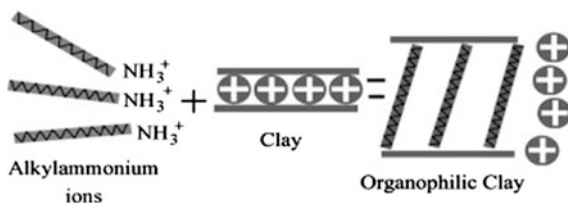
polymer/clay nanocomposite microstructure. XRD provides almost quantitative and TEM provides qualitative informations about the exfoliation and d-spacing of clay layers in the polymer matrix compared to that of in pure clay material. Also other techniques such as those based on thermal analysis, can be used to evaluate the interfacial interactions between clay layers and polymer chains.

5   Modification of Clay Materials

The preparation of polymer/clay nanocomposites with good dispersion of clay layers within the polymer matrix is not possible by physical mixing of polymer and clay particles. It is not easy to disperse nanolayers in most polymers due to the high face to face stacking of layers in agglomerated tactoids and their intrinsic hydrophilicity which make them incompatible with hydrophobic polymers. The intrinsic incompatibility of hydrophilic clay layers with hydrophobic polymer chains prevents the dispersion of clay nanolayers within polymer matrix and causes to the weak interfacial interactions. Incompatibility and weak interfacial interactions hinders the exfoliation and preparation of dispersed stable nanocomposite with improved properties. Therefore, organic modification of clay layers with hydrophobic agents is necessary in order to render the clay layers more compatible with polymer chains. The organoclays so formed having lowered surface energy are more compatible with polymers and polymer molecules are able to intercalate within their interlayer space or galleries under well-defined experimental conditions. The surface modification of clay layers can be achieved through a cation exchange process by the replacement of sodium and calcium cations present in the inter-layer space or clay galleries by alkylammonium or alkylphosphonium (onium) cations (Ahmad et al. 2009). In addition to the surface modification and increasing the hydrophobicity of clay layers, the insertion of alkylammonium or alkylphosphonium cations into the galleries causes to some degree of increasing in the inter-layer spacing which promotes the following intercalation of polymer chains into the galleries during nanocomposite preparation (Fig. 6) (Chigwada et al. 2006).

Clays containing divalent counter cations such as calcium cannot be easily hydrated and therefore their replacement by ion exchange process is not efficient. Therefore, in these clays, the divalent cations should be ion exchanged with easily exchangeable sodium cations prior to modification by onium cations (Ray and Okamoto 2003). The efficiency of organic modification by ion exchange process in

the increasing of basal spacing and consequently the exfoliation of clay and formation of stable nanocomposite systems depends also on the surface charge of clay layers. The surface charge density of clay layers depends on the clay nature and its preparation (growth) conditions. Surface modification of clay can also carried out through functionalization of clay layers by using alkoxysilane compounds. In this process, organic functional groups are introduced onto the surface of silicate particles through the condensation reaction between silanol group (Si-OH) of the silica surface and the alkoxysilane compounds.

Clays have also been modified with the help of organic acids to synthesize biocompatible nanocomposites for applications in tissues engineering and drug delivery (Ambre et al. 2011; Armentano et al. 2010; Chung et al. 2010; Floody et al. 2009; Suresh et al. 2010). The intercalation of clays is a result of interaction between the three phases, clay, polymer and the modifier (acid), which led the formation of an altered phase. Thus when the MMT clay was modified with 5-aminovaleric acid (Katti et al. 2010) and had improved qualities. These polymer scaffolds further promoted the growth of osteoblast cells in humans. MMT clay template had thus a very good potential for applications in bone tissue engineering (Ambre et al. 2010). The MMT clay modified with 5-aminovaleric acid has also been used for preparing chitosan/polygalacturonic acids which were found to proliferate osteoblast cells (Ambre et al. 2010). The modification of nanosize MMT clay with organic molecules and its subsequent incorporation for synthesizing nanocomposites has been found to be an effective method for improving the mechanical properties of PCNs (Ambre et al. 2011).

6 Polymer Clay Nanocomposites (PCN)

PCN are materials composed from polymer matrix and clay filler in nano dimension particles. The inexpensive clay can be easily modified due to its inherent properties viz ion exchange, metal, metal complex impregnation, pillaring and acid treatments to develop composites of desired functions. Further incorporation of small quantities of clay brings about substantial improvement in mechanical and physical properties of nanocomposites (Chowdary and Kumar 2015). Clays could be surface modified by the replacement of the inorganic exchangeable cations in the interlayer spacing of the layered silicates by alkyl ammonium surfactants (Cygan et al. 2009). Composite material can be tailored to have specific properties that will meet special requirements. This makes composites different from the other multi component systems such as blends and alloys. Composites are widely used in such diverse as transportation, construction and consumer products.

PCN gained immense interest in industry as well as in academic world. Organoclays played an important role in the formation of nanocomposite as it has been incorporated into various polymer systems including epoxy (Chen et al. 2003; Ratna et al. 2003), polyimides (Delozier et al. 2003; Nah et al. 2003; Su et al. 2004), polyesters (Lee et al. 2002; Wagener and Reisinger 2003), polyolefins

(Chang et al. 2004; Garca-Lopez et al. 2003; Koo et al. 2002; Manias et al. 2001), polystyrene (Hoffmann et al. 2000; Manias et al. 2000) and others. The clay nanolayers must be uniformly dispersed and exfoliated in the polymer matrix for their complete preparation. As a result, the improvement in properties can be observed in terms of decreased solvent uptake, flame retardance, enhanced barrier properties, increased thermal stability and an increase in tensile properties (Wang and Wilkie 2003; Giannelis 1996). Advances in polymer nanocomposites continue to be done using carbon nanotubes, carbon nanofillers, exfoliated graphite, nanocrystaline metals and fibers modified with inorganic fillers (Paul and Robeson 2008). But, layered silicates in their pure state are hydrophilic whereas most of the engineering polymers are hydrophobic in nature. Therefore, dispersion of native clays in most polymers is not easily achieved due to the intrinsic incompatibility of hydrophilic-layered silicates and hydrophobic engineering polymers (Patel et al. 2006; LeBaron 1999).

6.1 PCN Structure

Conventional composites or nanocomposites can be formed depending on the nature of the components, processing condition and strength of the interfacial interactions between polymer and layered silicates (Fig. 4) (Giannelis 1996; Pavlidou and Papaspyrides 2008; Pinnavaia 2001; Ray and Okamoto 2003; Zeng et al. 2005).
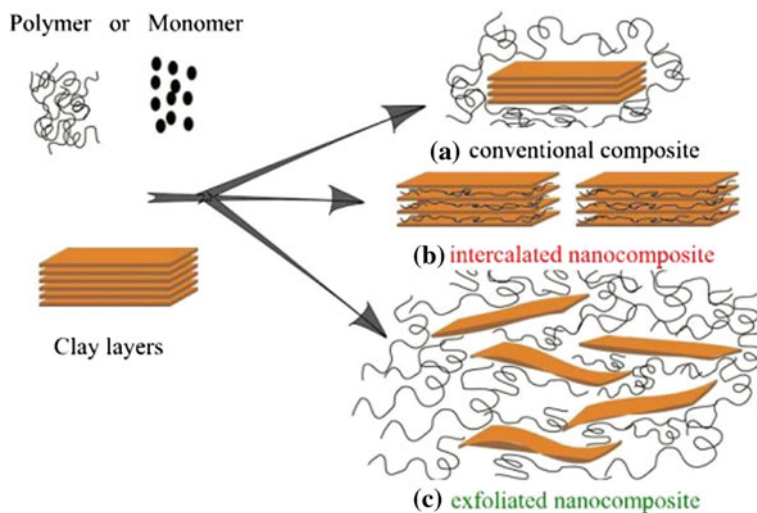
Fig. 4 Schematic diagram showing synthesis of different types of polymer clay nanocomposites

In the formation of conventional composite, the clay particles exist in their original aggregated state as the polymer cannot diffuse between the clay layers (Fig. 4a). These conventional composite revealed similar properties like micro particle filled composites. Normally, they showed improvement in modulus but this reinforcement benefit is usually followed by a deficiency in other properties such as strength or toughness. But, if a favourable condition for the mixing of clay minerals with polymer achieved, it results in the formation of two important PCN, i.e., intercalated and exfoliated nanocomposites. The clay layers retain the well-ordered multi structure of alternating polymeric and clay layers in intercalated nanocomposites (Fig. 4b). While, in exfoliated nanocomposites, the clay layers are well separated and randomly distributed in the continuous polymer matrix (Fig. 4c) (Azeez et al. 2013).

6.2 Preparation of PCN

In order to have a successful development of clay-based nanocomposites, it is necessary to modify natural clay chemically. Many efforts have been made for the preparation of intercalated and exfoliated polymer/clay nanocomposites with improved properties. A variety of polymer characteristics including polarity, molecular weight, hydrophobicity, reactive groups as well as clay characteristics such as charge density and its modified structure and polarity are affective on the intercalation of polymer chains within the clay galleries. Therefore different synthetic approaches have been used for the preparation of polymer/clay nanocomposites. In general there are four preparation methods including pre-swell or exfoliate (solution intercalation), in situ polymerization and melt intercalation. Three methods have been considered to synthesise polymer/layered silicate nanocomposites as follows:

6.2.1 Pre-Swell or Exfoliate

In this method, PCN are prepared by using a suitable solvent such as water, acetone, N,N-dimethylformamide, toluene and chloroform. The clay is allowed to pre-swell, or exfoliate in a suitable solvent; it is then added to the polymer suspended in the same solvent. When the layered silicate is dispersed within a solution of the polymer, the polymer chains intercalate and displace the solvent within the gallery of the silica. The intercalated nanocomposite is formed from which the solvent is removed by gentle heating or after putting it under vacuum. Large quantities of volatile solvent necessary for this approach (Quang and Donald 2006). It has been observed that the increase in entropy by desorption of solvent molecules is the driving force for the intercalation of polymer from solution (Vaia et al. 1997). This method have been used to intercalate water soluble polymers such as poly (ethylene oxide) (Aranda 1992), and poly(ethylene vinyl alcohol) (Zhao 1989), between the

clay layers. Nanocomposites based on cellulose (Delhom 2010), high-density polyethylene (Jeon 1998), polyimide (Yano et al. 1993), etc. have been synthesized by this method using non-aqueous solvents. The major advantage of this method is that it offers the possibility to synthesize intercalated nanocomposites based on polymers with low or even without polarity.

The drawbacks of this method are the requirement of suitable monomer/solvent or polymer solvent pairs and the high costs associated with the solvents, their disposal, and their impact on the environment. Aranda and Ruiz-Hitzky (Aranda 1992) reported the first preparation of polyethylene oxide (PEO)/MMT nanocomposites by this method. This technique was used for the preparation of nanocomposites of nitrile-based copolymer and polyethylene-based polymer with organically modified MMT (Jeon 1998). This technique was employed to prepare polysulfone (PSF)-organoclay nanocomposites (Sur et al. 2001). The exfoliation of silicate nanoclays in organic solvents such as xylene and toluene has also been explored (Quang and Donald 2006).

6.2.2 In Situ Polymerization

In situ polymerization method has been effectively used for nylon-6 and epoxy systems. The modified organoclay is pre swollen with the monomer or a monomer/solvent mixture and then initiated using heat, radiation or an appropriate initiator. First time in 1993, Usuki et al. successfully synthesised exfoliated Nylon-6/clay hybrid (NCH), by in situ ring-opening polymerization of ε-caprolactam, in which alkylammonium-modified layered silicate was thoroughly dispersed in advance (Usuki et al. 1993). It was found that organophilic clay that had been ion-exchanged with 12-aminododecanoic acid could be swollen by molten ε-caprolactam (Fig. 5).
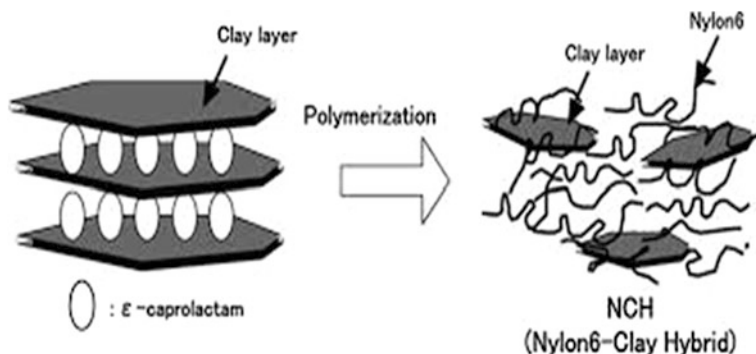

Fig. 5 Schematic diagram of polymerization to NCH (Nakano and Usuki 2014)

Messersmith et al. also synthesised NCH in the same manner and observed an appreciable decrease in gas permeability on clay addition (Messersmith and Giannelis 1995). In situ polymerization was further applied to lactones and lactides to produce polymer/clay nanocomposites (Kubies et al. 2002; Paul et al. 2003). In particular, reported the intercalative polymerization of ε-caprolactone between silicate layers in the presence of supercritical carbon dioxide. This dry process enables a complete exfoliation of clay platelets in the matrix, resulting in improved thermo-mechanical properties. Besides polyamide and aliphatic polyester nanocomposites, in situ polymerization method also used to synthesis epoxy resins. Pinnavaia and coworkers described the polymerization of a liquid epoxy resin, such as diglycidyl ether of bisphenol A, in the presence of polyetheramine and an organoclay (Lan and Pinnavaia 1994). Also, Giannelis et al. used ammonium salts where one alkyl chain contains a functional group capable of reacting and bonding with the epoxy upon crosslinking, such as hydroxy, epoxy or carboxylic functional groups. This results in direct attachment of the epoxy matrix to the silicate layers, thereby maximizing adhesion between the two phases and yielding a good dispersion.

Polyolefin's also prepared following in situ intercalative polymerization method. This implies intercalation of silicate layers by an olefin catalyst system, such as Ziegler-Natta or metallocene catalyst, followed by the polymerization of olefin in the presence of clay. This method was started by Bergman et al. who used a palladium-based complex and managed to polymerize ethylene (Fig. 6) (Bergman et al. 1999).

In situ intercalative polymerization, especially when carried out with clay specifically organo modified to promote polymer grafting or polymer growth from the clay surface is probably the best method to insure individual exfoliation of the clay layers in the final nanocomposite materials (Fig. 7).

6.2.3 Melt Intercalation

The third route of PCN synthesis is the melt intercalation. This method was first introduced by Vaia et al. (Vaia et al. 1993) in 1993, it does not required any solvent,
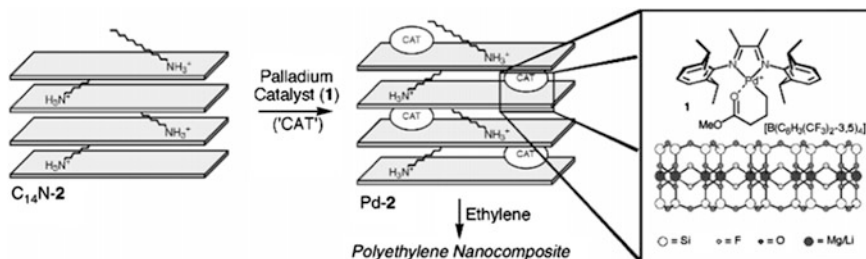

Fig. 6 Polyethylene nanocomposite synthesis by in situ polymerization (Bergman et al. 1999)
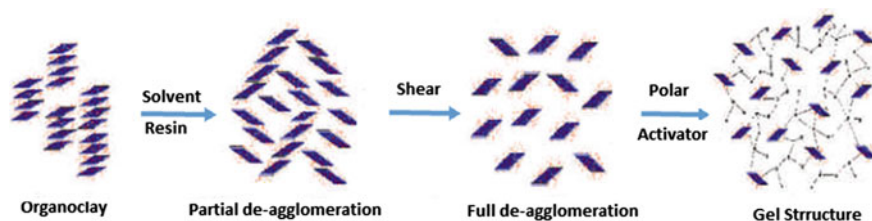
Fig. 7 Showing mechanism of gel formation (Patel et al. 2006)

only polymer matrix like molten thermoplastics are blended with the organoclay. But, sometimes curing agent like maleated polypropylene oligomers are required (Liu 1999). If the clay layer surfaces have enough attraction with the polymer, the polymer can diffuse between the clay layers and form either an intercalated or an exfoliated nanocomposite. Melt intercalation technique has been used to synthesis nanocomposites based on polyamide such as nylon 6 (Lim 2010) and nylon 66 (PA66) (Timmaraju 2011), and polyethylene terephthalate (PET) (Wang et al. 2006). This method is more opted because of its simplicity, cost effectiveness and the environment friendly approach than other methods. The melt intercalation method got high popularity due to its immense potential of application in rapid processing methods such as injection molding (Ferreira et al. 2011) and twin screw extrusion (Aristéia de Lima 2012).

7 Applications

Clay minerals found applications in many fields, including medicine, pharmacy and catalysis as well as in the manufacture of cosmetics, paint and ink, due to their abundance, low cost and environmentally friendly nature. These materials are also useful for the removal of grease, oil and nitrogen from water and waste-water and the sequestration of heavy metals in contaminated soils (Floody et al. 2009). The applications are closely related to their structure and compositions. Some of these clay applications are discussed below.

7.1 Drug Delivery

Extraordinary properties of clay or layered silicates like adsorption and desorption of organic molecules and surfactants indicates that these materials can be used for drug delivery. The clay has capacity to entrap polar organic compounds between their layers and also form intercalated compounds. As the release of the intercalated drugs is potentially controllable, these materials have potential applications in the pharmaceutical industry as a drug vehicle. However, the particles have to be

modified first before they can find application in drugs delivery (Batraet al. 2011). For that the clay particles are dispersed in aqueous drug solutions which are allowed to equilibrate. The solid phase is then dried. The bioactive molecules are entrapped by inducing coagulation in nanoclay dispersions or in capsules (Natarajan 2015) or the dry method is employed when the drug and clay are ground together. Calcium MMT showed acceptable results in the treatment of pain, open wounds, colitis, diarrhea, hemorrhoids, stomach ulcers, intestinal problems, acne and anemia (Fejer et al. 2001; Lee and Chen 2004, 2003; Lin et al. 2002). Yuancai and Si-Shen (Dong and Feng 2005) studied the novel poly (D, L-lactide-co-glycolide)/MMT nanoparticle drugdelivery system to formulate the drug carrier from a material, which can also have therapeutic effects, either synergistic with or capable to mediate the side effects of the encapsulated drug. In addition, layered double hydroxides are also used as drug carrier in various applications like surface unmodified and modified MMT. Intercalation of fenbufen in a layered double hydroxide followed by coating with Eudragit®S 100 gives a composite material which shows controlled release of the drug under in vitro conditions which model the passage of a material through the gastrointestinal tract (Sheng-Ping 2005). Intercalations of anti-inflammatory drug in layered double hydroxide have the advantage of gradual release over a longer period of time (Li et al. 2004; Min 2004). Also, it has been observed that novel layered double hydroxide could form a nanohybrid by intercalating with bimolecular anion such as mononucleotides, DNA which can enter cells, presumably through phagocytosis or endocytosis. The leukemia cells were used to explore the layered double hydroxide's potential as gene carriers (Kwak 2002; Patel et al. 2006). Various drugs like Paclitaxel, a drug used in cancer are loaded in poly D, L lactide co-glycolide/montmorillonite. It was observed that after an initial release of 22 % on the first day, there was slow release of 36 % of drug in the first week (Vaia et al. 1993). Medical devices such as drug delivery patch, implants, insert able devices with intercalated drug silicates provide controlled release of drugs.

Other than that clay minerals may be administered orally as antacids, gastrointestinal protectors, antidiarrhoeaics, osmotic oral laxatives, antianemics and mineral supplements. They also could absorb dietary toxins and bacterial toxins (Williams and Haydel 2010). Calcium montmorillonite has been reported to be of extensive use in pain, colitis, stomach ulcers and other health problems (Suresh et al. 2010). They are also used in formulations used for topical application in both dermopharmacy and dermo cosmetics (Patel et al. 2006).

7.2 Treatment of Waste Water

Organoclays have been used extensively in wastewater treatment in industry. It exhibits a synergistic effect with many water treatment unit processes like granular-activated charcoal, reverse osmosis, and air strippers. A number of organic molecules can be removing by granular activated carbon, but it is unable to remove

large molecules from wastewaters such as humic acid, emulsified oil and grease. Organoclays have proved a good technology for the treatment of oily wastewaters (Jasra et al. 1999). Humic acid being a common contaminant in potable water is difficult to remove with conventional flocculation techniques commonly used for the treatment of drinking water. On the other hand, activated carbon is not efficient due to its weak interaction with humic acid. As a result, subsequent chlorination produces unacceptable levels of trihalomethanes due to the presence of humic acid in drinking water which are known carcinogens (Beall 2003). Kokai reported the ability of organoclays to sorbs organic pollutants from waste water. Layered structure of organoclays is responsible for the sorption of organic pollutants from waste water. The organoclay contains alternating organic and inorganic layers which comprised of the quaternary ammonium compounds ion exchanged on the surface. These hydrophobic layers are responsible to trap organic pollutants dissolved in waste water. Presently, the disposal of industrial waste became more difficult and expensive because the disposal of such waste leaves the waste having a high potential with long-term problem. Column treatment of the waste with organoclay has been proved the best alternative method (Patel et al. 2006). Also, organoclays has been extensively used to treat military base effluent, oil well acid returns, boiler feed water, steam condensate among others (Patel et al. 2006).

7.3   Enzyme Immobilizer

Enzyme immobilization on solid supports has been used in order to facilitate product purification, continuous operation and catalyst recycling. Different methods have been studied for enzyme immobilization, such as solgel entrapment, glycolipids encapsulation, absorption into polymers and membrane encapsulation (Moelans et al. 2005). Immobilized enzymes also show great stability in the presence of organic solvents (Wu 2005), however, the low efficiency of immobilized enzymes in large-scale bioprocessing, is often a problem (Bai et al. 2006; Kim 2006). In order to improve catalytic efficiency, many supporting materials having different composition, shape, structure and surface modification have been investigated, among them inorganic materials such as silica gel, alumina and zeolites showed promising results, because of their non-toxicity and high resistance to microbial attack and organic solvents (Bai et al. 2006). Furthermore, nanomaterials are more capable candidates for enzyme immobilization than conventional supports because they can carry a high enzyme load and substrate diffusion do not face any hindrance (Kim 2006; Wang 2006). Enzymes immobilized on nanoparticles results in high mobility and activity, which suggest that the molecules are not rigidly attached to the support materials (Wang 2006). Moreover, a stabilizing effect on the immobilized enzyme observed due to effective resemblance between the pore dimension of nanomaterials and enzyme molecular size (Vamvakaki 2007). First theoretical study linking protein stabilization and confinement into nano-cages was reported by (Zhou and Dill 2001). They observed that entrapment of a protein into a

cage, having higher diameter, significantly increases its stability towards irreversible unfolding or denaturation. Consequently, porous materials such as porous carbon, mesoporous silica and aluminosilicates as suitable candidates for protein adsorption and stabilization (Vamvakaki 2007). Mesoporous materials have their pores size in the range 2–50 nm and therefore, they are included in the nanoscale range. Evidently, mesoporous silica showed good opportunity as possible supports for enzyme immobilization because the size of most enzyme molecules is comparable with the diameter of this mesoporous silica (Kim 2006; Moelans et al. 2005; Wang 2006). Additionally, allophane 'nanoballs' seem well suited for enzyme immobilization due to their similar physical properties as those of mesoporous silica. MMT nanoclays also revealed the same features as they have been used for enzyme immobilization by using layer-by-layer deposition and core-shell nanoclustering techniques (Li 2003; Liu 2005).

8 Conclusion

Nanoclays are natural nanomaterials that occur in the clay fraction of soil. In past decades, significant progress has been made in the development of clay/polymer nanocomposites. The manufacture of polymer-clay nanocomposites have opened up new vistas. In most cases, layered silicates first need to be modified with cationic-organic surfactants, in order to become miscible with polymeric matrices. Together with their advantages and limitations we have fact that clay/polymer nanocomposites show concurrent improvement in various material properties at very low filler content following the ease of preparation through simple processes such as melt intercalation, melt extrusion or injection moulding which opens up a new dimension for plastics and composites. Organoclays as drug vehicle for controlled release of drug is one of the born age area in medicinal application, nanoclays have great potential as compared to polymer and carbon nanotubes for drug delivery applications. The use of organoclays has proven to be very viable for many water treatment applications. Organoclays operate via partitioning phenomena and have a synergistic effect with activated carbon and other unit processes such as reverse osmosis. They have proven to be superior to any other water treatment technology in applications where the water to be treated contains substantial amounts of oil and grease or humic acid. The commercial application of organoclays to trihalomethane control in drinking water has not yet occurred. The field of nanoclays is one of the oldest methodologies as rheological modifier in industries and have been extensively used worldwide. The development of polar activator free organoclays made tremendous impact in the field of paint, ink and greases.

References

Abdel-Rahman, A.-F.M.: Chlorites in a spectrum of igneous rocks: mineral chemistry and paragenesis. Mineral. Mag. **59**, 129–141 (1995)

Ahmad, M.B., Hoidy, W.H., Ibrahim, N.A.B., Al-Mulla, E.A.J.: Modification of montmorillonite by new surfactants. J. Eng. Appl. Sci. **4**(3), 184–188 (2009)

Alexandre, M., Dubois, P.: Polymer-layered silicate nanocomposites: preparation, properties and uses of a new class of materials. Mater. Sci. Eng. R **28**, 1–63 (2000)

Ambre, A.H., Katti, K.S., Katti, D.R.: Nanoclay based composite scaffolds for bone tissue engineering applications. J. Nanotechnol. Eng. Med. **1**(3), 031013 (2010)

Ambre, A., Katti, K.S., Katti, D.R.: In situ mineralized hydroxyapatite on amino acid modified nanoclays as novel bone biomaterials. Mater. Sci. Eng. C-Mater. Biol. Appl. **31**(5), 1017–1029 (2011)

Aranda, P., Eduardo, R.-H.: Poly(ethylene oxide)-silicate intercalation materials. Chem. Mater. **4**, 1395–1403 (1992)

Ardenne, M., Endell, K., Hofmann, U.: Investigation of the finest fraction of bentonite and clay soil with the universal electron microscope. Ber. Deut. Keram. Ges. **21**, 207–227 (1940)

Armentano, I., Dottori, M., Fortunati, E., Mattioli, S., Kenny, J.M.: Biodegradable polymer matrix nanocomposites for tissue engineering: a review. Polym. Degrad. Stab. **95**(11), 2126–2146 (2010)

Azeez, A.A., Rhee, K.Y., Park, S.J., Hui, D.: Epoxy clay nanocomposites—processing, properties and applications: A review. Compos. Part B-Eng. **45**(1), 308–320 (2013)

Bai, Y.-X., Li, Y.-F., Yong Y., Yi, L.-X.: Covalent immobilization of triacylglycerol lipase onto functionalized nanoscale SiO_2 spheres. Process. Biochem. **41**, 770–777 (2006)

Batra, M., Gotam, S., Dadarwal, P., Nainwani, R., Sharma, M.: Nano-clay as polymer porosity reducer: a review. J. Pharm. Sci. Technol. **3**(10), 709–716 (2011)

Beall, G.W.: The use of organo-clays in water treatment. Appl. Clay Sci. **24**, 11–20 (2003)

Becker, O., Varley, R.J., Simon, G.P.: Thermal stability and water uptake of high perfmormance epoxy layered sili-cate nanocomposites. Euro. Polym. J. **40**, 187–195 (2004)

Bergman, J.S., Chen, H., Giannelis, E.P., Thomas, M.G., Coates, G.W.: Synthesis and characterization of polyolefin-silicate nanocomposites: a catalyst intercalation and in situ polymerization approach. Chem. Commun. (21), 2179–2180

Chang, J.H., Kim, S.J., Joo, Y.L., Im, S.: Poly(ethylene terephthalate) nanocomposites by in situ interlayer polymerization: the thermo-mechanical properties and morphology of the hybrid fibers. Polymer **45**(3), 919–926 (2004)

Chen, Y.-M., Tsao, T.-M., Wang, M.-K.: Removal of Crystal Violet and Methylene Blue from Aqueous Solution using Soil Nano-Clays Paper presented at the Proceedings of Conference on Environmental Science and Engineering (2011)

Chen, C.G., Khobaib, M., Curliss, D.: Epoxy layered-silicate nanocomposites. Prog. Org. Coat. **47**(3–4), 376–383 (2003)

Chigwada, G., Wang, D., Jiang, D.D., Wilkie, C.A.: Styrenic nanocomposites prepared using a novel biphenyl-containing modified clay. Polym. Degrad. Stab. **91**, 755–762 (2006)

Chowdary, M.S., Kumar, M.S.R.N.: Effect of nanoclay on the mechanical properties of polyester and S-Glass fiber (Al). Int. J. Adv. Sci. Technol. **74**, 35–42 (2015)

Chu, D.: The effect of matrix molecular weight on the dispersion of nanoclay in unmodified high density polyethylene (2006)

Chung, Y.L., Ansari, S., Estevez, L., Hayrapetyan, S., Giannelis, E.P., Lai, H.M.: Preparation and properties of biodegradable starch-clay nanocomposites. Carbohydr. Polym. **79**(2), 391–396 (2010)

Cygan, R.T., Greathouse, J.A., Heinz, H., Kalinichev, A.G.: Molecular models and simulations of layered materials. J. Mater. Chem. **19**(17), 2470–2481 (2009)

de Lima J.A., Pinotti, C.A., Felisberti, M.I., Gonçalves, M.C.: Blends and clay nanocomposites of cellulose acetate and poly(epichlorohydrin). Compos. Part B-Eng. **43**(23), 75–81 (2012)

Delhom C.D., White-Ghoorahoo. L.A., Pang, S.S.: Development and characterization of cellulose/clay nanocomposites. Compos. Part B-Eng. **41**(4), 75–81 (2010)

Delozier, D.M., Orwoll, R.A., Cahoon, J.F., Ladislaw, J.S., Smith, J.G., Connell, J.W.: Polyimide nanocomposites prepared from high-temperature, reduced charge organoclays. Polymer **44**(8), 2231–2241 (2003)

Deshmanea, C., Yuan, Q., Perkins, R.S., Misra, R.D.K.: On striking variation in impact toughness of polyethylene-clay and polypropylene-clay nanocomposite systems: the effect of clay-polymer interaction. Mater. Sci. Eng. A-Struct. Mater. Prop. Microstruct. Process. **458** (1–2), 150–157 (2007)

Dong, Y.C., Feng, S.S.: Poly(D, L-lactide-co-glycolide)/montmorillonite nanoparticles for oral delivery of anticancer drugs. Biomaterials **26**(30), 6068–6076 (2005)

Ewell, R.H., Insiey, Herbert: Hydrothermal synthesis of kaolinite, dickite, beidellite, and nontronite. Notl. Bur. Stand. Jour. Res. **15**, 173–185 (1935)

Fejer, I., Kata, M., Eros, I., Berkesi, O., Dekany, I.: Release of cationic drugs from loaded clay minerals. Colloid Polym. Sci. **279**(12), 1177–1182 (2001)

Ferreira, J.A.M., Reis, P.N.B., Costa, J.D.M., Richardson, B.C.H., Richardson, M.O.W.: A study of the mechanical properties on polypropylene enhanced by surface treated nanoclays. Compos. Part B-Eng. **42**(6), 1366–1372 (2011)

Floody, M.C., Theng, B.K.G., Mora, M.L.: Natural nanoclays: applications and future trends-a Chilean perspective. Clay Min. **44**(2), 161–176 (2009)

Fukushima, Y., Inagaki, S.: Synthesis of an intercalated compound of montmorillonite and 6-polyamide. J. Incl. Phenom. **5**(4), 473–482 (1987)

Garca-Lopez, D., Picazo, O., Merino, J., Pastor, J.: Polypropylene-clay nanocomposites: effect of compatibilizing agents on clay dispersion. Eur. Polymer J. **39**, 945 (2003)

Giannelis E.P: Polymer layered silicate nanocomposites. Adv. Mater. **8**(1), 29–35 (1996)

Grim, R.E., Guven, N.: Bentoniles–Geology, Mineralogy, Properties, and Uses. Elsevier, Amsterdam, p. 256 (1978)

Grim, R.E.: The history of the development of clay mineralogy clays and clay minerals **36**(2), 97–101 (1988)

Grim, R.E., Bradley, W.F.: A unique clay from the Goose Lake, Illinois, area. J. Am. Ceram. Soc. **22**, 157–164 (1939)

Gruner, J.W.: The crystal structure of kaolinite. Z. Kristallogr. **83**, 75–88 (1932)

He, H., Ma. Y., Zhu, J., Yuan P., Qing Y.: Organoclays prepared from montmorillonites with different cation exchange capacity and surfactant configuration. Appl. Clay Sci, **48**, 67–72 (2009)

Hendricks, S.B., Teller, E.: X-ray interference in partially ordered layer lattices. J. Phys. Chem. **10**, 147–167 (1942)

Hewitt, D.F.: The origin of bentonite. J. Wash. Acad. Sci. **7**, 196–198 (1917)

Heydari, A., Alemzadeh, I., Vossoughi, M.: Functional properties ofbiodegradable corn starch nanocomposites for food packaging applications. Mater. Des. **50**, 954–961 (2013)

Hoffmann, B., Dietrich, C., Thomann, R., Friedrich, C., Mulhaupt, R.: Morphology and rheology of polystyrene nanocomposites based upon organoclay. Macromol. Rapid Commun. **21**(1), 57–61 (2000)

Hofmann, U., Endell, K., Wilm, D.: Kxistalstrucktur und Quellung yon Montmorillonit. Z. Kristallogr. **86**(340), 348 (1933)

Houdry, E., Burr, W.F., Per Jr., A.E., Peters Jr., E.W.A.: Catalytic processing by the Houdry process. Natl. Petrol. News **30**, 570–580 (1938)

Hunt, P.G., Poach, M.E., Matheny, T.A., Reddy, G.B., Stone, K.C.: Denitrification in marsh-pond-marsh constructed wetlands treating swine wastewater at different loading rates. Soil Sci. Soc. Am. J. **70**(2), 487–493 (2006)

Jasra, R.V., Bajaj, H.C., Mody, H.M.: Clay as a versatile material for catalysts and adsorbents. Bull. Catal. Soc. India **9**, 113–121 (1999)

Jeon, H.G., Jung, H.T., Lee, S.W., Hudson, S.D.: Morphology of polymer/silicate nanocomposites-high density polyethylene and a nitrile copolymer. Polym. Bull., **41**, 107 (1998)

Jordan Jr., J.W.: Organophilic bentonites. I. Swelling in organic liquids. J. Phys. Colloid Chem. **53**, 294–306 (1949)

Kandola, B.K., Smart, G., Horrocks, A.R., Joseph, P., Zhang, S., Hull, T.R., Cook, A.: Effect of different compatibilisers on nanoclay dispersion, thermal stability, and burning behavior of polypropylene-nanoclay blends. J. Appl. Polym. Sci. **108**(2), 816–824 (2008)

Kashiwagi, T., Harris, R.H., Zhang, X., Briber, R.M., Cipriano, B.H., Raghavan, S.R., Shields, J. R.: Flame retardant mechanism of polyamide 6-clay nanocomposites. Polymer **45**(3), 881–891 (2004)

Katti, K.S., Ambre, A.H., Peterka, N., Katti, D.R.: Use of unnatural amino acids for design of novel organomodified clays as components of nanocomposite biomaterials. Philos. Trans. R. Soc. Math. Phys. Eng. Sci. **368**(1917), 1963–1980 (2010)

Ke, Y.C., Stroeve, P.: Polymer-Layered Silicate and Silica Nanocomposites. Elsevier Inc, Netherlands (2005)

Khater, A.E., Al-Mobark, L.H., Aly, A.A., Al-Omran, A.M.: Natural radionuclides in clay deposits: concentration and dose assessment. Radiat. Prot. Dosimetry. **156**(3), 321–330 (2013)

Kim, J., Grate, J.W., Wang, P.: Nanostructures for enzyme stabilization. Chem. Eng. Sci. **61**, 1017–1026 (2006)

Knight, W.C.: Bentonite. Eng. Min. J. **66**, 491 (1898)

Koo, C.M., Ham, H.T., Kim, S.O., Wang, K.H., Chung, I.J., Kim, D.C., Zin, W.C.: Morphology evolution and anisotropic phase formation of the maleated polyethylene-layered silicate nanocomposites. Macromolecules **35**(13), 5116–5122 (2002)

Kubies, D., Pantoustier, N., Dubois, P., Rulmont, A., Jerome, R.: Controlled ring-opening polymerization of epsilon-caprolactone in the presence of layered silicates and formation of nanocomposites. Macromolecules **35**(9), 3318–3320 (2002)

Kwak, S.Y., Jeong, Y.J., Park, J.S., Choy, J.H.: Bio-LDH nanohybrid for gene therapy. Solid State Ionics. Solid State Ionics **151**(1), 229–234 (2002)

Lan, T., Pinnavaia, T.J.: Clay-reinforced epoxy nanocomposites. Chem. Mater. **6**(12), 2216–2219 (1994)

LeBaron, P.C., Wang, Z., Pinnavaia, J.T.: Polymer-layered silicate nanocomposites: on overview. Appl. Clay Sci. **15**, 11 (1999)

Lee, W.F., Chen, Y.C.: Effect of bentonite on the physical properties and drug-release behavior of poly (AA-co-PEGMEA)/bentonite nanocomposite hydrogels for mucoadhesive. J. Appl. Polym. Sci. **91**, 2934 (2004)

Lee, W.F., Fu, Y.T.: Effect of montmorillonite on the swelling behavior and drug-release behavior of nanocomposite hydrogels. J. Appl. Polym. Sci. **89**(13), 3652–3660 (2003)

Lee, S.R., Park, H.M., Lim, H., Kang, T.Y., Li, X.C., Cho, W.J., Ha, C.S.: Microstructure, tensile properties, and biodegradability of aliphatic polyester/clay nanocomposites. Polymer **43**(8), 2495–2500 (2002)

Lepoittevin, B., Devalckenaere, M., Pantoustiera, N., M., Alexandrea, Kubies, D., Calberg, C., Jérôme, R., Dubois, P.: Poly(e-caprolactone)/clay nanocomposites prepared by melt intercalation: mechanical, thermal and rheological properties. Polymer **43**, 4017–4023 (2002)

Li, Z., H.N.: Direct electrochemistry of heme proteins in their layer-by-layer films with clay nanoparticles. J. Electroanal. Chem. **558**, 155–165 (2003)

Li, B.X., He, J., Evans, D.G., Duan, X.: Enteric-coated layered double hydroxides as a controlled release drug delivery system. Int. J. Pharm. **287**(1–2), 89–95 (2004)

Lim, S-H., Dasari, A., Wang, G.-T., Yu, Z.-Z., Mai, Y.-W., Yuan, Q.: Impact fracture behaviour of nylon 6-based ternary nanocomposites. Compos. Part B-Eng. **41**, 67–75 (2010)

Lin, F.H., Lee, Y.H., Jian, C.H., Wong, J.M., Shieh, M.J., Wang, C.Y.: A study of purified montmorillonite intercalated with 5-fluorouracil as drug carrier. Biomaterials **23**(9), 1981–1987 (2002)

Liu, L., Qi, Z., Zhu, X.: Studies on nylon 6/clay nanocomposites by melt-intercalation process. J. Appl. Polym. Sci. **71**, 1133–1138 (1999)

Liu, Y., Liu, H., Hu N.: Core-shell nanocluster films of hemoglobin and clay nanoparticle: direct electrochemistry and electrocatalysis. Biophys. Chem., **117**, 27–37 (2005)

Manias, E., Touny, A., Wu, L., Lu, B., Strawhecker, K., Gilman, J., Chung, T.: Polypropylene/silicate nanocomposites, synthetic routes and materials properties. Polym. Mater. Sci. Eng. **82**, 282 (2000)

Manias, E., Touny, A., Wu, L., Strawhecker, K., Lu, B., Chung, T.C.: Polypropylene/Montmorillonite nanocomposites. Review of the synthetic routes and materials properties. Chem. Mater. **13**(10), 3516–3523 (2001)

Mehmel, M.: Uber die Struktur yon Halloysit und Metahalloysit. Z. Kristallogr. **90**, 35–43 (1935)

Messersmith, P.B., Giannelis, E.P.: Synthesis and barrier properties of poly (ε-caprolactone)-layered silicate nanocomposites. J. Polym. Sci. Part A: Polym. Chem. **33**, 1047–1057 (1995)

Min, W., Shi. S., Wang, J., Li, Y., Duan, X.: Studies on the intercalation of naproxen into layered double hydroxide and its thermal decomposition by in situ FT-IR and in situ HT-XRD. Solid State Chem. **177**(7), 2534–2541 (2004)

Moelans, D., Cool, P., Baeyens, J., Vansant, E.F.: Using mesoporous silica materials to immobilise biocatalysis-enzymes. Catal. Commun. **6**(4), 307–311 (2005)

Mota, M.F., Silva, J.A., Queiroz, M.B., Laborde, H.M., Rodrigues, M.G.F.: Organophilic clay for oil/water separation process by finite bath tests. Braz. J. Pet. GAS **5**(2), 97–107 (2011)

Nah, C., Han, S.H., Lee, J., Lee, M., Lim, S., Rhee, J.: Intercalation behavior of polyimide/organoclay nanocomposites during thermal imidization. Compos. Part B, **35**(2), 125 (2003)

Nakano, M., Usuki, A.: Clay Nanohybrid Materials. In: Kobayashi, S., Müllen, K. (eds.) Encyclopedia of Polymeric Nanomaterials, pp. 1–4. Springer, Berlin (2014)

Natarajan, K., Anu, K.S.: Nanoclay Reinforced polyurethane-epoxy blend: a review. Int. J. Res. Eng. Adv. Technol. **3**(1), 78–90 (2015)

Nguyen, Q.T., Baird, D.G.: An improved technique for exfoliating and dispersing nanoclay particles into polymer matrices using supercritical carbon dioxide. Polymer, **48**(23), 6923–6933 (2007)

Niwas, S., Gupta, P.K., De Lima, O.A.L.: Nonlinear electrical conductivity response of shaly san14d reservoir. Curr. Sci. **92**(5), 612–617 (2007)

Okada, A., Kawasumi, M., Usuki, A., Kojima, Y., Kurauchi, T., Kamigaito, O.: Synthesis and properties of nylon-6/clay hybrids. In: Schaefer, D.W., Mark, J.E. (eds.) Polymer Based Molecular Composites. MRS Symposium Proceedings, vol. 171, pp. 45–50 (1990)

Olad, A., Rashidzadeh, A.: Preparation and anticorrosive properties of PANI/Na-MMT and PANI/O-MMT nanocomposites. Prog. Org. Coat. **62**(3), 293–298 (2008)

Patel, H.A., Somani, R.S., Bajaj, H.C., Jasra, R.V.: Nanoclays for polymer nanocomposites, paints, inks, greases and cosmetics formulations, drug delivery vehicle and waste water treatment. Bull. Mater. Sci. **29**(2), 133–145 (2006)

Paul, D.R., Robeson, L.M.: Polymer nanotechnology: nanocomposites. Polymer **49**(15), 3187–3204 (2008)

Paul, M.A., Alexandre, M., Degée, P., Calberg, C., Jérôme, R., Dubois, P.: Exfoliated polylactide/clay nanocomposites by in-situ coordination-insertion polymerization. Macromol. Rapid Commun. **24**(9), 561–564 (2003)

Pauling, L.: The structure of micas and related minerals. Proc. Natl. Acad. Sci. Soc. **16**, 123–129 (1930)

Pavlidou, S., Papaspyrides, C.D.: A review on polymer–layered silicate nanocomposites. Prog. Polym. Sci. **33**(12), 1119–1198 (2008)

Pinnavaia, T.J., Beall, G.W.: Polymer Clay Nanocomposites. Wiley (2001)

Quang, T., Donald, G.: Preparation of Polymer-Clay Nanocomposites and Their Properties. Adv. Polym. Technol. **25**(4), 270–285 (2006)

Ratna, D., Becker, O., Krishnamurthy, R., Simon, G.P., Varley, R.J.: Nanocomposites based on a combination of epoxy resin, hyperbranched epoxy and a layered silicate. Polymer **44**(24), 7449–7457 (2003)

Ray, S.S., Okamoto, M.: Polymer/layered silicate nanocomposites: a review from preparation to processing. Prog. Polym. Sci. **28**, 1539 (2003)

Reddy, B.: Advances in diverse industrial applications of nanocomposites (2011)

Reichenbach, H.G., Bayer, J.: Dehydration and rehydration of vermiculites: IV. Arrangement of interlayer components in the 1.43 nm and 1.38 nm hydrates of mgvermiculite. Clay Miner. **29**, 327–340 (1994)

Ries, H.: Clays and shales of Virginia, west of the Blue Ridge. Va. GeoL Surv. Bull. **20**, 118 (1920)

Ross, C.S., Kerr, P.F.: Optical and tr-ray research on clay minerals (abs.). Am. Mineral. **13**, 110 (1928)

Ross, C.S., Kerr., P.F.: The clay minerals and their identity. J. Sediment. Petrol. **1**, 35–65 (1930)

Ross, C.S., Kerr., P.F.: The kaolin minerals. U.S. Geol. Surv. Prof. Pap. **165F**, 151–175 (1931)

Ross, C.S., Shannon, E.V.: The chemical composition of optical properties of bentonite. J. Wash. Acad. Sci. **15**, 467–468 (1925)

Ross, C.S., Shannon, E.V.: Minerals of bentonite and related clays and their physical properties. J. Amer. Cer. Soc. **9**, 77–96 (1926)

Sadegh-Hassani, F., Mohammadi Nafchi, A.: Preparation and characterization of bionanocomposite films based on potato starch/halloysitenanoclay. Int. J. Biol. Macromol. **67**, 458–462 (2014)

Sheng-Ping, Z.: US Patent 0181015 A1 (2005)

Somani, R.S., Shukla, D.B., Bhalala, B.J.: Indian Patent NF No. 572/DEL/2000 (2000)

Stagnaro, S.M., Volzone, C., Huck, L.: Nanoclay as adsorbent: evaluation for removing dyes used in the textile industry. Procedia Mater. Sci. **8**, 586–591 (2015)

Su, S., Jiang, D.D., Wilkie, C.A.: Polybutadiene-modified clay and its nanocomposites. Polym. Degrad. Stab. **84**(2), 279–288 (2004)

Subramani S., Lee, J.Y., Kim, J.H., Cheong, I.W.: Crosslinked aqueous dispersion of silylated poly(-urethane urea)/clay nanocomposites. Compos. Sci. Technol. **67**, 1561–1573 (2007)

Sur, G.S., Sun, H.L., Lyu, S.G., Mark, J.E.: Synthesis, structure, mechanical properties, and thermal stability of some polysulfone/organoclay nanocomposites. Polymer **42**(24), 9783–9789 (2001)

Suresh, R., Borkar, S., Sawant, V., Shende, V., Dimble, S.: Nanoclay and drug delivery. Int. J. Pharm. Sci. Nanotechnol. **3**(2) (2010)

Tatum J. P., Wright, R.C.: US Patent 4752342 (1988)

Tcherbi-Narteh, A., Hosur, M., Triggs, E., Jeelani, S.: Thermal stability and degradation of diglycidyl ether of bisphenol A epoxy modified with different nanoclays exposed to UV radiation. Polym. Degrad. Stab. **98**(3), 759–770 (2013)

Theng, B.K.G.: Formation and Properties of Clay-Polymer Complexes. Elsevier Scientific publishing Company, Amsterdam (1979)

Timmaraju, M.V., Gnanamoorthy, R., Kannan, K.: Influence of imbibed moisture and organoclay on tensile and indentation behavior of polyamide 66/hectorite nanocomposites. Compos. Part B-Eng. **42**(4), 66–72 (2011)

Torabi, Z., Mohammadi Nafchi, A.: The effects of SiO_2 nanoparticles onmechanical and physicochemical properties of potato starch films. J. Chem. Health Risks **3**(1), 33–42 (2013)

Uddin, F.: Clays, nanoclays, and montmorillonite minerals. Metall. Mater. Trans. A **39**(12), 2804–2814 (2008)

Usuki, A., Kawasumi, M., Kojima, Y., Okada, A., Kurauchi, T., Kamigaito, O.: Swelling behavior of montmorillonite cation exchanged for V-amino acids by Ecaprolactam. J. Mater. Res. **8**(5), 1174–1184 (1993)

Vaia, R.A., Giannelis, E.P.: Lattice model of polymer melt intercalation in organically-modified layered silicates. Macromolecules, **30**, 7990–7999 (1997)

Vaia, R.A., Ishii, H., Giannelis, E.P.: Synthesis and properties of two-dimensional nanostructures by direct intercalation of polymer melts in layered silicates. Chem. Mater. **5**(12), 1694–1696 (1993)

Vaia, R.A., Ishii, H., Giannelis, E.P.: Synthesis and properties of 2-dimensional nanostructures by direct intercalation of polymer melts in layered silicates. Chem. Mater. **5**(12), 1694–1696 (1993)

Vamvakaki V., Chaniotakis, N.A.: Immobilization of enzymes into nanocavities for the improvement of biosensor stability. Biosens. Bioelectron. **22**, 2650–2655 (2007)

Voon, H., Bhat, R., Easa, A., Liong, M.T., Karim, A.A.: Effect of addition ofhalloysite nanoclay and SiO₂ nanoparticles on barrier and mechanicalproperties of bovine gelatin films. Food Bioprocess Technol. **5**(5), 1766–1774 (2012)

Wagener, R., Reisinger, T.J.G.: A rheological method to compare the degree of exfoliation of nanocomposites. Polymer **44**(24), 7513–7518 (2003)

Wang, P.: Nanoscale biocatalyst systems. Curr. Opin. Biotechnol. **17**, 574–579 (2006)

Wang, D., Wilkie C.A.: A stibonium-modified clay and its polystyrene nanocomposite. Polym. Degrad. Stab. **82**, 309–315 (2003)

Wang, Y., Gao, J., Ma, Y.A.: Study on mechanical properties, thermal stability and crystallization behavior of PET/MMT nanocomposites. US Compos. Part B-Eng. **37**, 399–407 (2006)

Williams, L.B., Haydel, S.E.: Evaluation of the medicinal use of clay minerals as antibacterial agents. Int. Geol. Rev. **52**(7/8), 745–770 (2010)

Wu, S., Liu, B., Li, S.: Behaviors of enzyme immobilization onto functional microspheres. Int. J. Biol. Macromol. **37**, 263–267 (2005)

Yano, K., Usuki, A., Okada, A., Kurauchi, T., Kamigaito, O.: Synthesis and properties of polyimide-clay hybrid. J. Polym. Sci. Part A. Polym. Chem. **31**(249), 3–8 (1993)

Yeh, J.M., Chang, K.C.: Polymer/layered silicate nanocomposite anticorrosive coatings. J. Ind. Eng. Chem. **14**(3), 275–291 (2008)

Zeng, Q.H., Yu, A.B., Lu, G.Q., Paul, D.R.: Clay-based polymer nanocomposites: research and commercial development. J. Nanosci. Nanotechnol. **5**, 1574 (2005)

Zeng, Q.H., Yu, A.B., Lu, G.Q., Paul, D.R.: Clay-based polymer nanocomposites: research and commercial development. J. Nanosci. Nanotechnol. **5**(10), 1574–1592 (2005)

Zhao, X., Urano, K., Ogasawara, S.: Adsorption of polyethylene glycol from aqueous solution on montmorillonite clays. Colloid Polym. Sci. **267**, 899–906 (1989)

Zhou, H.X., Dill, K.A.: Stabilization of proteins in confined spaces. Biochemistry **40**(38), 11289–11293 (2001)

Geology and Mineralogy of Clays for Nanocomposites: State of Knowledge and Methodology

I. El Amrani El Hassani and C. Sadik

Abstract The present chapter focuses on the scientific and technical research on clay-based nanocomposites. It begins with an introduction reminding the definition of clay nanocomposites reinforcement, the history of evolution of their field of research and development, their properties and their application fields. A synthesis is then presented on the mineralogy of natural clays specifying their classification and their physicochemical properties. This synthesis also includes the geology of argillaceous rocks citing their mode of genesis and their geographical distribution according to climatic zones. The last part of this paper shows, through the example of Morocco, the spatial distribution of clay deposits and the relationship that may exist between the nature of clay minerals of a deposit and its geological context. The note ends with a brief presentation on the different techniques of purification of natural clays and their organophilic transformation to make them finally ready to be used for the preparation of nanocomposites.

Keywords Nanocomposites · Clay · Geology · Mineralogy · Purification

1 Introduction

Scientific and technical research on nanocomposites has continued to develop and intensify in recent decades. Different raw materials (polymers and fillers) and several processing technics have been proposed (Cognard 1987; Burnside and

I. El Amrani El Hassani (✉)
Department of Earth Sciences, Scientific Institute, University Mohammed V of Rabat, Rabat, Morocco
e-mail: izdinelamrani@gmail.com

C. Sadik
Laboratory of Physical Chemistry of Applied Materials (LPCMA), Department of Chemistry, Faculty of Sciences Ben Msik, University Hassan II of Casablanca, Casablanca, Morocco

Giannelis 1995; Berthelot 2005; El Achaby et al. 2013; Ayana et al. 2014; Eesaee and Shojaei, 2014; Chang and Lee 2015; Lee and Won 2015).

Clay-based nanocomposites are very interesting in the fact that the clay minerals are of nanometer size and are capable to undergoing a large expansion. Indeed, the incorporation of a low content of nanoclay (montmorillonite) perfectly exfoliated in a polymeric matrix maintains the lightness of the composite by improving its physical, mechanical and thermal properties, etc. (Kojima et al. 1993; Messersmith and Giannelis 1995; Kawasumi et al. 1997; Sherman 1999; Cho and Paul 2001; Gloaguen and Lefebvre 2007). It is also necessary that the preparation of nanoclays and nanocomposites elaboration requires perfect control, both geology and physical chemistry of materials.

The contribution of geology is an important step of nanocomposite synthesis process, and consists first, to guide the prospecting work on the field of interesting clay deposits, then, to clearly identify the nature of mineralogical clays for each deposit to extract and purify the species clay minerals.

The present chapter is a synthesis of clays and clay minerals, from an abundant literature accumulated over several decades (Grim 1953; Millot 1964, 2001; Caillère et al. 1982; Deer et al. 1983; Velde 1985, 1995; Meunier 2005; Bergaya et al. 2006; Bouchet et al. 2000). Its aim is to provide maximum practical information's on the main families of clays, their formation context and their chemical-mineralogical properties as a basis for further work of nanocomposites elaboration.

Furthermore, the aim of this chapter is to facilitate communication and enhance cooperation between geologists, chemists and physicists in order to optimize their research on the synthesis of innovative and more efficient nanocomposites elaborated from nanoclays.

2 Clay-Based Nanocomposites

Composite materials based on a polymeric matrix (thermoplastic or thermosetting resin) and a solid filler (organic or inorganic) are promising, having a double interest: economic and technical. The addition of a volumic fraction of low cost charge in a high-cost polymeric matrix reduces the overall cost of the composite. Furthermore, the intervention on nature, size and the processing techniques allows to improve their mechanical, thermal, optical, electrical and magnetic properties (Cognard 1987; Daviaud and Filliatre 1987; Gay 1987; Berthelot 2005; Renard 2005).

The main research carried out on improving properties of composite materials showed that among the various fillers (calcium carbonate, quartz, glass fiber, carbon tubules, etc.), the use of clay as mineral fillers, in particular montmorillonite, significantly strengthens the composite and gives it a clear mechanical (Young's modulus, shock and wear resistance, etc.), thermal (pyroscopic temperature) as well

as optical, electrical and magnetic improvement. (Usuki et al. 1993; Kato et al. 1997; Doh and Cho 1998; Solomon et al. 2001).

Later, a big step was taken in the field of synthesis of composite materials, from the early 90s, with the first works of Burnside and Giannelis (1995), Giannelis (1996), Kawasumi et al. (1997), Giannelis et al. (1998, 2005) and Sherman (1999), which showed that the composite properties can be significantly improved by incorporating the lamellar clay mineral in the polymer matrix at nanometric scale. In fact, the reinforcing "nanoclay" pretreated and properly exfoliated and dispersed by a controlled manner in the polymer matrix provides greater atomic exchange interface between the two components. In addition, a very small amount of nanoclay (1–10 wt%) proves to be sufficient to improve the performance of the nanocomposite, which has no major consequence on density and the production process (Kojima et al. 1993; Cho and Paul 2001; Marchant and Jayaraman 2002).

Also, progress and control of the synthesis of nanocomposites polymer/nanoclay allows to invest several industrial applications areas such as automobile, aerospace, electronics, textile, construction, etc.

Regarding the automobile field, in particular, the major manufacturers, such as Toyota, Mitsubishi, Ford and General Motors have launched since the early 90s in the use of nanocomposites to manufacture some accessories (timing belts, boards steps, lateral protective strips) arranged in series on their vehicles (Usuki et al. 1993; Kawasumi et al. 1997; Gloaguen and Lefebvre 2007). Indeed, the use of these nanocomposites from nanoclays allows improving the surface state and the mechanical properties without increasing their density. This contributes to weight reduction of the vehicle and therefore its consumption of energy. In addition, the small amount of nanoclay incorporated into the polymer matrix makes it easily recyclable.

Because of their water and gas barrier properties (Yano et al. 1993), the nanocomposites have very interesting applications: the non-refrigerated packaging capable of providing a longer period conservation; tennis balls coatings to maintain a more durable internal pressure; fuel reservoir walls at very high tightness (Messersmith and Giannelis 1995; Sherman 1999; Gloaguen and Lefebvre 2007).

The reinforcement of nanocomposites by nanoclay shows a very good heat resistance (resistance to degradation). For example, the incorporation of 3 wt % by weight of montmorillonite increases the polymer temperature decomposition of more than 30 °K, which makes them very competitive compared to conventional insulating nanocomposites materials in the fields of building, technical textiles and other materials fearing flammability (Lee et al. 1997; Zhu et al. 2001; Bourbigot et al. 2006; Gloaguen and Lefebvre 2007).

Today, scientific researches on nanocomposites are becoming more sustained. This research covers all aspects related to the raw mineral and organic material, technical methods of elaboration and characterization, with the main objective to achieve innovative and more efficient nanocomposites (El Achaby et al. 2013; Ayana et al. 2014; Eesaee and Shojaei 2014; Chang and Lee 2015; Lee and Won 2015).

3 Clays and Clay Minerals

3.1 Definitions

Clay, from the Latin "*argilla*" corresponds to a sedimentary rock mainly composed of clay minerals which combine with various other constituents such as carbonates, quartz, feldspar, mica, organic matter, etc. However, it qualifies as clay, any material where clay minerals are predominant to the point of giving to these material two fundamental properties: plasticity and hardening. Indeed, the clay has a tendency to change in the presence of water in an easily malleable plastic paste. Heated to a moderate temperature (<300 °C), the clay undergoes a hardening that remains reversible but beyond this temperature (>500 °C) the clay is transformed by sintering to ceramic product (irreversible hardening).

The other constituents of clays, generally regarded as impurities, may act according to their nature and abundance to a behavior "plasticity/hardening" of the clay material. Clays shows a close association with the calcareous to give marl (35 % limestone and 65 % clay); abundant materials in nature and constitute the basis for the production of pottery, tiles, red bricks and floor tiles. Quartz is also a common mineral in clays and acts as a degreasing agent to reducing the plasticity of the clay paste. Feldspars, particularly sodi-potassic (albite and orthose), also present in some natural clays, act as a fluxing agents to reduce the temperature of sintering during the transformation of clay to ceramic.

Clay minerals correspond to phyllosilicates whose size is generally less than 2 microns. And it is also the fineness of these clay minerals that made their crystallographic characterization possible only after the development of some technics as X-ray diffraction (XRD) to the early XXth century. Indeed, thanks to XRD and other analysis techniques (differential thermal analysis, FTIR spectroscopy, Raman spectroscopy, X Fluoresce, electron microscopy, etc.) it became possible to analyze the fine structures of clay minerals and classify them according to the crystallographic nature and the lattice spacing of their constituent layers.

3.2 Classification of Clay Minerals

Clay minerals (phyllosilicates) consist of a stack of several hundreds of elementary sheets whose lateral extension is between 500 and 700 nm and having a thickness of one nanometer (1 nm = 10^{-9} m). These elementary sheets have specific structures and are composed in turn by 2 or 3 layers. Also, different species of clay minerals are distinguished according to the structure and the combination of their elementary sheets. Two types of layers are known: the tetrahedral layer and the octahedral layer.

- The tetrahedral layer (T) of structural formula $Si_4O_6(OH)_4$, is composed of tetrahedra $(SiO_4)^{4+}$ in which the atom of silica occupies the center of the
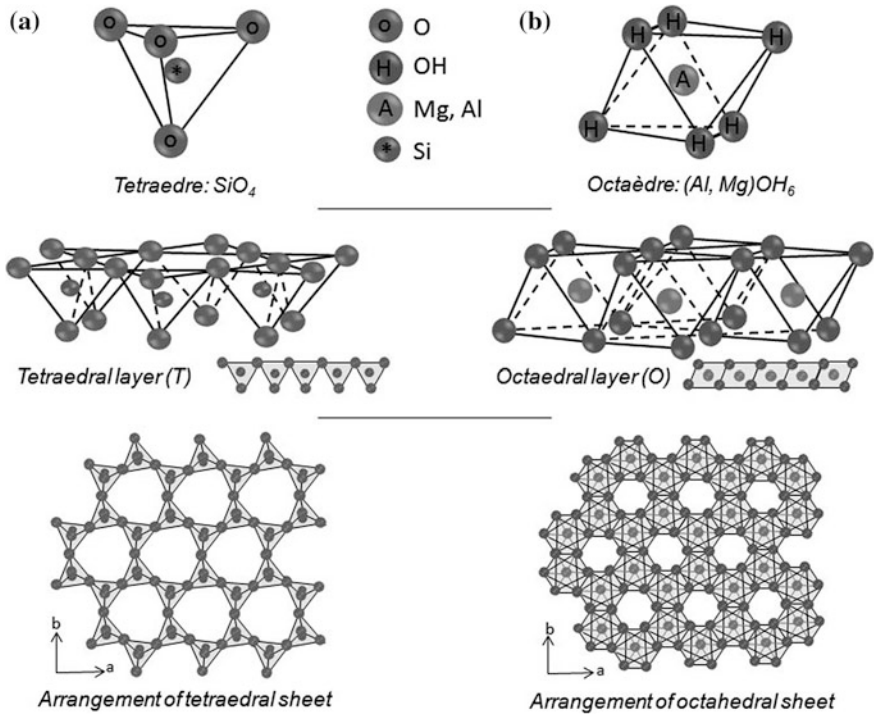
Fig. 1 Schematic representation of structure of tetrahedral (**a**) and octahedral (**b**) layers of clay minerals

tetrahedra and the four oxygen atoms are placed at the vertices of this tetrahedra. The pseudohexagonal arrangement of six tetrahedras having each three vertices in common with neighboring tetrahedras leads to the formation of a layer T. The thickness is about 0.3 nm (Fig. 1a).

- The octahedral layer (O) of structural formula $(Al_2/Mg_3)(OH)_6$ is composed of octahedra which alumina and magnesium atoms are in the center and hydroxides at the vertices. Tetrahedra sharing only edges to form the layer T, the thickness is relatively high (0.4 nm) than the layer O (Fig. 1b).

O and T layers can be combined together by placing connections in common to form two types of elementary sheets (Fig. 2a, b): two Tetrahedral-Octahedral sheets (T-O or 1: 1) and three Tetrahedral-Octahedral-Tetrahedral sheets (T-O-T or 2: 1).

The isomorphic substitutions that can take place between the cations (Si^{4+}, Al^{3+}, Fe^{3+}, Fe^{2+}, Mg^{2+}) at the T and O layers allows the loss of electronic neutrality. To compensate the leaf electric charge, cations are lodged between the sheets (interlayer space) to provide electronic charge balance. And that is exactly what gives to the clay minerals their cations exchange capacity and adsorbent power.
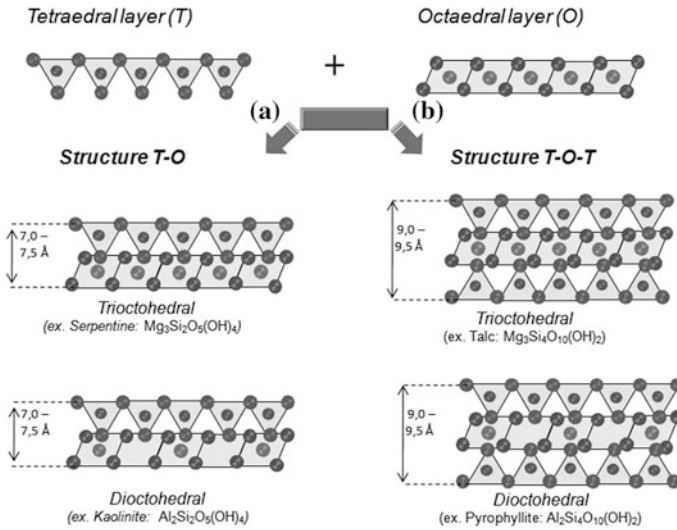
Fig. 2 Possible schematics representations of combinations between Tetrahedral (**a**) and Octahedral (**b**) layers of clays

Furthermore, cationic substitutions of phyllosilicates are used to distinguish between two classes of clay minerals:

- The dioctahedral (DO) in which two of three octahedra are filled with trivalent cations such as Al^{3+} and Fe^{3+} for a net charge of 6^+.
- The trioctahedral (TO) in which all octahedral sites are filled with divalent cations such as Mg^{2+} or Fe^{2+} for a net charge of 6^+.

Table 1 shows an example of classification of clay minerals on the basis of crystallographic configurations sheets (TO and TOT) and the nature of the cations of the octahedral sites (DO and TO). Among the fifty species of clay minerals, kaolinite, illite and the smectites are the most abundantly minerals found in nature.

- **Kaolinite**, $Si_2Al_2O_5(OH)_4$, it is in the hexagonal particles. The sheets have a neutral charge with tetrahedral layers of silicon heart and octahedral layers of aluminum heart. The distance from the surface of a sheet to the other (reticular equidistance) is equal to 0.7 nm (Fig. 3a).
- **Illite** have the following structural formula: (Si_{4-x}) $(Al,M_1,M_2)_2O_{10}(OH)_2K$. The isomorphic substitutions Si–Al and Al-(Mg, Fe) intervening in tetrahedra and octahedra give to sheets a negative charge. This charge is compensated by potassium ions which is located in interlaminar position and remain low exchangeable. The reticular equidistance is equal to 1 nm (Fig. 3b).
- **Smectite** group of clays has a T-O-T structure that is similar to that of pyrophyllite, but can also have significant amounts of Mg and Fe substituting into the octahedral layers. Thus, the smectites can be both dioctahedral and

Table 1 Summary classification of clay minerals family

Phyllosilicates	Dioctahedral (DO)	Trioctahedral (TO)
2 layers : T-O (or 1:1)	Group of Kaolinite	Group of Serpentinite
	- Kaolinite (Al)	- Antigorite (Mg)
	- Halloysite (Al)	- Chrysotile (Mg)
	- Dickite (Al)	- Cronstedite (Fe)
	- Nicrite (Al)	- Lizardite (Mg, Al)
3 layers : T-O-T (or 2:1)	- Pyrophyllite (Al)	- Talc (Mg)
		- Minnestontaite (Mg, Fe)
	Group of Smectite	
	- Montmorillonite (Al)	- Saponite (Mg)
	- Beidillite (Al, Fe)	- Stevensite (Mg)
	- Nontronite (Fe)	- Hectorite (Mg)
		- Sauconite (Mg, Zn)
	Group of Illites and Vermiculite	
	- Illite (Al, K)	- Vermiculite (Ni)
	- Vermiculite (Al)	- Batavite (Mg)
	Group of Micas	
	- Illite (Al, K)	- Phlogopite (Mg)
	- Muscovite (Al, K)	- Illite (Mg, Fe, K)
	- Seriite (Al, K)	- Biotite (Mg, Fe, K)
	- Paragonite (Al Na)	- Lepidolite (Mg, Fe, K)
	- Glauconite (Al, Fe)	- Ledikite (Mg, Fe, K)
3 layers T-O-T (2:1) Fibrous structure		- Sepiolite
		- Attapulgite
4 layers T-O-T-O (2:1:1)	Group of Chlorites	
	- Dombassite	- Clinochlore
	- Cookeite	- Chamosite
	- Sudoite	- Ripidolite

trioctahedral. The most important particularity of the smectite group is the ability for H_2O molecules to be adsorbed between the T-O-T sheets, causing the increasing volume of the minerals when they come in contact with water. Thus, the smectites are expanding clays. The reticular equidistance can vary from 1 to 1.4 nm (Fig. 3c).

In addition to these main groups of clay minerals, there are many other minerals, relatively scarce, but which are very interesting for their structural configuration, their behavior and properties. Among these minerals we mention:

- **Chlorites** whose interlayer space is occupied by a positive charged layer of hydroxide octahedral of Mg or Al. Chlorites are stable at high temperature and have a reticular equidistance equal to 1.4 nm (Fig. 3d).
- **Mixed Layer Clay** are common, and consist of clays that change from one type to another through a stacking sequence. The sequences can be ordered and regular, or high unordered and irregular. For example montmorillonite layers
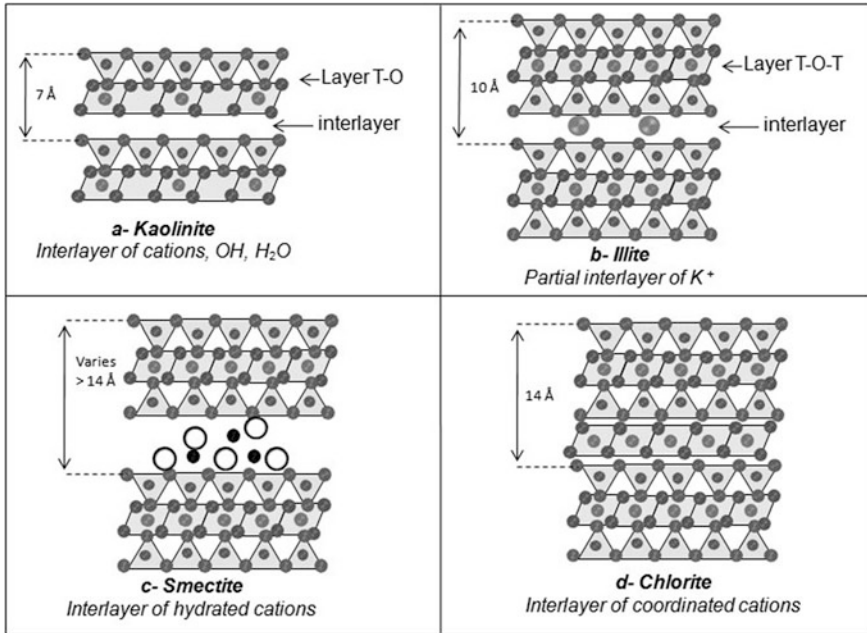
Fig. 3 Schematic representation of some clay minerals among the most common: kaolinite; illite; smectite and chlorite

can alternate with illite layers in an ordered way, or there can be several layers of montmorillonite with random layers of illite.

- **Sepiolite and attapulgite (palygorskite)** are a complex magnesium silicates, whose typical formula is $Mg_4Si_6O_{15}(OH)_2 \cdot 6H_2O$. They can appear as slats composed of a stack of three layers whose octahedral contains 3 to 5 cations (Mg, Al, Fe).
- **Halloysite** is a 1:1 aluminosilicate clay mineral with the empirical formula $Al_2Si_2O_5(OH)_4$. Its main constituents are aluminium (20.90 %), silicon (21.76 %) and hydrogen (1.56 %). Halloysite typically forms by hydrothermal alteration of alumino-silicate minerals. It can occur intermixed with dickite, kaolinite, montmorillonite and other clay minerals.

It should be noted, also, that some clay minerals such as kaolinite, pyrophyllite, smectite, chlorite and sepiolite may be obtained synthetically (Kloprogge et al. 1999; Zhang et al. 2011). The advantage of these synthetic mineral is that they are pure and have well defined structures and compositions. This constitutes a fundamental difference with natural clays which are often impure and whose the use in a specific application field as the composite and nanocomposite materials require works of purification and characterization. However, the market value of synthetic clays, prepared and marketed by specialized companies, remains very high compared to natural clays that can be extracted directly from deposits.

3.3 Properties of Clay Minerals

Phyllosilicates have very particular physicochemical properties because of their structural configurations and capacities of isomorphic substitutions. These are in fact the basis for the use of clay minerals in multiple industrial fields (pottery, ceramics, glassware, chemistry, composite, pharmaceutical, cosmetic, etc.). Here we remember the main properties of clay minerals, particularly those that make them very interesting in the field of preparation of nanocomposites.
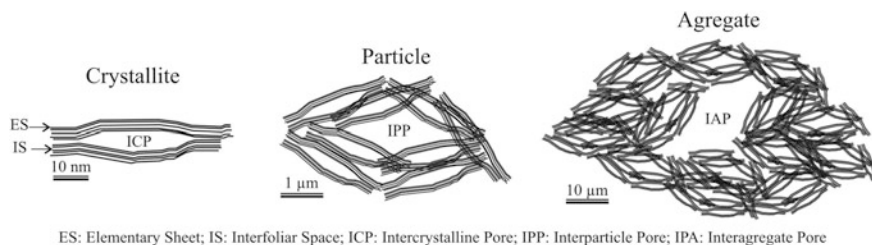
- **Form and specific surface.** It has already been noted above that the elementary unit of clay minerals is the sheet. It has a lateral extension of a few hundred nanometers (400–700 nm) for a thickness of 0.7–14 nm. The stack of these sheets giving crystallites whose thickness reaches 10 nm, then the aggregates and agglomerates which may exceed the micrometer (Fig. 4).

The sheets of different species of clays show vary extension reports lateral/thickness and show varying morphologies: Flake (kaolinite), lamellar (smectite), fiber (chrysotile), slats (sepiolite) or tubules (halloysite). The images of the scanning electron microscope (SEM) are used to characterize the morphology of the clay minerals (Fig. 5).

The very fine size and shape of sheets give to clay minerals a very large surface area relative to the volume compared to minerals of the same size and granular form (Velde 1995). This is the concept of specific surface (Sp) of mineral corresponding to the value of the ratio of its total surface area (St) on its mass (m) and is expressed in m^2/g (**Sp = St/m**).

In the case of clay minerals, in particular lamellar form (smectites), the surface area is very important because the total specific surface (St) which is expressed in m^2 comprises the outer surface of the sheets (Se) and the interfolaire surface (Si): (**St = Se + Si**).

Table 2 gives an indication of the average values of the specific surface of the most common clay minerals. Thus we can find that the specific surface of the smectites and vermiculite, in particular, are significantly higher than those of other phyllosilicates, which in turn have larger areas than other silicates.

ES: Elementary Sheet; IS: Interfoliar Space; ICP: Intercrystalline Pore; IPP: Interparticle Pore; IPA: Interagregate Pore

Fig. 4 Representation of the microstructures characteristics of a layered clay (Montmorillonite)
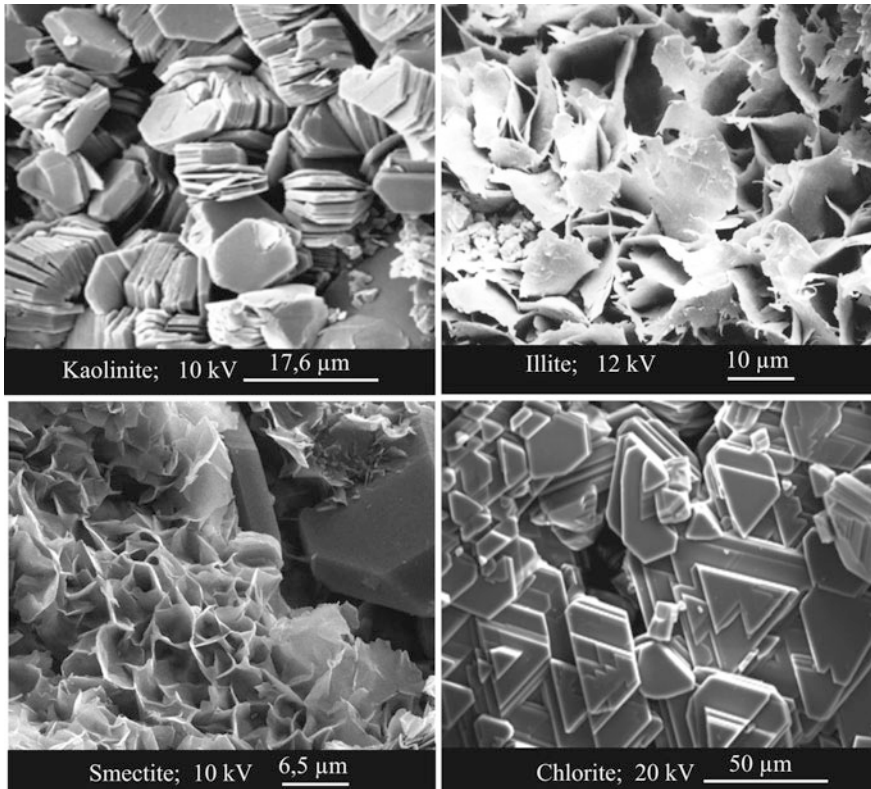
Fig. 5 SEM images showing the morphoscopy of some clay minerals: kaolinite; illite; smectite and chlorite

Table 2 Mean values of specific surfaces of clay and other silicate minerals (Eslinger and Peaver 1988)

	Specific surface (m^2/g)		
	External Surface	Internal surface	Total surface
Kaolinite	15	0	15
Illite	25	5	30
Smectite	50	750	800
Vermiculite	<1	750	750
Chlorite	15	0	15
Othor silicates	–	–	<5

- **Cation Exchange Capacity (CEC).** Clays have the property of fixing reversibly some cations contained in the surrounding solutions. The cation exchange capacity (CEC) corresponds to the number of negative charges likely to fix cations in this manner. It is expressed in centimols per kg (cmol/kg), which is a

translation in the international system of units of the milliequivalents per 100 g (meq/100 g), which have been traditionally used for decades. Cations can only be exchanged if they are weakly bonded to the external or internal surfaces (interlayer spaces) of crystals.

The CEC of the clays is related to two internal and external effects. The internal CEC reflects the charge deficiency of T-O-T (2:1) layers in the case of vermiculites and smectites. Consequently, the internal CEC depends on the permanent charges of clay species. The external CEC depends on the number of bonding sites of cations on the external surfaces. These negatively charged sites correspond to charges resulting from the tetrahedral or octahedral substitutions of those sheets forming the faces, or to defects emerging on these faces.

We note that the ionic radius of compensating cations influence the CEC: big highly charged cations are unable to be incorporated into the interlayer spaces of phyllosilicates and are therefore hardly exchangeable. Conversely, small and mobile cations are exchanged easily. The most common and easy exchangeable cations with clay in a decreasing order are: $Li^+ > Na^+ > Mg^{2+} > Ca^{2+} > Rb^+ > Cs^+$.

Table 3 summarizes, according to Eslinger and Peaver (1988), CEC of the most common varieties of clays and shows a very strong CEC of vermiculite and smectite compared with other clay minerals.

- **Swelling capacity**. In relation with their specific surface and CEC, some clay minerals, particularly those of the smectite group (montmorillonite, beidellite, saponite, hectorite, etc.), vermiculite and some interstratified minerals have a high hydrophilic affinity and ability to swelling. For these clay minerals, the weak bonds between the T-O-T (2:1) sheets and the moderate charge of these sheets (0.4–1.2 per unit cell) facilitate the separation of the interlayer spaces, increasing from 1 to 1, 8 nm, to adsorb a large amount of water molecules. For some varieties of montmorillonites, the water adsorption leads to an increase of volume up to 95 %.

3.4 Clays Genesis Process

Among the different geologic materials that make up the earth's crust, clays represent over 70 % of sedimentary rocks (Blatt et al. 1980) and cover about 1/3 of the surface of the continents (Meybeck 1987). Although research on the geology of clay goes back to the early 60s, with the fundamental work of Millot (1964), it is only more recently that a certain number of clarification and precision were made on their way of genesis, deposit and evolution. Among the most interesting references existing currently on clays we mention those of Millot (1970, 2001), Chamley (1989), Weaver (1989), Velde (1992, 1995), Hiller (1995), Allen (1997), Bergaya et al. (2006). The clays are found in the superficial range of the earth's crust, usually at a depth of 3.000 m and are classified into three categories.

Table 3 Indicative values of cation exchange capacity (CEC) of the most common clay minerals (Eslinger and Peaver 1988)

Clay minerals	CEC (meq/100 g)
Kaolinite	1–10
Illite	10–40
Smectites	80–150
Vermiculite	120–200
Chlorite	<10

- **Detrital clays**. The clay minerals can be considered as inherited phases of older rocks or minerals that have undergone mechanical disaggregation.
- The grain size and mineralogy of these clays depend on the nature of the parent rock, mechanisms of its alteration, as well as conditions of transport and deposition of detrital elements.

Depending on the nature rock (acid, basic or ultrabasic), the types of clays resulting from the fluid-rock interaction differ considerably. In the case of granite rocks, the hydrolysis of feldspar gives illite and aluminous smectite, plagioclase leads to kaolinite, while the mica is transformed into chlorites and vermiculites. For basic and ultrabasic rocks, alteration of their ferromagnesian minerals (olivine, pyroxene, amphibole and phlogopite) provides ferro-aluminous smectite (nontronite, beidellite), talc as well as fibrous clay minerals (chrysotile and antigorite). Furthermore, rock alteration and disintegration depend largely on climatic conditions, including the rate of precipitation and the tectonic regime (Allen 1997).

Inherited clay minerals can remain immobile (near of their bedrock) or undergo a transport and a deposit in a depressed area, located more or less far from the source region. In the latter case the topography and transportation factor (wind, fluvial and marine) play a important role in the lateral distribution of clays according to their particle size and mineralogy (Gibbs 1967; Eslinger and Peaver 1988).

- **Authigenic clays**. This clay crystallizes from interactions between saline solutions and silicates. Fresh sediment, composed of solid debris (inorganic and organic) impregnated with various ion rich solution, is a very favorable environment for the reactions of dissolution and formation of new mineral phases. Thus are formed carbonates, hydroxides, sulfates and also clays. However, these neoformation clays differ of dertital clays by their chemical composition and by their morphology. Different geological contexts and physico-chemical processes govern the genesis of different kinds of neoformation clay minerals. We will limit to remember some specific cases.

The lacustrine basins (salty Lakes and Sebkha) are particular environments that allow the formation of new magnesium phyllosilicates clay minerals of the smectite group (sepiolite, stevensite, hectorite) by direct evaporation of brackish water. This is the case of the formation of deposits of Ghassoul (stevensite) of Morocco. Concerning the bentonites (smectites and kaolinite association), it is widely accepted that their formation is related to the sedimentation of volcanic ash in closed and shallow environments (lakes, lagoons, inlets). Other examples of clay

neoformation we note: glauconites (ferriferous illite) which are in the form of green crystals sometimes associated with carbonates or coastal vases; red clays of ocean floor, rich in iron-smectite and containing zeolites and polymetallic nodules. These neoformation clays draw their raw material in products dissolution of limestone vases, siliceous vases and volcanic ash.

- **Transformed clay**. Over geological time, the primary formations of dertital or authigenic clays can undergo transformations after two geological phenomena: 1/deeper burying imposing a readaptation of initial mineral associations to new conditions of temperature and pressure; 2/interactions between fluids (hydrothermal or meteoric) and pre-existing mineral phases lead to a new state of chemical-mineralogical balance. In the two cases, the initial clay mineral assemblages are partially or completely erased and replaced by new minerals.

The transformation of clay according to the burying can be illustrated through the example of a drilling with 4.000 m of depth, made in a thick marl series of Cretaceous basin of Douala in Cameroon (Dunoyer de Segonzac 1964). This specific example shows that from 1.500 m montmorillonite completely disappears to give way to interbedded clays. Kaolinite remains up to 300 m before being relayed by chlorite and illite.

The hydrothermal alteration of clay minerals begins by fracturing allowing hydrothermal fluid flow in isolated or anastomosing veins (stockwerk). This gives rise to the creation of a small system with the apparition of an alteration which is propagated from the center of the vein into the clay rock. We can observe the following transformation reactions:

Smectite → Illite; showing an increase of the proportion of illite and a decrease of smectite in the mixed layers Illite-Smectite (I/S).

Montmorillonite → *Saponite* + Illite; assuming that the smectite layer induces directly the Illite layer.

Numerous experimental studies carried out on the kinetics of the hydrothermal transformation of clay minerals show that the transition from one phase to another are progressive in time and depend on temperature and the environments activity of K, Si, Al and Mg, chemical elements that can be made by the hydrothermal fluid or derived from destabilization of the existing phases in the system (Pytte and Reynolds 1889; Bouchet et al. 1988; Turpault et al. 1992).

3.5 Geographical Distribution of Clays

According to their genesis modes and following external geodynamic processes, primary clay formations can undergo mobilization and transport to depositing in other regions and giving high clay accumulations. This makes clays show a broad geographical distribution across the earth: surface of the continents and ocean floor.

Many research conducted on soil formation (Weaver 1989; Allen 1997) show the role of climate and meteoric alterations on the destruction of rocks. The

resulting components in solution moving the surface of the earth and are combined together to give new minerals, including clays.

- **In humid equatorial tropical climate**, heat and rains mean that the rocks are highly exposed to hydrolysis. A portion of the released chemical constituents are removed in the form of ion or complex ion by water trickling except iron, alumina and silica which remain in place. Iron precipitated to hydroxides giving, on site, iron hydroxides concentrations (hematite, magnetite, goethite, etc.). Alumina is deposited in gibbsite or combines with the silica to crystallize in the form of kaolinite. Thus develops the red soil rich in kaolinite, iron oxides and gibbsite called laterites.
- **In tropical-subtropical climate with alternating seasons**, the hydrolysis of rocks is mainly operational during the wet season but the evacuation of the ions is almost zero during the dry season. Under these conditions develops beidellite, mineral of the smectite group. This gives special types of clay soils, such as "vertisoil" and "fersiallitic".
- **In temperate climate**, low temperature and rainfall limit the alteration of silicate minerals except sensitive minerals (mica sericites, chlorite and clay). These latter undergo profound changes leading to varied mineral assemblages: vermiculite, smectite, interstratified chlorite-Al, etc.
- **In boreal climate**, prevailing in North Pole, the action of organic materials acid is so strong that it attacks the aluminosilicates. Thus were born podzol type of soils with their ashen backgrounds, rich in residues quartz.
- **In extreme, periglacial and desert climates**, Whether water is either frozen or absent, organic matter is lacking, the rocks are well protected from alteration. Soils in these regions are generally thin and composed of illite and chlorite resulting from the pulverization of preexisting phyllosilicates.

The diagram of the Fig. 6 summarizes the tight relationship between soil type and nature of the climate, relationship forms the basis of paleoclimatology, which use the results of clay study for the reconstruction of past climates.

Another question that also remains essential for understanding the distribution of clays on the surface of the globe refers to the transport process and clay deposits in the continental and marine environments. This question is largely discussed in the work of Eslinger and Peaver (1988), Chamely (1989), Weaver (1989), Velde (1995). For information, the scheme of Windom (in Velde 1995) gives a general idea about the distribution of the main clay minerals (illite, smectite, kaolinite and chlorite) in surface sediments of the different ocean basins (Fig. 7).

3.6 The Geological Cycle of Clays

Clay minerals that form clays materialize the geological history of recycling of the lithosphere. This story begins when the rocks of the earth's crust (basalt, granite, peridotite, shale, etc.), mainly composed of silicate minerals (quartz, feldspar, mica,
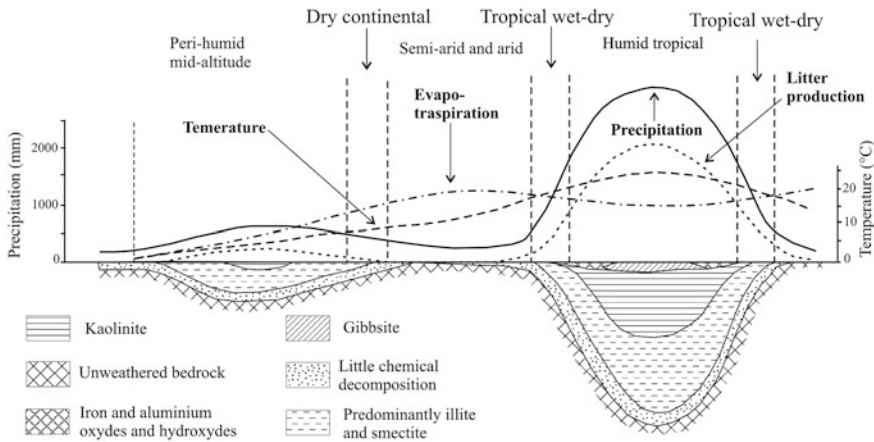
Fig. 6 Representation of the relationship between the type of soil (clay mineral composition) and the nature of the climate (in Allen 1997, digitized from origin diagram of Strakhov 1967)

pyroxene, olivine, etc.) come into contact with water (meteoric and/or hydrothermal). Thus, hydrolysis of silicate rocks contributes to the "birth" of clay minerals. The latters are then mobilized by wind and water currents animating the surface of the earth to reach the sedimentary basins, including ocean deep. These detrital clays will join authigenic ones formed locally by diagenesis. Sometimes, both inherited and neoformed clays may undergo transformations, which provide complex clay sequences.

Over geological time, which is counted in millions of years, clay deposits in ocean deep undergo a burying due to subsidence and tectonic. Arriving at great depths, where temperatures and pressures are significant, the various clays (kaolinite and smectite) recrystallized by diagenesis to give illite and chlorite. Exceeding the limit of diagenesis, all the clay minerals undergo general metamorphic leading to mineral assemblages of high temperature and pressure (mica, feldspar, etc.); what means the "death" of the clays. Beyond the metamorphism, partial melting of the materials from the base of the crust giving magmas which tend to progress gradually by gravity to the surface of the earth to give effusive and plutonic rocks. Once plutonic rocks outcrop on the surface of the earth by the tectonic movements, they exposed, in the presence of extrusive rocks; the clays cycle begins again.

Note also that the capacity of clays to retain water leads to the intervention of clay sediments on the mobility of the water from the surface of the earth to the depth of the crust, which has an essential consequence of the partial fusion of meta-sediments and magma genesis of subduction zones.
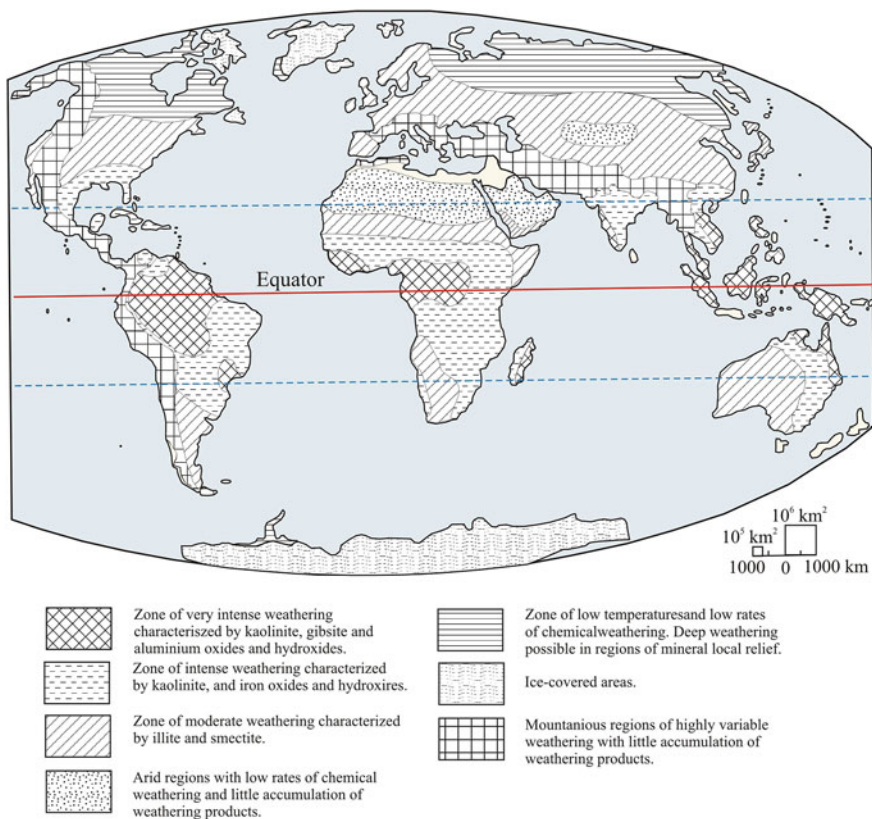
Fig. 7 Synthetic Scheme of the distribution of clay minerals on the surface of the continents (in Velde 1995, digitized from origin diagram of Strakhov 1967)

4 Clay for Nanocomposites

The use of clays as reinforcement in nanocomposites integrates two complementary research phases: a first preliminary phase is to search the most suitable clays and conditioned them to optimize its effect and; a second phase, more advanced, covers the elaboration and characterization of synthesized nanocomposites.

In this work, we look at the preliminary stage to remember the approach generally adopted to search and prepare the clay for the synthesis of nanocomposites. Three distinct but complementary steps can be distinguished: 1/geological prospecting clays; 2/purification of the clay material and 3/organophilic processing of clay.

4.1 Geological Prospecting Clays

Natural clays outcrop at the surface of the earth as an uncemented rock, sometimes compacted, with colors ranging from white to red or green, and variable modes deposits (in clusters, lenses or layers of varying thickness), according to the origin and the genesis mode of the clay.

In each country, cartographic documents (geological, geotechnical and thematic maps) as well as works and regional geological studies can guide the exploration towards areas rich in clays of different geological ages and petro-mineralogical nature.

To illustrate the spatial distribution of clay deposits at the scale of a country, we have chosen the case of Morocco. With its geographical position at the NW tip of Africa and a few kilometers of South of Europe, Morocco shows extreme geological and structural diversity (Fig. 8). All rock types are represented, from the Archean to Quaternary and retain the memory effects of the tectono-metamorphic that they have undergo through the different orogenesis: Panafrican, Caledonian, Hercynian and Alpine (Michard 1976; Piqué 1999; Michard et al. 2008).
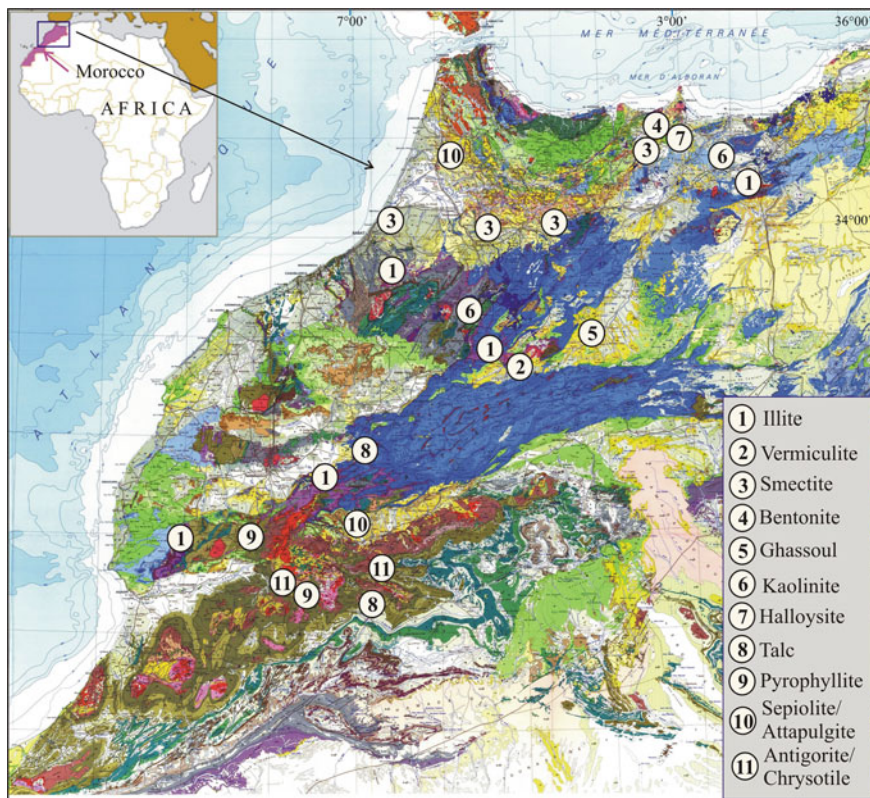
- *Illite and vermiculite group*
- The illitic clays are abundant and show a wide distribution across Morocco (Fig. 8). They correspond to continental deposits or shallow ocean floor, set up during the Triassic and Lower Cretaceous and form layers of a few meters to several hundred meters of thickness (Piqué and Laville 1993; El Ouahabi 2013; Sadik et al. 2014). Clay shows usually brick red colors, with fine or coarse grain and shows intercalations of greenstone and evaporites (rock salt, gypsum, sylvite). Clay mineral assemblage consists on average of 50 % of illite, 25 % of kaolinite and 25 % (+ chlorite + vermiculite + interstratified).
- Vermiculite concentrations are mainly found in 2 locations in Morocco: in the western Rif And Upper Moulouya (Fig. 8). In the Rif, vermiculite appears in decimeter filonets intersecting the Paleozoic massive of ultrabasic rocks (peridotite and amphibolites) of Beni-Bousera (Kornprobst 1974). While vermiculite of high Moulouya appears in accumulation or filonets in metric dimension associated with basic and alkaline igneous rocks (gabbro, diorite and syenite) altered in surface.
- *Smectite group*

The smectitic clays are also abundant in Morocco and can be divided into 3 main varieties:

- Marls of Southern Rif basin. These correspond to marine deposits of Miocene age, very fine-grained and light colored (yellow to gray). The marl which is very abundant in different regions of Morocco (Rif and Meseta) forms monotonous deposits exceeding sometimes 1.000 m (Fig. 8). These clays, relatively rich in carbonates are very operated by both the brick-makers and traditional potters. The composition of clay minerals is predominated by the smectite: 30–40 %

Fig. 8 Geological map of Morocco (Northern provinces) indicating the spatial distribution of the main types and clay deposits. (*1* Illite; *2* Vermiculite; *3* Marl; *4* Bentonite; *5* Ghassoul; *6* Kaolinite; *7* Halloysite; *8* Talc; *9* Pyrophyllite; *10* Sepiolite and Attapulgite; *11* Antigorite and Chrysotile)

smectite $+20$–30 % Kaolinite $+10$–20 % illite $+5$–10 % chlorite $+5$–10 % interstratified (Hilali and Jeannette 1981).

- Bentonite of Eastern Rif. Several deposits of bentonite are present in the region of Nador, around the Neogene volcanic complex of Gourougou (Fig. 8). These bentonites coming from the alteration of various volcanic products (ash, pyroclastic flows and glass) in different environments (air, marine and lacustrine) present various modes deposits (horizontal interbedded layers, clusters and lentils). Each type of deposit shows a typical composition that is dominated whether by beidellite, montmorillonite or montmorillonite-beidellite interstratified (El Bakkali et al. 1998; El Amrani et al. 2003).
- Ghassoul of Missour region. The ghassoul deposits of Missour outcrop in the SE of the Eastern Meseta at the junction of Upper and Middle Atlas (Fig. 8). Ghassoul, as a clod of earth brown, fine-grained and greasy, are present in lenses from 20 to 60 cm of thickness for several meters of long on top of Oligocene

clay-gypsum series (Trauth 1977; Barrakad 1981). The mineralogical and chemical analyzes reveal that the ghassoul consists mainly of trioctahedral magnesium smectite whose the aluminum content (Al_2O_3 = 4 %) confirms that it is stevensite of lacustrine origins (type Sebkha). Traces of illite and non-magnesian montmorillonite and quartz, carbonates and gypsum impurities are often associated with the dominant stevensite (85–90 %).

- ***Kaolinite group***
- Kaolinite. Moroccan soil does not contain a kaolin deposits except of some small concentrations which are associated with magmatic rocks acids. It is rich kaolin clay resulting from hydrothermal/meteoric alteration of alkali granite in the western Meseta (ex. Oulmès pluton) and East Mesta (ex. Beni Snassen pluton) (Fig. 8). This late-Hercynian granitic pluton, located in the Moroccan Meseta, is affected at its border, in contact with the surrounding rocks, by an intense hydrothermal alteration. This alteration caused the kaolinization of alkali-feldspar of the granitic rock and gives a friable material, rich in kaolin clay (10–20 %) with an appreciable quantity of quartz, flakes of muscovite, and chloritized biotite (Gmira 1994; Sadik et al. 2013).
- Halloysite. Some centimeter thick levels of halloysite exist in the volcanic region of Nador-Melilla (North-Eastern Rif). These levels are located on the Pliocene occurence between the top of the marl series and the base of the volcanic deposits of Gourougou (Fig. 8). Halloysite is derived from a hydrothermal transformation of inherited clay minerals by hot fluids related to volcanic activity. Montmorillonite and alunite, in substantial proportion (10–20 %) are frequently associated with halloysite (Hilali et Jeannette 1981).
- ***Talc and pyrophyllite groups***
- Talc. Interesting concentrations of talc are known in two regions of Morocco: the High Atlas and the Anti-Atlas. In the deposits of the High Atlas, in the regions of Aït Ouanergui and Ijoukak (Fig. 8), talc appears in layers or masses of metric thickness, white and intercalated in massive limestones and dolomites cut by acidic or basic magmatic rocks (microgranite, microdiorite, dolerite and gabbro). Against, talc which is located in the deposits of Anti-Atlas, near the localities of Bou-Azer and N'Kob (Fig. 8), of greenish color, shows an association with basic and ultrabasic rocks (gabbro, pyroxenite, serpentinite) and with dolomitized and serpentinized limestone. In the various cases, talc in very variable proportions of one deposit to the other is associated with limestone, chlorites, epidote, antigorite, etc. (Bouhaouli et al. 1981).
- Pyrophyllite. Different deposits of pyrophyllite exist in Morocco and are almost entirely situated in the Precambrian area of the Anti-Atlas, regions of Aït Baha, Aït Azegrouz, N'Kob, El Grara and Ougnat (Fig. 8) except a deposit that is located in the northern High Atlas, near to Tessaout river. Geologically, pyrophyllite shows a clear coloration, very fine grained and sometimes compact. It presents in layers or metric to decametric extension of accumulation associated with acid volcanic rocks (rhyolites and tuffs). This spatial association with

zonation often observed in the pyrophyllite rocks let admit their in situ formation by hydrothermal processing (pyrophylitisation) of acid volcanic rocks. About mineralogy, the different pyrophyllites rocks of the Anti-Atlas shows a binary or ternary association: quartz-pyrophyllite or quartz-pyrophyllite-kaolinite.

- *Fibrous clays group*
- Sepiolite and attapulgite (palygorskite). Interesting indexes of fibrous clays are described in two regions of Morocco. The first is in the region of Souk El Arbaa Gharb (Fig. 8). The series of marl of Eocene age, thicker at this area (>100 m), shows high levels of sepiolites which are associated with other clay minerals: attapulgite, smectite, illite, kaolinite and non-clay minerals: quartz, calcite, dolomite and hematite (Bensalem et al. 2014). The second index is in the Ouarzazate region (Fig. 8), where the sedimentary upper Cretaceous-Eocene of about 200 m of thickness, is mainly composed of carbonates, sulfates and phosphates with centimetric to decimetric alternations layers rich in attapulgite. The texture of attapulgite fibers suggests autochtonous (in situ) origin either by direct precipitation from solutions rich in magnesium or by transformation of magnesian smectite (Daoudi et al. 2009).
- Antigorite and chrysotile. Many asbestos indexes, mainly corresponding to chrysotile fibers with a lesser proportion of antigorites are reported in the Anti-Atlas, in the regions of Bou-Azzer and N'kob (Fig. 8). The Precambrian ophiolite complex of Bou-Azzer contains ultrabasics rocks (peridotite and pyroxenite) largely serpentinized and locally crosscut by rich veinlets of fibers with varying amounts of talc and magnetite (Leblanc 1981). In the region of N'Kob, the chrysotile develops in the magnesium limestone and serpentinized dolomite in association with antigorite, chlorite, talc and magnetite (Bouhaouli and Hilali 1981).

Table 4 summarizes the different clays groups well represented in Morocco by indicating their main geological characteristics. Through this example of Morocco, it is noted that clays may be related to various geological contexts (magmatic, sedimentary and metamorphic), presented in different deposit modes (layer, clusters, lentils, veinlets, etc.) and form complex associations of clay minerals (kaolinite $\pm$ smectite $\pm$ illite $\pm$ chlorite etc.).) and non-clay minerals (quartz, carbonate, magnetite, etc.).

In the case of the exploration of a variety of very specific clay, the geologist must target the most interesting clay area and conduct a thorough research, making use of suitable methods and techniques (geological sections, systematic sampling, sedimentological and particle size analysis, etc.) to clarify the nature of clay minerals, grain size of the rock, types of impurities, extension and exploitable reserves, etc.

Table 4 Summary table of different clays groups well represented in Morocco and their main geological characteristics

Clay groups	Geography n° / map	Geological Age	Deposit mode	Clay minerals Association
1/Illite/Vermiculite				
- Illite	1	- Trias - Low Cretac. - Late Alteration	- Layers - Filonets / Clusters	- Il ± Ka ± Ch ± Vr ± In
- Vermiculite	2			- Vr ± M c± In
2/ Smectites				
- Marl	3	- Upper Miocene.	- Layers	- Sm ± Ka ± Il ± Ch ± In
- Bentonite	4	- Neogene	- Layers / Lentils	- Sm ± Bd ± In
- Ghassoul	5	- Oligocene	- Lentils / Clusters	- Sm(St) ± Il ± Mt
3/ Kaolinite				
- Kaolinite	6	- Late alteration	- Clusters / Lentils	- Ka ± Ch ± Mc
- Halloysite	7	- Miocene-Pliocene	- Thin layers	- Ha ± Ka ± Mt
4/Talc/Pyrophullite				
- Talc	8	- Late alteration	- Layers / Clusters	- Tc ± Ch ± At ± Am
- Pyrophyllite	9	- Late alteration	- Layers / Clusters	- Pr ± Ka
5/ Fibrous clay				
- Sepiolite/Attapulgite	10	- Eocene - Cretaceous	- Layers	- Sp ± At ± Sm ± Il ± Ka
- Antigorite/Chrysotile	11	- Late alteration	- veinlets / Clusters	- Cr ± An ± Ch ± Tc

Abbreviation of clay minerals: Antigorite (An) ; Amiante (Am) ; Attapulgite (At) ; Beidellite (Bd) ; Chlorite (Ch) ; Chrysotile (Cr) ; Haloysite (Ha) ; Illite (Il) ; interbedded (In) ; Kaolinite (Ka) ; Micas (Mc) ; Montmorillonite (Mt) ; Pyrophyllite (Pr) ; Sepiolite (Sp) ; Smectite (Sm) ; Stevensite (St) ; Talc (Tc).

4.2 Purification of Clays

One of the major problems of natural clays is that they combine several species of clay minerals with a considerable amount of impurities (carbonates, quartz, feldspars, organic matter, rock fragments, etc.).

The great challenge of the use of these clays in the field of nanocomposites is, first, to purify them to keep only clay minerals concentrate, then, sort them to extract the desired clay mineral species (montmorillonite, kaolinite, illite, etc.). If the first purification step is technically easy, the second operation of clays sorting is more difficult.

We recall below the main methods and techniques conventionally used for purification of clays. Many patents exist on methods of separation and purification of minerals and more particularly clays (Fayolle 2006; El Amrani 2011).

Schematically, the purification of natural clay takes place following some steps that we try to describe briefly below:

- *Mechanical processing*. The compacted rock or as a lump of clay is dried in an oven at 110 °C for 24 h to eliminate the infiltrated and adsorbed water. The rock is then crushed to release the clay fraction of other coarse constituents (minerals, rock fragments). A dry sieving allows to eliminate the coarse fraction, usually higher than the millimeter.

- **Suspension in water**. The finely powdered rock is dissolved in distilled water and is subjected to a sufficiently strong agitation (500 tr/min during 24 h) accompanied by ultrasonic vibration (210 W, 10 kHz). These operations make it possible to disperse the lumps of clay minerals to liberate micro-flakes clays which are pressed against the surfaces of the non-clay mineral and at the same time dissolve the crystals evaporites (e.g. Rock salt and gypsum) which may be associated with clay rock.
- **Sedimentation and centrifugation**. A simple decantation can be useful, otherwise, we can use a centrifuge to separate the silty sand fraction, having a particle size greater than 2 μm, from the fraction mainly clayey which remains in suspension. The latter, filtered and dried in an oven, is our pre-concentrate clay which is still impure.
- **Elimination of organic matter**. The pre-concentrate clay is dissolved in hydrogen peroxide (H_2O_2) under moderate agitation (250 tr/min) during 24 h. The mixture is then heated at 70 °C during 1 h and then filtered by centrifugation at 3500 tr/min. Clay residue is rinsed with distilled water and then dried in an oven.
- **Elimination of carbonates**. The clay product free of any trace of organic matter is returned to acidic solution (0.1 N HCl). After agitation for 4–5 h, the clay was filtered by centrifugation (3500 tr/min) and then rinsed in several times with distilled water to remove traces of chloride before being dried.
- **Dissolution of hydroxides**. The presence of traces of iron, aluminum and magnesium hydroxides can be eliminated by performing an appropriate treatment of the clay such using a sodium citrate solution (50 ml, 0.3 M) and sodium hydrogen carbonate (10 ml, 1 M) for 30 min at a temperature of 80 °C. The addition of a small amount of sodium dithionite (1.5 g) leads to reduce the Fe^{3+} ions too Fe^{2+} which form a more stable complex with the citrate. The clay suspension is then rinsed with plenty of water with sodium chloride (2 M).
- **Elimination of the silica**. The various forms of silica, often present in the clays, can be properly dissolved by a treatment with a buffer solution (0.2 M) containing oxalic acid and ammonium oxalate. The treatment requires continuous agitation for a few hours, then rinsing with abundant water and centrifugation.
- **Control of purification**. The treated clay is subjected to analysis by X-ray diffraction (XRD) and infrared spectrometry (FTIR) to ensure its purification. Where undesirable elements still exist (dolomite, quartz, feldspar, iron oxides, etc.), appropriate chemical treatments can be applied.

Moreover, the operations of separation between the clay minerals of the same mixture are much more delicate and requires resources and sophisticated equipment. These, although they are technically possible in laboratory scale, their projections on an industrial scale for the preparation of a large quantity of pure clay, prove to be very costly.

Finally, it should be noted that a considerable saving of time and resources is still possible if the geologicals prospecting, previously well conducted, are used to identify deposits levels capable to provide the highest quality of the desired clay.

4.3 *Organophilic Modifications of Clays*

Hydroxides of octahedral layers provide natural clays hydrophilic character. Also, these clays exhibit no affinity with the organic polymer chains that constitute the composite matrix. We know that the essential properties of composite are relative to the physicochemical compatibility of clay interface (reinforcement)–polymer (matrix) and the ease of the mechanical stress transfer from the matrix to the reinforcement. This means that the use of natural clays for the preparation of the composites requires, first of all, an organophilic transformation of the hydrophilic clay.

This chemical transformation of clays is made possible by a cation exchange process "CE" (Lagaly 1981; 1986) which consists in substituting the charge-compensating cations in the interlayer galleries of the agile by cationic surfactants; molecules having a polar portion (hydrophilic head) and a apolar part (hydrophobic chain). The most commonly surfactants used for the "organophilisation" of lamellar natural clays are alkylammonium ions; derived molecules from the ammonium ion NH^{4+} and whose hydrogen atoms are replaced by one or two aliphatic hydrocarbon chains (6–20 carbon atoms) and by CH_3 or CH_2CH_2OH groups. The process of transformation is done in aqueous media where the phyllosilicates swell easily, which facilitates replacing at the interlayer space between the Na^{2+} and Ca^{2+} ions by alkylammoniums. After filtration and drying, we obtained organophilic clays whose interlayer space is occupied by the surfactant molecules.

We note that there is another organophilic technical transformation of clays which schematically consists of a covalent grafting of the organosilanes at the surface of the clay. In fact, after hydrolysis, silanes become silanols which can react with the hydroxide clays to form siloxane bonds. However, this technic is less controlled and therefore remains not often used.

Applied research on the case of montmorillonite, currently considered as the most suitable reinforcement for the synthesis of nanocomposites shows that the results of the transformation by the organophile method "EC" are influenced by three key factors:

- **The intrinsic parameters of the clay**. These parameters depend on the clay structure and CEC. As substitutions in montmorillonite are located in the octahedral layer, interaction with the compensating ions are attenuated by the tetrahedral layer. This facilitates the swelling of the layers in aqueous media and active the cation exchanges. However, when the density of the compensated sites is high (the case of vermiculite), the sheets are bounded by strong interaction, which limits the swelling and reduced the exchanges.
- **The type of compensating cation**. The type of compensating cation to substitute plays a decisive role on the interchanged ion rate during dispersion of clay in aqueous solution. Thus, large highly charged cations (e.g. K^+, Rb^+) limit the spacing of the interlayer spaces and resist to exchange. By cons, small ions (e.g. Na^+, Ca^{2+}) dissociated easily. As an example, alkylammoniums

exchanging is higher in sodium montmorillonite than in calcium and magnesium-montmorillonite.

- **The nature of the surfactant (alkyl ammonium ion)**. The length of the carbon chain, the size and shape of the polar head and the groups present in the surfactant plays an important role on cation exchange (Okada et al. 1987). Thus small NH^{4+} cations and those having 1 or 2 methyl groups can lodge easily in the interlayer spaces of the hexagonal cavities of clay, which strengthens interactions with the sheet and makes the exchange less reversible. Furthermore, the same studies show that the strength of amine-sheet interactions are more important for primary amines, which implies that the primary amines are exchanged more easily than others. Finally, the action of the groups present in the alkyl chains on the ion exchanged rate has a direct consequence on the variation of the interlayer distance.

According to work of Lagaly (1986), the alkyl ammonium ions arrangement at the interlayer spaces varies depending on the concentration of these ions in the media and the CEC of the clay in question. Thus, when the concentration of alkyl increases, the various layers are successively adsorbed on the surface of the sheets by cation exchange.

After these transformation process, we obtain organophilic clays whose interlayer spaces are occupied by surfactant ions arranged in 4 different configurations: monolayers; bilayers; pseudotrimoliculaire; and paraffin type (Fig. 9). These clays thus have a greater or lesser affinity with the organic matter will be ready to be used for the preparation of nanocomposites.

At the end of this review, we propose a general pattern that summarizes the different steps and techniques for treatment of natural clay to extract the desired clay mineral, purified it then make it organophylic to become directly usable for the preparation of nanocomposites (Fig. 10).

Fig. 9 Schematic representation of the possible configurations of the alkyl ions in the interlayer spaces of organophylic clays (Lagaly 1986)
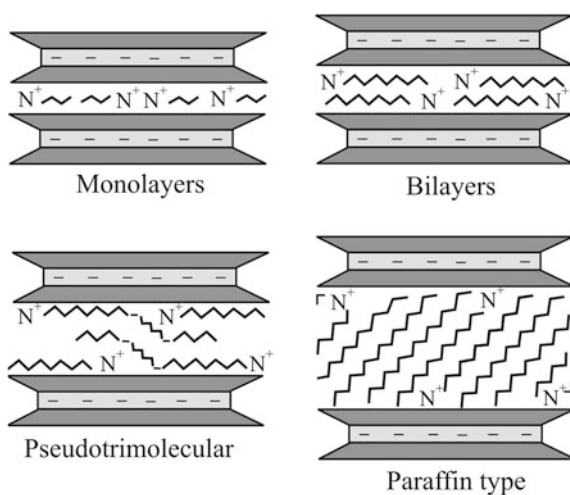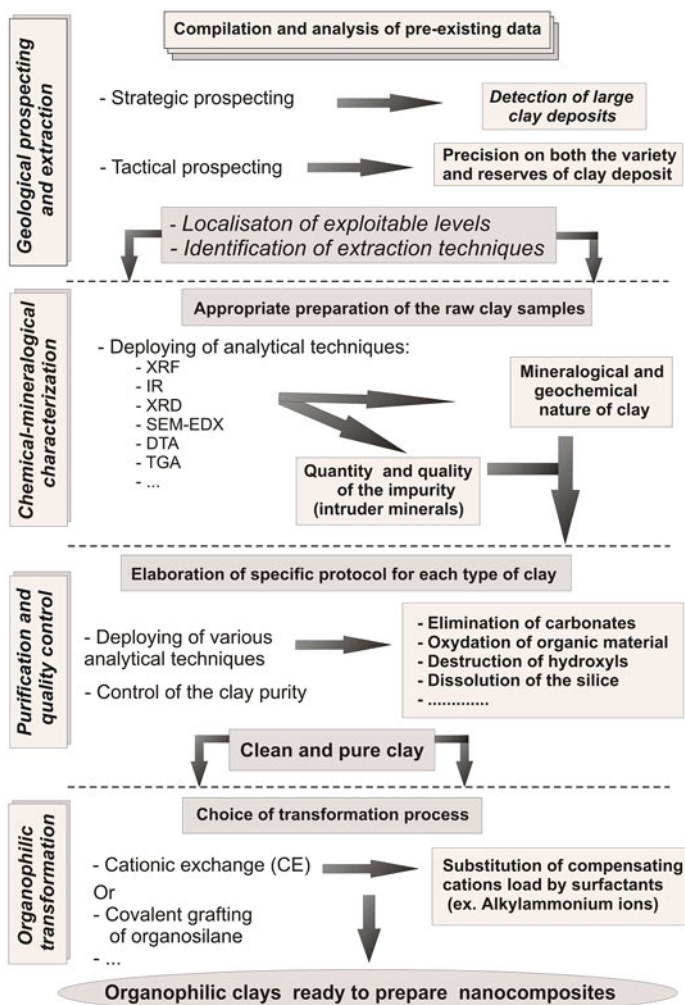
Fig. 10 General pattern of the prospecting, characterization, purification and organophilic transformation of a natural clays for application in nanocomposites

5 Conclusion

Scientific research on clay-based nanocomposites contributes to improving the prospects of technical and economic development. This is even more likely that the clay minerals have not yet delivered their entire secret. Indeed, the gradual advancement of knowledge on the properties and behavior of different species of clay minerals can better control their incorporation and dispersion as reinforcement in composites. Also the optimization of the matrix-reinforcement interface allows a

better transmission of mechanical stress from the matrix to the reinforcement (clay) and contributes to a continuous improvement in physical, mechanical, thermal and optical properties of the nanocomposite.

In this perspective, attention must not remain focused only on the use of montmorillonite and vermiculite (clay minerals actually having the greatest possibility of CEC and expansion), but exploration should be attempted on other clay minerals having particular structures and properties (halloysite, steveniste, sepiolite, etc.). This will eventually lead to original and innovative nanocomposites. Finally, on this review focused on the mineralogy and geology of natural clays and in contrast to other synthesis work that treat physicochemical aspects of nanocomposites, appears the interest of strengthening research, certainly promising, on nanocomposites through a larger federation of human and material resources and by engaging multidisciplinary research teams.

References

Allen, P.A.: Earth Surface Processus, pp. 404. Blackwell, Oxford (1997)

Ayana, B., Suin, S., Khatua, B.B.: Highly exfoliated eco-friendly thermoplastic starch (TPS)/poly (lactic acid)(PLA)/clay nanocomposites using unmodified nanoclay. Cabohydr. Polym. **110**, 430–439 (2014)

Barrakad, A.: Ghassoul. Mines, Géologie et Energie, numéro consacré aux roches et minéraux et industriels du Maroc, **49**, 138–142 (1981)

Bensalem, H., Aadjour, M., El Hadi, H., Saber, N., El Ouazzani, A., Mouttaqi, A.: Evaluation de la qualité industrielle des argiles fibreuses de Bled Rmel, bassin du Gharb, Maroc. Eur. Sci. J. **10** (18), 57–7881 (2014)

Bergaya, F., Theng, B.K.G., Lagaly, G.: Handbook of clay science, vol. 1 (Development in Clay Science). Elsevier, Amsterdam (2006)

Berthelot, J.M.: Matériaux composites, comportement mécanique et analyse de structures. 4ème édition, collection Lavoisier, Paris (2005)

Blatt, H., Middleton, G.V., Murray, R.C.: Origin of Sedimentary rocks. Prentice Hall, Englewood Cliffs, NJ (1980)

Bouchet, A., Meunier, A., Sardini, P.: Minéraux argileux. Mémoire 23, Edition Andra (2000)

Bouchet, A., Meunier, A., Velde, B.: Hydrothermal mineral assemblages containing two discrete illites/smectiteminerals. Bull Min. **111**, 587–599 (1988)

Bouhaouli, A., Jeannette, A., Mortaji, M., Nataf, M.: Talc et Pyrophyllite. Géologie et Energie, numéro consacré aux roches et minéraux et industriels du Maroc, **49**, 72–91 (1981)

Bouhaouli, A., Hilali, A.: Amiante. Mines, Géologie et Energie, numéro consacré aux roches et minéraux et industriels du Maroc, **49**,143–161 (1981)

Bourbigot, S., Delobel, R., Duquesne, S.: Comportement au feu des composites. Techniques de l'ingénieur, Référence AM5330 1–10 (2006)

Burnside, S.D., Giannelis, E.P.: Synthesis and properties of new poly (dimethylsiloxane) nanocomposites. Chem. Mater. **7**, 1597–1600 (1995)

Caillère, S., Hénin, S., Rautureau, M.: Minéralogie des argiles. 1. Structures et propriétés physico-chimiques, 2ème édition, Masson, Paris (1982)

Chamley, H.: Clay Sédimentology. Springer, pp. 623. Berlin Heidelberg, New York (1989)

Chang, M.K., Lee, H.C.: Effects of montmorillonite and compatibilizer on the mechanical and thermal properties of dispersing intercalated PMMMA nanocomposites. Int. Commun. Heat Mass Trans. **67**, 21–28 (2015)

Cho, J.W., Paul, D.R.: Nylon 6 nanocomposite by melt compounding. Polymer **42**, 1083–1094 (2001)

Cognard, P.: Les applications industrielles des matériaux composites, Edition du Moniteur (1987)

Daoudi, L., Jourani, E., Knidiri, A.: Les argiles fibreuses des formations phosphatées du bassin de Ouarzazate (Maroc): caractérisation et signification génétique. COVAPHOS III, **5**, 30–41 (2009)

Daviaud, R., Filliatre, C.: Introduction aux matériaux composites, 1- Matrices organiques. Editions du CNRS, Institut des matériaux composites (1987)

Deer, W.A., Howie, R.A., Zussman, J.: An Introduction to the Rock Forming Minerals. Fourteenth Impression, Longman (1983)

Doh, J.G., Cho, I.: Synthesis and properties of polystyrene-organoammonium montmorillonite hybrid. Polym. Bull. **41**, 511–518 (1998)

de Segonzac, G.D.: Les minéraux argileux dans la diagenèse, vol. 29. Passage au métamorphisme. In Mém. Serv. Carte géol. Als, Lorr (1964)

Eesaee, M., Shojaei, A.: Effect of nanoclay on the mechanical properties and durability of novolac phenolic resin/woven glass fiber composite at various chemical environments. Compos. Part A **63**, 149–158 (2014)

El Achaby, M., Ennajih, H., Arrakhiz, FZ., El Kadib, A., Bouhfid, R., Essasi, E., Qais, A.: Modification of montmorillonite by novel geminalbenzimidazolium surfactant and its use for the preparation of polymer organoclay nanocomposites. Compos. Part B **51**, 310–317 (2013)

EI Amrani: Séparateur de minéraux par effet combiné de la gravité et d'un jet d'air horizontal. OMPIC, Maroc n° MA 32519B1, Classification IPC B07B4/02 – B07B7/01 (2011)

El Amrani, E.I., El Bakkali, S., Haïmeur, J., Asebriy, L., Bourdier, J.L., Gourgaud, A., Vincent, P. M.: Genèse des gisements de fer, bentonite et perlite associés au volcanisme néogène du Rif nord-oriental (Maroc). Trav. Inst. Sci. Rabat **21**, 185–188 (2003)

El Bakkali, S., Gourgaud, A., Bourdier, J.L., Bellon, H., Gündogdu, N.: Post-collision neogene volcanism of Eastern Rif (Morocco): magmatic evolution through time. Lithos **45**, 523–543 (1998)

El Ouahabi, M.: Valorisation industrielle et artisanale des argiles du Maroc. Thèse de l'Université de Liège, pp. 189 (2013)

Eslinger, E., Peaver, D.: Clay Minerals for petroleum geologists and engineers. SEP short course 22, Soc Econ Paleonto Mineral, pp. 420 (1988)

Fayolle, D.: Procédé de purification d'une argile pour un usage thérapeutique. PCT n° WO2006032764 A1 (2006)

Gay, D.: Traité des Nouvelles Technologies–Série mécanique- Matériaux composites, Hermes (1987)

Giannelis, E.P.: Polymer layered silicate nanocomposite. Adv. Mater. **8**, 29–35 (1996)

Giannelis, E.P., Ferrara, G., Camino, G., Pellegatti, G., Rosenthal, J., Trombini, R.C.: Effect of matrix features on polypropylene layered silicate nanocomposite. Polymer **46**, 7037–7046 (2005)

Giannelis, E.P., Krishnamoorti, R., Manias, E.: Polymer-silicate nanocomposite: Model System for confined polymers and polymer brushes. Adv. Polym. Sci. **138**, 107–147 (1998)

Gibbs, R.J.: The geochemistry of the amazon river basin: Part I. The factors that control the salinity and the composition and concentration of suspended solids. Geol. Soc. Am. Bull. **78**, 1203–1232 (1967)

Gloaguen, J.M., Lefebvre, J.M.: Nanocomposites polymères/silicates en feuillets. Techniques de l'ingénieur, Référence AM5205 1–19 (2007)

Gmira, A.: Altération des granites d'Oulmès (Maroc central). Mécanismes et produits de la kaolinisation. Thèse de l'Université de Lyon (1994)

Grim, R.E.: Clay mineralogy. McGraw-Hill Inc., New York (1953)

Hilali, A., Jeannette, A.: Kaolin et argiles céramiques. Mines, Géologie et Energie, numéro consacré aux roches et minéraux et industriels du Maroc **49**, 30–57 (1981)

Hiller, S.: Erosion, sedimentation and sedimentary origin of clays.In Velde, B. (ed.) Clay and the environment, Springer, Berlin, pp. 162–219 (1995)

Kato, M., Usuki, A., Okada, A.: Synthesis of polypropylene oligomer-clay interaction compounds. J. Appl. Polym. Sci. **66**, 1781–1785 (1997)

Kawasumi, M., Hasegawa, N., Kato, M., Usuki, A., Okada, A.: Preparation and mechanical properties of polypropylene-clay hybrids. Macromolecules **30**, 6333–6338 (1997)

Kloprogge, J.T., Komarneni, S., Amonette, J.E.: Synthesis of smectite clay minerals: a critical review. Clays Clay Miner. **47**(5), 529–554 (1999)

Kojima, Y., Usuki, A., Kawasumi, M., Okada, A., Fukushima, Y., Kurauch, T., Kamigaito, O.: Mechanical properties of nylon 6-Clay hybrid. J. Miner. Res. **8**, 1185–1189 (1993)

Kornprobst, J.: Contribution à l'étude pétrographique et structurale de la zone interne du Rif (Maroc septentrional). Notes et Mém. Serv. Géol. Maroc, Rabat, n°251 (1974)

Lagaly, G.: Interaction of alkylamines with different types of layered compounds. Solid State Ion. **22**, 43–51 (1986)

Leblanc, M.: Ophiolites précambriennes et gites arséniés de cobalt. (Bou-Azzer, Maroc). Notes et M. Serv. Géol. Maroc, n°280 (1981)

Lee, J., Takekoshi, T., Giannelis, E.P.: Fire retardant polyetherimide nanocomposites. Mater. Res. Soc. Symp. Proc. **457**, 513–518 (1997)

Lee, S.J., Won, J.P.: Interfacial phenomena in structural polymeric nano-clay synthetic fiber reinforcedcementious composites. Compos. Struct. (2015)

Marchant, D., Jayaraman, K.: Strategies for optimizing polypropylene-clay nanocomposites structures. Ind. Eng. Chem. Res. **4**, 6402–6408 (2002)

Messersmith, P.B., Giannelis, E.P.: Synthesis and barrier properties of poly (ξ-caprolactone)-layered silicate nanocomposite. J. Polym. Sci., Part A: Polym. Chem. **33**, 1047–1057 (1995)

Meunier, A.: Clays. Springer (2005)

Meybeck, M.: Global chemical weathering of surfacial rocks estimated from river dissolved loads. Am. J. Sci. **287**, 401–428 (1987)

Michard, A.: Eléments de Géologie Marocaine, Notes et Mem. Serv. Géol. Maroc, n° 252, pp. 408 (1976)

Michard, A., Saddiqu, O., Chalouan, A., Frizon de la Motte, D.: Continental Evolution: The Geology of Morocco. Structure, Stratigraphy, and Tectonics of the Africa-Atlantic-Mediterranean Triple Junction. Edition Springer, pp. 404 (2008)

Millot, G.: Geology of cla. Chapman-Hall, London (1970)

Millot, G.: Argiles et Minéraux Argileux. Encyclopeadia Universalis et Edition Albin Michel, Paris, Dictionnaire des roches etminéraux (2001)

Millot, G.: Géologie des argiles. Masson, Paris (1964)

Okada, A., Kawasumi, M., Kurauchi, T., Kamigaito, O.: Synthesis and characterization of a nylon 6-clay hybrid. Am. Chem. Soc. Polym. Prepr. Div. Polym. Chem. **28**, 447–448 (1987)

Piqué, A.: Géologie du Maroc. Les domaines régionaux et leur évolution structurale. Edition Pumag, pp. 284 (1999)

Piqué, A., Laville, E.: Les séries triasiques du Maroc, marqueurs du rifting atlantique. C.R. Acad. Sci. Paris, série II **317**, 1215–1220 (1993)

Pytte, A.M., Reynolds, R.C.: The thermal transformation of smectite to illite. In: Naesser, N.D., MCCulloh, T.H. (eds.) The thermal history of a sedimentary bassin: methods and case history, pp. 133–140. Springer, Berlin Heidelberg New York (1989)

Renard, J.: Elaboration, microstructure et comportement des matériaux composites à matrice polymère, Collection Lavoisier, Paris (2005)

Sadik, C., Albizane, A., El Amrani, E.I.: Production of porous firebrick from mixtures of clay and recycled refractory waste with expanded perlite addition. J. Mater. Environ. Sci. **4**(6), 981–986 (2013)

Sadik, C., Albizane, A., El Amrani, E.I.: Composition and ceramic characteristics of Cretaceous clay from Morocco. Adv. Sci. Technol. **92**, 209–214 (2014)

Sherman, L.M.: Nanocomposites: A little goes a long way. Plastics Technol. **45**, 52–57 (1999)

Solomon, M.J., Almusallam, A.S., Seefeldt, K.F., Somwangthanaroj, A., Varadan, P.: Rhyology of polypropylene/clay hybrid materials. Macromolecules **34**, 1864–1872 (2001)

Strakhov, N.M.: Principles of lithogenesis Vol. 1. Oliver and Boyf Ltd, pp. 245 (1967)

Trauth, N.: Argile évaporitique dans la sédimentation carbonatée continentale et épicontinentale tertiaire. Bassin de Paris, de Mormoiron et de Salinelles (France) et du Jbel Ghassoul (Maroc). Sciences géologiques, Mémoires, 49, pp. 195 (1977)

Turpault, M.P., Berger, G., Meunier, A.: Dissolution-précipitation processes induced by hot water in fractured granite. Part 1: Wall-rock alteration and vein deposition processes. Eur. J. Mineral. **4**, 1457–1475 (1992)

Usuki, A., Kojima, Y., Kawasumi, M., Okada, A., Fukushima, Y., Kurauchi, T., Kamigaito, O.: Synthesis of nylon 6-Clay hybrid. J. Miner. Res. **8**, 1179–1184 (1993)

Velde, B.: Clay minerals. A physico-chemical explanation of their occurrence. Developments in sedimentology, vol. 40. Elsevier, Amsterdam (1985)

Velde, B.: Introduction to clay minerals. Chapman-Hall, London (1992)

Velde, B.: Origin and mineralogy of clays. Clays and environment. Springer, Berlin Heidelberg, New York (1995)

Weaver, C.E.: Clays, muds and shales. Developmentsin in sedimentology, vol. 44, p. 819. Elsevier, Amsterdam (1989)

Yano, K., Usuki, A., Okada, A., Kurauchi, T., Kamigaito, O.: Synthesis and properties of polyimide-clay hybrid. J. Polym. Sci.: Part A Polym. Chem. 312493–2498 (1993)

Zhanga, D., Zhoua, C.H., Linb, C.X., Tonga, D.S.: Synthesis of clay mineral. Appl. Clay Sci. **50** (1), 1–11 (2011)

Zhu, J., Morgan, A.B., Lamelas, F.J., Wilkie, C.A.: Fire properties of polystyrene-clay nanocomposites. Chem. Mater. **13**, 3774–3780 (2001)

Bioplastics and Bionanocomposites Based on Nanoclays and Other Nanofillers

A.H. Bhat, Imran Khan, Mohd Amil Usmani and Jahangir Ahmad Rather

Abstract This chapter provides an overall review on the latest progress in the research and development of bionanocomposites that are utilized in various applications such as packaging, durable goods, electronics and biomedical applications. The rise of biobased materials is guided by its renewability, low carbon footprint and biodegradability issues and by virtue of which vast applications of these materials are already available. The bionanocomposites provides a better alternative for the various drawbacks which can be found in the biobased polymer matrix materials. Some of the issues of low strength, poor barrier properties, hydrophilicity, low thermal stability and conductivity can be addressed by the development of bionanocomposites. The chapter will begin with the introduction and recent advances in the development of biobased materials from renewable resources and their usefulness. In the very next part, many types of bionanocomposites based on these fillers i.e. nanocellulose, carbon nanotubes and nanoclays, are discussed. This review also presents up-to-date progress in this area in terms of processing technologies, product development and applications.

Keywords Bionanocomposites · Nanocellulose · Nanoclays · Polymer

A.H. Bhat (✉)
Department of Fundamental and Applied Sciences, Universiti Teknologi Petronas,
31750 Bandar Seri Iskandar, Tronoh, Perak Darul Ridzuan, Malaysia
e-mail: aamir.bhat@petronas.com.my

I. Khan · J.A. Rather
Department of Chemistry, College of Science, Sultan Qaboos University,
PO Box 36, PC 123 Muscat, Oman

M. Amil Usmani
Department of Chemistry, Eritrea Institute of Technology,
P.O. Box 12676, Asmara, Eritrea

1 Introduction

The useful and the best biomaterial is the main challenge of the next decade. Such material can revolutionize and will address many global issues viz. petroleum shortage, global warming, and geopolitical conflicts that are linked to minerals or metals and incineration waste residues (Lavoine et al. 2012). Due to environment and sustainability issues, this century has witnessed remarkable achievements in green technology in the field of materials science through the development of bionanocomposites. Great interest was given to the development of renewable materials, particularly to packaging industries due to the problems involved recycling and the dwindling exhaustion of fossil resources (Morais et al. 2013).

Bioplastics represent a wide spectrum of thermoplastics that are obtained from biological resources and fossil resources, or combinations of both. Application of natural fibers as biofiller materials in composites have been focus of attention as they exhibit attractive advantages such as low cost and low density per unit volume, reduced tool wear and acceptable specific strength besides their renewable and degradable characteristics (Majeed et al. 2013). However, certain drawbacks such as incompatibility with the hydrophobic polymer matrix, the tendency to form aggregates during processing and water swellable nature of cellulose, especially in its amorphous regions, greatly reduce the potential of natural fibers to be used as reinforcement in polymers. Layered silicates also known as nanoclays are most commonly utilized nanofillers in the synthesis of polymer layered silicate nanocomposites. Among these layered silicates, phylloscilicates (2:1) are extensively used in preparing clay based nanocomposites. Therefore, new properties and functions, including uniformity and durability, are required for the next generation of biobased products and their engineering applications. Such features can be displayed by cellulose elementary "building blocks", known as nanocrystalline cellulose (NCC) (Brinchi et al. 2013). Nanocrystalline cellulose is a fine, white, odorless, crystalline powder, and biodegradable material, which can be isolated from cellulose (Mohamad et al. 2013). In the present review, our interest in this material is as a nanofiller, since it possess nanoscale dimensions, high specific area, and highly rigid crystalline structure (Chen et al. 2012). Consequently, it exhibit outstanding mechanical properties, such as high Young's modulus along with the longitudinal direction in the crystal region (Jonoobi et al. 2011).

Presently, academia and industries are investigating the use of nanostructures (cellulose nanostructures) as reinforcements in order to produce a new class of bionanocomposites. The inherent properties of these nanoparticles in enhancing the thermal, mechanical, dimensional stability and other types of functional properties (electrical/electromagneticshielding/barrier/fire retardant/triggered biodegradability/solvent resistance) of the composite materials with the added advantages of ecofriendliness were effectively utilized to create new class of materials. So, for the same purpose bio-based materials for packaging applications are being sought to

replace synthetic, non-degradable, thermoplastics due to rapid growth in municipal waste, consumer awareness and stricter government regulations.

2 Bioplastics

Bioplastics are a type of plastics derived from renewable biomass sources, such as vegetable oil, corn starch, pea starch or microbiota, rather than traditional plastics which are derived from petroleum. They are used either as a direct replacement for traditional plastics or as blends with traditional plastics. All bio-based and petroleum-based plastics are technically biodegradable, meaning they can be degraded by microbes under suitable conditions. Several starch-based plastics have been introduced into the market, and are used in some applications. Starch foam is one of the major starch-based packaging materials. It is produced by extrusion or compression/explosion technology. This product has been developed as a replacement for polystyrene which is used to produce loose-fillers and other expanded items. Another type of starch-based plastics is produced by blending or mixing starch with synthetic polyester. For this type of biodegradable plastics, granular starch can be directly blended with polymer, or its granular structure can be destructurized before being incorporated into the polymer matrix. The type of starch and synthetic polymer as well as their relative proportions in the blends influence the properties of the resulting plastics. The last group of starch-based plastics is polyesters that are produced from starch. The major starch-derived polyesters in the market now are polylactic acid and polyhydroxyalkanoate. The advantages of starch for plastic production include its renewability, good oxygen barrier in the dry state, abundance, low cost and biodegradability. The longstanding quest of developing starch-based biodegradable plastics has witnessed the use of different starches in many forms such as native granular starch, modified starch, plasticized starch and in blends with many synthetic polymers, both biodegradable and nonbiodegradable, for the purpose of achieving cost effectiveness and biodegradation respectively. In this regard, starch has been used as fillers in starch-filled polymer blends, thermoplastic starch (TPS) (produced from the combination of starch, plasticizer and thermomechanical energy), in the production of foamed starch and biodegradable synthetic polymer like polylactic acid (PLA) with varying results.

Poly (Lactic–acid) (PLA) is one of the matrix materials to be used in this research which is basically a type of thermoplastic aliphatic polyester derived from non-fossil renewable natural resources. On account of its biodegradability and biocompatibility, PLA has been widely used in biomedical applications. The inexpensive price of industrial grade PLA along with its high mechanical strength and good processability enables it to be used as a sustainable alternative to petrochemical-derived products in commodity applications (Lim et al. 2008). However, neat PLA exhibits brittleness and its fracture strain is only about 5 % in the tensile test, which results in poor impact and tear resistance. In addition, it also

shows poor heat stability with low levels of heat deflection temperature (HDT). These inherent deficiencies of PLA have greatly hindered its large-scale applications in both commodity and biomedical areas.

Another widely studied bioresourced family of polymer is bacterial polyhydroxyalkanoates. PHAs are natural biodegradable thermoplastics produced as intracellular energy and carbon storage materials by various microorganisms (Doi et al. 1990). Presently, only a few PHAs, mainly polyhydroxybutyrate (PHB) and poly (3-hydroxybutyrate-co-hydroxyvalerate) (PHBV), are commercially available and produced on an industrial scale. In the family of PHAs, PHBV has gained a lot of attentions because of its remarkable features including its excellent biodegradability, biocompatibility, and some properties similar to those of polypropylene. Moreover, compared to other biodegradable polyesters; PHBV shows excellent thermal resistance ability due to its high crystallinity. These fascinating properties make PHBV a potential substitute for petroleum-based polyolefin in many areas. Nevertheless, widespread application of PHBV is also limited because of its brittleness, low impact resistance, and high production cost. These complementary properties among PLA and PHBV blend components are very important and interesting that one can tailor the mechanical properties; processing properties and thermal performance by a simple melt blending method.

Bio-nanocomposites which are obtained from 100 % bio-based materials, in which the fillers are clay/renewable based and the matrix are obtained from renewable resources, are the focus of this chapter. This section presents three different nanofillers which are extensively used for the preparation of bio-nanocomposites: 1. Cellulose based nanofillers (Cellulose nanofibers and Cellulose nanowhiskers), 2. Carbon Nanotubes, 3. Nanoclays (Layered silicates).

2.1 Cellulose Based Nanofillers

As discussed in earlier sections, cellulose is a widely available and low cost material which is both renewable and biodegradable. These attributes combined with their environmentally benign nature makes the nanofibers obtained from cellulose very attractive for use as reinforcements in the preparation of bionanocomposites.

Cellulose is a sustainable, abundant and natural occurring biopolymer derived from a variety of living species such as plants, animals, bacteria and some amoebas. An attractive source of cellulose for industrial use is agricultural waste, as this use does not endanger food supplies and improves the rural economy (Chen et al. 2012; Lavoine et al. 2012). It is a classic example of a renewable and biodegradable structural plant polymer which can be processed into fibrils (Mohamad et al. 2013). Cellulose structure is organized into fibrils, which are surrounded by a matrix of lignin and hemicelluloses. There is a wide range of cellulose particle types that are being studied for various commercial applications. The diversity of cellulose

particle types depend on cellulose source and extraction processes (Brinchi et al. 2013).

Cellulose and hemicelluloses are polysaccharides having different monomer compositions and molecular arrangements as shown in Fig. 1. Cellulose is formed by cellobiose units (glucose dimer), and has no branched chains with high values of degree of polymerization and high crystallinity. Hemicelluloses are composed of different sugars precursors, have branched chain, rather low degree of polymerization compared to cellulose and are essentially amorphous.

Habibi et al. (2010) reported that the worldwide production of this biopolymer is estimated to be over 7.5×10^{10} tones each year. Of this, according to Lavoine et al. (2012) only about 6.0×10^{9} tones are processed by industries such as paper, textile, material and chemical industries (Figs. 2, 3).

In nature, cellulose does not occur as an isolated individual molecule in nature and is found as assemblies of individual cellulose chain-forming fiber cell wall. The microstructure of plant cell wall includes primary walls (the outer part which is very thin and generally less than 1_m) and secondary wall which consists of three layers
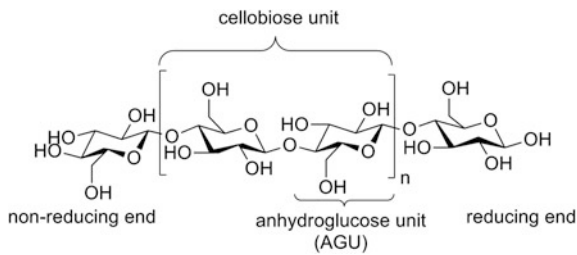

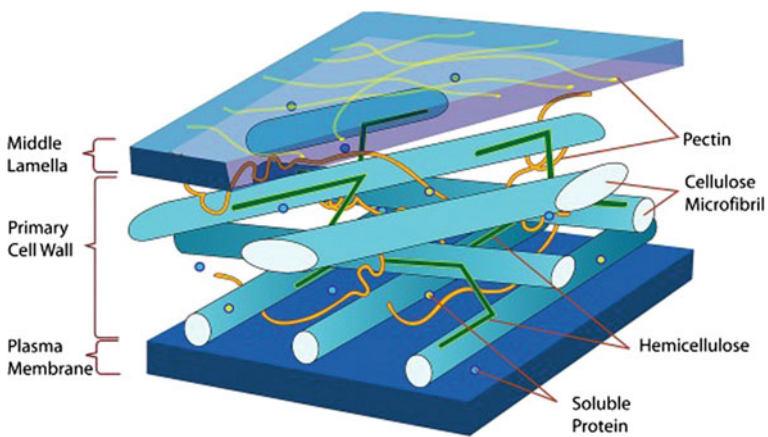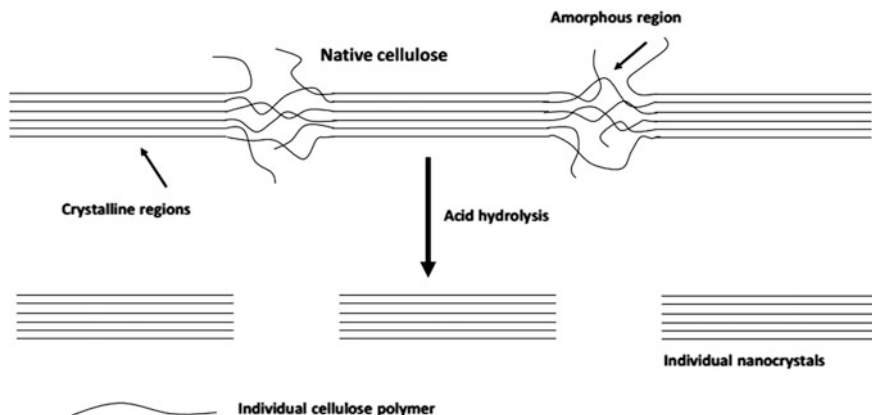Fig. 1 The cellulose polymer chain Structure

Fig. 2 A schematic diagram of plant cell wall structure

Fig. 3 Schematic of crystalline part of cellulose. (*Source* I. Filpponen, Hoeger, Lucia, Laine, and Rojas 2010)

(this layer contribute to the overall properties of fibers). The secondary layer is composed of microfibrils and these microfibrils include amorphous and crystalline regions. The size of crystal in lateral direction is around 5–30 nm and along the axis it is between 20 and 60 nm (Brinchi et al. 2013).

The morphological hierarchy in nanofibrillated cellulose (NFC) is labeled as elementary fibrils, which plug into larger units called microfibrils, which are then in turn assembled into fibers. This microfibrillar aggregates which allow the creation of highly ordered crystalline region form the core alternate with disordered amorphous domain which present at the surface. It is these crystalline regions that are extracted, resulting in nanocrystalline cellulose. The inter- and intra-molecular interactions networks and the molecular orientations of crystalline regions can vary, giving rise to cellulose polymorphs or allomorphs (Lavoine et al. 2012).

Nanocrystalline cellulose (NCC) are needle-shaped cellulose particles with It has relatively lower aspect ratio having a typical diameter of 2–20 nm. The length varies between 100 nm to several micrometers (Brinchi et al. 2013). The particles are 100 % cellulose and are highly crystalline varies between 54 and 88 % crystalline zones. The degree of crystallinity, dimensional diversity and morphology depends on the source of cellulosic material and preparation conditions as well as on the experimental technique used (Brinchi et al. 2013).

2.2 Carbon Nanotubes

Carbon nanostructures including fullerene (buckyballs), carbon nanotubes (single wall and multi wall), carbon nanofibers, carbon nanoparticles and graphene

nanosheets have been widely investigated due to their excellent physicochemical, mechanical and electrical properties (Dai 2006; Tasis et al. 2006). The allotropic behavior of carbon arises from different bonding states representing sp^3, sp^2, and sp hybridization. In general, the degree of carbon bond hybridization-n (sp^n) determines the structure of carbon nanomaterials and their functional properties (Dai 2006). Carbon nanotubes have been synthesized using many methods, among them (i) arc-discharge, (ii) ablation using laser (iii) chemical vapor deposition, (iv) high pressure of carbon monoxide are found to be most popular. In 1991, Sumio Iijima first demonstrated the arc discharge process for the fabrication of carbon nanotubes using two graphite rods with different potentials, which is kept in an argon filled enclosure. The optimum distance between anode and cathode caused the formation of arc. After a minute, carbon nanotubes can be collected on the cathode. Laser ablation was first used to grow high quality nanotubes by Guo and co-workers in 1995. In this process, a high intense laser pulse is used to ablate a carbon target, which is kept in argon filled tube-furnace at very high temperature of 1200 °C. Carbon nanotubes can be collected as deposition on the furnace wall. In chemical vapor deposition, a substrate coated with metal or metal oxide catalysis is heated up to 700 °C. Growth of carbon nanotubes occurs when the gaseous hydrocarbon (acetylene or methane) passes through along with the carrier gas (nitrogen or hydrogen or argon). An added advantage of chemical vapor deposition is the control of multi/single walled architectures in nanotubes through the suitable pre-treatment of the substrate surface. Constructive developments have been made on the chemical vapor deposition process for the development of carbon nanotubes, which promoted this process as a common one for industrial purposes. Among all of the above mentioned techniques, chemical vapor deposition has been established for industrial scale synthesis of carbon nanotubes with desired structures. Carbon nanotubes find many applications that include polymer nanocomposites, electrochemical energy storage/conversion, catalysis, hydrogen storage, health and environmental hygiene products and electronics. In polymer nanocomposites they have been utilized as high performance functional fillers, which not only improved thermal/mechanical performance but also provided additional functionalities such as fire retardant, moisture resistance, electromagnetic shielding and barrier performances. The field of polymer nanocomposites with carbon nonmaterial has highly diversified; carbon nanotubes based polymer composites have been widely explored in many aspects as described elsewhere. An exponential growth on polymer nanocomposites reinforced with carbon nanotubes occurred after the first research work published by Ajayan et al. This is happening not only because of their well-studied properties but also due to the advancement in recent years on their fabrication techniques at industrial scale. Especially for polymeric composites, carbon nanotubes impart several advantages: (i) versatility as reinforcement in both thermoplastic and thermoset regime (ii) extremely high theoretical/experimental tensile strength (150–180 GPa) and modulus (640 GPa to 1 TPa) (iii) one dimensional electronic structures, which enable significantly non scattering electron transport (iv) their compatibility with other chemical compounds, metal/metal oxides/chalcogenides nanoparticles and polymeric materials. Researchers have

effectively utilized these advantages of carbon nanotubes for the development of various composites systems from renewable resource based polymeric materials. Cao et al. reported the fabrication of plasticized starch/multiwalled carbon nanotubes composites with improved thermal, mechanical and water absorption properties. Improved performance of PLA bioplastic was reported by many researchers by reinforcing it with single wall and multiwall carbon nanotubes. Carbon nanotubes have also been utilized for the enhancement of polyurethane foams. For example, Liang et al. reported ~ 25–30 % property enhancement of soybased polyurethane foam reinforced with 0.1–1 % carbon nanotubes. A recent study on the carbon nanotube/epoxy soy oil composites was performed by Thielemans et al. in order to evaluate the ability of MWCNTs dispersion with their increasing content. Their research investigation found that composites displayed significant improvements in mechanical properties even at very low amounts of reinforcement of 0.28 wt%. They also identified that the addition of a higher weight fraction of carbon nanotubes to epoxy systems caused the agglomeration of fiber bundles. Reinforcement of carbon nanotubes into various polymer systems not only provides improvement in mechanical and thermal properties but also creates additional functional properties. Hapuarachchi et al., demonstrated multiwall carbon nanotubes as a successful flame retardant agent for PLA and their natural fiber reinforced biocomposites. They found a 58 % reduction in heat releasing rate (HRR) due to the addition of multiwall carbon nanotubes compared to virgin PLA. The development of high aspect ratio carbon nanotubes with better conductive properties created a new application for their polymer composites in electromagnet interference shielding and numerous reports were published on this aspect in different thermoplastic and thermoset platforms. Thomassin et al. demonstrated the exceptional EMI shielding properties of MWCNT reinforced poly(ε-caprolactone) nanocomposites. However, such research on renewable resource based biopolymer/CNT composites has not been extensively explored. One of the critical issues in the fabrication of CNT/polymer nanocomposites is their dispersion in a polymer matrix, as CNTs have the tendency to form agglomeration and remains in bundles because of their high aspect ratio and strong van der Waals interactions. In order to enhance their solubility, various attempts have been made: (i) oxidation of their surface by acid treatment (this will generate the carboxyl and hydroxyl groups), (ii) creation of long alkyl/polymer chains or biomolecules onto carbon nanotubes and (iii) physical treatments of sonochemical oxidation and plasma modification. An effective improvement on the surface functionalities of carbon nanotubes and their dispersion through fluorination was reported by Zhu. Eitan et al. demonstrated the functionalization of carbon nanotubes with epoxide-based functional groups for the effective reinforcement of the polymer matrix. Quantitative titrations were performed in order to confirm the attachment of epoxide-based functional groups on carbon nanotubes. Tseng et al. effectively demonstrated the plasma modification of carbon nanotubes for the fabrication of covalent-integrated epoxy composites. They also reported the improved mechanical and conductivity properties through the reinforcement of plasma modified carbon nanotubes. These functionalities will enable the compatibility of carbon nanotubes

with various polymeric matrixes and enhance the effectiveness of load transfer between polymer matrix and carbon nanotubes. Recent interest on carbon nanotubes has turned to combinations with various types of inorganic nanomaterials (metal/metaloxides/chalcogenides) and the resultant polymeric composites show additional properties, which enable diversified applications. Zhao et al. reported the microwave absorbing property of epoxy composites reinforced with functional carbon nanotubes combined with Ni and Ag. Their extensive research found that the microwave absorption of metal coated CNTs/epoxy composites was contributed by both the dielectric and magnetic losses of composite material. Ma et al. found that the incorporation of carbon nanotubes filled with silver nanoparticles into polymer matrices enhances their electrical conductivity significantly. Such high conducting polymer composites have potential applications in electronic industries. Such innovative developments will provide the opportunity for carbon nanotubes as high performance multi-functional fillers for new biobased composite systems.

2.3 Nanoclays

Layered silicates also known as nanoclays are most commonly utilized nanofillers in the synthesis of polymer layered silicate nanocomposites. Among these layered silicates, phylloscilicates (2:1) are extensively used in preparing clay based nanocomposites. The crystal arrangement in the silicate layers is made up of two tetrahedrally coordinated atoms amalgamated to edge-shared octahedral sheets. These sheets are made up either magnesium or aluminum hydroxide. These layers have thickness of 1 nm and their tangential dimensions range from 300 Å to a few microns. The variation in the dimensions depends on clay source, particulate silicate and preparation technique. Hence, these layers have a very high aspect ratio (length/thickness) and surface area. The van der Waals gap between these layers is due to the regular stacking of the layers; this gap is known as inter gallery spacing. The negative charges generated by isomorphic substitution (for e.g. Mg^{2+} replaced by Li^{1+}) within the layers are countered by inter-gallery alkali and alkaline cations. Generally, a moderate surface charge is found be associated with these layered silicates which is known as cation exchange capacity (CEC). CEC is commonly denoted as mequiv/100 gm. Also, CEC is not a constant value, but varies with layers and generally average values are considered. The end properties of nanocomposites are influenced by the dispersibility of silicates into their individual layers in the matrix. The dispersibility of layered silicates into individual layers is governed by its own ability for surface modification via ion exchange reactions that can replace interlayer inorganic ions with organic cations. Renewable polyesters are mostly organophilic compounds, while the pristine silicate layers are miscible only with hydrophilic polymers. The silicate layers can be made miscible with hydrophobic polymer by introducing/exchanging interlayer cations galleries (Na^+, Ca^{2+}, etc.) of layered silicates with organic compounds. Generally, phosphonium or ammonium cations with at least one long alkyl chain are used for this purpose. Ion

exchange silicates with organic cations results in an increased interlayer spacing due to bulkiness of alkyammoniums. These alkyammoniums cations can even provide certain functional groups that can initiate polymerization in presence of monomers and also they can compatibilize polymer matrix. The conducive chemical environment in the interlayer helps in the intercalation of polymer chains. Conversely, the organic modification improves both compatibilization between hydrophilic clay and hydrophobic polymer matrix and also increases interlayer spacing. Moreover, organic cations can be used as silicate-attached initiators or mediators for polymerization, thus providing a mechanism for improving interfacial adhesion between matrix and the silicate and a route for effective stress transfer. The separation between clay layers increases with the surfactant chain and charge density of the clay. A study on organoclays modified with alkylammonium chain lengths showed that higher the chain alkyamine chain length greater is the improvement in the interlayer spacing. This study also found that when same nanoclay was organically modified with alkyammoniums chain with 12,16,18 and 20 carbon atoms, the increase in the interlayer spacing increased were found to be 1.36, 1.79, 1.85 and 2.47 nm, respectively. These clays that are modified with organic ions are also known as organomodified layered silicates (OMLS). This way, it is feasible to compatibilize both polymer and the silicates and thereby improving the end properties of the nanocomposites.

3 Nanocomposites from Renewable Resources

Expansion of nanotechnology in recent years has influenced the scientific, technical and economical competitiveness of renewable resource-based polymers in developing a range of high performance engineering/consumer products. Recently scientists/engineers from academia and industries are investigating the use of nanostructures (cellulose nanostructures, carbon nanotubes and nano clays) as reinforcements in order to produce a new class of bionanocomposites. The inherent properties of these nanoparticles in enhancing the thermal, mechanical, dimensional stability and other types of functional properties (electrical/electromagnetic shielding/barrier/fire retardant/triggered biodegradability/solvent resistance) of the composite materials with the added advantages of eco friendliness were effectively utilized to create new class of materials. They also provide additional advantages like ease to process, transparent, low density and recyclable. These nano enabled functional properties are achieved by those biobased nanostructures due to their larger surface to volume ratio, improved surface reactivity at nano regime and molecular level distribution in the polymeric matrices. Many of these properties are precisely controlled by the size and the morphology of reinforced nanomaterials, which will enable tuning of desired properties for high performance applications including biomedical, sensor, and transducer, with relatively low concentration. In addition to materials development, deeper research should be focused on diversified application fields with prospects for commercialization of these novel bio

nanocomposites. Cost reduction and awareness of toxicological and environmental impacts of these nanocomposites should also be addressed. In this review biocomposites are classified into following major categories depends on the polymer matrix such as (i) nanocomposites based on starch plastics, (ii) nanocomposites using polylactic acid (PLA), which is synthesized using biomass-derived monomers, (iii) nanocomposites fabricated using polymers produced micro-organisms (polyhydroxyalkanoates (PHA)) and (iv) nanocomposites formulated using petroleum based biodegradable plastics. Further it can also be classified into various classes depending of the reinforced nanomaterials. This section describes a few important categories of bio-nanocomposites based on the reinforcements that are fabricated from various biobased plastics.

3.1 Cellulose Nanocomposites

The importance of cellulose nanocomposites arises from the unique properties of cellulose nanomaterials such as structural stability against various processing windows, excellent mechanical properties in terms of Young's modulus (about 138 GPa) compared to other lignocellulosic natural fibers (35–45 GPa for flax fiber) and very low coefficient of thermal expansion in longitudinal direction (10–7 K^{-1}). Structures of cellulose nanofibers are stabilized by hydrogen bonds with high levels of crystallinity, which makes cellulose nanofibers an ideal reinforcing material in polymeric materials. In general, cellulose nanocomposites made using renewable resource based biopolymers exhibit superior thermal, mechanical and barrier properties with minimum reinforcement (~ 5 wt%) compared to macro reinforcements with the added advantages of recyclability and biodegradability. Biopolymers of polysaccharides and proteins have been widely investigated due to their advantages of eco friendliness and biodegradability. The major challenge for their sustainability is their poor moisture resistance at higher humidity conditions. Incorporation of nanostructured materials with high aspect ratio as reinforcements reduced water-permeability compared to virgin matrix. In contrast, use of cellulose nanostructures into vast ranges of polysaccharides and protein biopolymers result in enhanced moisture resistance without compromising their immense advantages of biodegradability. Processing of starchbased materials with nano structured cellulose by traditional melt processing is always critical as the agglomeration of fiber materials has to be presented/controlled. Very few research reports are available on conventional melt processing of starch/cellulose fiber nanocomposites. Teixeira et al. reported the incorporation of nanofibers derived from cassava bagasse into cassava based starch thermoplastic. They were successful in employing a torque rheometer to study the effective dispersion of nanofibers in starch matrices. They also investigated the melt processing of thermoplastic corn starch with cotton derived cellulose nanofibers using a twin screw extruder. Their studies indicated that the existence of residual sugars and the plasticization of starch had heavily influenced the performance of the nanocomposites. Solution casting of

thermoplastic starch with cellulose nano fibrils derived from various renewable resources like wheat straw and flax was also explored for the fabrication of novel green nanocomposites. Cellulose based nanostructures has been utilized for improving PLA's. Microcrystalline cellulose (MCC) is the best source for cellulose nanowhiskers; however, dispersion of MCC into individual fibers is difficult especially in melt processing. Mathew et al. reported that the reinforcement of MCC in PLA processed through twin screw extrusion resulted in the retention of MCC as bundles and reduced in the mechanical properties. However, Nakagaito et al. experimented with the reinforcement of microfibrillated cellulose (nano to submicron wide fibers) in PLA through a solvent casting process, and concluded that cellulose was a promising reinforcing material. In order to address the challenges in melt compounding of cellulose nanofiber/nanowiskers, Oksman et al. developed a novel technique for the industrial scale processing of cellulose nanocomposite. They were using N,N-dimethylacetamide (DMAc) and LiCl as separation agent. It was found that the mechanical properties were not increased compared to virgin PLA, which is due to the presence of additives and unsuitable processing temperatures. Reinforcement of cellulose nanostructure into PLA creates a diversified impact that includes improvement in barrier properties, nucleation effects and foam formation. SanchezGarcia et al. reported the barrier properties of PLA/cellulose nanowhisker composites. Their research ensured that the addition of 3 wt% cellulose nanowhiskers into PLA was able to reduce the water and oxygen permeability by 82 % and 90 % respectively. Cellulose nanowhiskers acted as shield in PLA and caused the crystallinity development, which resulted in high barrier properties. Effects of microfibrillated cellulose-reinforcement in PLA on crystallization were studied by Suryanegara et al. They found that the microfibril acted as nucleating agent and altered the crystallization behavior of PLA, which resulted in the enhancement of storage modulus up to 1 GPa. Boissard et al. demonstrated the water functionalized microfibril cellulose as a foaming agent, and the formation of foamy PLA biocomposites with the lowest density of 0.49 g/cm^3. Water molecules absorbed in the microfibril cellulose were converted into vapor during the melt processing, serving as a blowing agent and causing the foam formation. Cellulose nanofibers that are produced by bacteria have been effectively used to tailor the surface of natural fibers for the development of hierarchical reinforcement. Pommet et al. developed a novel method to modify the surface of natural fibers with nanosized bacterial cellulose though the high number of hydrogen bonds. Furthermore, the reinforcement of modified natural fibers into PLLA created the new class of hierarchical composite with the enhanced properties. The technical challenges for PHA are its narrow processing window and high brittleness. This has been addressed by forming the copolymer of with valerate resulting in PHBV that exhibit lower crystallinity. The lower crystallinity of PHBV can be addressed by reinforcing it with nanostructured materials that can act as nucleating agents and result in enhanced crystallinity. Among them, cellulose nanostructures play a remarkable role in enhancing the performance of PHBV. Nanocomposites of PHBV/cellulose nanostructures were first reported by Jiang et al. using cellulose nanowhiskers as reinforcing material. In this study, a solution casting process was

used to fabricate PHBV/CNW composites and the obtained results were compared with the extrusion/injection molded samples. The extrusion process caused CNW agglomeration and resulted in reduced properties compared to the composite samples prepared using solution casting. Ten et al. reported the solution casting processing of PHBV/CNW nanocomposites using polyethylene glycol (PEG) as a compatibilizer between fiber and matrix. They confirmed the nucleating effect of cellulose nanowhisker and their positive impact in increasing their mechanical properties. Effects of CNW on other properties of PHBV such as dielectric and rheology were recently reported by Ten et al. The agglomeration of cellulose nanowhiskers in PHBV/CNW reflects in the reduction of real permittivity. In addition, the rheological analysis of PHBV/CNW composites exhibits a lower transition point (1.2 wt%) due to the possibility of PHBV-CNW network formation without geometrical overlapping.

3.2   CNT Nanocomposites

In general carbon nanostructures (including carbon nanotubes, nanofibers and graphene sheets) exhibit a range of properties, such as higher electrical conductivity, enhanced mechanical strength and better thermal behaviour, which make them desirable reinforcing materials for polymer nanocomposites. Especially carbon nanotubes receive more attention due their uniqueness in efficient load transfer, which arises from the enormous surface area and high aspect ratio. Mechanical behavior of carbon nanotubes composites is influenced by carbon nanotubes type, geometry of the carbon nanotubes and polymer nature (amorphous/crystalline/ semicrystalline), and the processing method (in situ polymerization/solvent casting/melt processing). In addition, other key factors in improving the properties of CNT based composites are the adhesion between carbon nanotubes and the polymer matrix, which can be tuned by imparting different functional groups on the walls of carbon nanotubes. The homogenous dispersion of nanotubes in the polymer matrix also helps in improving the properties. In bioplastic based composites, carbon nanotubes play a vital role in enhancing their thermal, mechanical, electrical and crystallization properties along with their biodegradation. In starch based plastic materials utilization of carbon nanotubes as nano reinforcement is limited by their effective distribution. One of the successful methods of dispersing CNTs into a starch matrix is functionalization. Famá et al. investigated the fabrication of starch/multi-walled carbon nanotubes composites and reported their improved mechanical properties. They were successful in dispersing MWCNTs into a starch matrix by adopting new strategies to wrap the carbon nanotubes surfaces with a starch–iodine complex. This also creased a strong adhesion between nanotubes and starch matrix, which caused an effective load transfer that improved their mechanical properties. They were able to achieve a 70 % increment in the stiffness with the MWCNTs reinforcement of only 0.055 wt%. Another investigation of Famá et al. on starch based nanocomposites using MWCNT modified with

starch–iodine complex resulted in lower water permeability with high storage modulus. These enhanced properties were obtained due to the uniform dispersion of MWCNT caused by the coating of same material that has been used for matrix. Liu et al. reported the effective usage of glycerol for the dispersion of MWCNTs in water solution, which lead to the formation of homogeneous thermo plastic starch/MWCNTs nanocomposites by a solution casting method. A significant improvement in pasting viscosity as well as thermal stability was observed on the thermo plastic starch by the effective reinforcement of MWCNTs. Improved electrical conductivity of glycerol plasticized starch polymer by the incorporation of MWCNT was reported by Ma and co-workers. A minimum reinforcement of MWCNT of about 4.75 wt% enhanced their electrical conductivity to 10° S/cm, which indicates that the starch/MWCNT nanocomposites would be a promising alternative to novel electroactive polymeric materials. This will also create a potential opportunity for such novel materials in various applications including biosensor, artificial muscles, and electronic shielding. As global research is moving towards the diversification of PLA based products, it is necessary to enhance their crystallization behaviour in order to achieve required thermal and mechanical properties as well as industrial scale processability. It is well understood that the crystallization kinetics of PLA obeys different mechanisms governed by various chemical and physical environments. In addition it also depends on the nucleating agent and its interface with the PLA matrix. Wu et al. studied both melt and cold crystallization of PLA/CNT composites and compared the obtained results with their biodegradation. They found that the addition of CNT to PLA plays dual roles as nucleating agent and physical barrier. Their results indicate that the addition of carbon nanotube to PLA accelerates the melt crystallization and hinders the cold crystallization. In addition, they identified that the composite samples with cold crystallization history exhibited higher degradation compared to the composite with melt crystallization history. This suggested that the crystallization behavior significantly influences the biodegradation. Xu et al. reported the improved nucleation effect of acid oxidized carbon nanotubes in PLA and investigated the effect of different aspect ratios of carbon nanotubes. Their result indicates that the addition of acid oxidized MWCNT increases the nucleation density of PLA. Comparing the effect of MWCNT with two different lengths, the lowest (0.5–2 μm) increase the nucleation density of PLA significantly since they offer more nucleating sites than MWCNT with 30 μm. Recent interest in the fabrication of porous structure in plastics, which contributes in altering their physical properties significantly along with material and cost savings, motivated the fabrication of porous PLA/CNT nanocomposites. Rizvi et al. developed the porous polylactide-multiwall carbon nanotube composites using two-stage batch foaming. They were able to obtain porous PLA-MWNT composites with highly expanded cores and denser skin. Increasing MWNT content caused the rise in degree of expansion compared to neat PLA. Addition of nanomaterials to PLA significantly improves the flame retardancy. Bourbigot and their research team investigated the reactive extrusion of PLA and its CNT nanocomposites using L,L-lactide precursor and catalysis in a co-rotating twin screw extruder and investigated their flame retardancy. They found

slight improvements in their flame retardancy. PLA fiber products are in large demand in packing, suture, and biomedical industries. In general, PLA fibers were prepared by melt spinning and solution spinning, which result in micron scale fibers. As the demand grows for nanosized fibers in many fields, the electrospinning process becomes a simple and versatile tool for the fabrication of many polymer fibers including PLA. Yang et al. reported the successful fabrication of polylactide/CNT composite fiber using electrospinning technique. His study indicated that the morphology of PLA/CNT composite fiber strongly depends on the solution concentration as well as solvent. The major issue in expanding commercial opportunities for PHB and related polymer materials is their crystallization behavior. Reviewing the work of PHB based blends, there is not much work has been done on the crystallization of PHB/CNT nanocomposites. Carbon nanotubes have been widely used as an excellent nucleating agent in PHB polymers and enhanced their crystallization properties. Xu et al. prepared PHB/MWCNTs nanocomposites and investigated the effect of various MWCNTs loadings on their thermal behavior, morphology and also kinetics of isothermal crystallization. They identified the heterogeneous nucleation effect of MWCNT, which improved the nonisothermal melt crystallization of PHB. Yun et al. reported the fabrication of PHB/CNT composite film for biomedical applications. They also studied their mechanical properties and found that the hardness and Young's modulus increased significantly with the addition of SWCNTs and resulted in the formation of film with more brittleness than the neat PHB films. This result confirms the nucleating effect of SWCNT on PHB polymer. Sanchez-Garcia et al. studied the solution casting synthesis of PHBV/CNT nanocomposites films and investigated their conductivity, thermal, mechanical and gas barrier properties. It was found that barrier, conductivity and mechanical properties of PHBV/CNT nanocomposites increased with 1 wt% carbon nanotubes. Shan et al. employed melt mixing process for the fabrication of PHBV/MWCNT nanocomposites and studied their crystallization process. They observed that the addition of CNT with PHBV increased the nucleation density of crystals and caused formation of smaller spherulites. Vidhate et al. reported the improved mechanical and electrical properties of PHBV/MWCNT nanocomposites fabricated by melt mixing. Their report indicated that the addition of MWCNT increases the recrystallization temperature significantly, which is about 70 % compared to virgin PHBV, and it varied substantially with the increase in MWCNT content in the composite.

3.3   Clay Nanocomposites

Bioplastic–clay nanocomposites have been receiving extensive attention due to their improved thermal, mechanical and barrier properties as well as reduced flammability compared to their respective virgin polymers. Nanoclays has been discussed above also. These clay materials were classified into many types based on their chemical nature, structure and their unique properties of swelling as well as

exfoliation. In composite fabrication montmorillonite, hectorite and saponite are the three most commonly used nanoclay minerals, which belong to the smectites family. Montmorillonite, saponite and hectorite are the three most commonly used nanoclays in the synthesis of polymer nanocomposites, these nanoclays belong to smectites family. Enhancement of polymer properties by individual clay layers can be obtained through their high aspect ratio and interfacial interactions with polymer networks. Also it requires very minimum reinforcement of about 3–6 wt% in order to achieve significant enhancement in their tensile and other physical properties. Versatility of layered silicates (clays) in composite fabrication is one of the most important composite fabrications not only due to their availability, low cost, and significant enhancement of properties but also their simple processability as well as adoptive nature with both thermoset and thermoplastic systems. Polymer–clay nanocomposites were commonly prepared by three different techniques. Starch based biodegradable materials have attracted tremendous interest for many applications, because of their cost effectiveness, easy availability, and their renewable origin. However, their applications have been limited due to their poor processability, weak material properties, lower moisture barrier and higher humidity sensitivity. Numerous research efforts address these issues/drawbacks to achieve better performance of starch-based biomaterials. The first starch–clay composite was made by Carvalho et al. using melt intercalation techniques. They showed that the starch-clay composite filled with 50 phr kaolin (clay) increased the tensile strength from 5 to 7.5 MPa and also reduced the water uptake. Thereafter several research works have explored starch/clay nanocomposites. Gao et al. investigated starch–clay nanocomposites using various clay materials with different hydrophilicities by the film blowing method. The properties of starch-nanoclay films were greatly influenced by the hydrophilicity of the clay, this study found that medium range hydrophilicity favored the nanocomposite formation. Zhang et al. investigated the thermal behaviour, morphology and crystallinity of starch/clay nanocomposites and compared the properties of composites made with pristine and organically modified clays. From this study, it was identified that the pristine clay enhanced the onset and maximum degradation temperatures of starch plastic, however modified clay enhanced the onset degradation temperature alone. A change in crystalline structure from B-type into Va-type was observed after melt extrusion. Over all they found that the compatibility is essential in addition to d-spacing of nanoclay for better intercalation. Magalhães et al. demonstrated the extrusion of glycerol-plasticized corn starch plastic with two types of clay with various formulations and investigated their processability as well as biodegradation. Their soil burial tests indicate that the addition of the clay enhanced their biodegradation rate compared to virgin starch plastic. Their detailed investigation revealed that the biodegradation of nanocomposites was influenced by their relative crystallinity as well as hydrophilicity. The challenge in establishing the food packaging technology with starch–clay nanocomposites is to understand the effect of food-nanocomposite contact. Avella et al. fabricated the biodegradable starch/clay nanocomposite films and extended their research for food packaging applications. This research revealed that optimum intercalation of polymeric chains into clay has enhanced the modulus

as well as tensile strength of the nanocomposites. They also performed the migration and food contact testing and confirmed that their samples are compatible with the European regulations and directives on biodegradable materials. PLA is becoming an attractive alternative to conventional polymers in many applications, however its processing window and barrier properties needs to be enhanced to widen its application window. Among most of the nanofillers, nanoclays are found improve the material properties and processing windows of the polymer even at a very low filler loading at 1 wt%. Rhim et al. processed PLA/clay nanocomposite films and investigated their tensile, moisture barrier and antimicrobial properties. They reported the increased moisture barrier properties suitable for food and beverage packaging. Their conclusion indicated that in PLA/clay nanocomposites the concentration of clay plays an important role in enhancing their properties. Wu et al. investigated melt rheology and thermal behavior of PLA/clay nanocomposites. Their study indicated the solid-like behaviour of composite material when the clay loading reaches 4 wt% or high, which indicates the percolation threshold of about 4 wt%. It is well known that PLA exhibits less flexibility and breaks down even at low deformation. Reinforcing clay with PLA further increases their stiffness, which is undesired for some featured applications. This can be overcome by its plasticization; Pluta et al. performed the plasticization of polylactide and fabricated their clay nanocomposites, and they were successful in reducing the brittleness of PLA. Tanoue et al. used poly (ethylene glycol) as plasticizing agent for PLA and fabricated the organoclay nanocomposites by melt processing. They investigated two different types of poly(ethylene glycol) with different molecular weights (2000 and 300,000–500,000). They found that the poly(ethylene glycol) with the molecular weight of 2000 is a good plasticizer for PLA in improving mechanical properties. Commercialization of PHB/HV copolymer and their composites can be achieved by improving their crystallization/processing behaviors, cost reduction and property enhancement. One possible approach is the reinforcement of layered clay nanostructures into polymer matrix. The major advantages of nano reinforcement are the possibility of significant enhancement of mechanical properties with a small amount of clay, along with complementary barrier properties, which is not possible using conventional glass fiber reinforcement. Choi et al. fabricated the PHB/HV–organoclay nanocomposites employing melt intercalation methods. They were successful in obtaining an intercalated structure, which is driven by the strong hydrogen bonding between polymer matrix and the nanoclay. Nanoclay played the role of nucleating agent and caused the enhancement of crystallization rate. Chen and his research team investigated the crystallization kinetics of PHBV/clay nanocomposites and reported that the addition of nanoclay enhanced the crystallization rates. However, it was found that the crystallization rate reduced with increase in clay content. Melt intercalation was employed by Bordes et al. for the fabrication of PHA/clay nanocomposites and the nucleating effect of clay and their influence in crystal size of PHA was reported. Three different techniques namely solvent casting, extrusion and melt mixing were compared for the fabrication of PHBV and clay nanocomposites by Cabedo et al. Solvent casting or melt mixing method of composite fabrication enabled the

Table 1 Physical properties of polymers

Property	Types of biopolymer				
	PLA	L-PLA	DL-PLA	PHB	PHBV
Density (Kg/m3)	1210	1240	1250	1180	1250
Tensile strength (MPa)	21	15.5	27.6	40	–
Young modulus (GPa)	0.35	2.7	1	3.5	0.9
Elongation (%)	2.5	3	2	5	15
Tg (°C)	45	55	50	5	5
Tm (°C)	150	170	–	168	153

formation of intercalated morphology, whereas melt blending result in sub-micron aggregates. PHBV degraded significantly during melt intercalation and this was influenced by filler concentration and residence time. The ultimate solution to control this degradation is using nitrogen gas environment during melt processing. It is well known that the compatibility between nanoclay and the polymer plays an important role in achieving the improvement in the nanocomposite properties. In order to enhance the compatibility between clay nanostructure and PHB matrix, Parulekar et al. experimented with the titanate modification of montmorillonite clay and obtained improved mechanical properties. They found that the addition of 5 wt% titanate-modified clay loading results in about 400 % improvement in impact properties in compared with virgin PHB. In addition the toughened and compatibilized PHB exhibits poor biodegradation compared to virgin PHB, which was enhanced several-fold by incorporating titanate-modified clay. Delamination of clay layers into individual layers and uniform dispersion in the matrix are the major challenges in nanocomposite fabrication. Organic cations such as distearyl dimethyl ammonium chloride and quaternary ammonium modified starches etc., are applied to improve the dispersion of nanoclay. Achieving miscibility and nanoclay dispersion are challenges till date (Table 1).

4 Applications

4.1 Packaging

Bioplastics suffer from three main disadvantages which are performance, processing, and cost compared to the petro-plastics. Narrow processing window, poor gas and water barrier properties, unbalanced mechanical properties, low softening temperature and weak resistivity of the plastics has limited their use in wide range of applications. As discussed previous sections, nanotechnology helps in overcoming these problems. Nanofillers help in improving the above discussed properties of the bioplastics. Bionanocomposites exhibit remarkable improvement compared to the neat matrix and conventional composites due to nano

reinforcements. Permeability properties apart from tensile properties are considered as the most important parameters in selecting materials for food packaging applications. High barrier to gases and vapours are key attribute found in glass and metal based packaging, the polymers are expected to perform on par with these materials. Polymers provide excellent balance in properties including mechanical, thermal and barrier properties. It is well recognized that the incorporation of nano-fillers especially nanoclay into the polymeric matrix can lead to significant enhancement in the barrier properties. This improved barrier properties in nanocomposites is explained on the basis of increased path length due to the presence of nanofillers that the same molecules needs to traverse while diffusing through the matrix. In nanoclay based nanocomposites, the clay layers create a more tortuous diffusive path and delays the transfer. Also the barrier properties of bionanocomposites depend on the orientation and the nanofillers state of dispersion in the polymer matrix. Nanoclays are more effective nanofillers compared to fibrillar nanocellulose for improving the barrier properties. Nanoclay based bionanocomposites have gained more importance by the packaging industry, due to the ease of availability, processing, and low costs compared to other nanocellulose, carbon nanotubes. PLA, PHB and starch based nanocomposites have been attractive for packaging applications. PLA fulfills the requirements for direct food contact with aqueous, acidic and fatty acids. Cups, cutlery and food containers are being manufactured using PLA by many companies. PLA can be laminated to paper and paperboard by extrusion coating for further use as packaging material. The insolubility of PLA in water limits its applications for use in paper products and industrial coatings. PLA is considered as a poor oxygen barrier; however its barrier property is high compared to all other bioplastics. Nanoclay has been used overcome this property of PLA. The effects of different organically modified nanoclays on the oxygen gas permeability of PLA has been studied by Chang et al. Melt intercalated nanocomposites were prepared and it was found that the permeability decreased for all the nanocomposites. In a study conducted by Plackett et al., PLA nanoclay based nanocomposites were studied for their suitability in cheese packaging. This study also showed the both water and oxygen properties have decreased significantly by the incorporation of nanoclay. Furthermore researchers have studied the effect of shear and feed rate on the permeability of PLA nanocomposite based films. It was found that films showed an improvement over PLA matrix. Oxygen barrier properties improved by a 15–48 % for PLA nanocomposites compared PLA. Also, both shear and feed rate had no influence on nanocomposites i.e. barrier properties were independent of these two factors. For neat PLA, the properties were dependent on the processing variables leading to conclusion that processing parameter needs to be optimized for PLA processing. Similar trend was observed for water vapor transmission rate, PLA nanocomposite films displayed a reduction of about 40–50 % in transmission rate. The observed improvement was again independent of processing variables. In case of PHAs their water resistant arises from their highly hydrophobic nature. It is interesting to note that PHAs are suitable for coating and film application. Also, the water vapour barrier property of PHAs is very close to that of the polyethylene, this makes them very attractive materials for the food packaging. However, the poor gas

barrier properties and narrow processing window limits their applications. Sanchez-Garcia et al. investigated the relationship between morphology and barrier properties in PHB/clay nanocomposites. In this study, the nanoclay showed a very high dispersion in the PHB matrix due to the organo modification of the clay layers. This high dispersed state has led to improvement in oxygen, Dlimonene, and water barrier proprieties of PHB/clay nanocomposites. Similarly, thermoplastic starch is also highly sensitive to water due to its high hydrophilicity. This is hindering its application in packaging which can be overcome by using nanocomposites technology. Park et al. focused their attention on water permeability. It appears that the relative water vapour transmission rate (WVTR) of the TPS nanocomposites was reduced by nearly a half compared to the neat TPS at only 5 wt% of montmorillonite. This result leads to exploration of TPS formulations for food packaging applications and protective coatings. The significant reduction in WVTR is attributed to the tortuous pathway created by nanoclay in the matrix. This pathway increases the time required for molecules to travel along the diffusion path, thus decreasing the WVTR. Park et al. also compared the effect of clay modification on WVTR and tensile properties of TPS by using unmodified montmorillonite (Cloisite Na$^+$ TM) and modified montmorillonite (Cloisite 30B TM). Surprisingly, this study revealed that the unmodified montmorillonite TPS showed improvement over modified montmorillonite TPS composites. The reason for observed improvement in unmodified montmorillonite TPS nanocomposites is the higher hydrophilicity of unmodified montmorillonite compared to modified montmorillonite. TPS used in the work is highly hydrophilic and has led to the intercalation along with better dispersion with hydrophilic unmodified montmorillonite than organophilic modified montmorillonite. This study leads to conclusion that the degree of clay dispersion is controls the water permeability rates in the nanocomposites. Cellulose nanofibers were found have the same reducing effect on barrier properties of TPS, this effect is attributed to the increase of the tortuosity induced by the presence of the nanofibers. However, the cellulose nanofibers are not as effective as that of nanoclay probably due to their shape which limits the increment in tortuous path. It is important to note that the decrease in permeability of nanocomposites, there are some contradictory observations in these properties for different solvents and gases. It is well known that the saturation is related to agglomeration phenomena of the nanofillers in the polymer matrix. Most of the times, different morphologies co-exist within the nanocomposites leading to different permeabilites that cause complex transport phenomena. Also, it is well known that the semi-crystalline polymers itself have two regions crystalline and amorphous leading to different permeabilities as crystalline regions are impermeable to penetrant molecules. It is well known that the decrease in the permeability is attributed to tortuous path created by nanofillers which increases the effective path length for vapors and gas molecules. However, these fillers also have an effect on the crystallinity and chain mobility of the polymer matrix leading to the reduction in permeation. Hence, both crystallinity changes and tortuous path has to be taken into consideration for analysing the effect of nanofillers on the permeability of nanocomposites.

4.2 Electronics, Sensor and Energy Applications

Polymers reinforced with engineered/functional nanostructures provide additional electrical, optical, electromagnetic shielding and magnetic properties and lead to the development of various advanced devices including light emitting, diodes, sensors, solar cells, display panels and other medical devices. As the global demand for flexible electronic devices increases polymer nanocomposites, receive extensive attention in developing various devices. Besides, ever-increasing uses of electrical and electronic equipment create environmental issues at the end of their life span and generate enormous waste products (e-waste). As a result, applications of bioplastics and their composites in electronic products are increasing due to their biodegradability and renewability with less environmental impact/carbon footprint. This section summarizes various device applications of bionanocomposites. (i) Advanced electronics: The advantage of cellulose nanofibers in fabricating transparent and flexible composites found wide applications not only for electronic devices such as displays, solar cells and organic light emitting diodes but also for roll-to-roll fabrication techniques. In roll-to-roll technique, continuous deposition of various functional components is facilitated leading to fabrication of electronic devices. The functional components used in this fabrication include metal wiring, active/gas barrier films. This technology has been widely used for the development of the flexible electronic devices. However, the application of this technology for plastic materials (while using as a substrate for active components) suffers due to a high coefficient of thermal expansion (CTE). Nogi et al. reported that the addition of bacterial cellulose nano fibers into polymeric resin caused the reduction in CTE. They also suggested that such new composite materials can be used as the potential substrate for roll-to-roll fabrication. A wide range of research has been performed in order to enhance the thermal and tensile properties of petro/bio based polymeric materials for the purpose of roll-to-roll fabrication. As an example, Petersson et al. reported fabrication of poly(lactic acid)/cellulose whiskers nanocomposites and found that the reinforcement of nanostructured cellulose whiskers enhanced their thermal and mechanical properties. They found that the both cellulose whiskers and their nanocomposites were thermally stable up to 220 °C, which indicating their suitability for various device applications. (ii) Sensors: Polymeric nanocomposites have been identified as suitable candidates to develop flexible sensors due to their advantages such as good electrical performance, simplicity in handling, light-weight, economic benefits, biocompatibility and eco friendliness while using biopolymers. In this perspective, a wide range of polymeric composites were fabricated and investigated with the reinforcement of various electric, magnetic, bio, optical and mechanical sensitive/active functional fillers for the development of various temperature, chemical, bio and humidity sensors. Cellulose based composite films (which are scientifically known as active paper) with active nanomaterials such as gold, silver and carbon nanotubes have been used to construct strain, chemical and bio sensors. Similarly PLA and their carbon nanotube-reinforced composite films were effectively used as the liquid sensing material. Yun et al.,

reported the fabrication MWNTs–cellulose composites as smart paper and demonstrated their application as chemical vapour sensors. Kobashi et al. have investigated the liquid sensing properties of melt-processed PLA/MWCNTs composite films by means of the electrical resistance variance on liquid contact. The sensing performance was optimized through the resistances of the composite due to the solvent transport in the structure. (iii) Electromagnetic shielding: Electromagnetic shielding is the action to block the electromagnetic field by using suitable barrier materials with efficient conductivity and/or magnetic properties. In recent years a number of polymer composites reinforced with high conductive fillers have been reported as EMI shielding materials. Such materials found applications in high performance shielded connectors, scientific/medical/consumer electronic devises and military/security products. Based on the conductivity range, materials can find applications in either electrostatic discharge (ESD) prevention (105–109 S/cm) or electromagnetic shielding (EMI) (greater than 100 S/cm). Profound research work has been reported for EMI shielding application using various types of petro-based polymer composites reinforced with many conducting fillers. Application of renewable resource based biocomposites for this purpose is just budding. Recently, Rizvi et al. reported the fabrication of solid and porous PLA-MWCNT composites and investigated their electrical conductivity. They have obtained low frequency complex conductivity of PLA-MWCNT composites reinforced with 5 % MWCNT that exhibited suitable conductivity for electrostatic discharge (ESD) prevention application. Duan et al. fabricated the polylactide based hybrid nanocomposites using graphite nanosheets and MWCNTs as reinforcement and demonstrated the enhancement of their electrical properties. Such enhancement of electrical properties indicates possible applications for EMI shielding. (iv) Thermoelectric systems: Thermoelectric systems are a very promising technology in harvesting electricity from any kind of heat sources, where the temperature gradient plays major role. Also, they offer additional advantages such as (i) reduced operational noise, (ii) long-term, maintenance-free operation and (iii) simplified structure with the absence of moving parts compared to traditional electricity generating systems. Thermoelectric semiconductors have been widely used for energy conversion; however they face disadvantages due to their expensive synthetic protocol. This motivated researchers to move towards polymer nanocomposites, since they are light and generally require relatively simple manufacturing processes relative to traditional semiconductor based thermoelectric materials. In general biobased polymers are electrical and thermal insulating materials, which could be altered to be highly conductive through the effective reinforcement of conductive carbon fillers. These nanocomposites materials with high electrical and thermal conductivity can be an excellent material for thermoelectric conversion. Antar et al. reported the thermoelectric behaviour of melt processed carbon nanotube/graphite co reinforced poly(lactic acid) composites and found that their thermal and electrical conductivity has increased compared to virgin plastic. (v) Solar cell: Another application of polymer nanocomposites reinforced with conducting carbon nanotubes is flexible photovoltaic cells. In polymer-based flexible photovoltaic cells, the challenging issue is to improve the

conductivity of polymer, which is directly influenced by the conduction of pho-togenerated carriers to the electrodes. Reinforcing high conducting carbon nan-otubes enhances the collecting performance of photogenerated electrons and improves the overall performance of flexible photovoltaic cells. For example, Valentin et al. made a novel approach to develop carbon nanotube based polymer nanocomposites and studied their electrical performance. They concluded that the polymer/SWNTs composite can perform as organic semiconducting material, which can be used to fabricate photovoltaic cells. Landi et al. also characterized the photovoltaic cell based on single-wall carbon nanotube– poly(3-octylthiophene)-(P3OT). Strange et al. have successfully fabricated PLLA–nanoclay composites films as bio degradable substrates for the solar cell application. However, extensive research on biobased polymer/carbon nanotubes composites for high performance photovoltaic applications has not been conducted.

4.3 Bionanocomposites for Medical Applications

The versatility and adaptability of bionanocomposites enable these materials to be utilized for biomedical applications. An essential characteristic of medical bioma-terials is biocompatibility, the ability to function appropriately in the human body to produce the desired clinical outcome, without causing adverse effects. Bionanocomposites are an intuitive choice for medical applications, given that such materials are constructed from bio-derived polymers, and such materials possess tunable mechanical properties. Bio-based polymers are increasingly being recog-nized as biocompatible materials for clinical use. For example, plastics and films made from corn-derived PDO have been shown to be non-cytotoxic and non-inflammatory to clinically relevant cell lines. Moreover, soy-derived polymers have been demonstrated to be useful as bone fillers. Bionanocomposites that combine the tissue compatibility of natural polymers and bio-derived polymers along with the physical and chemical properties of nano reinforcements will find widespread use in clinical medicine. In particular, three emerging areas of medical applications for bionanocomposites are tissue engineering, drug delivery, and gene therapy.

5 Conclusion

This review presents the current status of biobased plastics and their nanocom-posites. The usage of renewable resource based plastics can lead to the reduction of energy consumption and greenhouse gas emissions in certain applications. Biobased plastics are still at an early stage of commercialization, only starch-based bioplastics and PLA are available considerably for packaging and other industrial applications. A renaissance in producing traditional plastics by the use of bio-based

resources has led to new interest in polymers like PTT, PE, PP, PBS, PET and nylons. Advancements in microbial technology have led to the creation of new metabolic pathways to produce monomers/polymers in a cost-effective way. The price of PLA has reduced and currently competes with some petro-based polymers in the market place. It has found uses in various applications due to its renewable nature with added advantages of compostability. Also, many companies have been working on producing traditional polymers via biochemical pathways using renewable resources rather than petro-based resources. The inherent weaknesses of biopolymers are being overcome by different strategies. Bionanocomposites lead to dramatic improvements in the properties of the bioplastics. Addition of nanofillers (nanoclay, nanocellulose, carbon nanotubes and functional nano fillers) helps in tuning the properties of biopolymers as desired. Bioplastics are thermally sensitive and hence solvent-based processing techniques, especially solvent intercalation, have been widely updated for the preparation of bionanocomposites. Also, the irreversible agglomeration of nanocellulose when dried hinders it from being used in melt processing techniques. However, the melt intercalation technique is more industrially prevalent and helps in fine and uniform dispersion of nanofillers in the matrix. Also, to overcome the compatibility issues, often the nanofillers are organically modified using ammonium or phosphonium cations bearing at least one long alkyl chain. Extensive research has been explored for the fabrication of nanocomposites using renewable resource based biopolymers, which exhibit a remarkable increase in their thermal, mechanical and other functional properties (gas barrier, fire retardant, EMI shielding). Also, it is found that the addition of nanostructured fillers with biopolymers enhances their degradation rate significantly. In general, biopolymers experience various issues such as poor environmental stability, lower barrier properties, poor crystallization kinetics and narrow processing window, which inhibits their commercial opportunities. In starch based plastics the challenging issue is their poor stability against moisture, and it has been improved by reinforcing nanostructured fillers such as cellulose nanofibers, carbon nanotubes and nanoclay. It is well known that polylactide has shown much promise towards nanocomposites fabrication due to its cost effectiveness and comparable properties with conventional plastics. In polymer composites, nanostructure fillers act as an excellent nucleating agent and dominate in altering the crystallization behavior. In addition to PLA, PHBV also receives benefits from nanostructured materials as nucleating agents, which improves various properties. Bionanocomposites find great potential in many applications, remarkably in packaging, electronics and biomedical sectors. Currently food packaging films with high barrier properties are being explored. Even the applications of bionanocomposites in various electronic systems are budding, and it is expected to be a vibrant area of research in future. Significant research is in progress to extend the application of these nanocomposites for various consumer electronic systems, aiming at the reduction of global e-wastes. Polymer nanocomposites reinforced with carbon nanotubes show improved electrical conductivity, and extend their application as EMI shielding materials. Bionanocomposites with hydroxyapatite (HA) and layered double hydroxides (LDH) have been explored for various biomedical applications.

Given these functionalities, nanofillers in bioplastics have excellent potential to revolutionize the utilization of nanocomposites and expand their use in high value applications.

References

Brinchi, L., Cotana, F., Fortunati, E., Kenny, J.M.: Production of nanocrystalline cellulose from lignocellulosic biomass: technology and applications. Carbohydr. Polym. **94**(1), 154–169 (2013)

Chen, D., Lawton, D., Thompson, M.R., Liu, Q.: Biocomposites reinforced with cellulose nanocrystals derived from potato peel waste. Carbohydr. Polym. **90**(1), 709–716 (2012)

Dai, L.: From conventional technology to carbon nanotechnology: the fourth industrial revolution and the discoveries of C60, carbon nanotube and nanodiamond. In: Dai, L. (ed.) Carbon Nanotechnology: Recent Developments in Chemistry, Physics, Materials Science and Device Applications, pp. 3–11. Elsevier, Amsterdam (2006)

Doi, Y.: Microbial polyesters. Wiley-VCH, New York (1990). 166 pp

Guo, T., Nikolaev, P., Thess, A., Colbert, D., Smalley, R.: Catalytic growth of single-walled manotubes by laser vaporization. Chem. Phys. Lett. **243**, 49–54 (1995)

Jonoobi, M., Khazaeian, A., Tahir, P., Azry, S., Oksman, K.: Characteristics of cellulose nanofibers isolated from rubberwood and empty fruit bunches of oil palm using chemo-mechanical process. Cellulose **18**(4), 1085–1095 (2011)

Lavoine, N., Desloges, I., Dufresne, A., Bras, J.: Microfibrillated cellulose—its barrier properties and applications in cellulosic materials: a review. Carbohydr. Polym. **90**(2), 735–764 (2012)

Lim, L.T., Auras, R., Rubino, M.: Processing technologies for poly (lactic acid). Prog. Polym. Sci. **33**, 820–852 (2008)

Majeed, K., Jawaid, M., Hassan, A., Abu Bakar, A., Abdul Khalil, H.P.S., Salema, A.A., Inuwa, I.: Potential materials for food packaging from nanoclay/natural fibres filled hybrid composites. Mater. Des. **46**, 391–410 (2013)

Mohamad Haafiz, M.K., Eichhorn, S.J., Hassan, A., Jawaid, M.: Isolation and characterization of microcrystalline cellulose from oil palm biomass residue. Carbohydr. Polym. **93**(2), 628–634 (2013)

Morais, J.P., de Freitas Rosa, M.F., de Souza Filho Mde, S., Nascimento, L.D., do Nascimento, D. M., Cassales, A.R.: Extraction and characterization of nanocellulose structures from raw cotton linter. Carbohydr Polym **91**(1), 229–235 (2013)

Tasis, D., Tagmatarchis, N., Bianco, A., Prato, M.: Chemistry of carbon nanotubes. Chem. Rev. **106**, 1105–1136 (2006)

Oxygen Permeability of Layer Silicate Reinforced Polymer Nanocomposites

Sarat K. Swain, Niladri Sarkar, Gyanaranjan Sahoo and Deepak Sahu

Abstract Reinforcement of organically modified nanoclay into different synthetic and biopolymer matrices was performed by several techniques. For high density polyethylene (HDPE) and polyamide (PA6) based nanocomposites, single screw compounding process was adopted, whereas; for polymethylmethacrylate (PMMA), polyacrylonitrile (PAN) based nanocomposites in situ polymerization technique was taken into consideration. For protein and biopolymer based nanocomposites; nano clays were made to disperse through solution casting technique. The structural analysis of all the polymer/clay nanocomposites or bionanocomposites was performed through X-ray diffraction (XRD) and Fourier transform infrared (FTIR) studies, whereas; the morphological analysis was carried out through transmission electron microscope (TEM). The oxygen permeability of nano clay reinforced polymer nanocomposites was measured as function of clay content and pressure. It was found to be decreased with increase in clay content as compared to their neat polymers. Along with the clay content, ultrasonic treatment also affect the nature of dispersion of nanoclay and thereby the oxygen permeability of the fabricated nanocomposites. The enhanced obstacle towards the path of gas transportation within the fabricated polymer nanocomposite may enable the material for food packaging applications.

Keywords Nanoclay · FTIR · XRD · Gas barrier properties

S.K. Swain (✉) · N. Sarkar · G. Sahoo · D. Sahu
Department of Chemistry, Veer Surendra Sai University of Technology,
Burla, Sambalpur 768018, Odisha, India
e-mail: swainsk2@yahoo.co.in

1 Introduction

1.1 Polymer Composites: Opening the New Era of Material Chemistry

The idea of making composite by the combination of two or more materials is not a new concept; it was started from the inception of human civilization in order to fulfill the human desire and to get hybrid materials with superior properties than the individual one. According to IUPAC definition, composite materials are comprised of different non-gaseous phases in which at least one is a continuous phase and the other is dispersed in it. In terminology the continuous phase is called as matrix whether the discontinuous phase is called as reinforcing agent or filler. The combination of matrix and filler allows the development of new properties to composite. The low dense filler phase should be stiff, strong and thermally stable and should have high load capacity, whereas the load transfer and protection from chemical and mechanical damage are provided by the matrix part characterized with lower modulus and high elasticity. Depending on the nature reinforcing agent composite materials are classified into five categories and these are fiber, particle and flake, laminar or layered and filled composites. Reinforcement of nano-scale materials within composite is more beneficial as compared to macroscopic one as they contain less prominent defects. Modernization of this concept by introducing nano fillers to the matrix phase is a hot-field of recent research. As nanomaterials are characterized by nanometre dimension (1–100 nm) with high aspect ratio, these are very much affective to impart properties to the nanocomposite even with lower concentration. On the other hand, polymer based packaging materials are in lime light for industrial applications. So there is no doubt that the combination of these two will lead to different attractive properties to nanocomposites and it has already been proved for different polymer nanocomposites (Park et al. 2007; Zhang et al. 2007; Lv et al. 2007; Gilman 1999; Yang and Gu 2007; Rana et al. 2004; Sahoo et al. 2008; Osman and Atallah 2004; Abreu et al. 2007). Introduction of different nano fillers such as nano clay, carbon nanotube (CNT) and zirconium oxide(ZrO_2), boron nitride(BN), silicon carbide(SiC), calcium carbonate($CaCO_3$) nanoparticles to different synthetic and biopolymer matrix have already been done and an increase in mechanical, electrical, thermal properties have been observed with an additional influence in gas permeation and rheological properties(Zhong et al. 2007; Pradhan and Swain 2012; Swain et al. 2013; Dash et al. 2013a, b). Among all these properties, we are interested in gas barrier properties of polymer/clay nanocomposites as it has wide applications in liquid and food packaging. As polymeric materials shows many advantages over the glass containers that are usually used over the decades due to their low weight and high mechanical strength. Among different synthetic polymers, polypropylene (PP), polyethylene (PE) and poly (ethylene terephthalate) (PET) are widely used for making containers and bottles. But their poor barrier performances towards oxygen make them inappropriate for

products longevity. Due to nano structure dispersion and microscopic level interactions between nanoparticles and host polymers, high transparent polymer nanocomposites (polyester nanohybrids) show improved barrier performance to oxygen. These improved properties of polyester nanocomposites are suitable for use in the manufacture of closed containers (Kisku et al. 2014). Polymer blends with nanostructure dispersion are enormously used in recent years due to their high barrier performance to oxygen and organic solvents with improved mechanical strength (Barbee et al. 2002; Frounchi et al. 2006). Recently, organoclays incorporated polymer nanocomposites are used for hydrogen storage tanks (Kim and Lee 2006). As organoclay shows adsorptive properties to some bacteria like *Staphylococcus aureus* and *E-Coli* etc, organoclays incorporated polymeric materials are widely used for the development of microbial barrier properties in polymers (Jang 2006). Sometimes, the expected improvement in gas barrier properties of the layered silicate reinforced polymer nanocomposites for larger content of layered silicates; is not observed. This fact can be assigned from the agglomeration of layered silicates within the host polymer which leads to a decrease in the aspect ratio of nanoplatelets and results in the formation of numerous pores within the polymer nanocomposites. Due to creation of such porous microstructure, material shows the lower resistance towards gas transportation. To avoid such irreparable defects, a variety of processing techniques has been developed to improve desirable properties within polymer/clay nanocomposites.

In this chapter we report our published research contributions regarding the organically modified clay reinforced polymer nanocomposites. The method of fabrication, characterization and improved gas barrier properties of fabricated nanocomposites/bionanocomposites are discussed in detail. Effect of ultrasonication on the dispersion of clay platelets within high density polyethylene (HDPE) is explained. Improved gas barrier properties of cloisite®30B reinforced polyamide (PA6) nanocomposites is discussed. In situ polymerization technique is adopted to disperse the layered clay within the host polymers (PAN, PMMA, poly (MMA-co-AN) etc.). For various weight % of nanoclay the gas barrier properties of Albumin bovine, soy protein and chitosan based bionanocomposites has been successfully investigated.

1.2   Layered Silicate as Reinforcing Phase

The development of intercalated polymer nanocomposites with incorporation of modified and unmodified layered silicates by means of melt mixing method is a great achievement in material based research field. Today huge efforts have been devoted to incorporate nanoclay made in almost all type of polymeric matrix. The naturally occurring montmorillonite (MMT) are widely used for the fabrication of polymer nanocomposites. The large length (200–400 nm) to diameter ratio of

nanoclay makes them a suitable candidate for matrix reinforcement (Wang et al. 2006). Due to their unique layered structure with nano level thickness (1–100 nm); they are highly effective to improve mechanical and physical properties of polymers with low filler concentration (i.e. 3–6 wt%) and thereby used in automotive industry (Fukushima and Inagaki 1987). In nature, clays are generally existed with variable composition depending on their sources and groups. Nanoclays are generally prepared from smectite group (2:1 phyllosilicates) clays. Mainly, clays are montmorillonite {Si_4 [$Al_{1.67}Mg_{0.33}$] $O_{10}(OH)_2.nH_2O.X_{0.33}$ = Na, K or Ca} and hectorite {Si_4 [$Mg_{2.7}Li_{0.3}$]$O_{10}(OH)_2.nH_2O.X_{0.4}$ = Na}. In these two structures, octahedral sites are substituted isomorphically. On the other hand, other smectite group of clays include mainly beidillite {[$Si_{3.67}Al_{0.33}$] $Al_2O_{10}(OH)_2.nH_2O.X_{0.3}$ = Na, K or Ca}, nontronite with a structural formula {[$Si_{3.67}Al_{0.33}$] Fe_2O_{10} $(OH)_2.X_{0.33}$ = Na, K or Ca} and saponite {[$Si_{3.67}Al_{0.33}$] $Mg_3O_{10}(OH)_2$. $X_{0.33}$ = Na, K or Ca}. In these three types of layer silicates, tetrahedral sites are fund to be substituted isomorphically. The structural arrangement of smectite clays are composed with 1 nm thick 2-D layers. Each layer of smectite clays is constructed by the combination of two tetrahedral sheets of silica (SiO_2), which are fused together to form an edge shaped octahedral sheets of alumina. These silicate layers with lateral dimension varying from 30 nm to several μm are stacked with one another and form a regular vander Waals gap, known as interlayer or gallery. Negative charges are generally generated at the inter-layer gallery due to the isomorphic substitution with Fe^{3+}/Fe^{2+}, Mg^{2+} or Al^{3+} ions, and are normally counterbalanced by hydrated alkali or alkaline earth cations (Na^+, K^+, Ca^+ etc) residing in the interlayer. The high surface area (up to hundreds of m^2/g) and flexibility of clay platelets are the two another important characteristics which makes them useful in different applications. Before processing to nanoclay reinforced polymer nanocomposites, clay should be made pure from any impurities, like calcite, silica, kaolin, amorphous silica and crystalline quartz or silica. Clays can be purified by several methods, such as, centrifugation, sedimentation, hydrocyclone and chemical treatment. Clays can be characterized by means of their cation exchange capacities. Clays can be functionally modified by simple acid treatment or by metal/metal complex impregnation, ion exchange and pillaring techniques (Khan et al. 1991; Halligudi et al. 1992; Boricha et al. 1999). Due to the presence of charged ions into the interlayers, clays are hydrophilic in nature and therefore, naturally incompatible with a wide range of non-polar systems. This hydrophilic nature of clays can easily be converted to hydrophobic nature by means of ion-exchange treatment with organic cations such as an alkyl ammonium or phosphonium ion. The exchange of small size inorganic cations with more voluminous organic onium cations makes the inter-layer spacing wider than before. Modification of natural montmorillonite (MMT) with organic modifier generates a class of nanoclay named as Cloisite®10A, Cloisite®15A, Cloisite®20A, Cloisite®93A, Cloisite®30B (shown in Table 1). In our previous discussion it is already clear that clays or nanoclays are potential candidate for matrix reinforcement and compatible for the preparation of polymer nanocomposites.

Table 1 Properties of organically modified nanoclays

Sample code	Organic modifier	Modifier conc.	%weight Loss on ignition (%)	Density, g/cc	X-ray results
Cloisite®10A	2MBHT	125 meq/100 g clay	39	1.90	d_{001} = 19.2Å
Cloisite®15A	2M2θT	125 meq/100 g clay	43	1.66	d_{001} = 31.5Å
Cloisite®20A	2M2θT	95 meq/100 g clay	38	1.77	d_{001} = 24.2Å
Cloisite®93A	M2θT	95 meq/100 g clay	39.5	1.88	d_{001} = 23.6Å
Cloisite® 30B	MT2EtOH	90 meq/100 g clay	30	1.98	d_{001} = 18.5Å

2 Experimental Technique

2.1 Materials

Organically modified clay (Cloisite®15A, 20A, 93A and 30B) were purchased from Southern Clay Products (Austin, TX). The high density polyethylene (HDPE) was supplied from Chevron Phillips with specification of HMN 4550-03-Marlex. The specification of used polyamide 6 (PA6) was Ultramid B40LN (BASF). Prior to processing of polymer nanocomposites, PA6 was dried at 80 °C for 24 h. Acrylonitrile (AN) and methyl methacrylate (MMA) monomers were purchased from Merck, Germany and used after washing. Potassium persulphate ($K_2S_2O_8$) and ferrous ammonium sulphate were of analytical grade and obtained from Merck, Germany. Albumin bovine globules were purchased from Sisco Research Laboratory (SRL) Pvt. Mumbai, India. Soy protein sample was supplied by the HiMedia Laboratories Pvt. Ltd, Mumbai, India, whereas; chitosan powder, with DA (degree of deacetylation) of 90 %, was purchased from Fisher Scientific (Qualigens) Pvt. Ltd, Mumbai. Soy protein and chitosan powder were used without further purification. During all experimental works, solutions were prepared by double-distilled water.

2.2 Methods

Incorporation of organically modified nano clay into different synthetic and biopolymer matrix has been done by several methods, such as melt mixing, in situ polymerization and solution casting techniques. All these techniques lead to two types of orientation of layered structured nanoclay into polymeric matrix and these are named as intercalation and exfoliation. Nanoclay reinforced high density polyethylene (HDPE) nanocomposites with varying clay content (2.5 wt%, 5.0 wt% and 10.0 wt%) were fabricated by a single screw compounding extruder (Oh et al. 2003; Lapshin et al. 2008). This extruder is attached with a Maddock mixing section and a Melt Star mixing element along with an ultrasonic die attachment. For a better

processing purpose screw speed was maintained at 100 rpm and temperatures were set as 180 °C, 190 °C and 200 °C from the feeding section to the die zones, respectively. A continuous supply of ultrasound of frequency 20 kHz and amplitude of 10 μm was maintained by the insertion of two horns into a slit die of 4 mm gap size. The chosen HDPE was ultrasonically treated in the molten state at three different flow rates of 0.25, 0.50, and 0.75 g/s, corresponding to the residence time in the treatment zone of 21, 10, and 7 s, respectively. Similar synthetic protocol was adopted for the synthesis of nano clay reinforced polyamide (PA6/clay) nanocomposites. Composition of the polyamide nanocomposites was varied with varying clay content (2.5, 5.0, and 10.0 wt%) during the melt mixing process. Particularly for this nanocomposite, amplitudes of the supplied ultrasonic waves were varied as 5, 7.5, and 10 μm and temperatures was maintained 220, 225, and 230 °C during feeding process. Polyamide (PA6) was ultrasonically treated in the molten state at a flow rate of 0.50 g/s corresponding to a residence time of 14 s. In situ polymerization technique was applied for the synthesis of PAN/Cloisite®30B, PMMA/Cloisite®93A and Poly(MMA-co-AN)/cloisite®30B nanocomposites. For cloisite®30B reinforced polyacrylonitrile (PAN) nanocomposites were prepared by ultrasound assisted in situ emulsifier-free emulsion technique with varying clay loading (1 wt%, 2 wt%, 3 wt% and 4 wt%). During preparation of polymer nanocomposites, ultrasound waves of different powers and frequencies were used as 120/80, 120/60 and 80/80 W/KHz. The purified acrylonitrile (AN) was made to disperse in double distilled water through mechanical stirring with different wt% of clay for 1 h. Emulsifier free emulsion polymerization of acrylonitrile (AN) in water medium was initiated by slow addition of potassium persulphate and the mixture was allowed to stirring for 3 h at room temperature with continuous stirring. The polymerization process was ended up by the addition of 0.1 M solution of ferrous ammonium sulphate to the reaction mixture. The resultant product was then filtered and purified by washing with double distilled water followed by drying of the filter residue in a vacuum oven at 40–50 °C for 48 h. Same synthetic protocol was employed for cloisite®93A reinforced polymethylmethacrylate nanocomposite. Only the difference is in their polymerization temperature. For PMMA based nanocomposites polymerization temperature was maintained to 60 °C. The experimental parameters for synthesis of PMMA/clay nanocomposites are summarized in Table 2. For the preparation of nano clay reinforced poly (methylmethacrylate-co-acrylonitrile) different amount of the organoclay was dispersed in double-distilled water through continuous stirring at room temperature. After that, measured volumes of the two monomers methyl methacrylate (MMA) and acrylonitrile (AN), were added to the clay suspension. Then, the mixture was restirred with rise of temperature to 60 °C, after maintaining the desired temperature, the aqueous solution of KPS was added to start the copolymerization. The rest part of the synthetic protocol is same as PMMA/clay nanocomposites. In case of nano clay reinforced protein based nanocomposites, solution technique was adopted. According to this technique, calculated amount of protein powder (albumin bovine/soy protein) was well dispersed in double distilled water by continuous stirring at 50 °C for 30 min followed by ultrasonication (120 W/180 kHz) for another 30 min. Aqueous suspension of

Table 2 Experimental parameters for synthesis of PMMA and PMMA/Closite®93A nanocomposites (Patra et al. 2012)

Sample code	[MMA] (mol dm^{-3})	[KPS] (mol dm^{-3})	Cloisite®93A (wt%)	Ultrasound (W/kHz)	% age conversion
PMMA1	2.35	1×10^{-2}	0	0	28.6
PMMA2	2.35	1.5×10^{-2}	0	0	41.9
PMMA3	1.88	1.5×10^{-2}	0	0	43.5
PMMA4	1.88	1×10^{-2}	0	0	44.2
PMMA5	1.41	1.5×10^{-2}	0	0	30.6
PMMA6	1.41	1×10^{-2}	0	0	62.0
PMMA6-C1	1.41	1×10^{-2}	1	0	48.8
PMMA6-C2	1.41	1×10^{-2}	2	0	52.3
PMMA6-C3	1.41	1×10^{-2}	3	0	51.6
PMMA6-C3u1	1.41	1×10^{-2}	3	120/80	58.1
PMMA6-C3u2	1.41	1×10^{-2}	3	120/60	52.8
PMMA6-C3u3	1.41	1×10^{-2}	3	80/80	62.3

nano clay with different wt% of was prepared by stirring at 80 °C for 30 min, followed by ultrasonication for 30 min. Then the protein solution was added to different weight percentage clay solutions. For catalytic purpose, a mixture of CuSO$_4$/glycine (Sahoo et al. 1999; Sahoo et al. 2008; Kisku and Swain 2012) was added to the above mixture solution as a chelate complex and allowed stirring for 3 h at 50 °C. The final viscous product obtained through filtration was dried at room temperature for 2 days to obtain nanocomposite powder. For cloisite®30B reinforced soy protein nanocomposites sample was coded as BNC0, BNC1, BNC3, BNC5 and BNC8 for 0, 1, 3, 5 and 8 wt% of the clay content respectively. Nano clay (Cloisite®15A) reinforced chitosan bionanocomposites with enhanced gas barrier properties was prepared by the same solution casting technique and the synthesized chitosan/cloisite®15A bionanocomposites were coded as CBN1, CBN2, CBN3, CBN4, CBN5, and CBN8 for 1, 2, 3, 4, 5 and 8 wt% of clay, respectively.

2.3 Standard Techniques Used for Characterization and Study of Properties

To investigate the chemical interaction between the reinforced clay and the host polymer, Fourier transform infrared (FTIR) measurements of the fabricated nanocomposites/bionanocomposites were performed using a Shimadzu IRAffinity-1 Fourier Transform Infrared Spectrophotometer. Crystalline phases of the fabricated nanocomposites/bionanocomposites were identified through X-ray diffraction (XRD) patterns by using a Rigaku X-ray machine operating at 40 kV and 150 mA.

The mean interlayer spacing (d) of the reinforced (organically modified) clays in their pure form as well as in their nanocomposite/bionanocomposite were calculated using Bragg's formula: $n\lambda = 2d \sin\theta$. The nanostructure dispersion of layered clays within the host polymer was visualized from transmission electron microscopic (TEM) images, captured through transmission electron microscope, Tecnai 12, Philips, operating at 120 kV. For TEM analysis, an ultra cut low temperature sectioning system equipped with a diamond knife was used to cut ultra thin specimens of 75 nm by cryo-ultra microtome below T_g (glass transition temperature) of the sample. The oxygen barrier properties of nanocomposites/ bionanocomposites were measured with ASTM F 316-86 by using Oxygen Permeation Analyzer (PMI instrument, mode 1 GP-2 01-A, NY, USA). Sample specimens were converted to thin films of 0.5 mm thickness with the help of a Polymer Press at a pressure of 9 tons and a temperature of 210 °C for the barrier property measurement. The results were recorded as average of the values obtained from five same samples.

3   Characterization of Layer Silicate Reinforced Polymer Nanocomposites

3.1   FTIR Analysis

The chemical interaction between functional groups of layered silicate and host polymer was investigated by FTIR study. FTIR spectrum of Cloisite®30B shows the absorption peaks at 3645 cm^{-1} and 1032 cm^{-1} correspond to O-H and Si-O stretching, whereas; peaks at 2927 cm^{-1} and 1440 cm^{-1} are due to C–H and C–C stretching respectively. The FTIR peak at 517 cm^{-1} is assigned to stretching vibration of Al–O bond. In nano clay reinforced polymer nanocomposites the individual vibrational modes of different functional moiety attached to layered silicate are influenced by the functional groups of polymer. FTIR study is also carried out to realize the changes in the molecular structure due to the effect of ultrasound. FTIR spectra of ultrasonically treated and untreated HDPE/clay nanocomposites with 2.5 % clay content are shown in Fig. 1(I). It is observed that all absorption peaks are similar, except the peaks within the region of 1025– 1100 cm^{-1} assigned to the asymmetric stretching of C–C single bonds (Prasad and Grubb 1989). From the FTIR spectrum of untreated nanocomposites a broad absorption peaks at around 1072–1085 cm^{-1} is observed due to CH_2–CH_2 asymmetric stretching and CH_2 wagging of the polymer chain. For ultrasonically treated sample, the peak at 1072–1085 cm^{-1} is less intense as compared to ultrasonically untreated samples. This fact is attributed from the delamination of layered clays within the HDPE polymer by the application of ultrasonic waves of amplitude 10 µm. These changes in vibrational spectra with sonication were related to the structural modification of HDPE chain.
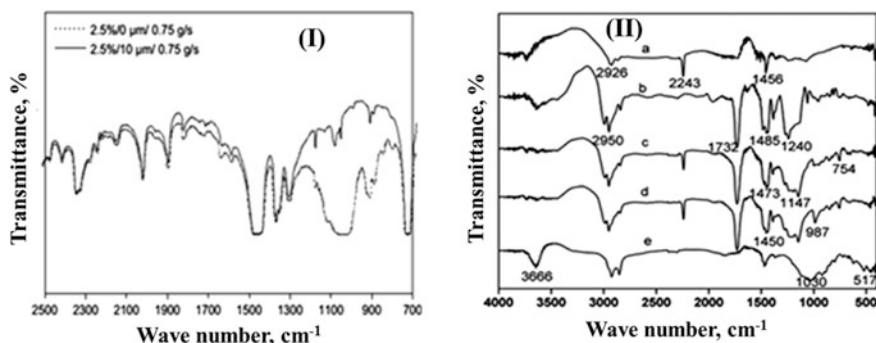
Fig. 1 FTIR spectra of (**I**) HDPE/clay (2.5 wt%) nanocomposites obtained at a feeding rate of 0.75 g/s without and with ultrasonic treatment at an amplitude of 10 µm; FTIR spectra (**II**) of poly (MMA-co-AN)/cloisite®30B nanocomposites [*a* PAN, *b* PMMA, *c* CP, *d* CP30B-3, *e* Cloisite®30B] (Swain and Isayev 2007; Patra and Swain 2012)

In the FTIR spectrum of cloisite®30B reinforced poly (methylmethacrylate-co-acrylonitrile), characteristic peaks of cloisite®30B are appeared at 3,666 cm^{-1} and 1,030 cm^{-1} with slight shifting in Si–O peak to 987 cm^{-1} (Fig. 1(II)). This shifting in peak position is occurred due to composite formation. The presence of absorption peaks between 2,924 cm^{-1} and 2,951 cm^{-1} is assigned to methylene groups of PMMA and evidenced in the FTIR spectra of all the nanocomposites. The observed FTIR bands at 1,732 cm^{-1} in Fig. 1 is due to the >C=O group stretching of polymethylmethacrylate. The peaks in the region 1,450–1,473 cm^{-1} indicate asymmetric bending vibrations due to methyl and methylene groups. Hence, the formation of copolymer and its nanocomposite is evidenced from FTIR study.

FTIR spectra (Fig. 2(I)) of pure Albumin bovine shows a strong absorption band at 1697 cm^{-1} due to >C=O stretching, which is also reflected for albumin/clay bionanocomposites around the same position (1695 cm^{-1}). For pure albumin bovine, the characteristic absorption peak of –OH is shown at 3546 cm^{-1}. This broad absorption band is also present in the albumin/clay composite. Due to coupling of bending vibration of N–H and stretching vibration of C–N, strong peaks at around 1540–1550 cm^{-1}, is observed for both, albumin bovine and albumin/clay nanocomposite (Fig. 2(I)) (Dons et al. 1995; Ball and Jones 1995). The absorption peak for Si–O vibration (1058 cm^{-1}) of pure clay is also reflected in the FTIR spectra of albumin bovine/clay bionanocomposites. But, the nature and intensity of the FTIR peaks of albumin bovine/clay bionanocomposite are different from that of the pure clay and pure albumin bovine. The broad –OH peak at around 3560 cm^{-1} of albumin bovine has become sharp in case of albumin bovine/clay bionanocomposite. Moreover, the sharp peak at 1500 cm^{-1} of nano clay is not seen in the FTIR spectra of the bionanocomposite. It results for the interaction between nanoclay and albumin matrix. For cloisite®30B reinforced soy protein bionanocomposites, appearance of Si–O stretching peak at 1045 cm^{-1} in the spectrum of the bionanocomposite (Fig. 2(II)) indicates the incorporation of organoclay into
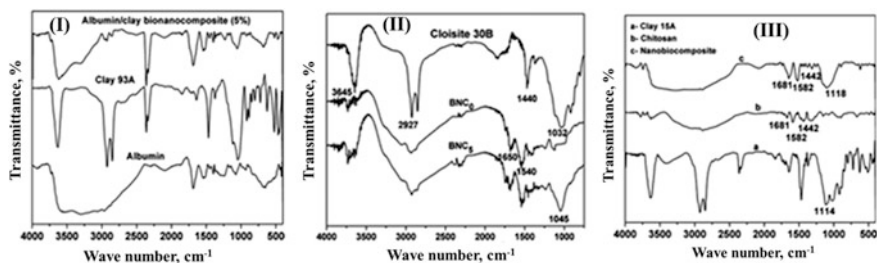
Fig. 2 FTIR spectra of (**I**) albumin, nanoclay, and albumin/clay (5 wt%) bionanocomposite; **II** Cloisite®30B, BNC0 (neat soy protein) and BNC5 (bionanocomposite with 5 % clay content); **III** clay, chitosan, and chitosan/clay nanobiocomposites with 5 % clay loading (Dash et al. 2012; Swain et al. 2012; Swain et al. 2014)

soy protein. Furthermore, the broad bands of very low intensity observed in the region of 3600–3750 cm^{-1} can be attributed to free and bound –OH and –NH groups, which are interacted via hydrogen bonding with the –OH group of Cloisite®30B.

The FTIR spectra of clay, chitosan and the chitosan/cloisite®15A nanobio-composites with 5 wt% nano clay loading are shown in Fig. 2(III). In FTIR spectrum of chitosan, two strong absorption peaks at around 1681 cm^{-1} and 1573 cm^{-1} has been observed due to amide (N–C=O) and C–N stretching vibration, respectively. Two another absorption peaks at 2877 cm^{-1} and 1442 cm^{-1} in chitosan is due to C–H stretching and C-H bending vibration. Moreover, the C-O-C asymmetric stretching at 1166 cm^{-1} and C–O stretching at 1082 cm^{-1} are also observed for chitosan. For cloisite®15A, the peaks at 1118 cm^{-1} is due to the Si–O stretching vibration. The presence of the Si–O stretching vibration peak of reinforced nanoclay along with all other peaks of chitosan in FTIR spectrum of chitosan/clay nanobiocomposite gives an evidence for the formation of composites.

3.2 XRD Analysis

The structural investigation of layered silicate reinforced polymer nanocomposites was performed by XRD analysis. The Fig. 3 shows the XRD patterns of HDPE/clay nanocomposites. According to Fig. 3b of HDPE/clay nanocomposites, 2.5 wt% of nano clay content within HDPE/clay nanocomposites shifted the crystalline peaks (001) to lower angles without the treatment of ultrasonication. As a consequence of this observed phenomenon, the interlayer distance is enlarged from 2.40 to 3.56 nm. This fact can be attributed from the intercalation of macromolecular chains (HDPE chains) within the inter-layer galleries of cloisite®20A. Moreover, the d-spacing value of HDPE/clay nanocomposites is observed to be decreased with increase in clay content. XRD patterns of HDPE/clay nanocomposites with 5 wt% clay at different amplitudes of ultrasound are shown in Fig. 3a. It seems that a
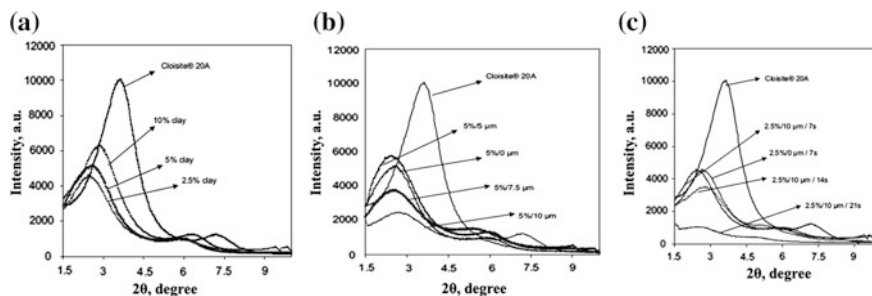
Fig. 3 XRD patterns of (**a**) nanoclay and HDPE/clay nanocomposites obtained without sonication at a feeding rate of 0.5 g/s, **b** clay and ultrasonically treated nanocomposites with 5 % clay content and a feeding rate of 0.5 g/s, **c** clay and HDPE/clay (2.5 %) nanocomposites obtained at an ultrasonic amplitude of 10 mm and different residence times (Swain and Isayev 2007)

contest between the effects of ultrasound to introduce both intercalation and exfoliation is evidently observed from the XRD patterns of ultrasonically treated and untreated samples. Moreover, the interlayer spacing of clay also undergoes changes with residence time of samples in the treatment zone (Fig. 3c). It is also found that the intensity of the peaks is substantially decreased with increase of residence times. The latter is a direct evidence of the tendency of clay to exfoliate with increase of residence times. In particular, the ultrasonically treated (amplitude 10 μm and mean residence time 21 s) nanocomposite shows a disappearance of this peak indicating a complete exfoliation of clay by HDPE matrix (Fig. 3c).

XRD patterns of polyamide (PA6)/clay nanocomposites and pure clay are summarized in Fig. 4(I)–(IV). From the XRD patterns of PA6/clay (cloisite®30B) nanocomposites, the characteristic peak pure clay disappears. This indicates that the fully exfoliated structure is obtained due to the insertion of polymer chains into the clay gallery. However, PA6/clay (cloisite®15A) and PA6/clay (cloisite®93A) nanocomposites show XRD peaks but at lower 2θ angles than those of respective pristine clays, indicating intercalated structures with less dispersion than in the case of clay (cloisite®30B). The interlayer distances for different clays, Cloisites® Southern clay Inc. (Ganjales, TX, USA) 15A, 93A, and 30B, along with corresponding PA6/clay nanocomposites are calculated by Bragg's law (nλ = 2d sinθ) and shown in Table 3.

X-ray diffraction data of pure clay (Cloisite®93A) and cloisite®93A reinforced polymethylmethacrylate nanocomposites is summarized in Table 4. With increase in clay concentration within the host polymethylmethacrylate, of the corresponding reinforced clay decreases with respect to its pure form. The decreased 2θ value results in an increase in d-spacing of the silicate layers. Moreover, for sonicated samples peak intensity is significantly reduced due to the formation of partial exfoliated structure because of the ultrasonic treatment. At 3 % clay content within the nanocomposite results an increase in basal spacing from 2.51 to 3.99 nm (Table 4). The enhancement of basal spacing corresponds to an intercalated structure. Reduction in intensity of the reflection of PMMA/clay may be due to
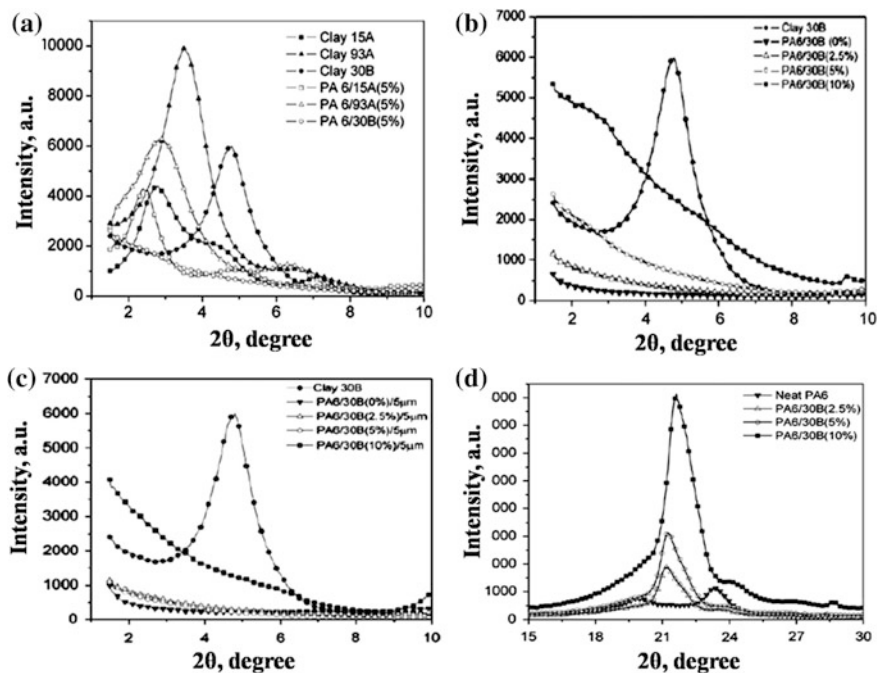
Fig. 4 XRD patterns of (**a**) cloisite15A, 93A, and 30B and PA6/clay (5 wt%) nanocomposites obtained without ultrasonic treatment, **b** clay (30B), PA6, and PA6/clay nanocomposites obtained without sonication and (**c**) with sonication at an amplitude of 5 μm, **d** PA6 and PA6/clay nanocomposites obtained without ultrasonic treatment (Swain 2011)

Table 3 Comparison of d-pacing of various clays and PA6/clay nanocomposites (Swain 2011)		

Sample	2θ (degree)	d-spacing (nm)
Cloisite®15A	2.81	3.16
PA6/ Cloisite®15A/0 μm	2.42	3.65
Cloisite®93A	3.48	2.36
PA6/ Cloisite®93A/0 μm	2.94	2.97
Cloisite®30B	4.80	1.84
PA6/ Cloisite®30B/0 μm	No clay peak	–
PA6/ Cloisite®30B/0 μm	No clay Peak	–

large X-ray absorption as well as due to delamination of silicate layers. Same type of XRD data is also observed for cloisite®30B reinforced polyacrylonitrile (PAN) nanocomposites and summarized in Table 5. XRD patterns of cloisite®30B and cloisite®93A reinforced poly(methylmethacrylate-co-acrylonitrile) nanocomposites are shown in Fig. 5(I), (II). The calculated d-spacing of different nanocomposites according to Bragg's formula are Summarized in Table 6. A decrease in 2θ value is observed with increase in clay content of the respective nanocomposites. With 3 % Cloisite®30B, copolymer/clay nanocomposites shows

Table 4 Interlayer (d) spacing of Clay and PMMA/Clay nanocomposites (Patra et al. 2011)

Samples	2θ (degree)	d-spacing (nm)
Closite®93A	3.52	2.51
PMMA6-C1	2.49	3.55
PMMA6-C2	2.40	3.68
PMMA6-C3	2.21	3.99
PMMA6-C3u1	No peak	–

Table 5 Evaluation of d-spacing of the clay and PAN/clay nanocomposites (Patra et al. 2011)

Sample	2θ (degree)	d-spacing(nm)
Cloisite®30B	4.8	1.84
PNC-1	2.8	3.15
PNC-2	2.6	3.39
PNC-3	2.5	3.53
PNC-2u1	No Peak	–
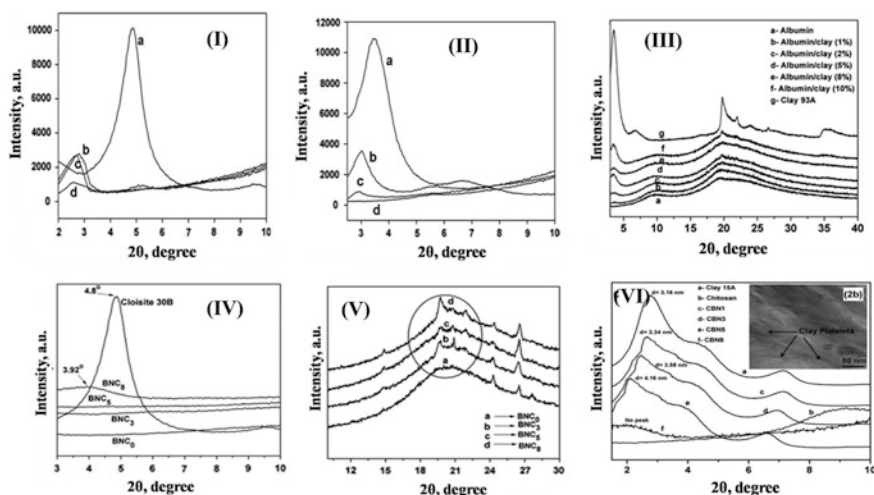
Fig. 5 XRD patterns of (**I**) *a* Cloisite®30B, *b* CP30B-1, *c* CP30B-2, *d* CP30B-3 **II** *a* Cloisite®93A, *b* CP93A-1, *c* CP93A-2, *d* CP93A-3, **III** *a* albumin, bionanocomposites of clay concentrations (*b*) 1 %, *c* 2 %, *d* 5 %, *e* 8 %, *f* 10 %, and *g* nanoclay, **IV** Cloisite®30B, soy protein (BNC0) and the soy protein/Cloisite®30B bionanocomposites in the 2θ range of 3 to 10 degrees and **V** soy protein bionanocomposites in the 2θ range of 10 to 30 degrees, **VI** XRD patterns of *a* clay 15A, *b* chitosan, nanobiocomposites *b* inset HRTEM image of chitosan/clay (8 wt%) nanobiocomposites (Patra and Swain 2012; Dash et al. 2012; Swain et al. 2012; Swain et al. 2014)

an increase in d-spacing of about double to that of the clay. It happens due to the intercalation of copolymer chains within the clay galleries. For copolymer/clay nanocomposites, the basal spacing is increased with increase in clay loading upto 2 %. Due to the exfoliation of clay platelets over the copolymer matrix in poly

Table 6 Interlayer (d)-spacing of copolymer/clay nanocomposites (Patra and Swain 2012)

Sample	2θ (degree)	d-spacing (nm)
Cloisite®93A	3.52	2.51
CP93A-1	3.02	2.92
CP93A-2	2.96	2.98
CP93A-3	No Peak	–
Cloisite®30B	4.80	1.84
CP30B-1	2.80	3.15
CP30B-2	2.72	3.24
CP30B-3	2.6	3.39

(methylmethacrylate-co-acrylonitrile) nanocomposites with 3 % clay content shows no crystalline peaks.

Albumin bovine shows (Fig. 5(III)) the structural peak at 2θ value of 2.18 degree. The characteristic peak at 2θ value of 3.488 degree is assigned for the layer structure of nanoclays corresponding to d-spacing of 2.36 nm. Moreover, the disappearance of nanoclay peak from the XRD of albumin bovine/clay nanocomposites (1 wt% and 2 wt%) may be assigned from the complete deformation of layered clays. For 5, 8, and 10 wt% nanoclay loaded albumin bovine a clear hump like peak is appeared just left to the crystalline peak of nanoclay. Such kind of shifting in peak position with low intensity may be due to intercalation (Swain and Isayev 2009) of protein matrix within the clay galleries. The intercalation at higher wt% of nanoclay may be due to local agglomeration of nanoclay. Further, the XRD patterns of soy protein and its composites were compared in Fig. 5(IV) with 2θ up to 30. It was noted that, the single broad peak of the diffraction pattern of the soy protein (Fig. 5(V)) is converted to multiple peaks in the diffraction patterns of the composites as shown as circular mark. It points to the change in crystallinity of soy protein in bionanocomposites due to dispersion of clay layers (Sikdar et al. 2007). The extent of exfoliation of clays within the composite is supported from HRTEM images. The XRD pattern of the clay (cloisite®15A) shows a peak at about 2θ value of 2.81, corresponding to basal spacing of 3.16 nm. After incorporation of chitosan matrix to clay the peaks of clay shifts to lower 2θ angle, indicating the formation of an intercalated nanostructure. The calculated basal spacing of cloisite®15A are summarized in Fig. 5(VI) (a). The results of XRD analysis in Fig. 5(VI) (b) are supported by the inset HRTEM. From the HRTEM images, uniform dispersion of clay platelets along with slight local agglomeration is observed.

3.3 Morphological Analysis

Morphological analysis of the synthesized polymer/clay nanocomposites was carried out using transmission electron microscope (TEM). For HDPE/clay nanocomposites, TEM micrographs are demonstrated in Fig. 6a, b. The regular layer structure of untreated 5 % clay samples (Fig. 6a) are found to be disrupted or
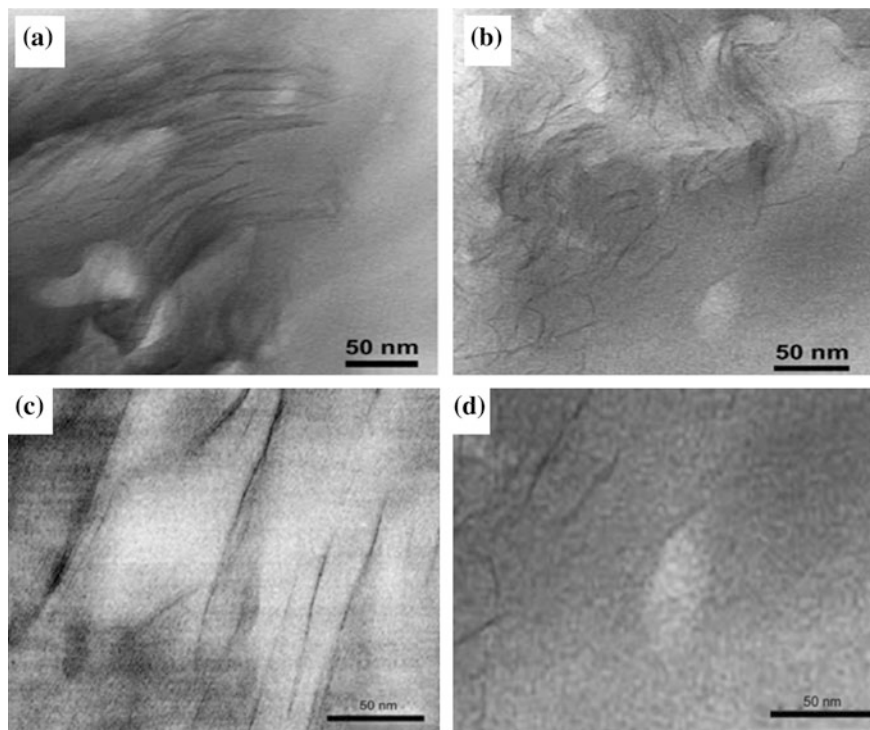
Fig. 6 TEM micrographs of HDPE/clay (5 %) nanocomposite obtained at a feeding rate of 0.5 g/s without (**a**) and with (**b**) ultrasonic treatment at an amplitude of 5 μm; TEM images of PA6/clay (Cloisite®30B) 5 wt% nanocomposites obtained without (**c**) and with (**d**) ultrasonic treatment at an amplitude of 5 μm (Swain and Isayev 2007; Swain 2011)

partially exfoliated by high power ultrasound showing that the polymer has entered into the inter-gallery spacing wherein individual clay layers are dispersed in the polymer matrix, as shown in Fig. 6b. Same type of exfoliated structure is resulted for nano clay reinforced polyamide (PA6/cloisite®30B) nanocomposites (Fig. 6c, d), TEM images are captured for PA6/clay nanocomposites with 5 wt% of nanoclay loading obtained with and without ultrasonic treatment at amplitude 5 μm. The effect of ultrasonic treatment for the exfoliation of layered structure within the host polymer was clearly evidenced from TEM images.

The effect of ultrasound on the exfoliation of nanoclay within polymethyl-methacrylate is also evidenced from the TEM images (Fig. 7e, f of PMMA/clay obtained with and without ultrasonic treatment. Figure 7c, d shows the nanostructural dispersion of nanoclay within polyacrylonitrile (PAN) matrix. Sometimes the nature of dispersion of nano clay within hydrophobic polymer is influenced by the organophilic nature of organically modified nano clay. TEM images of in situ synthesized nanostructure hybrid materials of poly (methylmethacrylate-co-acrylonitrile) with incorporation of organically modified clays, cloisite®30B and
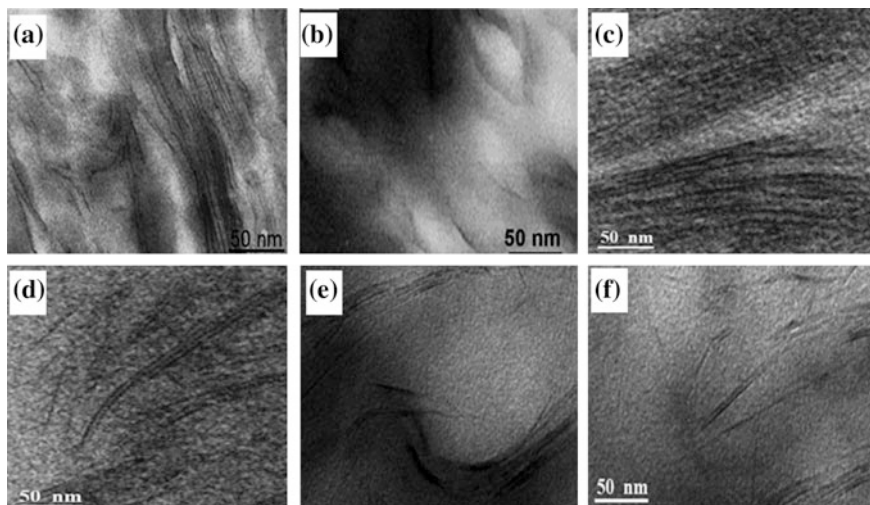
Fig. 7 TEM images of **a** CP30B-3 and **b** CP93A-3; TEM micrographs of PAN/clay nanocomposites **c** without and **d** with sonication; TEM micrographs of PMMA/clay nanocomposites: **e** without sonication and **f** with sonication (Patra and Swain 2012; Patra et al. 2011; Patra et al. 2012)
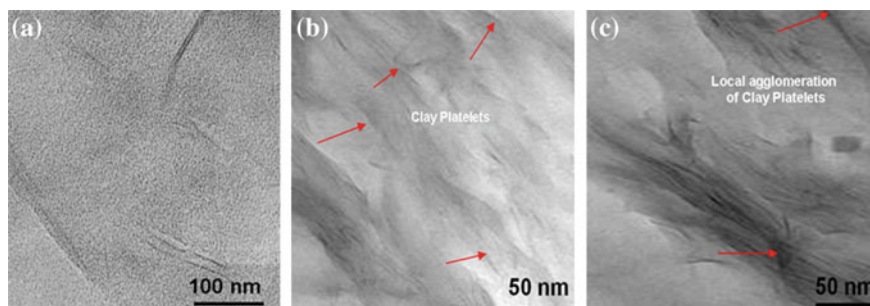
Fig. 8 TEM image of **a** soy/clay (5 wt%) bionanocomposite (BNC5); TEM images of **b** albumin/clay 2 % and **c** albumin/clay 10 % bionanocomposite (Swain et al. 2012; Dash 2012)

93A are shown in Fig. 7a, b. With same amount of filler loading (3 wt%), CP30B-3 shows local dispersion of the clay layers (Fig. 7a) whereas; CP 93A-3 shows the uniform distribution of delaminated clay layers within the copolymer matrix (Fig. 7b). This outcome can be attributed to the more organophilic nature of Cloisite®93A than Cloisite®30B.

Nanostructure dispersion of layered silicate within albumin bovine and soy protein has also been seen from Fig. 8a, b, c. Figure 8a presents the delaminated clays into some thin lamellas by soy protein with a dimension of about 2 nm in thickness. In TEM images, some black patches are appeared due to the local

agglomeration of clay layers within the protein matrix. For albumin/clay bio-nanocomposites with high and low percentages of nanoclay are compared in the Fig. 8b, c. For higher wt% of clay (10 wt%) albumin/clay nanocomposite (Fig. 8c) shows some extent of local agglomeration, whereas; for 2 wt% of clay content, a uniform dispersion of clay platelets within the albumin bovine matrix has been observed because of the exfoliation of clay layers (Fig. 8b).

4 Study of Oxygen Permeability of Layer Silicate Reinforced Polymer Nanocomposites

The main objective of preparing layered silicate reinforced polymer nanocomposites is their increased demand in food packaging applications. Due to special type layered structure and high aspect ratio of nano clay, when it subjected to polymer matrix, the resultant polymer nanocomposites show improved physical and chemical properties. Because of this reasons, nano clay reinforced polymer nanocomposites are used as an alternative of conventional plastic materials also for fabricating packaging films. Polymer-clay nanocomposites have an ordered nano-layer structure which provides the hurdles to oxygenentrance, whereas; conventional composites have voids for oxygen entrance in their microstructure. Oxygen permeability of HDPE/clay nanocomposites is conducted as a function of both, the clay content and ultrasonic amplitude at different feeding rates and summarized in Table 7 (Swain and Isayev 2007). From this Table 7 it is observed that oxygen permeability of HDPE/clay nanocomposites increases slightly as a function of clay content only. But a substantial decreased in oxygen permeability is observed for the combining effect of clay content and high ultrasonic amplitude (at 10 µm). The

Table 7 Oxygen permeability of HDPE/clay nanocomposites at different clay concentrations and ultrasonic amplitudes (Swain and Isayev 2007)

Sample	Clay (%)	Amplitude (µm)	Feeding rate (g/s)	Oxygen permeability (cm^{-3}day m^{-2})
1	0	0	0.75	75.9
2	2.5	0	0.75	76.2
3	5.0	0	0.75	76.4
4	10.0	0	0.75	79.7
5	2.5	5	0.75	76.8
6	2.5	7.5	0.75	80.6
7	2.5	10	0.75	69.7
8	5.0	10	0.75	71.2
9	10.0	10	0.75	73.3
10	2.5	10	0.5	65.9
11	2.5	10	0.25	61.8

Table 8 Oxygen permeability of PA6 and PA6/Clay®30B nanocomposites at different clay concentrations without and with ultrasonic treatment (Swain 2011)

SL no.	Samples (PA6/Cloisite®30B/amplitude)	Oxygen permeability (cm^3 mm/m^2/24 h)
1	Pure PA6	35.96
2	PA6/0 %/0 μm	23.05
3	PA6/2.5 %/0 μm	7.45
4	PA6/5 %/0 μm	5.16
5	PA6/10 %/0 μm	1.01
6	PA6/5 %/5 μm	10.38
7	PA6/5 %/7.5 μm	11.29
8	PA6/5 %/10 μm	12.37

nanocomposites of 2.5 % clay with treatment of ultrasound at amplitude of 10 μm with a feeding rate of 0.25 g/s (residence time 21 s) have oxygen permeability 20 % less than the neat HDPE matrix. The effect of ultrasound and clay content on the oxygen permeability of PA6/clay nanocomposites is summarized in Table 8 (Swain et al. 2011). With increasing the clay content, a significant improvement in the barrier properties of polymer nanocomposites has been observed and clearly evidenced from Table 8. The improvement in barrier properties can be assigned from the complete exfoliation of clay platelets during compounding process through single screw mixing extruder. At 10 wt% of clay loading within PA6 polymer, the gas barrier property of nano clay reinforced PA6 nanocomposites is found to be improved by 20 times as compared to pure PA6. Therefore, it can be concluded that the oxygen permeability of PA6/clay nanocomposites has been decreased tremendously with increasing clay content within PA6 matrix.

The oxygen permeability of in situ polymerized polymethylmethacrylate/clay nanocomposites and virgin polymethylmethacrylate are shown in Fig. 9a, b, c, d. The oxygen permeation through all the PMMA/clay nanocomposites are observed to be decreased as compared to the virgin PMMA and the decrement in the barrier properties is proportional to the clay content (Patra et al. 2012). With increasing pressure (up to 5 psi), the rate of oxygen flow is found to be increased as compared to the lower pressure. But the increment is less prominent for higher clay loading. It is observed that for 3 wt% clay loading within PMMA matrix, it shows a huge reduction in oxygen flow, near about 17 % as compared to virgin PMMA. Further air (oxygen) flow resistance (AR), which is the ratio of pressure to flow rate are calculated and found to be increased with increase in clay loading. It is attributed from the facts that during in situ polymerization of PMMA, the propagating chains of homopolymers is inserted within the inter-layer or gallery of the present clays and disrupted the layered clay and form an intercalated or partially exfoliated structure. The rate of oxygen flow is found to be reduced further for sonicated nanocomposites. The tremendous decrease in oxygen flow rate is due to the combined effect of power and frequency of the ultrasound and clay content. Due to ultrasonication during the synthesis of PMMA/clay nanocomposites, complete
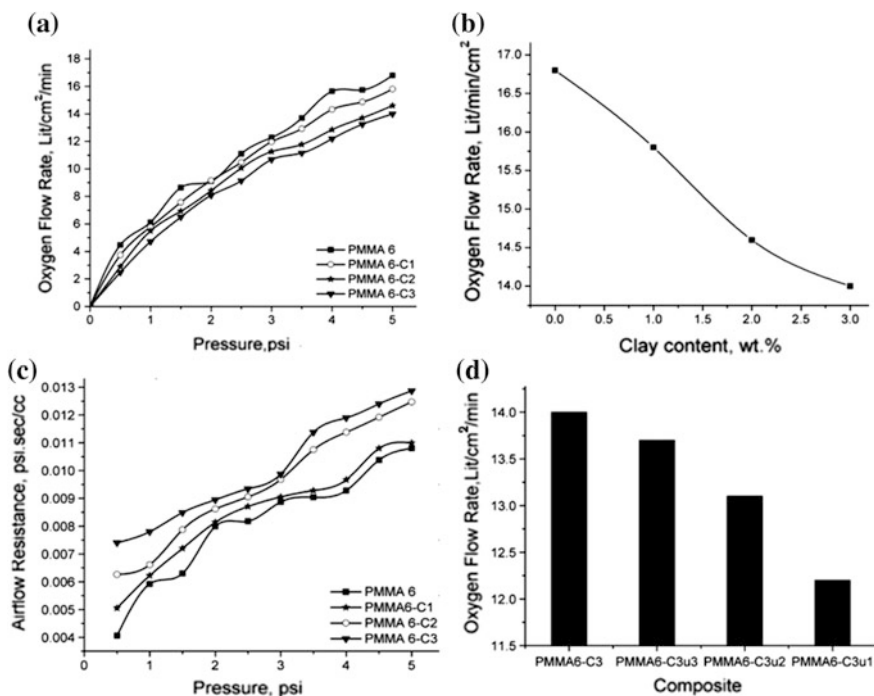
Fig. 9 Oxygen flow rate of **a** PMMA and PMMA/clay nanocomposites at different pressures; **b** Oxygen flow rate of PMMA and PMMA/clay nanocomposites with variation of clay content at 5 psi pressure; **c** Oxygen flow resistance of PMMA and PMMA/clay nanocomposites at different pressures; **d** Oxygen flow rate of sonicated samples as a function of power and frequency (Patra et al. 2012)

exfoliation of layered clays within polymeric network is occurred and results in a huge reduction in oxygen permeability. Same type of observation is also found for nanoclay reinforced polyacrylonitrile (Patra et al. 2011) nanocomposites and shown in Fig. 10a, b, c.

The observed oxygen flow rate of the copolymer poly(MMA-co-AN) is found to be less as compared to both the homopolymers, polymethylmethacrylate (PMMA) and polyacrylonitrile (PAN). This fact may be attributed from the polymer chain networking within the copolymer that develops some restriction to oxygen penetration. The incorporation of 3 wt% of both the organoclays, cloisite®30B and cloisite®93A shows a significant reduction in oxygen permeability as compared with the virgin copolymer (Patra et al. 2012). Figure 11a, b presents a comparative account of the effect of increase in the weight percent of Cloisite®30B and Cloisite®93A in copolymer matrix separately. It is observed that for both the organoclays, the oxygen permeability of poly(methylmethacrylate-co-acrylonitrile)/clay nanocomposites is decreased with increase in clay content. But, at all the percentages, Cloisite®93A reduces the permeability to a greater
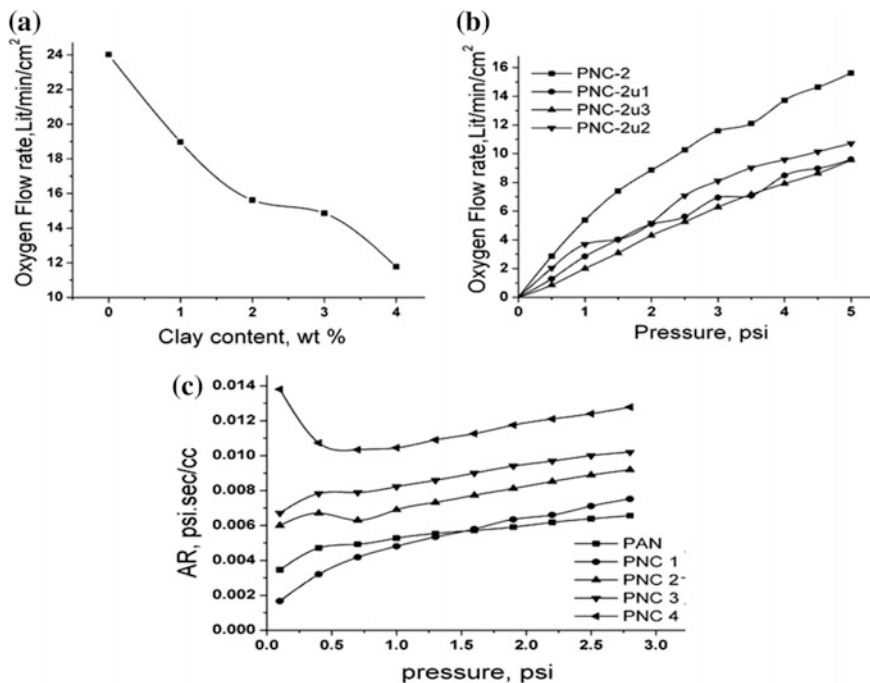
Fig. 10 Oxygen permeability of **a** PAN/clay nanocomposites as a function of clay content at 5 psi pressure; **b** Oxygen flow rate of PAN/clay (2 %) nanocomposites at different powers and frequency of ultrasound; **c** Air flow resistance (AR) of PAN/clay nanocomposites at various pressures (Patra et al. 2011)

extent in comparison to Cloisite®30B. In case of copolymer with reinforcement of 3 wt% cloisite®30B (CP30B-3), the oxygen permeability is reduced by 42 % when compared with the virgin copolymer, whereas at the same level of loading of cloisite®93A within the same copolymer (CP93A-3) shows 51.5 % reduction in oxygen permeability with respect to virgin copolymers. This variation in oxygen permeability is attributed from the more hydrophobic nature of cloisite®93A as compared to cloisite®30B.

The insertion of albumin chains within the gallery of layered clays creates hurdles to oxygen entrance due to the disruption of layered clays into clay platelets. But in case of virgin albumin bovine the greater extent of oxygen permeation as compared to its nanocomposites is attributed from the presence of micro-voids in the protein chains. In order to understand the effect of nano clay content on the gas barrier properties of albumin bovine, gas permeation measurement of all albumin bovine/clay nanocomposites is carried out at constant pressure of 1.5 psi (Dash et al.2012) and shown in Fig. 12a, b. At this pressure, observed oxygen flow rate is found to be decreased as compared to virgin albumin bovine and it is further decreased with increase in clay percentage. For 10 wt% of nano clay loading in
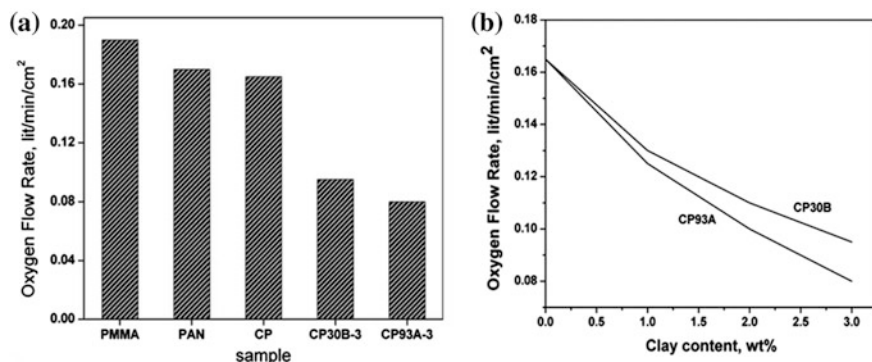
Fig. 11 A comparative account of oxygen permeabilities of **a** the individual homopolymers, copolymer, and copolymer/clay nanocomposites; **b** Oxygen permeability of the nanocomposites (at 5 psi pressure) as a function of wt% of Cloisite®30B and Cloisite®93A (Patra and Swain 2012)
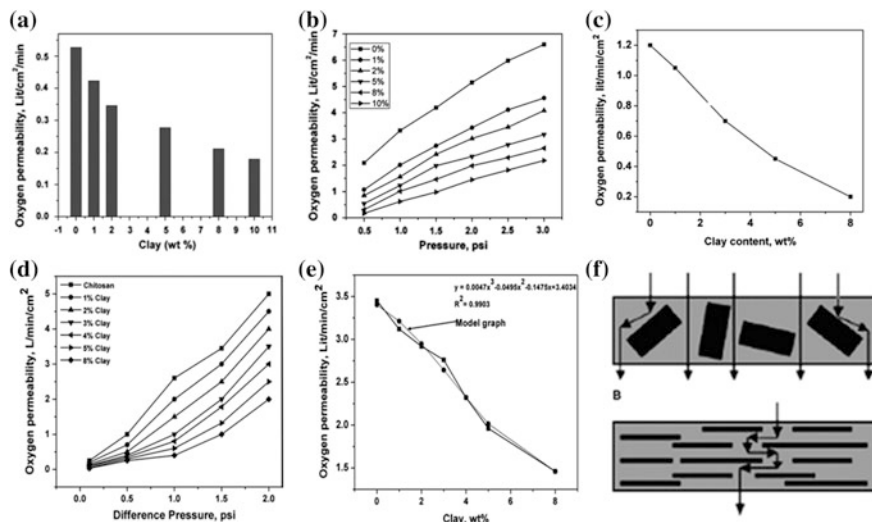
Fig. 12 Oxygen permeability of **a** albumin/clay bionanocomposites as a function of clay content at pressure 1.5 psi; **b** albumin/clay bionanocomposites as a function of wt% of clay at different pressure 3 psi; **c** albumin/clay bionanocomposites as a function of clay weight percent at a pressure of 5 psi; **d** chitosan/clay nanobiocomposites as a function of wt% of clay at difference pressure **e** chitosan/clay nanobiocomposites as a function of wt% of clay at constant pressure of 2 psi; **f** Scheme of gas permeation through polymer/clay nanocomposites (Dash et al. 2012; Swain et al. 2012; Swain et al. 2014; Patra and Swain 2012)

albumin bovine matrix, it shows reduction in oxygen permeation of about 1/3 with respect to the virgin polymer (Fig. 12a). With 8 % clay concentration, the oxygen permeability is observed to be reduced by 6 times as compared to the virgin protein.

The variation of oxygen permeability of all albumin/clay nanocomposites as a function of different pressure (upto 3 psi) has been carried out and observed an increase in gas permeation with increase in pressure (Fig. 12b). But the increment is not pronounced for albumin bovine/clay nanocomposites with higher wt% of clay loading. Due to the same analogy, oxygen permeability of nano clay reinforced soy protein bionanocomposites (Swain et al. 2012) is decreased with increase in clay content (Fig. 12c). Porous materials are more permeable to gases due to the presence of microscopic pores. As chitosan is known to be porous materials, it allows more and more oxygen within its porous network. But due to the dispersion of clay platelets within this porous network, a tortuous path is generated within chitosan/cloisite®15A nanocomposites which block the permeation of gas molecules by filling up the pores. The measurement of oxygen permeation gives the information regarding the nature of dispersion of clay platelets within nanocomposites. The observed oxygen flow rate through all chitosan/cloisite®30 B nanocomposites is observed to be less as compared to the virgin chitosan at constant pressure of 2 psi (Fig. 12d) (Swain et al. 2014). Like other bionanocomposites, the flow rate is decreased with increase in clay percentage (Fig. 12e). The suitability of the experimental data has been verified through a model graph with 3rd order regression polynomial equation (R^2 = 0.9903). The schematic representation of gas permeation through conventional and polymer/clay composites is shown in Fig. 12f.

Today, nano clay reinforced polymeric thin films are regarded as one of the most important materials for packaging based applications due to their enhanced barrier properties to oxygen, carbon dioxide and nitrogen and widely used for packaging food and carbonate drinks. The presence of impermeable clay layers creates a tortuous pathway for the incoming gaseous molecules. A huge reduction in oxygen permeability (50–500 times) has been reported for nanoclay reinforced polymer films. The permeation of gaseous penetrant to a polymeric membrane is a two stage complex process. Primarily, the gas molecules are adsorbed on the surface of the polymeric film and then they diffuse through the film. Different models have been done to account the gaseous diffusion through the polymeric membrane. At the time of adsorption, gas molecules are positioned in the free volume holes of the polymer that are created by Brownian motions of the chains or by thermal perturbations. As per this concept, diffusion process occurs by jumps through neighboring holes. Thereby, it depends on the number and the size of these holes (static free volume) and on the frequency of the jumps (dynamic free volume). The diffusion coefficient D (in $m^{-2}s^{-1}$) is related to the mobility of the gas molecules whiles the thermodynamic factor, solubility coefficient, S (in $mol\ m^{-3}\ Pa^{-1}$), is accounted from the interactions between the adsorbed gas molecules and polymer film. The gas permeability, P, of a polymer film is related to the diffusion coefficient (D) and sorption co-efficient (S) of a polymeric film. P = D · S. As per the model proposed on regular arrangement of parallel clay platelets, the general trend of diffusion is hampered due to the parallel orientation of clay platelets throughout the polymeric network and incoming gas molecules have travelled a longer and tortuous path. Hence, in polymer/clay nanocomposites, diffusion co-efficient is influenced by the

tortuosity, τ, $D = D_o/\tau$, τ depends on the shape, orientation and aspect ratio. The tortuosity (τ) is defined as $\tau = \ell'/\ell$.

The presence of nanoplatelets within the polymeric film also influence the solubility of the adsorbed gas molecules as, $S = S_o (1 - \Phi)$; where Φ is the volume fraction of the nanoplatelets that are dispersed in the matrix and S_o is the diffusion co-efficient of virgin polymer. Accounting of these two facts has led to a different result, $P_{composite}/P_{matrix} = (1 - \Phi)/\tau$. This model approximation is sufficient to predict the permeability of polymer/clay systems with lower level of clay loading (less than 1 %). But at higher concentration of clay the model fails to explain the experimental data. Three distinct regions within polymer/clay nanocomposites has been considered and named as surface modifier region (1–2 nm from clay), the unconstrained polymer region and constrained polymer region (50–100 nm from clay surface). The properties of the unconstrained polymer region are not affected by the insertion of clay platelets within the host polymer. These three regions are well enough to explain the increment or decrement in oxygen permeability of polymer/clay nanocomposites as the function of nanoclay content. But the expected outcome in many cases has been hampered due to poor clay orientation or for the incomplete exfoliation of the clay structure within the nano clay reinforced polymer composites.

5 Conclusions

Nano clay reinforced polymer nanocomposites are designed by several methods including solution casting, in situ polymerization etc. The structural orientation of nanoclay within polymeric network is highly dependent on the fabrication techniques. In case of in situ polymerization, the arrangement of layered structure within polymer is triggered by the insertion of polymer chain into the gallery of layered silicates. Due to such kind of propagation the ordered structure of the layered silicate is destroyed with an expansion in basal spacing. The increased basal spacing is eventually led the intercalation or exfoliation of silicate layers within polymeric phase. Intercalated and exfoliated layered silicate nanocomposites are two extreme states of silicate layer organization in the composite morphology. Actually the insertion of polymer chains in the galleries of the initial layered tactoids is termed as intercalated structure. Such structural orientation leads to a longitudinal expansion of basal spacing of the layered clay. The complete disruption of ordered clay into clay platelets is termed as exfoliation. Intercalated or exfoliated polymer/clay nanocomposites shows the improved barrier properties against diffusion of gas molecules and it is due to layered arrangement of nano clay throughout the polymeric matrix which creates hurdle in the path of gas permeation. The effect of ultrasound during preparation of polymer nanocomposites also affect the nature of dispersion of layered clay within host polymers. The structural orientation of layered clays within polymeric matrix was evidenced from the HRTEM and TEM images, whereas; delamination of ordered silicate layers with the loss of

crystallinity is confirmed from XRD analysis. Strong and effective chemical interaction between the functional groups of organically modified nanoclays and host polymer is realized from the FTIR spectrum. The variation of oxygen permeability for nanoclay reinforced polymer and biopolymer is accounted as a function of clay loading as well as a function of different pressure for a fixed clay loading. Depending on the nature of intercalation and exfoliation of clay layers within the host polymer different degree of obstacles in the path of gas permeation has been generated. A tremendous increase in barrier properties with increase in clay concentration is due to higher degree of exfoliation of clay platelets within polyamide matrix. This has been achieved through continuous ultrasonic extrusion method instead of chemical modification of the host polymer. For high density polyethylene (HDPE) nanocomposites, same synthetic protocol with high amplitude and residence times, is adopted to get the higher degree of exfoliation as evidenced from the substantial reduction in oxygen permeability. In case of protein network, oxygen permeability is found to reduce substantially with incorporation of nanoclay through solution casting techniques which lead to intercalated (for Albumin Bovine/cloisite®93A) and exfoliated structures (for soy/cloisite®93A) due to different functionality of protein and organically modified nanoclay. Whatever be the amount of clay dispersed in the polymeric phase, nanoclays are observed to be efficient filler for the improvement in gas barrier properties for polymer film.

References

Abreu, D., Losada, P., Angulo, I., Cruz, J.M.: Development of new polyolefin films with nanoclays for application in food packaging. Eur. Polym. J. **43**, 2229–2243 (2007)

Ball, A., Jones, R.A.L.: Conformational changes in adsorbed proteins. Langmuir **11**, 3542–3548 (1995)

Barbee, R., Matayabas, C.: Nanocomposites for high barrier applications (2002). United States Patent WO2000078855A1, 26 Nov 2002

Boricha, A.B., Mody, H.M., Das, A., Bajaj, H.C.: Facile dehydroxylation of styrene using clay based catalyst. Appl. Catal. A Gen. **179**, 5–10 (1999)

Dash, S., Kisku, S.K., Swain, S.K.: Effect of nanoclay on morphological, thermal, and barrier properties of albumin bovine. Polym. Compos. **33**, 2201–2206 (2012)

Dash, S., Swain, S.K.: Effect of nano-boron nitride on the physical and chemical properties of soy protein. Compos. Sci. Technol. **84**, 39–43 (2013a)

Dash, S., Swain, S.K.: Synthesis of thermal and chemical resistant oxygen barrier starch with reinforcement of nano silicon carbide. Carbohydr. Polym. **97**, 758–763 (2013b)

Dons, A., Steven, J., Prestrelski, S.J., Allison, S., Carpenter, J.F.: Infrared spectroscopic studies of lyophilization and temperature-induced protein aggregation. J. Pharm. Sci. **84**, 415–424 (1995)

Frounchi, M., Dadbin, S., Salehpour, Z., Noferesti, M.: Gas barrier properties of PP/EPDM blend nanocomposites. J. Membr. Sci. **282**, 142–148 (2006)

Fukushima, Y., Inagoki, S.: Synthesis of an intercalating compound of monontmorilonite and 6-polyamide. J Inclusion Phenom **5**, 473–482 (1987)

Gilman, J.W.: Flammability and thermal stability studies of polymer layered-silicate (clay) nanocomposites. Appl. Clay Sci. **15**, 31–49 (1999)

Halligudi, S.B., Bajaj, H.C., Bhatt, K.N., Krishnaratnam, M.: Hydrogenation of benzene to cyclohexane catalyzed by rhodium (I) complex supported an Montmorillonite clay. React. Kinet. Catal. Lett. **48**, 547–552 (1992)

Jang, B.Z.: Nanocomposite compositions for hydrogen storage and methods for supplying hydrogen to fuel cells (2006). US2006030483, 09 Feb 2006

Khan, B.T., Najmuddin, K., Shamsuddin, S., Annapooma, K., Bhatt, J.: synthesis, antimicrobial antitumor activity of a series of palladium (II) mixed ligand complexes. J. Inorg. Biochem. **44**, 55–63 (1991)

Kim, M.H., Lee, S.H.: Nanocomposite blend composition having excellent barrier property (2006). JP2006328426, 07 Dec 2006

Kisku, S.K., Sarkar, N., Dash, S., Swain, S.K.: Preparation of starch/PVA/CaCO$_3$ nanobiocomposite films: study of fire retardant, thermal resistant, gas barrier and biodegradable properties. Polym. Plast. Technol. Eng. **53**, 1664–1670 (2014)

Kisku, S.K., Swain, S.K.: Synthesis and characterization of chitosan/boron nitride composites. J. Am. Ceram. Soc. **95**, 2753–2757 (2012)

Lapshin, S., Swain, S.K., Isayev, A.I.: Ultrasound aided extrusion process for preparation of polyolefin-clay nanocomposites. Polym. Eng. Sci. **48**, 1584–1591 (2008)

Lv, J., Liu, W.: Flame retardancy and mechanical properties of EVA nanocomposites based on magnesium hydroxide nanoparticles/microcapsulated red phosphorus. J. Appl. Polym. Sci. **105**, 333–340 (2007)

Oh, J.S., Isayev, A.I., Rogunova, M.A.: Continuous ultrasonic process for in situ compatibilization of polypropylene/natural rubber blends. Polymer **44**, 2337–2349 (2003)

Osman, M., Atallah, A.: High-density polyethylene micro- and nanocomposites: effect of particle shape, size and surface treatment on polymer crystallinity and gas permeability. Macromol. Rapid Commun. **25**, 1540–1544 (2004)

Park, K., Chowdhury, S.R., Park, C., Kim, G.: Effect of dispersion state of organoclay on cellular foam structure and mechanical properties of ethylene vinyl acetate copolymer/ethylene-1-butenecopolymer/organoclay nanocomposite foams. J. Appl. Polym. Sci. **104**, 3879–3885 (2007)

Patra, S.K., Swain, S.K.: Effect of organoclays on the thermal, mechanical, and oxygen barrier properties of poly (methylmethacrylateco-acrylonitrile)/clay nanocomposites. Polym. Compos. **33**, 796–802 (2012)

Patra, S.K., Prusty, G., Swain, S.K.: Ultrasound assisted sythesis of PMMA/clay nanocomposites: study of oxygen permeation and flame retardant properties. Bull. Mater. Sci. **35**, 27–32 (2012)

Patra, S.K., Prusty, G., Swain, S.K.: Synthesis of PAN/clay nanocomposites: study of gas permeation properties. Int. J. Nanosci. **10**, 1101–1105 (2011)

Patra, S.K., Prusty, G., Swain, S.K.: Ultrasound assisted synthesis of PMMA/clay nanocomposites: study of oxygen permeation and flame retardant properties. Bull. Mater. Sci **35**, 27–32 (2012)

Pradhan, A.K., Swain, S.K.: Electrical conductivity and oxygen permeability of polyacrylonitrile/multiwalled carbon nanotubes composites. Polym. Compos. **33**, 1114–1119 (2012)

Prasad, K., Grubb, D.T.: Direct observation of taut tie molecules in high-strength polyethylene fibers by Raman spectroscopy. J. Polym. Sci. Part B Polym. Phys. **27**, 381–403 (1989)

Rana, P.K., Swain, S.K., Sahoo, P.K.: Synthesis, characterization, and properties of intercalated poly (2-ethyl hexylacrylate)/silicate nanocomposites: XRD, TEM, IR, TGA, superabsorbency, pressure-sensitive adhesion, and biodegradation. J. Appl. Polym. Sci. **93**, 1007–1011 (2004)

Sahoo, P.K., Dey, M., Swain, S.K.: Emulsifier-free emulsion polymerization of acrylonitrile: effect of in situ developed Cu (II)/glycine chelate complex initiated by monopersulfate. J. Appl. Polym. Sci. **74**, 2785–2790 (1999)

Sahoo, P.K., Samal, R., Swain, S.K., Rana, P.K.: Synthesis of poly (butyl acrylate)/sodium silicate nanocomposite fire retardant. Eur. Polym. J. **44**, 3522–3528 (2008)

Sikdar, D., Katti, D., Kalpana, K., Mohanty, B.: Effect of organic modifiers on dynamic and static nano-mechanical properties and crystallinity of intercalated clay-polycaprolactam nanocomposites. J. Appl. Polym. Sci. **105**, 790–802 (2007)

Swain, S.K.: Ultrasound assisted process of PA6/clay nanocomposites: mechanical, rheological and barrier properties. J. Polym. Eng. **31**, 185–189 (2011)

Swain, S.K., Isayev, J.S.: Effect of ultrasound on HDPE/clay nanocomposites: rheology, structure and properties. Polymer **48**, 281–289 (2007)

Swain, S.K., Kisku, S.K., Sahoo, G.: Preparation of thermal resistant gas barrier chitosan nanobiocomposites. Polym. Compos. **35**, 2324–2328 (2014)

Swain, S.K., Priyadarshini, P.P., Patra, S.K.: Soy protein/clay bionanocomposites as ideal packaging materials. Polym. Plast. Technol. Eng. **51**, 1282–1287 (2012)

Swain, S.K., Prusty, G., Jena, I.: Conductive, gas barrier, and thermal resistant behaviour of poly (methyl methacrylate) composite by dispersion of ZrO_2 nanoparticles. Int. J. Polym. Mater. Polym. Biomater. **62**, 733–736 (2013)

Swain, S.K., Isayev, A.I.: PA6/clay nanocomposites by continuous sonication process. J. Appl. Polym. Sci. **114**, 2378–2387 (2009)

Wang, X., Du, Y., Yang, J., Wang, X., Shi, Y., Hu, X.: Preparation, characterization and antimicrobial activity of chitosan/layered silicate nanocomposites. Polymer **47**, 6738–6744 (2006)

Yang, Y., Gu, H.: Preparation and properties of deep dye fibers from poly (ethylene terephthalate)/ SiO_2 nanocomposites by in situ polymerization. J. Appl. Polym. Sci. **105**, 2363–2369 (2007)

Zhang, J., Zhuag, W., Zhang, Q., Liu, B., Wang, W., Hu, B., Shen, J.: Novel polylactide/vermiculite nanocomposites by in situ intercalative polymerization. I. Preparation, characterization, and properties. Polym. Compos. **28**, 545–550 (2007)

Zhong, Y., Janes, D., Zhang, Y., Hetzer, M., Kee, D.: Mechanical and oxygen barrier properties of organoclay-polyethylene nanocomposite films. Polym. Eng. Sci. **47**, 1101–1107 (2007)

Bionanocomposite Materials Based on Chitosan Reinforced with Nanocrystalline Cellulose and Organo-Modified Montmorillonite

Meriem Fardioui, Mohamed El Mehdi Mekhzoum, Abou el Kacem Qaiss and Rachid Bouhfid

Abstract Recently, the research of materials based on bio-renewable and biodegradable polymers has been intensively increased since they are more friendly to the environment than the conventionally used petroleum-based polymers. Chitosan is globally the second most ubiquitous renewable natural polymer following cellulose. Chitosan is a biocompatible and biodegradable polymer characterized by unique structural, chemical, and biological properties. In the aim to obtain chitosan with ultimate properties, different nanofillers reinforcements were incorporated. The presences of nanosized filler result in very promising materials since they exhibit enhanced properties with preservation of the material biodegradability without eco-toxicity. Nowadays, chitosan bionanocomposites represent a class of materials that has attracted considerable attention especially in biomedical field thinks to their inherent properties such as nontoxicity, biodegradability as well as their improved structural and functional properties. This chapter highlights the recent advances in the development of chitosan bionanocomposite films. Preparative techniques, characterization and property improvements, these novel materials are discussed. A comparative study of chitosan-based bionanocomposite films prepared by incorporation with nanocrystalline cellulose (NCC), an organo-modified montmorillonite. The chemical and physical properties of the obtained bio-hybrid films with different concentration in terms of NCC and OMMT were discussed.

Keywords Chitosan · Organoclay · Nanocrystalline cellulose · Hybrid bionanocomposite films

M. Fardioui · M.E.M. Mekhzoum · A.e.K. Qaiss · R. Bouhfid (✉)
Moroccan Foundation for Advanced Science, Innovation and Research (MAScIR),
Laboratory of Polymer Processing, Rabat Design Center, Institute of Nanomaterial
and Nanotechnology (NANOTECH), Rue Mohamed El Jazouli,
Madinat Al Irfane, 10100 Rabat, Morocco
e-mail: r.bouhfid@mascir.com

1   Introduction

In order to avoid the problems generated by plastic waste, many attempts have been made to obtain an environmental friendly polymers (Bordes, Pollet, and Avérous 2009; Siracusa et al. 2008; Weber et al. 2010). Various researches are focused on the substitution of degradable polymers by renewable, biodegradable materials with low in cost retaining the similar properties (Singha and Thakur 2010; Thakur et al. 2014). These materials are often formulated with natural biopolymer sources, such as chitin, starch and cellulose or biodegradable synthetic polymers namely, polycaprolactone and polylactic acid, able to forming a cohesive and continuous matrix (Cieśla, Salmieri, and Lacroix 2006; Kalia et al. 2011; Le Tien et al. 2000). The obtaining of the bio-based materials with properties equivalent to those of fully synthetic products is the most challenging part of this approach (Othman 2014). In order to compete with synthetic plastics, they should have comparable mechanical and/or barrier properties. In this respect, organic compounds like chitosan, etc., are taken into considerations. Chitosan is one of the most widely exploited polysaccharides in various applications owing to its intrinsic properties that depend on environmental variables (Fernandes et al. 2010). Biofilms made of these materials do not create a threat to the environment and are cost-effective. However, the disadvantages of these films include poor thermo-mechanical and barrier properties. As a result, many studies are now attempting to resolve these drawbacks of the natural polymers to approach physicochemical attributes analogous to those of petrochemical polymers (Salmieri and Lacroix 2006). In general, the incorporation of nano-sized reinforcements for example nanoclays, carbon nanotubes, nanocrystalline cellulose, graphene and inorganic nanoparticles, into biopolymer has been widely exploited (Hussain 2006; Khan et al. 2012; Li et al. 2010). Nano-reinforcements are especially useful for biopolymers, because of their usually poor performance when compared to conventional petroleum-based polymers. As we know, the smaller the filler particles, the better is the interaction filler matrix (Ludueña et al. 2007), and usually the better is the cost price efficiency (Sorrentino et al. 2007). For making high performance bio-film materials with improved mechanical and barrier properties with better-controlled release plus bioactivity/functionality, nano-sized filler can be used. In our investigation, we studied nanocrystalline cellulose (NCC) and organo-modified montmorillonite (MMT-HD, Cloisite 20A and Cloisite 30B) as hybrid reinforcements, respectively. This chapter attempts to investigate the combined effect of NCC/OMMT bi-functional nano-sized filler on the functional properties of chitosan a current biodegradable polymer matrice through a solution casting method, the properties of the obtained bionanocomposites are discussed. A brief overview on Chitosan, NCC and OMMT is given below.

2   Chitosan: Structure and Properties

Chitin is the second most abundant natural polysaccharide after cellulose on earth, first identified in 1884, its composed of β(1 → 4)-linked 2-acetamido-2deoxy-β-D-glucose (N-acetylglucosamine) (Dutta et al. 2004) as shown in (Fig. 1a). Considering the amount of chitin produced annually in the world, it is the most bountiful polymer after cellulose (Kojima and Yoshikuni 1979). Similarly, the principle derivate of chitin, chitosan is a natural linear polysaccharide obtained from crustaceans consisting mainly of β-(1,4)-linked 2-deoxy-2-amino-D-glucopyranose units and partially of β-(1,4)-linked 2-deoxy-2-acetamido-D-glucopyranose. Chitosan is a partially deacetylated derivative of chitin (Rinaudo 2006; Srinivasa and Tharanathan 2007), which is primarily manufactured from exoskeleton of crustaceans namely crabs, shrimp and cell walls of fungi. Its chemical structure, presented in (Fig. 1b). Conventionally, the distinction between chitin and chitosan is based on the degree of acetylation (DA). In this respect. Several authors believe that chitosan is the biopolymer with at least 60 % of D residues (Acosta et al. 1993; Madihally and Matthew 1999). Besides, chitosan contains a large number of hydroxyl and amino groups. These two functional groups provide several possibilities for grafting of desirable bioactive groups (Yoshida and Franco 2009). Because of the great advantage provided by the use of polymers obtained from renewable sources, Chitosan has been one of the most attractive biopolymers due to its biocompatibility, biological activity and biodegradability (Kim et al. 2011; No et al. 2007; Rabea et al. 2003).
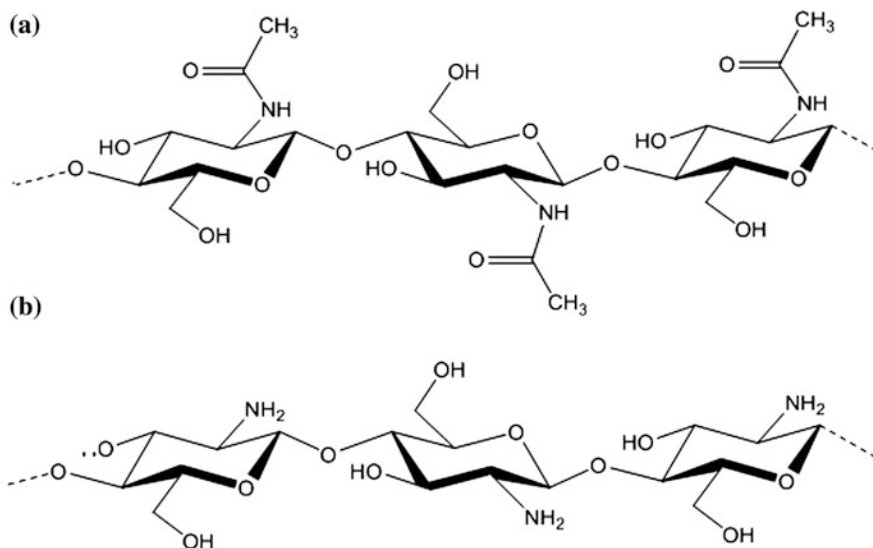
Fig. 1 Chemical structure of **a** chitin and **b** chitosan

3   Chitosan-Based Nanocomposites

Recently due to their biocompatibility and biodegradability behaviors, chitosan have been replacing synthetic polymer composites for various applications (Verma et al. 2008). The incorporation of nano-reinforcements into the chitosan matrix has been demonstrated as a powerful strategy to overcome the conventional drawbacks of the biopolymer (Depan et al. 2009). Nanocomposites of chitosan are potentially functional in a number of areas, including medicine, cosmetics, biotechnology, food industry, agriculture, environmental protection, paper industry, textiles, etc. (Hua et al. 2010). Depending on the nature and surface functionality of the nanofillers, nanocomposites of chitosan could show interesting structural and functional properties (Chen et al. 2011; Pal and Esumi 2007; Wang et al. 2006). Alternatively, chitosan extracted from different sources was used to prepare bionanocomposites with different properties (Jo et al. 2001; de Moura et al. 2009; Xu et al.2006). For instance, chitosan has been compared with other biopolymer-based films used in packaging fields, the results showed that chitosan has more advantages because of its antibacterial activity and bivalent minerals chelating ability (Casimiro et al. 2010; Chen et al. 2009). However, it's mechanical and water barrier properties should be improved (Kolhe and Kannan 2003). Thus, the enhancement of mechanical and barrier properties of chitosan films as well as the improvement of their dimensional stability has been achieved through the development of bio-nanocomposites obtained by adding plasticizer and various types of nanoreinforcing agents to the polymer matrix (Hong et al. 2008; Rao et al. 2010; Sánchez-González et al. 2010; Siripatrawan and Harte 2010). Currently, the addition of silicates nanolayeres especially montmorillonite in chitosan has been extensively studied (Dias et al. 2013; Silvestre et al. 2011). It was reported that the structure of chitosan/MMT nanocomposites and their thermal stability are strongly affected by the acetic acid (HAc) residue and the hydrogen bonds formed between chitosan and MMT on the nanocomposite properties. It was demonstrated that the residual acetic acid accelerates the chitosan thermal decomposition thus decreases its crystallinity level. In light of these facts. (Darder et al. 2003) synthesized functional CS/MMT nanocomposites, which been successfully used in the development of bulk-modified electrodes. In another work, (Dilip Depan, Annamalai Pratheep Kumar 2007) prepared nanocomposites of lactic acid grafted chitosan and layered silicates. They observed that nanocomposites are exhibiting better thermal and physical properties than do neat chitosan-g-lactic and poly(lactic acid). Currently, NCCs have started to take much attention as reinforcing materials in bionanocomposites because of their high disponibility, renewability, nanoscale dimensions, high specific surface, low density, fibrous morphology, ease of surface modification in the addition of the good mechanical properties (Park et al. 2007; Zoppe et al. 2009). The inelastic X-ray scattering was used to measure the transversal elastic modulus of the nanocrystallin cellulose, the transversal elastic modulus was about 220 GPa which reflect the efficiency of NCCs to enhance the mechanical properties of the polymeric matrix. The NCCs extracted from various

sources such as cotton, tunicate and wood for preparation of high performance nanocomposite have been investigated extensively (Azizi Samir et al. 2005). Both natural and synthetic polymers were explored as the matrices. For this reason, several papers on chitosan nanocomposites based on NCC have been reported in the literature (Azeredo et al. 2010; Klemm et al. 2009). To the best of our knowledge, no data has been reported about the studies of the combined effect of MMTs and nanocrystalline cellulose (NCC) on the final properties of chitosan.

4 Nanocrystalline Cellulose: Structure and Properties

Vegetable fibers are principally constituted by three different biopolymers namely cellulose, lignin and hemicelluloses (Escamilla-Treviño 2011). Each one of these components differs in their structure and properties. The cellulose is a semi-crystalline homopolysaccharide composed of two D-anhydroglucose ($C_6H_{11}O_5$) linked together by β-(1-4) glycosidic bonds which every glucose is corkscrewed 180° with respect to its neighbors (Fig. 2) (Habibi et al. 2010).

As can be seen in Fig. 2, many hydroxyl groups are responsible for the physical-chemical behaviors of the cellulose. They are capable of forming two types of hydrogen bonds depending on their position in the glucose unit. These hydrogen bonds exist between two adjacent hydroxyl functions present in the same cellulose chain (interamolecular bonds) that balance a linear arrangement in the cellulose molecule. In addition, they also exist between two adjacent chains (intermolecular
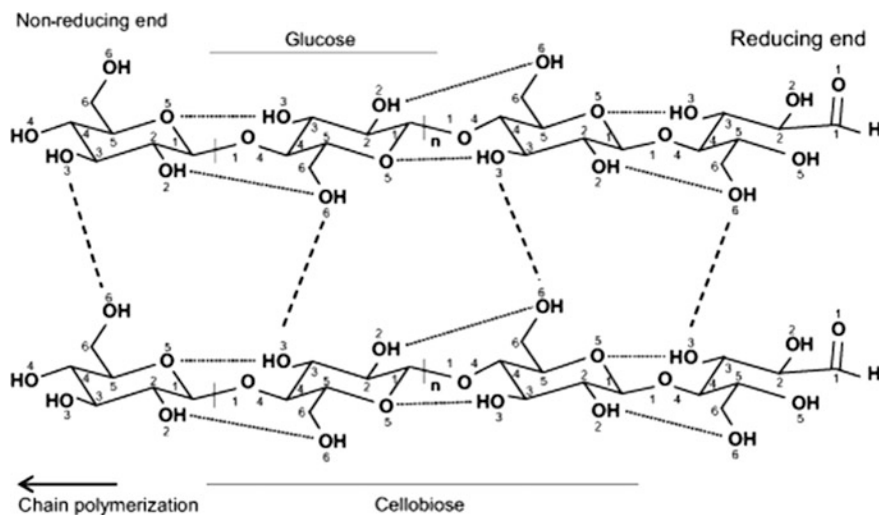
Fig. 2 The structure and the inter- and intra-chain hydrogen bonding pattern in cellulose I. *Dashed lines* inter-chain hydrogen bonding. *Dotted lines* intra-chain hydrogen bonding (Festucci-buselli et al. 2007)

bond) that explain the formation of the cellulose microfibrils in which certain regions are highly ordered; crystalline area (nanocrystalline cellulose) and other less ordered; amorphous areas (Santulli et al. 2014; Habibi et al. 2010).

These microfibrils are the structural component of plant fibers; they provide the major contribution to the strength of the plants which are built into a matrix of hemicellulose and lignin to form the cell wall (Thakur et al. 2014). On the other hand, lignin is a three-dimensional amorphous poly-phenolic which plays the role of the matrix in the vegetal fiber; it has three different units of phenyl propane types: p-coumaryl, coniferyl and sinapyl alcohols (Ramos 2003). Their composition is different depending on the plant species (Fig. 3).

Hemicellulose is a low molecular weight polysaccharide responsible for thermal degradation, biodegradation and moisture absorption of lignocellulosic fibers, it acts as a compatibilizer between the hydrophilic cellulose micro-fibrils and hydrophobic lignin (Ramos 2003), hemicellulose has the possibility to be interconnected with the lignin by covalent bonds, and to be associated with cellulose through hydrogen bonds and/or hydrophobic bond of Van der Waals type (Thakur et al. 2014). Therefore, the extraction of the nanocrystalline cellulose from vegetal fibers consisted to eliminate firstly the lignin and hemicellulose to obtain purified cellulose fibers followed by the degradation of amorphous cellulose area using for example chemical or enzymatic treatments (Le Normand et al. 2014), (Penttilä et al. 2013). The acid treatment is the most used method for extracting the NCC from the purified cellulose fibers, which it attacks the amorphous regions because of their low density compared to the crystalline regions (Kumar et al. 2014). The NCC as reinforcement in the polymeric matrix has several advantages because of their high
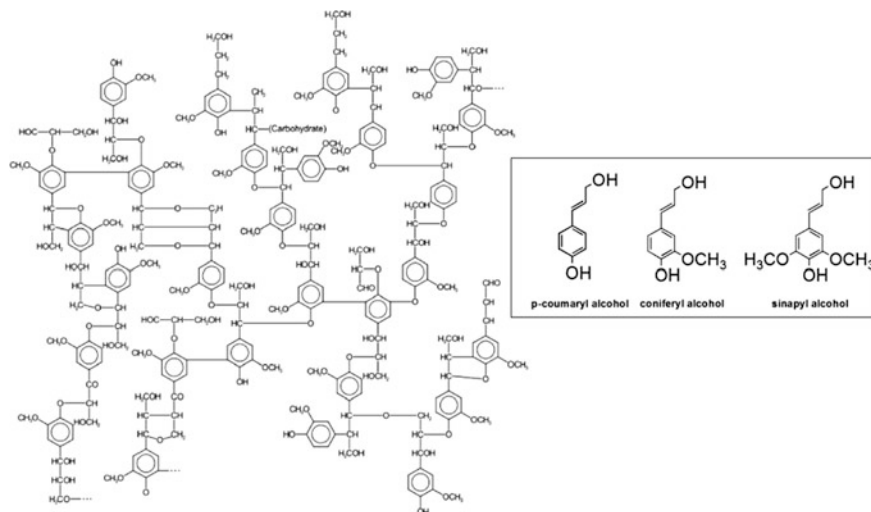
Fig. 3 Structure of lignin and lignin precursors of H-, G-, and S-units in lignin (Christopher et al. 2014)

surface area, low density, biodegradability, mechanical strength, renewability and low energy consumption in the extraction process of NCC (Rosli et al. 2013) which explain their incorporated into several polymer matrices, including polysiloxanes, polysulfonates, poly(caprolactone), styrene-butyl acrylate latex, poly(styrene-co-butyl acrylate) (poly(S-co-BuA)), cellulose acetate butyrate, carboxymethyl cellulose, poly(vinyl alcohol, poly(ethylene-vinyl acetate) (EVA), epoxides and polyethylene, polypropylene (Habibi et al. 2010).

5 Oragno-Modified-Montmorillonite: Structure and Proprieties

Clay particles as components of soil, are the smallest mineral inorganic fraction with size less than 2 μm in diameter without regard to crystallinity and composition of the particles, while the term clay mineral has generally applied to phyllosilicate (sheet or layer silicate) which is characterized by its layered structure and chemical composition (Giannelis 1998). In fact, they are naturally produced by chemical weathering of igneous, metamorphic and sedimentary rocks onto Earth's surface (Ahmadi et al. 2004). These layered minerals are hydrous aluminosilicates having continuous two-dimensional layers where each layer is made up of octahedral sheets based usually on magnesium or aluminum and silica tetrahedral sheets. Depending on the structure and layer types, the clay-sheets can be *organized* in different combination. When the unit silicate layer is build up from one octahedral sheet bonded to one tetrahedral sheet (TO) a 1:1 clay mineral results, while a 2:1 clay, is the arrangement of one octahedral sheet sandwiched by two tetrahedral sheets (TOT). As can be seen in Table 1, clay minerals may be divided into four major groups, mainly in terms of the variation in the layered structure.

Among different kinds of clay minerals. Montmorillonite (MMT), the name derived from Montmorillon, a town in the Poitou area, France are the most abundant minerals within the smectite group of 2:1 clay minerals (Lagaly and Ziesmer 2003). Montmorillonite is a clay mineral consisting of silicate layers. Its chemical structure is composed of two fused silica tetrahedral sheets sandwiching an edge-shared octahedral sheet of either aluminum or magnesium hydroxide and an interlayer region containing Na^+ or Ca^{2+} (Fig. 4) (Zeng et al. 2003). These sheets are stacked by weak Van der Waals forces leading to a layered structure and form a gap between layers called the interlayer space. In effect, montmorillonite clay has been investigated as excellent hydrophilic material with high cation exchange capacity (CEC = 80–120 meq/100 g). According to its layer dimensions, both length and width are from several hundreds of nanometers although its layer thickness can be only few nanometers. Montmorillonite is the most widely studied type of clay due to its swelling behavior, large specific surface area and peculiar layer charge characteristics (Ramsay et al. 1990). Due to its special layer structure, the Na^+ and Ca^{2+} residing in the interlayer regions can be replaced by ion exchange

Table 1 Major groups of clay minerals (Uddin 2008)

Solution	Group name	Member minerals	General formula	Remarks
1	Kaolinite	Kaolinite, dickite, nacrite	$Al_2Si_2O_5(OH)_4$	Members are polymorphs (composed of the same formula and different structure)
2	Montmorillonite or smectite	Montmorillonite, pyrophyllite, talc, vermiculite, sauconite, saponite, nontronite	$(Ca,Na,H)(Al,Mg,Fe,Zn)_2(Si,Al)_4O_{10}(OH)_2\text{-}XH_2O$	X indicates varying level of water in mineral type
3	Illite	Illite	$(K,H)Al_2(Si,Al)_4O_{10}(OH)_2\text{-}XH_2O$	X indicates varying level of water in mineral type
4	Chlorite	(i) amesite,	(i) $(Mg,Fe)_4Al_4Si_2O_{10}(OH)_8$	Each member mineral has separate formula; this group has relatively larger member minerals and is sometimes considered as a separate group, not as part of clays
		(ii) chamosite,	(ii)$(Fe,Mg)_3Fe_3AlSi_3O_{10}(OH)_8$	
		(iii) cookeite,	(iii) $LiAl_5Si_3O_{10}(OH)_8$	
		(iv) nimite etc.	(iv) $(Ni,Mg,Fe,Al)_6AlSi_3O_{10}(OH)_8$	
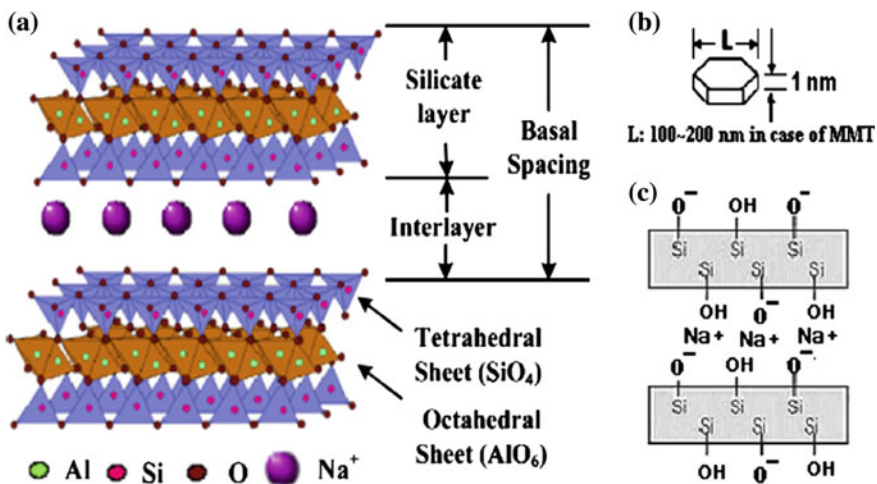
Fig. 4 **a** Molecular structure of MMT containing exchangeable sodium ion (MMT-Na +), **b** high aspect ratio clay platelet, and **c** schematic representation of side view between layers (Kim et al. 2006)

reactions with organic cations such as alkylammonium ions, sulfonium and phosphonium (Wang et al. 2003). The hydrophobic behavior and an increase in spacing between the layers of silicate are important factors which make organophilic montmorillonite compatible with the most hydrophobic polymers. Thus, this operation is named "organophilization of layered silicates". The earlier approaches in the field of modification of montmorillonite adopted ammonium surfactants. These commercially available organoclays incorporate short aliphatic chains, benzyl groups and usually a long alkyl chain (C_{12}–C_{18}) causing an increase in the interlayer spacing of the clay (Liu et al. 2005; Tanoue et al. 2004; Zha et al. 2005). However, the ammonium surfactants have low thermal stability and decompose at temperatures above 200 °C which are not suitable for high nanocomposites processing temperature between 200 and 300 °C. Table 2 lists different types of commercially available organically modified MMTs from Southern Clay Products, which differ in the nature of their counter cation and d-spacing. All four organoclays, Cloisite 20A, Cloisite 6A, Cloisite 93A and Cloisite 15A have the same surfactant in varying contents. In addition, the ammonium cations present in Cloisite 6A with two bulky tallow groups, are the most hydrophobic, whereas those in Cloisite 30B are the most hydrophilic. Furthermore, Many efforts have been made to obtain organo-modified clays with excellent thermal properties using different organic surfactants including single and dual cationic surfactants (Wang et al. 2004; Yilmaz and Yapar 2004), anionic–cationic surfactants (Zhu et al. 2000) and nonionic surfactants (Shen 2001). At present, there is a considerable amount of research on modification of montmorillonite using several kinds of organic surfactant especially heterocyclic compounds such as pyridinium, quinolinium
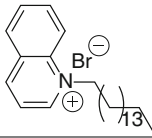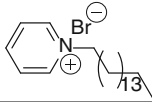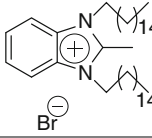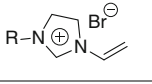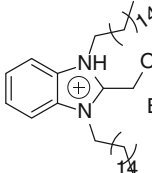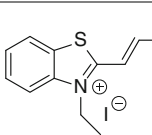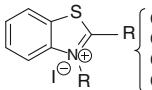
Table 2 Chemical structure of surfactant and the mean interlayer spacing (d_{001}) of organoclays available from southern clay products

Organoclay	Chemical structure of surfactant	$d001$ (nm)
Cloisite 30B	Methyl, tallow, bis-2-hydroxyethyl, quaternary ammonium chloride, MT2EtOH	1.85
Cloisite 6A	Dimethyl, dihydrogenated tallow, quaternary ammonium chloride, 2M2HT	3.51
Cloisite 10A	Dimethyl, benzyl, hydrogenated tallow, quaternary ammonium chloride, 2MBHT	1.92
Cloisite 15A	Dimethyl, dihydrogenated tallow, quaternary ammonium chloride, 2M2HT	3.15
Cloisite 20A	Dimethyl, dihydrogenated tallow, quaternary ammonium chloride, 2M2HT	2.42
Cloisite 25A	Dimethyl, dihydrogenated tallow, 2ethylhexyl quaternary ammonium, 2MHTL8	1.86
Cloisite 93A	Dimethyl, dihydrogenated tallow, ammonium, 2M2HT	2.36

T: tallow; HT: hydrogenated tallow; tallow: 65 % C_{18}, 30 % C_{16} and 5 % C

imidazolium and benzimidazolium in laboratory scale. These surfactants generally containing nitrogen heterocyclic structure with at least one long N-alkyl chain (C_{12} or greater). The incorporation of the aromatic surfactants into the gallery of clay layers show higher thermal stability compared to ammonium surfactant modified organoclays (Chigwada et al. 2006; Costache et al. 2007; El Achaby et al. 2013; Bottino et al.2003). Table 3 lists a few typical examples of these surfactants used in recent intercalation studies with d-spacing and their applications.

Table 3 Chemical structure of various heterocyclic surfactants with d-spacing and their applications

Heterocyclic compound structure	d(nm)	Application	Reference
	1.8	Polystyrene nanocomposite	Chigwada et al. (2006)
	2.0		
	2.9	Polystyrene nanocomposite	Costache et al. (2007)
	1.66 (R = C_{12}) 1.80 (R = C_{16}) 1.88 (R = C_{18})	Polystyrene nanocomposites	Bottino et al. (2003)
	3.54	High density Polyethylene and Polypropylene Nanocomposites	El Achaby et al. (2013)
	1.62	Polystyrene Nanocomposite/Chitosan biocomposites	(Unpublished paper)
	1.8 (R = C_{12})	Polyamide nanocomposites	

6 Molecular Design and Synthetic Procedures

In our case, *E*-3-dodecyl-2-(4-methoxystyryl)benzothiazol-3-ium iodide is new hemicyanine dye composed of an electron-donor *p*-anisaldehyde moiety and an electron acceptor that in this case is a benzothiazolium species bearing n-dodecyl chains (n = 12) where the hydrophobic alkyl chain substitution on the heterocyclic nitrogen of benzothiazole-derived hemicyanine dye. This compound which called push-pull system was synthesized in two steps from 2-methylbenzothiazole, 1-iodododecane, and *p*-anisaldehyde as a yellow solid, in 93 % overall yield (Tatay et al. 2006). For the synthesis of the benzothiazolium hemicyanine dye, the reaction route presented in Scheme 1 was applied. Details of the synthesis are given below. In general, the 2-methylheterocyclic ammonium salts are synthesized by heating the corresponding heteroaromatic base with a molar equivalent or an excess of an alkylating agent such as an alkyl iodide, bromide, sulphate or tosylate. With these considerations in mind. We first attempted several N-alkylation reactions of 2-methylbenzothiazole (n $\leq$ 12) with alkyl halides used as alkylating agent, but none of the N-alkylbenzothiazolium chlorides attempted could be isolated in satisfactory yields. In addition, the use of alkyl bromide affords hygroscopic salts with increased chain length (C_5-C_{12}). To counteract this problem, we decide to move forward and use alkyl iodide which is more reactive and achieve suitable yield relative to others. Hence, the quaternary salt 3-dodecyl-2-methylbenzothiazol-3-ium iodide was synthesized by reflux of available commercially 2-methylbenzothiazole with the corresponding 1-iodododecane in anhydrous acetonitrile. The solid crude product was obtained by the evaporation of the solvent and washing with diethyl ether. A key step in the synthesis of the target push-pull benzothiazoliumhemi-cyanine dye was a Knoevenagelaldo-type condensation of N-alkylbenzothiazolium and a substituted benzaldehyde. Therefore, the *E*-3-dodecyl-2-(4-methoxystyryl) benzothiazol-3-ium iodide was obtained upon interaction of the benzothiazolium salt with *p*-anisaldehyde in methanol in the presence of pyridine as catalyst. Methanol was chosen as a suitable solvent due to its good solvatation of the reactants.
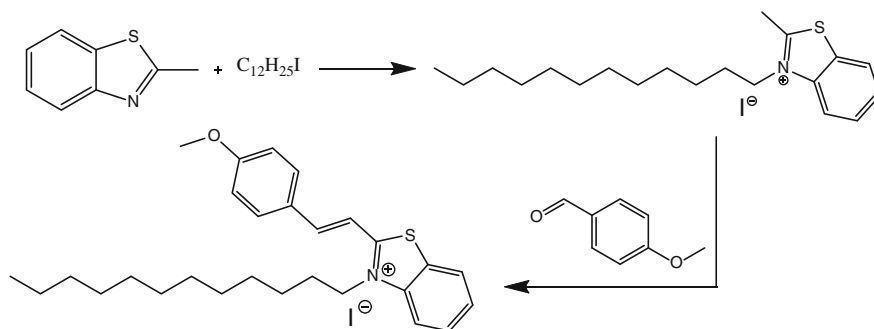
Scheme 1 The synthesis of 2-methylbenzothiazol-3-ium-based hemicyanine dye

The synthesis of hemicyanine dye has been performed in two steps. First, 3-dodecyl-2-methylbenzothiazol-3-ium iodide was prepared as previously reported (Das et al. 1993; Pardal et al. 2002): in a round bottom flask of 200 ml equipped with condenser. A mixture of 2-methylbenzothiazole (2.86 ml; 22.60 mmol) and1-iododododecane (12.25 ml; 42.20 mmol) in acetonitrile (25 ml) was heated under reflux for 24 h. After removal of acetonitrile by evaporation, diethyl ether was added to the residue. The benzothiazolium salt formed was collected by filtration, washed several times with diethyl ether and dried under vacuum to afford spectroscopically pure salt (4.5 g, 76.8 %). The second step of this synthesis was performed relates to previous (Basheer et al. 2006; Chen et al. 2005; Fedorova et al. 2002). In this respect, the benzothiazolium salt (1.5 g, 4.71 mmol) obtained is condensed with the corresponding p-anisaldehyde (1.94 g, 14.13 mmol) in methanol (30 ml) via in the presence of a catalytic amount of pyridine (0.4 ml). The mixture was stirred in an oil bath at reflux for 18 h. The reaction mixture was cooled to room temperature and the resulting precipitate was filtered, washed with diethyl ether and dried in vacuo, the primary solid was further purified by recrystallization in methanol to afford pure hemicyanine dye in the yield of 93 %. As stated before, a number similar 2-methylbenzothiazol-3-ium-based hemicyanine dye derivatives were reported in our previously patent. For the synthesis, we have adopted the catalytic free and solvent free reaction instead of the Knoevenagel reaction. The push–pull structures were obtained in good to high yields independent of substituent on the phenyl rings.

A general route for the synthesis of the prepared dye is shown in Scheme 1.

7 Montmorillonite-Hemicyane Dye (MMT-HD) Characterization

Initially, the hemicyanine dye-modified montmorillonite (MMT-HD) was prepared through cationic exchange of interfolar cation Na^+ in aqueous solution of surfactant as follows: in a two-neckround-bottom flask of 500 ml equipped with a condenser, a mixture of 150 ml of deionized water: ethanol (2:1) and 1.5 g of MMT-Na^+ was vigorously stirred for 5 h at 50 °C and sonicated forat least 30 min. Hereafter, the solution of E-3-dodecyl-2-(4-methoxystyryl)benzothiazol-3-ium iodide (2CEC) in ethanol (50 ml) was added dropwise to the suspension of MMT-Na^+ over 1 h after which refluxing and stirring were continued for 24 h at 80 °C. The resulting organoclay was isolated by centrifugation and washed with deioniwater–ethanol (1:1) solution and then by ethanol (several times). The organoclay powder was obtained by and drying at 80 °C in oven overnight.

Once the organo-clay was prepared. The FTIR analysis has been conducted to characterize the isolated solid material. As we know, the technique used to determine the structural properties of organo-modified clay is the Fourier transform infrared spectroscopy (FTIR). The Fig. 5 shows the procedure of the organophilization of
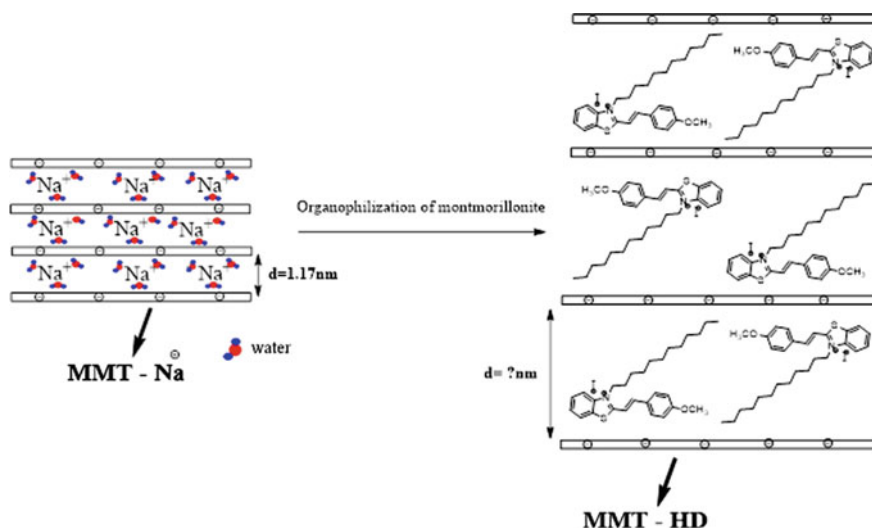
Fig. 5 Cation exchange reaction

montmorillonite using the above-mentioned hemicyanine dye surfactant (HD).The successful modification of montmorillonite by hemicyanine dye HD surfactant has been demonstrate by FTIR analysis. The Fourier transform infrared spectroscopy (FTIR) spectra of hemicyanine dye (HD), MMT-HD and MMT-Na are plotted in (Fig. 6). For the spectrum of the parent sodium-montmorillonite. Three bands absorption exist in the region 4000–1500 cm^{-1}. The band at 3625 cm^{-1} is assigned to the stretching vibration of structural (octahedral) hydroxyl (O-H) groups linked either to Al^{3+} or Mg^{2+}. The bands at 3370 cm^{-1} and 1627 cm^{-1}is assigned to the hydroxy group of interlayer water molecules. The absorption bands at 1118, 980 and

Fig. 6 FTIR spectra of HD, MMT-HD and MMT-Na clays
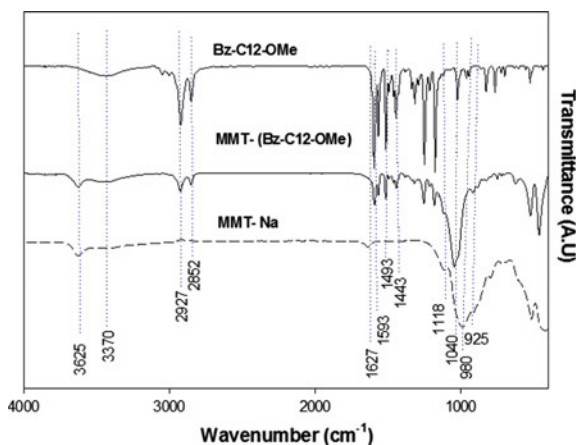
925 cm^{-1} are attributed to the stretching vibration of Si-O, Si-O-Si and the deformation of hydroxyl linked to either Al^{3+} or Mg^{2+} or Fe^{3+}(do Nascimento et al. 2004). Besides, the presence of the broad signal at 1040 cm^{-1} due to the presence of the Si–O–Si units of the corresponding hemicyanine dye-modified montmorillonite. Three new bands at 1593, 1492 and 1443 cm^{-1} can be attributed to the stretching vibrations of aromatic rings corresponding to C=C and C=N in the structure of hemicyanine dye. Additionally, the appearance in MMT-HD of new peaks at 2927, 2852 typical of C–H stretching vibration confirmed the presence of the organic guest intercalation agent.

8 Nanocrystalline Cellulose (NCC) Characterization

In this work, the NCCs were extracted from Coir fibers by chemical treatments; the alkali treatment was used to purify the cellulose by removing lignin and hemicelluloses from Coir fibers. Following washing with water at reflux, the residue was treated with alkali solution (4 wt% NaOH). The reaction mixture held in a round bottom flask for 3 h at reflux. The solid was then filtrated and washed using excess distilled water. This treatment was carried out three times. After alkali treatment, the bleaching process was completed by adding the sodium chlorite solution (1.7 wt%) plus eight drop of acetic acid at reflux for 5 h under continuous agitation. The mixture is let to cool and then filtered by using additionally distilled water in surplus. This treatment was performed tree times. The fibers results of the bleaching treatment were hydrolyzed using sulfuric acid (64 wt%) for 45 min at 45 °C under continuous stirring. The hydrolyzed material was water-washing and then centrifuge at 10.000 rpm at 10 °C for 20 min. This water washing step was repeated several times, the NCCs suspension was dialyzed against distilled water for several days until constant pH in the range of 6–7 was reached. Following dialysis treatment, the resulting suspension was sonicated for 30 min at 10°C before kept refrigerated for further used. The IR spectroscopy was performed to confirm the removing of the amorphous components from the Coir fibers by chemical treatments.

The IR spectroscopic spectra of the raw and chemically treated Coir fibers is presented in Fig. 7. All of the spectra show the presence of a broad band in the region of 3400–3300 cm^{-1}, which indicates the free O–H stretching vibration of the OH group in cellulose molecules and the band between 2900 and 2928 cm^{-1} indicates the aliphatic saturated C-H stretching associated with methylene groups in cellulose (Rosli et al. 2013). The important functional groups of lignin include carbonyls, phenol hydroxyl, aromatic rings, and methoxyl groups. The peak at 1722 cm^{-1} is assigned to the C=O stretching of carbonyl group of lignin and hemicelluloses and the peak at arrange to 1460 cm^{-1} reflected the C–C=C groups vibration of lignin, it reported that the intensity of these peaks decreased after alkali treatment and totally disappeared after bleached treatment which indicates the total elimination of lignin and hemicelluloses (Kargarzadeh et al. 2012).

Fig. 7 FTIR spectrum of the fibers after each chemical treatment
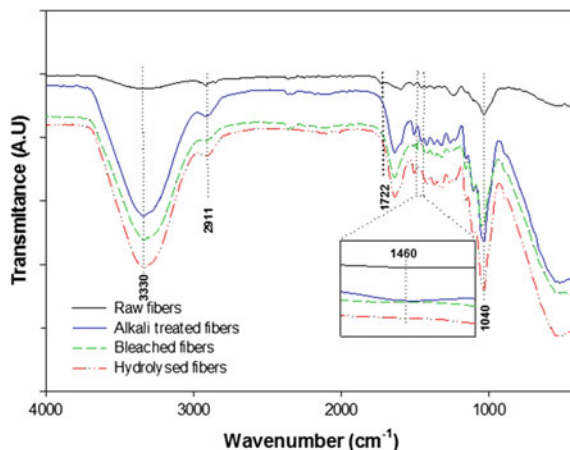
9 Hybrid Bionanocomposites Film Characterization (Cs/OMMT:NCC)

The structural, barrier, and mechanical properties of final bionanocomposite materials depend strongly on the nanofiller content, distribution/dispersion of the nanofiller into the matrix, and interfacial adhesion. In this study, the adhesion between hybrid-nanofillers (OMMT/NCC) and the chitosan was reached by the addition of glycerol as plasticizer (Fig. 8). To overcome the films brittleness, the

Fig. 8 The possible microstructure of the obtained CS/OMMT-NCC biofilms
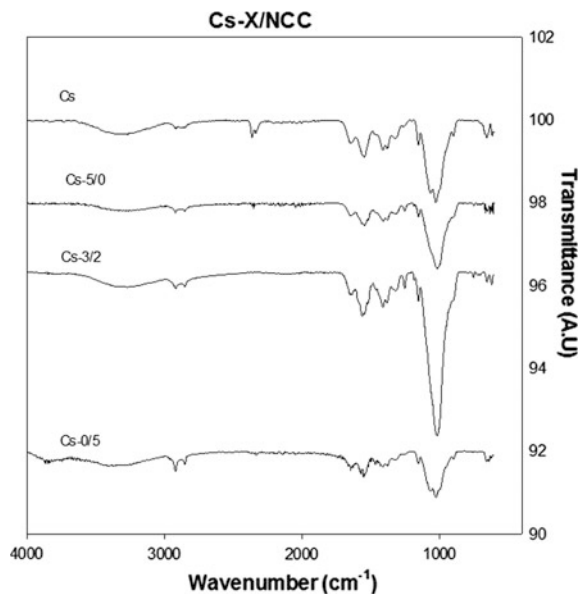
plasticizers are normally added to the film in the solution state (Müller et al. 2008) which increase the hydrophilicity, flexibility and modify the mechanical properties of films (Suyatma et al. 2005). The bionanocomposite samples in the form of films were produced using the solvent method. In this case, the chitosan solution was prepared using 1 % acetic acid solution. 0.7 g chitosan was dissolved in 40 ml acetic acid solution (1 %) and stirred at 50 °C for 3 h for homogenization. Then, chitosan solution was filtered under vacuum filter to remove impurities. Next, a 5 % of glycerol as plasticizer was added to the acidic chitosan solution. Initially, The hemicyanine-modified montmorillonite at different weight percentage (1, 2, 3, 4 and 5 wt%) were prepared by dispersing appropriate amounts of MMT-HD into 10 ml of deionized water–ethanol (1:1) and vigorously stirred. After 1 h, the MMT-HD suspension was treated with a high-performance dispersing instrument (T 25 digital ULTRA-TURRAX®—IKA) for 1 min and subsequently with an ultrasonic homogenizer for 4 min (Shinoda et al. 2012). It has to be mentioned that for both cloisite 20A/30B, the same procedure for dispersion as described above was followed to improve dispersibility of OMMT nanoplatelets. After that, the dispersion of OMMT nanoplatelets was added at a concentration of 0–5 wt%to the acidic biopolymer solution. On the other hand, a suspension of NCC (0,04 wt%) was sonicated for 30 min in water bath, and then added into the chitosan-organoclay solution and homogenized for 2 h at room temperature first by magnetic stirring followed by ultrasonic agitation. The solution was degassed to eliminate the air bulb. The applied method of homogenization/sonication improved dispersion of the modified clay nano-layers and NCCs into the chitosan matrix. Finally, the solution was cast on a Petri dish and left in ambient conditions to evaporate. Two control films as reference simples were prepared with chitosan and with chitosan/glycerol. Table 4 shows typical films composition.

After the preparation of the bio-films. The structural (FTIR), barrier (WVTR) and mechanical properties of the hybrid nanocomposites were carried out. When the compounds are blended, chemical interactions and physical links reflect changes in spectral peaks. Figures 9, 10 and 11 report FTIR spectra of chitosan/glycerol

**Table 4** Experimental design for composition of different hybrid bionanocomposites Cs/(OMMT-NCC)

Simple	Organoclay percentage (%w/w_{Cs})	n-cellulose percentage (%w/w_{Cs})
Cs/(5–0)	5	0
Cs/(4–1)	4	1
Cs/(3–2)	3	2
Cs/(2–3)	2	3
Cs/(1–4)	1	4
Cs/(0–5)	0	5

The Chitosan amount was 0.7 g/glycerol percentage added 5 %

Fig. 9 FTIR spectrum of the CS/MMT-HD:NCC hybrid nanocomposite films
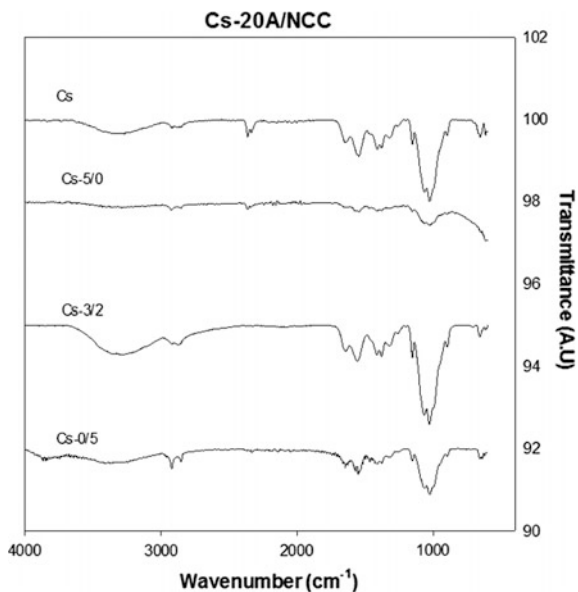
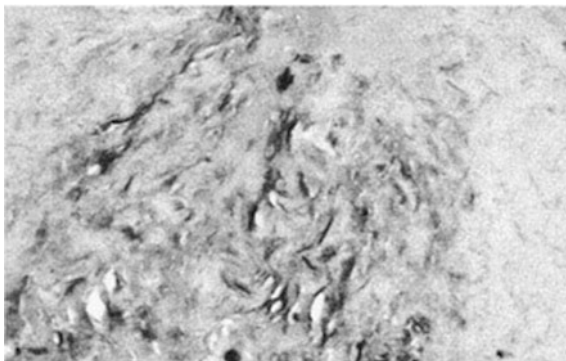Fig. 10 FTIR spectrum of the CS/Cloisite 20A: NCC hybrid nanocomposite films
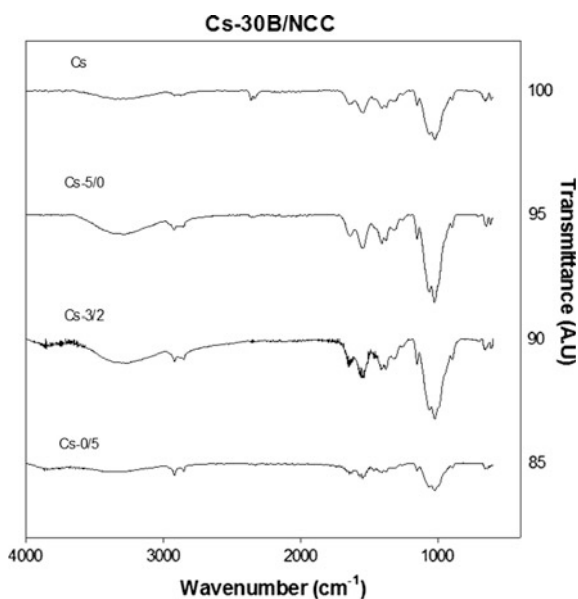
(Cs/Gly) and the Cs/OMMT:NCC of different hybrid bionanocomposite containing (0:5, 3:2, 5:0 wt%), respectively. For CS/Gly spectrum. It is well known that the bands between 3200 and 3500 cm^{-1} are assigned to –OH and –NH$_2$ groups of CS.

The bands appearing between 2750 and 3000 in the spectrum of chitosan film are due to stretching vibrations of C–H bond in –CH$_2$ (2918 cm^{-1}) and –CH$_3$ (2850 cm^{-1}) groups respectively.

In addition, strong bands at 1644 and 1568 cm^{-1} of the amide groups attributed respectively to the C=O stretching and NH bending modes corresponding to the structure of chitosan. Due to the presence of glycerol in all films. A peak at 1560 cm^{-1} has been previously ascribed to the presence of NH$_3^+$–CH$_3$COO$^-$ and disappears when glycerol was added (Brown et al. 2001). The plasticizer displace bound acetic acid from chitosan which increase the number of amine groups leading to the formation of hydrogen bonding with hydroxyl groups of organoclays, glycerol, NCCs and chitosan. For Cs/OMMT:NCC (5:0 wt%), due to the incorporation of 5 % of OMMT to the chitosan matrix, some differences can be observed in the FTIR spectra of the chitosan films, the characteristic stretching bands corresponding to the –OH and –NH$_2$ groups become more flattened when incorporating organoclay compared to CS/Gly. This observation indicates that hydroxyl and amine groups of chitosan formed hydrogen bonds with the –OH group of OMMT. In addition, two bands at 1541 and 1403 cm^{-1}, associated with –OH in-plane bending, decrease in the film incorporated with OMMT. For Cs/OMMT:NCC (3:2 wt%), a radical increase in the intensity of the band at 1025 cm^{-1} assigned to C–O stretching due to NCC incorporation. This fact indicates that hydrogen bonding, which is a strong interfacial interaction between fillers and polymer matrixes, formed between CS, OMMT and NCCs. Moreover, the effect of the addition of NCC into the chitosan-organoclay content are minor, as expected form the low amount of NCC incorporated (2 % wt%) to make the bio-films. For Cs/OMMT:NCC (0:5 wt%), the intensity of the absorption bands between 3000–2800 cm^{-1} originated from the C–H stretching vibrations was significantly increase suggesting more methylene groups from the high amount of NCCs incorporated (5 % wt%) which confirms that there was certain interaction between chitosan and nanocrystalline cellulose.

10 Mechanical and Microstructure Properties

The incorporation of nano-fillers to polymers matrix have been shown to substantially increase the final nanocomposite properties such as the mechanical properties. Indeed, the higher aspect ratio of the nano-fillers produces a large surface area for the polymer-nanofiller interaction to afford the needed reinforcement. However, the benefit of the nanofiller depends on the quantity added to the matrix which a large amount of the nano-fillers in the polymer tends to create the agglomeration. Thus, increasing the viscosity of the polymer, reduce the enthalpy and decrease the interface interaction filler/polymer which consequently tends to deteriorate the finale nanocomposite properties. Therefore, the distribution of the fillers and matrix/fillers adhesion are the importance parameter that allowed the improving or the deteriorating of the mechanical properties of the nanocomposites.

Scanning electron microscopy (SEM) and Transmission electron microscopy (TEM) were generally employed to reveal the homogeneity of the nanocomposite, the presence of voids, the adhesion/distribution level of the nanoparticles within the continuous matrix and the presence of aggregates. Chitosan nanocomposite with 3 wt% of MMT-Na (Fig. 12) presented a good and random dispersion of clay in chitosan matrix without obvious agglomeration between silicate layers (Xu, Ren,
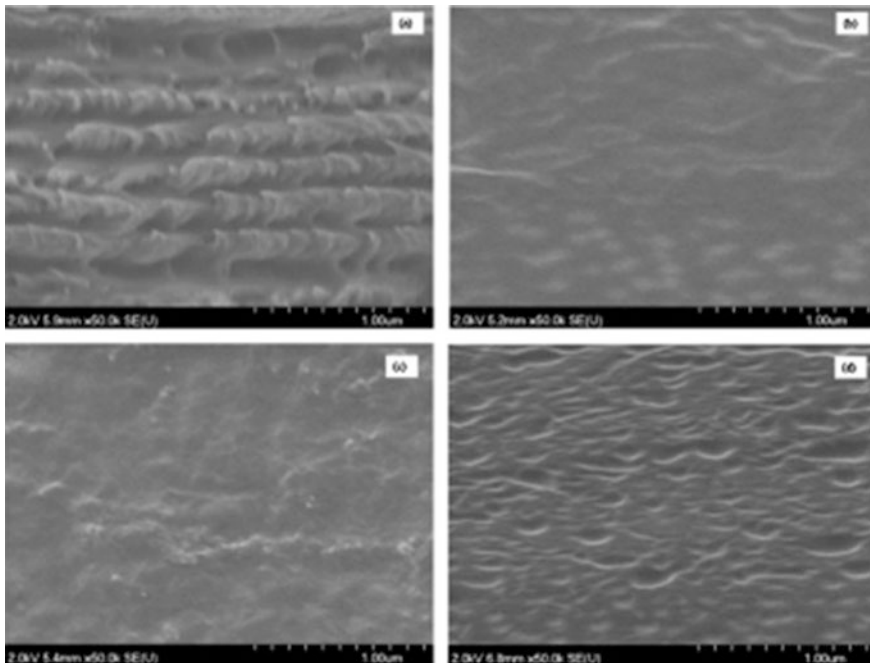
Fig. 12 TEM micrographs of chitosan and 3 wt% MMT-Na$^+$ nanocomposites film (Xu et al. 2005)

and Hanna 2006). A SEM micrograph of nanocomposite films with 5 wt% NCC content (Fig. 13c) exhibited a good dispersion of the NCC into chitosan matrix. The obtained mechanical results show an increase in tensile modulus and strength of chitosan films by 87 % and 16.5 %, respectively (Kamal and Lacroix 2015).

Fig. 13 SEM image of the cross section of **a** NCC, **b** chitosan, **c** chitosan +5 % NCC and **d** chitosan +10 % NCC (Kamal and Lacroix 2015)
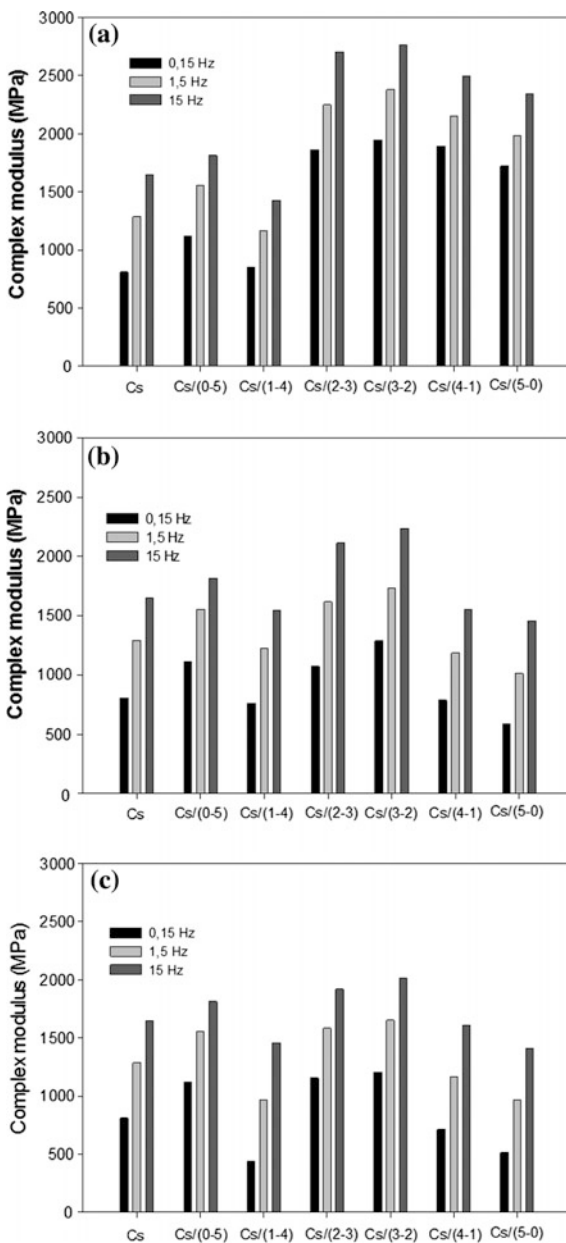
One of the essential objects of the combination of the nanocrystalline cellulose and the nano-clay is improving more the mechanical properties of the OMMT/NCCs system by progressively replacing the NCCs by the organo-nanoclays. The effect of the nano-layered silicates concentration on the dynamic mechanical behavior of the hybrid nanocomposites is shown in Fig. 14.

It can be concluded for all nanocomposites that the complex modulus increases with increasing of nanolayer amount, especially at clay contents above about 2 and 3 wt% (corresponding to 3 and 2 wt% of NCC, respectively), followed by a marked decrease. The dynamic mechanical behavior of the hybrid nanocomposites materials is related to the properties of the component, the morphology of the system, and the nature of the interface between the different nanofiller and polymer matrix. At low content of the nano-layer, the enhancement of properties is attributed to the lower percolation points created by the high aspect ratio of nanoclays, and at higher weight loading; decreases in this modulus may be attributed to the formation of agglomerated of the clay. The Table 4 presents the complex modulus for Cs/(0:5) and Cs/(3:2) and Cs/(2:3) for each hydride nanocomposites series at the quasi-static conditions (0.15 Hz).

As can be seen in Table 5, the enhancement of the mechanical properties is maximum for the hybrid nano-composites based on Cloisite 20A. It can be concluded that the chemical structure of surfactants, dispersion/morphology aspects and the interactions between organoclays/NCCs with chitosan matrix play a crucial role on the enhancement of the final mechanical properties of hybrid nanocomposites.

Fig. 14 The complex young's modulus of **a** Cs/Cloisite 20A-NCC, **b** Cs/Cloisite 30B:NCC and **c** Cs/MMT-HD:NCC hybrid nanocomposites
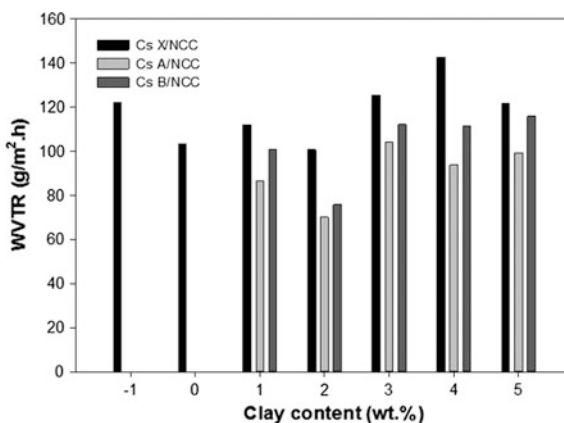
Table 5 The complex modulus of the Cs–0/5 and Cs–3/2 and Cs–2/3 hydrid nanocomposites at quasi-static conditions (0.15 Hz)

Nanocomposites	Complex modulus (MPa)	Complex modulus (MPa)	Complex modulus (MPa)
	Cs–0/5	Cs–3/2	Cs–2/3
Cs–20A/NCC	1117	1945	1864
Cs–30B/NCC		1286	1075
Cs-MMT-HD/NCC		1207	1156

11 Barrier Properties

Low water vapor transmission rate(WVTR) is a crucial property and an essential requirement for the films intended to be used in specific applications such as food packaging, protective coatings which exhibited the good barrier properties of the polymer. A significant reduction in water vapor transmission can result in either increased barrier efficiency, or a reduced thickness of the barrier layer for the same efficiency.

The WVTR across the hybrid nanocomposites films was determined according to the ASTM method E96-90, Procedure D. The tested nanocomposite films was positioned across the opening glass vial (diameter = 30 mm) containing 10 g of distilled water, and the glass vial was placed upright in a desiccator at 30 °C and with relative humidity maintained at 70 %. Evaporation of water through the test film was determined by weighing the glass vial. The weight loss of each cup was measured every hour for 6 h. Steady state weight loss curves were plotted and the slope of the linear portion was determined using a simple linear regression method. The WVTR of the material was determined by following equation:

$$WVTR = \frac{(\Delta w / \Delta t)}{A} = \frac{slope}{test\ area}$$

Where Δw is the weight change (g), Δt is the time (h), and A is the test area (mm^2). $\Delta w / \Delta t$ is the slope obtained from a chart of weight loss versus time.

Water vapor transmissionrate of the chitosan films incorporated with different concentrations of organoclay and nano-crystalline cellulose examined at 25 °C is showed in Fig. 15. The water vapor barrier property of the films was improved by clay incorporation in the film which the results showed that the minimum of WVTR is situated at 2 wt% of clay (corresponding to 3 wt% of NCCs) with a reduction of the WVTR of MMT-HD/NCC, Cloisite 20A/NCC and Cloisite 30B/NCC nanocomposites compared to pure chitosan film is about 17.3 %, 42.1 % and 37.2 %, respectively.

The decrease in WVTR of hybrid nanocomposite films is result of the presence of water vapor–impermeable silicate layers with large aspect ratios well dispersed in the polymer matrix at low weight content (Alboofetileh et al. 2013), the formation of hydrogen bond by a dipole–dipole force between the matrix and hydroxyl groups

Fig. 15 Water vapor transmission rate of the hydrid nanocomposites
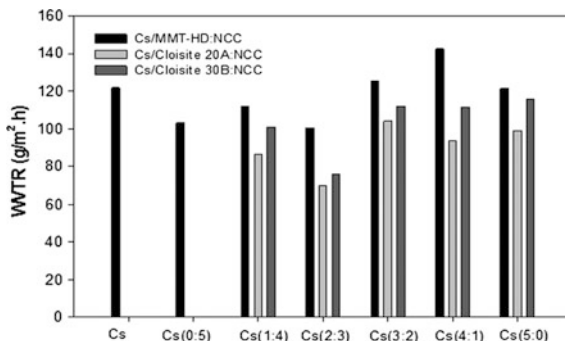
of NCCs and consequent the improvement of the biopolymer matrix cohesiveness (Rafieian and Simonsen 2015).

12 Conclusions

Cellulose, clay and chitosan are abundant, renewable and biodegradable bio-products which each one of them has a very large range of properties. The association of these materials offering new products that reunites their performances. In this study, chitosan/(OMMT-NCC) bionanocomposites were successfully prepared by the solvent method process. The chitosan/(nanolayer-nanocrystalline cellulose) films as hybrid bionanocomposites hold great promise in offering a performance films for the packaging applications. It has been clearly demonstrated that different parameters, such as OMMT/NCC dispersion (intercalated, or exfoliated), chitosan/(OMMT-NCC) affinity, and content, can affect the final structure and the bionanocomposite properties. The study of the mechanical properties and water barrier of these hybrid nanocomposites show that the chitosan matrix reinforced with 2 wt% of clay +3 wt% of NCCs gives the maximum improvement of the complex young's modulus and water vapor transmission rate. In addition, the properties of bio-films are more improved when the chitosan is reinforced with (Cloisite 20A/NCC), (Cloisite 30A/NCC) and (MMT-HD/NCC), respectively. Thus, the possibility of developing novel materials based on chitosan presents a very interesting and promising approach in the context of concerns about environmental waste problems. Based on the current literature on chitosan bionanocomposites, exceptionally strong future prospects can be predicted for these materials, which will broaden the scope of applications.

References

Acosta, N., Jiménez, C., Borau, V., Heras, A.: Extraction and Characterization of Chitin from Crustaceans. Biomass and Bioenergy **5**(2), 145–153 (1993)

Ahmadi, S.J., Huang, Y.D., Li, W.: Synthetic routes, properties and future applications of polymer-layered silicate nanocomposites. J. Mater. Sci. **39**(6), 1919–1925 (2004)

Alboofetileh, M., Rezaei, M., Hosseini, H., Abdollahi, M.: Effect of montmorillonite clay and biopolymer concentration on the physical and mechanical properties of alginate nanocomposite films. J. Food Eng. **117**(1), 26–33 (2013)

Azeredo, H., Mattoso, L., Avena-Bustillos, R., Filho, G., Munford, M., Wood, D., McHugh, T.: Nanocellulose reinforced chitosan composite films as affected by nanofiller loading and plasticizer content. J. Food Sci. **75**(1) (2010)

Azizi, M.A.S., Alloin, F., Dufresne, A.: Review of recent research into cellulosic whiskers, their properties and their application in nanocomposite field. Biomacromolecules **6**(2), 612–626 (2005)

Basheer, M.C., Alex, S., George Thomas, K., Suresh, C.H., Das, S.: A squaraine-based chemosensor for Hg^{2+} and Pb^{2+}. Tetrahedron **62**(4), 605–610 (2006)

Bordes, P., Pollet, E., Avérous, L.: Nano-biocomposites: biodegradable polyester/nanoclay systems. Prog. Polym. Sci. **34**(2), 125–155 (2009)

Bottino, F.A., Fabbri, E., Fragalà, I., Malandrino, G., Orestano, A., Pilatiand, F., Pollicino, A.: Polystyrene-clay nanocomposites prepared with polymerizable imidazolium surfactants. Macromol. Rapid Commun. **24**(18), 1079–1084 (2003)

Brown, C.D., Kreilgaard, L., Nakakura, M., Caram-lelham, N., Dean, K., Gombotz, W., Hoffman, A.: Release of PEGylated granulocyte-macrophage colony-stimulating factor from chitosan/glycerol films. J. Control. Release **72**, 35–46 (2001)

Casimiro, M.H., Gil, M.H., Leal, J.P.: Suitability of gamma irradiated chitosan based membranes as matrix in drug release system. Int. J. Pharm. **395**(1–2), 142–146 (2010)

Chen, F., Shi, Z., Neoh, K.G., Kang, E.T.: Antioxidant and antibacterial activities of eugenol and carvacrol-grafted chitosan nanoparticles. Biotechnol. Bioeng. **104**(1), 30–39 (2009)

Chen, Y.-S., Li, C., Zeng, Z., Wang, W., Wang, X., Zhang, B.: Efficient electron injection due to a special adsorbing groups combination of carboxyl and hydroxyl: dye-sensitized solar cells based on new hemicyanine dyes. J. Mater. Chem. **15**(16), 1654 (2005)

Chen, X., Wang, W., Song, Z., Wang, J.: Chitosan/carbon nanotube composites for the isolation of hemoglobin in the presence of abundant proteins. Anal. Methods **3**(8), 1769 (2011)

Chigwada, G., Wang, D., Wilkie, C.A.: Polystyrene nanocomposites based on quinolinium and pyridinium surfactants. Polym. Degrad. Stab. **91**(4), 848–555 (2006)

Christopher, L.P., Yao, B., Ji, Y.: Lignin biodegradation with laccase-mediator systems. Front. Energy Res. **2** (March), 1–13 (2014)

Cieśla, K., Salmieri, S., Lacroix, M.: Gamma-irradiation influence on the structure and properties of calcium caseinate-whey protein isolate based films. Part 2. Influence of polysaccharide addition and radiation treatment on the structure and functional properties of the films. J. Agric. Food Chem. **54**(23), 8899–8908 (2006)

Costache, M.C., Heidecker, M.J., Manias, E., Gupta, R.K., Wilkie, C.A.: Benzimidazolium surfactants for modification of clays for use with styrenic polymers. Polym. Degrad. Stab. **92** (10), 1753–1762 (2007)

Darder, M., Colilla, M., Ruiz-Hitzky, E.: Biopolymer-clay nanocomposites based on chitosan intercalated in montmorillonite. Chem. Mater. **15**(20), 3774–3780 (2003)

Das, S., Thomas, K.G., Ramanathan, R., George, M.V.: Photochemistry of squaraine dyes. 6. solvent hydrogen bonding effects on the photophysical properties of bis(benzothiazoly1idene) squaraines. 8: 13625–13628 (1993)

de Moura, M.R., Aouada, F.A., Avena-Bustillos, R.J., McHugh, T.H., Krochta, J.M., Mattoso, L. H.C.: Improved barrier and mechanical properties of novel hydroxypropyl methylcellulose edible films with chitosan/tripolyphosphate nanoparticles. J. Food Eng. **92**(4), 448–453 (2009)

Depan, D., Pratheep Kumar, A., Singh, R.P.: Bone tissue engineering with novel rhBMP2-PLLA composite scaffolds. J. Biomed. Mater. Res. Part A **81**(4), 771–780 (2007)

Depan, D., Kumar, A.P., Singh, R.P.: Cell proliferation and controlled drug release studies of nanohybrids based on chitosan-g-lactic acid and montmorillonite. Acta Biomater. **5**(1), 93–100 (2009)

Dias, M.V., Thomas, K.G., Ramanathan, R., George, M.V.: Use of allyl isothiocyanate and carbon nanotubes in an antimicrobial film to package shredded, cooked chicken meat. Food Chem. **141**(3), 3160–3166 (2013)

do Nascimento, G.M., Constantino, V.R.L., Temperini, M.L.A.: Spectroscopic characterization of doped poly(benzidine) and its nanocomposite with cationic clay. J. Phys. Chem. B **108**(18), 5564–5571 (2004)

Dutta, P.K., Duta, J., Tripathi, V.S.: Chitin and chitosan: chemistry, properties and applications. J. Sci. Ind. Res. **63**(1), 20–31 (2004)

El Achaby, M., Ennajih, H., Arrakhiz, F.Z., El Kadib, A., Bouhfid, R., Essassi, E., Qaiss, A.: Modification of montmorillonite by novel geminal benzimidazolium surfactant and its use for the preparation of polymer organoclay nanocomposites. Compos. B Eng. **51**, 310–317 (2013)

Escamilla-Treviño, L.L.: Potential of plants from the genus Agave as bioenergy crops. BioEnergy Res. **5**(1), 1–9 (2011)

Fedorova, O.A., Fedorov, Y., Vedernikov, A., Gromov, S., Yescheulova, O., Alfimov, M.: Thiacrown ether substituted styryl dyes: synthesis, complex formation and multiphotochromic properties. J. Phys. Chem. A **106**(25): 6213–6222 (2002)

Fernandes, S.C.M., et al.: Transparent chitosan films reinforced with a high content of nanofibrillated cellulose. Carbohydr. Polym. **81**(2), 394–401 (2010)

Festucci-buselli, R.A., Otoni, W.C., Joshi, C.P.: Structure, organization, and functions of cellulose synthase complexes in higher plants. **19**(1), 1–13 (2007)

Giannelis, E.P.: Polymer-layered silicate nanocomposites: synthesis, properties and applications. Appl. Organomet. Chem. **12**, 675–680 (1998)

Habibi, Y., Lucia, L.A., Rojas, O.J.: Cellulose nanocrystals: chemistry, self-assembly, and applications. Chem. Rev. **110**(6), 3479–3500 (2010)

Hua, S., Yang, H., Wang, W., Wang, A.: Controlled release of ofloxacin from chitosan-montmorillonite hydrogel. Appl. Clay Sci. **50**(1), 112–117 (2010)

Hussain, F.: Review article: polymer-matrix nanocomposites, processing, manufacturing, and application: an overview. J. Compos. Mater. **40**(17), 1511–1575 (2006)

Jo, C., Lee, J.W., Lee, K.H., Byun, M.W.: Quality properties of pork sausage prepared with water-soluble chitosan oligomer. Meat Sci. **59**(4), 369–375 (2001)

Kalia, S., Dufresne, A., Cherian, B.M., Kaith, B.S., Avérous, L., Njuguna, J., Nassiopoulos, E.: Cellulose-based bio- and nanocomposites: a review. Int. J. Polym. Sci. **2011**, 1–35 (2011)

Kamal, M.R., Lacroix, M.: Mechanical and barrier properties of nanocrystalline cellulose reinforced chitosan based nanocomposite films (2015)

Kargarzadeh, H., Ahmad, I., Abdullah, I., Dufresne, A., Zainudin, S.Y., Sheltami, R.M.: Effects of hydrolysis conditions on the morphology, crystallinity, and thermal stability of cellulose nanocrystals extracted from kenaf bast fibers. Cellulose **19**(3), 855–866 (2012)

Khan, A., Khan, R.A., Salmieri, S., Le Tien, C., Riedl, B., Bouchard, J., Chauve, G., Tan, V., Kamal, M.R., Lacroix, M.: Mechanical and barrier properties of nanocrystalline cellulose reinforced chitosan based nanocomposite films. Carbohydr. Polym. **90**(4), 1601–1608 (2012)

Kim, N.H., Malhotra, S.V., Xanthos, M.: Modification of cationic nanoclays with ionic liquids. Microporous Mesoporous Mater. **96**(1–3), 29–35 (2006)

Kim, K.W., Min, B.J., Kim, Y.-T., Kimmel, R.M., Cooksey, K., Park, S.I.: Antimicrobial activity against foodborne pathogens of chitosan biopolymer films of different molecular weights. LWT —Food Sci. Technol. **44**(2), 565–569 (2011)

Klemm, D., Schumann, D., Kramer, F., Heßler, N., Koth, D., Sultanova, B.: Nanocellulose materials—Different cellulose, different functionality. Macromol. Symp. **280**(1), 60–71 (2009)

Kojima, K., Yoshikuni, M.: Tributylborane-initiated grafting of methyl methacrylate onto chitin. **24**: 1587–1593 (1979)

Kolhe, P., Kannan, R.M.: Improvement in ductility of chitosan through blending and copolymerization with PEG: FTIR investigation of molecular interactions. Biomacromolecules **4**(1), 173–180 (2003)

Kumar, A., Negi, Y.S., Choudhary, V., Bhardwaj, N.K.: Characterization of cellulose nanocrystals produced by acid-hydrolysis from sugarcane bagasse as agro-waste. **2**(1), 1–8 (2014)

Lagaly, G., Ziesmer, S.: Colloid chemistry of clay minerals: the coagulation of montmorillonite dispersions. Adv. Colloid Interface Sci. 100–102(SUPPL.), 105–128 (2003)

Le Normand, M., Moriana, R., Ek, M.: Isolation and characterization of cellulose nanocrystals from spruce bark in a biorefinery perspective. Carbohydr. Polym. **111**, 979–987 (2014)

Le Tien, C., Letendre, M., Ispas-Szabo, P., Mateescu, M.A., Delmas-Patterson, G., Yu, H.L., Lacroix, M.: Development of biodegradable films from whey proteins by cross-linking and entrapment in cellulose. J. Agric. Food Chem. **48**(11), 5566–5575 (2000)

Li, L.-H., et al.: Preparation, characterization and antimicrobial activities of chitosan/Ag/ZnO blend films. Chem. Eng. J. **160**(1), 378–382 (2010)

Liu, G., Zhang, L., Zhao, D., Qu, X.: Bulk polymerization of styrene in the presence of organomodified montmorillonite. J. Appl. Polym. Sci. **96**(4), 1146–1152 (2005)

Ludueña, L.N., Alvarez, V.A., Vazquez, A.: Processing and Microstructure of PCL/clay Nanocomposites. Mater. Sci. Eng. A 460–461: 121–129 (2007)

Madihally, S.V., Matthew, H.W.T.: Porous chitosan scaffolds for tissue engineering. **20**: 1133–1142 (1999). (November 1998)

Müller, C.M.O., Yamashita, F., Laurindo, J.B.: Evaluation of the effects of glycerol and sorbitol concentration and water activity on the water barrier properties of cassava starch films through a solubility approach. Carbohydr. Polym. **72**(1), 82–87 (2008)

No, H.K., Meyers, S.P., Prinyawiwatkul, W., Xu, Z.: Applications of Chitosan for Improvement of Quality and Shelf Life of Foods: A Review. J. Food Sci. **72**(5) (2007)

Othman, S.H.: Bio-nanocomposite materials for food packaging applications: types of biopolymer and nano-sized filler. Agric. Agric. Sci. Procedia **2**, 296–303 (2014)

Pal, A., Esumi, K.: Photochemical synthesis of biopolymer coated Au_{core}–Ag_{shell} type bimetallic nanoparticles. J. Nanosci. Nanotechnol. **7**(6), 2110–2115 (2007)

Pardal, A.C., Ramos, S.S., Santos, P.F., Reis, L.V., Almeida, P.: Synthesis and spectroscopic characterisation of n-Alkyl quaternary ammonium salts typical precursors of cyanines. Molecules **7**(3), 320–330 (2002)

Park, W.I., Kang, M., Kim, H.S., Jin, H.J.: Electrospinning of poly(ethylene oxide) with bacterial cellulose whiskers. Macromol. Symp. **249–250**, 289–294 (2007)

Pei, H.N., Chen, X.G., Li, Y., Zhou, H.Y.: Characterization and ornidazole release in vitro of a novel composite film prepared with chitosan/poly(vinyl alcohol)/alginate. J. Biomed. Mater. Res. Part A **85**(2), 566–572 (2008)

Penttilä, P.A., Várnai, A., Pere, J., Tammelin, T., Salmén, L., Siika-aho, M., Viikari, L., Serimaa, R: Xylan as limiting factor in enzymatic hydrolysis of nanocellulose. Bioresour. Technol. **129**: 135–141 (2013)

Rabea, E.I., et al.: Chitosan as antimicrobial agent: applications and mode of action. Biomacromolecules **4**(6), 1457–1465 (2003)

Rafieian, F., Simonsen, J: The effect of carboxylated nanocrystalline cellulose on the mechanical, thermal and barrier properties of cysteine cross-linked gliadin nanocomposite. Cellulose **22**(2), 1175–1188 (2015)

Ramos, L.P.: The chemistry involved in the steam treatment of lignocellulosic materials. Quim. Nova **26**(6), 863–871 (2003)

Ramsay, J.D.F., Swanton, S.W., Bunce, J.: Swelling and dispersion of smectite clay colloids: determination of structure. J. Chem. Soc. Faraday Trans. **86**(23), 3919–3926 (1990)

Rao, M.S., Kanatt, S.R., Chawla, S.P., Sharma, A.: Chitosan and guar gum composite films: preparation, physical, mechanical and antimicrobial properties. Carbohydr. Polym. **82**(4), 1243–1247 (2010)

Rinaudo, M.: Chitin and chitosan: properties and applications. Prog. Polym. Sci. **31**(7), 603–632 (2006)

Rosli, N.A., Ahmad, I., Abdullah, I.: Solation and characterization of cellulose nanocrystals from agave angustifolia fibre. J. Bioresour. **8**: 1893–1908 (2013)

Salmieri, S., Lacroix, M.: Physicochemical properties of alginate/polycaprolactone-based films containing essential oils. J. Agric. Food Chem. **54**(26), 10205–10214 (2006)

Sánchez-González, L., González-Martínez, C., Chiralt, A., Cháfer, M.: Physical and antimicrobial properties of chitosan-tea tree essential oil composite films. J. Food Eng. **98**(4), 443–452 (2010)

Santulli, C., Sarasini, F., Fortunati, E., Puglia, D., Kenny, J.M. and Contents. . Okra fibres as potential reinforcement in biocomposites. In: Hakeem, K.R., Jawaid, M., Rashid, U.(eds.) Biomass and Bioenergy Processing and Properties, pp. 176–187. Springer International Publishing, Cham (2014)

Shen, Y.H.: Preparations of organobentonite using nonionic surfactants. Chemosphere **44**(5), 989–995 (2001)

Shinoda, R., Saito, T., Okita, Y., Isogai, A.: Relationship between length and degree of polymerization of TEMPO-oxidized cellulose nanofibrils. Biomacromolecules **13**(3), 842–849 (2012)

Silvestre, C., Duraccio, D., Cimmino, S.: Food packaging based on polymer nanomaterials. Prog. Polym. Sci. **36**(12), 1766–1782 (2011)

Singha, A.S., Thakur, V.K.: Mechanical, morphological, and thermal characterization of compression-molded polymer biocomposites. Int. J. Polym. Anal. Charact. **15**(2), 87–97 (2010)

Siracusa, V., Rocculi, P., Romani, S., Rosa, M.D.: Biodegradable polymers for food packaging: a review. Trends Food Sci. Technol. **19**(12), 634–643 (2008)

Siripatrawan, U., Harte, B.R.: Physical properties and antioxidant activity of an active film from chitosan incorporated with green tea extract. Food Hydrocoll. **24**(8), 770–775 (2010)

Sorrentino, A., Gorrasi, G., Vittoria, V.: Potential Perspectives of Bio-Nanocomposites for Food Packaging Applications. Trends Food Sci. Technol. **18**(2), 84–95 (2007)

Srinivasa, P.C., Tharanathan, R.N.: Chitin/chitosan—Safe, ecofriendly packaging materials with multiple potential uses. Food Rev. Int. **23**(1), 53–72 (2007)

Suyatma, N.E., Tighzert, L., Copinet, A., Coma, V.: Effects of hydrophilic plasticizers on mechanical, thermal, and surface properties of chitosan films effects of hydrophilic plasticizers on mechanical, thermal, and surface properties of chitosan films. J. Agric. Food Chem. **53**(10), 3950–3957 (2005)

Tanoue, S., Utracki, L.A., Garcia-Rejon, A., Sammut, P., Ton-That, M.-T., Pesneau, I., Kamal, M.R., Lyngaae-Jørgensen, J.: Melt compounding of different grades of polystyrene with organoclay. part 1: compounding and characterization. Polym. Eng. Sci. **44**: 1046–1060 (2004)

Tatay, S., Gaviña, P., Coronado, E., Palomares, E.: Optical mercury sensing using a benzothiazolium hemicyanine dye. Org. Lett. **8**(17), 3857–3860 (2006)

Thakur, V.K., Thakur, M.K., Raghavan, P., Kessler, M.R.: Progress in green polymer composites from lignin for multifunctional applications: a review. ACS Sustain. Chem. Eng. **2**(5), 1072–1092 (2014)

Uddin, F.: Clays, nanoclays, and montmorillonite minerals. Metall. Mater. Trans. A **39**(12), 2804–2814 (2008)

Verma, D., Katti, K.S., Katti, D.R., Mohanty, B.: Mechanical response and multilevel structure of biomimetic hydroxyapatite/polygalacturonic/chitosan nanocomposites. Mater. Sci. Eng. C **28**(3), 399–405 (2008)

Wang, S., Hu, Y., Zhongkai, Q., Wang, Z., Chen, Z., Fan, W.: Preparation and Flammability Properties of Polyethylene/clay Nanocomposites by Melt Intercalation Method from Na + Montmorillonite. Mater. Lett. **57**(18), 2675–2678 (2003)

Wang, C., Juang, L., Lee, C., Hsu, T., Lee, J., Chao, H.: Effects of exchanged surfactant cations on the pore structure and adsorption characteristics of montmorillonite. J. Colloid Interface Sci. **280**(1), 27–35 (2004)

Wang, S., Chen, L., Tong, Y.: Structure-Property Relationship in Chitosan-Based Biopolymer/montmorillonite Nanocomposites. J. Polym. Sci., Part A: Polym. Chem. **44**(1), 686–696 (2006)

Weber, C. J., Haugaard, V., Festersen, R., Bertelsen, G : Production and applications of biobased packaging materials for the food industry production and applications of biobased packaging materials for the food industry. 37–41 (2010). (May 2014)

Xu, Y., Ren, X., Hanna, M.A.: Chitosan/clay nanocomposite film preparation and characterization. J. Appl. Polym. Sci. **99**(4), 1684–1691 (2006)

Yilmaz, N., Yapar, S.: Adsorption properties of tetradecyl- and hexadecyl trimethylammonium bentonites. Appl. Clay Sci. **27**(3–4), 223–228 (2004)

Yoshida, C.M.P., Franco, T.T.: Chitosan tailor-made films : the effects of additives on barrier and mechanical properties and science. 161–170 (2009). (November 2008)

Zeng, Q.H., Yu, A.B., Lu, G.Q., Standish, R.K.: Molecular dynamics simulation of organic-inorganic nanocomposites: layering behavior and interlayer structure of organoclays. Chem. Mater. **15**(25), 4732–4738 (2003)

Zha, W., Choi, S., Lee, K.M., Han, C.D.: Dispersion characteristics of organoclay in nanocomposites based on end-functionalized homopolymer and block copolymer. Macromolecules **38**(20), 8418–8429 (2005)

Zhu, L., Chen, B., Shen, X.: Sorption of phenol, p-nitrophenol, and aniline to dual-cation organobentonites from water. Environ. Sci. Technol. **34**(3), 468–475 (2000)

Zoppe, J.O., Peresin, M.S., Habibi, Y., Venditti, R.A., Rojas, O.J.: Reinforcing poly (ε-caprolactone) nanofibers with cellulose nanocrystals. ACS Appl. Mater. Interfaces **1**(9), 1996–2004 (2009)

Hybrid Polymer Layered Silicate Nanocomposites

Hazizan Md Akil, Nur Suraya Anis Ahmad Bakhtiar and Nor Hafizah Che Ismail

Abstract This chapter highlights on recent development in general concept, preparation, characterization, properties, possibilities of polymers incorporated layered silicate nanocomposites and their applications in the field of nanotechnology. Polymer matrix based layered silicate nanocomposites have become a prominent area as it constitute a class of hybrid composites which the hybrid composite materials exhibit significant improvement in mechanical, decrease in gas permeability and flammability, heat distortion and thermal stability at very low filler content when compared with virgin polymers or conventional macro and micro composites. The wide range of polymer matrices is covered in this topic i.e. thermoplastic, thermosetting and elastomer. Preparative techniques of the polymer layered silicate nanocomposites include intercalation of polymers or pre-polymers from solution, sol-gel, in-situ polymerization and melt intercalation. The polymeric matrix with suitable filler and proper filler-matrix interaction will developed polymeric composites thus show great potential in wide range applications such as automotive, aerospace, packaging, construction and building.

Keywords Layered silicate · Polymer · Nanocomposites · Hybrid composites

H. Md Akil (✉) · N.S.A. Ahmad Bakhtiar · N.H. Che Ismail
School of Material and Mineral Resources Engineering,
Universiti Sains Malaysia, 14300 Seberang Perai Selatan,
Pulau Pinang, Malaysia
e-mail: hazizan@upm.my

H. Md Akil
Cluster for polymer composites (CPC), Engineering and Technology
Research Platform, Universiti Sains Malaysia, Engineering Campus,
14300 Nibong Tebal, Pulau Pinang, Malaysia

1   Introduction

In the past few decades, polymer nanocomposites especially polymer layered silicate nanocomposites (PLNS) have attracted considerable interest in research and industrial (Chrissopoulou and Anastasiadis 2011; Anastasiadis et al. 2008; Százdi et al. 2007; Sinha Ray and Okamoto 2003; Homminga et al. 2005). Compared to pristine polymers and conventionally modified composites, polymer nanocomposites often show improvement in mechanical, thermal, electrical and optical properties, flammability resistance and gas barrier properties. (Burmistr et al. 2005; Alexandre and Dubois 2000; Becker et al. 2002). Due to their superior and interesting properties, PLNS has been used for a wide range applications such as automotive, electronics and construction (Baksi and Basak 2012; Okada and Usuki 1995; Yeh and Chang 2008; Hackman and Hollaway 2006). Various polymer layered silicate nanocomposites, involving polypropylene, polyethylene, nylon, epoxy and rubber has been reported (Dominkovics et al. 2011; Dintcheva et al. 2009; Shen et al. 2004; Wang et al. 2015; Rezende et al. 2010). There are two major types in the morphological structure in polymer layered silicate nanocomposites; intercalated and exfoliated. Several method such as melt processing, solution blending and in situ polymerization has been carried out in order to prepare polymer layered silicate nanocomposites (Fernández et al. 2013; Yuan et al. 2010; Oh et al. 2013). In particular, montmorillonite (MMT), hectorite and saponite are among the most commonly used layered silicate in producing PLNS. This is due to their good swelling behaviour and ion exchange properties.

In recent years, great attention has been devoted to hybrid filler system especially the inclusion of nanoparticles. The concept of these hybrid system is to explore the improvement performance by combining the unique set properties of each filler in the final compound. The combinations of two nano fillers like CNTs and layered silicate (clay) has been reported before (Sinha Ray 2013; Li et al. 2009; Wang et al. 2008; Santangelo et al. 2011; Manikandan et al. 2012; Gorrasi et al. 2013). Some of the researcher combining of nanofiller with natural resources such as clay or natural fiber with clay to produce nanocomposites with enhanced properties (Guigo et al. 2009; Arrakhiz et al. 2013; Qiang et al. 2014; Mohamed 2013; Xu and Hoa 2008). This class of valuable hybrid nano fillers possess unexpected properties with higher added values offers applications in many fields such as electronic, optics and mechanics.

In this chapter, we introduce general concepts, classification of hybrid system and method of preparation of nanoparticles and nanocomposites. The application of hybrid polymer layered silicate nanocomposites are also be discussed in this topic.

1.1 Classification of Nanoparticles Using in Polymer Nanocomposites

Nanoparticles are considered as a high potential filler to improved mechanical and physical properties of polymer composites. Three different types of nanoparticles were usually incorporated into the polymer;

1. Zero dimensional polyhedral oligomeric silsesquioxanes such as (POSS)
2. One-dimensional nanofibers such as nanotubes and whiskers
3. Two-dimensional disc-like nanoparticles such as layered silicates
4. Three-dimensional spherical and polyhedral nanoparticles such as colloid silicates.

Among of these nanofillers, layered silicate has been widely study due to low cost and their variables applications in industries.

1.2 Layered Silicate

A clay mineral composed of layered silicates is a potential candidate for the construction of nanostructured hybrid composites. Inorganic nanoscale building blocks include nanotubes, layered silicates (e.g., montmo-rillonite, saponite), nanoparticles of metals (e.g., Au, Ag), metal oxides (e.g., TiO2, Al2O3), semiconductors (e.g., PbS, CdS), and so forth, among which SiO_2 is viewed as being very important (Pandey and Mishra 2011). However layered silicates is classified as one of inorganic fillers that is the most commonly reported in the literature. The growing interest in their use as functional fillers in most polymeric system is because they are inexpensive and easily available compared to other raw materials. This types of filler has 1 nm thick, undergoes intercalation with organic molecules precursors to form nanocomposites via ion exchange reaction. The possible intercalation and exfoliation exemplified by layered structure to be dispersed in polymer matrix creates a dramatically improved properties such as increased mechanical strength and scratching resistance, display flame retardancy properties and the most desirable part is producing new materials with lightweight properties. These magnificent properties acquire by layered silicates is due to its unique sheet structure that is classified into two different groups—(a) the 1:1 type crystal structure, and (b) the 2:1 crystal structure. Kaolinite is an example of 1:1 type crystal structure by which its tetrahedral sheet is fused with an octahedral sheet, whereby oxygen are shared. On the hand, the 2:1 phyllosilicate consists of two modular units: tetrahedral and octahedral sheets or sandwich- like on both sides. From the previous study, major inorganic layered silicates are coming from 2:1 phyllosilicate due to its special features. The variation in charges consist in 2:1 phyllosilicate will induces the occupancy of the interlayer space by exchangeable cations. Whereas, in the 1:1 phyllosilicate, the layer charge is close to zero has limits it's to be explored.

1.3 Hybrid Composites

Hybrid composites can be classified into three types; (i) the system where one type of filler materials added into a mixture of different matrices, (ii) two or more filler materials are present in a single matrix and (iii) by combining of both approaches. The hybridization of fiber with layered silicate have established to have a good result. From the previous work, it was shown that mechanical properties of the glass fiber/epoxy composites were improved by added nanoclay into the epoxy resin (Singh et al. 2014).

2 Polymer Layered Silicate Nanocomposites Preparation

At present there are four principal methods for producing polymer–layered silicate nanocomposites: (i) in situ template synthesis, (ii) intercalation of polymer from a solution, (iii) in situ intercalative polymerization and (iv) melt intercalation (Alexandre and Dubois 2000).

2.1 Intercalation of Polymer from a Solution

This technique based on a solvent system; the layered silicate is first swollen in the liquid monomer. In this case, the layered silicate are swellable meanwhile the polymer is soluble. When the polymer and layered silicate solutions are mixed, the polymer chains intercalate and remove the solvent inside the silicate interlayer. Previous researcher has studied the characterization of polymer/layered silicate pharmaceutical nanobiomaterials using high clay load exfoliation process. The exfoliation results reveals that toluene is a good solvent for the exfoliation process (Villaça et al. 2014).

2.2 Melt Intercalation

The principle of this method is based on homogenous mixing of silicates within the molten state. The product obtained then is subjected to subsequent cooling. There are several polymers were melt intercelated into clays such as Poly (L-lactic acid) (Fernández et al. 2013), Poly(vinylidene fluoride) (Song et al. 2008), polypropylene (Abdel-Goad 2011) and polyurethane (Barick and Tripathy 2010). In addition this method is favoured by most of industry as it avoids the use of monomers or solvents. This method is simpler, economical and sounds environmental friendly as no solvent are required. However melt intercalation experienced a compatability

issue when the matric use is less polar type. To overcome this problem a small amount of maleic anhydride grafted might be used to enhanced the mixing.

2.3   *In-Situ Polymerization*

There are various approaches in conducting in situ polymerization. It can be by relying on addition of monomer in solution or by exfoliating the layered silicates before polymerization occurs. The earliest example of exfoliated nanocomposite has been investigated by Toyota Research Central (Kojima et al. 1993). They disclosed the in-situ polymerization of caprolactam in the preparation of PA6/clay nanocomposites will increase the dispersion of the nanofiller as it is enables making in a single step. Next study conducted by Yuan et al. on the synthesis and properties of silicon/momtmorillonite nanocomposites. In this study, cetyltrimethylammonium bromide (CTAB) used as organic treatment agent and phenylmethylsilicone/organic monmorillonite (OMMT) nanocomposites was prepared by in-situ intercalative polymerization. The study shows that the molecules of silicone chain insert into the layer of the MMT (Yuan et al. 2010).

2.4   *Sol-Gel Method*

Processing methods for layered silicates hybrid nanocomposite include the sol-gel technology. The turning points on the development of hybrid materials starts since 1930s once sol-gel process has been used aggressively in processing method. In this technique, the clay minerals are synthesized within the polymer matrix, using an aqueous solution (or gel) containing the polymer and the silicate building blocks (Pavlidou and Papaspyrides 2008). However, sol gel is not often utilized since high temperature is needed while at the same time the inorganic components tends to aggregate. For instance, Tan et al. has study the intercalate epoxy groups into the layered silicate using sol-gel reaction of cationic APS and GPS. From the study, it was show that the epoxy-nanoclay composites exhibit high degree exfoliation of clay and have better thermal stability compared to disorder exfoliation.

3   Hybrid Layered Silicate Based Polymer Nanocomposites

Polymer is one of the most matrix used compared to metallic and ceramic. There are 3 types of polymers; thermoplastic polymers, thermosetting polymers and rubbers;

1. Thermoplastic—Often solvent soluble, melt easily and have little/no reticulation.

Table 1 Report on layer silicate/nanofiller hybrid composites

Clay/nanofiller	Matrix	References
Clay/carbon fibers	Epoxy	(Xu and Hoa 2008)
MMT/carbon fiber	Epoxy	(Zhou et al. 2007)
Nanoclay (MMT)/Glass fiber	Epoxy	(Sharma et al. 2012)
Clay/CNT	Poly(L-lactide)	(Gorrasi et al. 2013)
Smectite/CNT	PDLLA	(Santangelo et al. 2011)
MMT/CNT	Nafion	(Manikandan et al. 2012)

2. Thermoset—heavily cross linked, infusible and insoluble in solvent (Commonly used; epoxy resin, unsaturated polyester, amino resin and phenolic resins.
3. Rubber—Slightly cross linked. This properties will prevent the chain of the polymer to sliding when stretch.

Table 1 shows the summary report on layer silicate (clay)/nanofiller hybrid polymer nanocomposites.

3.1 Polypropylene-Clay Nanocomposites

Many reports on the different ways of preparations and characterization of PP/clay nanocomposites have been already published. Levchenko et al. has studied the influence of organo-clay on electrical and mechanical properties of PP/MWCNT/OC nanocomposites. From the research, it was found that the addition of organo-clay nanoparticles improves the carbon nanotubes dispersions and thus enhanced the electrical properties of the nanocomposites (Levchenko et al. 2011). Other study has reported that latex technique represents a good dispersion of exfoliated nanoclay particles The obtained results proved that the properties of nanocomposites are improved by the modification of structure and dynamics of the polymer (Raka et al. 2009).

3.2 Epoxy-Clay Nanocomposites

Epoxy, one of the thermosetting classes of polymer commonly used as it has better properties, such as high tensile strength, stiffness and hardness, low shrinkage during the curing process, good chemical and heat resistances, and high adhesive strength. There are many study has reported on epoxy filled hybrid filler composites. Wang et al. has reported on the fabrication and mechanical properties of exfoliated clay-CNTs/epoxy nanocomposites. The MMT/epoxy nanocomposites were prepared via in situ polymerization process. The result shows that the hardness and impact properties of the nanocomposites were increased effectively compared
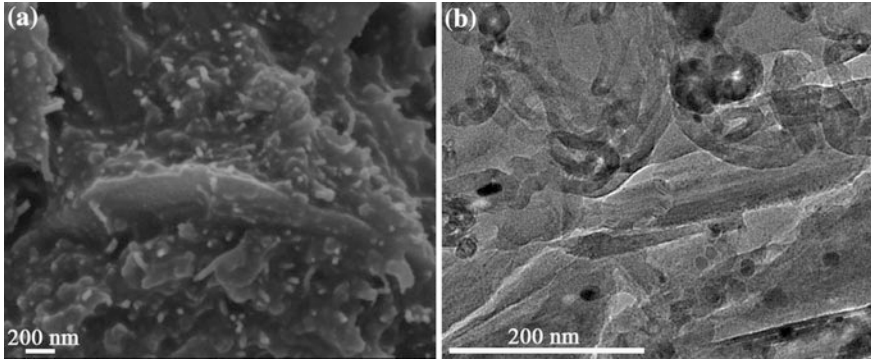
Fig. 1 **a** FESEM images of CNT-Muscovite/Epoxy and **b** HRTEM images of CNT-Muscovite/Epoxy

to pristine epoxy (Wang et al. 2008). Figure 1 shows FESEM and HRTEM images of CNT-Muscovite/Epoxy. The CNT-Muscovite was synthesis via chemical vapor deposition (CVD) and incorporated with epoxy resin.

3.3 Polystyrene-Clay Nanocomposites

Different techniques have been employed to form polystyrene nanocomposites. Melt intercalation and solution intercalation are the most practical method for polystyrene intercalate into the interlayer gallery of the clay. Previous researcher has developed nanocomposites by incorporated polystyrene-b-polyisoprene (PS-b-Pi) with organically modified montmorillonite and functionalized carbon nanotubes. The study reported on the preparation of polystyrene-b-polyisoprene copolymer with smectite clay and nanostructured clay-carbon nanotubes hybrid. Carbon nanotubes were growth on clay with nickel act as a catalyst by CCVD method. The CNT-clay/Ps-b-Pi nanocomposites were than prepared by solution intercalation. It was show that the hybrid filler (clay-CNT) exfoliated of the diblock copolymer Ps-b-PI nanocomposites were obtained from XRD analysis while the addition of semectite clay leads to intercalated structures (Litina et al. 2006).

3.4 Natural Rubber-Clay Nanocomposites

Natural rubber is one of the most important elastomers because of their interesting properties such as; high strength, elasticity, flexibility and abrasion resistance. Because of its low stiffness and high flexibility, natural rubber can be the best candidate to study the effect of the filler reinforcement in the nanocomposites.

Previous study has report on mechanical and structural properties of natural rubber latex based nanoclay nanocomposites prepared by latex method (Rezende et al. 2010). The nanocomposites were found contained exfoliated clay lamella in co-existance with tactoids which the presence of tactoid does not appear to damage the excellent reinforcement of the exfoliated platelets. The study showed that the ordering of the clay network affect thus enhance the mechanical properties of the composites. Other research by Rattanasom et al. studies the effect of natural rubber vulcanizates filled different clay types and hybrid clay/carbon ratios on the properties of the nanocomposites (Rattanasom and Prasertsri 2012). The hybrid natural rubber based nanocomposites were prepared by conventional rubber mixing technique. The addition of multiwalled carbon nanotubes into the natural rubber improved the tensile modulus, tensile strength and storage modulus meanwhile the addition of expanded organically modified montmorillonite shows gradual but permanent improvement of the tensile modulus, strength and storage modulus properties.

4   Applications and Prospective

The number of commercial applications of layered silicates hybrid nanocomposites has been growing at a rapid rate. The diversity of areas covers such as in automotive industry, filler technology, anti-corrosive barrier coating, optic, fire retardant materials and food packaging manufacturing. This can be seen by the earliest successes in the automotive industry developed by Ford Corporation where they successfully discovered the best to better disperse the clay within the polymer via sonication method. Relating to this matter, General Motors Corporation (GMC) apply this method of processing to nanocomposite based on clay and a thermoplastic olefin. The resulting material is not only lighter in weight and stiffer, but also more robust at low temperatures and more recyclable. The primary enhancement of layered silicates hybrid nanocomposite that has led to significant applications in automotive and other industries is modification and enhancement of mechanical properties. Automotive industries benefited the advances as many car components such as derived from this hybrid system produced significant improvement in various properties such as thermal, chemical and electrical properties. These include potential for utilization as mirror housings on various vehicle types, door handles, engine covers and intake manifolds and timing belt covers (Baksi and Basak 2012).

   This has been proven by work conducted by Okada et al. comprising nylon 6 and rubber clay hybrid. There have excellent mechanical properties once molded via melt compounding. This is due to the ionic bonding developed from negative charged silicates and positively charged polymer ends. In addition, timing belts is the most common products that have been manufactured in large quantities using injection molding processing technique. It is made from glass fibre reinforced nylon or polypropylene The belt cover showed good rigidity, excellent thermal stability

and no warp (Okada and Usuki 1995). Other examples, novel (PP-clay) hybrid materials were prepared using an organically modified layered silicate, namely Cloisite® 20A have allowed to simultaneously achieve higher moduli and improved process ability if their formulation includes compatibilizing agents (Zanoaga et al. 2015).

Next to the automotive industry, polymer nanocomposites are expected to find wide applications as barrier materials. The requirements to develop a sophisticated material for packaging especially in food packaging has prompted the researcher to investigate hybrid materials that has as barrier properties. The specific examples includes packaging of meats, nuts, dairy products, fruits and vegetables. The in cooperation of layered silicates in small quantities to polymer system creates a tortuous path by slow transmission of gases through composite. The tortuous path create delays the passage of molecules especially oxygen gases from penetrating the products. This enhance considerably the shelf life of many types of food. The famous supplier like Honeywell (Virginy, Southern Caroline) has developed a polyamide-based nanocomposite with specific active and passive barrier properties against oxygen.

Also quite interesting are potential applications of layered silicates intercalated with plastic materials. Plastic materials is always become a first choice once it comes to packaging purposes due to low cost, lightweight, easy availability and flexibility. However despite their attractive characteristics and large demand for this materials the fire risks and the rate of toxic gas release is a paramount factor that need to be considered. Therefore a lot of study has been conducted to reduce flammability of plastics. The innovation starts by the addition of flame retardation elements into plastic materials by Dr Jeff Gilman. Through their study, they concluded that the addition of layered silicates in nanometer range within a small volume of 2–6 % can enhance the flammability properties. The result shows that the heat release rate measure via calorimeter is significantly reduce up to 60 % suggesting a good prospect to be explored. The roles of layered silicates in plastic materials by means act as an insulation and mass transport barrier that promotes char formation.

In particular, Cardenas et al. reported the positive effects of the addition of organo-modified synthesized bentonite on the thermal stability and flame resistance of EVA (Miguel Angel Ca´rdenas et al. 2007).

Other potential applications of commercial hybrids with protective functions can be found in the painting industry. The first works start in 1950s where intense study developed on organically modified silane precursors led to resin formulations within the range of high-performance weather-resistant coatings (Sanchez et al. 2005).

5 Conclusion

This area shows immense potential for exploration due to many possible combinations of layered silicates and various polymer system. This field sounds promising, since it provides the opportunity to invent an almost unlimited set of new materials with multifunctional properties. The research opportunities offered by these materials have not ended after the huge number of literature reports on processing and properties of clay nanocomposites. In general, nanocomposite materials, particularly those with exfoliated structures present significant improvements of modulus and strength after modification of surface layer of layered silicates. Other interesting characteristics of this class of materials include improved barrier properties, thermal stability and flame retardancy.

References

Abdel-Goad, M.: Rheological characterization of melt compounded polypropylene/clay nanocomposites. Compos. Part B Eng. **42**(5), 1044–1047 (2011). doi:http://dx.doi.org/10.1016/j.compositesb.2011.03.025

Alexandre, M., Dubois, P.: Polymer-layered silicate nanocomposites: preparation, properties and uses of a new class of materials. Mater. Sci. Eng. R Rep. **28**(1–2), 1–63 (2000). doi:http://dx.doi.org/10.1016/S0927-796X(00)00012-7

Anastasiadis, S.H., Chrissopoulou, K., Frick, B.: Structure and dynamics in polymer/layered silicate nanocomposites. Mater. Sci. Eng. B **152**(1–3), 33–39 (2008). doi:http://dx.doi.org/10.1016/j.mseb.2008.06.008

Arrakhiz, F.Z., Benmoussa, K., Bouhfid, R., Qaiss, A.: Pine cone fiber/clay hybrid composite: mechanical and thermal properties. Mater. Des. **50**, 376–381 (2013). doi:http://dx.doi.org/10.1016/j.matdes.2013.03.033

Baksi, S., Basak, P.R.: Nanocomposites-Technology Trends & Application Potential. Technology Information, Forecasting and Assessment Council (2012)

Barick, A.K., Tripathy, D.K.: Thermal and dynamic mechanical characterization of thermoplastic polyurethane/organoclay nanocomposites prepared by melt compounding. Mater. Sci. Eng. A **527**(3), 812–823 (2010). doi:http://dx.doi.org/10.1016/j.msea.2009.10.063

Becker, O., Varley, R., Simon, G.: Morphology, thermal relaxations and mechanical properties of layered silicate nanocomposites based upon high-functionality epoxy resins. Polymer **43**(16), 4365–4373 (2002). doi:http://dx.doi.org/10.1016/S0032-3861(02)00269-0

Burmistr, M.V., Sukhyy, K.M., Shilov, V.V., Pissis, P., Spanoudaki, A., Sukha, I.V., Tomilo, V.I., Gomza, Y.P.: Synthesis, structure, thermal and mechanical properties of nanocomposites based on linear polymers and layered silicates modified by polymeric quaternary ammonium salts (ionenes). Polymer **46**(26), 12226–12232 (2005). doi:http://dx.doi.org/10.1016/j.polymer.2005.10.094

Chrissopoulou, K., Anastasiadis, S.H.: Polyolefin/layered silicate nanocomposites with functional compatibilizers. Eur. Polym. J. **47**(4), 600–613 (2011). doi:http://dx.doi.org/10.1016/j.eurpolymj.2010.09.028

Dintcheva, N.T., Al-Malaika, S., La Mantia, F.P.: Effect of extrusion and photo-oxidation on polyethylene/clay nanocomposites. Polym. Degrad. Stab. **94**(9), 1571–1588 (2009). doi:http://dx.doi.org/10.1016/j.polymdegradstab.2009.04.012

Dominkovics, Z., Hári, J., Kovács, J., Fekete, E., Pukánszky, B.: Estimation of interphase thickness and properties in PP/layered silicate nanocomposites. Eur. Polym. J. **47**(9), 1765–1774 (2011). doi:http://dx.doi.org/10.1016/j.eurpolymj.2011.06.010

Fernández, M.J., Fernández, M.D., Aranburu, I.: Poly(l-lactic acid)/organically modified vermiculite nanocomposites prepared by melt compounding: effect of clay modification on microstructure and thermal properties. Eur. Polym. J. **49**(6), 1257–1267 (2013). doi:http://dx.doi.org/10.1016/j.eurpolymj.2013.02.031

Gorrasi, G., Milone, C., Piperopoulos, E., Lanza, M., Sorrentino, A.: Hybrid clay mineral-carbon nanotube-PLA nanocomposite films. Preparation and photodegradation effect on their mechanical, thermal and electrical properties. Appl. Clay Sci. **71**, 49–54 (2013). doi:http://dx.doi.org/10.1016/j.clay.2012.11.004

Guigo, N., Vincent, L., Mija, A., Naegele, H., Sbirrazzuoli, N.: Innovative green nanocomposites based on silicate clays/lignin/natural fibres. Compos. Sci. Technol. **69** (11–12), 1979–1984 (2009). doi:http://dx.doi.org/10.1016/j.compscitech.2009.05.001

Hackman, I., Hollaway, L.: Epoxy-layered silicate nanocomposites in civil engineering. Compos. Part A Appl. Sci. Manuf. **37**(8), 1161–1170 (2006). doi:http://dx.doi.org/10.1016/j.compositesa.2005.05.027

Homminga, D., Goderis, B., Hoffman, S., Reynaers, H., Groeninckx, G.: Influence of shear flow on the preparation of polymer layered silicate nanocomposites. Polymer **46**(23), 9941–9954 (2005). doi:http://dx.doi.org/10.1016/j.polymer.2005.07.059

Kojima, Y., UA., Kawasumi, M., et al.: Mechanical properties of nylon 6-clay hybrid. J. Mater. Res. **8**, 1185–1189 (1993)

Levchenko, V., Mamunya, Y., Boiteux, G., Lebovka, M., Alcouffe, P., Seytre, G., Lebedev, E.: Influence of organo-clay on electrical and mechanical properties of PP/MWCNT/OC nanocomposites. Eur. Polym. J. **47**(7), 1351–1360 (2011). doi:http://dx.doi.org/10.1016/j.eurpolymj.2011.03.012

Li, M.K.S., Gao, P., Yue, P.-L., Hu, X.: Synthesis of exfoliated CNT–metal–clay nanocomposite by chemical vapor deposition. Sep. Purif. Technol. **67** (2), 238–243 (2009). doi:http://dx.doi.org/10.1016/j.seppur.2009.03.038

Litina, K., Miriouni, A., Gournis, D., Karakassides, M.A., Georgiou, N., Klontzas, E., Ntoukas, E., Avgeropoulos, A.: Nanocomposites of polystyrene-b-polyisoprene copolymer with layered silicates and carbon nanotubes. Eur. Polym. J. **42**(9), 2098–2107 (2006). doi:http://dx.doi.org/10.1016/j.eurpolymj.2006.03.025

Manikandan, D., Mangalaraja, R.V., Avila, R.E., Siddheswaran, R., Ananthakumar, S.: Carbon nanotubes rooted montmorillonite (CNT-MM) reinforced nanocomposite membrane for PEM fuel cells. Mater. Sci. Eng. B **177**(8), 614–618 (2012). doi:http://dx.doi.org/10.1016/j.mseb.2012.02.027

Miguel Angel Ca´rdenas DGa-Lp, J.F.F., Gobernado-Mitre, I., Merino, J.C., J.M.P., Martı´nez, J. D.D., Barbeta, J., D.C.: EVA nanocomposites elaborated with bentonite organo-modified by wet and semi-wet methods. Macromol. Mater. Eng. **292**, 1035–1046 (2007). doi:10.1002/mame.200700149

Mohamed, A.E.M.K.: Improvement of swelling clay properties using hay fibers. Constr. Build. Mater. **38**, 242–247 (2013). doi:http://dx.doi.org/10.1016/j.conbuildmat.2012.08.031

Oh, J.-K., Park, C.-H., Lee, S.-W., Park, J.-W., Kim, H.-J.: Adhesion performance of PSA–clay nano-composites by the in-situ polymerization and mechanical blending. Int. J. Adhes. Adhes. **47**, 13–20 (2013). doi:http://dx.doi.org/10.1016/j.ijadhadh.2013.09.002

Okada, A., Usuki, A.: The chemistry of polymer-clay hybrids. Mater. Sci. Eng. C **3**(2), 109–115 (1995). doi:http://dx.doi.org/10.1016/0928-4931(95)00110-7

Pandey, S., Mishra, S.B.: Organic–inorganic hybrid of chitosan/organoclay bionanocomposites for hexavalent chromium uptake. J. Colloid Interface Sci. **361**(2), 509–520 (2011). doi:http://dx.doi.org/10.1016/j.jcis.2011.05.031

Pavlidou, S., Papaspyrides, C.D.: A review on polymer–layered silicate nanocomposites. Prog. Polym. Sci. **33**(12), 1119–1198 (2008). doi:http://dx.doi.org/10.1016/j.progpolymsci.2008.07.008

Qiang, X., Hai-jun, L., Zhen-ze, L., Lei, L.: Cracking, water permeability and deformation of compacted clay liners improved by straw fiber. Eng. Geol. **178**, 82–90 (2014). doi:http://dx.doi.org/10.1016/j.enggeo.2014.05.013

Raka, L., Bogoeva-Gaceva, G/, Lu, K., Loos, J.: Characterization of latex-based isotactic polypropylene/clay nanocomposites. Polymer **50**(15), 3739–3746 (2009). doi:http://dx.doi.org/10.1016/j.polymer.2009.05.044

Rattanasom, N., Prasertsri, S.: Mechanical properties, gas permeability and cut growth behaviour of natural rubber vulcanizates: Influence of clay types and clay/carbon black ratios. Polym. Testing. **31**(5), 645–653 (2012). doi:http://dx.doi.org/10.1016/j.polymertesting.2012.04.001

Rezende, C.A., Bragança, F.C., Doi, T.R., Lee, L.-T., Galembeck, F., Boué, F.: Natural rubber-clay nanocomposites: Mechanical and structural properties. Polymer **51**(16), 3644–3652 (2010). doi:http://dx.doi.org/10.1016/j.polymer.2010.06.026

Sanchez, C., Julián, B., Belleville, P., Popall, M.: Applications of hybrid organic-inorganic nanocomposites. J. Mater. Chem. **15**, 3559–3592 (2005). doi:10.1039/b509097k

Santangelo, S., Gorrasi, G., Di Lieto, R., De Pasquale, S., Patimo, G., Piperopoulos, E., Lanza, M., Faggio, G., Mauriello, F., Messina, G., Milone, C.: Polylactide and carbon nanotubes/smectite-clay nanocomposites: Preparation, characterization, sorptive and electrical properties. Appl. Clay Sci. **53**(2), 188–194 (2011). doi:http://dx.doi.org/10.1016/j.clay.2010.12.013

Sharma, B., Mahajan, S., Chhibber, R., Mehta, R.: Glass fiber reinforced polymer-clay nanocomposites: Processing, structure and hygrothermal effects on mechanical properties. Procedia Chem. **4**, 39–46 (2012). doi:http://dx.doi.org/10.1016/j.proche.2012.06.006

Shen, L., Phang, I.Y., Chen, L., Liu, T., Zeng, K.: Nanoindentation and morphological studies on nylon 66 nanocomposites. I. Effect of clay loading. Polymer **45**(10), 3341–3349 (2004). doi:http://dx.doi.org/10.1016/j.polymer.2004.03.036

Singh, S.K., Singh, S., Sharma, S., Sharma, V.: Strength degradation of mechanical properties of unidirectional E- Glass fiber epoxy resin nanoclay composites under hygrothermal loading conditions. Procedia Mater. Sci. **5**, 1114–1119 (2014). doi:http://dx.doi.org/10.1016/j.mspro.2014.07.405

Sinha Ray, S.: 10—thermal stability and flammability of environmentally friendly polymer nanocomposites using biodegradable polymer matrices and clay/carbon nanotube (CNT) reinforcements. In: Environmentally Friendly Polymer Nanocomposites, pp 295–327. Woodhead Publishing (2013). doi:http://dx.doi.org/10.1533/9780857097828.2.295

Sinha Ray, S., Okamoto, M.: Polymer/layered silicate nanocomposites: a review from preparation to processing. Prog. Polym. Sci. **28**(11), 1539–1641 (2003). doi:http://dx.doi.org/10.1016/j.progpolymsci.2003.08.002

Song, Y.-M., Zhao, Z.-D., Yu, W.-X., Zheng, W.-T., Li, B., Yang, X.-W., Chen, X.-F.: Poly (vinylidene fluoride)/clay nanocomposites by melt compounding. Chem. Res. Chin. Univ. **24**(1), 116–119 (2008). doi:http://dx.doi.org/10.1016/S1005-9040(08)60024-0

Százdi, L., Pozsgay, A., Pukánszky, B.: Factors and processes influencing the reinforcing effect of layered silicates in polymer nanocomposites. Eur. Polym. J. **43**(2), 345–359 (2007). doi:http://dx.doi.org/10.1016/j.eurpolymj.2006.11.005

Villaça, J.C., da Silva, L.C.R.P., Barbosa, L.H.F., Rodrigues, C.R., Lira, L.M., do Carmo, F.A., de Sousa, V.P., Tavares, M.I.B., Cabral, e.L.M.: Preparation and characterization of polymer/layered silicate pharmaceutical nanobiomaterials using high clay load exfoliation processes. J. Ind. Eng. Chem. **20**(6), 4094–4101 (2014). doi:http://dx.doi.org/10.1016/j.jiec.2013.12.110

Wang, M., Fan, X., Thitsartarn, W., He, C.: Rheological and mechanical properties of epoxy/clay nanocomposites with enhanced tensile and fracture toughnesses. Polymer **58**, 43–52 (2015). doi:http://dx.doi.org/10.1016/j.polymer.2014.12.042

Wang, Z., Xu, C., Zhao, Y., Zhao, D., Wang, Z., Li, H., Lau, K.-T.: Fabrication and mechanical properties of exfoliated clay–CNTs/epoxy nanocomposites. Mater. Sci. Eng. A **490**(1–2), 481–487 (2008). doi:http://dx.doi.org/10.1016/j.msea.2008.01.040

Xu, Y., Hoa, S.V.: Mechanical properties of carbon fiber reinforced epoxy/clay nanocomposites. Compos. Sci. Technol. **68**(3–4), 854–861 (2008). doi:http://dx.doi.org/10.1016/j.compscitech.2007.08.013

Yeh, J.-M., Chang, K.-C.: Polymer/layered silicate nanocomposite anticorrosive coatings. J. Ind. Eng. Chem. **14**(3), 275–291 (2008). doi:http://dx.doi.org/10.1016/j.jiec.2008.01.011

Yuan, X., Li, X., Zhu, E., Hu, J., Cao, S., Sheng, W.: Synthesis and properties of silicone/montmorillonite nanocomposites by in-situ intercalative polymerization. Carbohydr. Polym. **79**(2), 373–379 (2010). doi:http://dx.doi.org/10.1016/j.carbpol.2009.08.014

Zanoaga, M., Tanasa, F., Darie, R.: Novel Polypropylene-clay Hybrid Materials for Automotive Industry. Effect of Compatilizing agent (2015)

Zhou, Y., Pervin, F., Rangari, VK., Jeelani, S.: Influence of montmorillonite clay on the thermal and mechanical properties of conventional carbon fiber reinforced composites. J. Mater. Process. Technol. **191**(1–3), 347–351 (2007). doi:http://dx.doi.org/10.1016/j.jmatprotec.2007.03.059

Rubber/Nanoclay Composites: Towards Advanced Functional Materials

Mohammad Khalid, Rashmi Walvekar, Mohammad Reza Ketabchi, Humaira Siddiqui and M. Enamul Hoque

Abstract In the recent years, nanoclay composites have drawn the attention of the researchers as well as manufacturers greatly because of their excellent capacity to withstand thermal and mechanical stress without significant compromise of impact and/or clarity. This chapter presents the preparation of nanoclay composites, characterization techniques, and the properties of the developed composites such as mechanical and thermal characteristics along with the recent applications of these nanocomposites. The rubber nanocomposite (RNC) and clay polymer nanocomposite (CPNC) have found their niche commercially in the tyre and sports industries providing reduced weight and energy dissipation, and enhanced air retention to the applied product.

Keywords Nanoclay · Nanocomposites · Functional material · Rubber · Polymer

1 Introduction

The unmodified clay mineral is a natural nanopolymer of high regularity, which has been existing in the earth since the time unmemorable. It is undoubtedly one of the oldest and most important fillers belonging to a large class of inorganic compounds.

M. Khalid · M.R. Ketabchi
Faculty of Engineering, Department of Chemical and Environmental Engineering,
University of Nottingham Malaysia Campus, 43500 Semenyih, Selangor, Malaysia

R. Walvekar
Energy Research Group, School of Engineering, Taylors University,
47500 Subang Jaya, Selangor, Malaysia

H. Siddiqui
School of Bioscience, Taylor's University, 47500 Subang Jaya,
Selangor, Malaysia

M.E. Hoque (✉)
Department of Biomedical Engineering, King Faisal University, Al-Hofuf 31982,
Al-Ahsa, Kingdom of Saudi Arabia
e-mail: mhoque@kfu.edu.sa

Clays are composed of extremely fine crystals, usually plate-shaped, less than 2 µm in diameter and less than 10 nm thick with high aspect ratio (100–500), and have large specific surface areas (750 m^2/g). They exhibit particular attributes of plasticity when mixed with water in certain proportions. The term "Nanoclay" is largely used as long as one of the dimensions is at nanometer scale. Clays are categorized based on the layers electrical charge (Table 1); either neutral-lattice structures, or low charged structures (negatively charged layers), or high charged structures (positively charged layers). Meanwhile, an equal amount of opposite charges situated in the interlayer space atone the layer charge in both high and low charged structures. These negatively or positively charged layers are named as cationic clays and anionic clays.

Generally, there are a constant number of anions expected in the clay. Therefore, the anion basis of $O_{10}(OH)_2$ for 2:1 clays and $O_5(OH)_4$ is largely used for 1:1 clays. Clay minerals are mainly described based on the cation composition and location. As presented in Fig. 1, they either fit into layered silicates or phyllosilicates classification. This categorization is based on the linked alumina sheets and silica layers; in different portions and in a certain way (Theng 2012). The most frequently used 2:1 phyllosilicate for a variety of non-ceramic and filler applications is smectites. The basic crystal structure of 2:1 phyllosilicate is a triple layer sandwich structure consisting of an octahedral alumina sheet between two tetrahedral silica sheets (Fig. 2). Atoms in these sheets common to both layers are oxygen. These three-layer units are loaded one above another with oxygen in neighboring layers adjacent to each other. In the tetrahedral coordination, silicon may be replaced by aluminum and possibly phosphorus; in the octahedral coordination, aluminum may be substituted by magnesium, iron, lithium, chromium, zinc, or nickel. Alterations in the substitutions within the lattice in terms of position and elemental composition give rise to numerous montmorillonite (MMT) clay minerals: montmorillonite, nontronite, saponite, hectorite, sauconite, beidellite, volkhonskoite, pimelite, and

Table 1 Classification of clays as a function of the electrical charge of the layer

Type of layers	Type of clay	Main features
Neutral layers	Pyrophyllite, talc, kaolinite	*Neutral clays*
		Layers joined together by van der Waals interactions and/or hydrogen bonds
Negatively charged layers	Phyllosilicates: e.g. bentonites (main component: montmorillonite)	*Cationic clays*
		The negative layer charge is exactly compensated by compensating cations are located in the interlayer space.
Positively charged layers	Hydrotalcite (HT). Layered double hydroxides (HT-like family)	*Anionic clays*
		The positive layer charge is exactly compensated by compensating anions located in the interlayer space
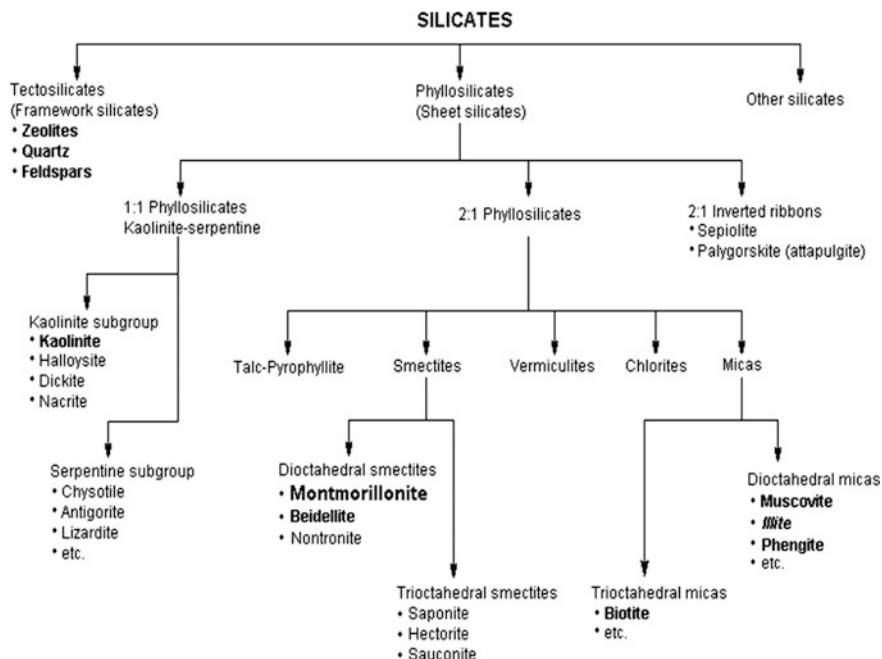
Fig. 1 Classification of silicates. Minerals that can be frequently found in bentonite or kaolin are in bold; the main components are in large typeface. Illite is a component of common soil and sediments and is classified as a mica.

griffithite. The MMT possesses great significance because of its swelling capabilities in water and other polar molecules and it is the most important species used for the production of commercial clay polymer nanocomposites (CPNC).

An idealized MMT has 0.67 units of negative charge so it behaves like a weak acid. The cation exchange capacity (CEC) is ~ 0.915 meq/g, i.e. one ion per 1.36 nm^2, i.e. anionic groups are spaced about 1.2 nm apart. MMT has a specific surface area of about 750–800 m^2/g (theoretical value is 834 m^2/g). Commercially, MMT is supplied in the form of powder with about an 8 μm particle size, each containing about 3000 platelets with a moderate aspect ratio of 10–300. Typical properties and applications are listed in Table 2. Layered silicates carry many advantages such as being natural inexpensive minerals. Their toxicologic profile is safe as they seem to have minor chance to cross biological barrier. They can thus lead to exceptional functional properties when incorporated into polymers, elastomers ceramics, inks, grease, paints and cosmetics (Patel et al. 2006).
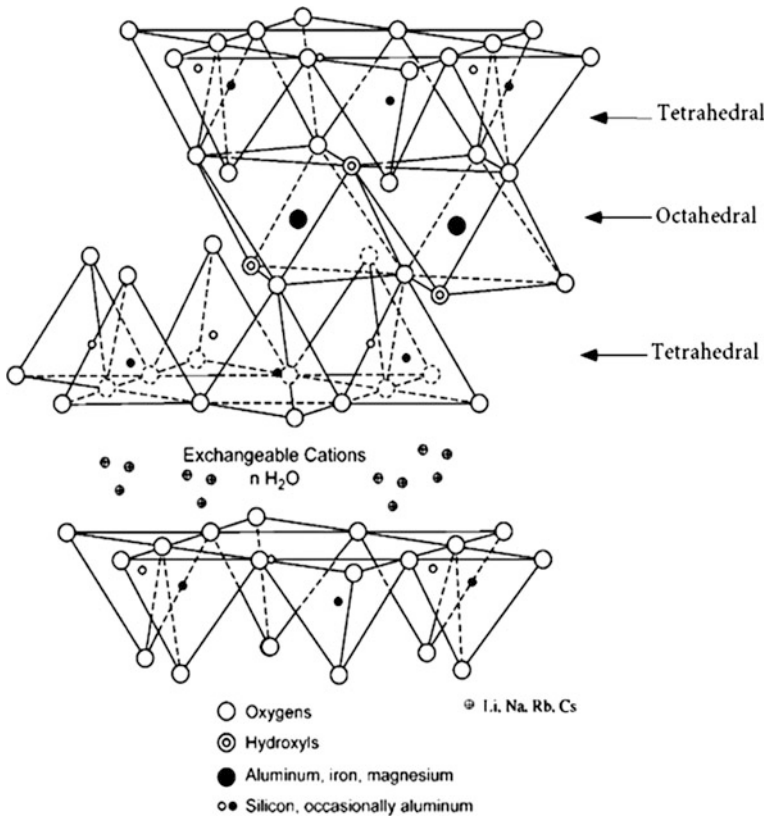
Fig. 2 Diagrammatic sketch of the structure of 2:1 phyllosilicates

2 Preparation and Properties

Natural clays are most commonly formed by the in situ hydrothermal alteration of alkaline volcanic ash and rocks of the Cretaceous period. Clay is usually mined in open pits. It is removed from the pit in layers, and stockpiled in multiple layers. Before the clay can be used, it has to be purified to eliminate the impurities. Typical contaminants include gypsum, anorthite, orthoclase, sodium carbonate, apatite, silica, albite, feldspar, halite, dolomite, siderite, calcite, biotite, chlorite, muscovite, stilbite, pyrite, hematite, kaolinite and many others. The purification often involves reduction of clay particle size either by mechanical means (milling, grinding, comminuting, etc.) or by application of hydrodynamic means (Morris 1967). Extensive early studies on clays synthesis has been reported (DeKimpe et al. 1961; Roy 1962; Weaver and Pollard 1973; Velde 1977; Linares and Huertas 1971).

Table 2 Properties and application of montmorillonite (MMT)

Physical constants		Applications
Unit cell molecular wt. (g/mol)	540.46	To slow down water flow through soil
Density (g/ml)	(2.5) 2.3–3.0	To produce nanocomposites
Crystal system and *d*-spacing (nm)	Monoclinic; $1.47 \times 0.442 \times 0.149$	To de-colour and purify liquids, viz. wines, juices, etc.
Moh's hardness @ 20 °C	1.5–2.0	As filler for paper or rubber
Appearance	White, yellow or brown with dull luster	In drilling muds to give the water greater viscosity
Cleavage	Perfect in one direction, lamellar	As a base for cosmetics and drugs
		As an absorbent
Characteristic	In H_2O its volume expands up to 30-fold	As a base for pesticides and herbicides
Field indicators	Softness, and soapy feel	As food additive for poultry and pets
DSC endothermic peaks, T (°C)	140, 700, 875	For thickening of lubricating oils and greases
DSC exothermic peak, T (°C)	920	For binding foundry sands
		To generate thixotropy
MMT swells in water more than any other mineral	Largest for Na-MMT, smaller for multivalent counter-ions	Absorption of ammonia, proteins, dyes and other polar, aromatic or ionic compounds

Linares and Huertas (1971) showed the effect of organic compounds in facilitating the synthesis of kaolin at low temperature by condensing aluminum hydroxide into octahedrally coordinated sheets. The detailed description of the early clay purification process is provided by Clocker et al. (1976) The purified clay with expanded interlayer spacing is treated with an onium intercalant (e.g. octadecyl ammonium chloride (ODA)). The initial interlayer distance is at about 1 nm while due to the large onium cations, this distance gradually widens. Therefore, the commercially available MMT based clays are presented with an interlayer distance of 1.5 and 2.5 nm. This space is typically known to be sufficient to produce exfoliated and intercalated assemblies. Nanoclay can also be made organophilic through a reaction between titanates (or organic silanes) with hydroxyl groups. This method is less popular as compared to ion exchange, and rarely accepted for rubber based composites (Galanti et al. 1999). The resulting organoclay has been used for thickening solutions in various solvents and paints. Organoclay suitable for use in CPNC must be purified and uniformly intercalated with great care. A more recent patent from AMCOL describes the detailed modern purification technology (Clarey et al. 2000). The important process control parameters are: concentration, counter ion level, purity, particle size, moisture ratio, dispersive characteristics, etc.

The idea of CPNC was first presented in 1987 by Toyota Central Research & Development Laboratories (TCRDL) in Japan, based on their pioneer investigations into nylon-6-clay nanocomposite (Kawasumi 2004). Ever since, numerous investigations have been conducted on these types of nanocomposites; an extensive review of these results has been reported elsewhere (Alexandre and Dubois 2000; Ray and Okamoto 2003). Research about rubber-clay nanocomposites (RCN) took place comparatively much later than those of CPNC. Initially, clays, especially kaolins were mainly used as non-active reinforcing filler for rubber (Hofmann 1989). The real significant research related to RCN started in early 2000 with hundreds of papers appearing in the scientific literature and numerous patents being filed. Since then, several rubbers were studied for preparation of RCC. Typical examples are styrene-butadiene-rubbers (SBR) (Galanti et al. 1999; Ganter et al. 2001; Mousa and Karger-Kocsis 2001), ethylene-propylene-diene-rubbers (EPDM) (Usuki et al. 2002; Zheng et al. 2004a, b), fluoro-rubbers (FKM) (Kader and Nah 2004), nitrile-butadiene-rubbers (NBR) (Hwang et al. 2004; Nah et al. 2001; Kim et al. 2003) and natural rubbers (NR) (Varghese et al. 2003; Magaraphan et al. 2003; Teh et al. 2004). A detailed review on the development with RCN can be found elsewhere (Sengupta et al. 2007; Lu et al. 2006).

In all these studies, the properties of RCN were reported to depend upon the dispersion of the clay layers. Major changes in composite structure could be attained following the nature of the employed components and the preparation technique. Four various types of clay dispersion in a hosting matrix have been presented in Fig. 3. Poor introduction of polymer to the silicate sheet results phase separated composites with least improvement in properties (Fig. 3a). Figure 3b is an example of intercalated structure where a single extended polymer penetrates between the layers. The exfoliated structures are obtained when $d_{001} > 8.8$ nm with the individual platelets either ordered (because of stress field or concentration effects) or not, respectively (Fig. 3c, d). It needs to be mentioned that in general, it is rare to obtain a fully exfoliated structure. In reality, an exfoliated structure is a mixed intercalated/exfoliated structure (Fig. 3d).

A decent interaction between the layers and the polymer matrix would certainly develop many properties of the nanocomposite such as impermeability (gas barrier capability) as well as mechanical properties. Nevertheless, this type of dispersion is
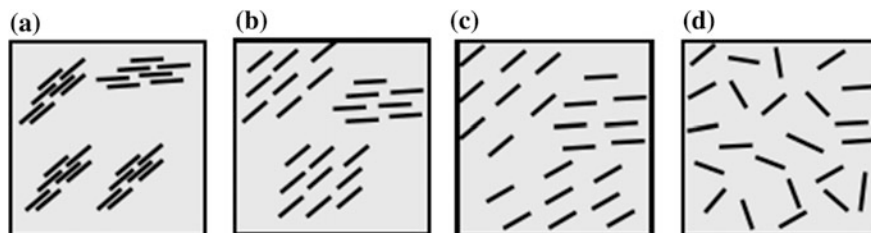

Fig. 3 Schematic representation of clay dispersion in polymer matrix

influenced by incongruity between the hydrophobic/hydrophilic behavior of components. Polymers/elastomers are naturally hydrophobic, while clays are hydrophilic. The enhancement in the specific properties and successful preparation of RCN requires that the surface of the clay is naturally improved in order to: (i) moderate the hydrophilicity, so that the clay becomes compatible with organic molecules; and (ii) to expand the intergallery distance at the same time (Fig. 4) this would enable introduction of rubber into the clay gallery.

The formation of CPNC/RCN can be described by thermodynamics of mixing through a balance of entropic and enthalpic factors which determines whether the nanofiller will be dispersed in a polymer/elastomer or not. Several studies have explained silicate clay nanocomposite formation mechanism. About polymer melt intercalation in organically modified clay (OMC), Vaia and Giannekis (1997a, b) were the first to establish the thermodynamic principle. In this principle, a lattice-based thermodynamic model is employed to study both enthalpic and entropic impacts during the development of a CPNC. This is to analyze the layered silicates driving forces for exfoliation and intercalation in long chain polymer matrix. Here, a decrease in the overall entropy of the polymer chains is observed which is believed to be due to the polymer isolation inside the interlayers. However, as the layers separate, the polymer confinement entropic loss could be atoned by the gain induced through the increase in conformational freedom of the tethered surfactant chains in a less isolated atmosphere. Slight increases in gallery height have minor influence on the total entropy; therefor modest variations in the system's total enthalpy define the possibility of thermodynamic intercalation. Complete layer separation, though, depends on the establishment of very favorable polymer-surface interactions to overcome the polymer confinement loss. It is understood that all free-energy considerations are dominated by the mixing enthalpy. Similar studies by Choudhury et al. (2010) demonstrated thermodynamics aspect of nanocomposite formation by the polymer melt intercalation mean field lattice based description (by

Fig. 4 Scheme of: **a** clay and **b** modified clay (Organoclay). Note that R can be replaced by any chemical unit
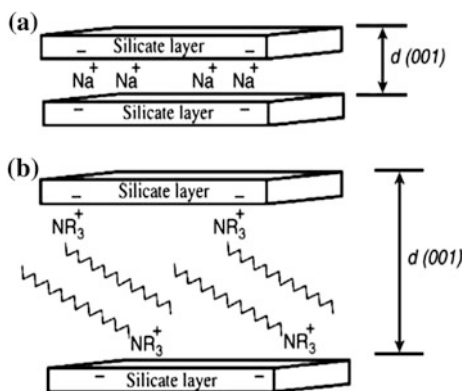
employing hydrogenated nitrile butadiene rubber (HNBR)-nanoclay nanocomposite). Another study by Mackay et al. (2006) linked the nanofiller dispersion in a polymer matrix to a favorable mixing enthalpy as molecular contacts increased between the dispersed nanofillers and the polymer. This increase was explained by the increased nanofiller accessible area which was due to the dispersion quality. Through this study, the nanofiller dispersion capability was directly linked to the nanofiller size; this size needs to be smaller than the polymers gyration radius.

To prepare RCN, certain stages are mainly followed: latex compounding (water assisted methods) (Wang et al. 2000; Wu et al. 2001; Potts et al. 2012), solution blending (solvent-assisted techniques) (López-Manchado et al. 2004; Pramanik et al. 2002; Jeon et al. 2003), melt compounding techniques (direct methods) (Gatos and Karger-Kocsis 2005; Gatos et al. 2004, 2005), and in situ polymerization (bulk, emulsion or suspension polymerization in the presence of nanoclay) (Nah et al. 2001; Kim et al. 2003; Varghese et al. 2003). Out of these processes, melt compounding is the most reliable technique following the present rubber compounding process. Although other routes are also viable, but they are complex and non-environment friendly, consequently not commonly used.

Bearing in mind the exfoliation/intercalation driving forces, to produce nanocomposites, rubbers have an edge over other polymer matrices. This is followed by the amine compounds (employed as low-molecular-weight intercalates/surfactants/in organophilic layered silicates) which act as activators in Sulphur curing rubber recipes. It is reported that by using octadecylamine (ODA) itself, the induction period, scorch time and optimum curing time were decreased in NR mixes (López-Manchado et al. 2003). Moreover, the vulcanization rate was further increased when ODA-modified clay was introduced in the same NR rubber recipe. Therefore, layered silicates intercalated by amine-compounds (containing different types of amines) could be involved in Sulphur curing reactions. This will favor rubber molecules and the silicate layers interaction ultimately leading to exfoliation process. Moreover, rubbers show high viscosities through melt compounding as they are very high molecular-weight elastomers. Therefore, they can apply high shear forces causing layered silicate stacks to peel-off and dispersed in the matrix (Fornes et al. 2001; Ko et al. 2002; Schön et al. 2002a). Furthermore, organophilic swelling behavior and pristine (non-organophilic layered silicates) could be exploited in organic and aqueous solutions to develop rubber-based nanocomposites via the solution and latex routes. Like many other nanomaterials (e.g. nanohydroxyapatite,) the properties of the rubber/nanoclay composites are influenced by various factors including process parameters (Michael et al. 2016a, b), Environmental Exposure etc. (Hoque et al. 2015). The characteristics of the rubber/nanoclay composites are described in proceeding sections.

3 Characterizations

A wide variety of nanofillers have been used for reinforcing rubber, generating the need for techniques that can accurately describe their dispersion degree and morphology of the obtained nanocomposite. In this aspect, the most prominent methods employed to analyze the nanocomposites structure are transmission electron microscopy (TEM), X-ray diffraction (XRD), small-angle X-ray scattering (SAXS), and wide-angle X-ray diffraction (WAXD). In the X-ray diffractogram, the clay basal signal position (001) of a nanocomposite sample is very beneficial to define the degree of clay layers dispersed in the matrix (Fig. 5). Generally speaking, a shift of this reflection towards small angles would be linked to the interlayer space widening, and also to intercalation accordingly. A collapse of layers (one onto the other) could be predicted if the (001) peak shifts to wider angles. This is mainly known to be due to the exchange, degradation or removal of the organomodificant interposed between the layers. The nanocomposites structure could be recognized either as intercalated or exfoliated following the basal reflection shape, position, and intensity. SAXS results are rarely used to determine the exfoliation directions as surface sensitivity and orientation of the platelets through the test can result in unclear analysis. In cases where SAXS is used, TEM inspection is further recommended to define unambiguously the presence of silicate exfoliation (Eckel et al. 2004).

TEM provides beneficial details based on the structure, spatial distribution, and morphology of the dispersed phase. Both, the low and high magnification micrographs are essential elements of the analysis. In this type of analysis two types of magnification are employed; higher magnification micrograph allows clay layers individual observation and assigns properties such as intercalated exfoliated morphology. On the other hand, low magnification micrograph focuses on the overall clay dispersion. In general, to characterize CPNC morphology, TEM and XRD techniques are viewed as complementary to each other. In addition to XRD and TEM, there are other methods that have been applied to gain more advanced details about the clay dispersion stage and interactions in the polymer nanocomposites including AFM (Morgan and Gilman 2003; Sadhu and Bhowmick 2005), NMR (Bourbigot et al. 2003), FTIR (Loo and Gleason 2003), neutron scattering (Hanley et al. 2003), rheology (Zhao et al. 2005) and dielectric spectroscopy (Bur et al. 2005). Another useful technique providing some indirect evidence on the silicate dispersion is known as the dynamic mechanical thermal analysis (DMTA) (Varghese and Karger-Kocsis 2003; Schön et al. 2002b; Schon and Gronski 2003). Enhanced intercalation/exfoliation are accurately indicated based on a strong reduction in the glass transition (T_g) relaxation along with the shoulder onset or further peaks above the T_g (Fig. 6).
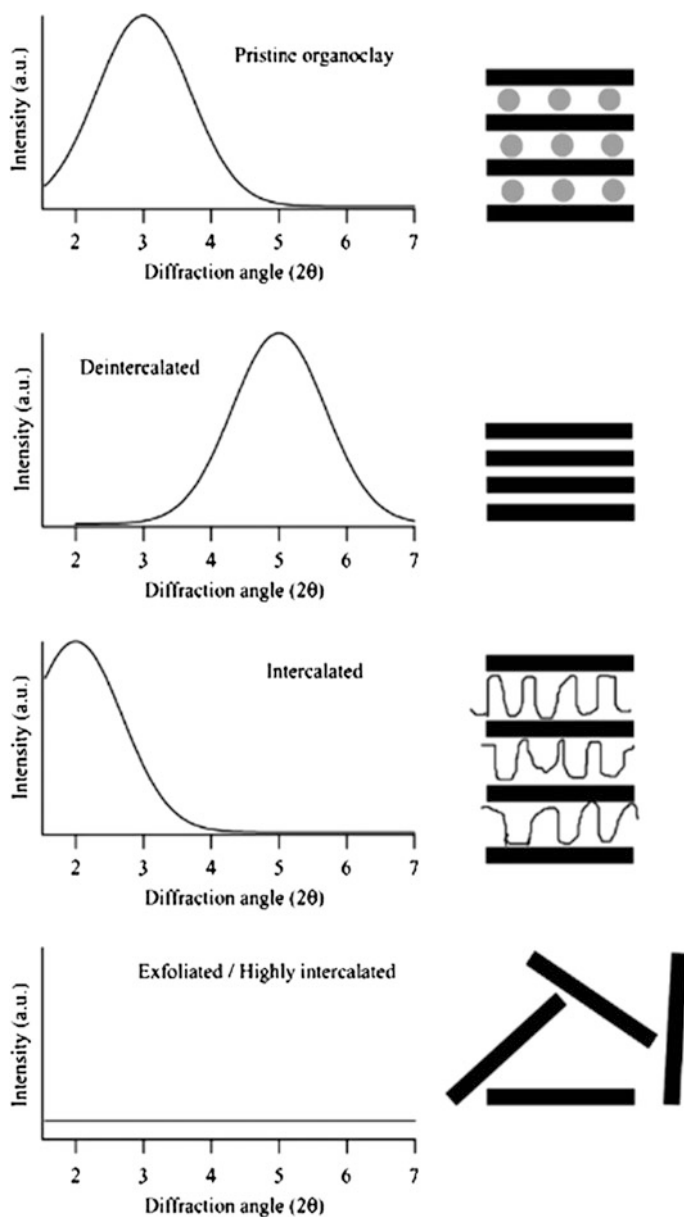
Fig. 5 Schematic of the WAXD patterns yielded by different filler morphologies. Gray circles in the pristine clay scheme represent the organomodificant molecules
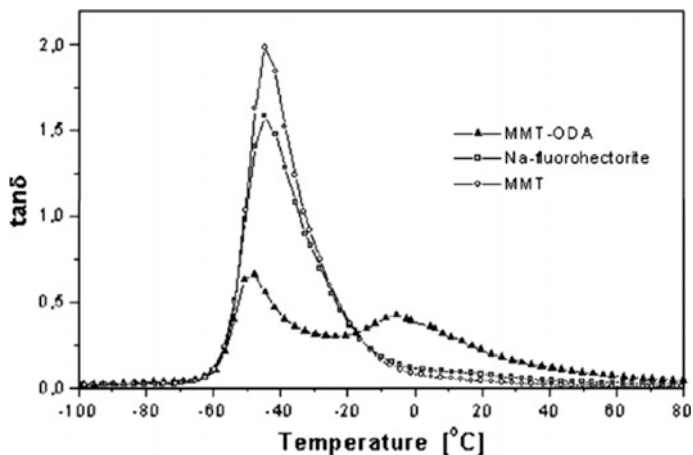
Fig. 6 Mechanical loss factor (tanδ) as a function of temperature for NR-systems with 10 phr pristine (MMT, Nafluorohectorite) and organoclay. Note that the aspect ratio of the synthetic Na-fluorohectorite was more than two times higher than that of the natural MMT

4 Applications

There are numerous application possibilities of this new class of RCN. However, the major commercial applications of RCN are in sport balls and vehicle tires. As for tire, RCN is applied in three main layers such as base (i.e. a part immediately before the tread in contact with the road), liner and tread. The position of such parts in tire and their role has been listed in Table 3. Combination of RCN provides many advantages like weight and energy dissipation reduction, air retention enhancement and extension in the magic triangle balance performances for a tire tread e.g. rolling resistance, wear and traction. This leads to considerable improvement in the properties and performance of the tires. In tire's base part,

Table 3 Tyre parts tested for RCN application

Tyre parts	Position in the tyre	Performances
Tread	In contact with road	Dry, wet, ice and snow traction
		Stability at high speed. Abrasion resistance. Protection of compounds below
Base (tread cushion)	Below the tread	Low hysteresis. Good adhesion
	Between tread and nylon 0°	Good fatigue, tear and durability. Compatibility
Liner or innerliner	Under the carcass	Impermeability to air and moisture. Prevention of degradation of tire structure (due to air and moisture)
Thin layer of impermeable rubber		Good flex fatigue, crack, and long term aging resistance

organoclay is used commonly referred to as "HP" (High Performance) or "UHP" (Ultra high performance) tires, belonging to classes "V" or "Z", designed to experience extreme driving conditions. Researches on organoclay incorporation were reported to have shown notable enhancement in mechanical properties of the tire part (Galimberti et al. 2003; Resmini et al. 2012; Giannini et al. 2003). In 2007, P zero tires containing organoclay were launched by Pirelli Tire for both HP and UHP types.

To fulfil the superior barrier properties, studies have been carried out to produce and enhance inner liner parts carrying organoclay. Through these studies, the oxygen transmission was notably reduced to about one fourth as organoclay was employed in BR (Elspass et al. 1998), BIMS (Elspass and Peiffer 2000), and SBR (Ishida and Fujiki 2005) production with an organoclay content as low as 9 phr (Elspass et al. 1998). Furthermore, during a study on nitrile rubber nanocomposite carrying organoclay (10 wt% organoclay), it was observed that the relative vapor permeability was remarkably reduced up to 85 % for water and 42 % for methanol. The most advanced applications of organoclays are linked with their flame resistance, fire retardance etc. Cable jacketing rubber mix already contains organoclays. A possible contribution of clay to environmental issues is that, in its presence, the ZnO (an ecotoxic compound) content of the recipes can be reduced.

Nanoclay based barrier coating technology has also gained fame through tennis ball manufacturing. Double core Wilson tennis ball is a good example in this field which has recently found a large commercial success. The Wilson tennis balls clay nanocomposite coating preserves the internal pressure for an extended time period. This is taking place while maintaining properties such as the feel, bounce and reproducibility of performances. In this coating technique, a butyl rubber-vermiculite clay nanocomposite is used to coat the core which traps the gas inside the ball and doubles its shelf life. By using RCN, coatings with higher flexibility and gas permeability 30–300 times lower than butyl rubber have been developed. The products in this field have shown notable resistance by strains up to 20 %. This type of coating keeps air longer, and allows the ball to bounce twice of the ordinary ones. This is due to the improvement in air retention. Takahashi et al. (2006) showed that a coating layer carrying vermiculite (20–30 wt%) in butyl rubber led to a reduction of the diffusion coefficients by two orders of magnitude and of gas permeability by 20–30 folds. This technique is expected to be extended to the rubber industry and be incorporated into footballs, and even in the tires of bicycle or automobiles (Hussain et al. 2006; Koo 2006; Balasubramanian and Jawahar 2015).

5 Summary and Future Perspectives

The nanoclay composites are considered to be the advanced functional materials with high regularity and safe toxicological profile that offer prominent mechanical and thermal stability. The properties of the nanoclay tend to become exceptionally

functional when incorporated with polymers due to good interfacial interaction. Commercially now, the nanoclay composites are used to improve the dynamic mechanical properties of tyre, and in coating tennis balls in which the clay nanocomposite acts as a gas barrier enabling it to increase its performance and durability. The nanoclay composites hold a promising future, and is likely to become an essential part in the rubber and automobile industries in coming times.

References

Alexandre, M., Dubois, P.: Polymer-layered silicate nanocomposites: preparation, properties and uses of a new class of materials. Mater. Sci. Eng.: R: Rep. **28**(1), 1–63 (2000)

Balasubramanian, M., Jawahar, P.: Nanocomposites Based on Inorganic Nanoparticles. Polym. Nanocompos. Based Inorg. Org. Nanomater. 257–346 (2015)

Bourbigot, S., VanderHart, D.L., Gilman, J.W., Awad, W.H., Davis, R.D., Morgan, A.B., Wilkie, C.A.: Investigation of nanodispersion in polystyrene–montmorillonite nanocomposites by solid-state NMR. J. Polym. Sci. Part B: Polym. Phys. **41**(24), 3188–3213 (2003)

Bur, A.J., Lee, Y.-H., Roth, S.C., Start, P.R.: Measuring the extent of exfoliation in polymer/clay nanocomposites using real-time process monitoring methods. Polymer **46**(24), 10908–10918 (2005)

Choudhury, A., Bhowmick, A.K., Ong, C.: Effect of different nanoparticles on thermal, mechanical and dynamic mechanical properties of hydrogenated nitrile butadiene rubber nanocomposites. J. Appl. Polym. Sci. **116**(3), 1428–1441 (2010)

Clarey, M., Edwards, J., Tsipursky, S.J., Beall, G.W., Eisenhour, D.D.: Method of manufacturing polymer-grade clay for use in nanocomposites. Google Patents (2000)

Clocker, E.T., Paterek, W., Farel, N.D., Selsley, M.J.: Conversion of clay to its colloidal form by hydrodynamic attrition. Google Patents (1976)

DeKimpe, C., Gastuche, M., Brindley, G.W.: Ionic coordination in alumino-silicic gels in relation to clay mineral formation. Am. Mineral. **46**(11–2), 1370–1381 (1961)

Eckel, D.F., Balogh, M.P., Fasulo, P.D., Rodgers, W.R.: Assessing organo-clay dispersion in polymer nanocomposites. J. Appl. Polym. Sci. **93**(3), 1110–1117 (2004)

Elspass, C.W., Peiffer, D.G.: Nanocomposite materials formed from inorganic layered materials dispersed in a polymer matrix. Google Patents (2000)

Elspass, C.W., Peiffer, D.G., Kresge, E.N., Wright, P.J., Chludzinski, J.J., Wang, H.C.: Tactoidal elastomer nanocomposites. Google Patents (1998)

Fornes, T., Yoon, P., Keskkula, H., Paul, D.: Nylon 6 nanocomposites: the effect of matrix molecular weight. Polymer **42**(25), 09929–09940 (2001)

Galanti, A., Laus, M., Fiorini, M.: Reinforcement of SBS by organophilic clay fillers. Kautsch. Gummi Kunstst. **52**(1), 21–25 (1999)

Galimberti, M., Fino, L., Verona, M.: Tyre for vehicle wheels with tread band of cap and base construction. Google Patents (2003)

Ganter, M., Gronski, W., Reichert, P., Mulhaupt, R.: Rubber nanocomposites: morphology and mechanical properties of BR and SBR vulcanizates reinforced by organophilic layered silicates. Rubber Chem. Technol. **74**(2), 221–235 (2001)

Gatos, K., Apostolov, A., Karger-Kocsis, J.: Compatibilizer effect of grafted glycidyl methacrylate on EPDM/organoclay nanocomposites. In: Materials Science Forum, 2005. Trans Tech Publ, pp. 347–350

Gatos, K.G., Karger-Kocsis, J.: Effects of primary and quaternary amine intercalants on the organoclay dispersion in a sulfur-cured EPDM rubber. Polymer **46**(9), 3069–3076 (2005)

Gatos, K.G., Thomann, R., Karger-Kocsis, J.: Characteristics of ethylene propylene diene monomer rubber/organoclay nanocomposites resulting from different processing conditions and formulations. Polym. Int. **53**(8), 1191–1197 (2004)

Giannini, L., Fino, L., Galimberti, M., Bizzi, S.: High-performance tyre for vehicle wheels. Google Patents (2003)

Hanley, H., Muzny, C., Ho, D., Glinka, C.: A small-angle neutron scattering study of a commercial organoclay dispersion. Langmuir **19**(14), 5575–5580 (2003)

Hofmann, W.: Rubber Technology Handbook. Hanser Publishers. Distributed in the USA by Oxford University Press (1989)

Hoque, M.E., Jin, T.W., Mohamed, S.H.: Physical and mechanical characteristics of conventional dental porcelain: effects of exposure environments. Mater. Lett. **143**, 67–70 (2015)

Hussain, F., Hojjati, M., Okamoto, M., Gorga, R.E.: Review article: polymer-matrix nanocomposites, processing, manufacturing, and application: an overview. J. Compos. Mater. **40**(17), 1511–1575 (2006)

Hwang, W.G., Wei, K.H., Wu, C.M.: Mechanical, thermal, and barrier properties of NBR/organosilicate nanocomposites. Polym. Eng. Sci. **44**(11), 2117–2124 (2004)

Ishida, K., Fujiki, K.: Rubber composition for inner liner and tire. US Patent 20,050,148,718 (2005)

Jeon, H., Rameshwaram, J., Kim, G., Weinkauf, D.: Characterization of polyisoprene–clay nanocomposites prepared by solution blending. Polymer **44**(19), 5749–5758 (2003)

Kader, M.A., Nah, C.: Influence of clay on the vulcanization kinetics of fluoroelastomer nanocomposites. Polymer **45**(7), 2237–2247 (2004)

Kawasumi, M.: The discovery of polymer-clay hybrids. J. Polym. Sci. Part A: Polym. Chem. **42**(4), 819–824 (2004)

Kim Jt, Oh, Ts, Lee Dh: Preparation and characteristics of nitrile rubber (NBR) nanocomposites based on organophilic layered clay. Polym. Int. **52**(7), 1058–1063 (2003)

Ko, M.B., Jho, J.Y., Jo, W.H., Lee, M.S.: Effect of matrix viscosity on clay dispersion in preparation of polymer/organoclay nanocomposites. Fibers Polym. **3**(3), 103–108 (2002)

Koo, J.H.: Polymer Nanocomposites. McGraw-Hill Professional Publisher (2006)

Linares, J., Huertas, F.: Kaolinite: synthesis at room temperature. Science **171**(3974), 896–897 (1971)

Loo, L.S., Gleason, K.K.: Fourier transform infrared investigation of the deformation behavior of montmorillonite in nylon-6/nanoclay nanocomposite. Macromolecules **36**(8), 2587–2590 (2003)

López-Manchado, M., Arroyo, M., Herrero, B., Biagiotti, J.: Vulcanization kinetics of natural rubber–organoclay nanocomposites. J. Appl. Polym. Sci. **89**(1), 1–15 (2003)

López-Manchado, M., Herrero, B., Arroyo, M.: Organoclay–natural rubber nanocomposites synthesized by mechanical and solution mixing methods. Polym. Int. **53**(11), 1766–1772 (2004)

Lu, Y.L., Liang, Y.R., Wu, Y.P., Zhang, L.Q.: Effects of Heat and Pressure on Microstructures of Isobutylene-Isoprene Rubber (IIR)/Clay Nanocomposites. Macromol. Mater. Eng. **291**(1), 27–36 (2006)

Mackay, M.E., Tuteja, A., Duxbury, P.M., Hawker, C.J., Van Horn, B., Guan, Z., Chen, G., Krishnan, R.: General strategies for nanoparticle dispersion. Science **311**(5768), 1740–1743 (2006)

Magaraphan, R., Thaijaroen, W., Lim-Ochakun, R.: Structure and properties of natural rubber and modified montmorillonite nanocomposites. Rubber Chem. Technol. **76**(2), 406–418 (2003)

Michael, F.M., Khalid, M., Ratnam, C., Rashmi, W., Hoque, M.E., Ketabchi, M.R.: Nanohydroxyapatite synthesis using optimized process parameters for load-bearing implant. Bull. Mater. Sci. **39**(1), 133–145 (2016a)

Michael, F.M., Khalid, M., Ratnam, C., Chee, C.Y., Rashmi, W., Hoque, M.E.: Sono-synthesis of nanohydroxyapatite: effects of process parameters. Ceram. Int. **42**(5), 6263–6272 (2016b)

Morgan, A.B., Gilman, J.W.: Characterization of polymer-layered silicate (clay) nanocomposites by transmission electron microscopy and X-ray diffraction: a comparative study. J. Appl. Polym. Sci. **87**(8), 1329–1338 (2003)

Morris, C.: Reducing particle size of clay and rheology control of clay-water systems. Google Patents (1967)

Mousa, A., Karger-Kocsis, J.: Rheological and thermodynamical behavior of styrene/butadiene rubber-organoclay nanocomposites. Macromol. Mater. Eng. **286**(4), 260–266 (2001)

Nah, C., Ryu, H.J., Han, S.H., Rhee, J.M., Lee, M.H.: Fracture behaviour of acrylonitrile–butadiene rubber/clay nanocomposite. Polym. Int. **50**(11), 1265–1268 (2001)

Patel, H.A., Somani, R.S., Bajaj, H.C., Jasra, R.V.: Nanoclays for polymer nanocomposites, paints, inks, greases and cosmetics formulations, drug delivery vehicle and waste water treatment. Bull. Mater. Sci. **29**(2), 133–145 (2006)

Potts, J.R., Shankar, O., Du, L., Ruoff, R.S.: Processing–morphology–property relationships and composite theory analysis of reduced graphene oxide/natural rubber nanocomposites. Macromolecules **45**(15), 6045–6055 (2012)

Pramanik, M., Srivastava, S., Samantaray, B., Bhowmick, A.: Synthesis and characterization of organosoluble, thermoplastic elastomer/clay nanocomposites. J. Polym. Sci. Part B: Polym. Phys. **40**(18), 2065–2072 (2002)

Ray, S.S., Okamoto, M.: Polymer/layered silicate nanocomposites: a review from preparation to processing. Prog. Polym. Sci. **28**(11), 1539–1641 (2003)

Resmini, E., Baione, F., Tirelli, D., Fino, L., Galimberti, M., Citterio, A.: Tire and crosslinkable elastomeric composition. Google Patents (2012)

Roy, R.: The preparation and properties of synthetic clay minerals. Genese et Synthese des Argiles, Colloques Intern Centre Nat Recherche Sci (1962)

Sadhu, S., Bhowmick, A.: Morphology study of rubber based nanocomposites by transmission electron microscopy and atomic force microscopy. J. Mater. Sci. **40**(7), 1633–1642 (2005)

Schon, F., Gronski, W.: Filler networking of silica and organoclay in rubber composites: reinforcement and dynamic-mechanical properties. Kautsch. Gummi Kunstst. **56**(4), 166 (2003)

Schön, F., Thomann, R., Gronski, W.: Shear controlled morphology of rubber/organoclay nanocomposites and dynamic mechanical analysis. In: Macromolecular Symposia, vol. 1, pp. 105–110. Wiley Online Library (2002a)

Schön, F., Thomann, R., Gronski, W.: Shear controlled morphology of rubber/organoclay nanocomposites and dynamic mechanical analysis. Macromol. Symp. **189**(1), 105–110 (2002b)

Sengupta, R., Chakraborty, S., Bandyopadhyay, S., Dasgupta, S., Mukhopadhyay, R., Auddy, K., Deuri, A.: A short review on rubber/clay nanocomposites with emphasis on mechanical properties. Polym. Eng. Sci. **47**(11), 1956–1974 (2007)

Takahashi, S., Goldberg, H., Feeney, C., Karim, D., Farrell, M., O'leary, K., Paul, D.: Gas barrier properties of butyl rubber/vermiculite nanocomposite coatings. Polymer **47**(9), 3083–3093 (2006)

Teh, P., Mohd Ishak, Z., Hashim, A., Karger-Kocsis, J., Ishiaku, U.: On the potential of organoclay with respect to conventional fillers (carbon black, silica) for epoxidized natural rubber compatibilized natural rubber vulcanizates. J. Appl. Polym. Sci. **94**(6), 2438–2445 (2004)

Theng, B.K.G.: Formation and Properties of Clay-Polymer Complexes, vol. 4. Elsevier (2012)

Usuki, A., Tukigase, A., Kato, M.: Preparation and properties of EPDM–clay hybrids. Polymer **43**(8), 2185–2189 (2002)

Vaia, R.A., Giannelis, E.P.: Lattice model of polymer melt intercalation in organically-modified layered silicates. Macromolecules **30**(25), 7990–7999 (1997a)

Vaia, R.A., Giannelis, E.P.: Polymer melt intercalation in organically-modified layered silicates: model predictions and experiment. Macromolecules **30**(25), 8000–8009 (1997b)

Varghese, S., Karger-Kocsis, J.: Natural rubber-based nanocomposites by latex compounding with layered silicates. Polymer **44**(17), 4921–4927 (2003)

Varghese, S., Karger-Kocsis, J., Gatos, K.: Melt compounded epoxidized natural rubber/layered silicate nanocomposites: structure-properties relationships. Polymer **44**(14), 3977–3983 (2003)

Velde, B.: Clays and Clay Minerals in Natural and Synthetic Systems. Elsevier Scientific Publishing Company (1977)

Wang, Y., Zhang, L., Tang, C., Yu, D.: Preparation and characterization of rubber–clay nanocomposites. J. Appl. Polym. Sci. **78**(11), 1879–1883 (2000)

Weaver, C.E., Pollard, L.D.: The chemistry of clay minerals (1973)

Wu, Y.P., Zhang, L.Q., Wang, Y.Q., Liang, Y., Yu, D.S.: Structure of carboxylated acrylonitrile-butadiene rubber (CNBR)–clay nanocomposites by co-coagulating rubber latex and clay aqueous suspension. J. Appl. Polym. Sci. **82**(11), 2842–2848 (2001)

Zhao, J., Morgan, A.B., Harris, J.D.: Rheological characterization of polystyrene–clay nanocomposites to compare the degree of exfoliation and dispersion. Polymer **46**(20), 8641–8660 (2005)

Zheng, H., Zhang, Y., Peng, Z., Zhang, Y.: A comparison between cure systems for EPDM/montmorillonite nanocomposites. Polym. Polym. Compos. **12**(3), 197–206 (2004a)

Zheng, H., Zhang, Y., Peng, Z., Zhang, Y.: Influence of clay modification on the structure and mechanical properties of EPDM/montmorillonite nanocomposites. Polym. Testing **23**(2), 217–223 (2004b)

Clay, Natural Fibers and Thermoset Resin Based Hybrid Composites: Preparation, Characterization and Mechanical Properties

Hind Abdellaoui, Rachid Bouhfid and Abou el Kacem Qaiss

Abstract Combining two or more kinds of reinforcement into the same matrix in order to enhance the mechanical properties of natural fiber composite is one of the attractive ways employed in this sense. Natural hybridization has also the target of promoting the natural resources, particularly local resources not exploited industrially. This chapter presents a study of the mechanical behavior of hybrid composite based on natural components, the first and third parts contain our own results on the mechanical behavior of the hybrid matrix epoxy/clay and the mechanical behavior of double hybrid composites using a hybrid matrix (epoxy/clay) and hybrid reinforcement jute/coir and jute/doum. About the second part, it focuses an overview of works of literature dealing hybrid composites based on natural fiber/natural fiber and natural fiber/synthetic fiber. Other than the hybridization of the reinforcement, it may also involve the hybridization of architecture and orientation of the reinforcement, which is also the subject of this chapter in its third part.

Keywords Clay · Natural fibres · Thermoset resin · Hybrid composites · Mechanical properties

1 Introduction

The composite materials based on thermosetting matrix are increasingly used in a variety of industrial fields such as aerospace, automotive and civil applications. Considering the environmental aspects, composite materials are currently at the core of sustainable development thanks to the use of natural constituents that either in terms of reinforcements, fillers or even the matrix. Many researchers were focused on development of composites with natural matrix (John and Thomas 2008; Martins et al. 2009; Behera et al. 2012). Consequently, the barrier resides

H. Abdellaoui · R. Bouhfid · A.e.K. Qaiss (✉)
MAScIR Foundation, Laboratory of Polymer Processing, Rabat Center Design,
Rue Mohamed Jazouli Madinat al Irfane, 10100 Rabat, Morocco
e-mail: a.qaiss@mascir.com

well in the marketing of these green composites because of the costly price of the biodegradable matrix, which the large part of these resins costs more than the usual thermoset resins (John and Thomas 2008). To remedy, the suggestion to add natural fillers in the matrix is sufficiently ambitious. Generally, the use of fillers improves mechanical, electric or thermal properties, and also reduces the price of onerous matrices. Clay with all its varieties (Illite, montmorillonite, kaolinite…) is one of the most abundant natural fillers and widely used in commercial applications (Cyras et al. 2008; Jeong et al. 2011). The study of the mechanical behavior of the hybrid matrix (thermoset matrix/clay) is increasingly considered by many researchers (Jeong et al. 2011; Arrakhiz et al. 2013; Nekhlaoui et al. 2015).

Concerning the composites reinforced with natural fibres, they earned a crucial interest in recent decades and still located on top research and development in this area. Various natural fibres have been used as reinforcement in composite materials such as jute, coir, pine cone, henna, doum and alfa (Mwaikambo and Ansell 2002; Bessadok et al. 2007; Charlet et al. 2007; Bessadok et al. 2009; Le Duigou et al. 2010; Defoirdt et al. 2010), and prove their proficiency thanks to their well know advantages: renewable and biodegradable character, low density and low cost (Megiatto et al. 2010; Jawaid et al. 2010; Boujmal et al. 2014). Several studies mentioned in the literature demonstrate that the employ of natural fibres in the composite increase the mechanical properties of the used matrix and give not at all similar properties to the glass fiber composite (Mwaikambo and Ansell 2002; Jawaid et al. 2011; Abdellaoui et al. 2015a), which it is gracefully recommended to improve the mechanical behavior of this kind of composite.

Hybridization is a way to enhance the mechanical properties of composites based on natural fibres. The hybrid composite may be designed by the combination of a synthetic fibres and natural fibres (woven or no woven) in a matrix (De Rosa et al. 2009; Khan et al. 2009), a combination of two natural fibres in a matrix (Jawaid et al. 2011), also a combination of synthetic matrix and natural fillers such as clay, henna (Cyras et al. 2008; Jeong et al. 2011; Arrakhiz et al. 2013; Nekhlaoui et al. 2015; Nekhlaoui et al. 2014; Boujmal et al. 2014). The hybridization is surely beneficial thanks to the complementarity effect, which the properties of each kind of fiber is complemented by the properties of the other kind. Thus far, the performed experimental works indicate an improvement of the mechanical behavior of composites through the hybridization effect (Jawaid et al. 2010; Jawaid et al. 2011; Arrakhiz et al. 2013).

Contextually, this chapter will be an opportunity to address and develop hybrid composites with hybrid natural constituents, we also take the opportunity to expose our own and recent experimental results achieved in this respect.

This chapter is architecturally routed to develop firstly the clay loaded thermoset matrices, which we quote our own experimental work on the mechanical characterization of the hybrid matrix (epoxy/clay), while drawing inspiration from literature to take into account different means of improving the mechanical properties of the hybrid matrix. Secondly, we briefly summarized the results of some literary works done on hybrid reinforcements composites to move directly to the third party, which treat the bi-hybrid composite, i.e., based on hybrid matrix and hybrid

reinforcement. As the first part of the hybrid matrix, this third part is also the subject of our own work on hybrid composites based on hybrid matrix epoxy/clay and natural hybrid reinforcement jute/doum and jute/coir.

## 2 Hybrid Matrix: Thermoset Matrix and Natural Filler (Clay)

Enhancing the mechanical properties of the thermosetting matrix is generally carried out by adding fillers such as calcium carbonate and talc. Filler is a mineral or vegetable substance, added to the base polymer. It basically allows modify the mechanical, thermal and electrical properties, or merely reduce the cost of the thermosetting matrix (Jeong et al. 2011).

The environmental setting requires the production of environmentally friendly parts using natural ingredients such as clay. In this chapter, our focus is devoted to clay loaded thermoset matrices.

2.1 Preparation

The clay purification is generally carried out by mixing rock clay and water in order to obtain a homogenous suspension. Then the suspension was filtered with a sieve of 100 µm and dried at 110 °C in an oven. The obtained particles were again crushed and sieved with a sieve of 1 µm or using cyclone to separate different particle size. The Fig. 1 shows the clay at rock and particle forms.

In this work, the used clay is Ilite with a density of 2.14 g/cm3.
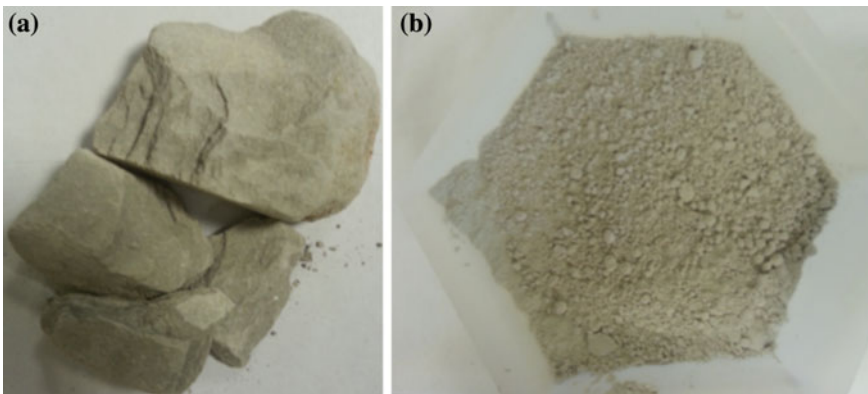
Fig. 1 Ilite's Clay; **a** Rock clay, **b** clay powder

Table 1 Experimental conditions

Hybrid matrix		
Case (%)	Epoxy (g)	Illite (g)
0	**10**	**0**
5	**9.5**	**0.5**
10	**9**	**1**
15	**8.5**	**1.5**
20	**8**	**2**

The prepared hybrid matrix is a mixture of epoxy matrix and different clay content (0, 5, 10, 15, 20) wt% as shown in the Table 1. The aim of using different clay content is to determine at which content, the mechanical properties of hybrid matrix are maximal, and to obtain an optimal viscosity, which is mandatory for processing and fiber impregnation.

After the cure of the hybrid matrix composites, the samples were cut and placed in an oven MTI (KSL 1400X) at a temperature of 150 °C for a period of 15 min to ensure their crosslinking.

2.2 Morphological Characteristics

The morphology of hybrid matrices made by epoxy mixed to different clay content (0, 5, 10, 15 and 20) wt% was illustrated by using the optical microscopy at 10 magnifications. The microscopy is supported with Leica QWin V3 analysis software as presented in Fig. 2.

According to the results of the optical microscope, it appears that the clay particles are highly distributed and dispersed in the epoxy thermoset matrix, mainly
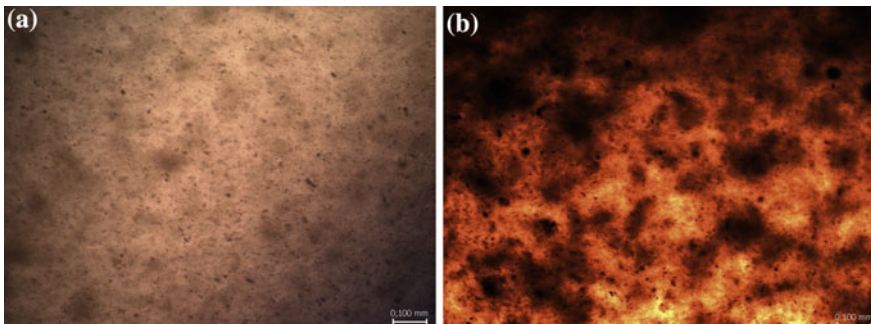
Fig. 2 Morphology of hybrid matrix at ×10 magnifications: **a** at 5 % of clay content, **b** at 20 % of clay content

at 5, 10 and 15 % clay content. At 20 % clay content, it is ascertained the formation of Agglomerations in the matrix. The presence of these agglomerations can cause structural defects in the final part and affects the mechanical properties.

2.3 Complex Viscosity of Hybrid Matrix

The viscosity of hybrid matrix was characterized by using a fluid rheology. The viscosity values were obtained in oscillatory tests performed in sweep frequency mode (0, 1–500 Hz).

The Fig. 3 illustrates the viscosity of different matrix with different clay content (0, 5, 10, 15 and 20) wt%. At low clay content (5 and 10 %), the epoxy matrix loses its viscous character. An increase of clay content permits an increasing of matrix viscosity until 15 % of clay. At 20 %, a significant increasing of matrix viscosity was observed. This increase can be explained by the high dispersion of clay particles and the dominance of Illite character in the epoxy matrix.

Knowing the viscosity of different hybrid matrices gives an idea of the impregnation and the flow of the matrix into the natural fiber reinforcement. More the matrix viscosity is higher; the impregnation is more demanding in terms of time and compression pressure (Abdellaoui and Echaabi 2014; Abdellaoui et al. 2015b). In fact, high matrix viscosity leads to poor impregnation of the reinforcement.

2.4 Mechanical Properties of Hybrid Matrix

2.4.1 Tensile Properties

The mechanical properties of the prepared composites are influenced by the size, distribution and clay content in epoxy matrix.

Fig. 3 Complex viscosity at different clay percent
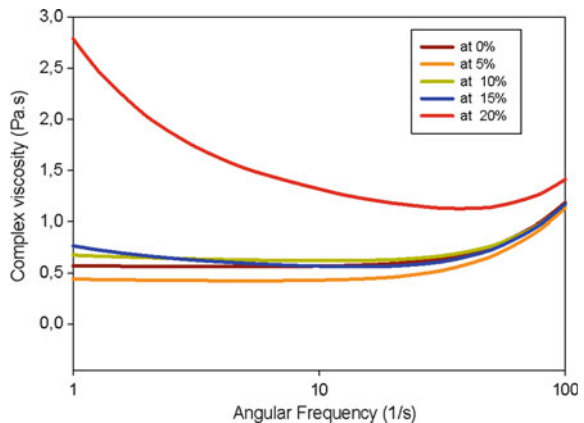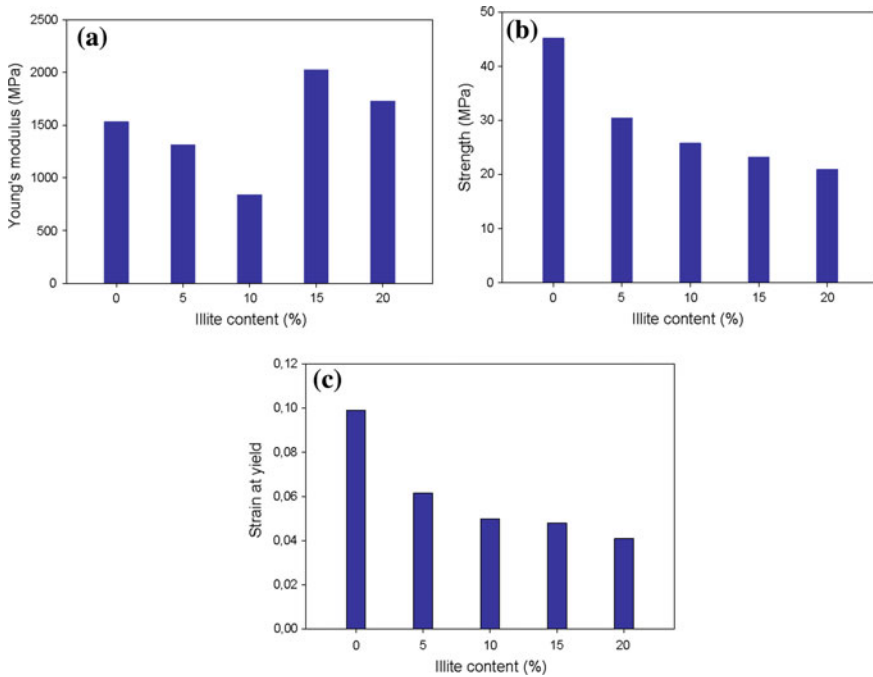
Fig. 4 Tensile measurements: **a** Young's modulus, **b** strength, **c** strain at yield

The tensile test was performed on a universal testing machine INSTRON 8821S (Instron, USA) at a crosshead speed of 3 mm/min. The samples were cut to following dimensions (120 × 15) according to ISO 527-12.

Figure 4 shows the evolution of tensile measurements (Young's modulus, strength, and strain at yield) on the clay content. It was observed (Fig. 4a) that the Young's modulus decreases with low clay content. Against, an increase of clay content (the 10 % beyond) leads to an increase of the Young's modulus (case of 15 and 20 %). the Young's modulus reaches its maximum in the case of hybrid matrix at 15 % clay content.

For a low clay content (5 and 10 %), a decrease in the Young's modulus was observed, which is explained by the poor dispersion of clay particles in polymeric epoxy. The clay particles are dispersed randomly in the matrix, breaking the molecular chains. Subsequently, it leads to a low bonding epoxy-clay, and therefore a decrease in Young's modulus. Beyond a 10 % Illite content, the Young's modulus increases and becomes higher than that of pure epoxy. However, at high clay content (20 %), the Young's modulus decreases, but remains higher than that of pure epoxy. The decrease in the Young's modulus is explained by the formation of agglomerates and the dominance of rigid clay behavior (Jeong et al. 2011; Boujmal et al. 2014).

Figure 4b shows the evolution of the tensile strength in function of clay content. It was observed that the tensile strength decreases with an increase in the clay content. The pure epoxy has a high tensile strength compared to epoxy doped by Illite. Therefore, the epoxy loses nearly 30 % of its stiffness by adding different clay content.

The ductility is expressed by the evolution of the strain at yield in function of clay content. The Fig. 4c shows that the ductility of various composites decreases with increasing of clay content. The pure epoxy has a fairly high ductility compared to other composites. The epoxy ductility decreases by almost 40 % by adding clay. This decrease is due to the decrease in epoxy plastic energy (Jeong et al. 2011). The rigid behavior of clay limits the plastic behavior of epoxy loaded with different clay content (Cyras et al. 2008; Arrakhiz et al. 2013; Nekhlaoui et al. 2015).

2.4.2 Rheological Properties

The rheological properties of different hybrid matrix were determined by torsional tests. The tests were carried out on an ARES-LS Rheometer with rectangular torsion mode. The torsional modulus G* is obtained in oscillatory tests performed in sweep mode (0.1–40 Hz) and defined by the Eq. (1):

$$G^* = \sqrt{G'^2 + G''^2} \tag{1}$$

where G′ and G″ are respectively the storage and loss modulus measured experimentally by the Rheometer.

Figure 5a shows the evolution of the complex modulus as a function of frequency and clay content (0, 5, 10, 15, 20) wt%. It is noted that the complex modulus G* increases by increasing the clay content, which is maximal at 15 % clay content. It expresses the strong interaction between the epoxy and clay particles (Arrakhiz et al. 2013; Boujmal et al. 2014). Thus, the complex modulus

Fig. 5 Complex modulus for the manufactured samples
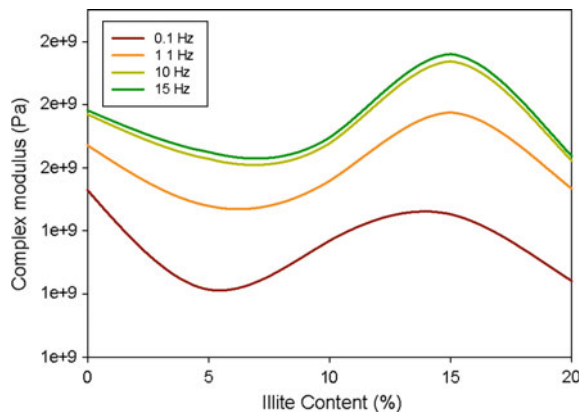
Fig. 6 Loss factor tanδ of different hybrid matrices
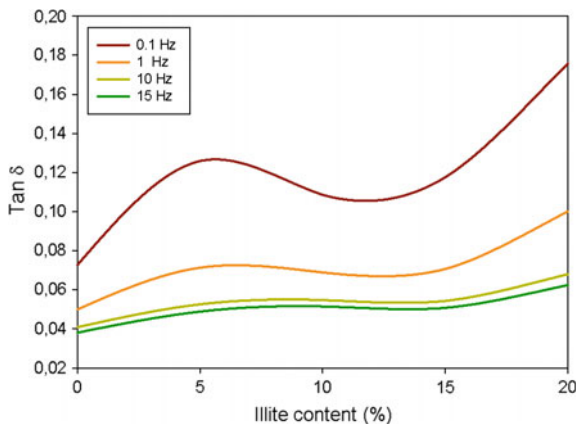
increases with the increase in frequency (0.1–15 Hz). At low frequency, the polymer chains have the time to relax. In contrast, at high frequency the molecules do not have enough time to rearrange for achieving the permanent deformation (Boujmal et al. 2014).

The evolution of the loss factor $\tan \delta = \frac{G''}{G'}$ versus the clay content and frequency for different hybrid matrices is illustrated in the Fig. 6. The loss factor decreases with increasing frequency and doesn't exceed 18 % for all hybrid matrices. These results explain the dominance of the elastic nature of the material, leading to the conclusion that the different hybrid matrices behave as an elastic solid (Jeong et al. 2011).

2.5 Mechanical Properties of Hybrid Matrix

Improving the compatibility between the hydrophobic organic matrix and hydrophilic inorganic filler as clay may be realized by many ways, especially by treating the inorganic filler by chemical modification.

Alkoxysilanes and amines are generally used to make more organophilic clays, which the amine treatment uses cationic exchange capacity of clays by exchanging interlayer-cations like K^+ et Na^+ (Jeong et al. 2011). The size reduction treatment can be on other way to boost the clay dispersion into the matrix, because it's logically that the homogeneity of mixture clay/matrix is obtained by decreasing the clay particle size. Also, the wet ball-milling is an resourceful process to reduce the clay particle size by exfoliation of clay as reported in literature (Jeong et al. 2011).

Hence, Improving the adhesion and compatibility between matrix and clay has directly repercussion on enhancement of mechanical properties of hybrid matrix.

In an interesting work, Jeong et al. (Jeong et al. 2011) have focused their study on the effects of physico chemical treatment of clay type Illite on improvement of

thermo-physical properties of the hybrid matrix epoxy/clay. The physico chemical treatment consists to modify chemically the Illite by octadecylamine (ODA) in order to transform it to organophilic material. The thermo-mechanical properties were performed by Dynamic Mechanical Analysis (DMA). The DMA results show that the storage and loss modulus of composites Epoxy/Illite are very higher than others of virgin epoxy as illustrated in the Figs. 7 and 8. According to the literature, many researchers were reported to obtain similar increase in storage and loss modulus of epoxy/clay. Its have also noted that the storage modulus increase with increasing of clay content, which this increasing is explained by the high stiffness of clay filler.

Generally, the dispersion of clay into the polymeric matrix can be realized y considering three different manners (Jeong et al. 2011) as illustrated in the Fig. 9.

Fig. 7 Storage modulus of composite Epoxy/Illite with treated and untreated Illite
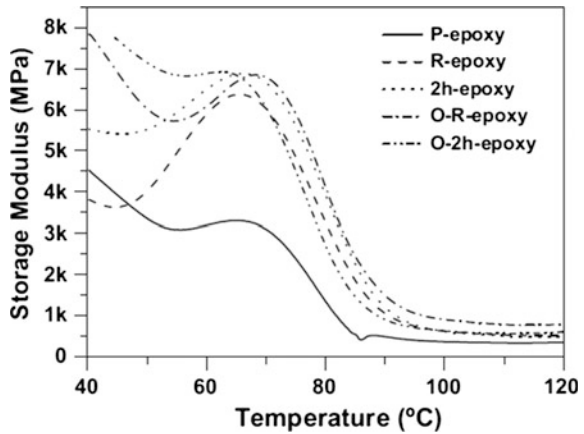
Fig. 8 Loss modulus of composite Epoxy/Illite with treated and untreated Illite
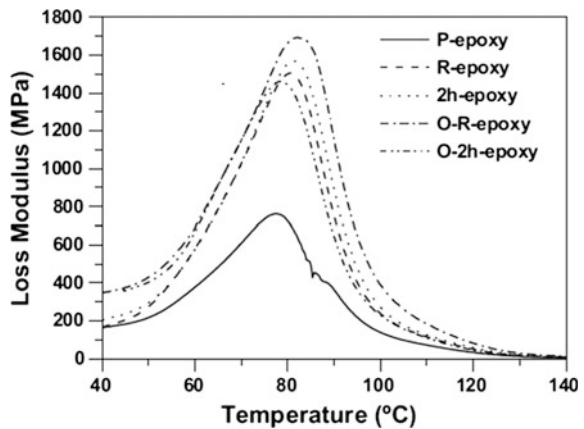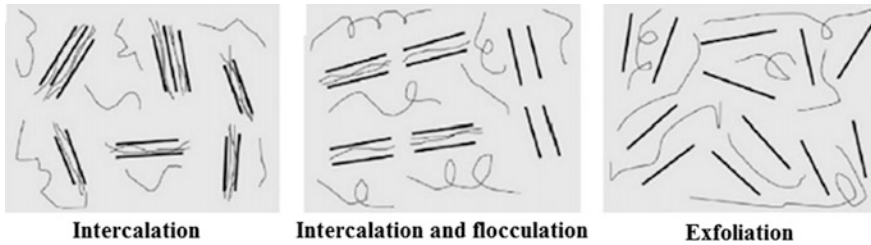
Fig. 9 Illustrative schema of clay dispersion into the polymeric matrix

Intercalation:	the polymeric matrix was incorporated into the layered clay in a crystographically regular model, despite of the matrix to the clay ratio. The hybrid matrix (matrix/clay) properties are usually equivalent to the clay properties
Intercalation and flocculation:	is the same as intercalation in the conceptual form. The difference exists particularly in the flocculation of some layered clays into the matrix
Exfoliation:	the clay layers were separately divorced into the polymeric matrix, having an average distances with small deviation. Also, the hybrid matrix (polymer/exfoliate clay) properties are equivalent to the clay properties

3 Thermoset Composites with Hybrid Reinforcement

The hybrid composite is defined by integration of two or more types of fibres into the same matrix. The hybrid fibrous reinforcement may be employed by using natural fiber/natural fiber or natural fiber/synthetic fiber in order to improve some materials properties as mechanical, and rheological properties, and also to make these materials more environmental friendly.

The major aim of hybridization is the complementary nature effect, which each kind of fiber could complement with what are lacking in the other.

3.1 Hybrid Composites with Natural/Synthetic Reinforcement

Using the glass fiber with natural fiber for hybridization provides a way to enhance the mechanical properties of natural fiber composites.

Table 2 Comparative study of water absorption in case of hybrid and non hybrid composites (Panthapulakkal and Sain 2007)

Samples	Water absorption %	
	Nonhybrid (coir–polyester composite) (20 wt%)	Hybrid [coir/glass–polyester composite]
Untreated	8.53	5.186
Alkali treated (5 %)	4.994	3.147
PMMA grafted (5 %)	3.98	2.663
PAN grafted (10 %)	4.119	2.997
Cyanoethylated	3.6	3.138
Bleached	5.8	3.718

In a study, Panthapulakkal et al. (Panthapulakkal and Sain 2007) noted that the hybridization with glass fiber improves the performance properties of composite based on hemp fiber/glass fiber. The flexural modulus reaches 5.5 GPa from 25wt% of hemp fiber and 15wt% of glass fiber. Then, the thermal properties and resistance to water absorption properties of hybrid composites were improved with incorporating glass fiber.

The water absorption of hybrid composite with 7 wt% of glass fiber and 13 wt% of natural fiber were compared to the water absorption of non hybrid composite and summarized in the Table 2.

In other investigation, Bakar et al. (Makssoudi et al. 2014) have studied the tensile behavior of oil palm fiber/glass fiber reinforced the epoxy matrix. The results indicate that the hybridization increased the tensile strength and Young's modulus of hybrid composite.

In a new recent study, Yahaya et al. (2015) have manufactured composites based on kenaf and aramid fibres in order to study the effect of kenaf fiber orientation on the mechanical characteristics of the hybrid composite for military vehicle's spall liner applications. The physical properties of hybrid composites are shown in the Table 3. The results illustrate that the tensile strength of woven kenaf hybrid composite is greater that the tensile strength of unidirectional and mat samples respectively. Also, the morphological results show that the employment of kenaf woven architecture can produce hybrid composite with high tensile properties.

Table 3 Physical properties of hybrid composites

Samples	Density (g cm^{-3})	Void %	Water %	Dimension stability %
Woven	1.10	7.32	7.21	2.04
UD	1.10	8.39	8.07	2.20
Mat	0.87	26.70	26.84	2.04

Table 4 Physical and mechanical properties of used fibres (Jawaid et al. 2010)

Properties	Oil palm EFB fiber	Jute fiber
Density (g/cm^3)	0.7–1.55	1.3
Tensile strength (MPa)	50–400	393–773
Young's modulus (GPa)	1–9	26.5
Elongation at break	8–18	1.5–1.8
Cellulose content (%)	49.6	58–63
Lignin content (%)	21.2	12-14

3.2 Hybrid Composites with Natural/Natural Reinforcement

Employing the hybrid natural reinforcement natural/natural fiber inside the same matrix can also enhance the mechanical behavior of elaborated composite thanks to the complementarity effect of combined fibres.

In this context, Jawaid et al. (2010) have realized hybrid composites on the basis of Empty Fruit Bunch (EFB) fiber and jute woven, which the Table 4 presents the physical and mechanical properties of both used fibres. The results of flexural and tensile tests illustrate that the utilization of jute woven in the pure EFB composite improved the mechanical properties of hybrid composites.

In another investigation, Idicula et al. (2005). were elaborated composites based on sisal and banana fibres in sandwich structure, which the banana fibres are the skin and the sisal fiber is the core material. The hybrid fibres reinforced polyester composite with reference to the relative volume fraction of the two fibres at a constant total fiber loading of 0.4 V_f. The authors note a positive effect of hybridization in flexural strength and modulus of the hybrid composite as shown in the Fig. 10. The tensile strength increased also with hybridization, which the maximum was reached at a ratio of sisal and banana 1:4.

Fig. 10 Flexural strength versus volume fraction of fibres
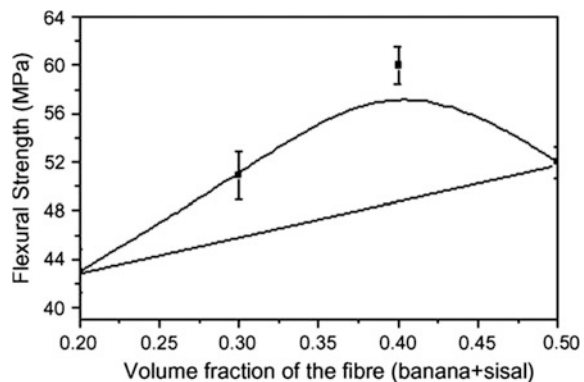
4 Bi Hybrid Composites: Hybrid Matrix and Hybrid Reinforcement

This part of chapter contains our own experimental work performed on composites based on hybrid matrix (epoxy/clay) and hybrid natural reinforcement jute/coir and jute/doum. The aim of this part is to study the effect of hybridization on the mechanical properties of elaborated composites and also to know if the hybridization permits to enhance the properties of natural fiber composites.

4.1 Materials and Preparation

4.1.1 Materials

Jute fibres are cut to dimensions of (120×120) cm^2. The jute fibres were used at two fiber directions, i.e. 0° and 45°as shown in the Table 5.

Raw Doum and Coir fibres with an average of length of 25 cm were collected from rural areas of Morocco. The coir fibres of mat architecture, and a mass content of 16 %, are made alternately with the jute woven to elaborate laminate composites. The doum fibres are extracted using the extraction method at hot water with forced immersion. The dry doum plant is placed in a basin with hot water at a temperature of 90° for 6 h, to facilitate the fiber extraction. Thereafter, the fibres are dried in an oven at 60 °C for 24 h.

Ilite's clay extracted from the region Rhamna in Morocco, is purified and mixed with epoxy matrix at different clay content (0, 5, 10, 15, 20) wt% using dispersed system (Fig. 11).

Table 5 Experimental conditions

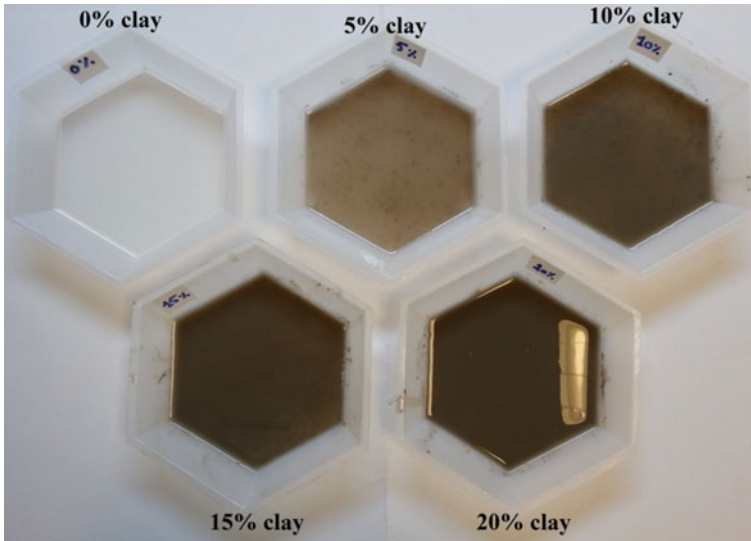| Layer's stacking Doum/Jute fibres	Layer's stacking Coir/jute fibres	Clay content (wt%)	Cutting direction
[0/DF/45/DF/0]	[0/CF/45/CF/0]	0	0°
			45°
		5	0°
			45°
		10	0°
			45°
		15	0°
			45°
		20	0°
			45°

Fig. 11 Hybrid matrix at different clay content

4.1.2   Composite Preparation

Layer Stacking

Two types of laminates were made: laminates based on jute/doum fibres and laminates based on jute/coir fibres to reinforce the hybrid matrix epoxy/clay.

For each laminate, the different fibres are alternately arranged. Jute fibres for the first, third and fifth layers; and other fibres (coir or doum) are for the second and fourth layers as shown in Fig. 12.

The samples are prepared in a stainless mold, Impregnating jute woven/coir fibres and jute woven/doum fibres by a doped resin at different clay content (0, 5, 10, 15, and 20) wt%, eventually the closing mold under a hydraulic press until desired thickness as shown in the Fig. 13. The samples were demolded after cure phase and cut at 0° and 45° directions. The crosslinking is carried out at temperature of 150 °C for 15 min.
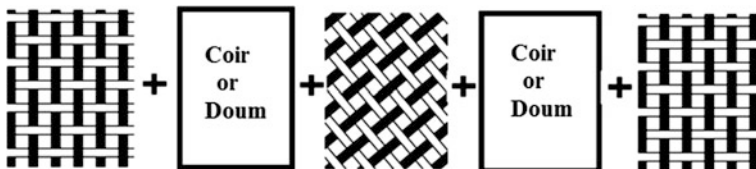
Fig. 12 Layers sequence
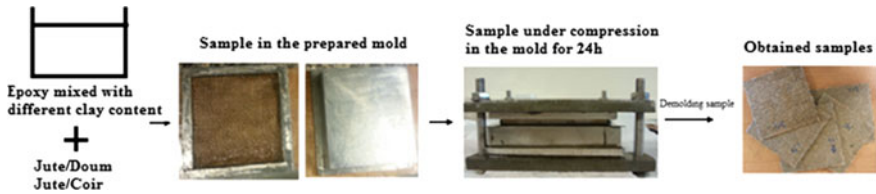
Fig. 13 Preparation steps

4.2 Experimental and Theoretical Densities

The average thickness for the prepared samples is generally about 2.65 mm. The weight of samples at different clay content is shown in Table 6.

The intrinsic characteristics of elaborated laminates were determined, which are summarized in the Table 7, as:

Table 6 Weight of different samples

Clay content (wt%)	Weight (g)	
	Jute/Coir composite	Jute/Doum composite
0	42.25	40.96
5	44.23	42.66
10	42.39	42.81
15	46.52	42.29
20	44.38	40.84

Table 7 Characteristics of different laminates

M_{clay} (%)	V_{clay} (%)	$\rho_{matrice}$ (g/cm^3)	M_f (%)	M_m (%)	$V_{f\ moyen}$ (%)	$\rho_{Theroretical}$ (g/cm^3)	$\rho_{experiment}$ (g/cm^3)
Jute/Coir composite							
0	0	1.08	38	62	31	1.19	1.06
5	2	1.11	36	64		1.21	1.07
10	5	1.14	38	62		1.23	1.11
15	8	1.17	34	66		1.25	1.13
20	11	1.2	36	64		1.27	1.14
Jute/Doum composite							
0	0	1.08	40	60	33	1.20	1.07
5	2	1.11	38	62		1.22	1.11
10	5	1.14	38	62		1.24	1.12
15	8	1.17	38	62		1.26	1.10
20	11	1.2	40	60		1.28	1.07

4.2.1 Experimental Density of Laminated Composite

$$\rho_{s\,Exp} = \frac{Weight\ of\ laminated}{Volume\ of\ laminated} \tag{1}$$

4.2.2 Theoretical Density of Laminated Composite

$$\rho_{s\,Theo} = \rho_f V_f + \rho_{clay} V_{clay} + \rho_e V_e \tag{2}$$

where V_f, V_{clay} and V_e are the fiber volume fraction, clay volume fraction and epoxy volume fraction for the used materials, respectively.

$$V_f = \frac{M_f/\rho_f}{M_f/\rho_f + M_{clay}/\rho_{clay} + M_e/\rho_e}$$

And

$$V_{clay} = \frac{M_{clay}/\rho_{clay}}{M_f/\rho_f + M_{clay}/\rho_{clay} + M_e/\rho_e} \tag{3}$$

where ρ_f ($1.45\,\text{g/cm}^3$), ρ_e ($1.08\,\text{g/cm}^3$) and ρ_{clay} ($2.14\,\text{g/cm}^3$) are the fiber, epoxy and clay density, respectively, obtained from literature (Abdellaoui et al. 2015a):

With: $\rho_m = \rho_{clay} V_{clay} + (1 - V_{clay})\rho_e$

The results of composite density show that the theoretical density is slightly higher that the experimental one. This difference is mainly due to the void content in elaborated composite, which in theory, the structure is supposed perfect.

4.3 Mechanical Properties of bi Hybrid Composites

4.3.1 Tensile Properties

The tensile measurements of different elaborated laminates are influenced by the fiber orientation, clay percent, architecture and size of used fibres.

Effect of Clay Content

The Fig. 14a, b show the evolution of Young's modulus of different laminates in function of clay content. An increase of Young's modulus with increasing of clay content was noted. Namely, an increase of almost 14 % in case of laminates
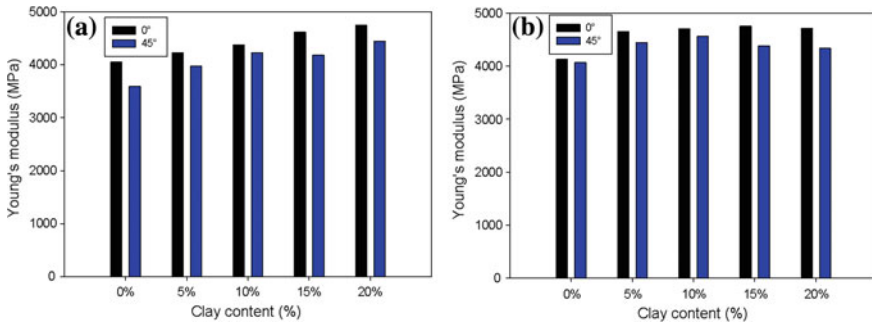
Fig. 14 Young's modulus of laminates, **a** laminates with (jute/coir), **b** laminates with (jute/doum)
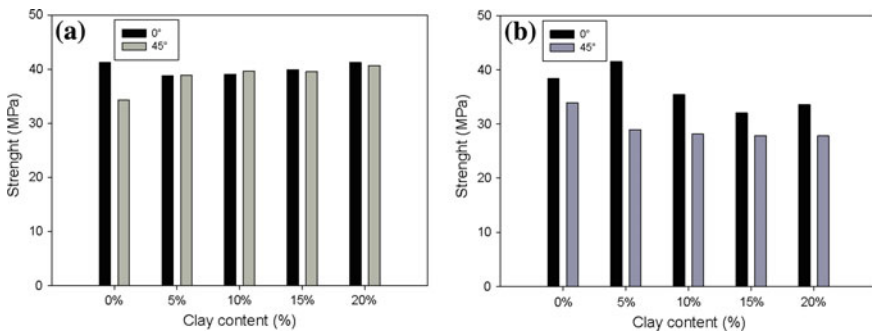

Fig. 15 Tensile strength of laminates, **a** laminates (jute/coir), **b** laminates (jute/doum)

(jute/doum) and 17 % in case of laminates (jute/coir). This is mainly due to the good distribution/dispersion of clay particles throughout the epoxy polymeric chains, which led to the good compatibility between clay and epoxy and the rigidity of each one of Doum and Coir fibres (Hariharan and Khalil 2005; Panthapulakkal and Sain 2007; Yahaya et al. 2015; Abdellaoui et al. 2015b).

Regarding the stiffness of the laminates (Fig. 15a, b), it was noted an increase in the tensile strength with increasing of clay percent. This increase is explained by the good wettability of the fibrous reinforcement by the hybrid matrix (epoxy/clay). Also, it was observed that the strain at yield decreases very lightly with increasing of clay percent (Fig. 16a, b). This is due to the fragile character of the fibres and the rigid nature of the clay (Hariharan and Khalil 2005).

Effect of the Fiber Orientation

It was observed (Fig. 14) that the Young's modulus is slightly higher in the case of laminates at 0° fiber orientation. These results seem logical because the load is carried by the length of unidirectional fibres in the longitudinal direction of fibres.
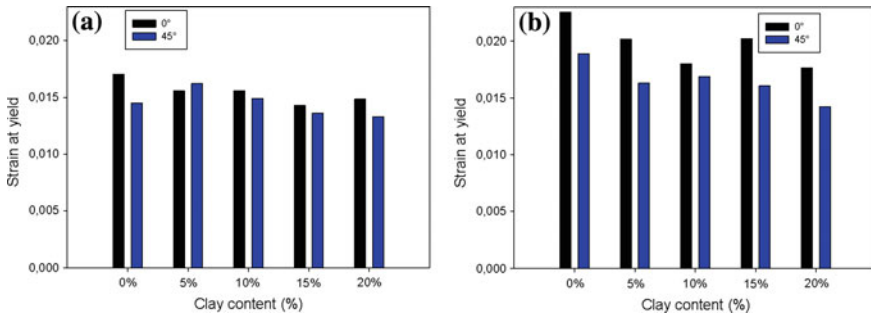
Fig. 16 Strain at yield of laminates, **a** laminates (jute/coir), **b** laminates (jute/doum)

Effect of the Fiber Size

Concerning the effect of fiber size, it is noted (Fig. 17) the Young's modulus is relatively high in the case of laminates with (Jute/Doum) fibres. This amounts to the difference in size of each fiber, which the coir is used in the form of small diameter fibres, and the doum is used in the form of fiber bundles. Therefore, the rigidity of the reinforcement increases progressively using fiber bundles. It's concluded that the small reinforcement size improves the composite ductility (Jute/coir), and the bundles or big size improve the composite rigidity (Megiatto et al. 2010).

Effect of the Fiber Architecture

About the reinforcement architecture, these results of laminates with (woven fabric/mat) were compared with those obtained in another work that we have recently realized on laminates based on (woven/woven) fabrics. This comparison reveals that the use of hybrid architecture (woven fabric/mat) allows to slightly

Fig. 17 Young's modulus of laminates
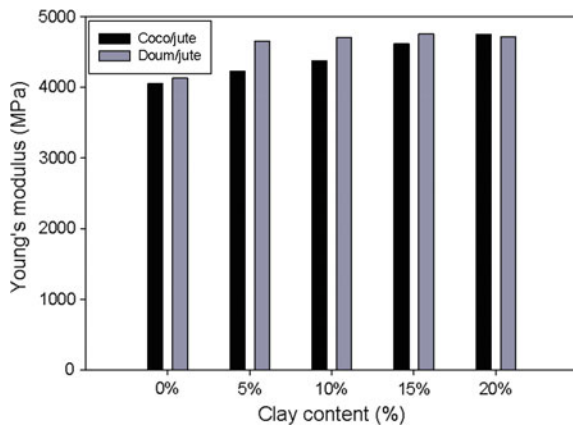
Fig. 18 Young's modulus of laminates with different architectures
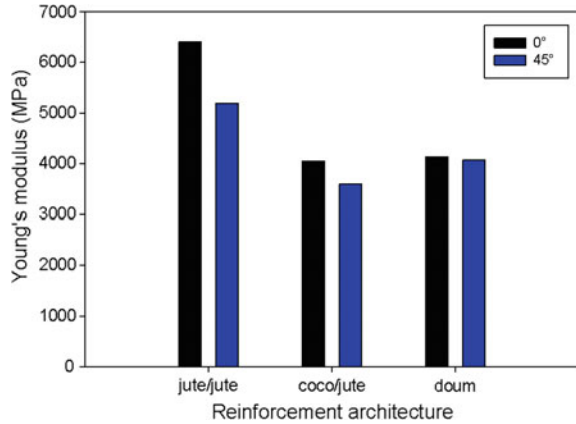
reducing the anisotropic character passing from laminates oriented at 0° to others oriented at 45° as illustrated in the Fig. 18. However, the mechanical properties decrease of almost 32 %, from laminates with reinforcement (woven fabric/mat) to laminates with (woven fabric/woven fabric). Generally, the load is supported by the unidirectional fibres in the longitudinal direction (Idicula et al. 2005).

4.3.2 Torsional Properties

This rheological test is used to determine the viscoelasticity of the laminates realized in different conditions.

As mentioned above, the complex Torsional modulus G* is given by:

$$G^* = \sqrt{G'^2 + G''^2} \tag{4}$$

where G′ and G″ are respectively the storage and loss modulus measured by the ARES-LS Rheometer, and the ratio of the storage modulus G′ and loss modulus G″ is the loss factor δ.

$$tan\delta = \frac{G''}{G'}$$

The Fig. 19a, b show the evolution of the loss factor according to the clay percent and frequency (0.1–40 Hz) in case of the two laminates reinforcement (Jute/doum) and (jute/coir). It is noted a slight decrease in the loss factor δ by increasing the clay percent. This confirms that the realized laminates behave as elastic solids, and the viscous component doesn't exceed an average of 8 %. This elasticity is essentially due to the elastic nature of the fibres and the matrix.
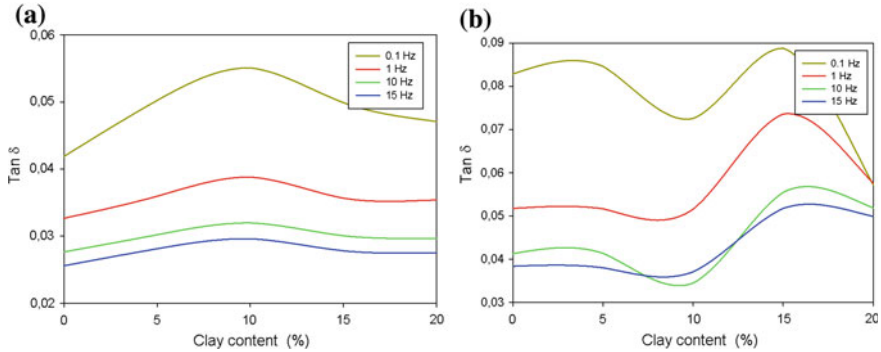
Fig. 19 Loss factor versus clay percent and frequency **a** Laminates with Coir/jute fibres, **b** laminates with Doum/jute fibres

Also, it is noted that the loss factor decreases with increasing frequency (0.1–15 Hz). A high frequency, the polymer chains don't have time to relax and re-arrange them, which reduces the viscous nature of the developed material (Abdellaoui et al. 2015a).

5 Conclusion

This chapter covers experimental studies performed on hybrid composites based on natural components, which the aim is to detect the effect of natural hybridization on the global mechanical properties of natural fiber composites. In this chapter, we treated successively hybrid matrices loaded with a natural material'clay, and hybrid composites of hybrid natural reinforcement and finally bi hybrid composites based on a hybrid matrix and reinforcing a natural hybrid. The mechanical behavior of these composite hybrids was studied, the results of preparation and characterization of the hybrid matrix and the bi hybrid composites, are our own experimental work. The hybridization effect will only be complete by prior knowledge of the mechanical properties of two types of fibres used in order to achieve complementarity. All the results summarized in this chapter reveals a stimulating ambition to further develop hybrid natural composites for applications industrially profitable.

References

Abdellaoui, H., Bensalah, H., Echaabi, J., Bouhfid, R., Qaiss, A.: Fabrication, characterization and modelling of laminated composites based on woven jute fibres reinforced epoxy resin. Mater. Des. **68**, 104–113 (2015a)

Abdellaoui, H., Bouhfid, R., Echaabi, J., Qaiss, A.: Experimental and modeling study of viscoelastic behaviour of woven dried jute under compressive stress. J. Reinf. Plast. Compos. **34**, 405–420 (2015b)

Abdellaoui, H., Echaabi, J.: Rheological models for modeling the viscoelastic behavior in liquid composite molding processes (LCM) review. J. Reinf. Plast. Compos. **33**, 714–732 (2014)

Arrakhiz, F.Z., Benmoussa, K., Bouhfid, R., Qaiss, A.: Pine cone fiber/clay hybrid composite: mechanical and thermal properties. Mater. Des. **50**, 376–381 (2013)

Behera, A.K., Avancha, S., Basak, R.K., Sen, R., Adhikari, B.: Fabrication and characterizations of biodegradable jute reinforced soy based green composites. Carbohydr. Polym. **88**, 329–335 (2012)

Bessadok, A., Marais, S., Gouanvé, F., Colasse, L., Zimmerlin, I., Roudesli, S., Métayer, M.: Effect of chemical treatments of Alfa (Stipa tenacissima) fibres on water-sorption properties. Compos. Sci. Technol. **67**, 685–697 (2007)

Bessadok, A., Roudesli, S., Marais, S., Follain, N., Lebrun, L.: Alfa fibres for unsaturated polyester composites reinforcement: Effects of chemical treatments on mechanical and permeation properties. Compos. Part A Appl. Sci. Manuf. **40**,184–195 (2009)

Boujmal, R., Essabir, H., Nekhlaoui, S., Bensalah, M.O., Bouhfid, R., Qaiss, A.: Composite from polypropylene and henna fiber: structural, mechanical and thermal properties. J. Biobased Mater. Bioenergy **8**, 246–252 (2014)

Charlet, K., Baley, C., Morvan, C., Jernot, J.P., Gomina, M., Bréard, J.: Characteristics of Hermès flax fibres as a function of their location in the stem and properties of the derived unidirectional composites. Compos. Part A Appl. Sci. Manuf. **38**, 1912–1921 (2007)

Cyras, V.P., Manfredi, L.B., Ton-That, M.-T., Vázquez, A.: Physical and mechanical properties of thermoplastic starch/montmorillonite nanocomposite films. Carbohydr. Polym. **73**, 55–63 (2008)

De Rosa, I.M., Santulli, C., Sarasini, F., Valente, M.: Post-impact damage characterization of hybrid configurations of jute/glass polyester laminates using acoustic emission and IR thermography. Compos. Sci. Technol. **69**, 1142–1150 (2009)

Defoirdt, N., Biswas, S., De, Vriese L., Tran, L.Q.N., Van, Acker J., Ahsan, Q., Gorbatikh, L., Van, Vuure A., Verpoest, I.: Assessment of the tensile properties of coir, bamboo and jute fibre. Compos. Part A Appl. Sci. Manuf. **41**, 588–595 (2010)

Hariharan, A.B.A., Khalil, H.P.S.A.: Lignocellulose-based hybrid bilayer laminate composite: Part I—studies on tensile and impact behavior of oil palm fiber-glass fiber-reinforced epoxy resin. J. Compos. Mater. **39**, 663–684 (2005)

Idicula, M., Neelakantan, N.R., Oommen, Z., Joseph, K., Thomas, S.: A study of the mechanical properties of randomly oriented short banana and sisal hybrid fiber reinforced polyester composites. J. Appl. Polym. Sci. **96**, 1699–1709 (2005)

Jawaid, M., Abdul Khalil, H.P.S., Bakar, A.A.: Mechanical performance of oil palm empty fruit bunches/jute fibres reinforced epoxy hybrid composites. Mater. Sci. Eng. A **527**, 7944–7949 (2010)

Jawaid, M., Abdul Khalil, H.P.S., Bakar, A.A.: Woven hybrid composites: tensile and flexural properties of oil palm-woven jute fibres based epoxy composites. Mater. Sci. Eng. A **528**, 5190–5195 (2011)

Jeong, E., Lim, J.W., Seo, K., Lee, Y.-S.: Effects of physicochemical treatments of illite on the thermo-mechanical properties and thermal stability of illite/epoxy composites. J. Ind. Eng. Chem. **17**, 77–82 (2011)

John, M., Thomas, S.: Biofibres and biocomposites. Carbohydr. Polym. **71**, 343–364 (2008)

Khan, M.A., Ganster, J., Fink, H.-P.: Hybrid composites of jute and man-made cellulose fibers with polypropylene by injection moulding. Compos. Part A Appl. Sci. Manuf. **40**, 846–851 (2009)

Le Duigou, A., Davies, P., Baley, C.: Interfacial bonding of Flax fibre/Poly(l-lactide) bio-composites. Compos. Sci. Technol. **70**, 231–239 (2010)

Makssoudi El, A., Abdellaoui, H., El Ouatib, R., Tahiri, M.: Development of composite materials based on expanded perlite and plastic wastes. Mechanic-chemical properties. In: 2nd Annual International Conference on Chemistry, Chemical Engineering and Chemical Process (CCECP 2014), pp. 38–46 (2014)

Martins, I.M.G., Magina, S.P., Oliveira, L., Freire, C.S.R., Silvestre, A.J.D., Neto, C.P., Gandini, A.: New biocomposites based on thermoplastic starch and bacterial cellulose. Compos. Sci. Technol. **69**, 2163–2168 (2009)

Megiatto, J.D., Ramires, E.C., Frollini, E.: Phenolic matrices and sisal fibers modified with hydroxy terminated polybutadiene rubber: Impact strength, water absorption, and morphological aspects of thermosets and composites. Ind. Crops Prod. **31**, 178–184 (2010)

Mwaikambo, L.Y., Ansell, M.P.: Chemical modification of hemp, sisal, jute, and kapok fibers by alkalization. J. Appl. Polym. Sci. **84**, 2222–2234 (2002)

Nekhlaoui, S., Essabir, H., Bensalah, M.O., Fassi-Fehri, O., Qaiss, A., Bouhfid, R.: Fracture study of the composite using essential work of fracture method: PP–SEBS–g–MA/E1 clay. Mater. Des. **53**, 741–748 (2014)

Nekhlaoui, S., Essabir, H., Kunal, D., Sonakshi, M., Bensalah, M.O., Bouhfid, R., Qaiss, A.: Comparative study for the talc and two kinds of moroccan clay as reinforcements in polypropylene-SEBS-*g*-MA matrix. Polym. Compos. **36**, 675–684 (2015)

Panthapulakkal, S., Sain, M.: Injection-molded short hemp fiber/glass fiber-reinforced polypropylene hybrid composites—Mechanical, water absorption and thermal properties. J. Appl. Polym. Sci. **103**, 2432–2441 (2007)

Yahaya, R., Sapuan, S.M., Jawaid, M., Leman, Z., Zainudin, E.S.: Effect of fibre orientations on the mechanical properties of kenaf–aramid hybrid composites for spall-liner application. Def. Technol. **12**, 52–58 (2015)

Wear Properties of Nanoclay Filled Epoxy Polymers and Fiber Reinforced Hybrid Composites

A. Jumahat, A.A.A. Talib and A. Abdullah

Abstract Polymeric material is one of the best materials, which has been used in many applications. This is owing to its excellent properties such as low density, good mechanical properties and good chemical resistance. The main objective of this research is to evaluate the effect of nanoclay on wear properties of epoxy polymer and fibre reinforced composites. The nanoclay/epoxy composites with 1, 3 and 5 wt% nanoclay contents were fabricated using high shear mixing system at 60 °C and speed of 12.7 m/s, while glass fiber reinforced nanocomposite panels were fabricated using vacuum bagging system. The effect of nanoclay on wear properties was evaluated using dry sliding wear and slurry tests. Dry sliding wear test was conducted using vitrified bonded silicon carbide abrasive wheels and Slurry test was conducted using a mixture of sand and water as slurry items. The mass loss and specific wear rate curves showed that wear properties of pure epoxy system and fiber reinforced polymer were enhanced when the weight fraction of nanoclay in the system reached up to certain weight percentage. Epoxy system with 3 wt% nanoclay has highest wear properties when compared to pure, 1 and 5 wt% nanoclay content in epoxy systems, while fiber reinforced polymer composite with 5 wt% nanoclay content has the highest wear properties compared to pure, 1 and 3 wt% nanoclay content. The results were affected by the agglomeration of nanoparticles and weak compatibility of nanoclay, glass fiber and epoxy.

Keywords Polymer · Nanoclay · Specific wear rate · Abrasive dry sliding test · Slurry test

A. Jumahat (✉) · A.A.A. Talib · A. Abdullah
Faculty of Mechanical Engineering, Universiti Teknologi MARA,
40450 Shah Alam, Selangor, Malaysia
e-mail: aidahjumahat@salam.uitm.edu.my

A.A.A. Talib
e-mail: anisadilah86@gmail.com

1 Introduction

Polymer composites have been used in many applications since decades ago until today. Epoxy resin is one of the most popular thermoset polymers, among other thermoset class polymers and thermoplastic polymers. Epoxy resins are used extensively as matrices for applications such as surface coatings, structural adhesives, encapsulation, and engineering composites (Mirmohseni and Zavareh 2010; Ahmad et al. 2012; Zulfli et al. 2012). Upon curing, epoxy resins possess excellent chemical and heat resistance, high adhesive strength, good impact resistance, high strength and hardness and high electrical insulation (Abdul et al. 2013). However, in all these applications, there are still limitation to end-use applications since epoxy resins are brittle and rigid in nature, thus have poor resistance to crack propagation (Mirmohseni and Zavareh 2010). Therefore, numerous study have been conducted to improve the properties of epoxy resins, one of the effective ways is by inclusion of nanoparticle into the matrix resin to produce polymer nanocomposite. Researchers have shown that polymer nanocomposite can provide high mechanical and tribological performance with variety of application without supressing other existing mechanical properties (Lam et al. 2005; Lam and Lau 2007; Mirmohseni and Zavareh 2010; Rashmi et al. 2011; Ahmad et al. 2012; Jumahat et al. 2012, 2013; Suresha et al. 2012; Žukas et al. 2012; Abdul et al. 2013; Esteves et al. 2013; Kanny and Mohan 2014; Amir et al. 2015; Dorigato et al. 2015). According to Callister (2001), some properties of cured epoxy resins were improved when they were upgraded into polymer nanocomposites.

Clay is one of the most widely used and investigated nanofillers in polymer nanocomposite applications. Its availability and nature make it one of the increasing nanofillers used to improve mechanical properties and also tribological properties of composites. When clay is mixed with water in correct proportion, it can form a plastic mass that are amendable to shaping (Callister and Rethwisch 2014). As montmorillonite is one type of clay, the dominant constituents in montmorillonite are silica and alumina (Koo 2006). It has high elastic modulus, low materials cost, low density, high thermal stability, low thermal expansion coefficient and high specific surface area (Jumahat et al. 2013). All these properties will significantly improve strength, stiffness, fracture toughness, dimensional stability and thermo-mechanical behaviour of polymer (Jumahat et al. 2012). The main factor affecting these properties is good dispersion rate of nanoparticle into epoxy resin system and the large interfacial interaction between the nanoparticle layer and the matrix of the system, which for nanoclay system is the degree of exfoliation (Sapiai et al. 2015b). Other factors affecting the final properties of nanocomposites are type and size of fillers, volume percentage of fillers, compatibility between nanofillers and polymer matrix, processing parameters and curing conditions.

Fiber reinforced polymer (FRP) composites are also widely used in various applications such as fuel tanks, sport equipment, satellites, aircraft and aerospace structure, advanced marine vessels, high-end automobile structure and other strength/weight critical applications. Addition of fiber into epoxy/nanoclay

composites offer improved thermal and mechanical properties and improved fiber-matrix interface (Zulfli et al. 2012; Kanny and Mohan 2014; Amir et al. 2015). However, despite the growing research done on mechanical properties of fiber reinforced nanocomposites, the study on wear properties is still far behind. The wear properties for fiber reinforced composites are depending of fiber orientation, fiber content, fiber length, compatibility of fiber and resin, layering pattern of fiber, and extent of intermingling of fibers (Sapiai et al. 2015a).

The importance of wear properties is as equal as the importance of mechanical properties of the materials. Wear is defined as the loss of material from contact surface when subjected to relative motion. There are five main types of wear which usually observed for polymer composites such as fatigue wear, fretting, erosion, adhesive and abrasive wear, whereas for fiber reinforced polymer, there are matrix wear, fiber sliding wear, fiber fracture and interfacial debonding (Suresha et al. 2010). The work conducted on the influence of nanofillers and matrix material on mechanical and tribological properties, especially wear resistance, hardness and coefficient of friction are in interests of many researchers. Variety combination of filler reinforcement into polymer resulted in better wear life for example, CNT (Campo et al. 2015), Nanosilica (Zhang et al. 2013), NanoZrO$_2$ (Kurahatti et al. 2014), NanoTiO$_2$ (Chang et al. 2005) and PTFE (Chang and Friedrich 2010).

Chun and Kin (Lam and Lau 2007) reported that the wear properties and micro-hardness of nanocomposite were increased with increasing content of nanoclay up to 4 wt% when tested with 5131 Abraser of Taber Industries. In another experiment, Suresha et al. (2012) reported that the abrasive wear resistance is at its best when only 5 wt% content of organo-modified montmorillonite (oMMT) filled epoxy nanocomposite as compared to other weight percentage of oMMT filled epoxy nanocomposites and neat epoxy. Higher filler content (7.5 wt%) produced agglomerated oMMT. However, different results have been found by Esteves, Ramalo, Ferreia and Nobre where only 1 wt% of nanoclay/epoxy composite exhibit better wear resistance than pure epoxy resin when tested using linear reciprocating ball-on-flat tribotester (Esteves et al. 2013). Even with higher hardness and Young's modulus, 3 and 6 wt% of nanoclay showed decrease in wear resistance, believed to cause by the localised defect of particle agglomeration. Whereas Rashmi, Renukappa, Suresha, Devarajaiah and Shivakumar reported the same result as (Suresha et al. 2012) where the most effective nanoclay content is up to only 5 wt %, when tested using pin-on-disc tester (Rashmi et al. 2011). Further increase in nanoclay content (7 wt%) has reduced the wear performance of nanoclay/epoxy composite.

For other polymer resin matrix, several research works are also reported. A PVDF/nanoclay composite, research done by Peng, Cong, Liu, Liu, Huang and Sheng found that nanoclay content are only effective at 1–2 wt% to improve mechanical and tribological properties of PVDF (Peng et al. 2009). Nanocomposite with 5 wt% exhibit higher wear suspected from weak compatibility between nanoclay and PVDF and decreased crystallinity. On the other hand, Jawahar et al. (2006) found that the least coefficient of friction and highest wear resistance of nanoclay/polyester composite is of only 3 wt%. They exhibit 85 % of improvement

in wear resistance and 35 % decrease in coefficient of friction when compared to pure polyester. Further addition of nanoclay (5 wt%) increases the wear rate since micropores formed in matrix system by agglomerated nanoclay.

In the present work, nanoclay filled epoxy polymer and advanced GFRP composite with different amount of nanoclay (1, 3 and 5 wt%) were prepared and the their specific wear rate were studied by carrying out dry sliding test and slurry test.

2 Experimental

2.1 Materials

The epoxy resin (Miracast 1517 A) with density of 1.30 g/cm^3 and its hardener (Miracast 1517 B), used for fabricating composite panels, were supplied by Miracon (M) Sdn. Bhd. The mixing ratio was set at 100:30. The nanoclay used was Nanomer I.30E supplied by Sigma-Aldrich (M) Sdn. Bhd, while glass fiber used was woven type fiber supplied by Vistec Technology Service (M) Sdn. Bhd.

2.2 Sample Fabrication

The desired amount of nanoclay (1, 3 and 5 wt%) was measured and pre-dispersed in epoxy resin by hand-stir for 15 min. To ensure homogenous dispersion and exfoliated structure, the mixture was then milled using high shear three roll mill machines at 12.7 m/s with temperature of 60 °C, as shown in Fig. 1. The gap between rollers was set to approximately 15 μm. The mixture was then degassed in vacuum oven for 1 h to remove entrapped air. Finally, the mixture was blended with hardener at ratio of 100:30 for 15 min before it was poured into released-agent coated silicon moulds. The silicon moulds were prepared based on sample dimensions as shown in Fig. 2. The sample was cured at room temperature for 24 h.

Fig. 1 High shear three roll mill machine
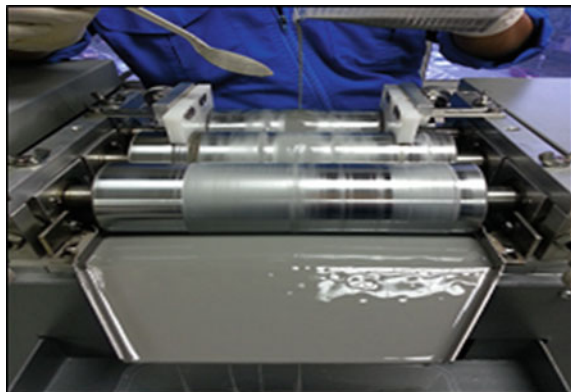
Fig. 2 Dimensions of **a** Dry sliding wear test and **b** Slurry wear test
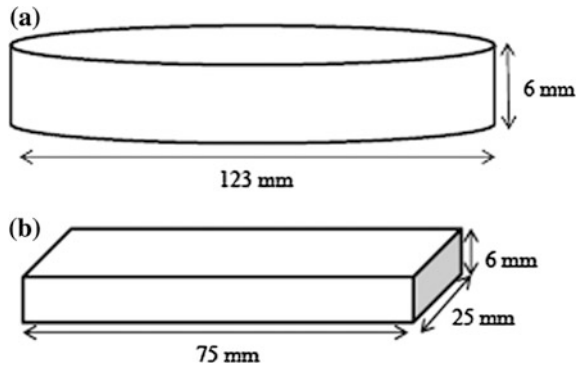

The nanomodified-FRP composites laminates were produced using vacuum bagging system using woven glass fiber and nanoclay-modified epoxy resin. The nanoclay modified epoxy resin of 1, 3 and 5 wt% was prepared based on the procedure mentioned above. There were 24 sheets of woven glass fiber layered with the mixture of nanomodified epoxy resin to reach a thickness of 6 mm. The laminates were then degassed by vacuum for 1 h to remove trapped air. Finally, the laminates were cured at room temperature for 24 h. The cured laminates were cut in accordance to specific dimensions, as shown in Fig. 2.

2.3 Dry Sliding Wear Test

Dry sliding wear test was done by using Abrasion Resistance Tester (TR-600). The tester and its schematic diagram are as shown in Fig. 3. The disc specimen was polymer, with size of 123 mm diameter and 6 mm thickness as shown in Fig. 2a. The sample was located in contact with two vitrified bonded silicon carbide abrasive wheels. Before each test, the wheels were cleaned by using dry brush in order to eliminate any dust on the abrasive wheels. The initial weight of each samples were taken before performing the test by using precision balance. The sample was rotating at a constant speed and load of 267 rpm and 20 N respectively for 2000 m distance travel before the mass of the sample was taken again. The mass of sample was taken at an interval of 2000 m for total of 10,000 m distance travel. Thus, the specific wear rate was measured by the loss in mass, based on Archad wear model;

$$W_s = (\Delta m)/(L \times \rho \times F) \tag{1}$$

where W_s in (mm^3/Nm), Δm is weight loss (g), L is sliding distance (m), ρ is density (g/mm^3) and F is applied load (N). The summary of operational conditions is given in Table 1.
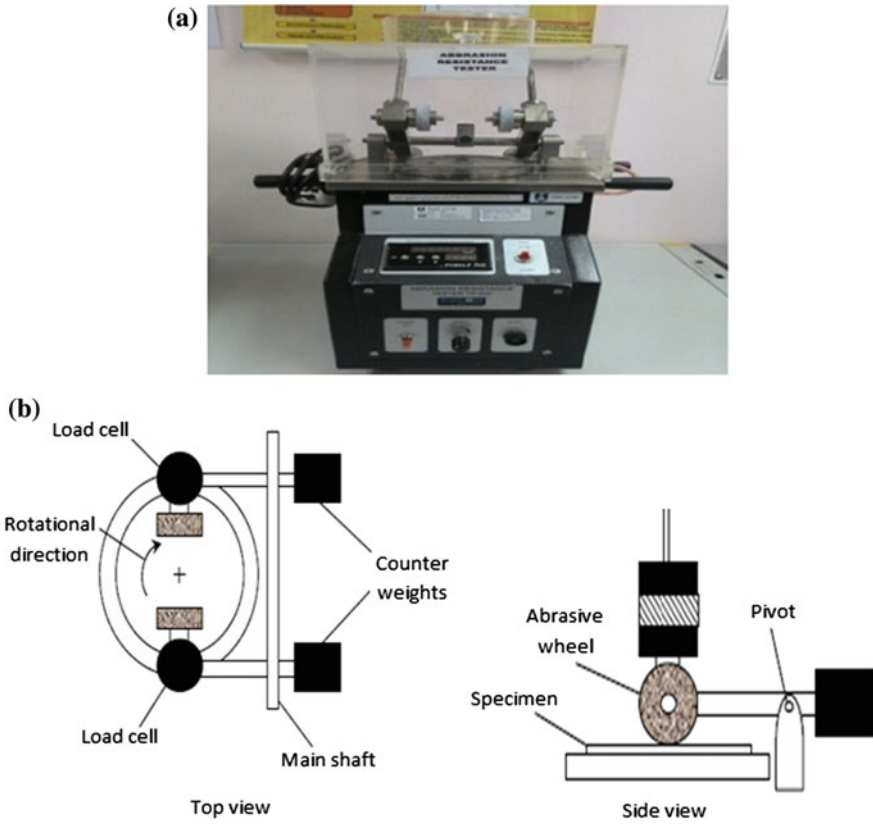
Fig. 3 **a** Abrasion Resistance Tester (TR-600) and **b** schematic diagrams of the Abrasion Resistance Tester

Table 1 Operational parameters of dry sliding test

Parameters	Experimental conditions
Contact geometry	Cylinder on flat
Type of motion	Unidirectional sliding
Applied load	20 N
Sliding speed	267 rpm
Sliding distance	10,000 m at interval 2000 m

2.4 Slurry Test

Slurry test was conducted using Slurry Erosion Test Rig (TR-40), as shown in Fig. 4, and sand was used as slurry media/condition. The dimension of specimen for this test is 75 mm × 25 mm × 6 mm as shown in Fig. 2b. The samples were attached to rotational holder in a container which contains the mixture of water and

Fig. 4 Slurry Erosion Test
Rig (TR-40)

Table 2 Operational
parameters of slurry test

| Parameters	Experimental conditions
Type of motion	Unidirectional sliding
Type of sand	Medium size (0.2–0.63 mm)
Sliding speed	267 rpm
Sliding time	20 h at interval 4 h
Sliding distance	10,000 m at interval 2000 m

sand with size ranged from 0.2 to 0.63 mm. The surface of samples was in contact
with sand particles that caused erosion on the surface of samples. The initial mass of
each samples were recorded before performing the test by using precision balance.
The amount of mass loss was recorded at every 2000 m distance intervals for
10,000 m distance travel. Based on the mass loss recorded, the specific wear rate
was calculated using Eq. (1). The summary of operational parameters is shown in
Table 2.

3 Results and Discussions

3.1 Mass Loss and Specific Wear Rate Measured Using Dry Sliding Wear Test

Mass loss over distance of the polymer nanocomposite and advanced GFRP nanocomposite were obtained from dry sliding test as shown in Fig. 5a and b, respectively. According to the graph, the mass loss for both nanocomposite and nanomodified-GFRP composite have a similar increasing trend as the distance travel increased. In Fig. 4a and b, a nanoclay composite with 3 wt% has the lowest mass loss, while pure epoxy resin shows the highest mass loss for both composite systems. It is also shown clearly that the addition of nanoclay has reduced the amount of mass loss for both systems.
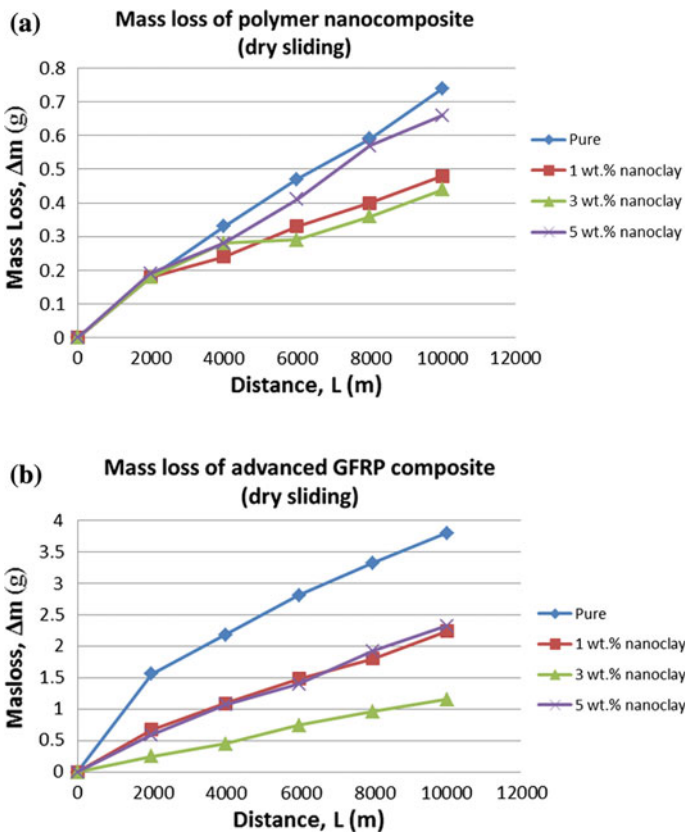
Fig. 5 Mass loss versus distance in dry sliding test of two different systems; **a** epoxy polymer with and without nanoclay, **b** GFRP composite with and without nanoclay

For polymer nanocomposite, pure epoxy polymer system has the highest mass loss after travelled for 10,000 m which 0.74 g, whereas the lowest mass loss is at 3 wt% of nanoclay filled epoxy polymer, which is only 0.44 g. On the other hand, pure epoxy system in advanced GFRP nanocomposite recorded the highest mass loss after travelled for 10,000 m which is 3.8 g while 1.15 g of mass loss was recorded for 3 wt% of nanoclay filled epoxy polymer in advanced GFRP composite which is the lowest mass loss after travelled 10,000 m. Further addition of nanoclay to 5 wt% has caused agglomeration of nanoclay particle in the system thus leads to easier surface removal. The 3 wt% of nanoclay content of polymer nanocomposite and advanced GFRP nanocomposites might have the best dispersion of nanoclay in epoxy, which improves the load carrying capacity, thus having the lowest mass loss. On the other hand, the data shows that mass loss increased with increasing distance for all nanocomposites is probably caused by the deeper grooving of the composite surface resulting more material being removed by the abrasion wheel (Suresha et al. 2012). However, the results also pointed out that the advanced GFRP nanocomposite has higher mass loss compared to the polymer nanocomposite. This is caused by the glass fiber orientation that introduced more friction heat to the system, causing further debonding which leads to more surface removal.

After the mass loss of each system was obtained by dry sliding test, the specific wear rate of each system was determined by using Eq. (1). Figure 6a, b shows the specific wear rate of nanocomposite and advanced GFRP nanocomposite system respectively. There is a sharp decreased at the beginning of the curve for both systems due to the run-in stage condition of composite that usually occurred on new material.

According to Fig. 6, the lowest specific wear rate is by 3 wt% of nanoclay filled epoxy polymer and the highest specific wear rate is by pure epoxy system for both polymer nanocomposite and advanced GFRP composite. In polymer nanocomposite, the lowest specific wear rate of 3 wt% of nanoclay filled epoxy polymer is 1.1×10^{-3} mm^3/Nm at distance of 4000 m. For pure epoxy system, the lowest specific wear rate was recorded at distance of 8000 m which is 2.7×10^{-3} mm^3/Nm. While for 1 and 5 wt% of nanoclay, the lowest specific wear rate of each system is 1.3×10^{-3} mm^3/Nm and 2.0×10^{-3} mm^3/Nm, respectively.

Similar as Fig. 6a, the graph in Fig. 6b also follows the typical trend. From the graph, it can be concluded that the 3 wt% of nanoclay filled epoxy polymer in advanced GFRP composite have the lowest specific wear rate. The lowest specific wear rate is 3.1×10^{-3} mm^3/Nm which is at 10,000 m travel distance while the highest specific wear rate, which is 4.8×10^{-3} mm^3/Nm, was recorded at 6000 m travel distance. The highest specific wear rate in the advanced GFRP composite for this dry sliding test was recorded by pure epoxy of advanced GFRP composite. It was recorded at 2000 m travel distance which is 24.5×10^{-3} mm^3/Nm while the lowest specific wear rate is 7.5×10^{-3} mm^3/Nm at distance 10,000 m. For 1 and 5 wt% of nanoclay filled epoxy polymer in advanced GFRP composite, the lowest specific wear rate was recorded are 5.2×10^{-3} mm^3/Nm and 5.4×10^{-3} mm^3/Nm respectively. The lower specific wear rate shows the better performance to resist the wear. According to the obtained result for dry sliding test, the increasing of
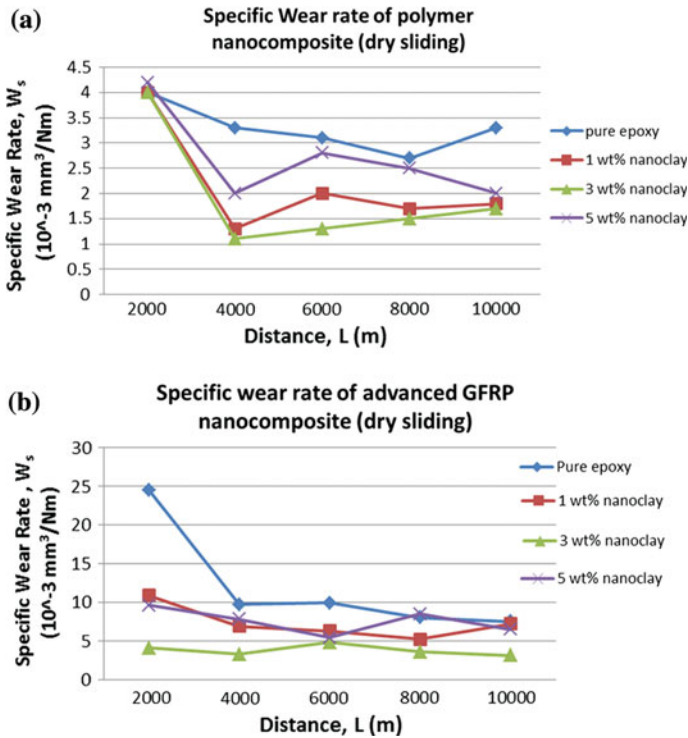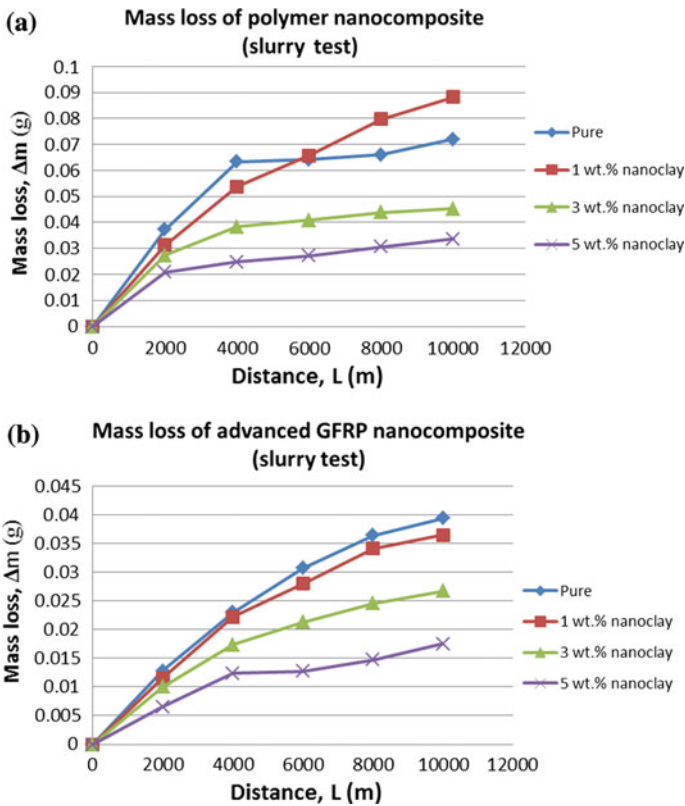
Fig. 6 Specific wear rate in dry sliding test of two different systems; **a** epoxy polymer with and without nanoclay, **b** GFRP composite with and without nanoclay

nanoclay particle up to 3 wt% in the epoxy polymer enhanced the wear properties of the system. Further increase of nanoclay in epoxy polymer system will form agglomeration which caused the surface removal become easier, thus increasing the wear rate (Suresha et al. 2012).

## 3.2 Mass Loss and Specific Wear Rate Measured Using Slurry Test

The mass loss and its corresponding wear rate of polymer nanocomposite and advanced GFRP nanocomposite are shown in Figs. 7 and 8. The results of polymer and FRP composite systems were compared to those of nanomodified systems as have been analysed before using dry sliding wear technique. In Fig. 7a, b, the curves show an almost similar increasing trend for all samples in polymer nanocomposites and advanced GFRP nanocomposites with 1, 3 and 5 wt% of nanoclay contents, except for 1 wt% nanoclay content of polymer nanocomposite.

Fig. 7 Mass loss versus distance in slurry test of two different systems; **a** epoxy polymer with and without nanoclay, **b** GFRP composite with and without nanoclay

The mass loss of 1wt% nanoclay-epoxy polymer specimen is higher than that of pure polymer system. This might be due to poor dispersion of nanoclay in the matrix which resulted in low matrix-particle bonding.

The mass loss of 1 wt% of nanoclay filled epoxy polymer is 0.0882 g after travelled for 10,000 m. For pure epoxy system, 3 and 5 wt% of nanoclay filled epoxy polymer, each system has 0.072, 0.0452 and 0.0337 g of mass loss, respectively, where 5 wt% of nanoclay filled epoxy polymer shows the lowest mass loss. Similar as nanocomposite, the mass loss of advanced GFRP nanocomposite also increased with increasing of travel distance. In this system, pure epoxy polymer system shows the highest mass loss compared to 1, 3 and 5 wt% of nanoclay filled epoxy polymer. The mass loss recorded for pure epoxy polymer system is 0.0396 g while the lowest mass loss in this system is for 5 wt% of nanoclay filled epoxy polymer which is only 0.0175 g. The mass loss after 10,000 m of travel distance of polymer nanocomposite system is higher compared to advanced GFRP nanocomposite system.

(a)

(b)
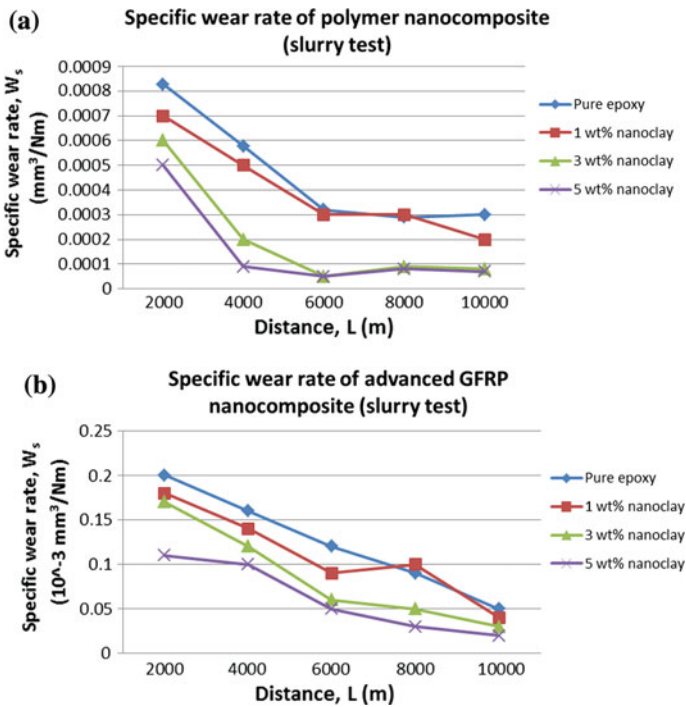
Fig. 8 Specific wear rate in slurry test of two different systems; **a** epoxy polymer with and without nanoclay, **b** GFRP composite with and without nanoclay

Figure 8a, b shows the specific wear rate of nanocomposite and advanced GFRP nanocomposite system which were obtained using slurry test. Based on the graph showed in Fig. 8, 5 wt% of nanoclay filled epoxy polymer shows the lowest specific wear rate for both polymer nanocomposite and advanced GFRP composite systems. In polymer nanocomposite system, the lowest value of specific wear rate recorded is 0.05×10^{-3} mm^3/Nm at distance of 6000 m, whereas the highest value of specific wear rate is recorded by pure epoxy polymer at 2000 m with 0.8×10^{-3} mm^3/Nm.

Specific wear rate of pure epoxy system is the highest when compared to the other systems. For advanced GFRP composite system, 5 wt% of nanoclay has the specific wear rate of 0.02×10^{-3} mm^3/Nm at 10,000 m travel distance, which is the lowest among all. The lowest specific wear rate recorded by pure system, 1 wt% of nanoclay and 3 wt% of nanoclay was at 10,000 m, which are 0.05×10^{-3} mm^3/Nm, 0.04×10^{-3} mm^3/Nm and 0.03×10^{-3} mm^3/Nm, respectively. In this slurry test, advanced GFRP nanocomposite showed a better performance of wear resistance compared to nanomodified-polymer systems.

4 Conclusion

The specific wear rate of nanocomposite system and advanced GFRP system was successfully determined using dry sliding and slurry tests. It can be concluded that the addition of nanoclay can reduce the specific wear rate of the polymer. For dry sliding test, the addition of nanoclay in epoxy polymer up to 3 wt% enhanced the wear properties of polymer nanocomposite and advanced GFRP composite. Further addition of nanoclay to 5 wt% reduced the wear properties of the system due to the agglomeration of nanoclay particle in the system that caused easier surface removal. It is suggested that, the addition of nanoclay in epoxy polymer provides good thermal stability of the polymer system which causes less surface removal on samples. For slurry test, the addition of nanoclay into epoxy polymer up to 5 wt% is the ideal case to enhance wear properties of both polymer nanocomposite system and advanced GFRP composite. Based on the results obtained, nanoclay filled polymer and fibre composites are very promising materials to be used in various applications, especially surface coatings, structural adhesives, encapsulation and engineering structures, due to their improved wear properties.

References

Abdul, A., Yop, K., Jin, S., Hui, D.: Epoxy clay nanocomposites—processing, properties and applications: a review. Compos. Part B **45**, 308–320 (2013)

Ahmad, K.Z.K., Ahmad, S.H., Tarawneh, M.A., Apte, P.R.: Evaluation of mechanical properties of Epoxy/Nanoclay/Multi-walled carbon nanotube nanocomposites using Taguchi method. Proc. Chem. **4**, 80–86 (2012)

Amir, W.W., Jumahat, A., Mahmud, J.: Effect of nanoclay content on flexural properties of glass fiber reinforced polymer (GFRP) composite. J. Teknol. **76**, 31–35 (2015)

Callister, W.D.J., Rethwisch, D.G.: Materials Science and Engineering: An Introduction, 9th edn. Wiley (2014)

Campo, M., Jimenez-Suarez, A., Ureña, A.: Effect of type, percentage and dispersion method of multi-walled carbon nanotubes on tribological properties of epoxy composites. Wear **324–325**, 100–108 (2015)

Collister, J.: Commercialization of polymer nanocomposites. In: Krishnamoorti, R., Vaia, R.A. (eds.) Polymer Nanocomposites: Synthesis, Characterization, and Modeling, pp. 7–14. American Chemical Society, Washington, DC (2001)

Chang, L., Friedrich, K.: Enhancement effect of nanoparticles on the sliding wear of short fiber-reinforced polymer composites: a critical discussion of wear mechanisms. Tribol. Int. **43**, 2355–2364 (2010)

Chang, L., Zhang, Z., Breidt, C., Friedrich, K.: Tribological properties of epoxy nanocomposites I. Enhancement of the wear resistance by nano-TiO_2 particles. Wear **258**, 141–148 (2005)

Dorigato, A., Morandi, S., Pegoretti, A.: Effect of nanoclay addition on the fiber/matrix adhesion in epoxy/glass composites. J. Compos. Mater. (2015)

Esteves, M., Ramalho, A., Ferreira, J.A.M., Nobre, J.P.: Tribological and mechanical behaviour of epoxy/nanoclay composites. Tribol. Lett. **52**, 1–10 (2013)

Jawahar, P., Gnanamoorthy, R., Balasubramanian, M.: Tribological behaviour of clay—thermoset polyester nanocomposites. Wear **261**, 835–840 (2006)

Jumahat, A., Soutis, C., Ahmad, N., Wan Mohamed, W.M.: Fracture toughness of nanomodified-epoxy systems. Appl. Mech. Mater. **393**, 206–211 (2013)

Jumahat, A., Soutis, C., Jones, F.R., Hodzic, A.: Compressive behaviour of nanoclay modified aerospace grade epoxy polymer. Plast. Rubber Compos. **41**, 225–232 (2012)

Kanny, K., Mohan, T.P.: Resin infusion analysis of nanoclay filled glass fiber laminates. Compos. Part B **58**, 328–334 (2014)

Koo, J.H.: Polymer Nanocomposites. McGraw-Hill (2006)

Kurahatti, R.V., Surendranathan, A.O., Ramesh Kumar, A.V., Wadageri, C.S.: Dry sliding wear behaviour of epoxyreinforced with nanoZrO$_2$ particles. Proc. Mater. Sci. **5**, 274–280 (2014)

Lam, C.K., Cheung, H.Y., Lau, K.T., et al.: Cluster size effect in hardness of nanoclay/epoxy composites. Compos. Part B **36**, 263–269 (2005)

Lam, C.K., Lau, K.T.: Tribological behavior of nanoclay/epoxy composites. Mater. Lett. **61**, 3863–3866 (2007)

Mirmohseni, A., Zavareh, S.: Preparation and characterization of an epoxy nanocomposite toughened by a combination of thermoplastic, layered and particulate nano-fillers. Mater. Des. **31**, 2699–2706 (2010)

Peng, Q.Y., Cong, P.H., Liu, X.J., et al.: The preparation of PVDF/clay nanocomposites and the investigation of their tribological properties. Wear **266**, 713–720 (2009)

Rashmi, Renukappa N.M., Suresha, B., et al.: Dry sliding wear behaviour of organo-modified montmorillonite filled epoxy nanocomposites using Taguchi's techniques. Mater. Des. **32**, 4528–4536 (2011)

Sapiai, N., Jumahat, A., Mahmud, J.: Flexural and tensile properties of kenaf/glass fibres hybrid composites filled with carbon nanotubes. J. Teknol. **76**, 115–120 (2015a)

Sapiai, N., Jumahat, A., Manap, N., Usoff, M.A.I.: Effect of nanofillers dispersion on mechanical properties of clay/epoxy and silica/epoxy nanocomposites. J. Teknol. **76**, 103–109 (2015b)

Suresha, B., Ravishankar, B., Sukanya, L.: Dynamic mechanical analysis and three-body abrasive wear behavior of epoxy nanocomposites. J. Reinf. Plast. Compos. **00**, 1–11 (2012)

Suresha, B., Shiva Kumar, K., Seetharamu, S., Sampath Kumaran, P.: Friction and dry sliding wear behavior of carbon and glass fabric reinforced vinyl ester composites. Tribol. Int. **43**, 602–609 (2010)

Zhang, J., Chang, L., Deng, S., et al.: Some insights into effects of nanoparticles on sliding wear performance of epoxy nanocomposites. Wear **304**, 138–143 (2013)

Žukas, T., Jankauskaitė, V., Žukienė, K., Baltušnikas, A.: The influence of nanofillers on the mechanical properties of carbon fibre reinforced methyl methacrylate composite. Mater. Sci. **18**, 250–255 (2012)

Zulfli, N.H.M., Abu Bakar, A., Chow, W.S.: Mechanical and thermal behaviors of glass fiber reinforced epoxy hybrid composites containing organo-montmorillonite clay. Malays. Polym. J. **7**, 8–15 (2012)

Synthesis of Natural Rubber/Palygorskite Nanocomposites via Silylation and Cation Exchange

N.A. Mohd Nor, S.N.A. Muttalib and N. Othman

Abstract This aim of this work is to study the synthesis of the natural rubber (NR)/palygorskite (PAL) nancomposites through silylation and cation exchange method. The properties of the vulcanizates are observed to investigate how different surface modification affects the properties of the nanocomposites. The results for curing characteristics, tensile properties, tear strength, hardness, crosslink density, rubber-filler interaction, fourier transform infrared spectroscopy (FTIR), x-ray diffraction analysis (XRD), scanning electron microscopy (SEM), transmission electron spectroscopy (TEM) and dynamic mechanical analysis (DMA) are discussed. It is found that the NR/PAL nanocomposites have improved properties compared to NR. NR/PAL using silylation method shows higher tensile strength, elongation at break and tear strength than NR/PAL using cation exchange method whereas NR/PAL using cation exchange method has higher modulus, hardness, crosslink density and lower rubber—filler interaction. The results are supported by SEM and TEM images. FTIR result shows new peaks signify the surface modification occurred. XRD pattern indicates that the modified PAL intercalates in the rubber matrix and the T_g values of NR/PAL nanocomposites decreased as a function of temperature.

Keywords Silylation · Cation exchange · Palygorskite · Natural rubber

1 Introduction

In the past few years, the use of clay incorporated with rubber (NR) has been widely studied due to the nanoparticles structure exhibit which can provide the reinforcement when rubber/clay nanocomposites formed (He et al. 2014; Yan et al.

N.A. Mohd Nor · S.N.A. Muttalib · N. Othman (✉)
School of Materials and Mineral Resources Engineering, Engineering Campus,
Universiti Sains Malaysia, Seri Ampangan, 14300 Nibongtebal, Pulau Pinang, Malaysia
e-mail: srnadras@usm.my

2004). Rubber clay nanocomposites have attracted more attention due to the excellent properties present in the system such as an improvement in the physical-mechanical properties, thermal stability, gas permeability and flammability compared to the unfilled rubber compounds (Das et al. 2014; Ali et al. 2013; Wang et al. 2013; Wang and Chen 2013; Jacob et al. 2007; Rajasekar et al. 2009). The major advantages of the nanocomposites system are the filler properties which are low cost and lighter weight (Sengupta et al. 2007).

The formation of rubber clay nanocomposites could be prepared using several methods like melt intercalation (Ren et al. 2005; Barick and Tripathy 2010; Azline et al. 2012; Irfan Fathurrohman et al. 2015; Shen et al. 2002), insitu polymerization (Gong et al. 2005; Ahmad et al. 2011; Tan et al. 2012; Sinha and Okamoto 2003) solution intercalation (Sinha and Okamoto 2003; Vijayalekshmi 2009; Shen et al. 2002; Paul et al. 2013) and latex compounding method (Jinghua et al. 2012; Anoop et al. 2010; Varghese and Karger-Kocsis 2003). Out of the four techniques, combination of melt mixing and latex compounding method have been widely used. This is because, melt mixing is environmentally friendly where no presence of the organic solvent is found in the system. It is also the popular method to choose by current industry because of the direct technique and its compatibility with current system such as extrusion and injection moulding (Jinghua et al. 2012). The latex compounding method was chosen because of many researchers were convinced that this technique can homogeneously disperse clay in the polymer matrix at the nano level (Wu et al. 2003; Wang et al. 2005). Well dispersion of clay in the polymer matrix is compulsory in order to increase the properties of the system. According to Jinghua et al. (2012), the basic idea of the latex compounding method is to increase the clay interlayer spacing during the first stage of the process. In the first stage, the polymerization of monomers or the dispersion of the clay in water was occurring. After that, the matrix will intercalates in this widened clay spacing.

However, the dispersion of fillers at nano level has a strong tendency to form agglomeration. Therefore, the surface adhesion and compatibility between filler and matrix need to be increased. In this study, two methods were used to overcome this problem. First, by using a silane coupling agent and second by using cation exchange method. Silanization is a process to modify clay mineral fillers and to induce a strong polymer-filler interaction. The importance of this process is to introduce a reaction of the surface of hydroxyl groups of the mineral with silane-coupling agents. On the surface of a PAL single crystal structure, there are abundant −OH groups, which are complimentary to form a reaction with silane coupling agent (Duan et al. 2011). He et al. (2014) studied the effect of silane coupling agent on the structure and mechanical properties of nano-dispersed clay filled styrene butadiene rubber. In their study, Bis [3−(triethoxysilyl) propyl] tetrasulfide silane was used and the results showed an improvement occurred in the dispersion of nanoclay in the SBR matrix, which proven by TEM and XRD. The interfacial interaction, processability of the nanocomposites and crosslink density of the clay filled SBR had also increased although some step of their study was time

consuming. The study on the nano-attapulgite functionalization by a silane modification for preparation of covalently-integrated epoxy/trimethylol-1,1,1-propane trimethacrylate (TMPTMA) nanocomposites was reported by Duan et al. (2011). The mechanism of their study could be basically described in the two steps. First, the −Si−OCH$_3$ groups in the silane structure were hydrolyzed by water into −Si −OH groups and second, the condensing reaction occured between the −Si−OH groups of silane and −OH groups of the PAL surface. This reaction indicated the grafting process of silane into the surface of PAL. The results of their study showed the uniform dispersion of PAL in the matrix and was proven by TEM and SEM. The glass transition temperature, mechanical properties and thermal stability of the nanocomposites of PAL modified by silane coupling agent had increased. However, higher filler loading was used in order to get these results.

Cation exchange method is the process of ion exchange between PAL and alkyl-ammonium ions. Alkyl ammonium surfactants are generally used as an organic surfactants. Usually the ion exchange reaction is affected by the length of alkyl chain and the number of alkyl tails on the surfactant molecules. The reaction between PAL and alkyl ammonium ion will modify the surface properties by ionically bound organic monolayer (Olalekan et al. 2004). The reason for choosing cations instead of anion in this ion exchange method is because cations are not strongly bound to the clay surface, so, small molecules cations can replace the cations present in the clay. By exchanging ions present in between layers with organic cations, PAL clay can be compatibilized with a wide variety of polymer matrix. In the meantime, this process enables the clay platelets to be separated so that they can be more easily intercalated and exfoliated. Ion exchange reactions depend on the type of organic surfactant and the cation exchange capacity (CEC) of the clay. The CEC of clay is very important factor for producing nanocomposite as it determines the amount of surfactants required for intercalation between the silicate layers to occur (Sinha and Okamoto 2003). There are various modifiers and different processes that have been used by researchers in the production of organoclay using ion exchange process. Olalekan et al. (2004) used octadecylamine, dodecylamine and cetyltrimethylammonium bromide in clay modification and the result showed that octadecylamine has better surface properties after modification. Zaharri et al. (2013) also used octadecylamine to their study on mechanical, thermal and morphological properties of ethylene vinyl acetate (EVA)/ zeolite composite.

In general, the aim of this study is to investigate the effect of two different types of surface modifications namely silylation and cation exchange methods on the curing characteristics, mechanical, physical, thermal and morphological properties of palygorskite (PAL) filled natural rubber (NR) nanocomposites. In order to achieve the objectives of this study, the composites undergo curing, tensile, hardness, swelling, rubber-filler interaction, x-ray diffraction (XRD), fourier transform infrared spectroscopy (FTIR), dynamic mechanical analysis (DMA), scanning electron microscopy (SEM) and transmission electron microscopy (TEM) testings. The result of the testing will be discussed in detail later in the next section.

2 Experimental

2.1 Materials

Natural rubber (SMR 20), which acts as a matrix and HA latex with 60 % of total solid content were purchased from Zarm and Chemical Supplier Sdn Bhd. The materials used for clay dispersion, such as palygorskite (PAL), anchoid, potassium hydroxide (KOH), and calcium chloride (CaCl) were supplied by Sigma Aldrich (M) Sdn Bhd. The materials used for silylation method such as Bis [3-(triethoxysilyl) propyl] Tetrasulfide-silane (TESPT), ethanol and Octadecylamine (OCT) were also purchased from Sigma Aldrich (M) Sdn Bhd. In addition, the materials such as sulfur, zinc oxide (ZnO), stearic acid, tetramethyl thiuram disulfide (TMTD), zinc diethyldithiocarbamate (ZDEC), and 2,2′-Methylenebis (6-tert-butyl-4-methylphenol) (BKF), which were used in the rubber compounding method were also provided by Zarm and Chemical Supplier Sdn Bhd.

2.2 Clay Treatment and Sample Preparation

2.2.1 Treatment of Clay

Silylation Method

Silane coupling agent was used for surface modification treatment of palygorskite. The TESPT coupling agent was hydrolyzed in the mixture of diluent/water (90/10 % vol) by stirrer at the room temperature. Then, the palygorskite was added and treated with hydrolyzed solutions. The mixture of these combinations was stirred for 30 min in the water bath at 50 °C. Next, the treated palygorskite was washed with ethanol and dried in the oven at 120 °C. The weight before and after entering the oven was taken. Finally, the dried attapulgite was placed in the dessicator to prevent water molecules absorption.

Cation Exchange Method

1000 ml of distilled water was measured into 2 litre capacity beaker, heated and maintained at a temperature of 80 °C in a water bath. 20 g of PAL was measured into the hot water and allowed to disperse under mixer rotating at 300 rpm for 1 h. A solution containing 7.5 g OCT with 4.2 ml of concentrated hydrochloric acid (HCl) in 500 ml hot distilled water maintained at 80 °C was subsequently added into the mixture and allowed to mix for another 1 h with the speed adjusted to 400 rpm. After that, the solid was filtered and washed severally with 1000 ml hot distilled water using vacuum filtration apparatus. The organoclay produced was

dried in an oven maintained at 60 °C for 36 h. The procedure was repeated for the remaining alkyl-ammonium salts (Olalekan et al. 2004).

2.2.2 Clay Dispersion Preparation

Palygorkite (PAL) dispersion was prepared by dispersing PAL with water, anchoid and KOH as shown in Table 1. The mixing time of PAL dispersion with silylation method (NR/PAL-SM) and cation exchange (NR/PAL-CE) was 1 h and 2 h, respectively. Then, the PAL dispersion had gone through sonication using Q Sonica Sonicators for SM (Nor et al. 2015a, b). Whereby for CE, the PAL dispersion was mixed using ball milling with ball to weight ratio (BPR) of 5:1 using ceramic ball (Muttalib and Othman 2015). This parameters is referred to our previous study. Time taken for NR/PAL-SM and NR/PAL-CE mixing in this process was 30 min and 48 h, respectively. The sonication and ball milling process were used to produce a good dispersion of PAL in the NR matrix in the next process. Before this study was carried out, the effect of PAL loading on the NR/PAL nanocomposites was performed to determine the optimum loading of PAL for both technique. The results displayed that optimum PAL loading for sonication process was 4 phr and for ball milling mixing was 6 phr.

Next, the PAL dispersion was mixed together with high ammonia (HA) latex for another 15 min for latex compounding process. Then, the PAL masterbatch was co-coagulated by calcium chloride solution and washed several times with water until it reach the pH 7. Finally, the masterbatch was dried in the oven at 100 °C for 2 h until the weight was constant. The same process was carried out for both methods.

2.2.3 Rubber Compounding Preparation

Rubber compounds were prepared using a laboratory, two-roll mill machine at 70 °C. Before the mixing process occur, the cleaning process of two roll mill must be done by using rubber cleaning materials. This is the important part to remove contaminants that remaining in the two roll mill which might affect the final properties of this compound. The temperature of the two roll mill was controlled by the flow of water

Table 1 Formulation of palygorskite dispersion

Materials	Part per hundred (phr)—silylated method	Part per hundred (phr)—cation exchange method
Palygorskite clay	4	6
10 % KOH	3	3
Anchoid	5	5
Water	88	86

Table 2 Formulation of rubber compounding

Materials	phr
Natural rubber, NR (SMR 20)	100
Zinc oxide (ZnO)	5
Stearic acid	2
BKF	2
ZDEC	0.5
TMTD	1
Sulphur	2.5

through a pipe into the machine. Both method, NR/PAL-SM and NR/PAL-CE were prepared using the same method and step to produce the sample. NR, PAL masterbatch and rubber compounding ingredient were mixed by following these steps; NR, masterbatch, activator (ZnO and stearic acid), antioxidant, accelerator and finally sulphur. The formula of these steps was tabulated in Table 2.

The control sample, NR was also prepared by using two roll mill machine. No filler was added in the control sample. The sequence of adding ingredient in this sample was similar to masterbatch sample but no PAL masterbatch was added. This sample was used to compare the properties between NR/PAL-SM and NR/PAL-CE. In this work, NR/PAL nanocomposites were cured with conventional (CV) curing systems. 25 to 30 min was needed in order to complete this process. Nip gap, time of mixing and the sequence of adding ingredients were kept constant for all formulations. The sheets of rubber compound were kept in a closed container before curing by Monsanto Moving die (MDR 2000) at 160 °C.

2.2.4   Vulcanization Process

The vulcanization process was done by using hot press machine. The temperature used was 160 °C which was similar to cure characteristics temperature. The rubber compounds was vulcanize from their respective t_{90} value into a flatter sheet mould with 2.0 mm thickness. The bumping is needed before the mould is close during moulding. The purpose of bumping is to remove the trapped air during compression. This step is important to avoid the air bubble on the compounds surface that can affect their properties.

2.2.5   Testing

Curing Characteristics

The cure characteristics of the NR/PAL nanocomposites for both method were acquired by using a Monsanto Moving Die Rheometer (MDR 2000). The test was used to determine minimum torque (M_L), maximum torque (M_H), torque difference,

scorch time (t_{s2}) and curing time (t_{90}) according to ASTM: D2084. The cure rate index was calculated as follows:

$$CRI = \frac{100}{(t90 - ts2)}$$

Torque difference was calculated based on the equation below:

$$\Delta H \;=\; M_H - \; M_L(Nm)$$

Tensile Test

The test specimen of tensile properties, referred to tensile strength, elongation at break and tensile modulus at 100, 300 and 500 % elongation, for the NR/PAL nanocomposites were studied using Universal Tensile Machine, Instron 3366. Dumb-bell shape was cut out for this testing following ASTM D412 and the cross-head speed was set at 500 mm/min. The testing was conducted at room temperature. Five samples were tested and average value was calculated for tensile properties.

Tear Test

The tear test was conducted using Universal Tensile Machine Instron 2266 according to the ASTM D624. The cross-head speed was set at 50 mm/min and trousers shape was cut out from the sample plate. Five samples were tested and average value were recorded and calculated in order to get the tear strength results.

Hardness Test

The hardness test for NR/PAL nanocomposites was tested by following ASTM D2240 using a hardness durometer (Shore A).

Crosslink Density

The swelling test was conducted to determine the crosslink density of NR/PAL nanocomposites. The test was carried out for 72 h at a room temperature. Test specimens was weighed before and after immersed in toluene solution using a weighing machine in order to determine the mass change. Finally, the crosslink density was calculated through Flory-Rehner equation:

$$Mc = \frac{-\rho_p Vs Vr^{\frac{1}{3}}}{\ln(1 - Vr) + Vr + \chi Vr^2}$$

where Mc is the molecular weight between crosslinks, ρ_p is the density of rubber, Vs is the molar volume of solvent (toluene), Vr is the volume fraction of the swollen rubber, χ is the interaction parameter between the rubber and toluene.

$$Vr = \frac{\frac{Xr}{\rho_r}}{\frac{Xr}{\rho_r} + \frac{Xs}{\rho_s}}$$

where, Xr is the mass fraction of rubber, Xs is the mass fraction of solvent, ρs is the density of solvent and ρr is the density of rubber. The crosslinking density can be calculated from the equation:

$$v = \frac{1}{2Mc}$$

where, Mc is the molecular weight between crosslinks.

Rubber-Filler Interaction

The Lorenz and Park equation was used to study the rubber-filler interaction in the NR/PAL nanocomposites of sample NR/PAL-SM and NR/PAL-CE. The equation was shown below. The symbol f and g were referring to the filled and unfilled NR vulcanizes, respectively. The symbol Z, a and b are the ratio by weight of fillers to rubber hydrocarbon in NR/PAL nanocomposites, and a constants, respectively. The lower value of swelling ratio (Qf/Qg) indicates a better interaction between the filler and the rubber matrix. The equation to find the rubber-filler interaction as follow:

$$\frac{Qf}{Qg} = ae^{-z}$$

The weight of toluene uptake per gram of rubber material, Q, was determined according to the following equation:

$$Q = \frac{Swollen\,Weight - Dried\,Weight}{100\,\frac{Original\,Weight}{Formula\,Weight}}$$

Field Emission Scanning Electron Microscope (FESEM)

The morphology of tensile fractured surface of the NR/ATP nanocomposite samples were examined using Field Emission Scanning Electron Microscopy (FESEM)

using model Zeiss SUPRA 35VP. The sample's fracture ends were coated with a thin layer of gold-palladium by using an SEM sputter coater. This coating was used to prevent the occurrence of electrostatic charge and poor resolution during examination.

High Resolution Transmission Electron Microscope (HRTEM)

The dispersion morphology of PAL in the NR matrix was analysed using High-Resolution Transmission Electron Microscopy (HRTEM, 200 kV Technai G2 20 S-Twin, Fei). The test specimens were cut out into ultra-thin cross-sections with approximately 80 nm in thickness using a Leica Ultra cut UCT ultramicrotome, equipped with a diamond knife. The temperature of the samples was maintained at −50 °C using liquid nitrogen for sample preparation. Afterwards, the samples prepared were placed onto a copper grid for testing.

X-Ray Diffraction (XRD)

The XRD patterns of NR/PAL nanocomposites were analysed using a radiation of X'pert diffractometer with Cu-K, model Siemens D5000 (40 kV generator voltages and 30 mA). The NR/PAL nanocomposites samples were scanned in step mode by $2 °/\text{min}^{-1}$ scan rate in the range from 10 to 30°. The d-spacing of the layered particle was then calculated using Bragg's equation $n\lambda = 2d \sin \theta$, where $\lambda = 0.1541$ nm is the wavelength of the x-ray, d is the interlayer distance and θ is the angle of incident x-ray radiation.

Fourier Transform Infrared Spectroscopy (FTIR)

A study of NR/PAL nanocomposites by FTIR was applied in order to differentiate the changes between the PAL modified and unmodified. The blends of PAL powder with KBr powders were pressed into pellets by a hydraulic pressure machine. The pellets were measured using a Paragon 1000 (Perkin Elmer, USA) with the resolution of 2 cm^{-1}, and the spectra were recorded in $400{-}4000 \text{ cm}^{-1}$ region.

Dynamic Mechanical Analysis (DMA)

The dynamic mechanical analysis of NR/PAL nanocomposite was carried out in a dynamic mechanical analyser (Mettler Toledo: model DMA861^e). The testing operated in a large tension mode with forceamplitude of 1 N at a frequency of 1 Hz. The temperature ranged from −100 to 100 °C, with a heating rate of 3 °C/min. DMA was used to evaluate the storage modulus (E'), loss modulus (E") and damping factor (Tan δ) as a function of temperature.

3 Results and Discussions

3.1 *Fourier Transform Infrared Spectroscopy (FTIR)*

The FTIR spectra of different modified PAL are shown in Fig. 1. As clearly seen in Fig. 1, the spectra of PAL-SM and PAL-CE are very similar to the raw PAL, however some variances in both spectra can still be detected. In all samples, vibrations of a group with very strong bands coming from Si–O–Si bond was observed in the range of $900-1000$ cm^{-1} (Rath et al. 2012). According to Wang et al. (2011), the Si–O–Si group was also presence at 797 cm^{-1}. The presence of the zeolite water was detected by the formation of band at 1654 cm^{-1}. The characterisation peak of the PAL at the range of $3397-3615$ cm^{-1} represented the hydroxyl groups of coordinated water. There were four hydroxyl groups present in the PAL which were located at 3613, 3578, 3540 and 3419 cm^{-1} (Wang et al. 2011). Each band was associated to different characterisation of hydroxyl groups which were band at 3613 cm^{-1} and was related to the hydroxyl group that were connected with the magnesium. The symmetric and antisymmetric stretching modes of molecular water was located at the bands of 3578 and 3540 cm^{-1}. Both bands linked the molecular water with magnesium at the edges of the channels. The bands at 3419 cm^{-1} was related to the water hydroxyl stretching in the PAL structure.

Compared to the spectra of PAL, the new bands at the range of $2800-3000$ cm^{1} were slightly observed in the spectra of PAL-SM and clearly observed in the sample of PAL-CE. The spectra was developed due to the oscillation of C−H bond in the PAL after treatment (Jinghua et al. 2012). Meanwhile, the presence of bands at 1447 cm^{-1} in the PAL-SM spectra corresponds to the –CH$_2$– scissoring and −CH3− asymmetric bending deformation vibration of TESPT (Jinghua et al. 2012; Duan et al. 2011). The presents of bands at 2918 cm^{-1} and 2850 cm^{-1} in the sample containing octadecylamine are recognized (Arroyo et al. 2003a, b). The presence of both bands are due to the the C−H asymmetric and symmetric stretching vibrations of octadecylamine, respectively. Furthermore, they added that the band present at 1467 cm^{-1} corresponded to the ammonium salt where this salt had been

Fig. 1 The FTIR spectra of NR PAL nanocomposites
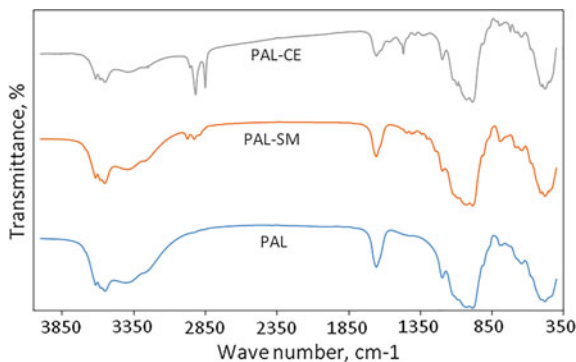
incorporated within the silicate layers. In addition, the presence of bands around 721 cm^{-1} was probably a silicon based ester such as R−OSi−O−(Olalekan et al. 2010).

3.2 X-Ray Diffraction (XRD)

The X-Ray diffractions patterns of NR, pure PAL, NR/PAL-SM and NR/PAL-CE from 10 to 30° are presented in Fig. 2a, b, c and d, respectively. The diffractions of Fig. 2a show that there was a broad peak presence in this sample. This is because NR is exhibit as amorphous structure where there is no crystalline peaks presence. The diffractions peaks at Fig. 2b of PAL were presence at $2\theta = 13.93^\circ$, 16.2°, and 19.70° which correspond to the primary diffraction of the (200), (040), and (400) planes of PAL, respectively while the diffraction peaks of SiO_2 at the same figure were presence at 20.90 and 26.67° (Wang et al. 2011; Wang and Sheng 2005; Lai et al. 2010).

However, after PAL underwent the treatment process, the crystal structure of PAL was destroyed. Only diffractions peaks at 19.70° was almost unchanged. This might be due to the diffraction peaks between $Mg_8Si_{12}O_{30}(OH)_4$ and PAL were overlapping in the nanocomposites (Wang and Chen 2013). They also added that the change in the crystal structure of PAL as well as the disappearance of PAL interlayer space happened in the nanocomposites. Chakraborty et al. (2010) and Kim et al. (2012) had reported that the unchanged of the peaks at sample treated by TESPT might be due to the formation of a conventional composite at microscopic level. The polymer will not intercalate into the silicate galleries after this formation. It was expected that there were silanol groups on the edges of the clay surfaces rather than the flat surfaces. The broad peaks were also present in the sample NR/PAL-SM. These peaks can be related to the nearly complete intercalation

Fig. 2 The X-Ray diffractions of a NR, b PAL, c NR/PAL-SM nanocomposites and d NR/PAL-CE nanocomposites
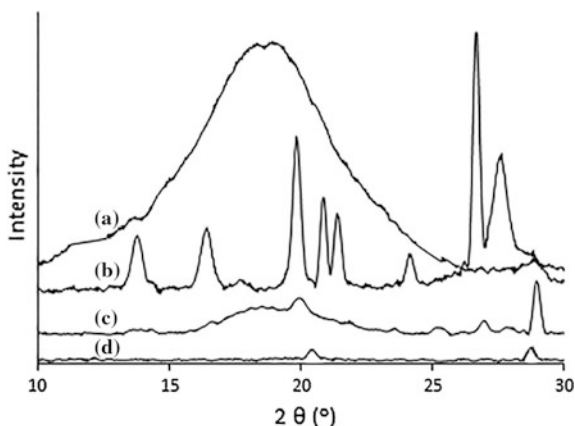
process of PAL in the NR matrix. These results also indicate that the distribution of PAL in NR/PAL-SM is better than NR/PAL-CE. These results can be correlated with the morphology properties in the next section.

3.3 Curing Characteristics

The vulcanization characteristics, expressed in terms of the minimum torque, M_L, maximum torque, M_H, torque difference, scorch time, ts_2, optimum cure time, t_{90}, and cure index, for NR and NR/PAL systems using different modification methods are reported in the Table 3. The minimum torque, M_L, is related to the viscosity of the NR nanocomposites before vulcanization. NR and NR/PAL-CE nanocomposite have similar values of M_L with 0.02, and NR/PAL-SM has lower torque value of 0.01 dNm. The lower minimum torque, M_L signifies that the viscosity is low, consequently, an improvement of material processability (Rooj et al. 2012).

For maximum torque, M_H, NR has the highest value with 7.29 dNm, followed by NR/PAL-CE and NR/PAL-SM with 6.87 and 5.23 dNm, respectively. NR has the highest value and NR/PAL-CE has higher M_H value than NR/PAL-SM. Generally, the M_H value for filled rubber is higher than unfilled rubber. However, in current study, the M_H value of NR/PAL nanocomposites is lower than NR gum. M_H values are obtained during rheometric study and depended on the degree of cross-linking. This is possibly due to clay minerals adsorbed curatives onto their surfaces and inhibited the curing process (Rooj et al. 2010). Hence, the decline in torque values could be associated to the intercalation of rubber chains into the interlayer space, which further prevented the formation of cross-links. This lowering of M_H is an indication of improved filler dispersion in the NR matrix (Rooj et al. 2010).

NR has the highest torque difference with 7.27 dNm, followed by NR/PAL-CE and then NR/PAL-SM, respectively. The ΔM value was the rough measurement of the crosslinking degree of rubber during vulcanization which could be used as an indirect indication of the crosslink density of the rubber compound (Wang and Chen 2013). As we compared both SM and CE nanocomposites, CE has higher ΔM value. This indicates that CE has higher crosslink density compared to CE and the theory is supported by crosslink density results later.

Table 3 Cure Characteristics for NR and NR/PAL nanocomposites

Cure characteristics	NR	NR/PAL-SM	NR/PAL-CE
Minimum torque (M_L) (dNm)	0.02	0.01	0.02
Maximum torque (M_H) (dNm)	7.29	5.23	6.87
Torque difference (ΔM) (dNm)	7.27	5.22	6.85
Scorch time (t_{s2}) (min)	1.19	1.38	1.04
Cure time (t_{90}) (min)	1.91	1.85	1.51
Cure index (min^{-1})	138.89	212.76	212.76

The scorch time, ts_2 of NR is 1.19 min. NR/PAL-SM has the highest ts_2 with 1.38 min while NR/PAL-CE has the lowest value, which is 1.04 min as compared to NR gum. The ts_2 of NR/PAL-SM is higher because of the high specific surface areas and the charges on the lattices. These two factors allowed PAL to easily adsorb the vulcanizing and curing agents (Wang and Chen 2013; Ismail and Ahmad 2014). NR/PAL-CE has shorter ts_2 value because more physical crosslink were formed between PAL and NR.

The cure time, t_{90} of NR/PAL nanocomposites are lower than NR. The t_{90} value of NR is 1.91 min. NR/PAL-CE has lower cure time compared to NR/PAL-SM which is 1.51 min and 1.85 min respectively. The value of t_{90} increases in NR/PAL-SM because silane prevents crosslinking reaction to occur (Rooj et al. 2010). The decrease in the cure time in NR/PAL-CE is possibly related to the interaction of the curing agents with PAL. On the other hand, a study has reported that the presence of ammonium groups of the organic cations intercalated into PAL and facilitates the curing reactions (Gu et al. 2009).

The cure indexes for NR/PAL nanocomposites are higher than NR. Both NR/PAL-SM and NR/PAL-CE have similar cure index value which is 212.76 min^{-1}, while the cure index for NR is 138.89 min^{-1}. The higher the value of cure index, the faster is the curing process. The curing rate was significantly increasing in the PAL filled NR nanocomposites as compared to NR gum without any fillers. This showed that the organoclay participated in the cure reaction and changed the curing rate by accelerating the curing process. The increasing cure rate is due to the availability of more thermal energy for the cure reaction (Choi et al. 2005).

3.4 Tensile Test

The stress-strain curve, tensile strength, elongation at break and tensile modulus of the pure NR, NR/PAL-SM and NR/PAL-CE are shown in Figs. 3, 4, 5 and 6 and Table 4, respectively. In the Fig. 3, it is observed that the ultimate strength and elongation at break of NR/PAL-SM is the highest compared to NR and NR/PAL-CE. The ultimate strength of sample NR/PAL-SM has increased by 17.16 % and the elongation at break has increased by 20.14 % compared to NR. It was discovered that the silane surface treatment of PAL has a significant effect on the strength of the NR/PAL-SM nanocomposites as can be seen clearly in Fig. 4. The interface interaction between the matrix macromolecular chains and the silicate layers of the clay had improved after going through silane surface treatment (He et al. 2014). The enhancement in the tensile strength and the elongation at break in the presence of silane also due to better filler dispersion in the nanocomposites (Manna et al. 1999). From this figure, it is also noted that sample NR/PAL-CE exhibits slightly higher at 500 % tensile modulus which is an increase of 4.52 % compared to NR. These results reveal that sample underwent cation exchange treatment can provide higher stiffness compared to sample that had undergone

Fig. 3 The stress-strain curves of NR/PAL nanocomposites

Fig. 4 The illustration of interface interaction between rubber and clay. The molecular structure of TESPT (He et al. 2014)

Fig. 5 The tensile strength of NR/PAL nanocomposites

Fig. 6 The elongation at break of NR/PAL nanocomposites
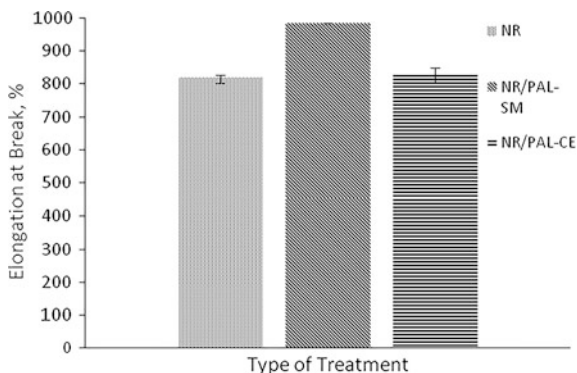
Table 4 The tensile modulus of NR/PAL nanocomposites

Properties	100 % tensile modulus, MPa	300 % tensile modulus, MPa	500 % tensile modulus, MPa
NR	0.88	2.33	5.08
NR/PAL-SM	0.83	2.23	4.45
NR/PAL-CE	0.99	2.45	5.31

silane surface treatment. Arroyo et al. (2003a, b) had reported similar results which the tensile modulus of sample containing organoclay with the presence of octadecylamine displayed higher stiffness compared to sample contain carbon black with similar filler loading (10 phr). Furthermore, the strain of NR/PAL-SM can go up to 1000. Meanwhile, the strain of NR/PAL-CE and NR is shown up to 800 only. This shows that the increase in the stiffness of NR/PAL-CE sample restricts the mobility of the chain in the nanocomposites. Thus, the strain of this sample is low compared to NR/PAL-SM. Meanwhile, sample that had undergone silane surface treatment exhibited the highest strain because of better filler dispersion and a strong rubber filler interaction between NR and PAL in NR/PAL-SM sample which had led to increase in strain.

The sample NR/PAL-SM displays the highest tensile strength and the highest percentage of elongation at break. However, the value for tensile modulus of NR/PAL-SM is the lowest compared to the other two samples, NR and NR/PAL-SM. Compared to NR, the tensile properties for sample contain PAL shows higher value. This indicates that PAL acted as the reinforcing filler to the NR matrix. The increase in the tensile strength in the sample NR/PAL-SM owed to the increase in the interfacial interaction between filler and matrix after undergoing the treatment. Such improvement of tensile strength might be ascribed to the well dispersion of the filler in the NR matrix. This statement can be supported with the data taken from SEM micrograph that will be discussed later.

He et al. (2014) also described the same trend which showed an increase in tensile strength of their samples after undergoing filler treatment. They also reported that the higher strength would produce a rougher surface of the tensile fracture

sample. The highest tensile strength of sample NR/PAL-SM may contribute to the better dispersion states of fillers in the polymer matrix as compared to the dispersion of filler in sample NR/PAL-CE (Tian et al. 2005). The illustration of the interface interaction between rubber and clay layer and the molecular structure of TESPT are shown in Fig. 4.

TESPT is a bi-functional coupling agent. This coupling agent contains the silyloxy groups which will react with the active hydroxyls on the silicate layers of the clay to form the covalent connection (He et al. 2014). From this reaction, it will form strong interaction with clay. This result is contributed by the modification, which had modified the affinity between the inorganic particles and polymer matrix. Thus, it will lead to a better dispersion of modified PAL (Wang et al. 2013).

On the contrary, the lower tensile strength exhibits by NR/PAL-CE may be due to the primary ammonium ions, $R-NH^{3+}$ in octadecylamine surfactant. This ion can form hydrogen bond with the clay surface and the results will decrease the number of available surface areas for interacting with the NR molecules (Zhang and Loo 2008). Tian et al. (2005) also stated that the better dispersion of clay and strong interfacial adhesion are needed in order to increase the strength. If the dispersion of PAL is poor and the interfacial adhesion is weak, the chance of slippage to occur between the interfaces at high deformation is higher. This result may cause low stress of the nanocomposite at a definite strain.

Generally, about 20.14 % increment in elongation at break is shown by NR/PAL-SM, meanwhile a significant change is observed in sample NR/PAL-CE. The increase in elongation at break of NR/PAL-SM was caused by the higher polymer-filler interaction between the treated PAL and NR matrix. This statement is also supported with the findings from Shanmugharaj et al. (2007). They reported that the increasing in mechanical properties of the silanized carbon nanotube and NR vulcanizates might be due to the high interaction between polymer and matrix. The incorporation of silane on the surface of PAL gives rise to the formation of excess chemical crosslinks between the silane and NR. This result will restrict the polymer slippage with an increase in deformation of nanocomposites. In contrast, the lower amount of increment in the NR/PAL-CE might be due to the stiffness of the filler produced from the cation exchange treatment preventing the high elongation at break from occurring in the sample NR/PAL-CE. The non-homogenous dispersion of PAL in the NR matrix could be the reason for the low elongation at break. This statement supported by SEM data in next section. This type of dispersion will restrict the NR chain orientation. Thus, it leads to the decrease in elongation at break of the NR/PAL nacocomposite. However, as compared to NR, the elongation at break of NR/PAL-CE was slightly higher. This is because the large amount of long alkyl amine ions in the PAL treated with octadecylamine may act as plasticizers in NR nanocomposites. Thus it will facilitate the movement of NR molecules and increase the elasticity in the NR chains (Kim et al. 2007).

The sample NR/PAL-CE shows the highest tensile modulus at 100, 300 and 500 % compared to the other two samples. The tensile modulus results at various percentages can be correlated to crosslink density and hardness data. As can be observed clearly, the highest tensile modulus at 500 % for example, is achieved by

NR/PAL-CE > NR > NR/PAL-SM. The sample undergone this treatment tends to become stiff compared to sample NR/PAL-SM. The result is also supported by the cure characteristics in Table 3 and hardness results, where the maximum torque, M_H value was 6.87 dN m and the hardness value of this sample was 49.5, the highest among all the samples. The result from elongation at break also shows the elasticity of this sample decreases because of the stiffness of filler. This reveals that, the PAL that has undergone this treatment can provide higher stiffness to the sample. It also reveals that the compatibility between the PAL and NR in sample NR/PAL-CE was higher than other samples. Nayak et al. (2009) described that the enhancement in the modulus can be attributed to the resistance exerted by clay layers against the matrix deformation and the stretching resistances of polymer chains with an extended conformation in the gallery. They also added that the insertion of silicate layers into the polymer chain will increase the surface interaction between clay and polymer matrix. Thus, it will increase the modulus of nanocomposites.

3.5 Crosslink Density

The crosslink density of pure NR and NR/PAL nanocomposites of sample NR/PAL-SM and NR/PAL-CE were calculated based on the nanocomposites swelling test. Figure 7 shows the crosslink density results of all samples in this study. The trend of this crosslink results are same as those of tensile modulus, where sample NR/PAL-CE shows the highest crosslink density. The result may be ascribed to the lower number of crosslink available for the chains. The highest crosslink density of the sample NR/PAL-CE was due to the cation exchange treatment on the filler, which work as the crosslinking agent. Therefore, it can enhance the modulus of the compounds. This observation also can be supported by the maximum torque value, M_H in the cure characteristics. Rooj et al. (2010) made an assumption that a rubber vulcanizate with a higher modulus has a higher

**Fig. 7** The crosslink density of NR/PAL nanocomposites
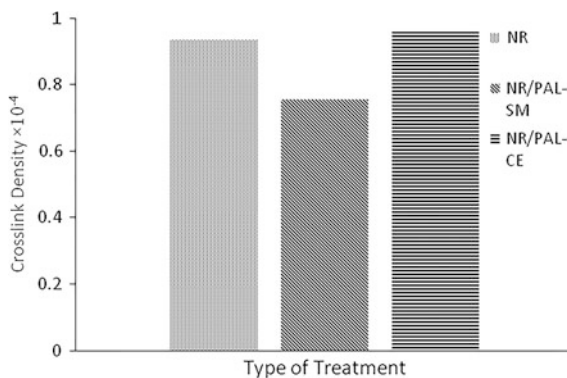
crosslink density than a rubber vulcanizate with lower crosslink density. They also added that the elongation at break decreases with the increasing crosslink density.

In contrast, sample NR/PAL-SM displayed the lowest crosslink density although the filler had undergone surface treatment. The clay undergone TESPT modification has lower crosslink density. This is because some of the methyl groups in natural rubber (NR) are used up by the reaction of tetra sulfide groups (TS) in TESPT modified clay, which has lessened the number of intermolecular crosslinking sites. Therefore, the enhancing in tensile properties of the nanocomposites merely comes from the interfacial interaction between TESPT modified clay and NR (Kim et al. 2012). It is also possibly due to the better dispersion and distribution of clay into polymer matrix, which delocalizes the stress successfully during tensile testing. The lower crosslinking density for NR/PAL-SM also may be due to the lower number of sites for sulfur crosslinks available on NR chains which it reflects this results as compared to NR/PAL-CE.

3.6 Tear Test

Tear strength of nanocomposites is usually present the same trend as tensile strength. Figure 8 shows the tear strength of the pure NR, NR/PAL-SM and NR/PAL-CE sample. Apparently, there is an insignificant result shown by all the three samples. The factors that influenced the tear strength is the same as factors affecting the tensile strength, which are the particle size and the surface area of the filler (Da Costa et al. 2002). A good dispersion of the filler in the matrix will also contribute to the higher result of tear strength. The result of tear strength in the samples can be correlated to the tearing energy in the nanocomposite. The fine particle filler size of the PAL might represent as a barrier for crack propagation during the tearing process (Gatos et al. 2007). The large aspect ratio of PAL could also influence the tear strength because of its needle like structure. This statement was also reported by Wang et al. (2005). They stated that clay with large aspect

Fig. 8 The tear strength of the NR/PAL nanocomposites
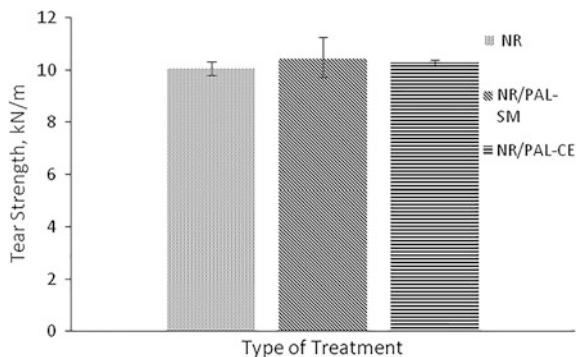
ratio will be more effective in limiting the rubber chain movement and in resisting the development of the crack in the nanocomposites compared to spherical structure.

3.7 Hardness Test

Hardness is one of a good indicator for reinforcement efficacy. Figure 9 shows result of Shore A hardness measurements for NR and NR/PAL composites of different PAL surface modification method. From Fig. 9, it can be seen that the hardness of NR/PAL-CE is higher than NR and NR/PAL-SM composite. This shows that NR/PAL-CE is stiffer than NR-PAL-SM and the treated PAL had acted as reinforcing filler in NR matrix. The hardness results correlate with the modulus results in the Table 4 and crosslink density in Fig. 7 where NR/PAL-CE has higher modulus and crosslink density than NR and NR/PAL-SM. High modulus and crosslink density means that the nanocomposite is stiffer due to interaction between PAL and NR matrix. Bindu sharmila et al. (2014) reported that hardness value represents the degree of compatibility and crosslink density. The enhancement in hardness by addition of PAL is potentially due to the increase confinement of NR in the composites because exfoliated/partially exfoliated NR/PAL nanocomposites restrict surface deformation.
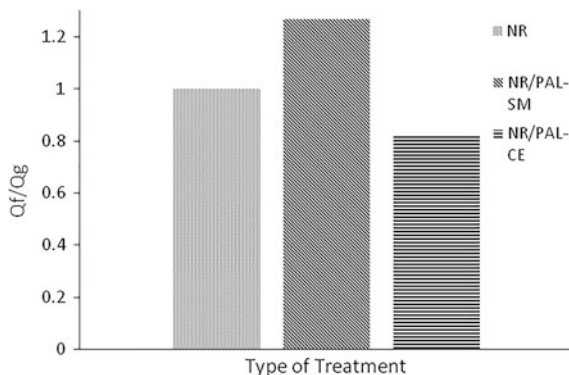
3.8 Rubber-Filler Interaction

The rubber-filler interaction of NR and NR/PAL nanocomposites of different PAL surface modification method are presented in Fig. 10. The data was calculated using Lorenz and Park's equation. It can be seen that the Q_f/Q_g ratio for NR/PAL-CE is lower than NR and NR/PAL-SM. The Q_f/Q_g ratio represents the degree of


Fig. 9 The hardness of NR/PAL nanocomposite
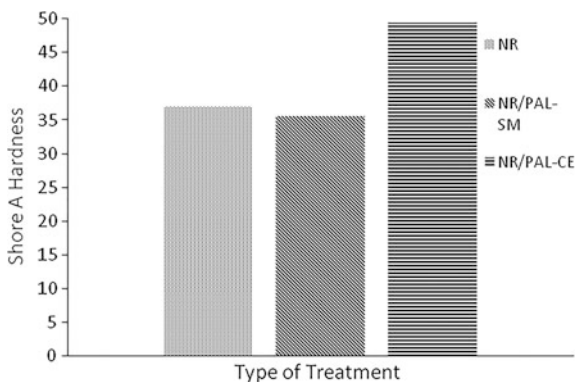
restriction of the rubber matrix swelling due to the interaction of the NR with PAL. Lower Q_f/Q_g values indicate a greater extent of rubber-filler interaction (Ooi et al. 2013). Therefore, according to the results shown in Fig. 10, NR/PAL-CE has stronger rubber-filler interaction compared to NR and NR/PAL-SM. High Q_f/Q_g value for NR/PAL-SM indicates that the toluene uptake is increased and the rubber-filler interaction is poorer than NR/PAL-CE composite. Higher degree of cross-linking should be able to reduce the rubber-filler interaction and lower the toluene uptake. However, the cross-link chain inside the NR/PAL-SM composites was unable to resist the expansion force in order to avoid swelling. This is because the latex added in the masterbatch method help to improve the dispersion of PAL in the rubber matrix but the interaction between the filler and the rubber matrix did not occur which led to the production of less crosslinks. Rubber-filler interaction is correlated with the degree of crosslinking, where high degree of crosslink will reduce the rubber-filler interaction (Jordan et al. 2005). This result supports the crosslink density result in the Fig. 7 where NR/PAL-CE has the highest crosslink density yet the lowest rubber-filler interaction value.

3.9 *Field Emission Scanning Electron Microscope (FESEM)*

SEM micrographs of PAL, NR and NR/PAL nanocomposites are shown in Fig. 11. Figure 11a shows the micrograph of palyorskite at 10 K X magnification. The micrograph indicates that palygorskite has around 1.399 µm and appearing in a needle-like structure. Normally clay was found with sphere particulate shape. However some of the clay have different shape of particle other than sphere, such as fibrous or needle like structure. Apart from being needle-like structure, palygorskite also exists in layers that stack together and is called layered silicates which can be observed clearly using TEM micrograph. To have better performance, palygorskite
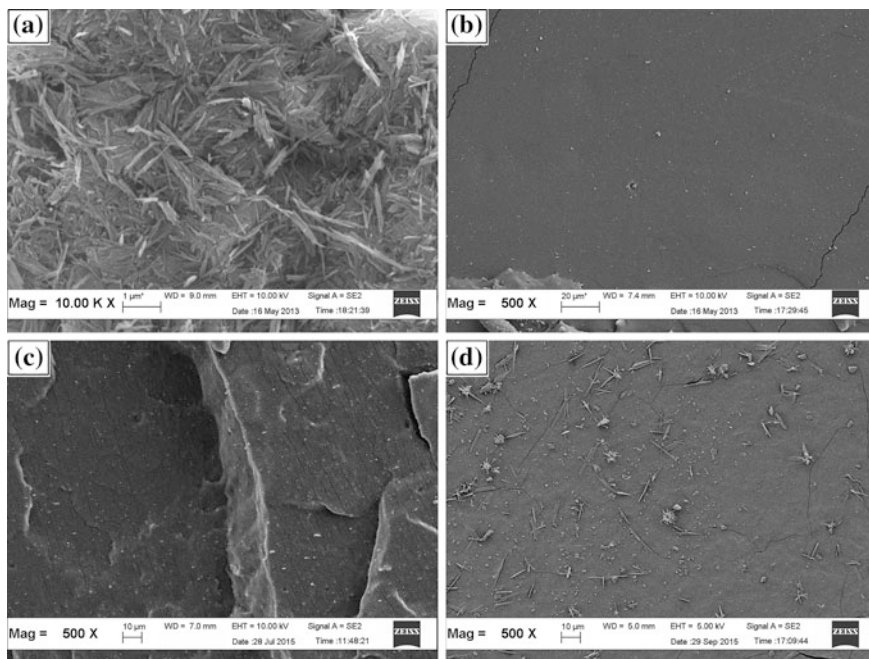
Fig. 11 SEM micrographs of **a** PAL, **b** NR, **c** NR/PAL-SM nanocomposites, and **d** NR/PAL-CE nanocomposites

needs to be dispersed in order to delaminate the stacked layers into discrete single or thinner layers.

Figure 11b shows the morphology of the natural rubber gum at 500X magnification. The SEM micrograph of NR gum has a smooth surface since there was no filler added. Smooth surface indicates that all materials are homogenously distributed in the matrices. However, the observation of SEM micrograph in Fig. 11b shows a smooth surface with small particles. The particles that are exhibited on the NR gum surface are believed to be the compounding ingredients used in rubber compounding.

Figure 11c and d are the SEM micrograph of NR/PAL-SM and NR/PAL-CE at 500X magnification respectively. It can be observed that the NR/PAL-SM micrograph exhibits rougher fracture surface consisting of tear paths compared to the NR/PAL-CE surface. There is no clear aggregate spotted on the surface indicating that the PAL silicate layers intercalated and dispersed in the NR matrix. Figure 11d micrograph shows that the palygorskite is dispersed in the NR matrix. But, still there are some aggregates can be seen on the surface. From the micrographs, it can be observed that the palygorskite which is in the needle-like structure stacks together. In comparison, Fig. 11c has smoother surface with no aggregates while Fig. 11d image consists of aggregates of PAL on the surface. This signifies that PAL treated with silylation method has better dispersion in NR matrix. SEM results

correlates with the tensile strength results shown in Fig. 3 where NR/PAL-SM nanocomposite has the highest strength compared to NR/PAL-CE and NR.

3.10 High Resolution Transmission Electron Microscope (HRTEM)

TEM micrographs provide other evidences to support the improvement of the dispersion of PAL particles in NR when they are modified (Fig. 12). The light phase in the TEM micrograph represents the NR matrix and the dark phase corresponds to the PAL particles. From Fig. 12a and c, it can be seen that the PAL particles disperse in the NR matrix. Figure 12b shows that the measured PAL
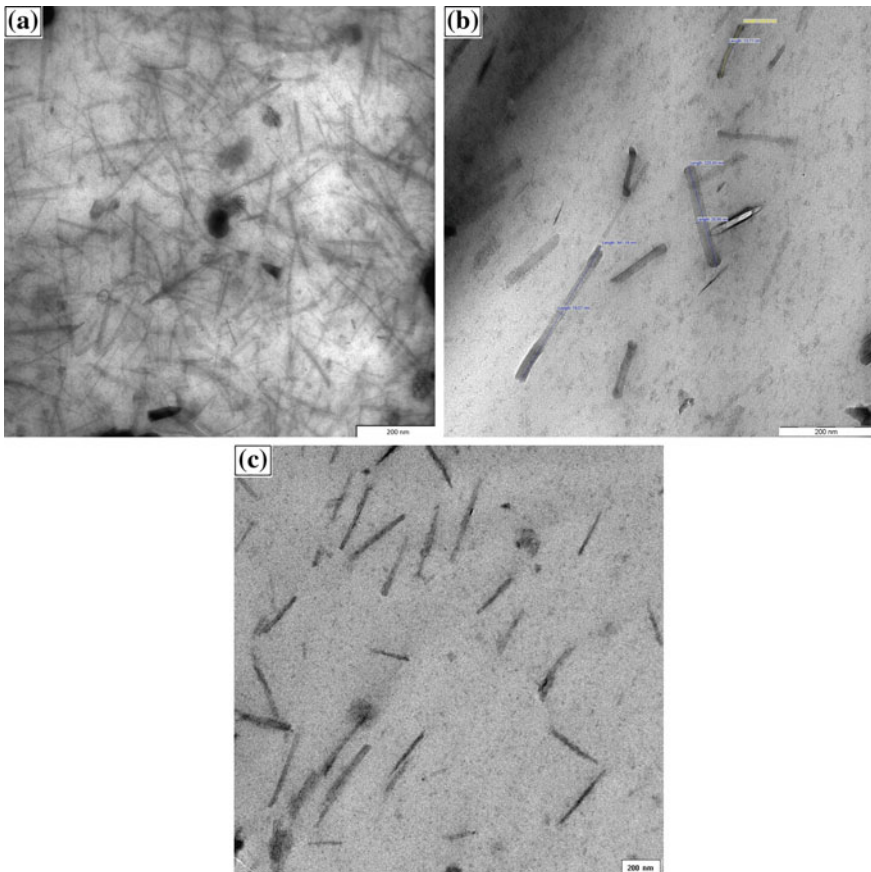
Fig. 12 TEM micrographs of **a** NR/PAL-CE nanocomposites, **b** measured NR/PAL-CE nanocomposites, and **c** NR/PAL-SM nanocomposites

particles. As mentioned in SEM discussion, it has been stated that the size of unmodified PAL particles is about 1399 nm or 1.399 μm. After modification, the size of the PAL particles in the composites shows reduction in size. The size of the modified PAL is in the range of 400−200 nm (Fig. 12b).

TEM characterization demonstrates that after modification, the size of PAL particles in NR matrix significantly decreases. Apart from that, the dispersion of PAL was improved and the interaction between rubber and PAL was enhanced. A better dispersion of PAL and the discrete single layers displayed in the Fig. 12b and c correlated with a good mechanical properties and a better performance of NR/PAL nanocomposites. According to Rath et al. (2012), PAL is categorized as a fibrillar silicate clay. This clay is much easier to separate into individual layers and can be uniformly distributed in polymer matrices because the spacing of single crystals is much larger and the interaction of van der Waals' force is considerably weaker than the silicate layers in montmorillonite. Thus, the dispersion of PAL was easy to disperse. The better dispersion of PAL in the NR/PAL-SM might due to the modifications of PAL occurred by silane coupling agent. In this process, the silane coupling agent coated on the surface of PAL which could reduce the surface free energy of PAL. These phenomena can improve the adhesion between PAL and matrix and it also help with separation of PAL layers (Gao et al. 2005). In addition, the surface –OH groups presence on the PAL was also modified by silane groups which it will increase the compatibility of clay with the rubber (Rath et al. 2012).

3.11   Dynamic Mechanical Analysis (DMA)

Dynamic mechanical analysis (DMA) is used to evaluate the viscoelastic properties of NR and NR/PAL nanocomposites. DMA is a reliable approach to illustrate the interaction between NR and PAL. Figure 13a, b, and c show the DMA test results of NR and NR/PAL nanocomposites including storage modulus (E'), loss modulus (E") and damping factor (tan δ) as a function of temperature.

The variation in storage modulus, E' with temperature of NR and NR/PAL nanocomposites is shown in Fig. 13a. The shape of curves show that the E' value decreases with the increasing temperature for all compounds. NR has higher storage modulus as compared to the NR/PAL nanocomposites. Meanwhile, the NR/PAL-CE has higher storage modulus than NR/PAL-SM nanocomposite. This shows that NR/PAL-CE has better thermo-mechanical stability of the material at higher temperature. Furthermore, the long alkyl chain in the ammonium salt, which modified the surface of PAL, increased the compatibility between NR and PAL and led to improved dispersion and interfacial interaction (Qiao et al. 2015). The results clearly show that PAL that is modified using cation exchange method gives higher stiffness compared to PAL treated by silylation method. The increase in stiffness of
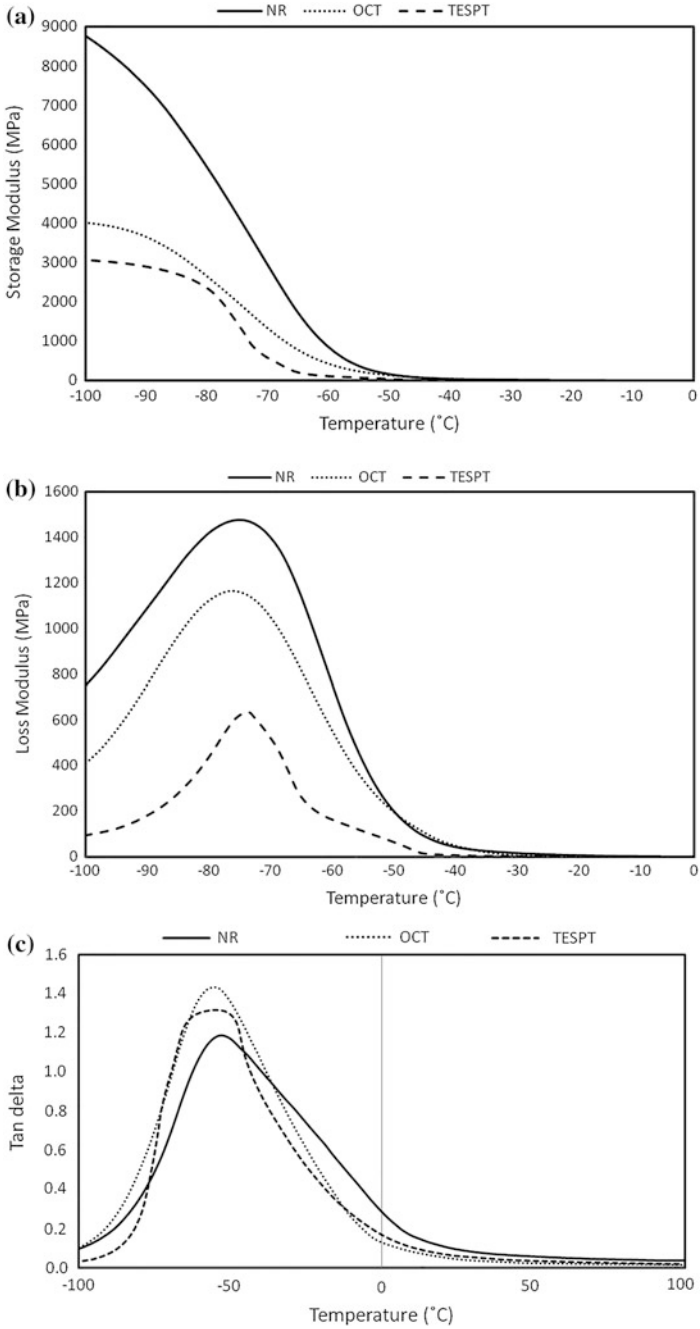
Fig. 13 **a** Storage modulus (E') versus temperature for NR and NR/PAL nanocomposites, **b** Loss modulus (E") versus temperature for NR and NR/PAL nanocomposites, and **c** Tan δ versus temperature for NR and NR/PAL nanocomposites

material indicates that a good reinforcing effect of the layered silicate. This result correlates with the hardness results in Fig. 6 where NR/PAL-CE shows the highest value of hardness.

The variation of loss modulus, E" with temperature of the NR gum sample and NR/PAL nanocomposites is displayed in Fig. 13b. E" is the viscous modulus of the polymeric material and is related to the ability of the material to dissipate energy as the function of temperature. E" is also associated with internal friction and is sensitive to different kinds of molecular motions, relaxation processes, transitions, morphology and other structural homogeneities. It can be seen that E" curve exhibits similar trend to E' curve. NR has higher loss modulus compared to NR/PAL nanocomposites and NR/PAL-CE has higher loss modulus than NR/PAL-SM. The increase in loss modulus as the result of filler addition can be explained in terms of friction between the PAL particles and NR molecules when the PAL particles are uniformly dispersed in the NR matrix. It has been noticed that NR/PAL-CE enhanced the loss modulus of the nanocomposites as compared to NR/PAL-SM. This indicates that PAL modified using cation exchange method has higher surface area per unit volume of layered silicates that resulting in higher friction between PAL and NR matrix.

The damping coefficient (tan δ) of pure NR and NR/PAL of different surface modification with temperature is recorded in Fig. 13c. Figure 13c shows NR exhibit a damping peak (tan δ = 1.19) at T_g = −52.6 °C. More significant changes occurred upon addition of PAL of different surface modification. NR/PAL-SM shows a peak of much increased intensity (tan δ = 1.31) at lower T_g of −56.6 °C. NR/PAL-CE shows the most intense peak (tan δ = 1.43) at T_g of −56.5 °C. The peak of the curve is regarded as the α transition corresponding to the T_g value of the compound. Most researchers reported the increase in T_g as fillers are added to the polymer due to good rubber-filler interaction (Rooj et al. 2012).

However, in this study, the T_g value of the composite decreased as PAL was added. The T_g value of NR/PAL nanocomposites have decreased about 4 °C. The value of tan δ at T_g is related to the volume of constrained NR within NR/PAL nanocomposites (Wilkinson et al. 2006). The constrained volume fraction of chain segments is due to either incorporation into crystallites or polymer-clay interaction. Thus, the value of tan δ at T_g is an indicator of the volume fraction of unconstrained, amorphous chain-segments within the materials. Similar argument has been made by Ash et al. (2002) as they found that the T_g value did not change with filler weight fraction less than 0.5 %, but above that, the T_g value dropped more than 20 °C. They stated that there are various reasons that lead to the reduction of T_g value. T_g value could decreased due to the changes in tacticity, molecular weight and retained monomer. In this study, the reduction of T_g is believed to occur due to solely the interaction of the polymer and palygorskite since the nanocomposite preparation does not alter either the tacticity or the molecular weight of the composites. Furthermore, aside of rubber-filler interaction, the crosslink density must also be considered when the precursors, like amine and stearic acid are presence on the surface of the clay mineral (Ivanoska-Dacikj et al. 2015). This is because they can affect the crosslink density and hence change the T_g compared to the NR gum.

4   Conclusion

This work studies the preparation and the characterization of the NR/PAL nan-composites through silylation and cation exchange method. The vulcanizates were subjected to curing characteristics, mechanical and morphological testing to inves-tigates how different surface modification affect the properties of the nanocompos-ites. From the results obtained, FTIR curves for treated PAL show new peaks signify that the surface modification occur in the PAL. NR/PAL-SM has higher tensile strength, elongation at break and tear strength compared to NR/PAL-CE. These results signify that NR/PAL-SM has better interfacial interaction. High tensile strength would produce rougher surface on the tensile fracture surface. From SEM images, it can be seen that NR/PAL-SM micrograph has rougher surface without PAL aggregates which supports the claim that NR/PAL-SM has better interfacial interaction than NR/PAL-CE. The X-Ray diffractions of NR/PAL–SM also showed the broad peak presence in this sample. It indicated that the intercalation of PAL in sample NR/PAL-SM is nearly complete. However, NR/PAL-CE has higher modulus than NR/PAL-SM indicating that it is stiffer. This statement is supported by maxi-mum torque and hardness test where the results obtained show that NR/PAL-CE has higher M_H value and hardness than NR/PAL-SM. Composites with high modulus will have higher crosslink density. Therefore, the crosslink density test shows that NR/PAL-CE has higher density which supports the statement. The crosslink density is related to rubber-filler interaction, where composite with high crosslink density will have lower rubber-filler interaction. It is shown that NR/PAL-CE has lower rubber-filler interaction than NR/PAL-SM and hence, again supports the previous statement. From DMA result, it is observed that NR/PAL nanocomposites have similar T_g value but the T_g is reduced as compared to NR and NR/PAL-CE higher storage and loss modulus than NR/PAL-SM.

References

Ahmad, M., Gharayebi, Y., Salit, M.S., Hussein, M.Z., Shameli, K.: Comparison of in situ polymerization and solution-dispersion techniques in the preparation of polyimide/montmorillonite (MMT) nanocomposites. Int. J. Mol. Sci. **12**, 6040–6050 (2011)
Ali, Z., El-N Emr, K., Youssef, H., Bekhit, M.: Mechanical and physicochemical properties of electron beam irradiated rubber/clay nanocomposites. Polym. Compos. 1600–1610 (2013)
Anoop, A.K., Sunil, J.T., Rosamma, A., Rani, J.: Natural rubber-carbon nanotube composite through latex compounding. Int. J. Polym. Mater. **59**, 33–44 (2010)
Arroyo, M., Lopez-Manchado, M.A., Herrero, B.: Preparation and characterization of organoclay nanocomposites based on natural rubber. Polym. Int. **52**, 1070–1077 (2003a)
Arroyo, M., Lopez-Manchado, M.A., Herrero, B.: Organo-montmorillonite as substitute of carbon black in natural rubber compounds. Polymer **4**, 2447–2453 (2003b)

Ash, B.J., Schadler, L.S., Siegel, R.W.: Glass transition behavior of alumina/polymethylmethacrylate nanocomposites. Mater. Lett. **55**, 83–87 (2002)

Barick, A.K., Tripathy, D.K.: Preparation and characterization of thermoplastic polyurethane/organoclay nanocomposites by melt intercalation technique: effect of nanoclay on morphology, mechanical, thermal, and rheological properties. J. Appl. Polym. Sci. **117**, 639–654 (2010)

Bindu Sharmila T.K., Ayswarya, E.P., Abraham, B.T., Sabura Begum, P.M., Thachil, E.T.: Fabrication of partially exfoliated and disorderd intercalated cloisite epoxy nanocomposites via in situ polymerization: mechanical, dynamic mechanical, thermal and barrier properties. Appl. Clay Sci. **102**, 220–230 (2014)

Chakraborty, S., Kar, S., Dasgupta, S., Mukhopadhyay, R., Bandyopadhyay, S., Joshi, M., Ameta, S.C.: Effect of treatment of bis(3-triethoxysilyl propyl)tetrasulfane on physical property of in situ sodium activated and organomodified bentonite clay—SBR rubber nanocomposite. J. Appl. Polym. Sci. **116**, 1660–1670 (2010)

Choi, D., Kader, M.A., Cho, B.-H., Huh, Y.-I., Nah, C.: Vulcanization kinetics of nitrile rubber/layered clay nanocomposites. J. Appl. Polym. Sci. 98 (2005)

Da Costa, H.M., Visconte, L.L.Y., Nunes, R.C.R., Furtado, C.R.G.: Mechanical and dynamic mechanical properties of rice husk ash-filled natural rubber compounds. J. Appl. Polym. Sci. **83**, 2331–2346 (2002)

Das, A.K., Suin, S., Shrivastava, N.K., Maiti, S., Mishra, J.K., Khatua, B.B.: Effect of nanoclay on the morphology and properties of acrylonitrile butadiene styrene toughened polyoxymethylene (Pom)/clay nanocomposites. Polym. Compos. 273–282 (2014)

Duan, J., Shao, S., Jiang, L., Li, Y., Jing, P., Liu, B.: Nano-attapulgite functionalization by silane modification for preparation of covalently-integrated epoxy/TMPTMA nanocomposites. Iran. Polym. J. **20**(11), 855–872 (2011)

Gao, X., Mao, L.X., Jin, R.G., Zhang, L.Q., Tian, M.: Preparation and characterization of polycarbonate/poly(propylene)/attpulgite ternary nanocomposites with morphology of encapsulation. Macromol. Mater. Eng. **290**, 899–905 (2005)

Gatos, K.G., Kameo, K., Karger-Kocsis, J.: On the friction and sliding wear of the rubber/layered silicate nanocomposites. Express Polym. Lett. **1**, 27–31 (2007)

Gong, F.L., Feng, M., Zhao, C.G., Zhang, S.M., Yang, M.S.: Particle configuration and mechanical properties of poly (vinyl chloride)/montmorillonite nanocomposites via in situ suspension polymerization. Polym. Testing **23**, 847–853 (2005)

Gu, Z., Song, G., Liu, W., Li, P., Gao, L., Li, H., Hu, X.: Preparation and properties of styrene butadiene rubber/natural rubber/organo-bentonite nanocomposites prepared from latex dispersions. Appl. Clay Sci. **46**, 241–244 (2009)

He, S., Xue, Y., Lin, J., Zhang, L., Du, X., Chen, L.: Effect of silane coupling agent on the structure and mechanical properties of nano-dispersed clay filled styrene butadiene rubber. Polym. Compos. (2014)

Ismail, H., Ahmad, H.S.: Effect of halloysite nanotubes on curing behavior, mechanical, and microstructural properties of acrylonitrile-butadiene rubber nanocomposites. J. Elastomer Plast. **46**(6), 483–498 (2014)

Irfan Fathurrohman, M., Soegijono, B., Budianto, E., Rohman, S., Ramadhan, A.: The effect of orga noclay on curing characteristic, mechanical properties, swelling and morphology of natural rubber/organoclay nanocomposites. Macromol. Symp. **353**, 62–69 (2015)

Ivanoska-Dacikj, A., Bogoeva-Gaceva, G., Rooj, S., Weibner, S., Heinrich, G.: Fine tuning of the dynamic mechanical properties of natural rubber/carbon nanotubes nanocomposites by organically modified montmorillonite: a first step in obtaining high-performance damping material suitable for seismic application. Appl. Clay Sci. **118**, 99–106 (2015)

Jacob, A., Philip, K.P., Aprem, A.S.: Cure characteristics and mechanical properties of natural rubber-layered clay nanocomposites. Int. J. Polym. Mater. Polym. Biomater. **56**, 593–604 (2007)

Jinghua, W., Xiaoping, L., Yuanfang, Demin, J.: Rubber/Clay nanocomposites by combined latex compounding and melt mixing: a masterbatch process. Mater. Des. **34**, 825−831 (2012)

Jordan, J., Jacob, K.I., Tannenbaum, R., Sharaf, M.A., Jasiuk, I.: experimental trends in polymer nanocomposites—a review. Mater. Sci. Eng. A **393**, 1–11 (2005)

Kim, E.S., Kim, E.J., Lee, T.H., Yoon, J.S.: Clay modification and its effect on the physical properties of silicone rubber/clay composites. J. Appl. Polym. Sci. **125**, E298–E304 (2012)

Kim, M.S., Kim, G.H., Chowdhury, S.R.: Polybutadiene rubber/organoclay nanocomposites: effect of organoclay with various modifier concentrations on the vulcanization behaviour and mechanical properties. Polym. Eng. and Sci. **47**, 308–313 (2007)

Lai, S., Yue, L., Zhao, X., Gao, L.: Preparation of silica powder with high whiteness from palygorskite. Appl. Clay Sci. **50**(3), 432–437 (2010)

Manna, A.K., Tripathy, D.K., De, P.P., De, S.K., Chatterjee, M.K., Peiffer, D.G.: Bonding between epoxidized natural rubber and clay in presence of silane coupling agent. J. Appl. Polym. Sci. **72**, 1895–1903 (1999)

Mohd Nor, N.A., Othman, N., Ismail, H.: Mechanical & morphological properties of attapulgite/nr composites: effect of mixing time variation. AIP Conf. Proc. **1669**, 020048 (2015a)

Mohd Nor, N.A., Othman, N.: Effect of filler loading on curing characteristic and tensile properties of palygorskite natural rubber nanocomposites. In: The 5th International Conference on Recent Advances in Materials, Minerals and Environment (RAMM) and 2nd International Postgraduate Conference on Materials, Mineral and Polymer (MAMIP) (2015b)

Muttalib, S.N.A., Othman, N.: Effect of ball milling parameters on properties of attapulgite filled natural rubber composite. In: The 5th International Conference on Recent Advances in Materials, Minerals and Environment (RAMM) and 2nd International Postgraduate Conference on Materials, Mineral and Polymer (MAMIP) 2015

Nayak, S.K., Mohanty, S., Samal, S.K.: Effect of clay types on the mechanical, dynamic mechanical and morphological properties of polypropylene nanocomposites. Polym.Plast. Technol. Eng. **48**, 976–988 (2009)

Azlina, H.N., Sahrim, H.A., Rozaidi, R.: Effect of nanoclay on the microstructure and the properties of thermoplastic natural rubber (TPNR)/OMMT nanocomposites. J. Thermoplast. Compos. Mater. **25**, 351–362 (2012)

Olalekan, S.T., Muyibi, S.A., Kazeem, S.K.: A comparative study on the effect of different alkylammonium. J. Sci. Innov. Dev. **1**(1), 1–11 (2004)

Olalekan, S.T., Qudsieh, I.Y., Kabbashi, N.A., Alkhatib, M., Muyibi, S.A., Yusof, F., Shah, Q.H.: Effect of modification on the physicochemical and thermal properties of organophilic clay modified with octadecylamine. Int. J. Eng. Technol. IJET-IJENS **10**(1), 23–3 (2010)

Ooi, Z.X., Ismail, H., Abu Bakar, A.: The effect of hydrochloric acid treatment on properties of oil palm ash-filled natural rubber composites. BioResources **8**(4), 5133–5144 (2013)

Paul, P.K., Hussain, S.A., Bhattacharjee, D., Pal, M.: Preparation of polystyrene-clay nanocomposite by solution intercalation technique. Bull. Mater. Sci. **36**(3), 361–366 (2013)

Qiao, H., Wang, R., Yao, H., Wu, X., Lei, W., Zhou, X., Zhang, L.: Design and preparation of natural layered silicate/bio-based elastomer nanocomposites with improved dispersion and interfacial interaction. Polymer **79**, 1–11 (2015)

Rajasekar, R., Pal, K., Heinrich, G., Das, A., Das, C.K.: Development of nitrile butadiene rubber-nanoclay composites with epoxidized natural rubber as compatibilizer. Mater. Des. **30**, 3839–3845 (2009)

Rath, J.P., Chaki, T.K., Khastgir, D.: Development of natural rubber-fibrous nano clay attapulgite composites: the effect of chemical treatment of filler on mechanical and dynamic mechanical properties of composites. Procedia Chemistry **4**, 131–137 (2012)

Ren, J., Huang, Y.X., Liu, Y., Tang, X.Z.: Preparation, characterization and properties of poly (vinyl chloride)/compatibilizer/organophilicmontmorillonite nanocomposites by melt intercalation. Polym. Testing **24**, 316–323 (2005)

Rooj, S., Das, A., Stockelhuber, K.W., Mukhopadhyay, N.A., Bhattacharyya, A.R., Jehnichen, D.: Pre-Intercalation of long chain fatty acid in the interlayer space of layered silicates and preparation of montmorillonite/natural rubber nanocomposites. Appl. Clay Sci. 50–56 (2012)

Rooj, S., Das, A., Thakur, V., Mahaling, R.N., Bhowmick, A.K., Heinrich, G.: Preparation and properties of natural nanocomposites based on natural rubber and naturally occurring halloysite nanotubes. Mater. Des. **31**, 2151–2156 (2010)

Sengupta, R., Chakraborty, S., Bandyopadhyay, S., Dasgupta, S., Mukhopadhyay, R., Auddy, K., Deuri, A.S.: A short review on rubber/clay nanocomposites with emphasis on mechanical properties. polymer engineering and science (2007)

Shanmugharaj, A.M., Bae, J.H., Lee, K.Y., Noh, W.H., Lee, S.H., Ryu, S.H.: Physical and chemical characteristics of multiwalled carbon nanotubes functionalized with aminosilane and its influence on the properties of natural rubber composites. Compos. Sci. Technol. **67**, 1813–1822 (2007)

Shen, Z., Simon, G.P., Cheng, Y.B.: Comparison of solution intercalationand melt intercalation of polymer-clay nanocomposites. Polymer **43**, 4251–4260 (2002)

Sinha, R.Y., Okamoto, M.: Polymer/Layered silicate nanocomposite: a review from preparation and processing. Prog. Polym. Sci. **28**, 1539–1641 (2003)

Tan, J., Wang, X., Luo, Y., Jia, D.: Rubber/Clay nanocomposites by combined latex compounding and melt mixing: a masterbatch process. Mater. Des. **34**, 825–831 (2012)

Tian, M., Liang, W., Rao, G., Zhang, L., Guo, C.: Surface modification of fibrillar silicate and its reinforcing mechanism on FS/rubber composites. Compos. Sci. Technol. **65**, 1129–1138 (2005)

Varghese, S., Karger-Kocsis, J.: Natural rubber-based nanocomposites by latex compounding with layered silicates. Polymer **44**, 4921–4927 (2003)

Vijayalekshmi, V.: Studies on natural rubber/clay nanocomposites: effect of maleic anhydride grafting of rubber. Ochin University of Science and Technology, Kochi 22, Kerala, India, August 2009

Wang, J., Chen, D.: Mechanical properties of natural rubber nanocomposites filled with thermally treated attapulgite. J. Nanomater. Article ID 496584, 11 (2013)

Wang, J., Liu, H., Wen, S., Shen, Y.: The mechanical properties of modified attapulgite reinforced nature rubber and styrene-butadiene rubber nanocomposites. Adv. Mater. Res. **150–151**, 762–765 (2011)

Wang, L., Sheng, J.: Preparation and properties of polypropylene/org-attapulgite nanocomposites. Polymer **46**, 6243–6249 (2005)

Wang, R., Li, Z., Wang, Y., Liu, W., Deng, L., Jiao, W.,Yang, F.: Effects of modified attapulgite on the properties of attapulgite/epoxy nanocomposites. Polym. Compos. (2013)

Wang, Y.Q., Zhang, H.F., Wu, Y.P., Yang, J., Zhang, L.Q.: Structure and properties of strain-induced crystallization rubber-clay nanocomposites by cocoagulating the rubber latex and the aqueous suspension. J. Appl. Polym. Sci. **96**, 318–323 (2005)

Wilkinson, A.N., Man, Z., Standford, J.L., Matikainen, P., Clemens, M.L., Lees, G.C., Liauw, C. M.: Structure and dynamic mechanical properties of melt intercalated polyamide 6—montmorillonite nanocomposites. Macromol. Mater. Eng. **291**, 917–928 (2006)

Wu, Y.P., Jia, Q.X., Yu, D.S., Zhang, L.Q.: Structure and properties of nitrile rubber (NBR)-clay nanocomposites by cocoagulating NBR latex and clay aqueous suspension. J. Appl. Polym. Sci. **89**, 3855–3858 (2003)

Yan, H., Sun, K., Zhang, Y., Zhang, Y., Fan, Y.: Effects of silane coupling agents on the vulcanization characteristics of natural rubber. J. Appl. Polym. Sci. **94**, 1511–1518 (2004)

Zaharri, N.D., Othman, N., Ishak, Z.M.: Effect of zeolite modification via cationic exchange method on mechanical, thermal, and morphological properties of ethylene vinyl acetate/zeolite composites. Adv. Mater. Sci.Eng. **2013** (2013)

Zhang, X., Loo, L.S.: Morphology and mechanical properties of a novel amorphous polyamide/nanoclay nanocomposite. J. Polym. Sci. Part B: Polym. Phys. **46**, 2605–2617 (2008)

Impact of Nanoclay on the Properties of Wood Polymer Nanocomposites

Md. Saiful Islam, Irmawati Binti Ramli, Sinin Hamdan, Rezaur Rahman, Ahmad Adib Aiman, Abdul Rasyid and Amyrah Auni

Abstract In this chapter, the influences of nanoclay on the attributes of tropical wood polymer nanocomposites (WPNCs) were discussed. The impregnation of wood samples with nanoclay and in situ polymerization were employed by vacuum-pressure method. The comparisons of improvement in different properties have been showed between the raw wood, wood plastic composites (WPC), and WPNC. The FTIR result confirmed the interaction and incorporation of nanoclay inside wood. The exfoliation of nanoclay has been identified by Transmission electron microscopy result. The formation of wood polymer nanocomposites was proven through X-ray diffraction (XRD) pattern and Scanning electron microscopy (SEM) images, respectively. Significant improvement in mechanical properties was found through nanoclay treatment. The Dynamic mechanical thermal analysis (DMTA) result also indicated the improvement of thermo-mechanical properties after nanoclay treatment. The storage modulus (E') of the WPNC specimen also unveiled notable enhancement in both rubbery plateau and glassy region in alliance to their parallel wood polymer composites and raw wood samples. The wood's Dynamic Young's modulus (E_d) also indicated significant increment for PF-nanoclay impregnated WPNC samples. Whereas, the treatment by PF-nanoclay system seem to lower the damping (loss $Tan\delta$) peaks of woods. Furthermore, the WPNC samples shown significant improved compared to WPC and raw ones against white-rot white-rot (polyporous versicolor) and brown-rot (postia placenta) exposed.

Md. Saiful Islam (✉) · I.B. Ramli · A.A. Aiman · A. Rasyid · A. Auni
Department of Chemistry, Faculty of Science, Universiti Putra Malaysia, 43400 Serdang, Selangor, Malaysia
e-mail: msaifuli2007@gmail.com

S. Hamdan
Faculty of Engineering, Department of Mechanical and Manufacturing Engineering, Universiti Malaysia Sarawak, Kota Samarahan, Malaysia

R. Rahman
Faculty of Engineering, Department of Chemical Engineering, Universiti Malaysia Sarawak, Kota Samarahan, Malaysia

1 Introduction

The study of wood modification has been intensively investigated resulting significant improvement in the wood's properties. Several types of wood have not been adequately developed and utilized as it is due to numerous drawbacks including pysico-mechanical properties, high moisture intake and biodegradation changing with the variation of environment (Vetter et al. 2009; Yalinkilic et al. 1998). Therefore, wood modification becomes one of approach to respond against the deficiencies of wood properties. The establishment of wood polymer composites (WPCs) from the result of impregnation of polymer was investigated over decades (Cai et al. 2003, 2007a, b, 2008a, b) Wood modification that used suitable chemical treatment and chemicals such as acrylic monomer, urethane, methyl methacrylate, styrene, urea formaldehyde resin, vinyl, phenol formaldehyde resin and epoxy resin have been approved to enhance the properties of wood though its face some limitation (Islam et al. 2011; Yildiz et al. 2005; Rowell 2005; Islam et al. 2010). WPCs have raised dimensional stability, boosted strength properties and higher resistance to biodeterioration.

Wood polymer nanocomposites (WPNCs) manufacturing from several kinds of particular wood species was based on impregnation with prepolymer mixture and in situ polymerization by vacuum-pressure method. An enhancement in the stiffness and strength were taking the effect from exfoliation of diverse kinds of nanoclay for example hectorite, saponite and montmorillonite which have an overlay structure (Bordes et al. 2009). Moreover, various thermoset nanocomposites and thermoplastic at low silicates content have been observed, lead to significant enhancements in mechanical and physical properties, as well as strength and tensile modulus, thermal stability, flexural modulus and strength, barrier resistance and flame retardant (Ray and Okamoto 2003). Because of the promising potential in refining the solid wood properties, thus nanocomposite technology can be significant approach to acquire better product.

Malaysia as the third largest tropical forest in the world has abundance of numerous types of tropical wood species but cannot be consumed due to disadvantages for examples low thermo-mechanical, physical, and mechanical properties (Islam et al. 2012b). Hence, a proper treatment should be done depend on specific uses in order to achieve satisfied utilization of woods. Recently, studies have been profound to chemical alteration of tropical light hardwood species with a nanoclay combination and PF resin which generally in nanotechnological modification.

Regarding the effect of nanoclay on the tropical wood nanocomposites properties, different perspective have been look through. The mechanical properties investigated in terms of modulus of compressive modulus and elasticity (MOE) whereas the
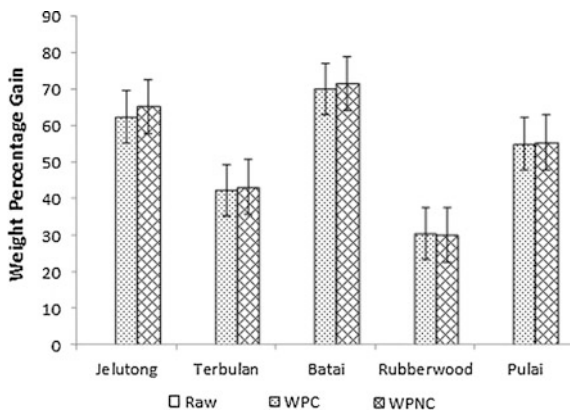
dynamic mechanical thermal analysis (DMTA) study has been done to analyze the wood samples thermo-mechanical feature. Analysis from DMTA has been showing the morphology of the structure, the description of interface between the stage and the fundamental properties of the components. Therefore, DMTA is an extremely versatile thermal analysis since there is no other method that offers more evidence in one test. DMTA also allows the resolve the form of viscoelastic in WPCs and delivers treasured perceptions into the affiliation between physiology, arrangements and wood polymers composites and their properties (Manchado and Arroyo 2000). Numerous studies about the DMTA properties of WPC materials and chemically altered wood have been determined (Sugiyama et al. 1996). Storage modulus E′, loss modulus E″, dynamic modulus E*, and mechanical damping tanδ of nanocomposite materials are the temperature-dependent dynamic parameters which indicate an understanding into the level of interaction and interface among the polymer medium and the coated silicate nanoclay. The free-free vibration testing was used to calculate the Dynamic Young's modulus (E_d) of wood. The energy dissipation and elastic properties of wood can use this technique as an alternative. It also provides quick information about the superiority of the materials. Three kinds of vibration, longitudinal (axial), torsion and bending (flexural) are comprises in these method which the flexural vibration is the most commonly used. It is due to the easiest way to excite and sense the vibrations under analysis (Islam et al. 2012a). The untreated wood seem to be less deterioration resistance since decrease weight due to the wood exposure with two kinds of fungi; brown-rot (postia placenta) and white-rot (polyporous versicolor) (Islam et al. 2013a).

In this chapter, pure PF resin and combined with Nanoclay prepolymer mixture were used to improve their aforesaid drawback properties of five designated species of tropical light hardwoods. Thus, the first objective of this study is to fabricate WPNCs as of particular tropical light hardwoods and second, to study the properties in mechanical, thermo-mechanical and decay resistance.
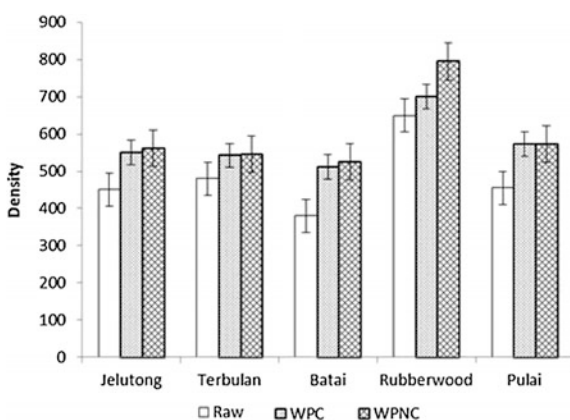
2 Density Measurement and WPG

Density and weight percentage gain (WPG) of the composites were calculated when the samples were dried properly after being polymerized. The results obtained for polymerized and raw wood samples are listed in Fig. 1. From the average value of densities and WPG shown, all wood species were successfully incorporated with PF and PF-Nanoclay as the highest percentage of polymer gained compared to other tested wood samples was Batai species. These result also point out that the density of wood species influence by the amount of polymer can be introduced into the woods, because of higher density wood species gain lower amount of polymer and vice versa (Yap et al. 1990). Thus, the polymerization of wood influenced by the density of wood species that plays such a crucial role in as well as the formation of WPC.

According Fig. 2, the treatments gave highest increment to Batai wood species
meanwhile as well as major increase in density of other wood species. These result
indicated that as the density of wood composites increased, the polymer inserted
into the wood species also increase. However there were no significant differences
between pure PF and PF-Nanoclay shown by the WPG of wood composites
samples. It also shown the incorporation of polymer and the formation of WPC
gained a small effect as the nanoclay mixed with PF resin.

3   Fourier Transform Infrared Spectroscopy (FTIR)

Deka and Maji (2013) have studied the impact of nanoclay to the polymer com-
posites which can be observed at the FTIR result (Fig. 1). The absorption peaks for
–CH_2 stretching of the N-cetyl-N,N,N-trimethyl ammonium bromide (curve a) were
at 2918, 2848, and 1475 cm^{-1} respectively (Li and Tripp 2002). The spectrum of

unchanged SiO_2 shows −OH stretching absorption peaks at 3424 cm^{-1} and −OH group adsorbed the particles surface at 1632 cm^{-1}. The other peaks were observed in range of 1087–465 cm^{-1} because of the presence of Si–O–Si group of SiO_2.

The FTIR spectra of N-cetyl-N,N,N-trimethyl ammonium bromide incorporated SiO_2 seems to be decreased of −OH. This is due to the absorption of −OH group on SiO_2 and interaction with CTAB. It can also be seen from the spectra that the two new peaks for –CH$_2$ stretching of CTAB were allocated at 2923 and 2854 cm^{-1}. The symmetric and asymmetric CH$_3$–N$^+$ deformation of CTAB group are the reason of this result (Li and Tripp 2002). Qu et al. (2010) modified TiO_2 with CTAB and identified that the interaction between TiO_2 and Br- of CTAB were due to formation of hydrogen bond or electrostatic forces interaction. These results had shown the combination of CTAB on the surface of SiO_2 particles (Fig. 3).

Various types of wood samples—raw wood, nanoclay, WPC, PB/G5 and WPC filled with nanoclay (3 wt%) and SiO_2 (1−5 wt%) FTIR result are shown in Fig. 4. The FTIR spectra (a) displays the presence of −OH stretching bands at 3434 cm^{-1}, 2931 cm^{-1} and –CH stretching at 2849 cm^{-1}, 1730 cm^{-1} for C=O stretching, 1635 cm^{-1} for −OH bending, 1163 cm^{-1} and 1045 cm^{-1} C–O stretching and 1000–645 cm^{-1} for C–H bending (out of plane) of the wood sample. Naturally improved nanoclay (spectra b) showed the peak at 3470 cm^{-1}, 2935 cm^{-1} and 2849 cm^{-1} (due to –CH stretching), 1620 cm^{-1} (−OH bending) and 1030–

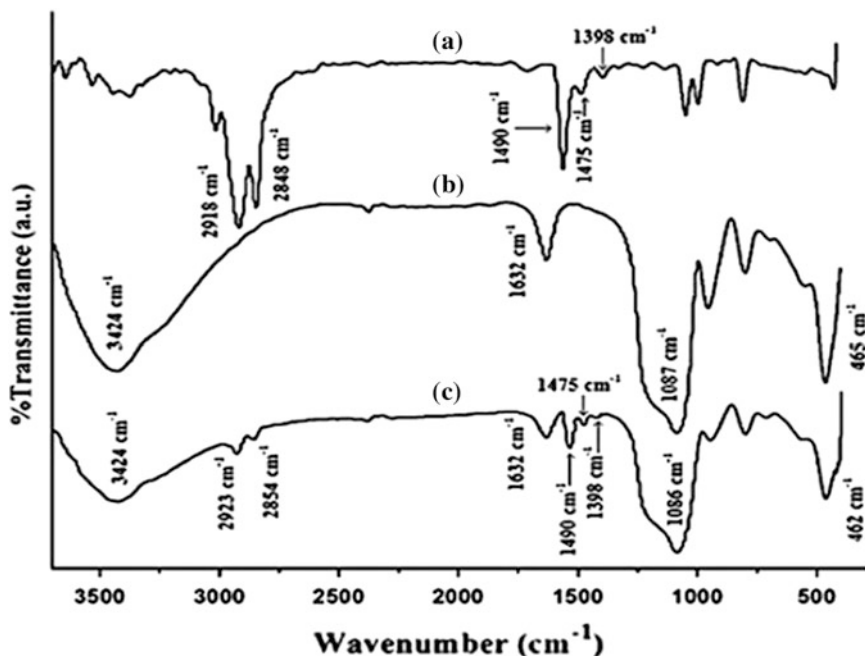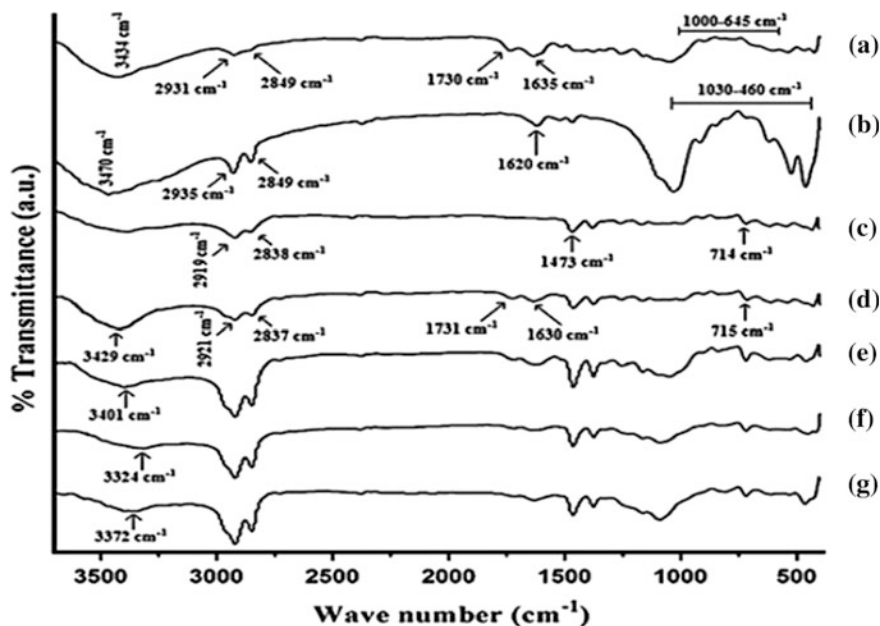**Fig. 3** FTIR spectra of *a* CTAB, *b* unmodified SiO_2, and *c* CTAB-modified SiO_2 [Permission has been taken]
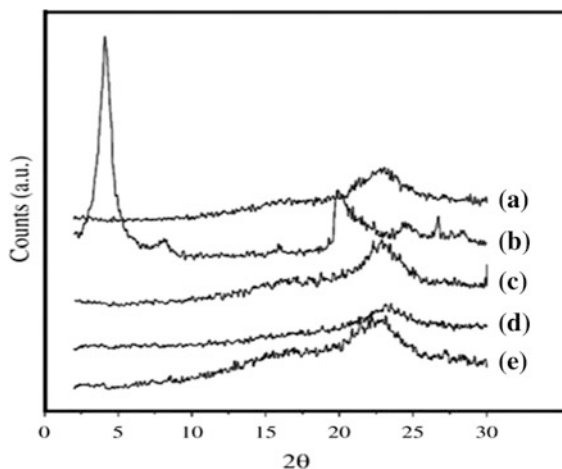
Fig. 4 FTIR spectra of *a* wood, *b* Nanoclay, *c* PB/G5, *d* PB/G5/W40, *e* PB/G5/W40/N3/S1, *f* PB/G5/W40/N3/S3, and *g* PB/G5/W40/N3/S5 [Permission has been taken]

460 cm^{-1} (due to Si, Al, Mg, etc. band). Polymer mixture filled with compatibilizer (spectra c) shows peaks at 2919 and 2838 cm^{-1} (–CH stretching), 714 cm^{-1} (–CH$_2$ bending) and 1473 cm^{-1} (–CH bending). PB/G5/W40 (curve d) shown peaks at 2921 and 2837 cm^{-1} (–CH stretching), 3429 cm^{-1} (−OH stretching), 1731 cm^{-1} (C=O stretching), 1630 cm^{-1} (−OH bending), and 715 cm^{-1} (–CH$_2$ bending).

The FTIR spectra of WPC filled with 3 wt% nanoclay and 1, 3, and 5 wt% of SiO$_2$ were also shown respectively. It was identified that the intensity of –OH stretching reduced and shifted to 3401 cm^{-1} (spectra e), 3324 cm^{-1} (spectra f) and 3372 cm^{-1} (spectra g) from 3434 cm^{-1} for wood and 3470 cm^{-1} for nanoclay. The intensities decreases and shifting to lower wavenumber proves that there were bond formation between the hydroxyl groups of wood, nanoclay and SiO$_2$. Furthermore, the intensities increases of –CH stretching at 2921 and 2837 cm^{-1} (spectra e–g) compared to those of wood indicated an interaction between polymer, wood and compatibilizer. Similar type of reduction in intensity of –OH absorption peak, a shifting to lower wavenumber and rise in –CH peak intensities was reported by Deka and Maji (2010). FTIR spectra of WPC (spectra e–g), shows peaks at 1030–460 cm^{-1} due to metal oxides bond equivalent to nanoclay and SiO$_2$. This indicating the formation of bond among wood, polymers, clay and SiO$_2$.

4 X-Ray Diffraction Study

The study of wood polymer nanocomposite by Devi R. and Maji T. via in situ polymerization explained the influence of additives and nanoclay in the mechanical and thermal properties. In Fig. 5 shows the X-Ray diffraction of treated wood, nanoclay and wood sample treated with S/G5/N1, S/G5/N1/V1 and S/G5/N1/V2 respectively. At 2.15 nm, interlayer distance was found for nanoclay at $2\theta = 4.1°$. Similarly the wood sample indicated a peak at $2\theta = 23.05°$ that caused by the crystal plane (002) of cellulose. Wood sample that been modified with S/G5/N1 shows only cellulose properties peak while the spike for nanoclay was found to be vanished. Therefore, it can be assume that either the nanoclay layers became delaminated or the interlayer distance had fully expanded. The position of diffraction peak in wood samples unchanged despite of the vinyl trichlorosilane (VTCS) was added to GMA/nanoclay. This suggested that the dispersion of nanoclay in the polymer did not disturb by VTCS due to the nanoclay immersed into the amorphous region of wood cellulose.

5 Morphological Studies

5.1 Scanning Electron Microscopic (SEM)

Devi et al. (2012) studied about impregnation of styrene acrylonitrile copolymer (SAN), SiO_2 nanoparticles modified with c-trimethoxy silyl propyl methacrylate (MSMA), and nanoclay into wood. Figure 6 shows the SEM micrograph untreated wood (a), treated wood (b–f). Empty parenchyma, the pit, and cell wall were observed for controlled wood. Thus, for the modified wood, the empty spaced were
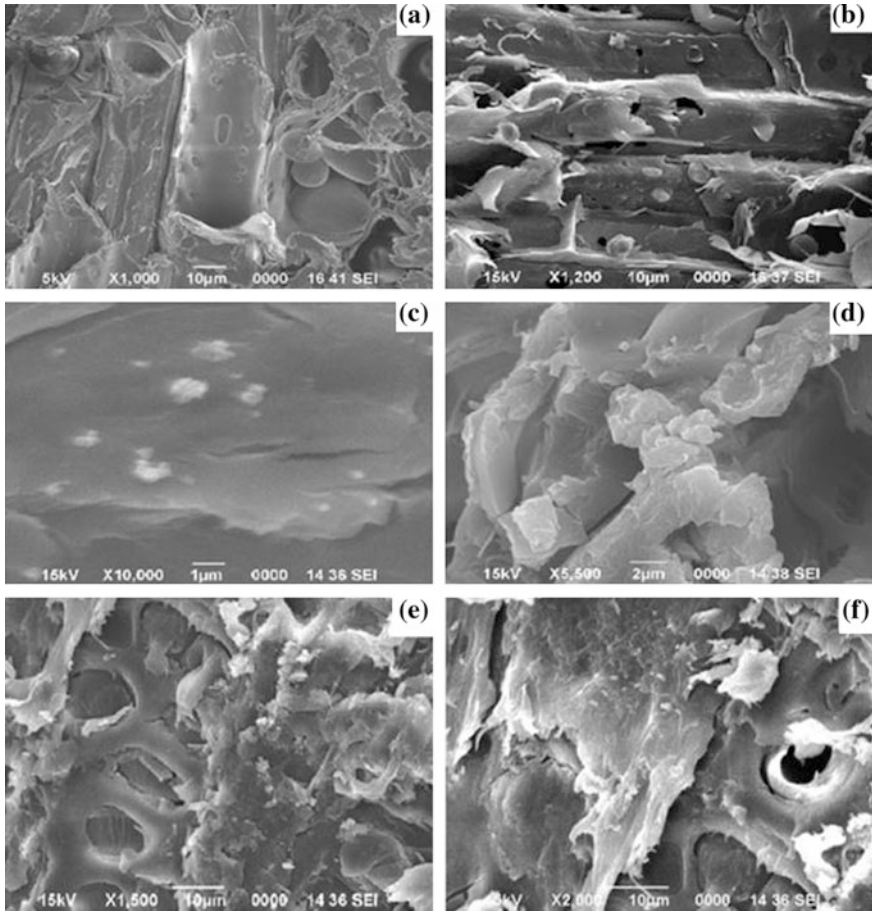
Fig. 6 Scanning electron micrographs of **a** untreated, **b** SAN, **c** SAN/SiO$_2$ (0.5 %), **d** SAN/nanoclay (0.5 %), **e** SAN/SiO$_2$ (0.5 %)/nanoclay (0.5 %), and **f** SAN/SiO$_2$ (0.5 %) nanoclay (2.0 %)-treated wood samples. [Permission has been taken]

filled with SAN polymer (b), SAN SiO$_2$ 0.5 % (c), and SAN/nanoclay 0.5 % materials. The treated nanoparticles can be spotted as white spots were either located in the cell walls or filled in the cell lumen. The existence of nano-SiO$_2$ and nanoclay was observed in the wood cell wall and wood pit which can be spotted in figure e and f.

5.2 Transmission Electron Microscopy (TEM)

From research of the synthesized composites that been done by Iman and Maji (2012) which is to prove the extent of exfoliation of nanoclay. The dark lines
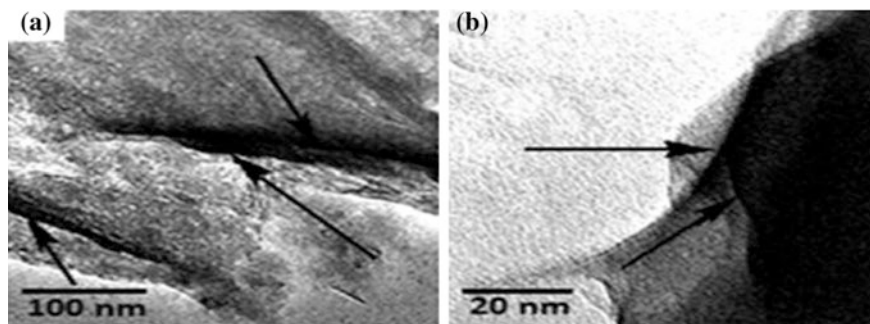
Fig. 7 TEM micrograph of S/clay composite with 5 % clay **a** 100 nm and **b** 20 nm scale [Permission has been taken]

indicated the spreading of the clay films which can be observed in both images as shown by arrow marks. The TEM micrograph of composites that been incorporated with nanoclay are shown in Fig. 4. The Fig. 7a, b represent the TEM micrograph in 100 to 20 nm range. The TEM micrograph shows the starch has delaminated the clay layer to turn into thin lamellas with thickness dimension of 2−3 nm. This proves that the nanoclay were exfoliated into the starch matrix moderately and well dispersed. This similar result was also reported by Chen and Zhang (2006); Yoonesi et al. (2004) which we can assumes that the nanoclay successfully intercalated into the composites.

6 Mechanical Properties

6.1 Modulus of Elasticity (MOE) and Compressive Modulus

Islam et al. (2013a) studied about morphological and mechanical properties of tropical wood polymer nanocomposite (WPNC). In Figs. 8 and 9, it represent the mechanical properties—MOE and mean compressive modulus of WPC and WPNC samples respectively. As the mechanical test result shown, the treatment with PF resin (WPC) and PF-Nanoclay (WPNC) lead to considerable improvement in MOE and compressive modulus. Even so it is worth noting that the MOE and compressive modulus were significantly affected by the PF-Nanoclay treatment. It can be deduced that WPNC samples of all wood species appeared to have higher MOE and compressive modulus compared to WPC samples. For WPNC samples, it was about 50−65 % of MOE values increment, whereas WPC samples show around 15−21 % that for the untreated references. A significant increase in compressive modulus of WPNC samples is shown while WPC samples only slightly increased.

The reinforcement nanoclay improved the interphase interaction between nanoclay, PF and also the density increases due to the reduction of void spaces in the
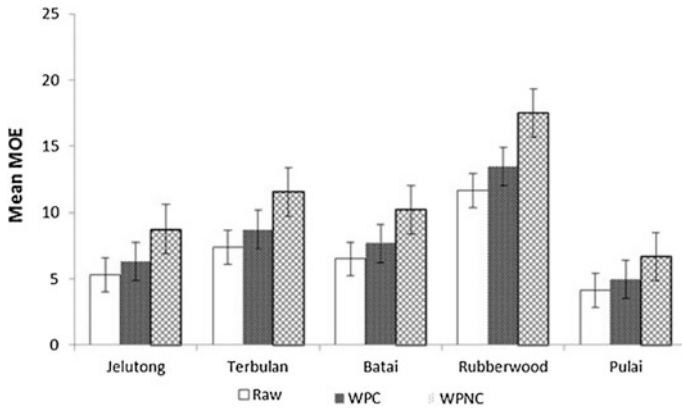
Fig. 8 Mean for Modulus of Elastic (MOE)
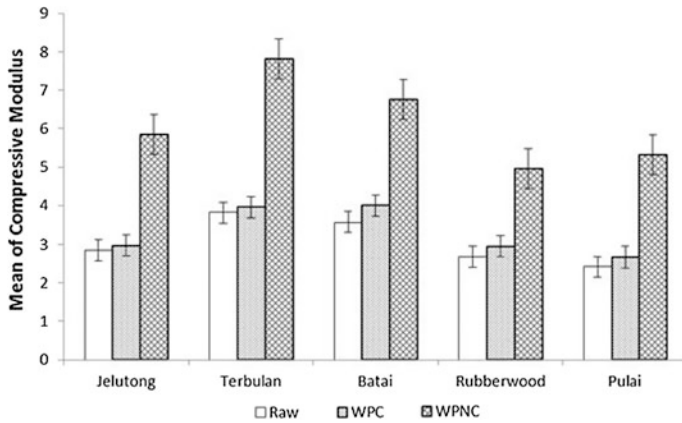
Fig. 9 Mean of compressive modulus

wood caused the improvement in MOE and compressive strength of WPNC samples (Cai et al. 2007a). However, due to high density of Rubberwood species a slight increase was found for WPC and WPNC and inside the cell wall a small amount of prepolymer incorporated (Deka et al. 2000).

6.2 Dynamic Young's Modulus (E_d)

Rahman et al. (2012) studied about the influence of nanoclay/phenol formaldehyde resin on wood polymer composites. 5 types of wood were tested and each will have a control which is the raw wood. From the result obtained (Fig. 10), nanofiller with

Fig. 10 Dynamics young's modulus of raw wood, WPNC for all species. [Permission has been taken]
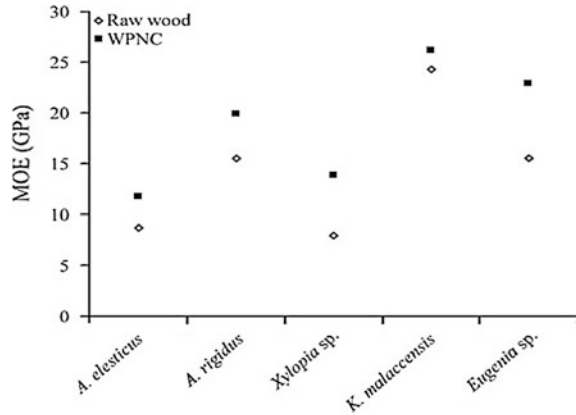
phenol formaldehyde enhance the Young's modulus as observed in all species which was according to his previous work. After the impregnation of the monomer, *Eugenia* sp., *Xylopia* sp., *Artocarpus* rigidus and *Artocarpus* elasticus have higher Young's modulus than the raw one. But, for Koompassia malaccensis the values was slightly higher which is due to the hard cell wall (nanofiller effect on all wood species).

6.3 Storage Modulus (E′)

The research of wood polymer nanocomposites by Cai et al. (2008a) on the effect of interphase between wood, melamine-urea-formaldehyde and layered silicate on the performance. The storage modulus (E′) of raw woods and their composites indicated in Fig. 11 (a–e) were determined by dynamic mechanical thermal analysis (DMTA) test. The increased in temperature will decrease the E′ values of all woods and their composite due to increase chain movement of the wood cell wall polymeric components (i.e. lignin, hemicelluloses and cellulose).Whereas, around 50 −120 °C showed a drop in E′ values was sharp next to the glass transition (Tg) of the raw wood. Generally, this decreasing value inclination in modulus is common to show the behavior of wood viscoelasticity. A considerable improvement in the E′ of the WPC and WPNC samples over the untreated controlled woods can be seen in Fig. 11. This improvement caused by the better interface interaction between wood fiber, PF and nanoclay that permitted larger force transfer at the interphase (Cai et al. 2008b). Nonetheless, Fig. 11 showed the difference between E′ values of the WPNC samples, WPC and raw wood samples were remarkably high. In the glassy state region, there was higher increment in E′ value than the rubbery state. The storage modulus of WPNC samples clearly showed greater value below Tg and this disposition uniformly reduced in the rubbery plateau.
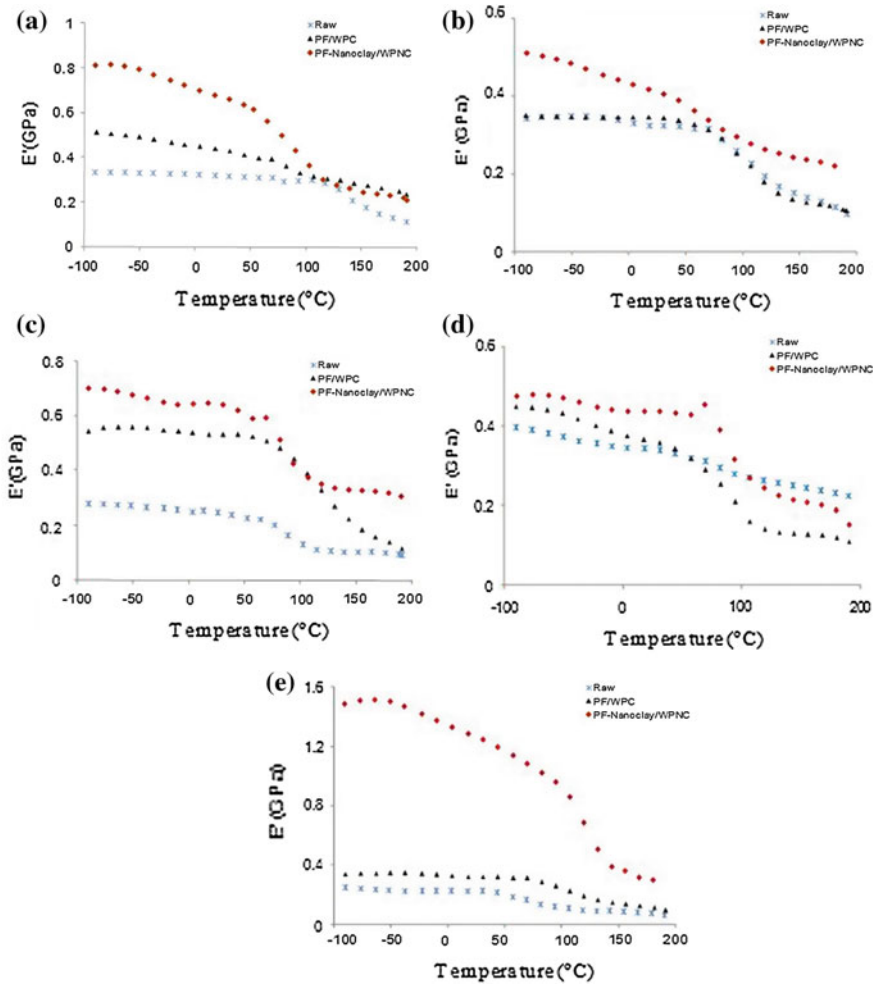
Fig. 11 Variation of storage modulus (E′) as a function of temperature for raw wood, WPC and WPNC samples of **a** Jelutong, **b** Terbulan, **c** Batai, **d** Rubberwood, and **e** Pulai. [Permission has been taken]

Moreover, the WPNC samples had higher overall percentage changes for E′(% ΔE′) over the range of temperature between −50 and 150 °C compared to those of WPC and raw wood samples. These can be interpreted as inside the wood, the integration of nanoparticles provided extra support that in turn playing role as a reinforcement in enhancing the surface compatibility between polymer matrix and wood fiber (Cai et al. 2007b, 2008b). It was also stated that the increment in E′ value for WPNC of Rubberwood was lowest compared to other WPNC samples due to its lower polymer matrix incorporation and high density.

6.4 Loss Tangent (Tanδ)

Cai et al. (2008b) research on the influence of the nature of nanofiller on the performance of wood polymer nanocomposite reported that the weak interphase interaction of NF3 (Cloisite Na$^+$, a pristine nanoclay, hydrophilic) with the cured MUF(melamine-urea-formaldehyde) matrix was also resulted from the loss tangent (tanδ) of the material which can be observed at Fig. 12. Broad shoulder, with nearly identical maximum peak of about 185 °C can be visibly observed for the MUF and NF3/MUF treated wood. Yet, within the range of the temperature measured, there is no noticeable tanδ peaks could be noticed for pure wood. This shows that the wood impregnated with MUF rised the transition (T_g, max) and the hydrophilic nanoclay NF3 had nearly no outcome on the T_g, indicating NF3 has weak interactions with the impregnated MUF matrix. We also can observe relatively lower tanδ peak was perceived for the NF3/MUF treated sample compare to the pure MUF impregnated wood. These might because of the relatively lesser amount of MUF impregnated into the wood as indicated for other NF3/MUF treated samples and also due to the consequence of the impregnated nanoparticles. As we can see, the restricted polymeric chain movement of the polymeric matrix lead to the stiff fiber reduced the tanδ peak (Salehi et al. 1998; Cai et al. 2003). From the result obtained, eventhough for the NF2(Claystone APA)/MUF impregnated wood have quite the similar weight gain as the MUF impregnated wood, greatly lower height of tanδ curve was observed and no tanδ could be spotted. It proves that the interphase interactions of the nanofiller and the polymer matrix have been formed strongly.
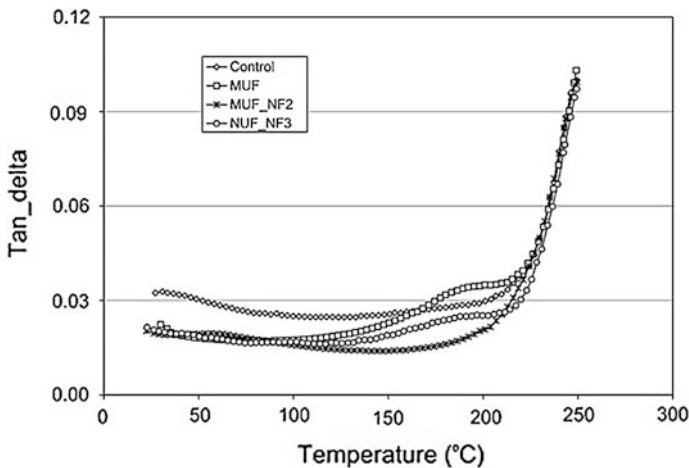
Fig. 12 tanδ profiles of pure wood, and MUF, NF2/MUF and NF3/MUF impregnated wood. [Permission has been taken]

7 Decay Resistance

The research of tropical wood polymer nanocomposites (WPNC) has done by Islam et al. (2013a) on their decay resistance and thermal stability properties. Laboratory decay resistance test was conducted and weight loss because of white-rot (poly-porous versicolor) and brown-rot (postia placenta) fungi attacks for raw wood, WPC and WPNC samples are presented in Figs. 13 and 14. As illustrated in the figures, both decay fungi attacked the untreated wood severely causing great weight loss, thus that all raw wood species generally were non-resistant to decay exposure. Whereas, WPC and WPNC samples indicated remarkable and significant resistance towards both decay fungi. However, PF-Nanoclay treatment was shown to yield the excellence result for decay resistance of all species. The PF-Nanoclay treatment resulted significantly superior decay resistance. These due to its great efficiency of water exclusion and inhibition of mycelial spread as stated also in earlier chapter (Yalinkilic et al. 1998). These expected result caused by the barrier properties of

Fig. 13 Weight losses of raw wood and wood composites samples after white rot fungi exposed
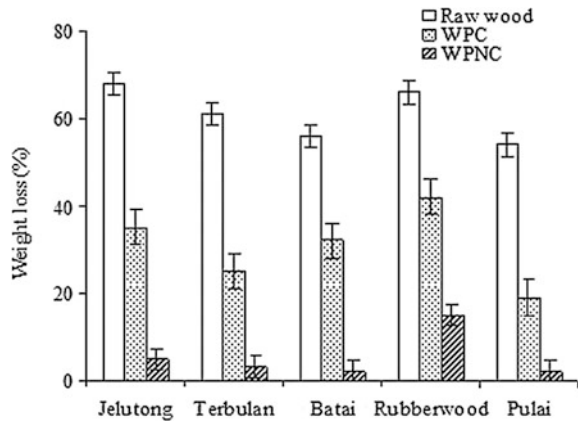
Fig. 14 Weight losses of raw wood and wood composites samples after brown rot fungi exposed
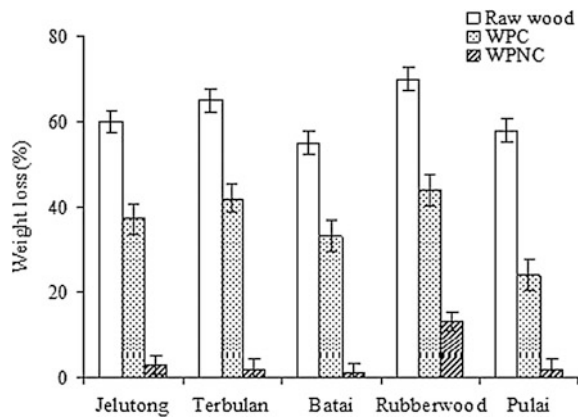
nanofiller nanoclay that significantly reduced the water uptake capacity of the WPNC same as claimed by the other researchers (Yildiz et al. 2005; Williams and Hale 2003).

8 Conclusion

Considerable improvements in mechanical, dynamic mechanical and decay resistance properties were obtained for WPNC. FTIR results confirmed that the nanoparticles successfully incorporated into wood surfaces and formation of WPNC. The XRD results of WPNC reveal an improved degree of crystallinity and a thorough polymer covered surface quality. The SEM micrographs showed the better interphase interactions between wood, PF, nanoclay and wood component, which ominously improved the mechanical and dynamic mechanical possessions of all particular tropical light hardwoods. While the TEM results show that the nanoclay were partially exfoliated and well dispersed into the starch matrix which can be presumed that the intercalation of the nanoclay into the composites was effective. Moreover, the resistance towards fungi deterioration exposure of WPNC samples was advanced compared to WPC and untreated samples. Dynamic mechanical properties in term of storage modulus, and glass transition temperature (Tg) was significantly changed by the PF-Nanocaly treatment.

Although some new insight has been gained with respect to the chemical modifications of tropical wood, many issues still need to be resolved to utilize the value-added application. Therefore, it is recommended that there are many research scope till exist in this area which could be carried out in future.

References

Bordes, P., Pollet, E., Avérous, L.: Nano-biocomposites: biodegradable polyester/nanoclay systems. Prog. Polym. Sci. **34**(2), 125–155 (2009)

Cai, X., Riedl, B., Ait-Kadi, A.: Cellulose fiber/poly(ethylene-co-meth-acrylic acid) composites with ionic interphase. Compos. A **34**, 1075−1084 (2003)

Cai, X., Riedl, B., Zhang, S.Y., Wan, H.: Formation and properties of nanocomposites made up from solid aspen wood, melamine-urea-formaldehyde, and clay. Holzforschung **61**, 148–154 (2007a)

Cai, X., Riedl, B., Zhang, S.Y., Wan, H.: Effects of nanofillers on water resistance and dimensional stability of solid wood modified by melamine-urea-formaldehyde resin. Wood Fiber Sci. **39**(2), 307–318 (2007b)

Cai, X., Riedl, B., Zhang, S.Y., Wan, H.: The impact of the nature of nanofillers on the performance of wood polymer nanocomposites. Compos. A Appl. Sci. Manuf. **39**(5), 727–737 (2008a)

Cai, X., Riedl, B., Zhang, S.Y., Wan, H.: The impact of interphase between wood, melamine-urea-formaldehyde and layered silicate on the performance of wood polymer nanocomposites. Compos. A **39**, 727–737 (2008b)

Chen, P., Zhang, L.: Interaction and properties of highly exfoliated soy protein/montmorillonite nanocomposites. Biomacromolecules **7**(6), 1700–1706 (2006)

De Vetter, L., Stevens, M., Van Acker, J.: Fungal decay resistance and durability of organosilicon-treated wood. Int. Biodeterior. Biodegradation **63**(2), 130–134 (2009)

Deka, M., Saikia, C.N.: Chemical modification of wood with thermosetting resin: Effect on dimensional stability and strength property. Bioresour. Technol. **73**, 179–181 (2000)

Deka, B.K., Maji, T.K.: Effect of coupling agent and nanoclay on properties of HDPE, LDPE, PP, PVC blend and Phargamites karka nanocomposite. Compos. Sci. Technol. **70**, 1755–1761 (2010)

Deka, B.K., Maji, T.K.: Effect of SiO_2 and nanoclay on the properties of wood polymer nanocomposite. Polym. Bull. **70**(2), 403–417 (2013)

Devi, R.R., Maji, T.K.: Effect of nano-SiO_2 on properties of wood/polymer/clay nano composites. Wood Sci. Technol. **46**, 1151–1168 (2012a)

Devi, R.R., Maji, T.K.: Effect of nano-ZnO on various physical, thermal, mechanical properties, and UV stability of wood polymer composites. Ind. Eng. Chem. Res. **51**, 3870–3880 (2012b)

Hamdan, S., Islam, M.S., Ahmed, A.S., Rahman, M.R., Rusop, M.: Study on thermal and biodegradation resistance of tropical wood material composites. J. Appl. Polym. Sci. (2013)

Islam, M.S., Hamdan, S., Rahman, M.R., Jusoh, I., and Ibrahim, N.F.: Dynamic Young's modulus and dimensional stability of Batai tropical wood impregnated with polyvinyl alcohol. J. Sci. Res. **2**(2), 227–236 (2010)

Islam, M.S., Hamdan, S., Rahman, M.R., Jusoh, I.: The effect of crosslinker on mechanical and morphological properties of tropical wood material composites. Mater. Des. **32**(4), 2221–2227 (2011)

Islam, M.S., Hamdan, S., Jusoh, I., Rahman, M.R.: Effect of coupling reaction on the mechanical and biological properties of tropical wood polymer composite (WPC). Biodeterior. Biodegradation **72**, 108–113 (2012a)

Islam, M.S., Hamdan, S., Talib, Z.A., Ahmed, A.S., Rezaur, M.R.: Tropical wood polymer nanocomposite (WPNC): The impact of nanoclay on dynamic mechanical thermal properties. Compos. Sci. Technol. **72**(2012), 1995–2001 (2012b)

Islam, M.S., Hamdan, S., Rusop, M., Rahman, M.R.: Mechanical and morphological properties of tropical wood polymer nanocomposite (WPNC). Adv. Mater. Res. **667**, 200–205 (2013a)

Islam, M.S., Hamdan, S., Rusop, M., Rahman, M.R.: Thermal stability and decay resistance properties of tropical wood polymer nanocomposites (WPNC). Adv. Mater. Res. **667**, 482–489 (2013b)

Iman, M., Maji, T.K.: Effect of crosslinker and nanoclay on starch and jute fabric based green nanocomposites. Carbohydr. Polym. **89**(1), 290–297 (2012)

Li, H., Tripp, C.P.: Spectroscopic Identification and dynamics of adsorbed cetyltrimethylammonium bromide structures on TiO_2 surfaces. Langmuir **18**, 9441–9446 (2002)

López-Manchado, M.A., Arroyo, M.: Thermal and dynamic mechanical properties of polypropylene and short organic fiber composites. Polymer **41**(21), 7761–7767 (2000)

Yap, M.G.S., Chia, L.H.L., Teoh, S.H.: Wood polymer composites from some tropical hardwood. J. Wood Chem. Technol. **10**(1), 1–19 (1990)

Qu, Y., Wang, W., Jing, L., Song, S., Shi, X., Xue, L., Fu, H.: Surface modification of nanocrystalline anatase with CTAB in the acidic condition and its effects on photocatalytic activity and preferential growth of TiO_2. Appl. Surf. Sci. **257**, 151–156 (2010)

Rahman, M.R., Hamdan, S., Islam, M.S., Ahmed, A.S.: Influence of nanoclay/phenol formaldehyde resin on wood polymer nanocomposites. J. Appl. Sci. **12**(14), 1481 (2012)

Ray, S.S., Okamoto, M.: Polymer/layered silicate nanocomposites: a review from preparation to processing. Prog. Polym. Sci. **28**(11), 1539–1641 (2003)

Rowell, R.M.: Chemical Modification of Wood. Handbook of Wood Chemistry and Wood Composites, 381 (2005)

Salehi-Mobarakeh, H., Brisson, J., Ait-Kadi, A.: Ionic interphase of glass fiber/polyamide 6,6 composites. Polym. Compos. **19**, 264–274 (1998)

Sugiyama, M., Norimoto, M.: Temperature dependence of dynamic visco elasticities of chemically treated woods. Mokuzai Gakkaishi. **42**, 1049–1056 (1996)

Williams, F.C., Hale, M.D.: The resistance of wood chemically modified with isocyanates: The role of moisture content in decay suppression. Int Biodeterior. Biodegradation **52**, 215–221 (2003)

Yalinkilic, M.K., Imamura, Y., Takahashi, M., Kalaycioglu, H., Nemli, G., Demirci, Z., Ozdemir, T.: Biological, physical and mechanical properties of particleboard manufactured from waste tea leaves. Int. Biodeterior. Biodegradation **41**(1), 75–84 (1998)

Yildiz, Ü.C., Yildiz, S., Gezer, E.D.: Mechanical properties and decay resistance of wood–polymer composites prepared from fast growing species in Turkey. Bioresour. Technol. **96**(9), 1003–1011 (2005)

Yoonessi, M., Toghiani, H., Kingery, W.L., Pittman, C.U.: Preparation, characterization, and properties of exfoliated/delaminated organically modified clay/dicyclopentadiene resin nanocomposites. Macromolecules **37**(7), 2511–2518 (2004)

Mechanical and Thermal Properties of Hybrid Graphene/Halloysite Nanotubes Reinforced Polyethylene Terepthalate Nanocomposites

Ibrahim Mohammed Inuwa, Tan Boon Keat and Azman Hassan

Abstract In this work, the effects of graphene nanoplatelets (GNP) and halloysite nanotubes (HNT) constant ratio content and processing methods on the mechanical and thermal properties of polyethylene terepthalate (PET) nanocomposites were investigated. The GNP/HNT filled PET nanocomposites were prepared by melt process using single screw extruder and counter rotating twin screw extruder followed by injection molding to produce test samples. The mechanical properties of the nanocomposites was investigated by comparing the effect of extruder types on tensile, flexural and impact test. The results show that the nanocomposites with the ratio of 2 wt% GNP and 1 wt% HNT hybrids have the highest tensile strength, flexural strength and impact strength. By comparing the two processing methods, PET nanocomposites prepared by single screw extruder exhibits higher tensile strength than those prepared using twins screw extruder. Furthermore, the results of differential scanning calorimetry (DSC) shows that the melting temperature of PET is not essentially affected by the presence of the hybrid nanofillers. However, the degree of crystallinity (X_c) and cold crystallization temperature (T_{cc}) were lower than pure PET with GNP2/HNT1 having the lowest X_c and T_{cc}. Overall the results show that the maximum improvement in mechanical and thermal properties were achieved by the combination of GNP and HNT in the nanocomposites with 2 wt% and 1 wt% respectively using the single screw extruder.

Keywords Graphene · Halloysite nanotubes · Polyethylene terepthalate · Thermal properties · Mechanical properties

I.M. Inuwa · T.B. Keat · A. Hassan (✉)
Department of Polymer Engineering, Faculty of Chemical and Energy Engineering,
Universiti Teknologi Malaysia, 81310 Johor, Malaysia
e-mail: azmanh@cheme.utm.my

1 Introduction

In the last twenty years, there has been wide spread interest to use nanoparticles dispersed in polymer matrices. The field of nanotechnology is one of the most popular areas for current research and development in basically all technical disciplines. This obviously includes polymer science and technology and the importance for nanotechnology will increase as miniaturization becomes more important in areas, such as computing, sensors, biomedical and many other applications. Advances in science, medicine and engineering depend largely on the ability to synthesize nanoparticles of various materials, sizes and shapes as well as assemble them efficiently into complex architecture (Kuilla et al. 2010). This would include microelectronics as the critical dimension scale for modern devices is now below 100 nm and interfacial phenomena in blends and nanocomposites involve nanoscale dimensions (Paul and Robeson 2008).

Graphene is a two-dimensional, one-atom-thick carbon sheet of sp2 bonded carbon atoms with a planar honeycomb network structure. It is the strongest material ever measured with tensile strength of 130 GPa and Modulus of 1 TPa (Kuilla et al. 2010). Graphene was discovered by scientist in Manchester in 2004. Graphene is predicted to have remarkable properties, such as thermal and flame retardant (Paul and Robeson 2008), superior mechanical properties (Paul and Robeson 2008) and excellent electronic transport properties (Zhang et al. 2010). Rheological and barrier properties of polymer nanocomposites are also improved by incorporation of graphene nanofillers. This versatility of graphene/polymer nanocomposites indicates their potential application in automotive, aerospace, electronics, and packaging (Kim et al. 2010).

Halloysite nanotubes (HNTs) are natural occurring aluminosilicate clays with hollow nanotubular structure mined from natural deposits in countries such as China, America, New Zealand, Brazil and France. HNT deposits have been found in many geographic areas where they are present in a variety of particle shapes and hydration states. HNTs have an empirical chemical formula of $Al_2Si_2O_5(OH)_4.2H_2O$, which is chemically similar to kaolin clay (Singh 1996). HNTs are a potential alternative to CNTs as a reinforcing filler for polymers because HNTs are much less expensive than CNTs. HNT is expected to be an effective impact modifier for brittle polymers at a much lower cost (Ye et al. 2007). HNT is predicted have remarkable properties, such as thermal stability and flame retardancy (Du et al. 2006), crystallinity (Du et al. 2010), and mechanical properties (Prashantha et al. 2011). In this study, graphene and halloysite nanotubes (HNT) are incorporated into PET with the aim of improve the mechanical, thermal and flame retardant properties. It is also intended to to investigate the effect of processing method on the properties of PET/GNP/HNT composites by comparing single screw and counter rotating twin screw extruders.

2　Experimental

2.1　Materials and Sample Preparation

Three materials used are PET, GNP and HNT. Extrusion grade, medium viscosity polyethylene terephthalate (PET) with intrinsic viscosity of 0.82 g/dl were secured for the experiment. Halloysite nanotube (HNT) clay, was purchased from Aldrich. The HNT tube dimension was 30–70 nm × 1–4 µm. PET/GNP and PET/GNP/HNT/were premixed in sealed containers and shaken manually.

　　PET was dried in a vaccum oven for 24 h to remove all the moisture content that could cause hydrolytic degradation during the compounding process. PET, PET/GNP and PET/GNP/HNT were placed in a mixer for 5 min before compounding. In this research, 3, 2 and 1 wt% of GNP, and 2 and 3 wt% HNT content were used. The mixture was compounded by techtuder nano 30 single screw extruder and Brabender PL2000 counter rotating twin screw extruder at 50 rpm. The four zones temperature profile were set at 205, 230, 230 and 250 °C. The extrudates were pelletized using laboratory scale pelletizing machine and dried in a dryer for 24 h at 120 °C and then injection molded to produce standard test specimens. The machine used was JSW Model NIOOB II with the barrel temperature of 240−280 °C.

2.2　Testing and Characterization

2.2.1　Tensile Test

Tensile test can be defined as force required in breaking a specimen and it extend and elongate until its breaking point. The tests were carried out according to ASTM D638. The crossed speed of 5 mm/min was used for testing. Five specimens for each formulation were tested and average values were recorded.

2.2.2　Flexural Test

The flexural test was conducted using Instron Universal Testing Machine according to the ASTM D790, a three-point bending system. The specimens were tested at the crosshead of 3.0 mm/min with a support span of 100 mm. The data were recorded electronically and the load-deflection curve were shown on the computer screen as a visual representation. Flexural strength and flexural modulus values were determined. Five specimens of each formulation were tested and the average values reported.

2.2.3   Impact Test

The specimens with varying proportions were subjected to notched Izod impact test using a pendulum type impact tester according to ASTM D4812. Prior to the test, all the specimens were notched at mid section using a notching machine with the depth of the notch at 0.25 mm. After taking the dimensions of the specimens, end of the specimens were clamped into position with the notched side facing the striking edge of the pendulum. The pendulum was released and allowed to strike through the specimens. The swing angle was recorded. Five specimens of each formulation were tested and the average values reported.

2.2.4   Differential Scanning Calorimetry

The thermal cure behaviour of PET, PET/GNP and PET/GNP/HNT were measured using a Perkin–Elmer differential scanning calorimeter (DSC-7) interfaced to a PC running Pyris software. DSC were carried out at a heating rate of 10 °C/min within the range of 30 to 300 °C using a sample size of 8 to 10 mg. The crystallization process was then followed as the sample was cooled at the same rate. Two basic parameters were obtained in this testing which was heat flow and temperature. In addition, a heat flow-temperature curve with a peak values of the crystallization exotherms and melting endotherms were obtained. The percentage of crystallinity Xc (PET) was calculated using the following equation:

$$\% \text{ Crystallinity} = 100\% \times \Delta H_M / \left(f \Delta H_M^\circ \right) \tag{3.1}$$

where, ΔH_M is measured heat fusion, f is the weight fraction PET, and ΔH°_M is the enthalpy of fusion for 100 % crystalline polymer (ΔH_M (PET) = 138.5 J/g).

3   Results and Discussion

3.1   Tensile Test

Table 3.1 shows the values of tensile properties of PET, PET/GNP, PET/GNP/HNT nanocomposites. The tensile strength and Young's modulus were significantly increased compared to pure PET. However, the elongation at break is reduced compared to pure PET.

3.1.1 Tensile Strength

Table 1 shows the tensile properties of PET, PET/GNP, PET/HNT and PET/GNP/HNT hybrid nanocomposites. Analyses of the results show that in general, all the nanocomposites have higher tensile strength than pure PET. Figure 1 shows the tensile strength of PET nanocomposites prepared using single screw extrusion. It can be seen that the nanocomposites containing 2 wt% GNP and 1 wt% HNT shows a significant increase from 37.6 MPa for pure PET to 50.8 MPa for PET/GNP2/HNT1 that is about 35.1 % increase. It can be concluded that the optimum concentration of GNP and HNT for best reinforcement effect of PET is 2/1 GNP/HNT ratio using a single screw extruder. This may suggest a possible interaction between remnant of hydroxyl group of GNP and HNT or between hydroxyl group of HNT and terminal hydroxyl group of PET. However, when 1 wt % GNP and 2 wt% HNT were incorporated into PET the tensile strength decreased considerably to 45.6 MPa. This shows that mechanical reinforcement of GNP is better than that of HNT. This can be attributed to high aspect ratio of GNP compared to HNT and also due its platelet geometry as against HNT which is tubular.

Table 1 Tensile properties of PET/GNP/HNT nanocomposites

Sample	Tensile strength (MPa)	Young's modulus (MPa)	Elongation at break (%)
PET	37.6 ± 3.3	1151.9 ± 57.5	4.59 ± 0.14
PET/GNP3 (Single screw)	40.8 ± 2.4	2557.3 ± 76.6	1.92 ± 0.19
PET/GNP2/HNT1 (Single screw)	50.8 ± 3.3	2363.7 ± 77.2	2.84 ± 0.26
PET/GNP1/HNT2 (Single screw)	45.6 ± 3.6	2490.6 ± 25.8	2.16 ± 0.20
PET/GNP3 (Twin screw)	40.1 ± 2.8	2625.8 ± 56.5	1.75 ± 0.16
PET/GNP2/HNT1 (Twin screw)	44.7 ± 3.9	2576.0 ± 65.0	2.10 ± 0.22
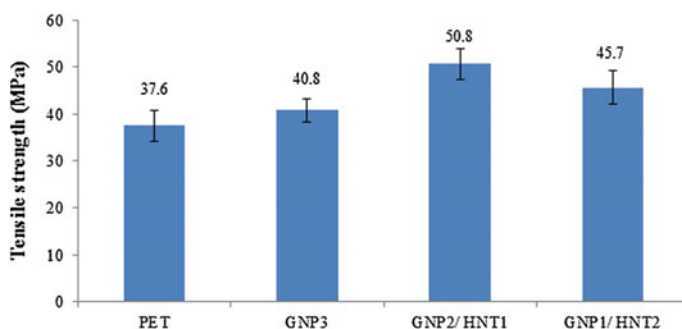
Fig. 1 Tensile strength of PET nanocomposites prepared using single screw extruder
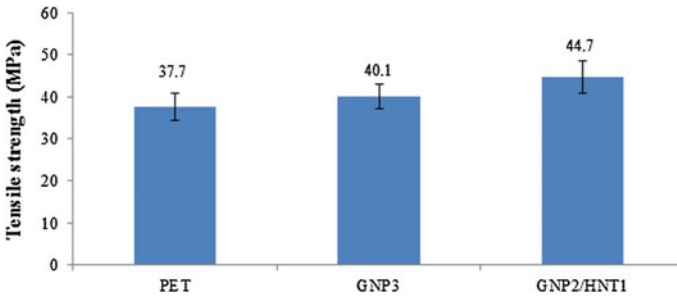
Fig. 2 Tensile strength of PET nanocomposites prepared using twin screw extruder

Figure 2 shows the tensile strength of PET nanocomposites prepared using twin screw extruder. It can be seen that the nanocomposites containing 2 wt% GNP and 1 wt% HNT shows a considerable increase from 37.6 MPa for pure PET to 44.7 MPa for PET/GNP2/HNT1 that is about 18.9 % increase. Thus, it can be concluded that the trend of enhancement was relatively same as with single screw extruder.

Effect of Extruder Type on Tensile Strength of PET Nanocomposites

Figure 3 shows the tensile strength of the PET nanocomposites prepared using single crew extruder and twin screw extruder. In general, the tensile strength of PET nanocomposites prepared using single screw extruder is higher than those using twin screw extruder. The tensile strength of PET/GNP3 using single screw extruder is 40.789 MPa while for twin screw extruder is 40.142 MPa. The tensile strength of PET/GNP2/HNT1 using single crew extruder is 50.8 MPa while for twin screw extruder is only 44.7 MPa. Thus, PET nanocomposites produced by single screw extruder have better tensile strength than PET nanocomposites produced by twin screw extruder. This is because the presence of barrier in the single screw surface that increase the retention times of the materials in the screw. This special screw

Fig. 3 Effect of extruder on tensile strength of PET nanocomposites
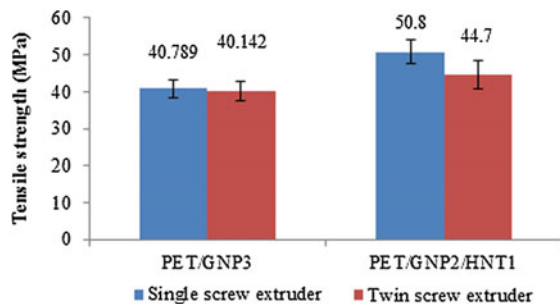
characteristic of single screw is more suited to the nanoparticles dispersion than twin screw (Kim and Kwon 1996).

3.1.2 Young's Modulus

Figure 4 shows the Young's modulus of PET nanocomposites using single screw extrusion. In general all the PET nanocomposites have higher Young's modulus which is more than 100 % increase of Young's modulus compared to neat PET. It can be seen that the nanocomposites containing 3 wt% GNP shows a dramatic increase of Young's modulus from 1151.0 MPa for pure PET to 2557.3 MPa for PET/GNP3. Therefore, it can be concluded that the optimum formulation for the best Young's modulus of PET is 3 wt% GNP. However, the Young's modulus of PET/GNP2/HNT1 and PET/GNP1/HNT2 comes down considerably to 2363.7 MPa and 2490.6 MPa respectively compared to PET/GNP3. This indicates that GNP is much stronger than HNT. Young's modulus of GNP is 1 TPa (Lee et al. 2008) which is significantly higher than HNT with only 140 GPa of Young's modulus (Lecouvet et al. 2013). Since the Young's modulus is a function of concentration of fillers and types of fillers, thus replacement of 1 wt% or 2 wt% of GNP with HNT were considerably bring down the Young's modulus of the nanocomposites.

Figure 5 shows the Young's modulus of PET nanocomposites prepared using twin screw extrusion. It can be seen that the nanocomposites containing 3 wt% GNP shows a highest increase of Young's modulus which is about 2625.8 MPa. This is the highest value of Young's modulus that was obtained. Therefore, it can be concluded that the trend of enhancement was relatively same as using single screw extruder.

Effect of Extruder on Young's Modulus of PET Nanocomposites

Figure 6 shows the Young's modulus of PET nanocomposites prepared using single screw extruder and twin screw extruder. The Young's modulus for all the
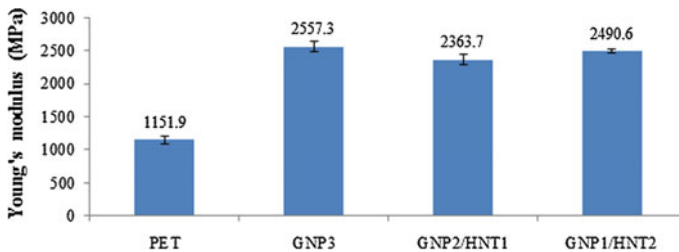
Fig. 4 Young's modulus of PET nanocomposites prepared using single screw extruder
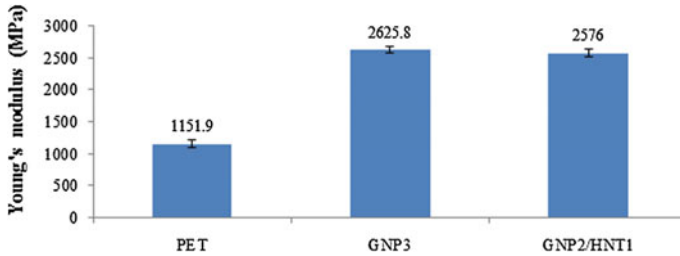
Fig. 5 Young's modulus of PET nanocomposites prepared using twin screw extruder

Fig. 6 Effect of extruder on Young's modulus of PET nanocomposites

formulation was comparable. For example, the Young's modulus of PET/GNP3 prepared by single screw extruder and twin screw extruder were 2557.3 MPa and 2625.8 MPa respectively. These values are comparable and it shows that type of machine does not affect the Young's modulus of the PET nanocomposites. The Young's modulus of PET nanocomposites was determined by type of fillers and concentration of the fillers rather than the orientation and dispersion of the fillers.

3.1.3 Elongation at Break

The elongation at break of all formulations were reduced when compared with neat PET. Figure 7 shows the elongation at break of PET nanocomposites prepared using single screw extruder. It shows that the elongation at break was significantly reduced from 4.59 % for pure PET to 1.92 % for PET/GNP3. This is due to the rigid or stiffness characteristics of fillers that restrict the motion of polymer molecular chain. However, it was significantly increased to 2.85 % for PET/GNP2/HNT1. This can be attributed to the presence of HNT in the formulation.
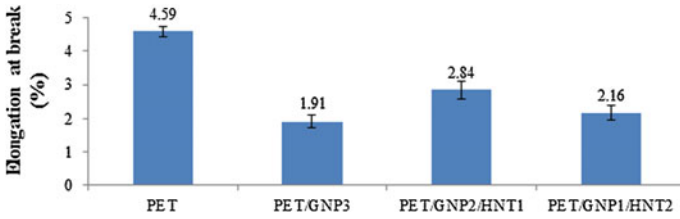
Fig. 7 Elongation at break of PET nanocomposites prepared using single screw extruder
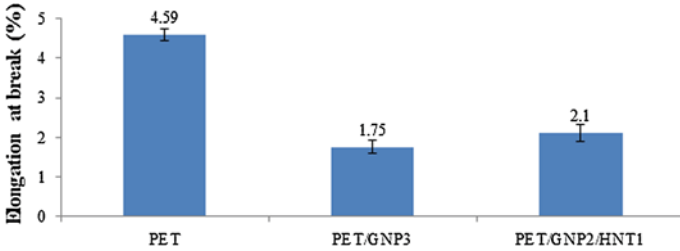
Fig. 8 Elongation at break of PET nanocomposites prepared using twin screw extruder

Figure 8 shows the elongation at break of PET nanocomposites prepared using twin screw extruder. The elongation at break shows similar trend with PET nanocomposites prepared using single screw extruder where the elongation at break was dramatically reduced from 4.59 % for pure PET to 1.75 % for PET/GNP3 and then considerable increased to 2.10 % for PET/GNP2/HNT1 due to the interaction between GNP and HNT fillers.

Effect of Extruder Type on Elongation at Break of PET Nanocomposites

Figure 9 show the elongation at break of PET nanocomposites prepared using single screw extruder and twin screw extruder. In general, the elongation at brea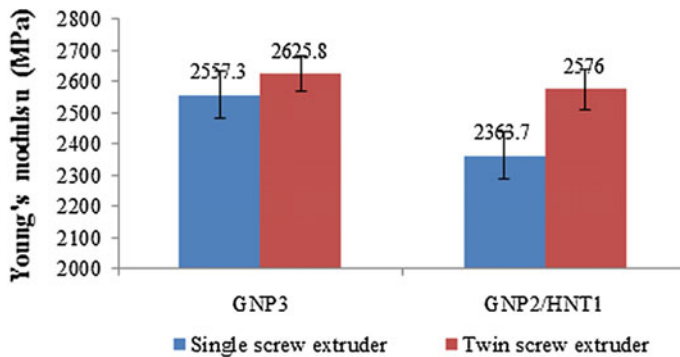k of PET nanocomposites prepared using single screw extruder is higher than using those prepared using twin screw extruder. For example, the elongation at break of PET/GNP2/HNT1 using single screw extruder is 2.84 % while for twin screw extruder is 2.10 %. This can be attributed to the screw design where the screw of single screw is surrounded by flights which act as barrier to the materials inside the screw leading to a higher resident time (Kim and Kwon 1996). Thus, the degree of dispersion is higher for single screw extruder.
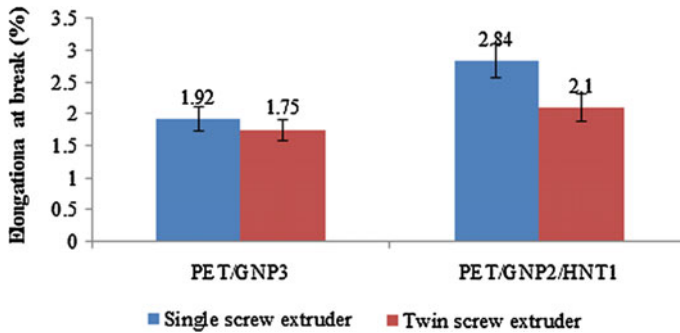
Fig. 9 Effect of extruder on elongation at break of PET nanocomposites

3.2 *Flexural Test*

Table 2 shows the values of flexural strength and flexural modulus of PET, PET/GNP, PET/GNP/HNT nanocomposites. In general, flexural strength was reduced when compared with pure PET. However, flexural modulus was significantly increased compared to pure PET.

3.2.1 Flexural Strength

Figure 10 shows the flexural strength of the PET nanocomposites prepared using single screw extruder. It can be seen that the nanocomposites containing 3 wt% GNP shows a dramatic reduction of flexural strength from 73.0 MPa for pure PET to 49.9 MPa for PET/GNP3. In general, the flexural strength of the PET nanocomposites was reduced when compared to pure PET. By contrast, the tensile strength of PET/GNP shows an improvement when compared to pure PET. This is because the specimens for the tensile test are thinner than specimens for the flexural test which are thick. Therefore, dispersion and alignment of the graphene plates in tensile specimens is better than flexural specimens (Kalaitzidou et al. 2007). Hence, the tensile strength of PET/GNP is improved compared to the pure PET while flexural strength of PET/GNP is reduced compared to pure PET. Similar deduction can be

Table 2 Flexural properties of PET/GNP/HNT nanocomposites

Sample	Flexural strength (MPa)	Flexural modulus (MPa)
Pure PET	73.0 ± 1.0	2347.5 ± 48.4
PET/GNP3 (Single screw)	49.9 ± 5.0	3032.3 ± 130.4
PET/GNP2/HNT1 (Single screw)	63.7 ± 5.0	2982.9 ± 148.8
PET/GNP1/HNT2 (Single screw)	59.7 ± 2.0	2964.3 ± 140.1
PET/GNP3 (Twin screw)	64.1 ± 3.3	2953.3 ± 63.8
PET/GNP2/HNT1 (Twin screw)	71.0 ± 3.0	2924.5 ± 25.1
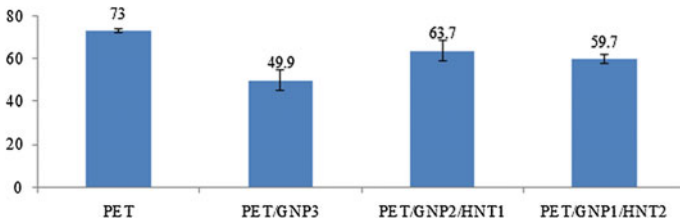
Fig. 10 Flexural strength of PET nanocomposites prepared using single screw extruder
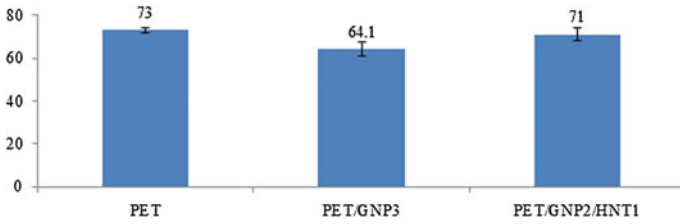
Fig. 11 Flexural strength of PET nanocomposites prepared using twin screw extruder

applied to other PET/GNP/HNT nanocomposites with various ratios. However, the flexural strength is significantly increased from 49.9 MPa for PET/GNP3 to 63.7 MPa for PET/GNP2/HNT1. This may suggest a possible interaction between remnants of hydroxyl group attached to the basal surface of GNP and the hydroxyl attached to the walls of HNT tubes or between hydroxyl group of HNT and terminal hydroxyl group of PET. The flexural strength of the PET/GNP1/HNT2 was reduce slightly to 59.7 MPa compared to PET/GNP2/HNT1. This can be attributed to the alignment of the GNP is better than HNT due its platelet geometry as against HNT which is tubular.

Figure 11 shows the flexural strength of the PET nanocomposites prepared using twin screw extruder. In general, the flexural strength of the PET nanocomposites was reduced when compared to pure PET. However, the reduction of flexural strength is less than PET nanocomposites prepared by single screw extruder. The flexural strength of PET/GNP3 was slightly reduced to 64.1 MPa and then increased to 71.0 MPa for PET/GNP2/HNT1 which is almost same value to pure PET (73.0 MPa). This may also be attributed to the interaction between hydroxyl groups as mention earlier.

Effect of Extruder Type on Flexural Strength of PET Nanocomposites

Figure 12 shows the flexural strength of PET nanocomposites prepared using single screw extruder and twin screw extruder. In general, the flexural strength of PET nanocomposites prepared using twin screw extruder is higher than using those

Fig. 12 Effect of extruder on flexural strength of PET nanocomposites

prepared using single screw extruder. For instance, flexural strength of PET/GNP3 using twin screw extruder is 64.1 MPa while for single screw extruder is 49.9 MPa. The flexural strength for PET/GNP2/HNT1 using twin screw extruder is 63.7 MPa while for single screw extruder is 71.0 MPa. This can be attributed to the higher mechanical shear generated in the twin screw extruder compared to single screw extruder which caused the alignment of the PET nanocomposites prepared by twin screw extruder is better than those prepared by single screw extruder. This orientation is responsible for better properties of the twin screw extruder samples compared to the single screw extruder (Kim and Drzal 2009).

3.2.2 Flexural Modulus

Figure 13 shows the flexural modulus of PET nanocomposites prepared using single screw extruder. In general, all the PET nanocomposites have higher flexural modulus which is more than 24 % increase of flexural strength compared to neat PET. It can be seen that the flexural strength increase significantly from 2347.5 MPa for pure PET to 3032.3 MPa for PET/GNP3. This is the highest value of flexural modulus that was obtained. Therefore, it can be concluded that the optimum formulation for the best flexural modulus of PET is 3 wt%
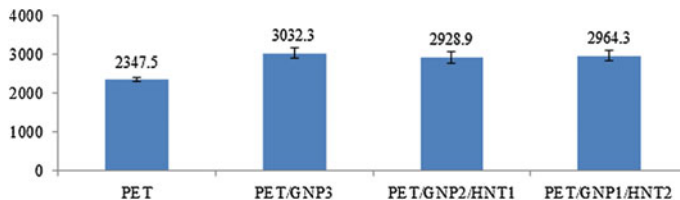
Fig. 13 Flexural modulus of PET nanocomposites prepared using single screw extruder

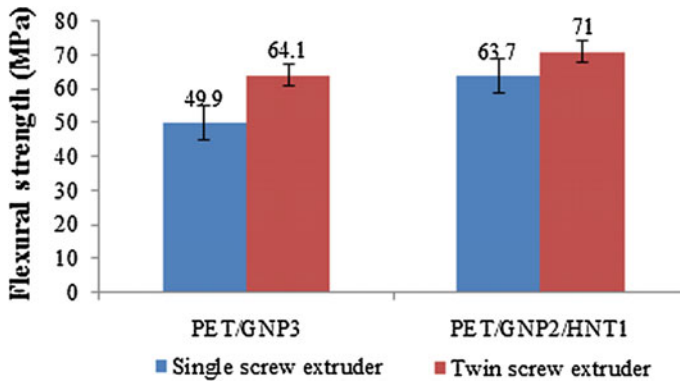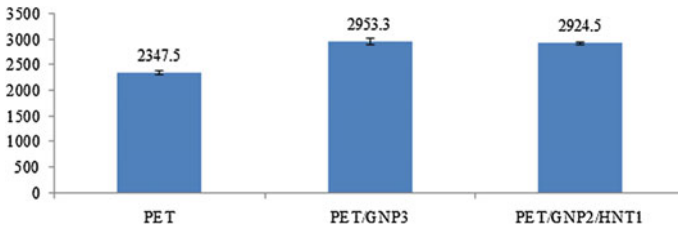**Fig. 14** Flexural modulus of PET nanocomposites prepared using twin screw extruder

GNP. However, the flexural modulus of PET/GNP2/HNT1 and PET/GNP1/HNT2 are slightly lower than PET/GNP3 with 2928.9 MPa and 2964.3 MPa respectively. This indicates that GNP is much stronger than HNT. Since the flexural modulus is a function of concentration of fillers and types of fillers, thus replacement of 1 wt% or 2 wt% of GNP with HNT were slightly bring down the flexural modulus of the nanocomposites.

Figure 14 shows the flexural modulus of PET nanocomposites prepared using twin screw extrusion. It can be seen that the flexural modulus was increased significantly from 2347.5 MPa for pure PET to 2964.3 MPa for PET/GNP3. However, the flexural modulus of PET/GNP2/HNT1 was slightly lower than PET/GNP3 which is about 2924.5 MPa. This observation is similar to the discussion presented for PET/GNP nanocomposites prepared by single screw.

Effect of Extruder Type on Flexural Modulus of PET Nanocomposites

Figure 15 shows the flexural modulus of PET nanocomposites prepared using single screw extruder and twin screw extruder. The flexural modulus for all the formulation was comparable. For example, the flexural modulus of PET/GNP3 prepared by single screw extruder and twin screw extruder were 3032.3 MPa and
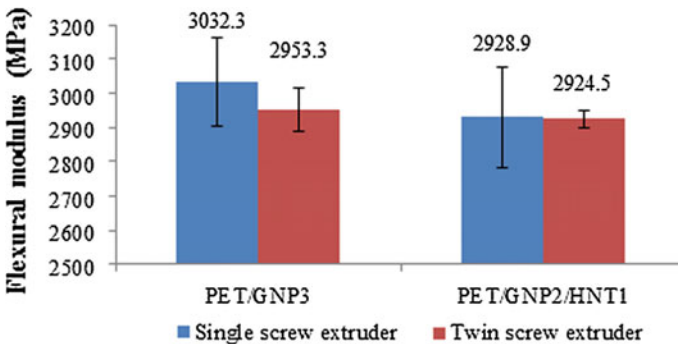
Fig. 15 Effect of extruder on flexural modulus of PET nanocomposites

2953.3 MPa respectively. These values are comparable and it shows that type of machine does not affect the flexural modulus of the PET nanocomposites. The flexural modulus of PET nanocomposites was determined by type of fillers and concentration of the fillers rather than the orientation and dispersion of the fillers.

3.3 Impact Test

Table 3 shows the impact strength of PET, PET/GNP, PET/GNP/HNT nanocomposites. In general, impact strength was reduced when compared with pure PET.

Figure 16 shows the impact strength of PET nanocomposites prepared using single screw extruder. In general, impact strength of PET nanocomposites was lower than pure PET. This can be attributed to the presence of fillers which act as stress concentration sites for crack initiation and growth. For example, the impact strength of PET/GNP3 was reduced dramatically from 35.1 J/m to 17.7 J/m. However, the impact strength of PET/GNP2/HNT1 was significant increased to 27.6 J/m when compared with PET/GNP which is the optimum concentration for PET nanocomposites. Chatterjee et al. (2012) reported that increase in toughness observed in the case of GNP/CNT hybrid was attributed to the crack deflection and crack bridging mechanisms between GNP and CNT. Similar conclusion may apply in this case due similarities in geometry between GNP and HNT. However, the impact strength of PET/GNP1/HNT2 was lower than PET/GNP2/HNT1 which is

Table 3 Impact strength of PET/GNP/HNT composite

Sample	Impact strength (J/m)
PET	35.1 ± 3.4
PET/GNP3 (Single screw)	17.7 ± 2.0
PET/GNP2/HNT1 (Single screw)	27.6 ± 1.7
PET/GNP1/HNT2 (Single screw)	19.3 ± 2.0
PET/GNP3 (Twin screw)	17.7 ± 2.0
PET/GNP2/HNT1 (Twin screw)	23.4 ± 1.6
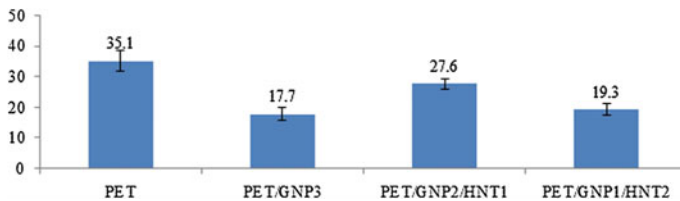
Fig. 16 Impact strength of PET nanocomposites prepared by single screw extruder
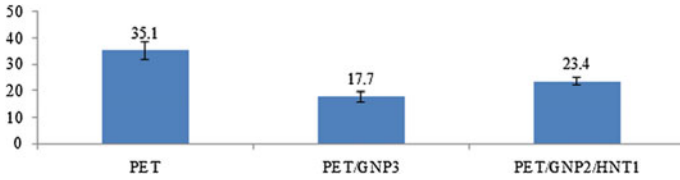
Fig. 17 Impact strength of PET nanocomposites prepared using twin screw extruder

about 19.3 J/m. This can be explained the GNP has higher aspect ratio than HNT due to its platelet geometry as against HNT which is tubular.

Figure 17 shows the impact strength of PET nanocomposites prepared using twin screw extruder. The impact strength was reduced dramatically from 35.1 J/m for pure PET to 17.7 J/m for PET/GNP3. However, the impact strength of PET/GNP2/HNT1 was considerable increased to 23.4 J/m when compared to PET/GNP3. Hence, the trend of changes of impact strength is same as PET nanocomposites prepared by single screw extruder.

3.3.1 Effect of Extruder Type on Impact Strength of PET Nanocomposites

Figure 18 shows the impact strength of PET nanocomposites prepared using single screw extruder and twin screw extruder. In general, the impact strength of PET nanocomposites prepared by single screw extruder is same or slightly higher than those prepared by twin screw extruder. Although the impact strength of PET/GNP3 is same for both machine which is 17.7 J/m, but for the impact strength of PET/GNP2/HNT1 prepared by single screw extruder is slightly higher than those prepared by twin screw extruder. This indicated that the dispersion of GNP and HNT fillers in polymer matrix for single screw extruder is better than twin screw
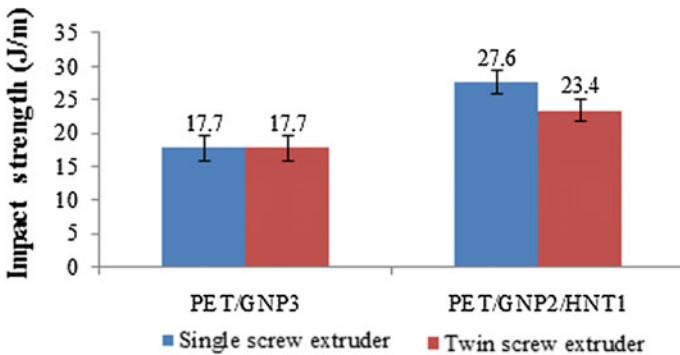
Fig. 18 Effect of extruder on impact strength of PET nanocomposites

extruder. This can be explained by the special screw design of single screw in which the presence of barrier in the surface of screw that increases the retention times of the materials in the screw (Kim and Kwon 1996).

3.4 Differential Scanning Calorimetry Analysis

Table 4 shows the glass transition temperature (T_g), melting temperature (T_m), crystallization temperature (T_c), cold crystallization temperature (T_{cc}), enthalpy change (ΔH_m) and degree of crystallinity (X_c) of PET, PET/GNP, PET/GNP/HNT nanocomposites.

From Table 4 it is evident that there was no any significant change in the melting temperature (T_m) of all PET nanocomposites compared to the neat PET. This indicated that these nanofillers have no much effect on T_m of PET. The crystallization temperatures (T_c) for PET/GNP3 prepared by single screw decreased by just 1 °C compared to pure PET and that of PET/GNP2/HNT1 and PET/GNP1/HNT2 were decreased by about 3 compared to pure PET. However, the T_c for PET/GNP3 and PET/GNP2/HNT1 prepared by twin screw extruder was significant increased from 208.60 °C for pure PET to 216.97 °C and 218.30 °C respectively. This indicated that the mechanical shear generated by the twin screw extruder was higher than the single screw extruder which consequently led to a better mixing process compared to those prepared by single screw extruder (Kim and Drzal 2009).

In general, the degree of crystallinity (X_c) was reduced for PET nanocomposites prepared by both types of extruders compared to pure PET. This is a typical characteristic of nano particles in polymer matrix in most cases. The X_c for PET/GNP3, PET/GNP2/HNT1, PET/GNP1/HNT2 prepared by single screw extruder was 22.2 %, 18.7 % and 24.4 % respectively which a significant reduction

Table 4 Glass transition temperature (T_g), crystallization temperature (T_c), melting temperature (T_m), cold crystallization temperature (T_{cc}), enthalpy change (ΔH_m) and degree of crystallinity (X_c) values for PET, PET/GNP, PET/GNP/HNT nanocomposites

Sample	T_g (°C)	T_m (°C)	T_{cc} (°C)	T_c (°C)	ΔH_m (J/g)	X_c (%)
PET	61.61	247.67	175.14	208.60	39.57	28.6
PET/GNP3 (Single screw)	63.66	248.67	128.27	207.60	29.80	22.2
PET/GNP2/HNT1 (Single screw)	62.30	249.07	127.27	205.27	25.13	18.7
PET/GNP1/HNT2 (Single screw)	61.90	248.47	130.00	205.27	32.80	24.4
PET/GNP3 (Twin screw)	62.77	246.27	229.00	216.97	20.21	15.0
PET/GNP2/HNT1 (Twin screw)	62.07	245.77	119.20	218.30	28.04	20.9

compared to 28.6 % for pure PET. Similarly, the X_c of PET/GNP3 and PET/GNP2/HNT1 prepared by twin screw extruder was also reduced to 15.0 % and 20.9 % respectively. These results indicate that GNP and HNT may act as vast nucleation sites due to their nanosized particles and accelerate the crystallization process in PET matrix. Subsequently less crystalline regions are formed due to shorter time available. This may significantly lower degree of crystallinity of the nanocomposites (Karevan and Kalaitzidou 2013).

For PET nanocomposites prepared by single screw extruder, the lower degree of crystallinity of PET/GNP2/HNT1 with 18.7 % can be attributed to a better dispersion of GNP/HNT into polymer matrix which provides many nucleation sites for crystallization. Since the nucleation sites are many, there will be numerous sites for spherulite growth with each particle exhibiting incomplete growth due to competition. Consequently, the degree of crystallinity is lower. However, the PET nanocomposites prepared by twin screw extruder showed an opposite trends which PET/GNP3 have a lowest X_c value. This can be attributed to the higher shearing force of the twin screw extruder compared to the single screw extruder. This may have caused the GNPs to disperse and align better to the direction of flow than those prepared by single screw extruder (Kim and Drzal 2009). Therefore, more nucleation sites results with higher rates of crystallization and lower degree of crystallinity (Guo and Chuan 2012). In addition, the higher aspect ratio of graphene also helped the graphene formed more nucleating site for crystallization.

In general, the cold crystallization temperature (T_{cc}) of PET nanocomposites was lower than pure PET except PET/GNP3 prepared by twin screw extruder which is significantly higher than pure PET. For PET nanocomposites prepared by single screw extruder, the T_{cc} for PET/GNP3, PET/GNP2/HNT1 and PET/GNP1/HNT2 were 128.27 °C, 127.27 °C and 130.00 °C respectively which is much lower than T_{cc} for pure PET which is about 175.14 °C. This can be attributed that the presence of GNP and HNT nanofillers strongly affect the T_{cc} by acting as heterogeneous nucleation site for crystallization process (Al-Jabareen et al. 2013). The T_{cc} for PET/GNP2/HNT1 is lower than PET/GNP3 can be explained by the increased no of particles and better dispersion of the hybrid fillers. Hence, the degree of crystallization is lower. Nevertheless, T_{cc} of PET/GNP1/HNT2 is slightly higher than PET/GNP2/HNT1 is due to nature of the fillers, shape, particle size effects, and interactions between the fillers (Todorov and Viana 2007).

For PET nanocomposites prepared by twin screw extruder, the T_{cc} for PET/GNP3 is 229.00 °C which is much higher than T_{cc} for pure PET which is about 175.14 °C. In contrast, the T_{cc} of PET/GNP2/HNT1 prepared by twin screw extruder is 119.20 °C which was significant lower than pure PET. The higher T_{cc} of PET/GNP3 can be attributed to agglomeration of GNP in the polymer matrix. Due to this agglomeration GNP fillers acts as inhibitor which inhibit the crystallization process and hence higher T_{cc} (Todorov and Viana 2007). Furthermore, the lower value of T_{cc} for PET/GNP2/HNT1 prepared by twin screw extruder can be explained by better dispersion of hybrids fillers and also between nanofiller and matrix as mentioned above.

Generally, the glass transition temperature T_g for PET nanocomposites prepared by both type of extruders were slightly higher than pure PET. This indicated that the stiffness of GNP and HNT fillers restricted the motion of PET molecular chains thereby reducing the flexibility of the matrix. Similar effect can be seen in the case of percent elongation at break where characteristic stiffness of the nanofillers reduced the elongation at break.

4 Conclusion and Future Perspectives

This research investigated the effect of GNP/HNT hybrid nanofillers on the mechanical and thermal properties PET composites.

From the tensile test, the results showed that the optimum GNP/HNT content is 2 wt% GNP and 1 wt% HNT where there is better dispersion of the nanfillers in the polymer matrix which facilitated the interaction between remnants of hydroxyl group attached to the basal surface of GNP and the hydroxyl attached to the walls of outer walls HNT tubes or between hydroxyl group of HNT and terminal hydroxyl group of PET. By comparing type of extruders, PET nanocomposites produced by single screw extruder exhibits higher tensile stregth than those prepared by twin screw extruder. In contrast, PET nanocomposites prepared by twin screw extruder exhibits higher flexural strength than those prepared by single screw extruder. In the DSC, the melting temperature remain essentially unaffected. However, the cold crystallization temperature and degree of crystallinity of PET/GNP/HNT was lower than pure PET. This shows that GNP and HNT may act as vast nucleation sites due to their nanosized particles and accelerate the crystallization process in PET matrix. Subsequently less crystalline regions are formed due to shorter time available. PET/GNP2/HNT1 have lowest T_{cc} and X_c which showed that the degree of dispersion to polymer matrix is highest. This study has highlighted the potential applications of hybrid nanofillers consisting of graphene and haloysites nanotubes. Its believed however, that the moderate properties improvements achieved in this study can be further enhanced by the chemical modification of the nanofillers especially the nanoclay. This will improve their dispersion in polymer matrix and lead to even higher improvements in mechanical properties such as toughness and strengths. It will also be of interest to have a morphological analysis of specimens to assess the degree of filler dispersion.

References

Al-Jabareen, A., Al-Bustami, H., Harel, H., Marom, G.: Improving the oxygen barrier properties of polyethylene terephthalate by graphite nanoplatelets. J. Appl. Polym. Sci. **128**(3), 1534–1539 (2013)
Chatterjee, S., Nafezarefi, F., Tai, N.H., Schlagenhauf, L., Nuesch, F.A., Chu, B.T.T.: Size and synergy effects of nanofiller hybrids including graphene nanoplatelets and carbon nanotubes in mechanical properties of epoxy composites. Carbon **50**(15), 5380–5386 (2012)

Du, M.L., Guo, B.C., Jia, D.M.: Thermal stability and flame retardant effects of halloysite nanotubes on poly(propylene). Eur. Polymer J. **42**(6), 1362–1369 (2006)

Du, M.L., Guo, B.C., Wan, J.J., Zou, Q.L., Jia, D.M.: Effects of halloysite nanotubes on kinetics and activation energy of non-isothermal crystallization of polypropylene. J. Polym. Res. **17**(1), 109–118 (2010)

Guo, W.Y., Chuan, K.Y.: Crystallization, dispersion behavior and the induced properties through forming a controllable network in the crosslinked polyester-SiO2 nanocomposites. J. Appl. Polym. Sci. **123**(3), 1773–1783 (2012)

Kalaitzidou, K., Fukushima, H., Miyagawa, H., Drzal, L.T.: Flexural and tensile moduli of polypropylene nanocomposites and comparison of experimental data to Halpin-Tsai and Tandon-Weng models. Polym. Eng. Sci. **47**(11), 1796–1803 (2007)

Karevan, M., Kalaitzidou, K.: Understanding the property enhancement mechanism in exfoliated graphite nanoplatelets reinforced polymer nanocomposites. Compos. Interfaces **20**(4), 255–268 (2013)

Kim, H., Abdala, A.A., Macosko, C.W.: Graphene/Polymer nanocomposites. Macromolecules **43**(16), 6515–6530 (2010)

Kim, S., Drzal, L.T.: Comparison of exfoliated graphite nanoplatelets (xGnP) and CNTs for reinforcement of EVA nanocomposites fabricated by solution compounding method and three screw rotating systems. J. Adhes. Sci. Technol. **23**(12), 1623–1638 (2009)

Kim, S., Kwon, T.: Enhancement of mixing performance of single-screw extrusion processes via chaotic flows: Part I. Basic concepts and experimental study. Adv. Polym. Technol. **15**(1), 41–54 (1996)

Kuilla, T., Bhadra, S., Yao, D.H., Kim, N.H., Bose, S., Lee, J.H.: Recent advances in graphene based polymer composites. Prog. Polym. Sci. **35**(11), 1350–1375 (2010)

Lecouvet, B., Horion, J., D'Haese, C., Bailly, C., Nysten, B.: Elastic modulus of halloysite nanotubes. [Research Support, Non-U.S. Gov't]. Nanotechnology **24**(10), 105704 (2013)

Lee, C., Wei, X.D., Kysar, J.W., Hone, J.: Measurement of the elastic properties and intrinsic strength of monolayer graphene. Science **321**(5887), 385–388 (2008)

Paul, D.R., Robeson, L.M.: Polymer nanotechnology: nanocomposites. Polymer **49**(15), 3187–3204 (2008)

Prashantha, K., Lacrampe, M.F., Krawczak, P.: Processing and characterization of halloysite nanotubes filled polypropylene nanocomposites based on a masterbatch route: effect of halloysites treatment on structural and mechanical properties. Express Polym. Lett. **5**(4), 295–307 (2011)

Singh, B.: Why does halloysite roll?–A new model. Clays Clay Miner. **44**(2), 191–196 (1996)

Todorov, L.V., Viana, J.C.: Characterization of PET nanocomposites produced by different melt-based production methods. J. Appl. Polym. Sci. **106**(3), 1659–1669 (2007)

Ye, Y.P., Chen, H.B., Wu, J.S., Ye, L.: High impact strength epoxy nanocomposites with natural nanotubes. Polymer **48**(21), 6426–6433 (2007)

Zhang, H.B., Zheng, W.G., Yan, Q., Yang, Y., Wang, J.W., Lu, Z.H., Yu, Z.Z.: Electrically conductive polyethylene terephthalate/graphene nanocomposites prepared by melt compounding. Polymer **51**(5), 1191–1196 (2010)

Nanoclay Reinforced on Biodegradable Polymer Composites: Potential as a Soil Stabilizer

M.I. Syakir, N.A. Nurin, N. Zafirah, Mohd Asyraf Kassim and H.P.S. Abdul Khalil

Abstract Polymeric composites (biodegradable and non-biodegradable materials) have been extensively used in diverse types of applications ranging from automotive industries to packaging industries using natural fibres, man-made fibre and other biomass as reinforced materials. Soil erosion, triggered by two main events, anthropogenic activities and natural causes conceivably gives bad impacts to living things by altering the stability of the ecosystem and causing human to lose lives and damage their properties. Nanoclay reinforced on biodegradable polymeric is the preferred candidate for developing soil stabilizer materials as this material possesses hydrophilic properties that adsorb liquid molecules to handle erosion of soil. The capacity of the materials to retain a significant amount of water that releases gradually into the ground as it decays will not only mitigate soil erosion, but also improves soil fertility and productivity by enhancing the aeration of water and air in soil. Recent studies concerning nanoclay/biodegradable composite materials are cited in this paper. Overall, this chapter summarizes the definition, the properties, as well as the applications of nanoclay and biodegradable materials, to further generate the idea of combining both of these materials for soil erosion mitigation. Potentially, this fundamental study pertaining to special characteristics of nanoclay/biodegradable composite offers limelight on the green solution potentials for cost-effective and sustainable plantations management.

Keywords Nanoclay · Nanocomposites · Biodegradable · Soil stabilizer

M.I. Syakir (✉) · N.A. Nurin · N. Zafirah · M.A. Kassim · H.P.S. Abdul Khalil
School of Industrial Technology, Universiti Sains Malaysia, Penang, Malaysia
e-mail: misyakir@usm.my

M.I. Syakir
Centre for Global Sustainability Studies, Universiti Sains Malaysia, Penang, Malaysia

1 Nanoclay

Clay, which has grain size less than 4 μm, results from weathering and erosion of rocks over a long time. Clay minerals have a sheet-like structure connected by aluminium and are composed of tetrahedral silicon that consists of four oxygen atoms and one silica at the center. In fact, the four main groups of clays are kaolinite, illite, montmorillonite (MMT), and chlorite. Among the other clays, MMT, which has a 2:1 layered structure, owing to two silica tetrahedrons sandwiching an alumina octahedron (Pusch and Yong 2006) in its structure, is one of the most commonly used clays in the synthesis of nanocomposites (Li et al. 2005).

MMT expands largely more than other clays due to loosely bound individual crystals and elastic water content of MMT that increases extensively in volume when it absorbs water. Plus, the presence of sodium as the predominant exchangeable cation also can result in high amount of expansion in the samples. Furthermore, the existence of adjoining oxygen layers in each unit strengthens the bond between the layers and thus, all the minerals are susceptible to swelling and show a marked cation exchange capacity (Fayed and Attewell 1965).

In fact, the applications of nanocomposites have been growing at a rapid rate. Baksi et al. (2008) claimed that by 2010, the worldwide production of nanocomposite would have been expected to exceed 600,000 tons and cover the areas of drug delivery systems, anti-corrosion barrier coatings, ultraviolet (UV) protection gels, lubricants and scratch free paints, new fire retardant materials, new scratch/abrasion resistant materials, as well as superior strength fibers and films in the next 5–10 years.

Nanoclay, which has been modified from the surface of MMT mineral, has a high aspect ratio with at least one dimension of the particle in the nanometer range. Besides, the purity and the capacity of cation exchange are both critical characteristics of nanoclay as they respectively determine the mechanical properties and provide the surface activities of this mineral. Nanoclay, in fact, has been extensively used to modify polymer by reinforcing and improving the mechanical, the thermal, and the barrier properties of the polymer. Nonetheless, some of the unpredictable properties, including increasing strength of thermoplastics, reducing gas permeability, improving solvent resistance, and enhancing flame retardant properties, are exhibited by using only a small portion of nanoclay into the polymer matrix (Hussain et al. 2007; Chowdary and Kumar 2015). Moreover, coupling agents, such as silane, are used to stabilize the dissemination of nanoclay, as well as to enhance the bonding of nanoclay to the polymer matrix (You et al. 2011).

1.1 Definition of Nanoclay

The term 'nano' is derived from the Greek nanos, meaning dwarf and when used as a prefix indicates 10^{-9}. Nanotechnology is the design, the characterization, the

production, as well as the applications of materials, devices, and systems conducted at a nanoscale, which is about 1–100 nm (nm) (Allhoff et al. 2010; Ramsden 2014). Besides, materials with particle size less than 2 mm in equivalent spherical diameter is called 'clay fraction', which include nanoclay as particles with diameter less than 100 nm (Floody et al. 2009).

Moreover, the type of clay that is frequently used in nanocomposites belongs to the family of 2:1 layered silicates, such as MMT and saponite. Their structure composts of layers are made up of two tetrahedrally coordinated silicon atoms layer with octahedral sheet of either aluminium or magnesium hydroxide in intermediate. The thickness of the layered sheet is about 1 nm each, while its length ranges from tens of nanometers to more than one micron, depending on the layered silicate. Meanwhile, the Van der Waals gap located between the platelets of the stacked layer is called the interlayer or the gallery.

Furthermore, isomorphic substitution can occur in the layers where Al^{3+} and Mg^{2+} are exchanged with positively charged ions, Fe^{2+} and Li^+ respectively for both ions. The layers of many clay minerals carry a permanent negative charge. The exchangeable inorganic cations (Na^+, Ca^{2+}) balance the interlayer sites via isomorphic substitution. Moreover, alkali earth cations, such as Na^+ and Ca^{2+}, which are located in the interlayer galleries, increase the hydrophilic attribute of the clay by counteracting with global negatively charged platelets.

Besides that, most polymers, mainly the biopolyesters, are considered to be organophilic compounds; which means, they have an affinity for organic substances. Thus, in order to obtain better affinity between the filler and the matrix, the inorganic cations located inside the galleries (Na^+, Ca^{2+}, etc.) are generally exchanged by ammonium or phosphoniumcations bearing at least one long alkyl chain, and possibly, other substituted groups (Bordes et al. 2009). The resulting clays are called organomodified layered silicates (OMLS) makes MMT abbreviated as OMMT. The modification of layered silicate affects the nanostructure of the material, and subsequently, the properties of nanocomposites.

1.2   Properties of Nanoclay

The physical, the chemical, and the biological properties of nano materials differ from the properties of individual atoms and molecules or bulk matter. Hence, nano particles have the potential to remote all fundamental properties of materials, such as their melting temperature, magnetic properties, charge capacity, and even their color, without changing the chemical compositions of the material (Baksi et al. 2008). Nano materials are recognized for its low cost, low-to-moderate reinforcement (Morton 1987), versatilities, and stiffening properties (Barlow 1993). Table 1 shows few past researches regarding the properties of nanoclay.

The particle of clay that exists in nano form has particular and special features that make it different from other fillers. Nanoclay particle, which has a platelet shape, has thickness and width of only 1 nm and 70–150 nm respectively. Besides,

Table 1 Properties of nanoclay

Properties of nanoclay	References
Low cost, low-to-moderate reinforcement	Morton (1987)
Large surface area leads to special features, such as increased strength and chemical or heat resistance of the material	Holister et al. (2003)
Hydrophilic properties	Wang et al. (2006), Mohan and Kanny (2015)
High specific surface area due to its nanometer size and high aspect ratio	Litchfield and Baird (2008)

nanoclay has high surface interaction with polymer matrix due to its specific interfacial area and therefore, has the ability to alter the properties of the material drastically even inserted of only a few percent (2–7 %). The ratio of surface-area-to-volume ratio increases as the particle gets smaller.

In addition, when nanoclay is combined with polymers, it possesses enhanced mechanical and superconducting properties for advanced applications. A lot of interactions also happen between the hybrid materials in nanocomposites as large surface area leads to special features, such as increased strength and chemical or heat resistance of the material (Holister et al. 2003).

Furthermore, particles that are small enough may start to exhibit quantum mechanical behavior. However, the properties of nanoparticles cannot be easily described due to the increased influence of exterior atoms or quantum effects, for example, lately, it had been reported that perfectly-formed silicon 'nanospheres' with 40–100 nm diameters were found to be among the hardest material known, falling between sapphire and diamond (Holister et al. 2003).

Nanomaterials (nanoclay) too have properties in electronic, kinetic, magnetic, and optical, which are very particular from those of their bulk counterparts. For example, nanomaterials are translucent because their particles have smaller wavelength than light. Besides, clay has many interesting properties, such as high elastic modulus and easy to access at low cost. However, its application is largely restricted because clay dispersion cannot be easily achieved (Muzny et al. 1996).

1.3   *Applications of Nanoclay*

Nanoclay has recently attracted the interest of many researchers and scientists for its potential applications mainly ascribed to high aspect ratio and dimension of nanoscale silicate layers dispersed within the polymer matrix. Strong interactions can be established between the silicate layers and the polymer chains, even with incorporation of a very small amount of clay, which would in turn, lead to substantial changes in both thermal and mechanical properties of nanocomposites compared to common microcomposites.

The mechanical properties of nanocomposite materials have been improved, thus, leading to the various types of applications in automotive (e.g., door handles and engine covers), and other general industrials (e.g., power tool housings and covers for mobile phones). Nanoclay is also applied for food packaging, fuel tanks, films, and flammability reduction (Baksi et al. 2008).

In addition, small quantities of nanoclay have been improved to give significant impact to the gaseous barrier property of materials. Nanoclay particles slow down the transmission of oxygen through the composite and results in almost zero oxygen transmission in rather a long period of time. This special feature has sparked wide interest in nanoclay composites in food packaging applications. Significantly improved strength and barrier properties also make polymer-clay nanocomposites suitable for packaging materials (Baksi et al. 2008).

Polymer nanocomposite also has been proven to restrict flammability behavior with only 2 % of nanoclay loading. Though conventional microparticle filler incorporation is also capable to be used as flame retardant agents, this usually causes reduction in various other important properties. Nanoclay approaches, however, are able to either maintain or enhance other properties and characteristics of materials. Thus, it is assumed that the incorporated nanoclays accumulate at the surface of polymer and form a barrier to oxygen diffusion when the polymer matrix is burned and gasified during combustion, hence slowing down the burning process (Sen 2001).

For instance, a study revealed that nanoclay is capable in reducing solvent transmission through polymers and this comes with great concern in the automotive industry as incorporation of nanoclay in fuel tank had been found to reduce fuel transmission, thus contributing to significant material cost reductions. Nanoclay incorporation has also been shown to intensify transparency and to reduce haze characteristics of films through the alteration of crystallization behavior brought about by nanoclay particles.

Nanoclay also can be used to produce fibers that act as carriers for drugs, fragrances or other active agents and to enable the controlled release of the incorporated species (Ghosh 2011). Recently, clays have contributed to the protection and the remediation of environment, such as MMT, as effective barriers to isolate radioactive wastes, while clay particle as pollutants absorbent of organic compounds and inorganic trace metals from soils and groundwater (Ghosh 2011).

Meanwhile, in the rubber industry, clay has been widely used as a non-black filler (Barlow 1993; Zhu and Wool 2006). A few studies have been reported on the modification of polystyrene/polybutadiene (Subana et al. 2013), polypropylene (Vu et al. 2004; Lopattananon et al. 2014), and polysulfide (Pradhan et al. 2009) of elastomer by using nanoclay. The mechanical properties and the tensile strength of the bio-based elastomers have significantly improved (Zhu and Wool 2006) even with only a small amount of clay content is involved. Even at 8 wt% of nanoclay concentration, the nanoclay particles are very well-dispersed in the polymer matrix (Pradhan et al. 2009).

2 Biodegradable Polymer

Biodegradable polymers have gained vast interest in the past few years due to arising environmental awareness, the mark-up of oil prices in recent times, and declining fossil resources as synthetic polymers (Ghanbarzadeh and Almasi 2013). Biodegradable polymers like plant fibers are not justsustainable, but also flexible and easy to obtain and used for several different industrial products including pulp and paper, rope, cords, reinforcement in composite matrices (Abdul Khalil 2000). Plus, the improved properties of plant fiber reinforced composites make it competitive to the synthetic composites, hence, increased the use of it in diverseapplications (Abdul Khalil et al. 2007; Hariharan and Abdul Khalil 2005). Abdul Khalil and Suraya (2011) stated that, the natural fibers have the potential to replace glass fibers either alone or mix with many other materials.

This leads to the development of biopolymers produced from varies sources, eco-friendly with lower energy consumption, biodegradable, and non-toxic to the environment. Polylactic acid (PLA), biodegradable aliphatic polyester, which can be derived from 100 % renewable resources, such as corn and sugar beets, has attracted more attention among other biopolymers (Krishnamachari et al. 2009). Besides, the most significant advantages of biodegradable polymers are that they become degraded naturally, thus their decomposition helps to enrich the soil and stabilize landfills by reducing the volume of waste, besides lessening the labor cost for removal of plastic wastes in the environment.

Since biopolymers are biodegradable and the main productions are obtained from renewable resources, they perform an interesting alternative route to common non-degradable polymers for short-life range applications, such as packaging and agriculture (Muzny et al. 1996). Nonetheless, most biopolymers are expensive compared to thermoplastic and are still impractically used in daily life. Therefore, it is necessary to improve them to compete with this common thermoplastic. Nevertheless, at presence, many biopolymers have been turned into products that have further altered their structure, thus making them non-biopolymer. For example, crude oil tends to degrade itself in environment; however, once it is turned into plastic, it becomes an unsustainable product that is indecomposable and pollutes the environment.

2.1 Definition of Biodegradable Polymer

Biodegradable material, which can be derived from both naturally and synthetically, is a type of material that is capable to decompose into carbon dioxide, methane, water, inorganic compounds, and biomass under aerobic or anaerobic conditions where the major mechanism involved is enzymatic action of micro-organisms within a specific period of time (Kržan 2012; Leja and Lewandowicz 2010). It can be either biodegraded into air, soil or water. Oxidation and hydrolysis are the two

main degradation processes of biodegradable materials like proteins, polysaccharides, and nucleic acids (Leja and Lewandowicz 2010).

The properties and the breakdown mechanism are determined by their exact structure (e.g., bond type, solubility, and copolymers), and environment (e.g., pH, water, and microorganisms). Besides, the most important factor affecting the biodegradability of polymeric materials is the chemical structure of polymer as it is responsible to the stability, the reactivity, the hydrophilicity, and the swelling behavior of the functional group (Kyrikou and Briassoulis 2004). Moreover, physical and physico-mechanical properties, such as molecular weight, porosity, elasticity, and morphology, are the other vital aspects that determine the degradation mechanisms of polymer (Anderson and Shive 1999; Acemoglu 2004).

2.2 Types of Biodegradable Polymer

Biodegradable polymers can be classified into their chemical composition, origin, synthesis method, processing method, economic importance, application, etc. (Avérous and Pollet 2012). Generally, there are two groups of natural polymers; those obtained from natural resources and synthetic polymers produced from oil. On the other hand, Avérous and Boquillon (2004) reported that biodegradable materials are categorized into four different classes (Fig. 1); polymers that are obtained from renewable resources, biomass (e.g., starch, and cellulose), microbial production (e.g., polyhydroxyalkanoates) and chemically of agro-products (e.g., polylactic acid), as well as non-renewable resources, which are petrochemical resources (e.g., polyesteramides).
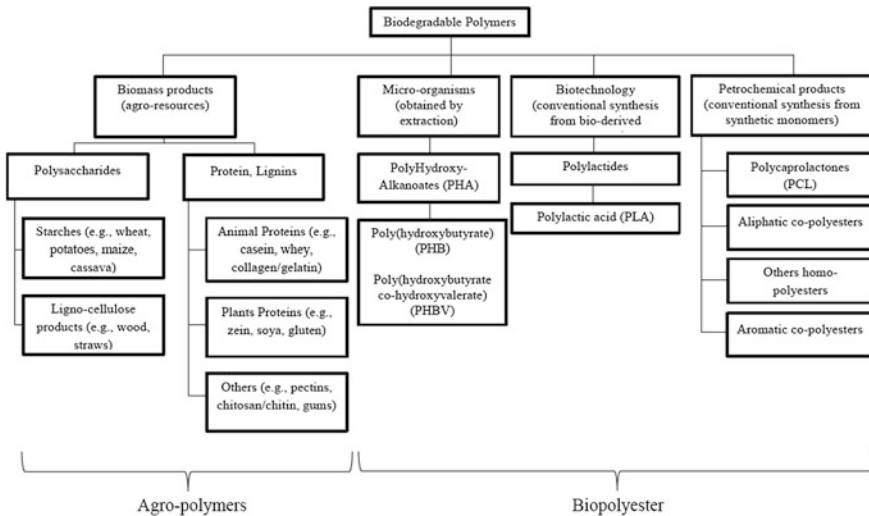

Fig. 1 Classification of biodegradable polymers (Avérous and Boquillon 2004)

The first family is agro-polymers (e.g., polysaccharides) obtained from biomass via fractionation. Polysaccharides and proteins are the two examples under this category. Polysaccharides are the most abundant macromolecules in the ecosystem, which comprise of long chains of monosaccharide units linked together with glycosidic bonds. Polysaccharides, such as starch, chitin, chitosan, and pectins, are some examples of the essential structural elements of plants and animals exoskeleton. Meanwhile, proteins are large biomolecules that consist of one or more long chains of amino acid and they are produced by animals, plants, and bacteria. Most proteins are comprised of linear polymers built from a series of up to 20 different amino acids. Soybean proteins, corn proteins, wheat gluten, casein, and gelatin are some examples of protein. In fact, there are four distinct aspects in the structure of a protein, which are primary structure, secondary structure, tertiary structure and quaternary structure. Primary structure refers to the linear sequence of amino acids in polypeptide chain that connected together by covalent bonds. Secondary structure is a regularly repeating local structures stabilized by hydrogen bonds, such as the alpha helix or the beta sheet while tertiary structure is the overall shape of a single protein molecule; the spatial relationship of the secondary structures to another and controls the basic function of the protein. Last but not least, the structure formed by many proteins and function as a single protein complex called quaternary structure.

The second and third families are polyesters, obtained via fermentation from biomass or from genetically modified plants (e.g., polyhydroxyalkanoate: PHA) and by synthesis from monomers obtained from biomass (e.g., polylactic acid: PLA), respectively. Meanwhile, the fourth family refers to polyesters that are totally synthesized by the petrochemical process (e.g., polycaprolactone: PCL, polyesteramide: PEA, and aliphatic or aromatic copolyesters). A large number of these biodegradable polymers (biopolymers) are commercially available. They show a large range of properties and they can compete with non-biodegradable polymers in different industrial fields (e.g., packaging).

Shah (2015) highlighted study done by Avérous and Boquillon (2004) and generalized the division of biodegradable polymers into natural polymers, synthetic polymers, and modified natural polymers. Natural polymers or biopolymers are produced naturally by living organisms and are all degradable type of polymers. Polysaccharides (e.g., starch, and cellulose), polyesters (e.g., polyhydroxyalkanoates), proteins (e.g., silk), and hydrocarbons (e.g., natural rubbers) are the most common natural polymers. On the other hand, synthetic polymers, which do not origin from natural resources, can be subdivided into carbon chain backbone and heteroatom chain backbones. Synthetic polymers can be identified from their polymer structure, polymer physical properties, and environmental condition. The degradation condition of synthetic polymers can be generalized as Table 2.

Modified natural polymers are the modification of natural polymers so that environmentally acceptable polymer can be developed. They can be further divided to blends and grafts, chemically modified, oxidation and esterification. Hence, the alteration should not interfere with the biodegradation process. Besides, the modification can be made by blending with other natural and synthetic polymers,

Table 2 Degradation condition of synthetic polymers depends on the properties of polymers (Shah 2015)

Properties of polymers	Degradation condition
Carbon-chained	Unfavorable for biodegradation
Chain branching	Non-biodegradable
Condensation polymerization	Unlikely to be biodegraded
Lower molecular weight	Susceptible to biodegradation
Crystallinity	Reduces biodegradability
Higher hydrophilic/hydrophobic	Better for degradation

grafting of other polymeric composition and chemical modification to introduce some desirable functional groups via oxidation or some other simple chemical reactions, such as esterification or etherification.

2.3 Properties of Biodegradable Polymer

According to Vroman and Tighzert (2009), biodegradable polymers should be biocompatible, bioabsorbable, and mechanically resistant to be used as biopolymers. Biocompatible is the ability of the substances to adapt in new environment without being treated as a foreign object. Bioabsorbable or biodegradable means the polymers should be able to decompose upon completing the intended purpose while mechanically resistant means the material should possess equivalent or greater mechanical stability to ensure high reliability in the period of use. Nevertheless, some properties of biodegradable materials may be varied, according to their chemical and physical structures that differ from one another. The general properties of biodegradable polymers are briefly tabulated in Table 3.

Table 3 Properties of biodegradable polymers based on past researches

Properties of biodegradable polymers	References
Degradable, high water vapor permeability, good oxygen barrier, not electrostatically chargeable, low thermal stability	Lörcks (1998), Petersen et al. (1999)
Intoxicant, high mechanical strength, capable of controlling degradation rates	Ratner et al. (2004)
Mostly soluble in water, poor mechanical properties	Ma et al. (2005)
Poor mechanical and barrier properties, sensitive to water, brittle, low mechanical strength properties and permeability, good mechanical and optical properties, very sensitive to moisture	Vroman and Tighzert (2009)
Solid, high molecular weights, comprised of repeating macromolecules, compostable	Kumar et al. (2011)
Hydrophilic and poor mechanical properties	Ghanbarzadeh and Almasi (2013)

All biodegradable polymers originate from renewable resources (such as starch, protein, fiber), readily available, and also offer low-cost materials compared to most synthetic plastics. Researches regarding these materials have begun a few years ago for they are low in cost, environmental friendly, and for the fact that they are able to compete in the context of strength per weight of material (John and Thomas 2008). Plus, biodegradable polymers have been used for medical purpose since a long time ago. These materials are the best choice rather than synthetic materials because they are intoxicant, have high mechanical strength, and are capable of controlling degradation rates (Ratner et al. 2004).

Besides, biodegradable materials must be stable and sturdy enough to be used in their particular application and upon completing their intended purpose; they should be broken down in the environment from the action of naturally occurring microorganisms (Kumar et al. 2011). When they degrade, they tend to accumulate until 95 % of dry weight of the bacteria. Biopolymers also limit the emission of carbon dioxide during the manufacturing process. The degradation properties of biopolymers give rise to good possibilities in crop management as the decomposition of biopolymers to soil increases soil fertility and productivity.

Moreover, biodegradable materials also can easily absorbed water; owing to hydrophillicity characteristics that allow them to easily interact with water-soluble enzyme. However, the hydrophilic characteristics of certain biodegradable polymers, such as soy protein, lead to poor mechanical and barrier properties of the polymers (Vroman and Tighzert 2009). Natural polymer like starch is mostly soluble in water, but has poor mechanical properties (Ma et al. 2005). Thus, mixing biopolymers with other materials is able to strengthen both the physical and the mechanical properties of biopolymers. Furthermore, reinforcement of fiber with polymers is a very good idea because it produces high mechanical properties and dimensional stability by merging with low weight fiber. This is very important in technical applications, such as automotive industry.

In fact, some biopolymers, such as starch-based materials, are sensitive to water, brittle, and have low mechanical strength properties (Vroman and Tighzert 2009). Plus, even though chitin and chitosan are insoluble in most solvents that limited their applications; chemical modifications can be carried out to chitosan since its chemical structure contains amino and hydroxyl reactive groups. Apart from chemical modification, the blending technique is also one of the approaches that can be employed to upgrade the mechanical properties of these materials.

Other than that, the attribute of low penetrability in starch film is suitable for application of food packaging. When the film is incorporated with proteins and polysaccharides, it possesses good mechanical and optical properties, but it is very sensitive to wetness; thus, has poor water barrier properties. In contrary to the combination of film with lipids, it makes the film to be more resistant to moisture.

Additionally, John and Thomas (2008) asserted that natural fibers can be considered as composite-by-nature due to the presence of cellulose fibrils that are aligned along the length of the fiber, which provides maximum flexibility strength and stiffness. They also mentioned that cellulose in natural fibers is insusceptible to high pH or oxidizing agents. Despite of that, it can be easily hydrolyzed by acid to

water-soluble sugars. In addition, Wollerdorfer and Bader (1998), based on their study, claimed that natural fibers have been identified as the potential materials to reinforce thermoplastic components and injection of moldable materials mainly due to their low density and ecological advantages.

2.4 Applications of Biodegradable Polymer

In recent years, biodegradable materials have attracted vast attention due to their various applications in many sectors, mainly in packaging, medicine, agriculture, ecological and automotive industries. However, biopolymers in the packaging industry have received more attention than those designated for any other application. In fact, many countries have begun to produce packaging materials by using biodegradable materials due to the increase in environmental awareness; acknowledging that synthetic packaging materials have a negative impact and are harmful to the nature. Therefore, scientists and researchers are now working on further development of biodegradable plastics based on polyester and starch. According to Janssen and Moscicki (2009), due to the high specialization and the values of the larger units, medical applications of biodegradable materials have developed faster than the others.

2.4.1 Packaging Material

Biodegradable materials can be employed to produce several types of packaging materials, such as garbage bags, disposable cutlery and plates, food packaging and shipping materials. Molecular weights, chemical structures, crystallinites, and processing conditions are some of the important factors that affect the physical characteristics of polymers for packaging. Nowadays, most consumers demand environmental friendly products from food industry companies, including supermarkets and processors, which lead the growth of biodegradable packaging industry to expand exaggeratedly. The common biodegradable polymers have two types of materials; polymers that originate from renewable plant raw materials, which are rather difficult to decompose, as well as polymers formed by chemical synthesis reactions, which are easily degraded and mineralized by microorganisms. A study conducted by Mitrus et al. (2009) showed that compostable packaging degrades faster than a banana skin, while plastic packages or carrier bags take longer time to do the same.

2.4.2 Medicine

The modern field of medicine would be impossible without the use of diverse natural or artificial materials. Some of these materials are meant to be stay forever in

the body, while some are only intended for temporary use and have to be removed or excreted from the body. This step can be avoided if the materials used have the ability to degrade themselves and are absorbed into the body cells after their intended purposes have been completed. This can be done through the application of biodegradable material for medical purpose. However, Ikada and Tsuji (2000) reported that most clinically used biopolymers lack biocompatibility and this is a huge problem, especially when they are used permanently as implants in our body.

In medicine, biodegradable polymers have great ability, primarily for controlled drug delivery, materials supporting surgical operation (adhesives, sutures, and surgical meshes), for orthopedic devices (screws, pins, and rods), dental applications (filler after a tooth extraction), tissue engineering (intraocular lens, dental implant, and breast implant), and artificial organs for temporary or permanent assistance (artificial kidney, artificial heart, and vascular graft), also not to mention typical applications for disposable products (e.g. syringe, blood bag, and catheter).

The application of biodegradable synthetic polymers has been initiated since past few years and since then, various studies have been conducted in view of the fact that the specifications are quite complex as it involves important organs in human, thus, the polymer must be biocompatible, not to induce an inflammatory response, and must have suitable mechanical, as well as processing characteristics. Plus, the degradation products must be sure to be harmless and easily reabsorbed or excreted by the human body.

2.4.3 Agriculture

The application of polymer in agriculture is catching attention in science, especially in the polymer chemistry field. The purpose of using polymer in agriculture is to maximize water and land efficiency without giving negative impact to the environment and natural resources. Polymer benefits agriculture by improving the physical properties of soil through the increment of water holding capacity, water use efficiency, and soil permeability, besides reducing the irrigation frequency, thus stopping erosion and water run-off.

Polymers are also used to increase the effectiveness of herbicide and pesticide by allowing lower doses to be used, as well as to protect the environment indirectly by lowering pollution and cleaning-up existing pollutants (Ekebafe et al. 2011). Polymer biocide, which is also known as antimicrobial polymers, is a class of polymer with the ability to inhabit the growth of microorganisms, such as protozoans, bacteria, and fungi. These polymers have been designed to copy antimicrobial peptides properties that are used in the immune system of biotic factors, such as humans, plants, and animals, to kill bacteria. Polymer biocide also enhances the efficiency of some existing antimicrobial agents, besides minimizing the environmental problem by lessening the remaining toxic agents, surging their efficiency and selectivity, as well as by extending the lifetime of antimicrobial agents, in addition to being nonvolatile and chemically stable. Thus, it cannot be lost via

volatilization, photolytic decomposition, and transportation (Ekebafe et al. 2011; Kenawy et al. 2007).

Meanwhile, in agriculture, biodegradable plastic mulches offer an alternative to polyethylene mulch production and disposal (Corbin et al. 2013; Huang et al. 1990). When the materials degrade, it acts as compose fertilizers, thus improving soil fertility and productivity. The polyethylene plastic mulch also benefits the production of crop by controlling weeds, conserving soil moisture, increasing soil temperature, increasing crop yield and quality, has a relatively low cost, and is readily available (Corbin et al. 2009; Miles et al. 2012). Moreover, plastic mulch, biodegradable plant pots, disposable composting containers, and bags also are used in this industry (Huang et al. 1990). The pots are inserted directly into the soil, and as the plants begin to grow, they will breakdown slowly.

2.4.4 Ecological

Biodegradable polymer has diverse advantages towards the preservation and the conservation of environment. The major application of this biopolymer is in the plastic-related industries as these industries are the main contributor to pollution even some plastic products can be re-used after adequate processing. Biodegradable plastic is not just low cost, but it also has high strength of mechanical properties, besides being harmless to the environment. Like other non-biodegradable plastics, biodegradable plastic also maintains the mechanical strength and other properties during their practical use, as well as being degraded to low-molecular-weight compounds, such as H_2O, CO_2 and non-toxic by-products with the aid of microorganisms (Gebelein and Carraher 1994).

2.4.5 Automotive

The environmental legislation restrained automakers to decrease the disposal of vehicle wastes, thus dramatically increasing the interest of automotive industry in producing vehicles from biodegradable composites. Campos et al. (2008) developed a front loudspeaker made from two different biodegradable composites; polylactic acid (PLA) and blend of starch, as well as cellulose acetate (SCA), which is reinforced by cellulose spent fibers. In fact, a study by Ashori (2008) revealed that wood–plastic composites (WPCs) are now being widely used for the replacement of some automotive components, such as fiberglass, dashboards, door panels, seat cushion, steels, etc. Moreover, attributes like low density, and high strength, modulus, stiffness, as well as biodegradability, are some of the special properties of plant fibers that make them compatible to be used in the automotive industry; not to mention, the unlimited availability of these raw materials that comes from renewable sources.

For instance, Mercedes-Benz Corporation has brought biodegradable materials to the next level as this company produces a completely biodegradable vehicle

named Mercedes-Benz BIOME. It is made of a material called BioFibre that is lighter than metal or plastic (around 394 kg), yet stronger than steel (Banks 2010). Kolybaba et al. (2003) also asserted that bio-based cars are more economical as they are lighter, thus reduce fuel costs. In addition, the vehicle can run on "BioNectar4534" stored in the car's BioFibre once it is on the road and the only by-product produced is oxygen. Although the use of biopolymer is still new in the automotive industry, a lot of researches should be conducted in order to ensure the evolution of this material in the future.

3 Nanoclay and Biodegradable Polymers

The revolution of polymer-clay nanocomposite was first achieved about 15 years ago. It involves the hybrid of nanometer-thick layers of clay and polymers to produce new materials. A composite material is formed when two or more materials with different physical or chemical properties are combined together to produce completely different characteristics from the original individual components. The properties of polymeric composite materials are mainly determined by three essential elements; the resin, the reinforcement (particles and fibers), and the interface between them (Huang and Netravali 2007). The technology, process, properties and applications of nanoclay/biodegradable polymer are briefly explained in this section.

3.1 Technology of Nanoclay and Biodegradable Polymers

Since 1990, Nylon-6 clay nanocomposites, which are one of the most important polymer-nanoclay composites, have been studied and analyzed. Since then, the materials have been slowly and widely used in various applications, particularly in automotive production, such as Toyota.

Researchers at the Toyota Central Research Laboratories had successfully studied Nylon-6 clay nanocomposites as these materials showed dramatic improvement for mechanical, thermal, and chemical properties, even only with small percent of nanoclay used, compared to pristine polymer (Floody et al. 2009; Alexandre and Dubois 2000; Kojima et al. 1993; Okada and Usuki 1995) and began them in their automobiles ever since. They prepared nylon-clay nanocomposite by inserting Ɛ-caprolactam into an organoclay and polymerizing the monomer by heating (Fukushima and Inagaki 1987).

The very first commercial application used for Nylon-6 clay nanocomposites was as timing belt cover for Toyota cars, in collaboration with Ube Industries in 1991 and shortly after that, engine covers on Mitsubishi's GDI engines was introduced by Unitika using the same nanocomposites (Edser 2002). The revolution was continued as in August 2001, General Motors and Basell announced the

application of clay/polyolefin nanocomposites as a step assistant component for GMC Safari and Chevrolet Astro vans (Cox et al. 2004). Noble Polymers also has developed clay/polypropylene nanocomposites for structural seat backs in the Honda Acura (Patterson 2004), while Ube is developing clay/nylon-12 nanocomposites for automotive fuel lines and fuel system components (Gao 2004).

3.2 Process of Nanoclay and Biodegradable Polymers

Generally, diverse processing techniques are available to prepare nanoclay/polymer composites. This chapter section briefly depicts the technique and the processes involved in producing these composites. Researchers, eventually, have successfully discovered various ways and techniques to produce these materials. Nanoclay can be produced through condensation from vapor, chemical synthesis, and solid-state processes, such as milling before being coated with hydrophilic or hydrophobic substances, depending on the desired application (Holister et al. 2003).

Meanwhile, the melt compounding technique has become the main choice of method for polymer/nanocomposites recently because it is the most industrially practicable approach as it offers advantages to both economic and environment (Krishnamachari et al. 2009). Polymer nanocomposites can be synthesized by using diverse methods, as in Fig. 2.
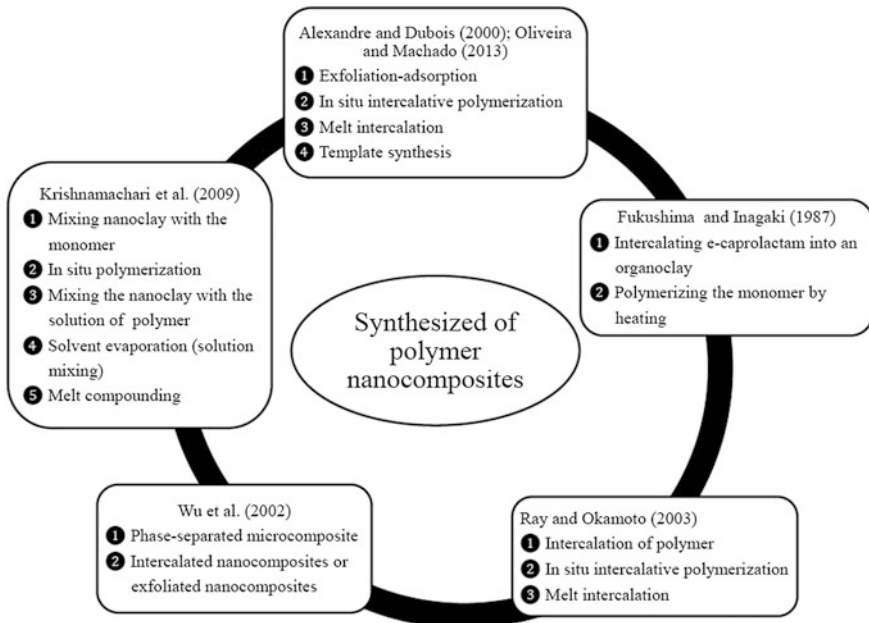

Fig. 2 Synthesization of polymer nanocomposites

Additionally, proper dispersion of the nanoparticles in the polymer matrix is a key component to achieve great improvements of final nanocomposites as uneven dispersion of nanoparticles decreases the mechanical properties of polymers. Abdul Khalil et al. (2009) mentioned that the modulus and tensile strength of hybrid compounds are affected by the arrangement of fillers in the compound itself. Normally, nanoclay agglomerates when mixed with water. This happens due to the interaction of different types of forces that occurs at the surrounding environment, including van der Waals forces and water surface tension. Agubra et al. (2013) mentioned that homogeneous dispersion of nanoclay created large surface area for the polymer/filler interaction thus, contributed to a strong interfacial bond between the fiber and the polymer.

Hence, in order to achieve proper dispersion of nanoclay in the polymer matrix, it must be deagglomerated by modifying the interaction between forces. The dispersion of nanoclay in polymer matrix can be done by using three different mixing combinations (Agubra et al. 2013; Bensadoun et al. 2011). The first one is by using ultrasonic sonication that uses ultra sound to detach the individual nanoparticles from the clay bundles that open up interlayer spacing to the material. Sound waves generated from ultrasonication spread into water resulting in irregular pressure cycles, which break the bonding forces, thus leading to deagglomeration of nanoclay. The second one is by thinky mixing, which involves centrifugal force rotation of nanoclay and the material under vacuum pressure to break the electrostatic force holding the clay bundles together, thus dispersing the nanoclay, and lastly, magnetic stirring that creates a vortex effect from the stirring magnet to break the bond that holds clay together. These three methods are then, followed by three roll-milling intended to enhance the efficiencies of the individual mixing methods. However, the combination of magnetic stirring and thinky mixing, followed by three roll-milling, was found to offer excellent clay exfoliation result, while the combination of ultrasound sonication and three roll-milling resulted in poor clay exfoliation (Agubra et al. 2013). This had been mainly because of the degradation of polymer network due to sonication process.

3.3 Properties of Nanoclay Reinforced on Polymers

Hybridization of polymer and nanocomposites is one of the newest revolutionary steps of the polymer technology, particularly in the reinforcement of nanocomposites and thermoplastic starch polymers (Ghanbarzadeh and Almasi 2013). The reinforcement, in fact, aims to create new properties of the materials besides strengthening mechanical structure of the polymers. Table 4 below simplifies the properties of nanoclay and polymers according to few past studies.

Excellent enhancement of properties had been discovered by Dufresne and Cavaille (1998), as well as Angles and Dufresne (2000), with reinforced microcrystalline whiskers of starch and cellulose in thermoplastic starch polymer, as well as synthetic polymer nanocomposites. This may be due to transcrystallisation

Table 4 Properties of nanoclay reinforced on polymers

No	Properties of nanoclay polymers	References
1	Improves fire, mechanical and barrier properties compared to polymer composites containing traditional fillers	Awad et al. (2009), Porter et al. (2000), Pinnavaia and Beal (2000)
2	Tensile strength increased by 25 % with addition of 2 wt%, fracture toughness increased by about 56 % and 77 % for the insertion of 1 and 2 wt% nanoclay, accordingly, critical strain energy release rates increased by 140 % and 190 % with incorporation of 1 and 2 wt%, nanoclay respectively	Wang et al. (2006)
3	High mechanical properties (tensile and modulus strength)	Okada et al. (1990), Lan and Pinnavaia (1994), Giannelis (1998), LeBaron et al. (1999), Gilman (1999), Liu et al. (1999), Chen et al. (2003), Fu and Naguib (2006), Wang et al. (2006), Ali et al. (2013)
4	Improved mechanical and water vapor permeability properties of nanocomposite films about 20 % to 60 %	Hashemi et al. (2014)
5	Enhanced thermal stabilities and water vapor barriers properties	Ferfera-Harrar and Dairi (2014)
6	High tensile modulus, notched impact strength significantly improved for samples with up to 2 wt% nanoclay additives	Hegde et al. (2013)
7	Improved mechanical properties of nanoclay loading at 2.5 wt% and reduced water absorption of polymer	Yadav and Yusoh (2015)

processes at the matrix/fiber interface. Moreover, a study conducted by Almasi et al. (2010), which tested the effect of nanoclay into starch/carboxymethyl cellulose blends, improved the film impermeability and tensile of the material properties. Mohan and Kanny (2015) claimed that corn starch films, when filled with nanoclay fillers, improved dimensional stability and plugging property, depending on the concentration of nanocomposite structure and clay concentration. They also observed better enhancement of material stability at only a small percentage of nanoclay concentration (2–3 wt%) as a result of exfoliated structure and proper dispersion of nanoclay in the matrix polymer. In addition, tensile strength of the polymers also was increased by 13 % with only 3 wt% of nanoclay. Moreover, Rhim et al. (2006) investigated the antimicrobial activity by using agar diffusion disk method and revealed that nanocomposite film prepared with the organically modified MMT (Cloisite 30B) demonstrated antimicrobial activity against *Listeria monocytogenes* and *Staphylococcus aureus*, which are gram-positive type bacteria, while the pristine MMT did not show any antimicrobial activity.

Other than that, Avella et al. (2005) homogeneously dispersed nanocomposites in thermoplastic starch through polymer melt processing technique to be used as

food packaging and the results also showed that nanoclay effectively increased the mechanical parameters of starch films, such as modulus and tensile strength. Nanoclay reinforced on modified starch enhanced tensile strength, improved the impermeability of materials (Almasi et al. 2010), and upgraded biodegradation properties of the biopolymers (Shayan et al. 2015). Nanoclay also has significantly boosted up the tensile strength and the elongation of quince seed mucilage (QSM) edible films by only 2 % concentration of nanoclay only (Shekarabi et al. 2014). It also significantly increased the glass transition temperatures of QSM-films to 83.4 °C with the same concentration of nanoclay compared to control films. Plus, incorporation of nanoclay on QSM-films also improved the gas barrier properties of the films.

Nanoclay also improved oxygen barrier properties, enhanced stiffness, and reduced extensibility of nanocomposite (Kuktaite et al. 2014). High amount of hydrogen bonds in natural polymers structure provided good barrier properties against oxygen and grease, especially in dry conditions compared to synthetic polymers.In fact, at present, biopolymer/nanoclay has been studied by numerous researchers to be applied in food packaging. This is because; bio-hybrid nanocomposite has been proven to intensify the barrier properties against oxygen, water vapor, and UV light transmission (Vartiainen et al. 2010), thus slowing down microorganism activity towards the food due to absence of air, water, and light. Above all, the researches and the results gained from the incorporation of nanoclay and biodegradable suggest that the addition of nanoclay is not just eco-friendly, but it also can increase the physical properties of biopolymer, thus, this hybridization materials can be applied in the future for more advanced applications.

3.4 Applications of Nanoclay and Biodegradable Materials

The revolution of replacing non-biodegradable petroleum-based plastic materials has gained vast attention as this synthetic material has a bad impact upon the environment due to non-biodegradability and non-renewable resources characteristics. This has led scientists to develop a new and environmental friendly product with satisfaction of physical structure, not to mention the accessibility to gain the raw materials of biopolymers, such as polysaccharides, proteins, and lipids.

To date, only a few studies have focused on the applications of nanoclay/biodegradable polymer composites for commercial use, especially in the packaging industry, because nanotechnology in biodegradable material is quite a new thing. In this section, the applications of this hybrid material have been tabulated as in Table 5 below and are discussed briefly accordingly.

A study conducted by Sothornvit et al. (2009), and supported by Alavi et al. (2014) revealed that whey protein isolate (WPI)/nanoclay composite films displayed a great potential in the food packaging industry. WPI, which is a by-product in cheese industries, has high potential as a food packaging material; owing to

Table 5 Applications of nanoclay on vary type of biodegradable materials

Applications of nanoclay and biodegradable polymers	References
Whey protein isolate (WPI)/nanoclay composite as a food packaging material	Sothornvit et al. (2009), Alavi et al. (2014)
Barley protein (BP)/nanoclay film containing grapefruit seed extract (GSE) used as an antimicrobial packaging for controlling mushroom quality during storage	Shin et al. (2013)
Sesame seed meal protein (SSMP)/nanoclay composite films in food packaging	Lee et al. (2014)
Chitosan (exoskeleton of crustaceans)/nanoclay composite film containing *Silybum marianum L.* extract (SME) used as an antioxidant food packaging	Ghelejlu et al. (2016)

transparent and long films shelf life, improving quality, and intensifying safety of food packaging. The use of bio-nanocomposite in food packaging is not only eco-friendly, but also protects the food and enhances its shelf life (Sozer and Kokini 2008).

On the other hand, Lee et al. (2014) suggested that sesame seed meal protein (SSMP)/nanoclay composite films were compatible to be applied in food packaging. Sesame (*Sesamumindicum L.*) is a type of flowering plant that belongs to the family of Pedaliaceae and it is cultivated for its edible seeds (Kafiriti and Mponda 2009). They found that the surface and the cross section of the SSMP/nanoclay composite film was flatter and had fewer pores and cracks than the SSMP film without nanoclays with the addition of only 5 % of nanoclay in the film, which resulted in the best physical properties of it.

Moreover, Shin et al. (2013) proposed that barley protein (BP)/nanoclay film containing grapefruit seed extract (GSE) can be used as an eco-friendly packaging for controlling mushroom quality during storage. They produced BP film by extracting barley flour. Nanoclay, then, was incorporated into BP film to improve the physical properties of the BP film. They found that the composite film of BP to Cloisite Na^+ with the ratio of 4:1 exhibited the best physical properties among the other films prepared. This is evidence that nanoclay has great ability to strengthen material structures even with a small percentage. Moreover, they demonstrated the ability of GSE to inhibit microbial growth in mushrooms during storage by reducing the populations of total aerobic bacteria, yeast, and molds.

In addition, Ghelejlu et al. (2016) revealed that reinforcement of nanoclay to chitosan (exoskeleton of crustaceans) matrix containing *Silybummarianum L.* extract (SME) improved water vapor permeability, water resistance, and mechanical features of the chitosan films. They noted that the presence of nanoclay increased the melting point of chitosan composite film, while the insertion of SME at minimal loading completely improved water vapor permeability and water solubility of the films, besides darkening the appearance of films. SME films also enhanced antioxidant activity and barrier properties of the material compared to other natural extracts. Incorporation of natural antioxidants into packaging materials

can preserve quality, safety, and sensory properties of food naturally rather than adding additives directly to the food, because oxidation is the main factor that affects the shelf life due to impairment of lipids in food (Imran et al. 2014).

Even though the applications of nanoclay in biodegradable materials are still lacking in other industries, researchers have begun to investigate these hybrid materials since past few years ago. Pauzi et al. (2014), in their study, tested the integration of organic nanoclay into palm-oil based polyurethane (PU) in foam industries and observed enhanced thermal stability and compressive strength of foam than pristine PU foam. Haq et al. (2014) also conducted a study by combining multiscale nanoclay with industrial unprocessed raw hemp. The combination for both elements successfully produced an outstanding stiffness–toughness balance, besides enhancing absorption and barrier properties.

4 Problems and Challenges of Nanoclay and Biodegradable Materials

Due to the low application of biodegradable materials with nanoclay, researchers have discovered some reasons on why this hybrid has failed to work with other any application, except in the packaging industry. With that, Muller et al. (2007) mentioned that even starch is the best candidate among other natural polymers that promises attractive combination on not just price, availability, and thermoplastic behavior, but also the ability of starch to biodegrade in environment. However, the hydrophilic feature of this biodegradable starch-based film has been identified as the main drawback as this material tends to reduce its stability and has poor mechanical properties (Almasi et al. 2010) when applied to different environmental conditions.

Furthermore, biodegradable polymers are well-known as materials that cause no harm to the environment as they are produced from natural resources, such as agricultural raw materials. Even so, they still encounter some obstacles to break through the commercialized market, such as cost and their ability to perform. According to Ray et al. (2003), fragility, unable to withstand changes of temperature, low melt viscosity, and high gas permeability, are some reasons that have restricted their extensive use in applications. They also show some restrictions in terms of thermal resistance, as well as barrier and mechanical properties (Ghanbarzadeh and Almasi 2013).

Vartiainen et al. (2010) said that hydrophilic properties also are the main challenge for packaging purposes that restricted further application of most biopolymers. Nevertheless, hydrophobic features owned by most of the synthetic polymers make them incompatible to be incorporated with hydrophilic starch, thus resulting in poor mechanical properties (Almasi et al. 2010). Hansen and Plackett (2008) claimed that films and coatings produced from natural materials usually are hygroscopic, which causes the materials to gain or lose water in order to reach

equilibrium at humidity condition (Yadav and Yusoh 2015). Therefore, numerous ways have been determined by researchers to ameliorate the functional characteristics of starch films. One way is through the combination of starch with other polymers or fillers like nanoclay. Proper dispersion through varies techniques should be giving more attention as it will determined the mechanical properties of the end product.

5 Potential in Soil Stabilizers

Reinforcement of nanoclay in biodegradable materials as a soil stabilizer should be given more attention and a detailed study should be conducted. With the hydrophilic characteristic of biodegradable materials being a problem to vast applications, soil stabilizers from biopolymers have high possibilities to be efficiently used due to their hydrophilic feature, especially when combined with nanoclay. Biopolymers, thus, could be used as absorbent materials in horticulture, healthcare, and agricultural applications because they are insoluble in water, but absorb water rather well (Kiatkamjornwong et al. 2000). In fact, some potential natural materials that have been identified for this purpose include palm oil empty fruit bunch (POEFB), jute, wood-stranded material, dried stalks of barley, oats, rice, and wheat.

Moreover, biopolymers with hydrophilic properties must be able to absorb a maximum amount of water, and to retain the water before slowly releasing it into the ground (Fig. 3). These materials then will be able to decompose in a specific period of time, depending on the shelf life of materials upon completing the intended purpose. This application is based on the concept of "back to nature" because instead of eliminating the waste product, it is used to protect the soil from
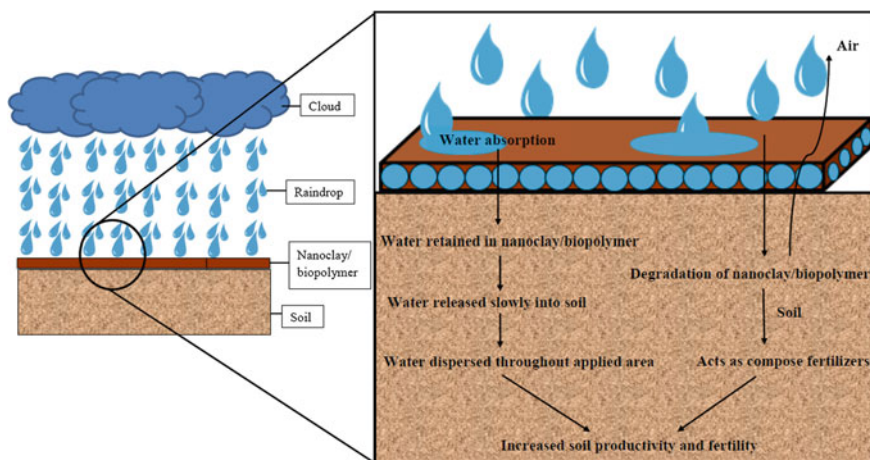
Fig. 3 Illustration of nanoclay reinforcing on biodegradable materials as soil stabilizer

erosion by stabilizing the soil structure. It also helps to improve soil fertility and productivity through degradation by providing nutrients to soil.

Other than that, biodegradable polymers are characterized by poor mechanical properties; therefore, reinforcing of nanomaterials must be added to overcome this deficit. Interaction between nanoclays surfaces with biopolymers assist dispersion of nanoclay within the polymer matrix, thereby resulting in greater properties advancements, even at lower filler loadings. However, homogenous dispersion of nanoclays into polymer matrix is still challengeable since they are hydrophilic in their natural state, unequally distributed, and require proper techniques to avoid aggregation between the platelets in the materials (Nazaré et al. 2006).

Additionally, development of biopolymers-based materials, such as the nano-biocomposites, can be developed, as at present, the industry is mostly concerned with sustainable development; resulting in low production cost of biopolymers (Bordes et al. 2009). Therefore, these materials will be financially and technically competitive towards synthetic polymer-based nanocomposites; opening a new revolution for the plastic industry.

6 Future Perspective

Natural material/nanoclay reinforced polymeric materials are the subject of many scientific and research projects. The mixed of these two materials will improve the physical properties of natural material not to mention, it is compostable which makes it environmentally-friendly product. Although there are many problems arise due to hydrophilicity of biopolymer, this hybrid shows great potential to be used in other applications other than packaging industry. Nanoclay/biopolymer has great potential as soil stabilizer as hydrophilicity is one of the crucial features because the material must be able to hold the water to reduce soil erosion. Hybrid material from natural material/nanoclay reinforced polymer materials can be developed at lower cost while increasing sustainability and functionality. Further study is needed in the future to determine the maximum water holding capacity of materials as well as the adsorption of water. Research and progress in this area will not only able to reduce natural disaster and enhance sustainability of nature, but also benefits the economy of agricultural industry. The compatibility of this hybrid to environment also should be investigated.

7 Conclusion

This study has simplified the major concerns pertaining to biodegradable polymers and nanoclay, their definition, types, properties, and applications. Environmental awareness and limitation of petroleum-based products have persuaded researchers to further discover new materials that originate from renewable biomass resources

and to enable natural recycling. This is due to the negative impact created by synthetic polymers to the ecosystem regarding waste accumulation and operation. Moreover, in line with the developments in technology, the production and the usage of such material should be dismissed as it is obviously perilous to the environment. Biopolymer wastes like jute, wood-strand materials, agricultural straw, and POEFB are now finding applications in a wide range of industries. Nanotechnology, particularly nanoclay, is another promising area to be integrated with biopolymers.

References

Abdul Khalil, H.P.S.: Effect of fiber treatments on mechanical properties of coir or oil palm fiber reinforced polyester composites. J. Appl. Polym. Sci. **78**, 1685–1697 (2000)

Abdul Khalil, H.P.S., Hanida, S., Kang, C.W., Fuaad, N.A.N.: Agro-hybrid composite: the effects on mechanical and physical properties of oil palm fiber (EFB)/glass hybrid reinforced polyester composites. J. Reinf. Plast. Compos. **26**, 203–218 (2007)

Abdul Khalil, H.P.S., Kang, C.W., Khairul, A., Ridzuan, R., Adawi, T.O.: The effect of different laminations on mechanical and physical properties of hybrid composites. J. Reinf. Plast. Compos. **28**(9), 1123–1137 (2009)

Abdul Khalil, H.P.S., Suraya, N.L.: Anhydride modification of cultivated kenaf bast fibers: morphological, spectroscopic, and thermal studies. Bioresources **6**, 1122–1135 (2011)

Acemoglu, M.: Chemistry of polymer biodegradation and implications on parenteral drug delivery. Int. J. Pharm. **277**(1–2), 133–139 (2004)

Agubra, V., Owuor, P., Hosur, M.: Influence of nanoclay dispersion methods on the mechanical behavior of e-glass/epoxy nanocomposites. Nanomaterials **3**(3), 550–563 (2013)

Alavi, S., et al. (eds.): Polymers for Packaging Applications. Apple Academic Press, New Jersey (2014)

Alexandre, M., Dubois, P.: Polymer-layered silicate nanocomposites: preparation, properties and uses of a new class of materials. Mater. Sci. Eng. R **28**(1–2), 1–63 (2000)

Ali, M.H.M., Kahder, M.M., Al-Saad, K.A., Al-Meer, S.: Properties of nanoclay PVA composites materials. QSci. Connect **1** (2013)

Allhoff, F., Lin, P., Moore, D.: What is Nanotechnology and Why Does it Matter?: From Science to Ethics. UK, Wiley-Blackwell (2010)

Almasi, H., Ghanbarzadeh, B., Entezami, A.A.: Physicochemical properties of starch-CMC-nanoclay biodegradable films. Int. J. Biol. Macromol. **46**, 1–5 (2010)

Anderson, J.M., Shive, M.S.: Biodegradation and biocompatibility of PLA and PLGA microspheres. Adv. Drug Deliv. Rev. **28**(1), 5–24 (1999)

Angles, M.N., Dufresne, A.: Plasticized starch/tunicin whiskers nanocomposites. Macromolecules **33**(22), 8344–8353 (2000)

Ashori, A.: Wood–plastic composites as promising green-composites for automotive industries. Bioresour. Technol. **99**(11), 4661–4667 (2008)

Avella, et al.: Biodegradable starch/clay nanocomposite films for food packaging applications. Food Chem. **93**(3), 467–474 (2005)

Avérous, L., Boquillon, N.: Biocomposites based on plasticized starch: thermal and mechanical behaviours. Carbohydr. Polym. **56**(2), 111–122 (2004)

Avérous, L., Pollet, E. (eds.): Biodegradable Polymers in Environmental Silicate Nano-Biocomposites, pp. 13–39. Springer, London (2012)

Awad, W.H., et al.: Material properties of nanoclay PVC composites. Polymer **50**(8), 1857–1867 (2009)

Baksi, S., Basak, P.R., Biswas, S.: Nanocomposites—technology trends and application potential. In: International Conference and Exhibition on Reinforced Plastics (ICERP-2008), Mumbai, 7–9 Feb 2008 (2008)

Banks, G.: Mercedes-Benz BIOME concept—could cars be grown in a lab? (2010). http://www.gizmagcom/mercedes-benz-biome-concept/17096/. Accessed 28 Mar 2016

Barlow, F.W.: Rubber Compounding: Principles, Materials, and Techniques, 2nd edn. CRC Press, Fluorida (1993)

Bensadoun, F., et al.: A study of nanoclay reinforcement of biocomposites made by liquid composite molding. Int. J. Polym. Sci. **2011**, 1–10 (2011)

Bordes, P., Pollet, E., Averous, L.: Nano-biocomposites: biodegradable polyester/nanoclay systems. Prog. Polym. Sci. **34**(2), 125–155 (2009)

Campos, A.R., Cunha, A.M., Tielas, A., Mateos, A.: Biodegradable composites applied to the automotive industry: the development of a loudspeaker front. [Abstract]. Mater. Sci. Forum **587–588**, 187–191 (2008)

Chen, L., Wong, S., Pisharath, S.: Fracture properties of nanoclay-filled polypropylene. J. Appl. Polym. Sci. **88**(14), 3298–3305 (2003)

Chowdary, M., Kumar, M.N.: Effect of nanoclay on the mechanical properties of polyester and s-glass fiber (Al). IJAST Int. J. Adv. Sci. Technol. **74**, 35–42 (2015)

Corbin, A., Miles, C., Hayes, D., Dorgan, J., Roozen, J.: Suitability of biodegradable plastic mulches. In: Certified Organic Production American Society of Horticulture Conference, St Louis, Missouri, 25–28 July 2009 (2009)

Corbin, A., et al.: Using biodegradable plastics as agricultural mulches. Washington State University Extension Fact Sheet FS103E, Washington State University, Pullman, WA (2013)

Cox, H., Dearlove, T., Rodgers, W., Verbrugge, M., Wang, C.S.: Nanocomposite systems for automotive applications. In: 4th World Congress in Nanocomposites, EMC, San Francisco, 1–3 Sept 2004 (2004)

Dufresne, A., Cavaille, J.Y.: Clustering and percolation effects in microcrystalline starch reinforced thermoplastic. J. Polym. Sci. Part B **36**(12), 2211–2224 (1998)

Edser, C.: Auto applications drive commercialization of nanocomposites. Plast. Addit. Compd. **4**(1), 30–33 (2002)

Ekebafe, L.O., Ogbeifun, D.E., Okieimen, F.E.: Polymer applications in agriculture. Biochemistry **23**(2), 81–89 (2011)

Fayed, L., Attewell, P.B.: A simplified, non-rigorous, tabular classification of clay minerals with some explanatory notes. Int. J. Rock Mech. Min. Sci. Geomech. **2**(3), 271–274 (1965)

Ferfera-Harrar, H., Dairi, N.: Green nanocomposite films based on cellulose acetate and biopolymer-modified nanoclays: Studies on morphology and properties. Iran. Polym. J. **23**(12), 917–931 (2014)

Floody, M.C., Theng, B.K., Mora, M.L.: Natural nanoclays: applications and future trends — a Chilean perspective. Clay Miner. **44**(2), 161–176 (2009)

Fu, J., Naguib, H.E.: Effect of nanoclay on the mechanical properties of PMMA/Clay nanocomposite foams. J. Cell. Plast. **42**(4), 325–342 (2006)

Fukushima, Y., Inagaki, S.: Synthesis of an intercalated compound of montmorillonite and 6-polyamide. J. Incl. Phenom. Macro **5**, 473–482 (1987)

Gao, F.: Clay/polymer composites: the story. Mater. Today **20**, 50–55 (2004)

Gebelein, C., Carraher, C. (eds.): Biotechnology and Bioactive Polymers. Plenum Press, New York (1994)

Ghanbarzadeh, B., Almasi, H.: Biodegradable polymers. Biodegradation—Life of Science, pp. 141–185. InTech, Croatia (2013)

Ghelejlu, S.B., Esmaiili, M., Almasi, H.: Characterization of chitosan–nanoclay bionanocomposite active films containing milk thistle extract. Int. J. Biol. Macromol. **86**, 613–621 (2016)

Ghosh, A.: Nano-clay particle as textile coating. Int. J. Eng. Technol. **11**(5), 34–36 (2011)

Giannelis, E.P.: Polymer-layered silicate nanocomposites: synthesis, properties and applications. Appl. Organomet. Chem. **12**, 675–680 (1998)

Gilman, J.W.: Flammability and thermal stability studies of polymer layered-silicate (clay) nanocomposites. Appl. Clay Sci. **15**, 31–49 (1999)

Hansen, N., Plackett, D.: Sustainable films and coatings from hemicelluloses: a review. Biomacromolecules **9**, 1493–1505 (2008)

Haq, M., Burgueño, R., Mohanty, A.K., Misra, M.: Hybrid bio-based composites from UPE/EML blends, natural fibers, and nanoclay. Macromol. Mater. Eng. **299**(11), 1306–1315 (2014)

Hariharan, A.B.A., Abdul Khalil, H.P.S.: Lignocellulose-based hybrid bilayer laminate composite: Part I—Studies on tensile and impact behavior of oil palm fiber-glass fiber-reinforced epoxy resin. J. Compos. Mater. **39**, 663–684 (2005)

Hashemi, J., Neves, M., Yoshino, T., Nakajima, M.: Investigation the effects of different composition of chitosan/clay on the nanocomposite film properties. In: Proceedings International Conference of Agricultural Engineering, Zurich, 6–10 July 2014 (2014)

Hegde, R.R., Bhat, G.S., Spruiell, J.E., Benson, R.: Structure and properties of polypropylene-nanoclay composites. J. Polym. Res. **20**(12) (2013)

Holister, P., Weener, J.W., Román, C., Harper, T.: Nanoparticles. Científica **3**, 1–11 (2003)

Huang, J.C., Shetty, A.S., Wang, M.S.: Biodegradable plastics: a review. Adv. Polym. Technol. **10**(1), 23–30 (1990)

Huang, X., Netravali, A.: Characterization of flax fiber reinforced soy protein resin based green composites modified with nano-clay particles. Compos. Sci. Technol. **67**(10), 2005–2014 (2007)

Hussain, F., Roy, S., Narasimhan, K., Vengadassalam, K., Lu, H.: E-glass polypropylene pultruded nanocomposite: Manufacture, characterization, thermal and mechanical properties. J. Thermoplast. Compos. Mater. **20**(4), 411–434 (2007)

Ikada, Y., Tsuji, H.: Biodegradable polyesters for medical and ecological applications. Macromol. Rapid Commun. **21**, 117–132 (2000)

Imran, M., Klouj, A., Revol-Junelles, A., Desobry, S.: Controlled release of nisin from HPMC, sodium caseinate, poly-lactic acid and chitosan for active packaging applications. J. Food Eng. **143**, 178–185 (2014)

Janssen, L.P., Moscicki, L.: Thermoplastic Starch: A Green Material for Various Industries. Wiley-VCH, Weinheim (2009)

John, M., Thomas, S.: Biofibres and biocomposites. Carbohydr. Polym. **71**(3), 343–364 (2008)

Kafiriti, E., Mponda, O.: Soil, plant and crop production-growth and production of sesame. In: Encyclopedia of Life Support System (EOLSS) (2009). http://www.eolss.net/eolsssample.aspx. Accessed 12 Mar 2016

Kenawy, E., Worley, S.D., Broughton, R.: The chemistry and applications of antimicrobial polymers: a state-of-the-art review. Biomacromolecules **8**(5), 1359–1384 (2007)

Kiatkamjornwong, S., Chomsaksakul, W., Sonsuk, M.: Radiation modification of water absorption of cassava starch by acrylic acid/acrylamide. Radiat. Phys. Chem. **59**(4), 413–427 (2000)

Kojima, et al.: Mechanical properties of nylon 6-clay hybrid. J. Mater. Res. **8**(5), 1185–1189 (1993)

Kolybaba, et al.: Biodegradable polymers: past, present, and future. Written for Presentation at the 2003 CSAE/ASAE Annual Intersectional Meeting, North Dakota, USA, 3–4 Oct 2003, Paper No RRV03-0007 (2003)

Krishnamachari, P., Zhang, J., Lou, J., Yan, J., Uitenham, L.: Biodegradable poly(lactic acid)/clay nanocomposites by melt intercalation: a study of morphological, thermal, and mechanical properties. Int. J. Polym. Anal. Charact. **14**(4), 336–350 (2009)

Kržan, A.: Biodegradable polymers and plastics. In: Innovative Value Chain Development for Sustainable Plastics in Central Europe (PLASTiCE) (2012). http://www.icmpp.ro/sustainableplastics/files/Biodegradable_plastics_and_polymers.pdf. Accessed 19 Mar 2015

Kuktaite, R., Türe, H., Hedenqvist, M.S., Gällstedt, M., Plivelic, T.S.: Gluten biopolymer and nanoclay-derived structures in wheat gluten–urea–clay composites: relation to barrier and mechanical properties ACS sustainable chemistry & engineering ACS sustainable. Chem. Eng. **2**(6), 1439–1445 (2014)

Kumar, A.A., Karthick, K., Arumugam, K.P.: Properties of biodegradable polymers and degradation for sustainable development international. J. Chem. Eng. Appl. **2**(3), 164–167 (2011)

Kyrikou, I., Briassoulis, D.: Biodegradation of agricultural plastic films: a critical review. J. Polym. Environ. **15**(3), 125 (2004)

Lan, T., Pinnavaia, T.J.: Clay-reinforced epoxy nanocomposites. Chem. Mater. **6**, 2216–2219 (1994)

LeBaron, P.C., Wang, Z., Pinnavaia, T.J.: Polymer-layered silicate nanocomposites: an overview. Appl. Clay Sci. **15**, 11–29 (1999)

Lee, J., Song, N., Jo, W., Song, K.B.: Effects of nano-clay type and content on the physical properties of sesame seed meal protein composite films. Int. J. Food Sci. Technol. **49**(8), 1869–1875 (2014)

Leja, K., Lewandowicz, G.: Polymer biodegradation and biodegradable polymers—a review polish. J. Environ. Stud. **19**(2), 255–266 (2010)

Li, X., et al.: Structural and mechanical characterization of nanoclay-reinforced agarose nanocomposites. Nanotechnology **16**(10), 2020–2029 (2005)

Litchfield, D.W., Baird, D.G.: The role of nanoclay in the generation of poly (ethylene terephthalate) fibers with improved modulus and tenacity. Polymer **49**(23), 5027–5036 (2008)

Lopattananon, N., Tanglakwaraskul, S., Kaesaman, A., Seadan, M., Sakai, T.: Effect of nanoclay addition on morphology and elastomeric properties of dynamically vulcanized natural rubber/polypropylene nanocomposites. Int. Polym. Process. **29**(3), 332–341 (2014)

Liu, L., Qi, Z., Zhu, X.: Studies on nylon 6/clay nanocomposites by melt-intercalation process. J. Appl. Polym. Sci. **71**, 1133–1138 (1999)

Lörcks, J.: Properties and applications of compostable starch-based plastic material. Polym. Degrad. Stab. **59**(1–3), 245–249 (1998)

Ma, X., Yu, J., Kennedy, J.F.: Studies on the properties of natural fibers-reinforced thermoplastic starch composites. Carbohydr. Polym. **62**(1), 19–24 (2005)

Miles, C., et al.: Durability of potentially biodegradable alternatives to plastic mulch in three tomato production regions. Hort. Sci. **47**(9), 1270–1277 (2012)

Mitrus, M., Wojtowicz, A., Moscicki, L.: Biodegradable polymers and their practical utility. In: Janssen, L.P., Moscicki, L. (eds.) Thermoplastic Starch: A Green Material for Various Industries. Wiley-VCH, Weinheim (2009)

Mohan, T., Kanny, K.: Thermoforming studies of corn starch-derived biopolymer film filled with nanoclays. J. Plast. Film Sheet **32**(2), 163–188 (2015)

Morton, M.: Rubber Technology. Van Nostrand Reinhold Company, New York (1987)

Muller, C.M.O., Yamashita, F., Laurindo, J.B.: Evaluation of the effect of glycerol and sorbitol concentration and water activity on the water barrier properties of cassava starch films through a solubility approach. Carbohydr. Polym. **10**, 1016–1021 (2007)

Muzny, C.D., Butler, B.D., Hanley, H.J.M., Tsvetkov, F., Peiffer, D.G.: Clay platelet dispersion in a polymer matrix. Mater. Lett. **28**(4–6), 379–384 (1996)

Nazaré, S., Kandola, B.K., Horrocks, A.R.: Flame-retardant unsaturated polyester resin incorporating nanoclays. Polym. Adv. Technol. **17**(4), 294–303 (2006)

Okada, A., Usuki, A.: The chemistry of polymer-clay hybrids. Mater. Sci. Eng. R **3**(2), 109–115 (1995)

Okada, et al.: Polymer-based molecular composites. In: Schaefer, D.W., Mark, J.E. (eds.) Materials Research Society Symposium Proceeding, vol. 171, pp. 45–50 (1990)

Oliveira, M., Machado, A.V.: Preparation of polymer-based nanocomposites by different routes. In: Wang, X. (ed.) Nanocomposites: Synthesis, Characterization and Applications, pp. 73–94. NOVA Publishers, New York (2013)

Patterson, T.: Forte™ Nanocomposites—our revolutionary breakthrough. In: 4th World Congress in Nanocomposites, EMC, San Francisco, 1–3 Sept 2004 (2004)

Pauzi, N.N., Majid, R.A., Dzulkifli, M.H., Yahya, M.Y.: Development of rigid bio-based polyurethane foam reinforced with nanoclay. Compos. B **67**, 521–526 (2014)

Petersen, et al.: Potential of biobased materials for food packaging. Trends Food Sci. Technol. **10**, 52–68 (1999)

Pinnavaia, T.J., Beal, G.W. (eds.): Polymer–Clay Nanocomposites. Wiley, Chichester (2000)

Porter, D., Metcalfe, E., Thomas, M.J.K.: Nanocomposite fire retardants—a review. Fire Mater. **24**, 45–52 (2000)

Pradhan, S., Guchhait, P.K., Kumar, K.D., Bhowmick, A.K.: Influence of nanoclay on the adhesive and physico-mechanical properties of liquid polysulfide elastomer. J. Adhes. Sci. Technol. **23**(16), 2013–2029 (2009)

Pusch, R., Yong, N.R.: Microstructure of Smectite Clays and Engineering Performance. Taylor & Francis, London (2006)

Ramsden, J.J.: What is nanotechnology? In: Ramsden, J.J. (ed.) Applied Nanotechnology—The Conversion of Research Results to Products, 2nd edn, pp. 3–12. Elsevier, William Andrew (2014)

Ratner, B.D., Hoffman, A., Schoen, F., Lemons, J. (eds.): Biomaterials Science: An Introduction to Materials in Medicine, 3rd edn. Elsevier, Amsterdam (2004)

Ray, S.S., Okamoto, M.: Polymer/layered silicate nanocomposites: a review from preparation to processing. Prog. Polym. Sci. **28**(11), 1539–1641 (2003)

Ray, S.S., et al.: New polylactide/layered silicate nanocomposites 5 designing of materials with desired properties. Polym. J. **44**(21), 6633–6646 (2003)

Rhim, J., Hong, S., Park, H., Ng, P.K.: Preparation and characterization of chitosan-based nanocomposite films with antimicrobial activity. J. Agric. Food Chem. **54**(16), 5814–5822 (2006)

Sen, A.K.: Coated Textiles: Principles and Application. Technomic, Pennsylvania [Chapter-Smart function in Textile] (2001)

Shah, G.D.: Classification of biodegradable polymers [Web log post] (2015). http://plasticlecturenotes.blogspot.my/2015/03/classificationofbiodegradablepolymers17html. Accessed 19 Mar 2016

Shayan, M., Azizi, H., Ghasemi, I., Karrabi, M.: Effect of modified starch and nanoclay particles on biodegradability and mechanical properties of cross-linked poly lactic acid. Carbohydr. Polym. **124**, 237–244 (2015)

Shekarabi, A.S., Oromiehie, A.R., Vaziri, A., Ardjmand, M., Safekordi, A.A.: Investigation of the effect of nanoclay on the properties of quince seed mucilage edible films. Food Sci. Nutr. **2**(6), 821–827 (2014)

Shin, Y., Song, H., Jo, W., Lee, M., Song, K.B.: Physical properties of a barley protein/nano-clay composite film containing grapefruit seed extract and antimicrobial benefits for packaging of Agaricus bisporus. Int. J. Food Sci. Technol. **48**(8), 1736–1743 (2013)

Sothornvit, R., Rhim, J., Hong, S.: Effect of nano-clay type on the physical and antimicrobial properties of whey protein isolate/clay composite films. J. Food Eng. **91**(3), 468–473 (2009)

Sozer, N., Kokini, J.L.: Nanotechnology and its applications in the food sector. Trends Biotechnol. **27**(2), 82–89 (2008)

Subana, P.S., Nair, P.P., George, K.E.: Studies on combined effect of nanoclay and elastomer on mechanical properties of polystyrene/polybutadiene blend. J. Acad. Ind. Res. **1**(8), 461–463 (2013)

Vartiainen, J., Tuominen, M., Nättinen, K.: Bio-hybrid nanocomposite coatings from sonicated chitosan and nanoclay. J. Appl. Polym. Sci. **116**, 3638–3647 (2010)

Vroman, I., Tighzert, L.: Biodegradable Polymers. Materials **2**, 307–344 (2009)

Vu, Y.T., Rajan, G.S., Mark, J.E., Myers, C.L.: Reinforcement of elastomeric polypropylene by nanoclay fillers. Polym. Int. **53**(8), 1071–1077 (2004)

Wang, L., Wang, K., Chen, L., Zhang, Y., He, C.: Preparation, morphology and thermal/mechanical properties of epoxy/nanoclay composite. Compos. A **7**(11), 1890–1896 (2006)

Wollerdorfer, M., Bader, H.: Influence of natural fibres on the mechanical properties of biodegradable polymers. Ind. Crops Prod. **8**(2), 105–112 (1998)

Wu, C.L., Zhang, M.Q., Rong, M.Z., Friedrich, K.: Tensile performance improvement of low
     nanoparticles filled-polypropylene composites. Compos. Sci. Technol. **62**(10–11), 1327–1340
     (2002)
Yadav, S.M., Yusoh, K.: Mechanical and physical properties of wood-plastic composites made of
     polypropylene, wood flour and nanoclay. In: Proceeding—Kuala Lumpur International
     Agriculture, Forestry and Plantation, Kuala Lumpur, Malaysia, 12–13 Sept 2015 (2015)
You, Z., et al.: Nanoclay-modified asphalt materials: preparation and characterization. Constr.
     Build. Mater. **25**(2), 1072–1078 (2011)
Zhu, L., Wool, R.P.: Nanoclay reinforced bio-based elastomers: synthesis and characterization.
     Polymer **47**(24), 8106–8115 (2006)

Development and Characterization of Nano Clay Reinforced Three-Phase Sandwich Composite Laminates

N.R.R. Anbu Sagar and K. Palanikumar

Abstract Polymer based sandwich composites are widely used in the development of components for aircraft, railway coaches and marine application. Among the varieties, Glass-Jute fiber hybrid and Glass fiber-PS foam core sandwich laminates find wider application in the railway coaches and building of boat hulls, because of its unique properties such as high strength and stiffness-to-weight ratio and good damping property. In the present investigation, PS foam-GFR sandwich laminates are fabricated with a total of four layers of glass fiber in the skin and PS foam as core, by varying wt% of nano clay in polyester resin so as to obtain four different combinations of PS foam-GFR sandwich laminates. Various tests are undertaken to study the properties. In general, the results of the various experiments have shown that, the nanoclay modified polyester resin sandwich laminates exhibit the highest mechanical properties when compared to the unmodified polyester resin composite laminates. In addition to the mechanical tests, X-ray Diffraction (XRD), Scanning Electron Microscopy (SEM) and Energy Dispersive X-ray Spectroscopy (EDS) have been carried out to examine the microstructure and elemental composition of the fabricated composites. From the analysis, it is observed that, the samples containing nanoclay contain more of Silicon and Aluminium due to nanoclay loading in the matrix. The relative comparison has also been made between Jute-GFR hybrid and GFR-PS foam sandwich laminates for suitable application of composites.

Keywords 3D sandwich · Nanoclay · Hybrid laminates · Hand layup · Scanning electron micrographs · Energy dispersive X-ray · X-ray diffraction (XRD)

N.R.R. Anbu Sagar
Mechanical Design and Manufacturing Engineering,
Adama Science and Technology University, Adama, Ethiopia

K. Palanikumar (✉)
Department of Mechanical Engineering, Sri Sai Ram Institute of Technology,
Chennai 600 044, India
e-mail: palanikumar_k@yahoo.com

1 Introduction

Nano Reinforcement of Polymers to attain nano composites has fascinated the attention of researchers for their prospective in property improvement. Since organically modified nanoclay having ultra-high strength and stiffness and they have become very popular during the last decade for nano reinforcement of polymers. Their nano-scale dimensions contribute enormous rheological benefits to the polymer resin systems. Nano particles at very small concentration dispersed in polymer resins often impart advanced mechanical properties. So, nano reinforcement of polymer has opened up a new horizon for different property development and their potentials in structural applications (Belingardi et al. 2003). Polymer nano composites are comparatively a new type of composite material, of which the possibilities are many, but they are not fully explored. Thermoset plastic continuous fiber reinforced composites laminate as skin and the low density materials as core sandwich panels are another comparatively new development within the field of composites.

In this chapter, the results of the two new combinations of composites have been described. These combinations consists of a three-phase (3D) of jute-glass fiber hybrid sandwich laminate and three-phase of skin sandwich laminate with soft core (Reis and Rizkalla 2008) is studied in detail. The studies on the mechanical characterization (static and dynamic) such as flexural, tensile, impact, post impact and damping properties etc., of polymer and nano polymer matrix composites have been carried out by many researchers. The studies on these mechanical characteristics are important, as these polymer based fiber reinforced composites are difficult to characterize the material due to their anisotropic and non linearity. The studies of these materials are needed to achieve near-net shape. Many researchers have also studied the characteristics of polymer and nano polymer based GFR hybrid and GFR—soft core sandwich composites which are used in aerospace and marine application.

Mubarak et al. (2009) have made a hybrid composites consists of jute fibers with polypropylene matrix and have tested for its strength. They have found that the strength (>70 MPa) and impact properties (>80 kJ/m^2) have been improved. Thwe and Liao (2003) have made a study on the resistance of Bamboo with and without glass fibers and found the fatigue properties behavior under cyclic tensile loading. Yongli Zhang et al. (2013) have studied the flax and glass fiber reinforced plastics. The results indicated that the properties improved by increasing the glass fiber and the stacking sequence have also influenced the tensile strength and tensile failure strain, but not the tensile modulus.

The effect of stacking sequence on mechanical properties is studied by Ahmed and Vijayarangan (2008). The results showed that, the properties of jute composites have considerably improved by the placing of glass fibres. Ramesh et al. (2013) have manufactured the sisal–jute–glass fiber with polyester matrix. The results indicated that, the inclusion of sisal–jute with GFRP improve the mechanical properties. Further, Boopalan et al. (2013) have inticated that the addition of banana fiber in jute/epoxy composites increased the mechanical properties and it has decreased the moisture absorption capacity.

The increased tensile properties of jute oil palm fiber hybrid composites are found by Jawaid et al. (2013). Multiple layers of jute and E-glass fibre reinforced laminates have been studied by Igor et al. (2009). The results have suggested that the T-hybrids presented better at low impact energies, which do not damage significantly the laminate core. In contrast, Q-hybrids are better suited to withstand an extensive damage produced by higher impact energies, in that they allow a more effective redistribution of impact damage in the structure. Nayak et al. (2009) have proved that, the hybridization increases the storage modulus. Manalo et al. (2010) have investigated the flexural behaviour of the glue-laminated fibre composite sandwich beams experimentally. Overall, it has been claimed that, the sandwich-glue-exhibit better properties than the composite sandwich beams.

Fam and Sharaf (2010) have explored the viability of fabrication and flexural strength of sandwich laminate developed from low density polyurethane foam core and GFRP skins. The strength and stiffness of the panels increased substantially. Jian Xiong et al. (2011) have investigated the failure of the sandwich panels which have been made of carbon fiber composite under axial compression loading. James Sargianis and Jonghwan Suhr (2012) have investigated the core thickness change on the vibrational properties. They have found that, there is a severe increase in concurrence frequency for the sandwich beam with the thinnest core thickness due to the low bending stiffness which leads to low damping values. Karippal et al. (2011) have studied the mechanical properties of epoxy/glass/nanoclay hybrid composites. They have indicated the improved mechanical properties with an increase in the nanoclay loading up to 5 wt%. Faguaga et al. (2012) have investigated and found that, the nanoclay included polyester matrix system show a harmful effect in degradation resistance, because of the degree of hydrophilicity of the selected clay which produces a weak interphase with the polymeric matrix.

Antonio et al. (2007) have investigated the effect of Montmorillonite silicate layers on glass-fiber-epoxy laminated composites by low-velocity impact and X-ray diffraction tests. Anbusagar et al. (2012) investigated the influence of nanoclay content on sandwich composites under flexural and impact loading. The measurement shows that, the flexural and impact properties are greatly increased, over the range of nanoclay loading. Further Anbusagar et al. (2013 a, b) have investigated the Effect of nanoclay modified polyester resin on flexural, impact, hardness and water absorption properties of untreated woven jute and glass fabric hybrid sandwich laminates experimentally. The testing results have indicated that, the flexural properties are greatly increased at 4 % of nanoclay loading while impact, hardness and water absorption properties are increased at 6 % of nanoclay loading.

The polymer based jute-glass hybrid and glass-soft core sandwich laminates have been used in building the railway coaches and boat hull but they continually suffer from static loading, dynamic loading and environmental effect, and are in service for many decades now. It is also critical that, the most stringent quality measurements are needed to study the mechanical properties of fabricated laminated composites. Reliability is an important criterion in the manufacture of railway coaches and boat hull, and therefore, these composite manufacturers need to maintain high-quality on a consistent basis. Hence, this research chapter focuses on

the manufacturing of high performance composites which are discussed above and evaluation of mechanical properties such as tensile, flexural, impact, water absorption, hardness and damping using experimentally. The microstructures of the fabricated laminates before and after fracture are assessed by using XRD, EDS and SEM analysis.

2 Materials and Methods

There are several factors which have been considered while selecting the materials for a composite structure. The most important factors are clay and resin chemistry, dispersion of the clay in resin, compatibility of fiber and resin, matrix formulation, processing parameters and curing conditions. In this chapter, the selected materials, their physical properties, dispersion method of nanoclay in matrix, laminate manufacturing method and experimental methods for static and dynamic characterizations are described.

Face sheet material: The plain weave E-glass fabric 600 g/m^2 is procured from Binani industries limited, Mumbai, India. Figure 1a shows the E-glass fiber that has been used for the present study.
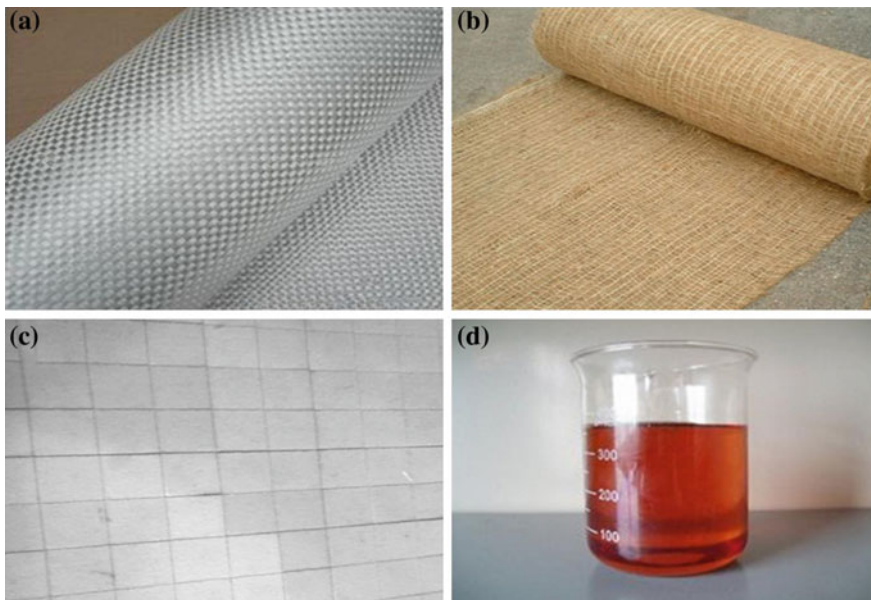
Fig. 1 Photograph view of materials used to fabricate various laminates. **a** Glass fiber. **b** Jute fiber. **c** Polystyrene foam. **d** Polyester resin

Core 1: Woven jute fabric of 22 yarns of Tex 310 in warp direction and 12 yarns of Tex 280 in weft direction, per inch having an average weight of 367 g/m^2 and average thickness of 0.8 mm, is directly procured from Kolkata, West Bengal, India. Figure 1b shows the jute fiber, which has been used for the present study.

Core 2: GEN-M-01-03002R04 Medium density polystyrene foam sheet in squares 10 mm are used as a core material for sandwich structure. This foam has a density and thickness of 60 kg/m^3 and 6 mm respectively. Figure 1c shows the polystyrene foam sheet used for the present study.

Resin and hardener: Polyester as resin and Methyl ethyl ketone peroxide and cobalt naphthanate are used as catalyst and accelerator. Figure 1d shows the polyester resin used for the present study.

Nano Clay: The nanoclay used in this study is procured from Southern Clay Products, Na$^+$ Montmorillonite modified with some concentration and octadecyl trimethyl ammonium chloride. According to the x-ray diffraction results provided by the supplier, the gallery spacing of Cloisite Na$^+$ is 11.7A˚and having CEC 2.6 meq/100 g clay. Figure 2 shows the commercial nanoclay, which has been used for the present study. The physical properties of the nanoclay used in this study are given Table 1.

Fig. 2 Photograph view of nanoclay

Table 1 Physical properties of Cloisite® Na$^+$ (Nanoclay)

Physical properties	Metric
Specific gravity	2.86 g/cc
Bulk density	0.1994 g/cc
Loss on ignition	7.00 %
Particle size	≤ 2.00 μm

3 Manufacturing of Nano Composites

3.1 Preparation of Organic Montmorillonite (OMMT)

Na^+-MMT is dispersed in distilled water with some concentration and octadecyl trimethyl ammonium chloride is vigorously stirred for few times at a given temperature. The white precipitates are washed with hot distilled water (above 80 °C) until no bromide ion has been detected with a 0–1 mol/l $AgNO_3$ solution. The product obtained is then vacuum–dried at 70 °C to a constant weight and then it has been grounded and screened with 300-mesh sieve to get the modified clay (OMMT) (Miyagawa et al. 2006).

3.2 Dispersion of Nanoclay with Matrix

The necessary amount (up to 6 wt%) of modified Na^+ Montmorillonite is mixed with resin made of polyester. The initial mixing is carried out by hand in a spatula, Mechanical mixer is used at a speed of 2000 rpm for 20 min for proper mixing. Figure 3 shows the mixing of nanoclay. The temperature is maintained below 100 ºC to avoid self-polymerization (Chandradoss et al. 2008).

3.3 Preparation of Nano Composites

The laminates prepared for the present study are GFRP face sheet laminate, hybrid sandwich laminate and GFRP face sheet sandwich laminate with soft core. Figures 4 and 5 show the tools that have been used and photographic view of preparation of nano composite laminate by hand lay-up process respectively. Moulding box is prepared with the required size and the use of wax polish and polyvinyl alcohol act as a releasing agent. Mixture of OMMT nano clay and polyester resin (2, 4, and 6 wt of clay) is applied over the fiber mat of 300 cm square for a setting period of 1 h. After curing the laminate, it has been removed from the mold and cured at room temperature for 48 h. Then the samples are carefully cut from the laminates by using a diamond saw with sufficient allowance for finishing. Final dimensions are obtained by finishing the samples by using the medium grade emery paper. The specimen details are provided in Table 2. Five different specimens are used and the average values are provided. the experimental data showing the maximum standard deviation also included.

Table 3 records the details of the samples that have fabricated for the present investigation and Tables 4 and 5 show the various sample configurations used for the present study. The hybrid sandwich laminates are made with total of 10 plies. Six plies consisting jute fiber have been replaced by polystyrene foam.

Fig. 3 Mixing of nanoclay with polyester resin

Fig. 4 Photograph view of tools used for hand layup process

The fiber volume fraction is obtained by (1).

$$V_f = \frac{\Sigma(w_f/\rho_f)}{\Sigma(w_f/\rho_f) + (W_r/\rho_r)} \tag{1}$$

where W_f and W_r are the weights of the glass and resin. ρ_f and ρ_r are respective densities. Figure 6a–d shows test samples prepared from various laminates. For the all laminates face sheet materials, E-glass fiber with cross ply fiber orientations have been applied.

Fig. 5 Preparation of nano composites by hand lay-up process

Table 2 Dimensions of the samples for various tests

Type of test	Width (mm)	Thickness (mm)	Length (mm)	Span length (mm)	Crosshead speed (mm/min)	ASTM standard
Tensile test	25	3	200	150	1.5	ASTM: D3039
Flexural test (GFRP face sheet)	10	3	150	64	2	ASTM: D790
Flexural test (Hybrid sandwich)	12	8	150	120	4	ASTM: D790
Flexural test (Soft core Sandwich)	25	8	160	130	4	ASTM: C393
Charpy impact test	12.5	8	120	–	–	ASTM: D6110
Water absorption test	25	8	76.2	–	–	ASTM: D570
Hardness test	25	8	25	–	–	ASTM: D2240
LVI test	50	8	50	–	–	ASTM: D2794
CAI test	50	8	50	–	–	ASTM: C364
Free vibration test	25	8	250	–	–	ASTM: E756

Table 3 Fabricated sample combinations and its sample codes

S. No	Type of laminate	Materials	Thickness (mm)	Sample code	Clay loading (wt%)
1	GFRP	Polyester + Clay + E-glass	3	F1	0
				–	2
				–	4
				–	6
2	PS foam Sandwich	Polyester + Clay + E-glass + PS foam	8	F2	0
				F2	2
				F4	4
				F6	6
3	Hybrid Sandwich	Polyester + Clay + E-glass + Jute core	10	S1	0
				S2	0
				S3	2
				S4	4
				S5	6

Table 4 Jute-GFR hybrid sandwich combination used for the fabrication process

Sample code	wt% of clay	wt% of fibers		Total volume fraction (%)
		Jute	Glass	Fiber
S1	0	100	0	37
S2	0	60	40	35.6
S3	2	60	40	33.3
S4	4	60	40	33.6
S5	6	60	40	33.2

Table 5 PS foam-GFRP face sheet sandwich combinations used for the fabrication process

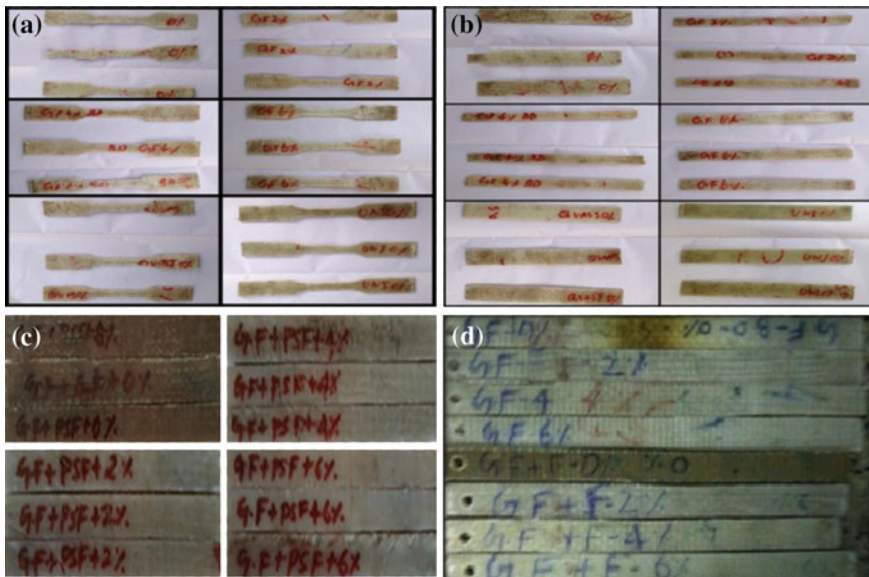| Sample code	wt% of clay	Core thickness (mm)	Total volume fraction (%) fiber
F1	0	0	33
F2	0	6	33
F3	2	6	33
F4	4	6	33
F5	6	6	33

Fig. 6 **a–d** Test samples prepared for various test. **a** Tensile test samples. **b** Flexural test samples. **c** Charpy impact test samples. **d** Free vibration test samples

4 Experimental Procedure

Experimental procedures to obtain the static and dynamic properties have been discussed in following sections.

4.1 Tensile Test

GFRP face sheet laminate property in tension is obtained by using the Universal Testing Machine, [(UTM) AG-IS-50 KN] accordance with ASTM standard given in Table 2. The test specimen is positioned as shown in Fig. 7. The speed of testing is set at the proper rate. A plotter is connected to the testing machine. The deflection of the specimen is continued until the fracture. A plotter plots the load–elongation curve results on the graph sheet. The flexural strength and modulus are calculated from the test results. The modulus of elasticity in static tension is calculated according to;
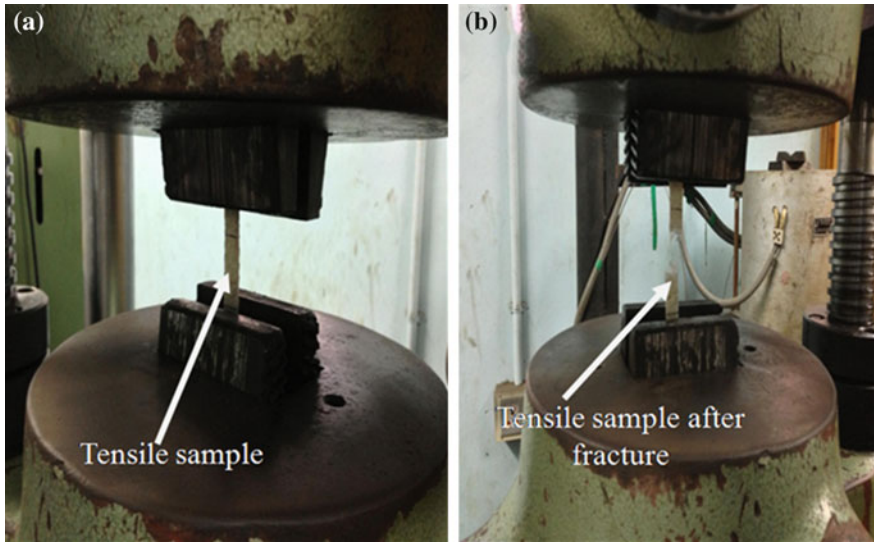
$$E_f = LG/A \tag{2}$$

Fig. 7 a–b Experimental set up for tensile test. **a** Sample before fracture. **b** Sample after fracture

Table 6 Tensile properties of GFRP face sheet laminates

| % of clay	0 %	2 %	4 %	6 %
Tensile strength (MPa)	153	183	189	181
Tensile modulus (GPa)	9.95	10.18	12.58	11.51

where A and G are the cross sectional area and slope of the tangent to the initial straight-line portion of the load-elongation curve (Meguid and Sun 2004). Observed tensile properties for GFRP face sheet laminate are given in Table 6.

4.2 Flexural Test Analysis

The flexural properties of the GFRP face sheet laminate and sandwich laminates are evaluated by using the Universal Testing Machine, [(UTM) LR-100K (Lloyd Instrument Ltd U.K)] accordance with ASTM standards and dimension given in Table 5. The test samples are positioned horizontally over the two supports as shown in Fig. 8. The deflection of the specimen has been continued until a rupture of the specimen is observed. A plotter plots the load–deflection curve results on the graph sheet. The flexural strength is calculated from the test results. The flexural strength of various sandwich laminates is reported in Ref. (Ahmed et al. 2006; Anbusagar et al. 2015; Younesi et al. 2013; Jawaid et al. 2013).

Fig. 8 Photo of flexural test setup
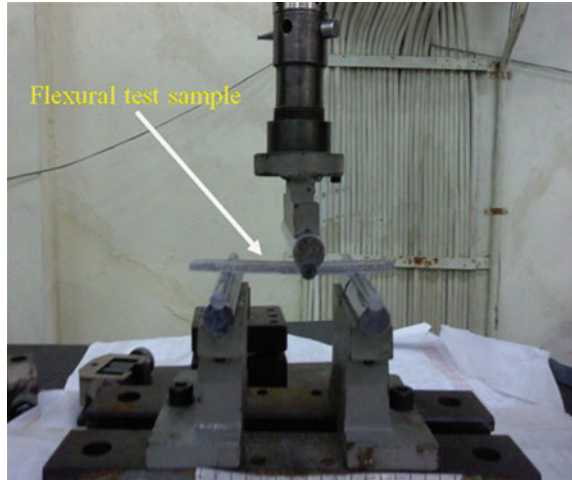
The maximum bending stress at failure on the tension side of the flexural sample is considered as the flexural strength of the material. The maximum bending stress in the outer fibers is calculated according to;

$$\sigma_m = 3FL/2bd^2 \tag{3}$$

where F is the load at a given point on the load deflection curve, L is the support span and b and d are the width and depth of the beam, respectively.

The modulus of elasticity in bending is calculated according to;

$$E_b = L^3M/4bd^3 \tag{4}$$

where M is the slope of the tangent to the initial straight-line portion of the load-deflection curve. Tables 7, 8 and 9 show the average flexural properties of hand layup samples of various laminates.

Table 7 Flexural properties of GFRP face sheet laminates

% of clay	0 %	2 %	4 %	6 %
Flexural failure load (N)	96	128	166	145
Flexural strength (MPa)	101	110	142	120
Flexural modulus (GPa)	6.10	6.32	9.62	7.94

Table 8 Flexural properties of Jute-GFR hybrid sandwich laminates

Sample code	Measured failure load (N)	Flexural strength (Mpa)	Flexural modulus (Gpa)
S1	307	85.6	8.13
S2	506.22	140	10.53
S3	586.66	162.81	13.63
S4	558.96	134.48	15.26
S5	449.65	113.67	16.35

Table 9 Flexural properties of PS foam-GFRP face sheet sandwich laminates

Sample code	Measured failure load (N)	Flexural strength (Mpa)	Flexural Rigidity $\times$ 10^3 (N-mm^2)	Observed failure mode
F1	96	101	3900	Compressive failure
F2	199.99	27.18	5409.6	Face yield
F3	207.34	28.21	6484.8	Face yield
F4	238.87	32.50	7694.4	Face yield
F5	170.81	23.24	5980.8	Face yield + wrinkling

Fig. 9 Photo of Charpy impact test setup

4.3 Charpy Impact Test

The Charpy impact tests (Mallick 2007) are performed on commercial impact test machine in which, a pendulum hammer is released from a standard height to contact a beam specimen (unnotched) with a specified kinetic energy. A horizontal simply supported beam specimen is used in the Charpy test is shown in Fig. 9. The energy

Table 10 Charpy impact properties of Jute-GFR hybrid sandwich laminates

Sample code	S1	S2	S3	S4	S5
Impact strength (kJ/m^2)	25.87	48.71	50.35	52.72	59.63

Table 11 Charpy impact properties PS foam-GFRP face sheet sandwich laminates

Sample code	F1	F2	F3	F4	F5
Impact strength (kJ/m^2)	20.35	24.32	25.68	25.83	36.59

absorbed in flouting the specimen, regularly indicates the position of a pointer on a calibrated dial attached to the testing machine. The energy absorbed is equal to the difference between the energy of the pendulum hammer at the moment of impact and the energy remaining in the pendulum hammer after breaking the specimen (Boopalan et al. 2013; Mallick 2007). Tables 10 and 11 show the observed. Charpy impact strength of sandwich laminates.
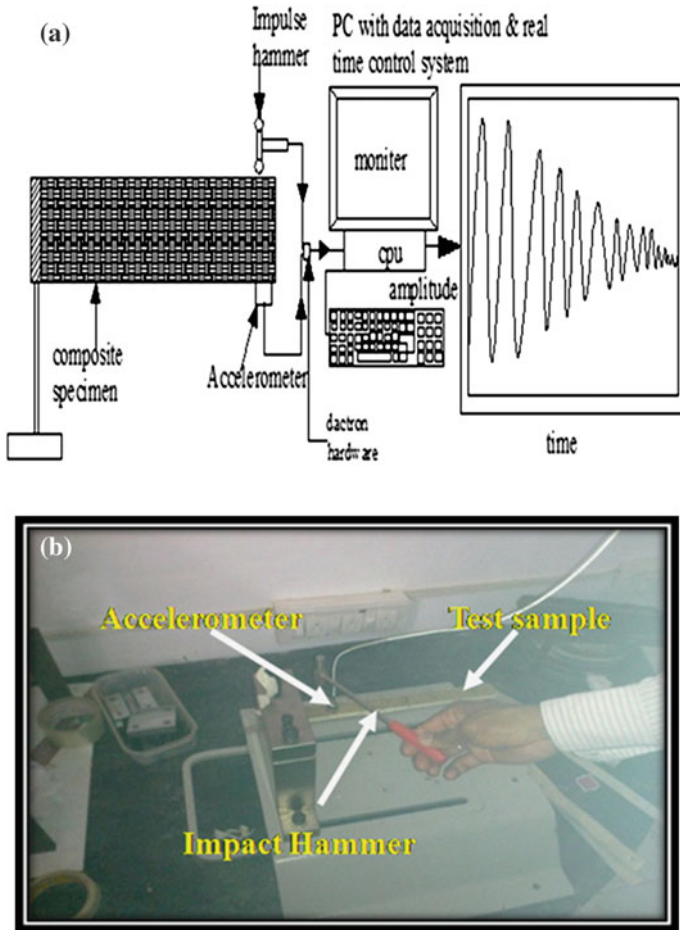
4.4 Free Vibration Test

The natural frequency and damping ratio are evaluated by using vibration testing equipment. It contain Kristler make accelerometer–model 87054250M1, Data Acquisition System (Dewetron-model DEWE501) and computer software (Dewesoft 7.0.5.). ASTM: E756 is used for making the specimen. A Fast Fourier Transform (FFT) is used for the signal and the software measures the lateral natural vibration modes (Fig. 10b).

The vibration test gives the free vibration time response and the Frequency Response Function (FRF), simultaneously as a result. In this analysis, two different moduli are determined. The first one is the storage modulus or elastic modulus usually denoted by E′, which represents the ability of the material to store energy. The second one is the loss modulus, which indicates the ability of the material to dissipate energy and it is usually defined by E″. The ratio of loss modulus E″ and the storage modulus E′ is called Tan delta (Tan δ), which represents the damping property of the material (Dipa Ray et al. 2002).

For free vibration a logarithmic damping (Δ) is used based on the following equation,

$$\Delta = 1/n \ \ln \ (A_0/A_n) \tag{5}$$

where n indicates the number of peaks; A_0 is the amplitude of the first peak and A_n is the amplitude of the final peak analyzed.

Fig. 10 a–b Free vibration test set up. **a** Free vibration test set up. **b** Free vibration test sample with equipment

The storage modulus (E′) is calculated for a specimen having 300 mm* 30 mm * 8 mm (James and Jonghwan 2012) is:

$$E' = \frac{4\pi^2 f^2}{3I}\left[M + \frac{33}{140}m\right]L^3\left[1 + \frac{\Delta^2}{4\pi^2}\right] \tag{6}$$

Where E′ indicates the storage modulus; f is the natural frequency; I is the inertial moment; M is the accelerometer weight; m is the specimen weight and L is the specimen length.

The loss factor, tanδ, is calculated from the decaying-oscillatory damping curve as follows;

$$\tan \delta = \frac{\ln(A_0/A_n)}{n\pi} \tag{7}$$

The loss modulus (E") is calculated by the Eq. (8)

$$\tan \delta = \frac{E''}{E'} \tag{8}$$

Damping factor (ζ) is calculated by the Eq. (9)

$$\zeta = 1/\sqrt{1 + (2\pi/\Delta)^2} \tag{9}$$

Dynamic stiffness (S) is calculated by the Eq. (10)

$$S = (f \times 2\pi)^2 m \tag{10}$$

Table 12 show the free vibration experimental test result for the laminates fabricated.

4.5 Post Impact Testing

For the evaluation of damage area and damage tolerance capability of fabricated laminates, the (a) low Velocity Impact (LVI) and (b) Compression After Impact (CAI) test have been carried out. Damage pattern and damage area are evaluated by using low velocity impacted test samples. From CAI test, the residual compressive strength and residual compressive modulus are measured to assess the damage tolerance capability of the impacted samples. Samples are impacted by using a non instrumented drop weight impact test system on size (50 × 50) mm cut from the laminates according to ASTM: D2794. The drop tower consists of a crosshead with height arrangement, a mechanical single impact round rebound brake, and circular

Table 12 Vibration test result of PS foam-GFR face sheet sandwich laminates

Sample code	Natural frequency (HZ)	Storage modulus (MPa)	Loss modulus (MPa)	Damping ratio	Dynamic stiffness (N/m)
F1	6.89	8.22	8.09	0.00898	56.223
F2	8.51	262.05	13.87	0.01218	142.95
F3	10.05	365.48	81.06	0.01545	199.37
F4	19.5	1375.96	271.1	0.02328	750.58
F5	17.97	1169.68	116.06	0.01717	637.42
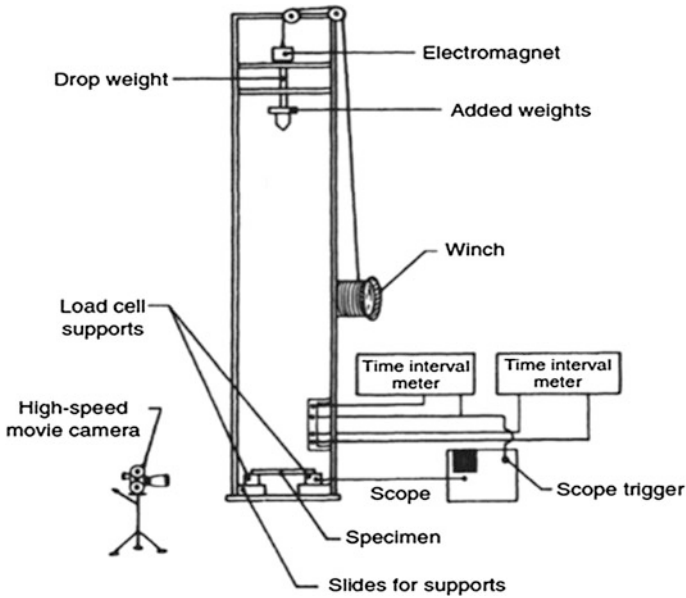
Fig. 11 Drop weight impact test system

fixture for supporting the test samples. For each type of laminate, the impact samples are divided into two groups with three samples in each group. Each group has impacted at energies of 10, 15 and 20 J. The typical arrangement of drop weight impact test system is shown in Fig. 11.

The machine is operated in gravity mode and the energies are obtained by changing the drop height, with constant impactor mass of 1 kg. The damaged area of the impacted samples is obtained by using high resolution camera to obtain over all envelopment of damaged area. The CAI tests are conducted in order to determine the degradation in compressive strength, modulus and compressive load carrying ability of the composite after impact. The CAI test is conducted according to ASTM: C364 using same impacted samples with the size of (50 × 50) mm. The rate of loading is 0.5 mm/min. The compressive modulus is evaluated from the slop of the load-stroke plot that has been generated by the software (Dear and Brown 2003). Post impacted test sample with equipment are shown in Fig. 12. Tables 13 and 14 show the damage area of post impact test samples for hybrid and PS foam core sandwich laminates respectively. Tables 15 and 16 shows the compressive residual properties result for hybrid and PS foam core sandwich laminates respectively.
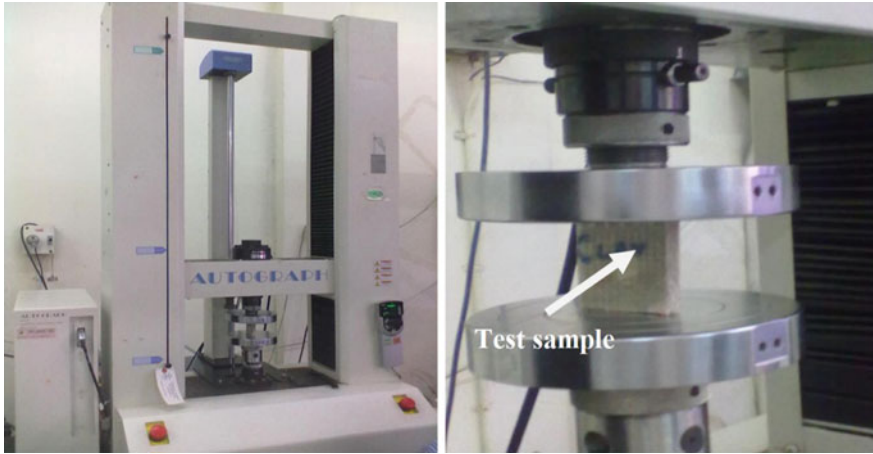
Fig. 12 CAI test set up

Table 13 Damage area measured for Jute-GFR hybrid sandwich laminates

Sample code		S1	S2	S3	S4	S5
Damage area (mm^2)	Impact energy (10 J)	1250	312	260	250	255
	Impact energy (20 J)	1300	370	353	320	333

Table 14 Damage areas measured for PS foam-GFR face sheet sandwich laminates

Sample code		F1	F2	F3	F4	F5
Damage area (mm^2)	Impact energy (10 J)	1122.6	719	695.6	325.3	632.6
	Impact energy (15 J)	1296	1036.6	839.3	426	796

Table 15 Compressive residual properties of Jute-GFR hybrid sandwich laminates

Sample codes	S1	S2	S3	S4	S5
CAI strength (MPa)	11.8	28.2	35.38	40.72	38.49
CAI modulus (MPa)	120.5	162.57	199.03	304.28	206.72

Table 16 Compressive residual properties of PS foam-GFR face sheet sandwich laminates

Sample codes	F1	F2	F3	F4	F5
CAI strength (MPa)	–	9.43	12.32	13.08	12.52
CAI modulus (MPa)	–	18.24	20.46	25.86	21.41

4.6 Water Absorption Testing

Water absorption testing is carried out with sandwich laminates as per ASTM: D570 to study the effect of nano clay loading on the water absorption behaviour of laminates. Samples with 76.2×25 mm dimension are cut from the sandwich laminated plate. Further, to avoid direct contact with water, resin coating has been given to all the edges of the samples. After that the samples are then dried in an oven at 75 ˚C for 24 h. These samples are weighed without delay in a single precision electronic balance with an accuracy of 0.0001 g. Three samples from each group are then immersed in water at a room temperature. The immersed samples are removed from water after 24 h. Then the surface of the samples is wiped off using a soft dry cloth. Again the samples are weighed by using the same electronic balance and these samples are immersed again in water. The same procedure is carried out till the saturation period is reached. The weight gained by the samples has been monitored with utmost care and proper attention has been given to change the water periodically. The water absorption percentage is calculated by using the equation Q (%) = $(W_1 - W_2)/W_1$, where W_1 and W_2 are weights of dry and wet samples respectively (Venkateshwaran et al. 2011; Fraga et al. 2003; Akil et al. 2009). Tables 17 and 18 show the water absorption properties for sandwich laminates.

Table 17 Water absorption properties of Jute-GFR hybrid sandwich laminates

Sample code	Water immersion period (hours)						
	24 h	144 h	264 h	384 h	504 h	624 h	744 h
S1	5.5	9.5	10.5	11.2	11.8	12.5	13
S2	3	6.25	7.35	8.5	9.5	10.8	11.25
S3	1.95	4.95	5.8	6.5	7.5	9.5	10
S4	1.5	3.8	4.5	5.9	7.1	7.2	8.3
S5	1.2	2.8	3.5	5.5	6.5	6	7.5

Table 18 Water absorption properties of PS foam-GFR face sheet sandwich laminates

Sample code	Water immersion period (hours)						
	24 h	144 h	264 h	384 h	504 h	624 h	744 h
F1	0.6	1.4	1.75	2.75	3	3.1	3.2
F2	2.5	4	4.75	6.2	6.5	6.7	6.9
F3	1.25	3.2	3.57	4.2	4.5	5	5.5
F4	1.2	2.5	3	3.2	3.5	4	5
F5	0.75	1.7	2.2	2.89	3	3.6	4

Fig. 13 Photo view of
Shore D hardness testing
model

Table 19 Shore D hardness
values of with and without
nanoclay polyester resin
laminates

Material property	% of nanoclay			
	0 %	2 %	4 %	6 %
Shore D hardness	80	90	100	118

4.7 Hardness Testing

Digital durometer pocketsize model probe has been used for measuring Shore D
hardness of the samples following standards ASTM: D2240. The Shore D hardness
testing model is shown in Fig. 13. Hardness measured for nanoclay polyester resin
is shown in Table 19.

4.8 Microstructure Analysis

Samples with and without nanoclay particles are analyzed by X-ray diffraction
(XRD) technique. The samples are scanned in the interval of $2\theta = 2–10$ at 40 kV
and 30 mA. Using XRD, intercalation behavior of clay particles loaded to matrix
with different concentration is analyzed. The measurement condition of the Rigaku
smart lab equipment is shown in Table 20. The Rigaku smart lab equipment is
shown in Fig. 14 which is used for XRD analysis.

In order to obtain microstructure, the samples are examined with CARLZEISS
high resolution microscope at different level of magnifications. Also, the samples
are given as gold vapor deposition onto the fractured surface of tensile specimens to
have a conductive layer over the samples. In addition to the polished surfaces, the

Table 20 Measurement condition of the Rigaku smart lab equipment

Description	Size
X-Ray	40 kV, 30 mA
Goniometer	Smart Lab
Attachment	Standard
Filter	Cu_K-beta
CBO selection slit	BB
Diffracted beam mono.	None
Detector	SC-70
Scan mode	Continuous
Scan speed/Duration time	1.0000 deg/min
Step width	0.0200 deg
Scan axis	Theta/2-Theta
Scan range	2.0000–10.0000 deg
Incident slit	2/3 deg
Length limiting slit	10.0 mm
Receiving slit #1	2/3 deg
Receiving slit #2	0.150 mm

Fig. 14 Photo view of Rigaku smart lab equipment

fractured surfaces of the mechanically tested samples are also studied under SEM to identify any change in adhesion between matrix and glass fibers because of the nanoclay. The CARLZEISS high resolution microscope equipment is shown in Fig. 15.

Energy Dispersive X-ray Spectroscopy (EDS) is utilized to analyze elemental composition analyses of the nanoclay by using the Oxford instrument with five iteration of each sample. The attachment of Oxford instrument is shown in Fig. 15.

**Fig. 15** Photo view of CARLZEISS high resolution microscope with Oxford instrument

5 Properties of Smart Materials

Advanced composite like nanoparticle infused polymer fiber, low density core sandwich structures are finding increased application in many different engineering and commercial fields of their unique static and dynamic properties. Mainly they are used for marine and aerospace applications. As a marine structure, they are subjected to static and dynamic loading during their operation and it has been avoided. So, the characteristic study on those materials has immense potential due to their different application fields and their excellent properties.

With the advent of composite materials and their wide use in the structural applications, it has become necessary to study the characteristic into the laminates to facilitate the design of structure to the main static and dynamic load bearing. The characteristic study of composites differs from the metal significantly in many aspects. The empirical relations are used to predict the various properties that have to be modified considerably when applied to the composite materials. The part of discussion based on the experimental analysis is presented as follows:

In this section, the mechanical properties such as flexural, Charpy impact, water absorption, damage tolerance capability of the two set of materials namely Jute-GFR sandwich hybrid and GFR-PS foam sandwich laminates are presented in the form of bar charts and the inference from the bar charts are narrated.

Fig. 16 a–b Comparison of flexural properties of sandwich laminates with respect to nanoclay loading. **a** Comparison of flexural strength of sandwich laminates. **b** Comparison of flexural modulus of sandwich laminates
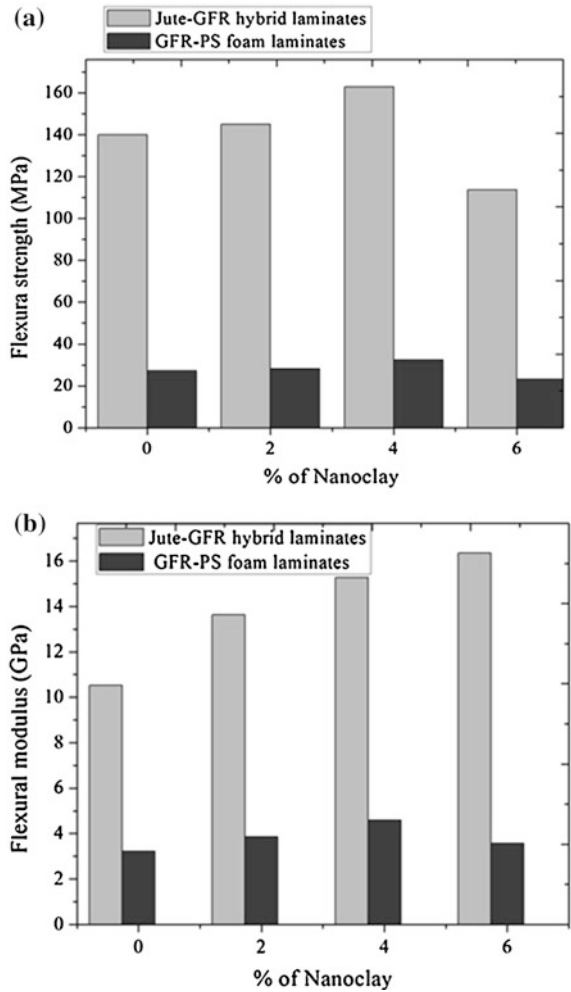
5.1 Flexural Properties

Flexural strength and modulus for sandwich laminates for different samples are compared in Fig. 16a–b. From Fig. 16a, b, it is observed that, the flexural strength and flexural modulus of 4 % nanoclay Jute-GFR hybrid laminate is 16 and 45 % which are more when compared with 0 % of nanoclay Jute-GFR hybrid laminate respectively. In case of GFR-PS foam sandwich laminate, the flexural strength and flexural modulus of 4 % nanoclay sample is 19.5 and 42 % more than 0 % nanoclay sample respectively (Karippal et al. 2011).

Furthermore, it is observed from Fig. 16a, b that, the 4 % of nanoclay Jute-GFR hybrid laminate sample has higher flexural properties when compared to 4 % of nanoclay GFR-PS foam sandwich laminate sample. However, it has to be clarified that, the weight to strength ratio is more in case of 4 % nanoclay GFR-PS foam sandwich laminate sample when compared to 4 % nanoclay Jute-GFR hybrid laminate sample. Hence, the Jute-GFR hybrid laminate is used where weight aspect is not considered as a deciding factor in structural application and GFR-PS foam sandwich laminate is used where strength is not considered as a deciding factor in structural application.

5.2 Charpy Impact Strength

Figure 17 shows the variation of impact strength of the different samples with respect to various clay combinations. From Fig. 17, it is observed that, the Charpy impact strength of 6 % nanoclay Jute-GFR hybrid laminate is 22.4 % more when compared with 0 % nanoclay Jute-GFR hybrid laminate sample. In case of GFR-PS foam sandwich laminate, the Charpy impact strength of 6 % nanoclay sample is 49 % more than 0 % nanoclay sample. Furthermore, it is observed from the figure that, the 6 % nanoclay Jute-GFR hybrid laminate sample has higher impact properties when compared to 6 % of nanoclay GFR-PS foam sandwich laminate sample due to higher absorption of nano modified polyester resin by Jute-GFR hybrid

Fig. 17 Comparison of impact strength of sandwich laminates with respect to nanoclay loading
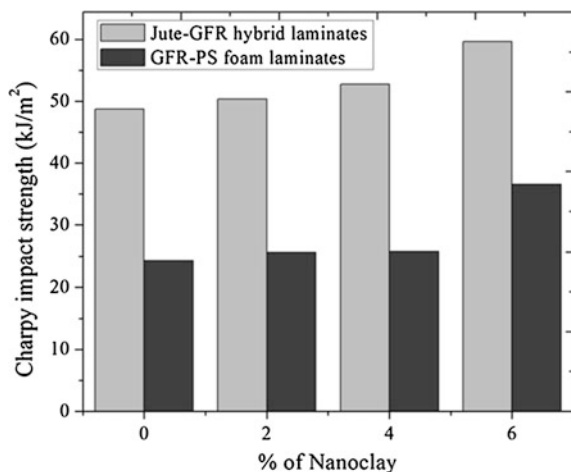
laminate. Achieving improvement in the impact strength also suggests the possibility of having uniformly dispersed, submicron nanoclay clusters, as mechanical performance which is known to be highly dependent on the particle size (Cardoso et al. 2002).

5.3 Water Absorption Behaviour

Figure 18 shows the variation of water absorption percentage of the different samples with respect to various clay combinations for the immersion period of 744 h. From Fig. 18, it is observed that the reduction in water absorption percentage of 6 % nanoclay Jute-GFR hybrid laminate is 50 % more when compared with 0 % nanoclay Jute-GFR hybrid laminate sample. In case of GFR-PS foam sandwich laminate, the reduction in water absorption percentage of 6 % nanoclay sample is 72 % more than 0 % of nanoclay sample. Furthermore, it is observed from the Fig. 18 that, the 6 % nanoclay GFR-PS foam sandwich laminate sample has lower water absorption percentage when compared to 6 % nanoclay Jute-GFR hybrid laminate sample due to the presence of non permeable PS foam as core material (Hazizan et al. 2009).

5.4 Low Velocity Impact Damage Area

Figure 19 shows the low velocity impact damage area of the different samples with respect to various clay combinations for 10 J of impact energy (Saha et al. 2008). From Fig. 19, it is observed that, the reduction in damage area of 4 % nanoclay

Fig. 18 Comparison of percentage of water absorption of sandwich laminates with respect to nanoclay loading
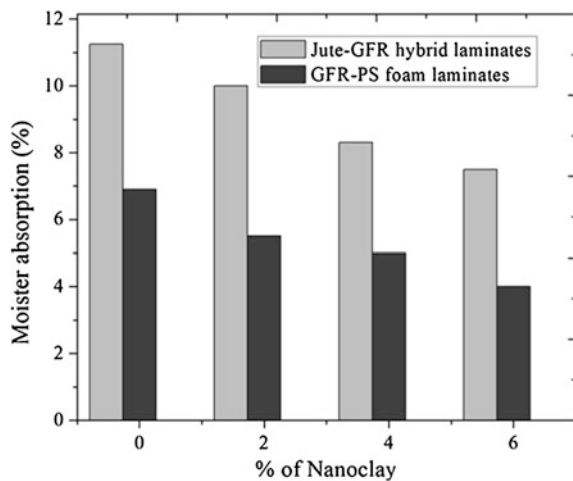
Fig. 19 Comparison of
damage areas of sandwich
laminates with respect to
nanoclay loading
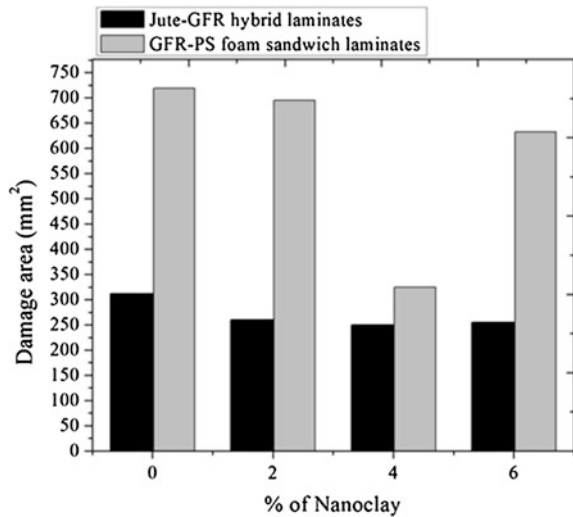
Jute-GFR hybrid laminate is 24 % more when compared with 0 % nanoclay
Jute-GFR hybrid laminate sample. In case of GFR-PS foam sandwich laminate, the
reduction in water absorption percentage of 4 % nanoclay sample is 2.2 times more
than 0 % of nanoclay sample. Furthermore, it is observed from Fig. 19 that, the
4 % nanoclay Jute-GFR hybrid laminate sample has lower damage area when
compared to 4 % nanoclay GFR-PS foam sandwich laminate sample due to higher
absorption of nano modified polyester resin by Jute-GFR hybrid laminate (Nunes
et al. 2004; Mines et al. 1998).

5.5   Comparison of Compression After Impact (CAI) Properties

Figure 20a, b show the comparison of Compression After Impact (CAI) properties
of post impact drop weight impact test sandwich laminate samples. From Fig. 20a,
b, it is observed that, the post impact compression strength and modulus of 4 %
nanoclay Jute-GFR hybrid laminate is 44 and 87 % more when compared with 0 %
of nanoclay Jute-GFR hybrid laminate respectively. In case of GFR-PS foam
sandwich laminate, the post impact compression strength and modulus of 4 %
nanoclay sample is 38 and 41 % more than 0 % of nanoclay sample respectively.
Furthermore, it is observed from Fig. 20a, b that, the 4 % nanoclay Jute-GFR
hybrid laminate sample has higher CAI properties when compared with 4 % of

Fig. 20 Comparison of CAI
properties of sandwich
samples with respect to
nanoclay loading.
a Compression strength of
CAI sandwich samples with
respect to nanoclay loading.
b Compression modulus of
CAI sandwich samples with
respect to nanoclay loading
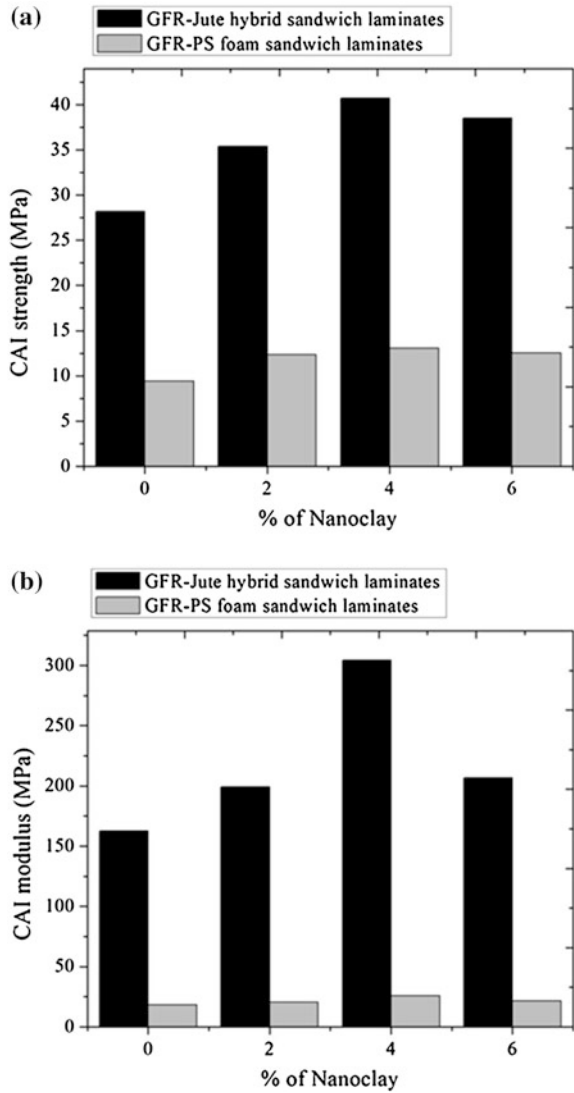
nanoclay GFR-PS foam sandwich laminate sample due to higher fiber volume
fraction in Jute-GFR hybrid laminate.

5.6 Microstructure Analysis

Microstructure of the fabricated samples has been carried out by XRD, EDS and
SEM analysis. The detailed studies of various microstructural analyses are dis-
cussed below.

5.6.1 XRD Analysis

The Fig. 21 shows results of the x-ray diffraction study of sample (0, 2 and 4 %) scanned at the interval $2\theta = 3–10$. The d–spacing of natural nanoclay particle is 11.7 A°. The d-spacing of sample with nanoclay particles is 18.6 A°. This 49 % increase in the gallery spacing of nanoclay is a clear indication of intercalation. The increase in gallery spacing is due to penetration of polyester resin molecules between the clay sheets. Due to the existence of high fraction of glass fibers and polyester matrix, the characteristic peaks from any agglomerated clay layers is not in the noticeable level when compared to the fraction of the clay particles in the composites. In order to understand the agglomeration tendency of nanoclay particles, backscattered SEM images has been obtained from the smooth and fracture surfaces of sample with and without nanoclay particle. Corroborating our findings,
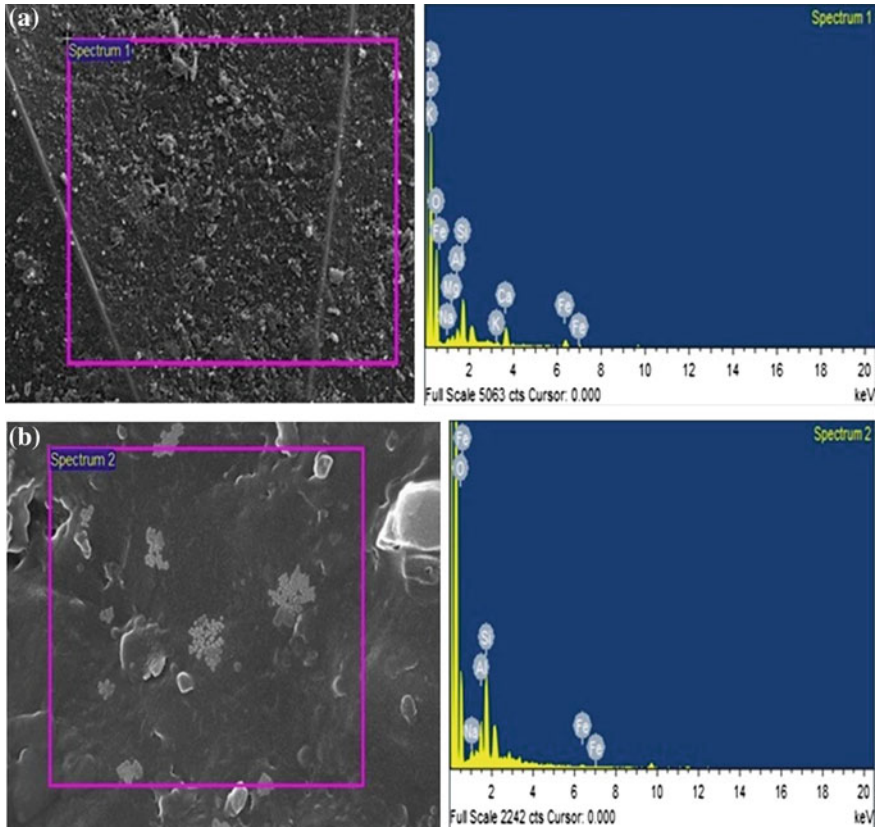

Fig. 21 X-ray diffractograms of laminates with respect to different samples scanned at the interval $2\theta = 3–10$
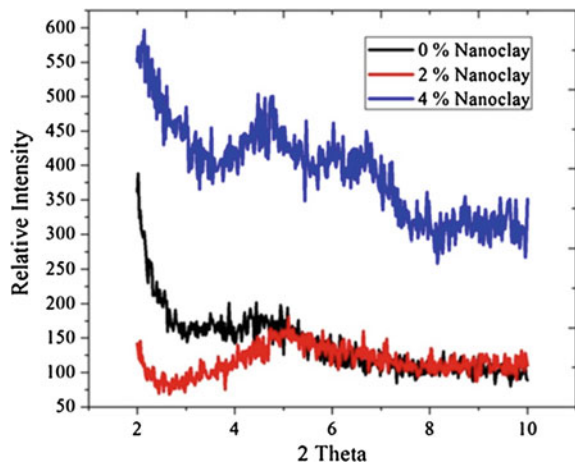
Fig. 22 X-ray diffractograms of laminates with respect to different samples scanned at the interval $2\theta = 3–8$
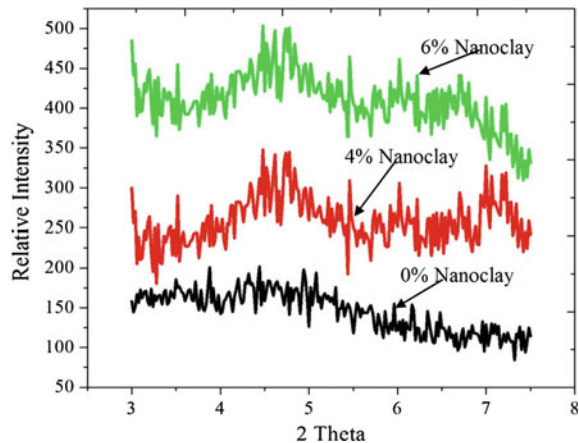
Fig. 23 SEM Images and its EDS analysis of **a** Sample without nanoclay **b** Sample with 4 % of nanoclay

the XRD spectrum of the samples with identical glass fiber reinforced in clay modified matrix is measured by Emrah Bozkurt et al. (2007). The results of the x-ray diffraction study of sample (0, 4 and 6 %) scanned at the interval $2\theta = 3$–8 are shown in Fig. 22.

5.6.2 EDS Analysis

Figure 23 illustrate the EDS allotment of material composition with SEM image of a polished cross section of the 0 and 4 % nanoclay sample. It is observed that, the 4 % of nanoclay sample containing more of Silicon and Aluminum due to reinforcement of nanoclay in the matrix.
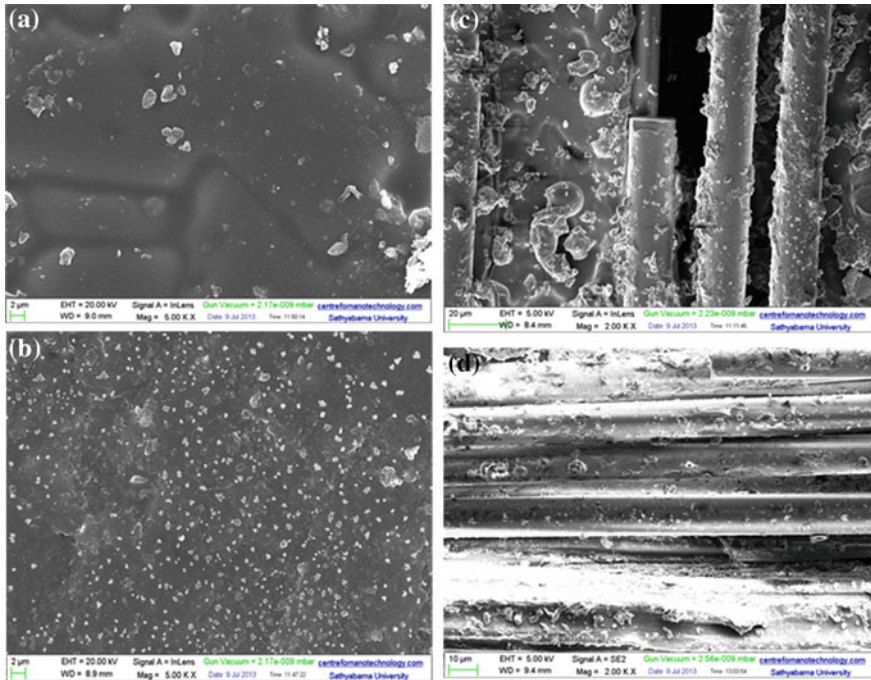
Fig. 24 a–d Scanning electron micrographs of composite samples with 0 and 4 wt% nanoclay.
a Images taken at 5 kx from the polished surfaces of 0 % nanoclay sample. **b** Images taken at 5 kx
from the polished surfaces of 4 % nanoclay sample. **c** Image taken 2 kx from fracture surface of
0 % nanoclay sample. **d** Image taken 2 kx from fracture surface of 4 % nanoclay sample

5.6.3 SEM Analysis

The Fig. 24a–d shows SEM image of before and after fracture surface of the
composite samples. It is often not possible to see individual nanoclay platelets
implanted in a polymer matrix system by using SEM. However, the image observed
in the nanocomposite samples is an indication of the homogeneity of the nanoclay
dispersion. From Fig. 24b, it is observed that, the samples containing 4 % nanoclay
display a granular surface topology with geometric features at smaller length scales,
compared with the sample without nanoclay. These Microstructural differences
similar to the ones observed herein which have been reported elsewhere for hand
lay–up glass/epoxy composites (Levent Aktas 2010). The composite sample
without nanoclay, having less matrix residues that are observed on the fiber surfaces
and between fibers is poor signs of good fiber-matrix adhesion which are observed
in Fig. 24c. Figure 24d also shows the fracture surfaces of the composite samples
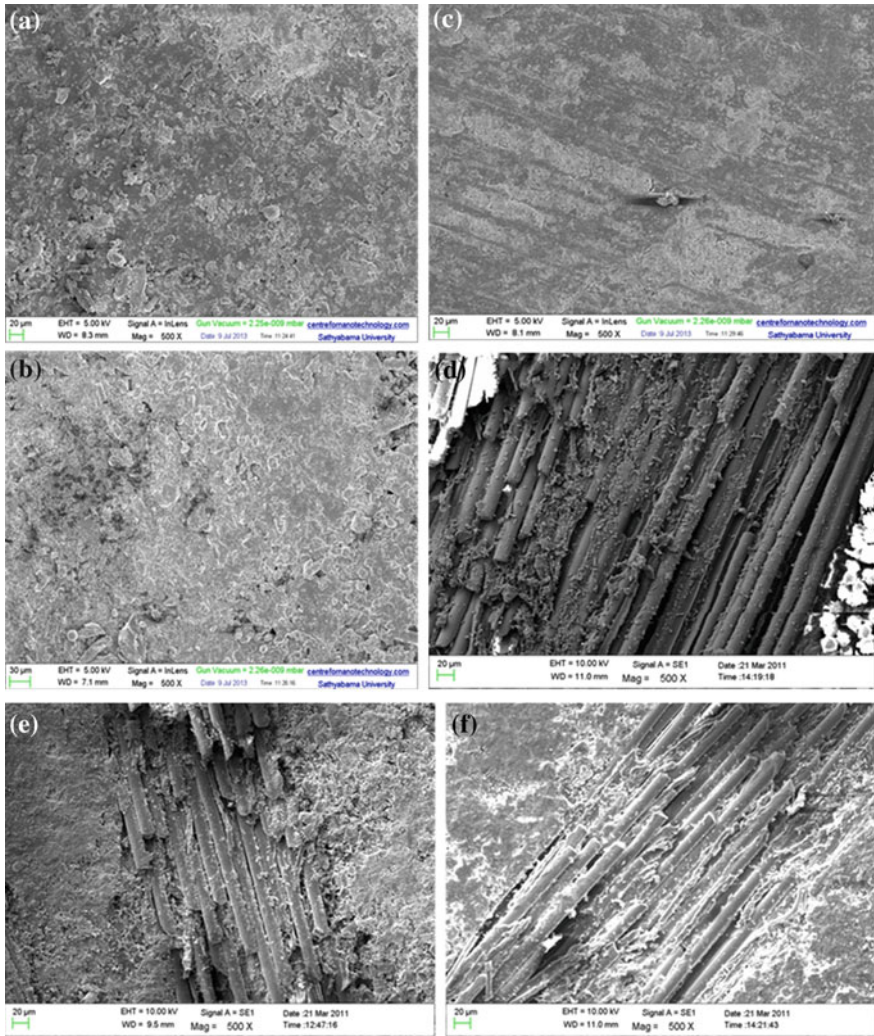
Fig. 25 a–f Scanning electron micrographs of composite samples with 0, 4 and 6 % nanoclay taken at 500x. **a** Images taken from the polished surfaces of 0 % nanoclay sample. **b** Images taken from the polished surfaces of 4 % nanoclay sample. **c** Images taken from the polished surfaces of 6 % nanoclay sample. **d** Image taken from fracture surface of 0 % nanoclay sample. **e** Image taken from fracture surface of 4 % nanoclay sample. **f** Image taken from fracture surface of 6 % nanoclay sample

with 4 % of nanoclay. The buildup of nano modified matrix residues around the fibers is considerably more compared to the sample without nanoclay. Existence of nano matrix material around the fibers after fracture indicates that effective

Table 21 Summary of results in terms of laminates S1 and F1 (S1: All Jute laminate without nanoclay, F1: PS foam-Glass sandwich laminate without nanoclay)

S. no	Material properties	Improvement found at (%)	Amount of improvement	
			Hybrid sandwich	PS foam sandwich
1	Flexural strength (MPa)	4	90 %	–
2	Flexural modulus (Gpa)	4	83.6 %	–
3	Flexural rigidity (N-mm$^{2)}$)	4	–	20 times
4	Charpy impact strength (kJ/m^2)	6	2.3 times	80 %
5	Shore D hardness	6	34 %	
6	% of moister absorption	6	73 % (744 h)	25 % (744 h)
7	Reduction of Damage area (mm^2)	4	5 times (10 J), 4 times (20 J)	3.4 times (10 J), 3 times (15 J)
8	CAI strength (MPa)	4	2.45 %	–
9	Natural frequency (Hz)	4	–	3 times
10	Storage modulus (MPa)	4	–	105 times
11	Loss modulus (MPa)	4	–	33 times
12	Dynamic stiffness (N/m)	4	–	14.4 times
13	Damping factor	4	–	2.6 times
14	d-spacing	4	49 %	

fiber-matrix adhesion is maintained after the addition of nanoclay. The scanning electron micrographs of before and after fracture surface of the 0, 4 and 6 % composite samples taken at 500× are shown in Fig. 25a–f.

6 Summary of Research Findings

In this section, experimental results obtained for various laminates are summarized. Tables 21 and 22 records the details of the summary of percentage improvement of static and dynamic properties for sandwich laminates when compared with the laminate without nano clay.

Table 22 Summary of results in terms of laminates S2 and F2 (S2: Jute-Glass hybrid laminate without nanoclay, F2: PS foam-Glass laminate without nanoclay)

S. no	Material properties	Improvement found at (%)	Amount of Improvement	
			Hybrid sandwich	PS foam sandwich
1	Flexural strength (MPa)	4	16.2 %	19.5 %
2	Flexural modulus (Gpa)	4	44.9 %	42 %
3	Flexural rigidity (N-mm$^{2)}$)	4	–	20 times of all glass
4	Charpy impact strength (kJ/m^2)	6	22.4 %	50 %
5	% of moister absorption	6	50 % (744 h)	72 % (744 h)
6	Reduction of damage area (mm^2)	4	24 % (10 J), 15.6 % (20 J)	2.2 times (10 J), 2.43 times (15 J)
7	CAI strength (MPa)	4	44 %	38 %
8	Natural frequency (Hz)	4	–	2.3 times
9	Storage modulus (MPa)	4	–	5.2 times
10	Loss modulus (MPa)	4	–	19 times
11	Dynamic stiffness (N/m)	4	–	5.2 times
12	Damping factor	4	–	1.9 times

References

Ahmed, K.S., Vijayarangan, S.: Tensile, flexural and interlaminar shear properties of woven jute and jute-glass fabric reinforced polyester composites. J. Mater. Process. Technol. **207**, 330–335 (2008)

Ahmed, K.S., Vijayarangan, S., Rajput, C.: Mechanical behavior of isothalic polyester-based untreated woven jute and glass fabric hybrid composites. J. Reinf. Plast. Compos. **25**, 1549–1569 (2006)

Akil, H.M., Cheng, L.W., Ishak, Z.A.M., Bakar, A.A., Rahman, M.A.: Water absorption study on pultruded jute fibre reinforced unsaturated polyester composites. Compos. Sci. Technol. **69**, 1942–1948 (2009)

Aktas, L., Cengiz Altan, M.: Characterization of nanocomposite laminates fabricated from aqueous dispersion of nanoclay. Polym. Compos. **31**, 620–629 (2010)

Anbusagar, N.R.R., Palanikumar, K., Giridharan, P.K.: Study of sandwich effect on nanoclay modified polyester resin GFR face sheet laminates. Compos. Struct. **125**, 336–342 (2015)

Anbusagar, N.R.R., Giridharan, P.K., Palanikumar, K.: Effect of nano modified polyester resin on hybrid sandwich laminates. Mater. Des. **54**, 507–514 (2013a)

Anbusagar, N.R.R., Giridharan, P.K., Palanikumar, K.: Influence of Nano Particle on Flexural and Impact Properties of Sandwich Structures. Adv. Mater. Res. **602**, 174–177 (2013b)

Anbusagar, N.R.R., Giridharan, P.K., Palanikumar, K.: Mechanical behavior of glass-jute sandwich nano polyester composites to flexural and impact loading. Eur. J. Sci. Res. **84**(2), 148–155 (2012)

Antonio, A.F., Soares, M.I., Neto, A.S.: A study on nanostructured laminated plates behavior under low-velocity impact loadings. Int. J. Impact Eng. **34**, 28–41 (2007)

Belingardi, G., Cavatorta, M.P., Duella, R.: Material characterization of a composite–foam sandwich for the front structure of a high speed train. Compos. Struct. **61**, 13–25 (2003)

Boopalan, M., Niranjanaa, M., Umapathy, M.J.: Study on the mechanical properties and thermal properties of jute and banana fiber reinforced epoxy hybrid composites. Compos. B **51**, 54–57 (2013)

Bozkurt, E., Kaya, E., Tanoglu, M.: Mechanical and thermal behavior of non-crimp glass fiber reinforced layered clay/epoxy nanocomposites. Compos. Sci. Technol. **67**, 3394–3403 (2007)

Cardoso, R.J., Shukla, A., Bose, A.: Effect of particle size and surface treatment on constitutive properties of polyester-cenosphere composites. J. Mater. Sci. **37**, 603 (2002)

Chandradoss, J., Ramesh Kumar, M., Velmurugan, R.: Effect of clay dispersion on mechanical, thermal and vibration properties of glass fiber-reinforced vinyl ester composites. J. Reinf. Plastics Compos. **27**, 1585–1601 (2008)

Igor, M., De Rosa., Santulli, C., Sarasini, F., Valente, M.: Post-impact damage characterization of hybrid configurations of jute/glass polyester laminates using acoustic emission and IR thermography. Compos. Sci. Technol. **69**, 1142–1150 (2009)

Dear, J.P., Brown, S.A.: Impact damage processes in reinforced polymeric materials. Compos. A **5**, 411–420 (2003)

Faguaga, E., Perez, C.J., Villarreal, N., Rodriguez, E.S., Alvarez, V.: Effect of water absorption on the dynamic mechanical properties of composites used for windmill blades. Mater. Des. **36**, 609–616 (2012)

Fam, A., Sharaf, T.: Flexural performance of sandwich panels comprising polyurethane core and GFRP skins and ribs of various configuration. Compos. Struct. **92**, 2927–2935 (2010)

Fraga, A.N., Alvarez, V.A., Vazquez, A., De la Osa, O.: Relationship between dynamic mechanical properties and water absorption of unsaturated polyester and vinyl ester glass fiber composites. J. Comp. Mater. **37**, 1553–1574 (2003)

Akil, H.M., Cheng, L.W., Ishak, Z.A.M., Bakar, A.A., Rahman, M.A.A.: Water absorption study on pultruded jute fibre reinforced unsaturated polyester composites Composites Science and Technology. **69**(11), 1942–1948 (2009)

Jawaid, M., Abdul Khalil, H.P.S., Hassan, A., Dungani, R., Hadiyane, A.: Effect of jute fiber loading on tensile and dynamic mechanical properties of oil palm epoxy composites. Compos. B **45**, 619–624 (2013)

Karippal, J.J., Narasimha Murthy, H.N., Rai, K.S., Sreejith, M., Krishna, M.: Study of mechanical properties of epoxy/glass/nanoclay hybrid composites. J. Compos. Mater. **451**, 893–1899 (2011)

Khan, M.A., Ganster, J., Fink, H.-P.: Hybrid composites of jute and man-made cellulose fibers with polypropylene by injection moulding. **C**ompos. Part A. **40**, 846–851 (2009)

Mallick, P.K.: Performance. Dekker Mechanical Engineering (2007)

Manalo, A.C., Aravinthan, T., Karunasena, W.: Flexural behaviour of glue-laminated fibre composite sandwich beams. Compos. Struct. **92**, 2703–2711 (2010)

Meguid, S.A., Sun, Y.: On the tensile and shear strength of nano-reinforced composite interfaces. Mater. Des. **4**, 289–296 (2004)

Mines, R.A.W., Worrall, C.M., Gibson, A.G.: Low velocity perforation behaviour of polymer composite sandwich panels. Int. J. Impact Eng **21**, 855–879 (1998)

Miyagawa, H., Jurek, R.J., Mohanty, A.K., Misra, M., Drzal, L.T.: Biobased epoxy/clay nanocomposites as a new matrix for CRFP. Compos. A **37**, 54–62 (2006)

Nayak, S.K., Mohanty, S., Samal, S.K.: Influence of short bamboo/glass fiber on the thermal, dynamic mechanical and rheological properties of polypropylene hybrid composites. Mater. Sci. Eng. A. **523**, 32–38 (2009)

Nunes, L.M., Paciornik, S.: M. d'Almeida, J.R.: Evaluation of the damaged area of glass-fiber-reinforced epoxy-matrix composite materials submitted to ballistic impacts. Compos. Sci. Technol. **64**, 945–954 (2004)

Ramesh, M., Palanikumar, K., Hemachandra Reddy, K.: Mechanical property evaluation of sisal–jute–glass fiber reinforced polyester composites. Compos. B **48**, 1–9 (2013)

Ray, D., Sarkar, B.K., Das, S., Rana, A.K.: Dynamic mechanical and thermal analysis of vinylester-resin-matrix composites reinforced with untreated and alkali-treated jute fibres. Compos. Sci. Technol. **62**, 911–917 (2002)

Reis, E., Rizkalla, S.: Material characteristics of 3-D FRP sandwich panels. Constr. Build. Mater. **22**, 1009–18 (2008)

Saha, M.C., Kabir, E., Jeelani, S.: Study of debond fracture toughness of sandwich composites with nanophased core. Mater. Lett. **62**, 567–570 (2008)

Sargianis, J., Suhr, J.: Effect of core thickness on wave number and damping properties in sandwich composites. Compos. Sci. Technol. **72**, 724–730 (2012)

Thwe, M.M., Liao, K.: Durability of bamboo-glass fiber reinforced polymer matrix hybrid composites. Compos. Sci. Technol. **63**, 375–387 (2003)

Venkateshwaran, N., ElayaPerumal, A., Alavudeen, A., Thiruchitrambalam, M.: Mechanical and water absorption behaviour of banana/sisal reinforced hybrid composites. Mater. Des. **32**, 4017–4021 (2011)

Xiong, J., Ma, L., Wu, L., Liu, J., Vaziri, A.: Mechanical behavior and failure of composite pyramidal truss core sandwich columns. Compos. Part B. **42**, 938–945 (2011)

Younesi, D., Mehravaran, R., Akbarian, S., Younesi, M.: Fabrication of the new structure high toughness PP/HA-PP sandwich nano-composites by rolling process. Mater. Des. **43**, 549–559 (2013)

Zhang, Y., Li, Y., Ma, H., Yu, T.: Tensile and interfacial properties of unidirectional flax/glass fiber reinforced hybrid composites. Compos. Sci. Technol. **88**, 172–177 (2013)